2019年5月27日(月)

[E] ポスター発表 | セッション記号 P (宇宙惑星科学)：P-PS 惑星科学

15:30 ~ 17:00 | ポスター会場 幕張メッセ国際展示場 8ホール_1

[P-PS05] Recent advances of Venus science

コンビーナ:佐藤 毅彦(宇宙航空研究開発機構・宇宙科学研究本部)、堀之内 武(北海道大学地球環境科学研究院)、山本 勝(九州大学応用力学研究所)、Kevin McGouldrick(University of Colorado Boulder)

[PPS05-P01] New thermal infrared camera for fine horizontal brightness temperature structures at the cloud-top level of Venus

*Tetsuya Fukuhara[1]、Makoto Taguchi[1]、Takeshi Imamura[2]、Sanjay S Limaye[3] (1.Rikkyo University、2.The University of Tokyo、3.University of Wisconsin)

[PPS05-P02] Temperature and wind variations in Venusian mesosphere and lower thermosphere by mid-infrared heterodyne spectrometer in 2018

*高見 康介[1]、中川 広務[1]、佐川 英夫[2]、村田 功[1]、笠羽 康正[1] (1.東北大学大学院理学研究科地球物理学専攻惑星大気物理学分野、2.京都産業大学大学院理学研究科物理学専攻)

[PPS05-P03] Local time dependence of limb darkening seen in the thermal infrared Venus disk

*秋場 聖浩[1] (1.立教大学院理学研究所物理学専攻)

[PPS05-P04] あかつき中間赤外画像の積算による金星雲頂の定在構造と帯状構造の抽出

*福谷 貴一[1]、今村 剛[1]、田口 真[2]、福原 哲哉[2]、神山 徹[3] (1.東京大学、2.立教大学、3.産総研)

[PPS05-P05] Akatsuki's IR2 Nightside Photometry Restoration by Deconvolution

*Choon Wei Vun[1]、Takehiko Satoh[2,1]、Kevin McGouldrick[3]、Takeshi Horinouchi[4]、Takao M. Sato[5] (1.SOKENDAI、2.ISAS/JAXA、3.University of Colorado Boulder、4.Hokkaido University、5.Hokkaido Information University)

[PPS05-P06] Enormous cloud cover as seen by Akatsuki/IR2 on the night-side disk of Venus

*佐藤 毅彦[1,2]、Vun Choon Wei[2]、佐藤 隆雄[3]、堀之内 武[4]、はしもと じょーじ[5]、McGouldrick Kevin[6] (1.宇宙航空研究開発機構・宇宙科学研究所、2.総合研究大学院大学・宇宙科学専攻、3.北海道情報大学・経営情報学部、4.北海道大学・地球環境科学研究院 、5.岡山大学・理学部地球科学科、6.LASP, University of Colorado Boulder)

[PPS05-P07] あかつき搭載IR1から明らかにする金星雲の全球変動

*高木 聖子[1]、岩上 直幹、高橋 幸弘[1]、佐藤 光輝[1] (1.北海道大学大学院理学研究院)

[PPS05-P08] 対流モデルに向けた金星雲計算スキームの開発

*杉山 耕一朗[1]、福原 望[1]、小高 正嗣[2]、中島 健介[3]、石渡 正樹[2]、今村 剛[4]、林 祥介[5] (1.松江高専・情報、2.北大・理・宇宙、3.九大・理・地惑、4.東大・新領域創成科学、5.神戸大・理・地惑)

[PPS05-P09] 放射伝達を陽に考慮した金星大気大循環モデルで見られる東西平均構造

★招待講演

*林 祥介[1]、塩尻 千里[1]、樫村 博基[1]、高橋 芳幸[1] (1.神戸大学・大学院理学研究科 惑星学専攻/惑星科学研究センター（CPS）)

[PPS05-P10] 電波掩蔽による金星大気温度データからの重力波の波束の抽出

*森 亮太[1]、今村 剛[1]、Javier Peralta[2] (1.東京大学、2.宇宙航空研究開発機構)

[PPS05-P11] **Status of lightning hunt in Venus with Akatsuki/LAC and Pirka telescope**

*高橋 幸弘[1,2]、佐藤 光輝[1,2]、今井 正尭[3]、Lorenz Ralph[4]、高木 聖子[1,2]、大野 辰遼[1] (1.北海道大学・大学院理学院・宇宙理学専攻、2.北海道大学・大学院理学研究院、3.産業技術総合研究所、4.ジョンズホプキンズ大学応用物理研究所)

[PPS05-P12] **Possibility of electric discharge in the Venusian atmosphere due to the super-rotation of clouds**

*Adhithiyan Neduncheran[1]、Ugur Guven[1,2]、Ananyo Bhattacharya[3] (1.University of Petroleum and Energy Studies, India、2.United Nations Centre for Space Science and Technology Education in Asia and the Pacific、3.Sardar Vallabhbhai National Institute of Technology,India)

[E] ポスター発表 | セッション記号 P (宇宙惑星科学)：P-PS 惑星科学

17:15 ~ 18:30 | ポスター会場 幕張メッセ国際展示場 8ホール_2

[P-PS05] Recent advances of Venus science

コンビーナ:佐藤 毅彦(宇宙航空研究開発機構・宇宙科学研究本部)、堀之内 武(北海道大学地球環境科学研究院)、山本 勝(九州大学応用力学研究所)、Kevin McGouldrick(University of Colorado Boulder)

[PPS05-P01] New thermal infrared camera for fine horizontal brightness temperature structures at the cloud-top level of Venus

*Tetsuya Fukuhara[1]、Makoto Taguchi[1]、Takeshi Imamura[2]、Sanjay S Limaye[3] (1.Rikkyo University、2.The University of Tokyo、3.University of Wisconsin)

[PPS05-P02] Temperature and wind variations in Venusian mesosphere and lower thermosphere by mid-infrared heterodyne spectrometer in 2018

*高見 康介[1]、中川 広務[1]、佐川 英夫[2]、村田 功[1]、笠羽 康正[1] (1.東北大学大学院理学研究科地球物理学専攻惑星大気物理学分野、2.京都産業大学大学院理学研究科物理学専攻)

[PPS05-P03] Local time dependence of limb darkening seen in the thermal infrared Venus disk

*秋場 聖浩[1] (1.立教大学院理学研究所物理学専攻)

[PPS05-P04] あかつき中間赤外画像の積算による金星雲頂の定在構造と帯状構造の抽出

*福谷 貴一[1]、今村 剛[1]、田口 真[2]、福原 哲哉[2]、神山 徹[3] (1.東京大学、2.立教大学、3.産総研)

[PPS05-P05] Akatsuki's IR2 Nightside Photometry Restoration by Deconvolution

*Choon Wei Vun[1]、Takehiko Satoh[2,1]、Kevin McGouldrick[3]、Takeshi Horinouchi[4]、Takao M. Sato[5] (1.SOKENDAI、2.ISAS/JAXA、3.University of Colorado Boulder、4.Hokkaido University、5.Hokkaido Information University)

[PPS05-P06] Enormous cloud cover as seen by Akatsuki/IR2 on the night-side disk of Venus

*佐藤 毅彦[1,2]、Vun Choon Wei[2]、佐藤 隆雄[3]、堀之内 武[4]、はしもと じょーじ[5]、McGouldrick Kevin[6] (1.宇宙航空研究開発機構・宇宙科学研究所、2.総合研究大学院大学・宇宙科学専攻、3.北海道情報大学・経営情報学部、4.北海道大学・地球環境科学研究院 、5.岡山大学・理学部地球科学科、6.LASP, University of Colorado Boulder)

[PPS05-P07] あかつき搭載IR1から明らかにする金星雲の全球変動

*高木 聖子[1]、岩上 直幹、高橋 幸弘[1]、佐藤 光輝[1] (1.北海道大学大学院理学研究院)

[PPS05-P08] 対流モデルに向けた金星雲計算スキームの開発

*杉山 耕一朗[1]、福原 望[1]、小高 正嗣[2]、中島 健介[3]、石渡 正樹[2]、今村 剛[4]、林 祥介[5] (1.松江高専・情報、2.北大・理・宇宙、3.九大・理・地惑、4.東大・新領域創成科学、5.神戸大・理・地惑)

[PPS05-P09] 放射伝達を陽に考慮した金星大気大循環モデルで見られる東西平均構造

★招待講演

*林 祥介[1]、塩尻 千里[1]、樫村 博基[1]、高橋 芳幸[1] (1.神戸大学・大学院理学研究科 惑星学専攻/惑星科学研究センター（CPS）)

[PPS05-P10] 電波掩蔽による金星大気温度データからの重力波の波束の抽出

*森 亮太[1]、今村 剛[1]、Javier Peralta[2] (1.東京大学、2.宇宙航空研究開発機構)

[PPS05-P11] **Status of lightning hunt in Venus with Akatsuki/LAC and Pirka telescope**

*高橋 幸弘[1,2]、佐藤 光輝[1,2]、今井 正尭[3]、Lorenz Ralph[4]、高木 聖子[1,2]、大野 辰遼[1] (1.北海道大学・大学院理学院・宇宙理学専攻、2.北海道大学・大学院理学研究院、3.産業技術総合研究所、4.ジョンズホプキンズ大学応用物理研究所)

[PPS05-P12] **Possibility of electric discharge in the Venusian atmosphere due to the super-rotation of clouds**

*Adhithiyan Neduncheran[1]、Ugur Guven[1,2]、Ananyo Bhattacharya[3] (1.University of Petroleum and Energy Studies, India、2.United Nations Centre for Space Science and Technology Education in Asia and the Pacific、3.Sardar Vallabhbhai National Institute of Technology,India)

[E] ポスター発表 | セッション記号 P (宇宙惑星科学)：P-EM 太陽地球系科学・宇宙電磁気学・宇宙環境

13:45 ~ 15:15 | ポスター会場 幕張メッセ国際展示場 8ホール_1

[P-EM10] Multi-scale Coupling in the Magnetosphere-Ionosphere-Thermosphere System

コンビーナ:Yue Deng(University of Texas at Arlington)、Toshi Nishimura(Boston University)、Liu Huixin(九州大学理学研究院地球惑星科学専攻 九州大学宙空環境研究センター)、Yanshi Huang(Harbin Institute of Technology, Shenzhen)

[PEM10-P01] 相対論的電子降り込みに対する南北両半球大気のレスポンス

*田中 良昌[1,13,14]、西山 尚典[1,14]、門倉 昭[1,13,14]、尾崎 光紀[2]、三好 由純[3]、大山 伸一郎[3,15]、片岡 龍峰[1,14]、堤 雅基[1,14]、西村 耕司[1,13,14]、佐藤 薫[4]、笠原 禎也[2]、熊本 篤志[5]、土屋 史紀[5]、吹澤 瑞貴[5]、疋島 充[6]、松田 昇也[6]、松岡 彩子[6]、篠原 育[6]、能勢 正仁[3]、長妻 努[7]、篠原 学[8]、藤本 晶子[9]、寺本 万里子[3]、野村 麗子[10]、行松 彰[1,14]、細川 敬祐[11]、小路 真史[3]、Ralph Latteck[12] (1.国立極地研究所、2.金沢大学理工研究域、3.名古屋大学宇宙地球環境研究所、4.東京大学大学院理学系研究科、5.東北大学大学院理学研究科、6.宇宙航空研究開発機構宇宙科学研究所、7.情報通信研究機構、8.鹿児島工業高等専門学校、9.九州工業大学、10.国立天文台、11.電気通信大学大学院情報理工学研究科、12.Leibniz-Institute of Atmospheric Physics e.V. at the University Rostock, Germany、13.情報・システム研究機構 データサイエンス共同利用基盤施設 極域環境データサイエンスセンター、14.総合研究大学院大学、15.University of Oulu, Finland)

[PEM10-P02] Comparison of precipitating particle energy of proton aurora at geomagnetic conjugate points

*田口 真[1]、西島 樹[1]、門倉 昭[2] (1.立教大学、2.情報・システム研究機構)

[PEM10-P03] A regularized deep convolutional general adversarial network (R-DCGAN) for total electron content map completion

*Mingwu Jin[1]、Zhou Chen[2,3]、Yue Deng[1]、Yang Pan[1]、Jin-Song Wang[2] (1.University of Texas at Arlington、2.Institute of Space Science and Technology, Nanchang University, Nanchang, China、3.Key Laboratory of Space Weather, National Center for Space Weather, China Meteorological Administration, Beijing, China)

[PEM10-P04] A long-lasting auroral bright spot around magnetic north pole: Is it the evidence of stable magnetic reconnection?

*Qing-He Zhang[1]、Guo-Cheng Shen[1]、Yong-Liang Zhang[2]、Kjellmar Oksavik[3]、Michael Lockwood[4]、Zan-Yang Xing[1]、Yu-Zhang Ma[1] (1.Institute of Space Sciences, Shandong University, Weihai, China、2.The Johns Hopkins University Applied Physics Laboratory, Laurel, Maryland, USA、3.Birkeland Centre for Space Science, University of Bergen, Bergen, Norway、4.Department of Meteorology, University of Reading, Earley Gate, Post Office Box 243, RG6 6BB, UK.)

[PEM10-P05] Statistical study of the relationship between ion upflow and field-aligned current in the topside ionosphere for both hemispheres during disturbed and quiet times

Shan-Yu Zhou[1]、*Qing-He Zhang[1]、P. T. Jayachandran[2]、Kjellmar Oksavik[3]、Larry Lyons[4]、Zan-Yang Xing[1]、Yu-Zhang Ma[1]、Marc Hairston[5]、Yong Wang[1] (1.Institute of Space Sciences, Shandong University, Weihai, China、2.Physics Department, University of New Brunswick, Fredericton, New Brunswick, Canada、3.Birkeland Centre for Space Science, University of Bergen, Bergen, Norway、4.Department of Atmospheric and Oceanic Sciences, University of California, Los Angeles, California, USA、5.William B. Hanson Center for Space Sciences, University of Texas at Dallas, Richardson, Texas, USA)

[PEM10-P06] SAPS in the 2013 March 17 Storm Event: Initial Results from the Coupled Magnetosphere-Ionosphere-Thermosphere Model

*Dong Lin[1,2]、Wenbin Wang[2]、Wayne Scales[1]、Kevin Pham[2]、Jing Liu[2]、Binzheng Zhang[2]、Viacheslav Merkin[3]、Xueling Shi[1] (1.Virginia Tech、2.High Altitude Observatory, NCAR、3.APL, John Hopkins Univ.)

[PEM10-P07] Westward turning motions of nighttime medium-scale traveling ionospheric disturbances (MSTIDs) at the equatorward side of the dusk side auroral oval associated with auroral brightening

*Sneha Yadav[1,2]、Kazuo Shiokawa[1]、Shin-ichiro Oyama[1,3,4]、Yuichi Otsuka[1] (1.ISEE, Nagoya University, Nagoya, Japan、2.SPL, VSSC, India、3.Ionosphere Research Unit, University of Oulu, Oulu, Finland、4.NIPR, Tachikawa, Japan)

[E] ポスター発表 | セッション記号 P (宇宙惑星科学)：P-EM 太陽地球系科学・宇宙電磁気学・宇宙環境

17:15 ~ 18:30 | ポスター会場 幕張メッセ国際展示場 8ホール_4

[P-EM10] Multi-scale Coupling in the Magnetosphere-Ionosphere-Thermosphere System

コンビーナ:Yue Deng(University of Texas at Arlington)、Toshi Nishimura(Boston University)、Liu Huixin(九州大学理学研究院地球惑星科学専攻 九州大学宙空環境研究センター)、Yanshi Huang(Harbin Institute of Technology, Shenzhen)

[PEM10-P01] 相対論的電子降り込みに対する南北両半球大気のレスポンス

*田中 良昌[1,13,14]、西山 尚典[1,14]、門倉 昭[1,13,14]、尾崎 光紀[2]、三好 由純[3]、大山 伸一郎[3,15]、片岡 龍峰[1,14]、堤 雅基[1,14]、西村 耕司[1,13,14]、佐藤 薫[4]、笠原 禎也[2]、熊本 篤志[5]、土屋 史紀[5]、吹澤 瑞貴[5]、疋島 充[6]、松田 昇也[6]、松岡 彩子[6]、篠原 育[6]、能勢 正仁[3]、長妻 努[7]、篠原 学[8]、藤本 晶子[9]、寺本 万里子[3]、野村 麗子[10]、行松 彰[1,14]、細川 敬祐[11]、小路 真史[3]、Ralph Latteck[12] (1.国立極地研究所、2.金沢大学理工研究域、3.名古屋大学宇宙地球環境研究所、4.東京大学大学院理学系研究科、5.東北大学大学院理学研究科、6.宇宙航空研究開発機構宇宙科学研究所、7.情報通信研究機構、8.鹿児島工業高等専門学校、9.九州工業大学、10.国立天文台、11.電気通信大学大学院情報理工学研究科、12.Leibniz-Institute of Atmospheric Physics e.V. at the University Rostock, Germany、13.情報・システム研究機構 データサイエンス共同利用基盤施設 極域環境データサイエンスセンター、14.総合研究大学院大学、15.University of Oulu, Finland)

[PEM10-P02] Comparison of precipitating particle energy of proton aurora at geomagnetic conjugate points

*田口 真[1]、西島 樹[1]、門倉 昭[2] (1.立教大学、2.情報・システム研究機構)

[PEM10-P03] A regularized deep convolutional general adversarial network (R-DCGAN) for total electron content map completion

*Mingwu Jin[1]、Zhou Chen[2,3]、Yue Deng[1]、Yang Pan[1]、Jin-Song Wang[2] (1.University of Texas at Arlington、2.Institute of Space Science and Technology, Nanchang University, Nanchang, China、3.Key Laboratory of Space Weather, National Center for Space Weather, China Meteorological Administration, Beijing, China)

[PEM10-P04] A long-lasting auroral bright spot around magnetic north pole: Is it the evidence of stable magnetic reconnection?

*Qing-He Zhang[1]、Guo-Cheng Shen[1]、Yong-Liang Zhang[2]、Kjellmar Oksavik[3]、Michael Lockwood[4]、Zan-Yang Xing[1]、Yu-Zhang Ma[1] (1.Institute of Space Sciences, Shandong University, Weihai, China、2.The Johns Hopkins University Applied Physics Laboratory, Laurel, Maryland, USA、3.Birkeland Centre for Space Science, University of Bergen, Bergen, Norway、4.Department of Meteorology, University of Reading, Earley Gate, Post Office Box 243, RG6 6BB, UK.)

[PEM10-P05] Statistical study of the relationship between ion upflow and field-aligned current in the topside ionosphere for both hemispheres during disturbed and quiet times

Shan-Yu Zhou[1]、*Qing-He Zhang[1]、P. T. Jayachandran[2]、Kjellmar Oksavik[3]、Larry Lyons[4]、Zan-Yang Xing[1]、Yu-Zhang Ma[1]、Marc Hairston[5]、Yong Wang[1] (1.Institute of Space Sciences, Shandong University, Weihai, China、2.Physics Department, University of New Brunswick, Fredericton, New Brunswick, Canada、3.Birkeland Centre for Space Science, University of Bergen, Bergen, Norway、4.Department of Atmospheric and Oceanic Sciences, University of California, Los Angeles, California, USA、5.William B. Hanson Center for Space Sciences, University of Texas at Dallas, Richardson, Texas, USA)

[PEM10-P06] SAPS in the 2013 March 17 Storm Event: Initial Results from the Coupled Magnetosphere-Ionosphere-Thermosphere Model

*Dong Lin[1,2]、Wenbin Wang[2]、Wayne Scales[1]、Kevin Pham[2]、Jing Liu[2]、Binzheng Zhang[2]、Viacheslav Merkin[3]、Xueling Shi[1] (1.Virginia Tech、2.High Altitude Observatory, NCAR、3.APL, John Hopkins Univ.)

[PEM10-P07] Westward turning motions of nighttime medium-scale traveling ionospheric disturbances (MSTIDs) at the equatorward side of the dusk side auroral oval associated with auroral brightening

*Sneha Yadav[1,2]、Kazuo Shiokawa[1]、Shin-ichiro Oyama[1,3,4]、Yuichi Otsuka[1] (1.ISEE, Nagoya University, Nagoya, Japan、2.SPL, VSSC, India、3.Ionosphere Research Unit, University of Oulu, Oulu, Finland、4.NIPR, Tachikawa, Japan)

[E] ポスター発表 | セッション記号 A (大気水圏科学)：A-OS 海洋科学・海洋環境

15:30 ~ 17:00 | ポスター会場 幕張メッセ国際展示場 8ホール_3

[A-OS12] Marine ecosystems and biogeochemical cycles: theory, observation and modeling

コンビーナ:伊藤 進一(東京大学大気海洋研究所)、平田 貴文(北海道大学地球環境科学研究院)、Enrique N Curchitser(Rutgers University New Brunswick)、Eileen E Hofmann(Old Dominion University)

[AOS12-P01] 日本海の生態系に対する対馬海峡を経由する栄養塩輸送の影響

*柴野 良太[1]、森本 昭彦[1]、髙山 勝巳[2]、滝川 哲太郎[3]、伊藤 雅[4] (1.愛媛大学沿岸環境科学研究センター、2.九州大学応用力学研究所、3.長崎大学大学院水産・環境科学総合研究科、4.水産研究・教育機構日本海区水産研究所)

[AOS12-P02] Revisiting vertical variations in stoichiometry during oceanic organic matter decomposition

*重光 雅仁[1]、青山 道夫[1]、土居 知将[1]、横川 太一[1]、村田 昌彦[1] (1.国立研究開発法人　海洋研究開発機構)

[AOS12-P03] Reproduction of iron-rich intermediate water in the Sea of Okhotsk by high resolution biogeochemical model.

*西川 はつみ[1]、三寺 史夫[1]、浩志 吉成[2]、拓也 中野渡[3]、中村 知裕[1]、内本 圭亮[4]、羽角 博康[5] (1.北海道大学　低温科学研究所、2.国立環境研究所、3.北海道区水産研究所、4.地球環境産業技術研究機構、5.東京大学　大気海洋研究所)

[AOS12-P04] The global oceanic iron distribution estimated by data assimilation approach

*土居 知将[1]、長船 哲史[1]、増田 周平[1]、小畑 元[2]、三角 和弘[3]、西岡 純[4] (1.海洋研究開発機構、2.東京大学、3.電力中央研究所、4.北海道大学)

[AOS12-P05] A high-resolution multi-purpose particle tracking framework for coastal areas near Japan

*松村 義正[1]、桂 将太[1]、黒木 聖夫[2]、中野 英之[3]、山岸 孝輝[4] (1.東京大学 大気海洋研究所、2.海洋研究開発機構、3.気象庁気象研究所、4.高度情報科学技術研究機構)

[AOS12-P06] Numerical study on seasonality of ocean litters collected at the Dongsha Island in the northern South China Sea

*Yi-Chia Hsin[1]、Chia-Ying Ko[2]、Ming-Shiou Jeng[3] (1.Research Center for Environmental Changes, Academia Sinica、2.Institute of Fisheries Science, National Taiwan University、3.Biodiversity Research Center, Academia Sinica)

[AOS12-P07] A key spot and timing to monitor chlorophyll-a in the Kuroshio western boundary current

*平田 貴文[1] (1.北海道大学地球環境科学研究院)

[AOS12-P08] **Impacts of cyclonic eddies on phytoplankton biomass and phenology in the Kuroshio Extension region**

*Eko Siswanto[1]、Yoshikazu Sasai[1] (1.Japan Agency for Marine-Earth Science and Technology)

[AOS12-P09] Diagnostic estimation and uncertainties of nutrient limitation of phytoplankton growth in Michaelis-Menten functional form

*橋岡 豪人[1]、相田 真希[1] (1.国立研究開発法人 海洋研究開発機構)

[AOS12-P10] Modeling productivity in lower trophic levels in Otsuchi Bay, northeast of Japan, using a nested OGCM with a biogeochemical component

*坂本 天[1]、浦川 昇吾[2]、伊藤 幸彦[1]、羽角 博康[1]、田中 潔[1] (1.東京大学大気海洋研究所、2.気象庁気象研究所)

[AOS12-P11] Change in lower trophic level ecosystems to decadal scale variation of climate system in the North Pacific Ocean

*相田 真希[1]、田所 和明[2]、小室 芳樹[3]、橋岡 豪人[1]、原田 尚美[1] (1.国立研究開発法人 海洋研究開発機構 地球環境観測研究開発センター、2.国立研究開発法人 水産研究・教育機構　東北区水産研究所、3.国立研究開発法人 海洋研究開発機構　北極環境変動総合研究センター)

[AOS12-P12] Estimation of experienced environment of jack mackerel in the East China Sea

*樋口 富彦[1]、高橋 素光[2]、白井 厚太朗[1]、伊藤 進一[1] (1.東京大学大気海洋研究所、2.国立研究開発法人 水産研究・教育機構 西海区水産研究所)

[E] ポスター発表 | セッション記号 A (大気水圏科学)：A-OS 海洋科学・海洋環境

17:15 ~ 18:30 | ポスター会場 幕張メッセ国際展示場 8ホール_5

[A-OS12] Marine ecosystems and biogeochemical cycles: theory, observation and modeling

コンビーナ:伊藤 進一(東京大学大気海洋研究所)、平田 貴文(北海道大学地球環境科学研究院)、Enrique N Curchitser(Rutgers University New Brunswick)、Eileen E Hofmann(Old Dominion University)

[AOS12-P01] 日本海の生態系に対する対馬海峡を経由する栄養塩輸送の影響

*柴野 良太[1]、森本 昭彦[1]、髙山 勝巳[2]、滝川 哲太郎[3]、伊藤 雅[4] (1.愛媛大学沿岸環境科学研究センター、2.九州大学応用力学研究所、3.長崎大学大学院水産・環境科学総合研究科、4.水産研究・教育機構日本海区水産研究所)

[AOS12-P02] Revisiting vertical variations in stoichiometry during oceanic organic matter decomposition

*重光 雅仁[1]、青山 道夫[1]、土居 知将[1]、横川 太一[1]、村田 昌彦[1] (1.国立研究開発法人　海洋研究開発機構)

[AOS12-P03] Reproduction of iron-rich intermediate water in the Sea of Okhotsk by high resolution biogeochemical model.

*西川 はつみ[1]、三寺 史夫[1]、浩志 吉成[2]、拓也 中野渡[3]、中村 知裕[1]、内本 圭亮[4]、羽角 博康[5] (1.北海道大学　低温科学研究所、2.国立環境研究所、3.北海道区水産研究所、4.地球環境産業技術研究機構、5.東京大学　大気海洋研究所)

[AOS12-P04] The global oceanic iron distribution estimated by data assimilation approach

*土居 知将[1]、長船 哲史[1]、増田 周平[1]、小畑 元[2]、三角 和弘[3]、西岡 純[4] (1.海洋研究開発機構、2.東京大学、3.電力中央研究所、4.北海道大学)

[AOS12-P05] A high-resolution multi-purpose particle tracking framework for coastal areas near Japan

*松村 義正[1]、桂 将太[1]、黒木 聖夫[2]、中野 英之[3]、山岸 孝輝[4] (1.東京大学 大気海洋研究所、2.海洋研究開発機構、3.気象庁気象研究所、4.高度情報科学技術研究機構)

[AOS12-P06] Numerical study on seasonality of ocean litters collected at the Dongsha Island in the northern South China Sea

*Yi-Chia Hsin[1]、Chia-Ying Ko[2]、Ming-Shiou Jeng[3] (1.Research Center for Environmental Changes, Academia Sinica、2.Institute of Fisheries Science, National Taiwan University、3.Biodiversity Research Center, Academia Sinica)

[AOS12-P07] A key spot and timing to monitor chlorophyll-a in the Kuroshio western boundary current

*平田 貴文[1] (1.北海道大学地球環境科学研究院)

[AOS12-P08] **Impacts of cyclonic eddies on phytoplankton biomass and phenology in the Kuroshio Extension region**

*Eko Siswanto[1]、Yoshikazu Sasai[1] (1.Japan Agency for Marine-Earth Science and Technology)

[AOS12-P09] Diagnostic estimation and uncertainties of nutrient limitation of phytoplankton growth in Michaelis-Menten functional form

*橋岡 豪人[1]、相田 真希[1] (1.国立研究開発法人 海洋研究開発機構)

[AOS12-P10] Modeling productivity in lower trophic levels in Otsuchi Bay, northeast of Japan, using a nested OGCM with a biogeochemical component

*坂本 天[1]、浦川 昇吾[2]、伊藤 幸彦[1]、羽角 博康[1]、田中 潔[1] (1.東京大学大気海洋研究所、2.気象庁気象研究所)

[AOS12-P11] Change in lower trophic level ecosystems to decadal scale variation of climate system in the North Pacific Ocean

*相田 真希[1]、田所 和明[2]、小室 芳樹[3]、橋岡 豪人[1]、原田 尚美[1] (1.国立研究開発法人 海洋研究開発機構 地球環境観測研究開発センター、2.国立研究開発法人 水産研究・教育機構　東北区水産研究所、3.国立研究開発法人 海洋研究開発機構　北極環境変動総合研究センター)

[AOS12-P12] Estimation of experienced environment of jack mackerel in the East China Sea

*樋口 富彦[1]、高橋 素光[2]、白井 厚太朗[1]、伊藤 進一[1] (1.東京大学大気海洋研究所、2.国立研究開発法人 水産研究・教育機構 西海区水産研究所)

[E] ポスター発表 | セッション記号 H (地球人間圏科学)：H-DS 防災地球科学

13:45 ~ 15:15 | ポスター会場 幕張メッセ国際展示場 8ホール_3

[H-DS11] Subaqueous Landslides and Their Anthropogenic Impact for Coastal Regions

コンビーナ:北村 有迅(鹿児島大学大学院理工学研究科地球環境科学専攻)、山田 泰広(海洋研究開発機構　海洋掘削科学研究開発センター)

[HDS11-P01] Deformed sediment gravity flow deposits associated with bypassing slides:an example from the Miocene Ushikiri Formation, Southwest Japan

*小林 未季[1]、酒井 哲弥[2] (1.日本工営株式会社、2.島根大学総合理工学部)

[HDS11-P02] 四国沖大陸棚斜面の海底地すべり調査と津波計算

*権 容大[1]、馬場 俊孝[1]、松野 哲男、林 美鶴、市原 寛 (1.徳島大学大学院)

[HDS11-P03] 八代海南部における白鳳丸KH-18-3次研究航海で採取された堆積物コアの物性から推定される堆積環境

*堀 航喜[1]、北村 有迅[2]、白鳳丸K-18-3次研究航海 乗船研究者一同 (1.九州大学大学院理学府地球惑星科学専攻、2.鹿児島大学大学院理工学研究科地球環境科学専攻)

[HDS11-P04] 「白鳳丸」KH-18-3次研究航海で採取された八代海の堆積物コア試料のベーンせん断強さと帯磁率

*北村 有迅[1]、影山 遼[2]、山﨑 楓[2]、後藤 滝弥[2]、堀 航喜[2]、池端 雄太[2]、川端 訓代[1]、小山 大輝[2]、白鳳丸KH-18-3 乗船研究者 (1.鹿児島大学大学院理工学研究科地球環境科学専攻、2.鹿児島大学理学部地球環境科学科)

[HDS11-P05] Identification of turbidites in the Yatsushiro Sea surface sediment core samples from non-destructive measurements: Hakuho-maru KH-18-3 Cruise, Yatsushiro Sea, Western Kyushu, Japan

*後藤 滝弥[1]、北村 有迅[2]、白鳳丸KH-18-3次研究航海 乗船研究者一同 (1.東京大学大気海洋研究所、2.鹿児島大学大学院理工学研究科地球環境科学専攻)

[HDS11-P06] Revised columnar section based on grain size distribution analysis of samples from Hakuho-maru KH-18-3 in Yatsushiro sea

*池端 雄太[1]、北村 有迅[2]、白鳳丸KH-18-3次研究航海乗船研究者 Family (1.九州大学大学院理学府地球惑星科学専攻、2.鹿児島大学大学院理工学研究科地球環境科学専攻)

[E] ポスター発表 | セッション記号 H (地球人間圏科学)：H-DS 防災地球科学

17:15 ~ 18:30 | ポスター会場 幕張メッセ国際展示場 8ホール_13

[H-DS11] Subaqueous Landslides and Their Anthropogenic Impact for Coastal Regions

コンビーナ:北村 有迅(鹿児島大学大学院理工学研究科地球環境科学専攻)、山田 泰広(海洋研究開発機構　海洋掘削科学研究開発センター)

[HDS11-P01] Deformed sediment gravity flow deposits associated with bypassing slides:an example from the Miocene Ushikiri Formation, Southwest Japan

*小林 未季[1]、酒井 哲弥[2] (1.日本工営株式会社、2.島根大学総合理工学部)

[HDS11-P02] 四国沖大陸棚斜面の海底地すべり調査と津波計算

*権 容大[1]、馬場 俊孝[1]、松野 哲男、林 美鶴、市原 寛 (1.徳島大学大学院)

[HDS11-P03] 八代海南部における白鳳丸KH-18-3次研究航海で採取された堆積物コアの物性から推定される堆積環境

*堀 航喜[1]、北村 有迅[2]、白鳳丸K-18-3次研究航海 乗船研究者一同 (1.九州大学大学院理学府地球惑星科学専攻、2.鹿児島大学大学院理工学研究科地球環境科学専攻)

[HDS11-P04] 「白鳳丸」KH-18-3次研究航海で採取された八代海の堆積物コア試料のベーンせん断強さと帯磁率

*北村 有迅[1]、影山 遼[2]、山﨑 楓[2]、後藤 滝弥[2]、堀 航喜[2]、池端 雄太[2]、川端 訓代[1]、小山 大輝[2]、白鳳丸KH-18-3 乗船研究者 (1.鹿児島大学大学院理工学研究科地球環境科学専攻、2.鹿児島大学理学部地球環境科学科)

[HDS11-P05] Identification of turbidites in the Yatsushiro Sea surface sediment core samples from non-destructive measurements: Hakuho-maru KH-18-3 Cruise, Yatsushiro Sea, Western Kyushu, Japan

*後藤 滝弥[1]、北村 有迅[2]、白鳳丸KH-18-3次研究航海 乗船研究者一同 (1.東京大学大気海洋研究所、2.鹿児島大学大学院理工学研究科地球環境科学専攻)

[HDS11-P06] Revised columnar section based on grain size distribution analysis of samples from Hakuho-maru KH-18-3 in Yatsushiro sea

*池端 雄太[1]、北村 有迅[2]、白鳳丸KH-18-3次研究航海乗船研究者 Family (1.九州大学大学院理学府地球惑星科学専攻、2.鹿児島大学大学院理工学研究科地球環境科学専攻)

[E] ポスター発表 | セッション記号 H (地球人間圏科学)：H-DS 防災地球科学

13:45 ~ 15:15 | ポスター会場 幕張メッセ国際展示場 8ホール_4

[H-DS12] Advanced Remote Sensing toward Mega-Disaster Response

コンビーナ:栄珠 郭(水災害リスクマネジメント国際センター)、竹内 渉(東京大学生産技術研究所)

[HDS12-P01] Satellite-based assessment of electricity restoration efforts in Puerto Rico after Hurricane Maria

*Miguel O Roman[1]、Eleanor Stokes[2,3]、Zhuosen Wang[2,3]、Virginia Kalb[3]、Ranjay Shrestha[4,3] (1.Earth from Space Institute, Universities Space Research Association、2.Earth System Science Interdisciplinary Center, University of Maryland、3.NASA Goddard Space Flight Center、4.Science Systems and Applications, Inc)

[HDS12-P02] Flood inundation forecasting coupled with in-situ water level and satellite data

*Young-Joo Kwak[1]、Jonggeol Park[2]、Wataru Takeuchi[3] (1.ICHARM-UNESCO: International Centre for Water Hazard And Risk Management、2.Tokyo University of Information and Sciences、3.University of Tokyo)

[HDS12-P03] バングラデッシュ海岸域における水害長期モニタリング

★招待講演

*朴 鍾杰[1]、栄珠 郭[2] (1.東京情報大学、2.土木研究所)

[HDS12-P04] Automatic shoreline detection and coastal change detection using multiple satellite data in Bangladesh

*Young-Joo Kwak[1] (1.ICHARM-UNESCO: International Centre for Water Hazard And Risk Management)

[E] ポスター発表 | セッション記号 H (地球人間圏科学)：H-DS 防災地球科学

17:15 ~ 18:30 | ポスター会場 幕張メッセ国際展示場 8ホール_14

[H-DS12] Advanced Remote Sensing toward Mega-Disaster Response

コンビーナ:栄珠 郭(水災害リスクマネジメント国際センター)、竹内 渉(東京大学生産技術研究所)

[HDS12-P01] Satellite-based assessment of electricity restoration efforts in Puerto Rico after Hurricane Maria

*Miguel O Roman[1]、Eleanor Stokes[2,3]、Zhuosen Wang[2,3]、Virginia Kalb[3]、Ranjay Shrestha[4,3] (1.Earth from Space Institute, Universities Space Research Association、2.Earth System Science Interdisciplinary Center, University of Maryland、3.NASA Goddard Space Flight Center、4.Science Systems and Applications, Inc)

[HDS12-P02] **Flood inundation forecasting coupled with in-situ water level and satellite data**

*Young-Joo Kwak[1]、Jonggeol Park[2]、Wataru Takeuchi[3] (1.ICHARM-UNESCO: International Centre for Water Hazard And Risk Management、2.Tokyo University of Information and Sciences、3.University of Tokyo)

[HDS12-P03] バングラデッシュ海岸域における水害長期モニタリング

★招待講演

*朴 鍾杰[1]、栄珠 郭[2] (1.東京情報大学、2.土木研究所)

[HDS12-P04] Automatic shoreline detection and coastal change detection using multiple satellite data in Bangladesh

*Young-Joo Kwak[1] (1.ICHARM-UNESCO: International Centre for Water Hazard And Risk Management)

[E] ポスター発表 | セッション記号 H (地球人間圏科学)：H-CG 地球人間圏科学複合領域・一般

15:30 ~ 17:00 | ポスター会場 幕張メッセ国際展示場 8ホール_9

[H-CG26] デルタとエスチュアリー：複雑な河口システムへの学際的取り組み

コンビーナ:齋藤 文紀(島根大学エスチュアリー研究センター)、Guan-Hong Lee(Inha University)、David L Dettman(University of Arizona)、堀 和明(名古屋大学環境学研究科地理学講座)

[HCG26-P01] Deltafront Clinoform of Abandoned Yellow River Delta in Jiangsu Province, China

*LIANGYONG ZHOU[1] (1.Qingdao Institute of Marine Geology China Geological Survey)

[HCG26-P02] Holocene evolution and Anthropocene destruction of the Krishna delta, east coast of India: delta lobe shifts, human impact, and sea-level history

Kakani Nageswara Rao[2]、*Yoshiki Saito[1]、K.Ch.V. Nagakumar[4]、Sumiko Kubo[3]、Shilpa Pandey[5]、 Zhen Li[6]、G. Demudu[2]、A.S. Rajawat[7] (1.Estuary Research Center, Shimane University、2.Andhra University、3.Waseda University、4.Centre for Water Resources and Management、5.Birbal Sahni Institute of Palaeosciences、6.University of Victoria、7.Space Applications Centre)

[HCG26-P03] 日本周辺の完新統中の海生生物遺体と陸生植物の放射性炭素年代値の差異

*中西 利典[1,2]、七山 太[3,4]、卜部 厚志[5]、堀 和明[6]、ホン ワン[7] (1.京都大学、2.日本原子力研究開発機構、3.産業技術総合研究所、4.熊本大学、5.新潟大学、6.名古屋大学、7.KIGAM)

[HCG26-P04] Assessment of MEIS for Marine Spatial Planning in the Nakdong River Estuary, Busan Metropolitan City, South Korea

*Jun-Ho Lee[1]、Han Jun Woo[1]、Hoi-Soo Jung[1]、Chan Mi Park[1] (1.Korea Institute of Ocean Science and Technology)

[HCG26-P05] Tidal changes at Asian deltas in response to future sea-level rise

*上原 克人[1] (1.九州大学)

[HCG26-P06] **A governing equation of non-deltaic transgressive profile: 2D numerical simulation and flume experiments**

*Junhui Wang[1,2,3]、Tetsuji Muto[3] (1.China University of Petroleum (Beijing)、2.State Key Laboratory of Petroleum Resources and Prospecting, China、3.Nagasaki University)

[E] ポスター発表 | セッション記号 H (地球人間圏科学)：H-CG 地球人間圏科学複合領域・一般

17:15 ~ 18:30 | ポスター会場 幕張メッセ国際展示場 8ホール_16

[H-CG26] デルタとエスチュアリー：複雑な河口システムへの学際的取り組み

コンビーナ:齋藤 文紀(島根大学エスチュアリー研究センター)、Guan-Hong Lee(Inha University)、David L Dettman(University of Arizona)、堀 和明(名古屋大学環境学研究科地理学講座)

[HCG26-P01] Deltafront Clinoform of Abandoned Yellow River Delta in Jiangsu Province, China

*LIANGYONG ZHOU[1] (1.Qingdao Institute of Marine Geology China Geological Survey)

[HCG26-P02] Holocene evolution and Anthropocene destruction of the Krishna delta, east coast of India: delta lobe shifts, human impact, and sea-level history

Kakani Nageswara Rao[2]、*Yoshiki Saito[1]、K.Ch.V. Nagakumar[4]、Sumiko Kubo[3]、Shilpa Pandey[5]、 Zhen Li[6]、G. Demudu[2]、A.S. Rajawat[7] (1.Estuary Research Center, Shimane University、2.Andhra University、3.Waseda University、4.Centre for Water Resources and Management、5.Birbal Sahni Institute of Palaeosciences、6.University of Victoria、7.Space Applications Centre)

[HCG26-P03] 日本周辺の完新統中の海生生物遺体と陸生植物の放射性炭素年代値の差異

*中西 利典[1,2]、七山 太[3,4]、卜部 厚志[5]、堀 和明[6]、ホン ワン[7] (1.京都大学、2.日本原子力研究開発機構、3.産業技術総合研究所、4.熊本大学、5.新潟大学、6.名古屋大学、7.KIGAM)

[HCG26-P04] Assessment of MEIS for Marine Spatial Planning in the Nakdong River Estuary, Busan Metropolitan City, South Korea

*Jun-Ho Lee[1]、Han Jun Woo[1]、Hoi-Soo Jung[1]、Chan Mi Park[1] (1.Korea Institute of Ocean Science and Technology)

[HCG26-P05] Tidal changes at Asian deltas in response to future sea-level rise

*上原 克人[1] (1.九州大学)

[HCG26-P06] **A governing equation of non-deltaic transgressive profile: 2D numerical simulation and flume experiments**

*Junhui Wang[1,2,3]、Tetsuji Muto[3] (1.China University of Petroleum (Beijing)、2.State Key Laboratory of Petroleum Resources and Prospecting, China、3.Nagasaki University)

[E] ポスター発表 | セッション記号 S (固体地球科学)：S-SS 地震学

13:45 ~ 15:15 | ポスター会場 幕張メッセ国際展示場 8ホール_5

[S-SS07] Rigorous Seismicity Modelling and Hypothesis Testing

コンビーナ:庄 建倉(統計数理研究所)、Schorlemmer Danijel(GFZ German Research Centre for Geosciences)、Matt Gerstenberger(GNS Science)、鶴岡 弘(東京大学地震研究所)

[SSS07-P01] **Development of Physics-based Ground Motion Simulation in A Hybrid Approach and Applications to Seismic Hazard Assessment in Taiwan**

*Hsieh Ming-Che[1]、Yen Yin-Tung[1]、Ma Kuo-Fong[2,3] (1.Disaster Prevention Technology Research Center, Sinotech Engineering Consultants (Inc.), Taiwan、2.Department of Earth Sciences, National Central University, Taiwan、3.Earthquake-Disaster & Risk Evaluation and Management Center, National Central University, Taiwan)

[SSS07-P02] Increasing Earthquake Forecast Testability - CSEP Future Developments

*Danijel Schorlemmer[1]、Naoshi Hirata[2]、Fabrice Cotton[1]、Matt Gerstenberger[3]、Thomas Jordan[7]、Warner Marzocchi[4]、William Savran[7]、Maximilian Werner[5]、Stefan Wiemer[6]、Thomas Beutin[1]、David D Jackson[8]、Philip Maechling[7]、Sum Mak[1]、Kazuyoshi Nanjo[9]、Yosihiko Ogata[10]、David Rhoades[3]、Hiroshi Tsuruoka[2]、Graeme Weatherill[1]、Jiancang Zhuang[10] (1.GFZ German Research Centre for Geosciences、2.Earthquake Research Institute, University of Tokyo, Japan、3.GNS Science, Lower Hutt, New Zealand、4.University of Naples, Naples, Italy、5.University of Bristol, Bristol, United Kingdom、6.ETH Zurich, Zurich, Switzerland、7.University of Southern California, Los Angeles, USA、8.University of California Los Angeles, Los Angeles, USA、9.University of Shizuoka, Shizuoka, Japan、10.Institute of Statistical Mathematics, Tachikawa, Japan)

[SSS07-P03] Precision versus uncertainty in regional seismic hazard mapping

*Gerstenberger Matt[1]、Schorlemmer Danijel[2] (1.GNS Science、2.GFZ-Potsdam)

[SSS07-P04] An extreme value analysis of seismograms designed for early forecast of aftershocks

*澤崎 郁[1] (1.防災科学技術研究所)

[SSS07-P05] **Spatio-temporal clustering of successive earthquakes: data analyses of global data.**

*THYSTERE MATONDO BANTIDI[1]、Takeshi Nishimura[1] (1.Tohoku University)

[SSS07-P06] CSEPJapanにおける関東3ヶ月予測結果

*鶴岡 弘[1]、平田 直[1] (1.東京大学地震研究所)

[SSS07-P07] Long-term earthquake risk in North China estimated from a modern catalogue

熊 子瑶[2]、*庄 建倉[1]、周 仕勇[2] (1.統計数理研究所、2.北京大学)

[SSS07-P08] **Distributions of focal mechanisms in background seismicity and earthquake clusters in Japan**

*庄 建倉[1,2]、蒔田 恵理[2] (1.統計数理研究所、2.総合大学院大学)

[SSS07-P09] New Ground Motion Prediction Equations for Western Saudi Arabia

*木内 亮太[1,2]、Walter Mooney[1]、Hani Zahran[3] (1.U.S. Geological Survey、2.京都大学防災研究所、3.Saudi Geological Survey)

[SSS07-P10] Study on the spatial and temporal change of velocity structure before and after 2003 Chengkung earthquake, Taiwan

*TING YA LIANG[1]、Wen-Yen Chang[1,2,3]、Strong Wen[4] (1.National DONG HWA University、2.Eastern Taiwan Earthquake Research Center、3.National Center for Research on Earthquake Engineering、4.National Chung Cheng University)

[E] ポスター発表 | セッション記号 S (固体地球科学)：S-SS 地震学

17:15 ~ 18:30 | ポスター会場 幕張メッセ国際展示場 8ホール_19

[S-SS07] Rigorous Seismicity Modelling and Hypothesis Testing

コンビーナ:庄 建倉(統計数理研究所)、Schorlemmer Danijel(GFZ German Research Centre for Geosciences)、Matt Gerstenberger(GNS Science)、鶴岡 弘(東京大学地震研究所)

[SSS07-P01] **Development of Physics-based Ground Motion Simulation in A Hybrid Approach and Applications to Seismic Hazard Assessment in Taiwan**

*Hsieh Ming-Che[1]、Yen Yin-Tung[1]、Ma Kuo-Fong[2,3] (1.Disaster Prevention Technology Research Center, Sinotech Engineering Consultants (Inc.), Taiwan、2.Department of Earth Sciences, National Central University, Taiwan、3.Earthquake-Disaster & Risk Evaluation and Management Center, National Central University, Taiwan)

[SSS07-P02] Increasing Earthquake Forecast Testability - CSEP Future Developments

*Danijel Schorlemmer[1]、Naoshi Hirata[2]、Fabrice Cotton[1]、Matt Gerstenberger[3]、Thomas Jordan[7]、Warner Marzocchi[4]、William Savran[7]、Maximilian Werner[5]、Stefan Wiemer[6]、Thomas Beutin[1]、David D Jackson[8]、Philip Maechling[7]、Sum Mak[1]、Kazuyoshi Nanjo[9]、Yosihiko Ogata[10]、David Rhoades[3]、Hiroshi Tsuruoka[2]、Graeme Weatherill[1]、Jiancang Zhuang[10] (1.GFZ German Research Centre for Geosciences、2.Earthquake Research Institute, University of Tokyo, Japan、3.GNS Science, Lower Hutt, New Zealand、4.University of Naples, Naples, Italy、5.University of Bristol, Bristol, United Kingdom、6.ETH Zurich, Zurich, Switzerland、7.University of Southern California, Los Angeles, USA、8.University of California Los Angeles, Los Angeles, USA、9.University of Shizuoka, Shizuoka, Japan、10.Institute of Statistical Mathematics, Tachikawa, Japan)

[SSS07-P03] Precision versus uncertainty in regional seismic hazard mapping

*Gerstenberger Matt[1]、Schorlemmer Danijel[2] (1.GNS Science、2.GFZ-Potsdam)

[SSS07-P04] An extreme value analysis of seismograms designed for early forecast of aftershocks

*澤崎 郁[1] (1.防災科学技術研究所)

[SSS07-P05] **Spatio-temporal clustering of successive earthquakes: data analyses of global data.**

*THYSTERE MATONDO BANTIDI[1]、Takeshi Nishimura[1] (1.Tohoku University)

[SSS07-P06] CSEPJapanにおける関東3ヶ月予測結果

*鶴岡 弘[1]、平田 直[1] (1.東京大学地震研究所)

[SSS07-P07] Long-term earthquake risk in North China estimated from a modern catalogue

熊 子瑶[2]、*庄 建倉[1]、周 仕勇[2] (1.統計数理研究所、2.北京大学)

[SSS07-P08] **Distributions of focal mechanisms in background seismicity and earthquake clusters in Japan**

*庄 建倉[1,2]、蒔田 恵理[2] (1.統計数理研究所、2.総合大学院大学)

[SSS07-P09] New Ground Motion Prediction Equations for Western Saudi Arabia

*木内 亮太[1,2]、Walter Mooney[1]、Hani Zahran[3] (1.U.S. Geological Survey、2.京都大学防災研究所、3.Saudi Geological Survey)

[SSS07-P10] Study on the spatial and temporal change of velocity structure before and after 2003 Chengkung earthquake, Taiwan

*TING YA LIANG[1]、Wen-Yen Chang[1,2,3]、Strong Wen[4] (1.National DONG HWA University、2.Eastern Taiwan Earthquake Research Center、3.National Center for Research on Earthquake Engineering、4.National Chung Cheng University)

[E] ポスター発表 | セッション記号 S (固体地球科学)：S-IT 地球内部科学・地球惑星テクトニクス

15:30 ~ 17:00 | ポスター会場 幕張メッセ国際展示場 8ホール_12

[S-IT21] 核-マントルの相互作用と共進化

コンビーナ:河合 研志(東京大学大学院理学系研究科地球惑星科学専攻)、飯塚 毅(東京大学)、太田 健二(東京工業大学大学院理工学研究科地球惑星科学専攻)、土屋 卓久(愛媛大学地球深部ダイナミクス研究センター)

[SIT21-P01] 茨城県稲田花崗岩における小スケールの岩石組成変化の検討 -日本列島地殻由来の地球ニュートリノフラックスの高精度推定に向けて-

★招待講演

*上木 賢太[1]、南 一輝[2]、飯塚 毅[3]、榎本 三四郎[4]、田中 宏幸[2] (1.海洋研究開発機構、2.東京大学地震研究所、3.東京大学地球惑星科学専攻、4.ワシントン大学)

[SIT21-P02] Towards a better estimation of the temperature distribution beneath the Japanese Islands

*田中 明子[1]、山野 誠[2]、濱元 栄起[3]、後藤 秀作[4]、松本 拓己[5] (1.産業技術総合研究所 活断層・火山研究部門、2.東京大学 地震研究所、3.埼玉県 環境科学国際センター、4.産業技術総合研究所 地圏資源環境研究部門、5.防災科学技術研究所)

[SIT21-P03] 日本列島地殻由来の地殻ニュートリノフラックス推定への地球化学データベース利用

*原口 悟[1]、上木 賢太[1]、岩森 光[1,2,3] (1.海洋研究開発機構、2.東京大学地震研究所、3.東京工業大学)

[SIT21-P04] **Viscosity of potassium titanosilicate melt at high pressure**

*鈴木 昭夫[1] (1.東北大学大学院理学研究科地学専攻)

[SIT21-P05] **Lattice thermal conductivity of wadsleyite and ringwoodite at the mantle transition zone pressures**

*木村 清二[1]、太田 健二[6]、川添 貴章[2]、廣瀬 敬[3]、鍵 裕之[4]、八木 貴志[5] (1.東京工業大学理学院地球惑星科学系、2.広島大学大学院理学研究科地球惑星システム学専攻、3.東京工業大学大学　地球生命研究所、4.東京大学大学院理学系研究科附属地殻化学実験施設 、5.国立研究開発法人産業技術総合研究所、6.東京工業大学大学院理工学研究科地球惑星科学専攻)

[SIT21-P06] In-situ X-ray observations of the olivine-spinel transformation under shear deformation: preliminary results on the reaction-induced weakening

*久保 友明[1]、森山 一哉[1]、森 悠一郎[1]、今村 公裕[1]、小泉 早苗[2]、西原 遊[3]、鈴木 昭夫[4]、肥後 祐司[5] (1.九州大学、2.東大地震研、3.愛媛大学GRC、4.東北大学、5.JASRI)

[SIT21-P07] Internally resistive heated diamond anvil cell experiments with metal encapsulated minerals

*山本 倫也[1]、太田 健二[1]、末広 翔[1]、井上 勇人[1] (1.東京工業大学)

[SIT21-P08] Shear deformation on post-spinel

*山崎 大輔[1]、辻野 典秀[1]、西原 遊[2] (1.岡山大学惑星物質研究所、2.愛媛大学地球深部ダイナミクス研究センター)

[SIT21-P09] **Lattice thermal conductivity of $CaSiO_3$ perovskite at high pressures and high temperatures**

*恩賀 皓太郎[1]、太田 健二[1]、長谷川 暉[1,2]、八木 貴志[2]、廣瀬 敬[3,4]、大石 泰夫[5] (1.東京工業大学理学院地球惑星科学系、2.産業技術総合研究所、3.東京工業大学地球生命研究所、4.東京大学大学院理学系研究科地球惑星科学専攻、5.高輝度光科学研究センター)

[SIT21-P10] **Polycrystalline diamond sintered from ultradispersed nanodiamonds**

*西 真之[1,2]、山本 幸一郎[1]、周 佑黙[1]、入舩 徹男[2,1] (1.愛媛大学地球深部ダイナミクス研究センター、2.東京工業大学地球生命研究所)

[SIT21-P11] Thermal conductivity measurements on iron and MgO periclase at high pressure and high temperature similar to the Earth's mid-lower mantle conditions

*長谷川 暉[1,2]、太田 健二[2]、八木 貴志[1]、廣瀬 敬[3,4] (1.産業技術総合研究所、2.東京工業大学、3.東京工業大学地球生命研究所、4.東京大学)

[SIT21-P12] Azimuthal anisotropy in the lowermost mantle beneath Philippine from ScS-S times

*田中 聡[1] (1.海洋研究開発機構　地球深部ダイナミクス研究分野)

[SIT21-P13] Detailed 3-D S-velocity structure within D" at the western Pacific LLSVP margin: smaller scale plumes and paleoslabs

*鈴木 裕輝[1]、河合 研志[1]、ゲラー ロバート[1]、田中 聡[2]、Weerachai Siripuvaraporn[3]、Songkhun Boonchaisuku[3]、Noisagool Sutthipong[3]、石原 靖[2]、Taweoon Kim、宮川 幸治[4]、竹内 希[4] (1.東京大学、2.海洋研究開発機構、3.Mahidol University、4.東京大学地震研究所)

[SIT21-P14] Possible interaction between the core and mantle inferred from a core surface flow model

*松島 政貴[1] (1.東京工業大学理学院地球惑星科学系)

[SIT21-P15] 高温高圧条件下での金属-ケイ酸塩メルト間の希ガス分配係数の実験的決定

*田中 友崇[1]、桑原 秀治[2]、貴志 智[1]、野村 龍一[3]、三部 賢治[5]、鍵 裕之[4]、舘野 繁彦[6]、角野 浩史[1] (1.東京大学大学院総合文化研究科広域科学専攻相関基礎科学系、2.愛媛大学　地球深部ダイナミクス研究センター、3.京都大学、4.東京大学大学院理学系研究科附属地殻化学実験施設、5.東京大学地震研究所、6.東京工業大学地球生命研究所)

[SIT21-P16] **Measurement of T-dependent electrical resistivity of solid and liquid Fe and Pt at fixed P**

*Innocent Ezenwa[1]、Takashi Yoshino[1] (1.Institute for Planetary Materials, Okayama University)

[SIT21-P17] Ancient, highly depleted mantle constrained by Re-Os isotope and highly-siderophile element compositions of French Polynesian xenoliths

*秋澤 紀克[1]、石川 晃[2]、鈴木 勝彦[3]、小木曽 哲[4] (1.東京大学　大気海洋研究所、2.東京工業大学　理学院地球惑星科学系、3.JAMSTEC　海底資源研究開発センター、4.京都大学　大学院人間・環境学研究科)

[SIT21-P18] First-principles prediction of hydrogen partitioning between the core and mantle

*大場 篤朗[1]、土屋 卓久[1] (1.愛媛大学 地球深部ダイナミクス研究センター)

[SIT21-P19] Microvolume stable isotope measuremetns and its applicaiton for high-pressure high-temperature experimental run products

*Madhusoodhan Satish-Kumar[1]、Shinnosuke Aoyama[1] (1.Department of Geology, Faculty of Science, Niigata University)

[SIT21-P20] Electrical resistivity of hcp Fe-Si alloys at high pressure and temperature

*井上 勇人[1]、末広 翔[1]、太田 健二[1]、廣瀬 敬[2,3]、大石 泰生[4] (1.東京工業大学理学院地球惑星科学系、2.東京工業大学地球生命研究所、3.東京大学大学院理学系研究科地球惑星科学専攻、4.高輝度光科学研究センター)

[SIT21-P21] Electrical resistivity and thermal conductivity of fcc Fe: Implications for the Mercury's core

★Invited Papers

*五味 斎[1]、芳野 極[1] (1.岡山大学)

[SIT21-P22] Lateral heterogeneity in the lowermost outer core (F layer) of the Earth revealed by seismic analyses

*大滝 壽樹[1]、金嶋 聰[2]、土屋 卓久[3] (1.産業技術総合研究所地質情報研究部門、2.九州大学大学院理学研究院地球惑星科学部門、3.愛媛大学地球深部ダイナミクス研究センター)

[SIT21-P23] 内核の不均一成長に伴う地球外核中の流れと軽成分分布

*竹広 真一[1]、佐々木 洋平[2] (1.京都大学数理解析研究所、2.京都大学大学院理学研究科数学教室)

[SIT21-P24] Sharpness of the hemispherical boundary in the inner core beneath the northern Pacific

*入谷 良平[1]、川勝 均[1]、竹内 希[1] (1.東京大学地震研究所)

[SIT21-P25] Stable carbon isotope fractionation in Fe-C system from first principles

*出倉 春彦[1]、土屋 卓久[1] (1.愛媛大学地球深部ダイナミクス研究センター)

[E] ポスター発表 | セッション記号 S (固体地球科学)：S-IT 地球内部科学・地球惑星テクトニクス

17:15 ~ 18:30 | ポスター会場 幕張メッセ国際展示場 8ホール_22

[S-IT21] 核-マントルの相互作用と共進化

コンビーナ:河合 研志(東京大学大学院理学系研究科地球惑星科学専攻)、飯塚 毅(東京大学)、太田 健二(東京工業大学大学院理工学研究科地球惑星科学専攻)、土屋 卓久(愛媛大学地球深部ダイナミクス研究センター)

[SIT21-P01] 茨城県稲田花崗岩における小スケールの岩石組成変化の検討 -日本列島地殻由来の地球ニュートリノフラックスの高精度推定に向けて-

★招待講演

*上木 賢太[1]、南 一輝[2]、飯塚 毅[3]、榎本 三四郎[4]、田中 宏幸[2] (1.海洋研究開発機構、2.東京大学地震研究所、3.東京大学地球惑星科学専攻、4.ワシントン大学)

[SIT21-P02] Towards a better estimation of the temperature distribution beneath the Japanese Islands

*田中 明子[1]、山野 誠[2]、濱元 栄起[3]、後藤 秀作[4]、松本 拓己[5] (1.産業技術総合研究所 活断層・火山研究部門、2.東京大学 地震研究所、3.埼玉県 環境科学国際センター、4.産業技術総合研究所 地圏資源環境研究部門、5.防災科学技術研究所)

[SIT21-P03] 日本列島地殻由来の地殻ニュートリノフラックス推定への地球化学データベース利用

*原口 悟[1]、上木 賢太[1]、岩森 光[1,2,3] (1.海洋研究開発機構、2.東京大学地震研究所、3.東京工業大学)

[SIT21-P04] **Viscosity of potassium titanosilicate melt at high pressure**

*鈴木 昭夫[1] (1.東北大学大学院理学研究科地学専攻)

[SIT21-P05] **Lattice thermal conductivity of wadsleyite and ringwoodite at the mantle transition zone pressures**

*木村 清二[1]、太田 健二[6]、川添 貴章[2]、廣瀬 敬[3]、鍵 裕之[4]、八木 貴志[5] (1.東京工業大学理学院地球惑星科学系、2.広島大学大学院理学研究科地球惑星システム学専攻、3.東京工業大学大学　地球生命研究所、4.東京大学大学院理学系研究科附属地殻化学実験施設 、5.国立研究開発法人産業技術総合研究所、6.東京工業大学大学院理工学研究科地球惑星科学専攻)

[SIT21-P06] In-situ X-ray observations of the olivine-spinel transformation under shear deformation: preliminary results on the reaction-induced weakening

*久保 友明[1]、森山 一哉[1]、森 悠一郎[1]、今村 公裕[1]、小泉 早苗[2]、西原 遊[3]、鈴木 昭夫[4]、肥後 祐司[5] (1.九州大学、2.東大地震研、3.愛媛大学GRC、4.東北大学、5.JASRI)

[SIT21-P07] Internally resistive heated diamond anvil cell experiments with metal encapsulated minerals

*山本 倫也[1]、太田 健二[1]、末広 翔[1]、井上 勇人[1] (1.東京工業大学)

[SIT21-P08] Shear deformation on post-spinel

*山崎 大輔[1]、辻野 典秀[1]、西原 遊[2] (1.岡山大学惑星物質研究所、2.愛媛大学地球深部ダイナミクス研究センター)

[SIT21-P09] **Lattice thermal conductivity of $CaSiO_3$ perovskite at high pressures and high temperatures**

*恩賀 皓太郎[1]、太田 健二[1]、長谷川 暉[1,2]、八木 貴志[2]、廣瀬 敬[3,4]、大石 泰夫[5] (1.東京工業大学理学院地球惑星科学系、2.産業技術総合研究所、3.東京工業大学地球生命研究所、4.東京大学大学院理学系研究科地球惑星科学専攻、5.高輝度光科学研究センター)

[SIT21-P10] **Polycrystalline diamond sintered from ultradispersed nanodiamonds**

*西 真之[1,2]、山本 幸一郎[1]、周 佑黙[1]、入舩 徹男[2,1] (1.愛媛大学地球深部ダイナミクス研究センター、2.東京工業大学地球生命研究所)

[SIT21-P11] Thermal conductivity measurements on iron and MgO periclase at high pressure and high temperature similar to the Earth's mid-lower mantle conditions

*長谷川 暉[1,2]、太田 健二[2]、八木 貴志[1]、廣瀬 敬[3,4] (1.産業技術総合研究所、2.東京工業大学、3.東京工業大学地球生命研究所、4.東京大学)

[SIT21-P12] Azimuthal anisotropy in the lowermost mantle beneath Philippine from ScS-S times

*田中 聡[1] (1.海洋研究開発機構　地球深部ダイナミクス研究分野)

[SIT21-P13] Detailed 3-D S-velocity structure within D" at the western Pacific LLSVP margin: smaller scale plumes and paleoslabs

*鈴木 裕輝[1]、河合 研志[1]、ゲラー ロバート[1]、田中 聡[2]、Weerachai Siripuvaraporn[3]、Songkhun Boonchaisuku[3]、Noisagool Sutthipong[3]、石原 靖[2]、Taweoon Kim、宮川 幸治[4]、竹内 希[4] (1.東京大学、2.海洋研究開発機構、3.Mahidol University、4.東京大学地震研究所)

[SIT21-P14] Possible interaction between the core and mantle inferred from a core surface flow model

*松島 政貴[1] (1.東京工業大学理学院地球惑星科学系)

[SIT21-P15] 高温高圧条件下での金属-ケイ酸塩メルト間の希ガス分配係数の実験的決定

*田中 友崇[1]、桑原 秀治[2]、貴志 智[1]、野村 龍一[3]、三部 賢治[5]、鍵 裕之[4]、舘野 繁彦[6]、角野 浩史[1] (1.東京大学大学院総合文化研究科広域科学専攻相関基礎科学系、2.愛媛大学　地球深部ダイナミクス研究センター、3.京都大学、4.東京大学大学院理学系研究科附属地殻化学実験施設、5.東京大学地震研究所、6.東京工業大学地球生命研究所)

[SIT21-P16] **Measurement of T-dependent electrical resistivity of solid and liquid Fe and Pt at fixed P**

*Innocent Ezenwa[1]、Takashi Yoshino[1] (1.Institute for Planetary Materials, Okayama University)

[SIT21-P17] Ancient, highly depleted mantle constrained by Re-Os isotope and highly-siderophile element compositions of French Polynesian xenoliths

*秋澤 紀克[1]、石川 晃[2]、鈴木 勝彦[3]、小木曽 哲[4] (1.東京大学　大気海洋研究所、2.東京工業大学　理学院地球惑星科学系、3.JAMSTEC　海底資源研究開発センター、4.京都大学　大学院人間・環境学研究科)

[SIT21-P18] First-principles prediction of hydrogen partitioning between the core and mantle

*大場 篤朗[1]、土屋 卓久[1] (1.愛媛大学 地球深部ダイナミクス研究センター)

[SIT21-P19] Microvolume stable isotope measuremetns and its applicaiton for high-pressure high-temperature experimental run products

*Madhusoodhan Satish-Kumar[1]、Shinnosuke Aoyama[1] (1.Department of Geology, Faculty of Science, Niigata University)

[SIT21-P20] Electrical resistivity of hcp Fe-Si alloys at high pressure and temperature

*井上 勇人[1]、末広 翔[1]、太田 健二[1]、廣瀬 敬[2,3]、大石 泰生[4] (1.東京工業大学理学院地球惑星科学系、2.東京工業大学地球生命研究所、3.東京大学大学院理学系研究科地球惑星科学専攻、4.高輝度光科学研究センター)

[SIT21-P21] Electrical resistivity and thermal conductivity of fcc Fe: Implications for the Mercury's core

★Invited Papers

*五味 斎[1]、芳野 極[1] (1.岡山大学)

[SIT21-P22] Lateral heterogeneity in the lowermost outer core (F layer) of the Earth revealed by seismic analyses

*大滝 壽樹[1]、金嶋 聰[2]、土屋 卓久[3] (1.産業技術総合研究所地質情報研究部門、2.九州大学大学院理学研究院地球惑星科学部門、3.愛媛大学地球深部ダイナミクス研究センター)

[SIT21-P23] 内核の不均一成長に伴う地球外核中の流れと軽成分分布

*竹広 真一[1]、佐々木 洋平[2] (1.京都大学数理解析研究所、2.京都大学大学院理学研究科数学教室)

[SIT21-P24] Sharpness of the hemispherical boundary in the inner core beneath the northern Pacific

*入谷 良平[1]、川勝 均[1]、竹内 希[1] (1.東京大学地震研究所)

[SIT21-P25] Stable carbon isotope fractionation in Fe-C system from first principles

*出倉 春彦[1]、土屋 卓久[1] (1.愛媛大学地球深部ダイナミクス研究センター)

[E] ポスター発表 | セッション記号 B (地球生命科学)：B-BG 地球生命科学・地圏生物圏相互作用

13:45 ~ 15:15 | ポスター会場 幕張メッセ国際展示場 8ホール_6

[B-BG01] Elemental cycling in terrestrial and coastal ecosystems- Carbon and Nitrogen perspectives

コンビーナ:Punyasloke Bhadury(Indian Institute of Science Education and Research Kolkata)

[BBG01-P01] Forest-CEW: A Forest Ecosystems Model for Carbon-Energy-Water Processes.

*Zhenghong Tan[1] (1.Hainan University China)

[BBG01-P02] **Interdependent Dynamics of LAI-ET across Roofing Landscapes: the Mongolian and Tibetan Plateaus**

*Li Tian[1] (1.Institute of Geographic Sciences and Natural Resources Research, Chinese Academy of Sciences)

[BBG01-P03] **Particle Phase Organic compounds (PAHs and VOCs) at Two Big Cities (Dhaka and Rajshahi) in Bangladesh**

*Islam Nazrul nazrulislam6727@gmail.com[1]、Tanzina Tul Karim[1]、Rasheda Nahida[1]、Nusrat Mousume[1]、Farha Jeba[1]、Abdus Salam[1] (1.Department of Chemistry, University of Dhaka, Dhaka-1000, Bangladesh)

[BBG01-P04] **Diversity and activity of diazotrophs in the coastal waters of Southeastern Arabian Sea (SEAS)**

*JABIR THAJUDEEN[1]、Mohamed Hatha Abdullah (1.Cochin University of Science and Technology India)

[BBG01-P05] **Bloom of *Palmerina hardmaniana*, a marine centric planktonic diatom in a coastal mangrove ecosystem- implication for coastal carbon cycling**

*Punyasloke Bhadury[1] (1.Centre for Climate and Environmental Studies and Department of Biological Sciences, Indian Institute of Science Education and Research Kolkata)

[BBG01-P06] Dynamics of Carbon and Nitrogen influx in large river system: Isotopic study from river Ganga, India

*Anurag Kumar[1]、Prasanta Sanyal[1,2]、Punyasloke Bhadury[3,2] (1.Department of Earth Sciences, Indian Institute of Science Education and Research Kolkata, Mohanpur 741246, India、2.Centre for Climate and Environmental studies, Indian Institute of Science Education and Research Kolkata, Mohanpur 741246, India、3.Department of Biological Sciences, Indian Institute of Science Education and Research Kolkata, Mohanpur 741246, India)

[E] ポスター発表 | セッション記号 B (地球生命科学)：B-BG 地球生命科学・地圏生物圏相互作用

17:15 ~ 18:30 | ポスター会場 幕張メッセ国際展示場 8ホール_31

[B-BG01] Elemental cycling in terrestrial and coastal ecosystems- Carbon and Nitrogen perspectives

コンビーナ:Punyasloke Bhadury(Indian Institute of Science Education and Research Kolkata)

[BBG01-P01] Forest-CEW: A Forest Ecosystems Model for Carbon-Energy-Water Processes.

*Zhenghong Tan[1] (1.Hainan University China)

[BBG01-P02] **Interdependent Dynamics of LAI-ET across Roofing Landscapes: the Mongolian and Tibetan Plateaus**

*Li Tian[1] (1.Institute of Geographic Sciences and Natural Resources Research, Chinese Academy of Sciences)

[BBG01-P03] **Particle Phase Organic compounds (PAHs and VOCs) at Two Big Cities (Dhaka and Rajshahi) in Bangladesh**

*Islam Nazrul nazrulislam6727@gmail.com[1]、Tanzina Tul Karim[1]、Rasheda Nahida[1]、Nusrat Mousume[1]、Farha Jeba[1]、Abdus Salam[1] (1.Department of Chemistry, University of Dhaka, Dhaka-1000, Bangladesh)

[BBG01-P04] **Diversity and activity of diazotrophs in the coastal waters of Southeastern Arabian Sea (SEAS)**

*JABIR THAJUDEEN[1]、Mohamed Hatha Abdullah (1.Cochin University of Science and Technology India)

[BBG01-P05] **Bloom of *Palmerina hardmaniana*, a marine centric planktonic diatom in a coastal mangrove ecosystem- implication for coastal carbon cycling**

*Punyasloke Bhadury[1] (1.Centre for Climate and Environmental Studies and Department of Biological Sciences, Indian Institute of Science Education and Research Kolkata)

[BBG01-P06] Dynamics of Carbon and Nitrogen influx in large river system: Isotopic study from river Ganga, India

*Anurag Kumar[1]、Prasanta Sanyal[1,2]、Punyasloke Bhadury[3,2] (1.Department of Earth Sciences, Indian Institute of Science Education and Research Kolkata, Mohanpur 741246, India、2.Centre for Climate and Environmental studies, Indian Institute of Science Education and Research Kolkata, Mohanpur 741246, India、3.Department of Biological Sciences, Indian Institute of Science Education and Research Kolkata, Mohanpur 741246, India)

[E] ポスター発表 | セッション記号 M (領域外・複数領域)：M-IS ジョイント

15:30 ~ 17:00 | ポスター会場 幕張メッセ国際展示場 8ホール_19

[M-IS02] 地球掘削科学

コンビーナ:山田 泰広(海洋研究開発機構　海洋掘削科学研究開発センター)、針金 由美子(産業技術総合研究所)、黒柳 あずみ(東北大学学術資源研究公開センター東北大学総合学術博物館)、山口 耕生(東邦大学, NASA Astrobiology Institute.)

[MIS02-P01] 地下生命圏研究における凍結コア試料の活用と名古屋議定書への対応

*肖 楠[1] (1.海洋研究開発機構)

[MIS02-P02] In-situ rock strength calculated from drilling parameters. Comparison of results from various sites.

*Adam Wspanialy[1]、Yasuhiro Yamada[1]、Saneatsu Saito[1]、KYAW MOE[1] (1.Japan Agency for Marine-Earth Science and Technology)

[MIS02-P03] Interaction between submarine landslides and subseafloor sedimentary microbiome: Chikyu SCORE Expedition 910 off Cape Erimo

*星野 辰彦[1]、浦本 豪一郎[2]、藤内 智士[2]、諸野 祐樹[1]、井尻 暁[1]、鈴木 志野[1]、久保 雄介[1]、稲垣 史生[1]、Chikyu SCORE Exp. 910 研究者一同 (1.独立行政法人海洋研究開発機構、2.高知大学)

[MIS02-P04] 襟裳岬沖SCORE掘削コアのXRFコアスキャナー連続化学分析

*村山 雅史[1]、矢生 晋介[3]、藤内 智士[2]、浦本 豪一郎[3]、山田 泰広[4]、稲垣 史生[4]、久保 雄介[5] (1.高知大学　農林海洋科学部海洋資源科学科、2.高知大学　理工学部、3.高知大学　海洋コア総合研究センター、4.海洋研究開発機構　海洋掘削科学研究開発センター, 、5.海洋研究開発機構　地球深部探査センター)

[MIS02-P05] 熊本地震震源断層掘削コアを用いた熱物性測定

*佐野 暉[1]、林 為人[1]、渋谷 奨[1,2]、神谷 奈々[1]、杉本 達洋[1]、石塚 師也[1]、林 愛明[3] (1.京都大学大学院工学研究科、2.地圏総合コンサルタント、3.京都大学大学院理学研究科)

[MIS02-P06] 東オーストラリア沖ロードハウライズ地域で採取された浅部コアの物性・強度試験結果：将来のロードハウライズライザー掘削に向けて

*杉原 孝充[1]、青池 寛[1]、斎藤 実篤[2]、村山 達也[1]、武田 研太郎[1]、小野寺 拓也[3]、澄川 あゆみ[3]、木戸 ゆかり[1]、真田 佳典[1] (1.海洋研究開発機構　地球深部探査センター、2.海洋研究開発機構　海洋掘削科学研究開発センター、3.日本海洋事業)

[MIS02-P07] ICDP DSeis 4: Drilling, core logging, and in-hole geophysical logging of ICDP DSeis drilling into the M5.5 aftershock zones in a South African gold mines.

*吉田 峻輔[1]、田所 遼悟[1]、杉村 幸祐[1]、兼松 慎[1]、東 充也[1]、Liebenberg Benni[2]、 van Heerden Esterhuizen[2]、Stephen Tau[3]、Siyanda Mngadi[3]、Ray Durrheim[3]、Martin Ziegler[4]、椋平 祐輔[5]、Ronald Conze[6]、矢部 康男[7]、金木 俊也[8]、Yokoyama Yuki[9]、Nomqhele Nkosi[10]、Dave Roberts[10]、Sifiso Buccio[11]、小笠原 宏[1] (1.Graduate school of science and engineering, Ritsumeikan、2.Moab Khotsong mine, Vijoenskroon、3.Univ. Witwatersrand, School of Geoscience、4.ETH, Zurich Dep. Earth Sciences、5.Inst. Fluid Science, Tohoku Univ.、6.GFZ, Potzdam、7.Graduate School of Science, Tohoku Univ.、8.Disaster Prevention Research Inst., Kyoto Univ.、9.Graduate School of Science,Osaka Univ.、10.Mandela Mining Precinct, CSIR、11.Council for Geoscience)

[MIS02-P08] ICDP DSeis 5: Diametrical Core Deformation Analysis of the M5.5 aftershock zone core - stress concentration at reflective intrusives and transition in stress regimes.

*杉村 幸祐[1]、吉田 峻輔[1]、田所 遼悟[1]、小笠原 宏[2]、石田 亮壮、矢部 康男[3]、伊藤 高敏[4]、明雄 船戸[5]、Siyanda Mngadi[6]、Ray Durrheim[6] (1.立命館大学大学院　理工学研究科、2.立命館大学　理工学部、3.東北大学　理学部、4.東北大学　流体科学研究所、5.深田地質研究所、6.Univ. Witwatersrand, School of Geoscience)

[MIS02-P09] ICDP DSeis 6: Deformation Rate Analysis of the M5.5 aftershock zone core - stress concentration at reflective intrusives

*兼松 慎[1]、東 充也[1]、矢部 康男[2]、阿部 周平[2]、Watson Bryan[3]、Durrheim Ray[3]、小笠原 宏[1] (1.立命館大学 理工学部物理科学科、2.東北大学理学研究科、3.Witwatersrand大)

[MIS02-P10] ICDP DSeis 7: compilation of stress information and comparison with calculated stresses in the M5.5 aftershock zones

*東 充也[1]、矢部 康男[2]、杉村 幸佑[1]、石田 亮壮、兼松 慎[1]、吉田 峻輔[1]、田所 遼悟[1]、伊藤 高敏[4]、船戸 明雄[5]、小笠原 宏[3] (1.立命館大学大学院理工学研究科、2.東北大学大学院理学研究科・理学部 附属地震・噴火予知研究観測センター、3.立命館大学理工学部、4.東北大学流体科学研究所、5.深田地質研究所)

[MIS02-P11] ICDP DSeis 8: the M5.5 fault structure and reflective intrusives in legacy 3D seismic reflection data

*野田 拓[1]、Manzi Musa[2]、Ogasawara Hiroyuki[1]、Linzer Lindsay[2]、Enslin Stephanie[2]、Durrheim Ray[2]、小笠原 宏[1] (1.立命館大学、2.Witwatersrand大)

[MIS02-P12] ICDP DSeis 9: are streaks in the M5.5 aftershocks potentially located on highly stressed intrusive?

*Ryogo Tadokoro[1]、Katsuya Ishibashi[2]、Horiuchi Shigeki[3]、Hiroshi Ogasawara[4] (1.Graduate School of Science and Engineering, Ritsumeikan Univ.、2.School of Science and Engineering, Ritsumeikan Univ.、3.Homeseismo ltd.、4.College of Science and Engineering, Ritsumeikan Univ.)

[E] ポスター発表 | セッション記号 M (領域外・複数領域)：M-IS ジョイント

17:15 ~ 18:30 | ポスター会場 幕張メッセ国際展示場 8ホール_32

[M-IS02] 地球掘削科学

コンビーナ:山田 泰広(海洋研究開発機構　海洋掘削科学研究開発センター)、針金 由美子(産業技術総合研究所)、黒柳 あずみ(東北大学学術資源研究公開センター東北大学総合学術博物館)、山口 耕生(東邦大学, NASA Astrobiology Institute.)

[MIS02-P01] 地下生命圏研究における凍結コア試料の活用と名古屋議定書への対応

*肖 楠[1] (1.海洋研究開発機構)

[MIS02-P02] In-situ rock strength calculated from drilling parameters. Comparison of results from various sites.

*Adam Wspanialy[1]、Yasuhiro Yamada[1]、Saneatsu Saito[1]、KYAW MOE[1] (1.Japan Agency for Marine-Earth Science and Technology)

[MIS02-P03] Interaction between submarine landslides and subseafloor sedimentary microbiome: Chikyu SCORE Expedition 910 off Cape Erimo

*星野 辰彦[1]、浦本 豪一郎[2]、藤内 智士[2]、諸野 祐樹[1]、井尻 暁[1]、鈴木 志野[1]、久保 雄介[1]、稲垣 史生[1]、Chikyu SCORE Exp. 910 研究者一同 (1.独立行政法人海洋研究開発機構、2.高知大学)

[MIS02-P04] 襟裳岬沖SCORE掘削コアのXRFコアスキャナー連続化学分析

*村山 雅史[1]、矢生 晋介[3]、藤内 智士[2]、浦本 豪一郎[3]、山田 泰広[4]、稲垣 史生[4]、久保 雄介[5] (1.高知大学　農林海洋科学部海洋資源科学科、2.高知大学　理工学部、3.高知大学　海洋コア総合研究センター、4.海洋研究開発機構　海洋掘削科学研究開発センター, 、5.海洋研究開発機構　地球深部探査センター)

[MIS02-P05] 熊本地震震源断層掘削コアを用いた熱物性測定

*佐野 暉[1]、林 為人[1]、渋谷 奨[1,2]、神谷 奈々[1]、杉本 達洋[1]、石塚 師也[1]、林 愛明[3] (1.京都大学大学院工学研究科、2.地圏総合コンサルタント、3.京都大学大学院理学研究科)

[MIS02-P06] 東オーストラリア沖ロードハウライズ地域で採取された浅部コアの物性・強度試験結果：将来のロードハウライズライザー掘削に向けて

*杉原 孝充[1]、青池 寛[1]、斎藤 実篤[2]、村山 達也[1]、武田 研太郎[1]、小野寺 拓也[3]、澄川 あゆみ[3]、木戸 ゆかり[1]、真田 佳典[1] (1.海洋研究開発機構　地球深部探査センター、2.海洋研究開発機構　海洋掘削科学研究開発センター、3.日本海洋事業)

[MIS02-P07] ICDP DSeis 4: Drilling, core logging, and in-hole geophysical logging of ICDP DSeis drilling into the M5.5 aftershock zones in a South African gold mines.

*吉田 峻輔[1]、田所 遼悟[1]、杉村 幸祐[1]、兼松 慎[1]、東 充也[1]、Liebenberg Benni[2]、 van Heerden Esterhuizen[2]、Stephen Tau[3]、Siyanda Mngadi[3]、Ray Durrheim[3]、Martin Ziegler[4]、椋平 祐輔[5]、Ronald Conze[6]、矢部 康男[7]、金木 俊也[8]、Yokoyama Yuki[9]、Nomqhele Nkosi[10]、Dave Roberts[10]、Sifiso Buccio[11]、小笠原 宏[1] (1.Graduate school of science and engineering, Ritsumeikan、2.Moab Khotsong mine, Vijoenskroon、3.Univ. Witwatersrand, School of Geoscience、4.ETH, Zurich Dep. Earth Sciences、5.Inst. Fluid Science, Tohoku Univ.、6.GFZ, Potzdam、7.Graduate School of Science, Tohoku Univ.、8.Disaster Prevention Research Inst., Kyoto Univ.、9.Graduate School of Science,Osaka Univ.、10.Mandela Mining Precinct, CSIR、11.Council for Geoscience)

[MIS02-P08] ICDP DSeis 5: Diametrical Core Deformation Analysis of the M5.5 aftershock zone core - stress concentration at reflective intrusives and transition in stress regimes.

*杉村 幸祐[1]、吉田 峻輔[1]、田所 遼悟[1]、小笠原 宏[2]、石田 亮壮、矢部 康男[3]、伊藤 高敏[4]、明雄 船戸[5]、Siyanda Mngadi[6]、Ray Durrheim[6] (1.立命館大学大学院　理工学研究科、2.立命館大学　理工学部、3.東北大学　理学部、4.東北大学　流体科学研究所、5.深田地質研究所、6.Univ. Witwatersrand, School of Geoscience)

[MIS02-P09] ICDP DSeis 6: Deformation Rate Analysis of the M5.5 aftershock zone core - stress concentration at reflective intrusives

*兼松 慎[1]、東 充也[1]、矢部 康男[2]、阿部 周平[2]、Watson Bryan[3]、Durrheim Ray[3]、小笠原 宏[1] (1.立命館大学 理工学部物理科学科、2.東北大学理学研究科、3.Witwatersrand大)

[MIS02-P10] ICDP DSeis 7: compilation of stress information and comparison with calculated stresses in the M5.5 aftershock zones

*東 充也[1]、矢部 康男[2]、杉村 幸佑[1]、石田 亮壮、兼松 慎[1]、吉田 峻輔[1]、田所 遼悟[1]、伊藤 高敏[4]、船戸 明雄[5]、小笠原 宏[3] (1.立命館大学大学院理工学研究科、2.東北大学大学院理学研究科・理学部 附属地震・噴火予知研究観測センター、3.立命館大学理工学部、4.東北大学流体科学研究所、5.深田地質研究所)

[MIS02-P11] ICDP DSeis 8: the M5.5 fault structure and reflective intrusives in legacy 3D seismic reflection data

*野田 拓[1]、Manzi Musa[2]、Ogasawara Hiroyuki[1]、Linzer Lindsay[2]、Enslin Stephanie[2]、Durrheim Ray[2]、小笠原 宏[1] (1.立命館大学、2.Witwatersrand大)

[MIS02-P12] ICDP DSeis 9: are streaks in the M5.5 aftershocks potentially located on highly stressed intrusive?

*Ryogo Tadokoro[1]、Katsuya Ishibashi[2]、Horiuchi Shigeki[3]、Hiroshi Ogasawara[4] (1.Graduate School of Science and Engineering, Ritsumeikan Univ.、2.School of Science and Engineering, Ritsumeikan Univ.、3.Homeseismo ltd.、4.College of Science and Engineering, Ritsumeikan Univ.)

[E] ポスター発表 | セッション記号 M (領域外・複数領域)：M-TT 計測技術・研究手法

13:45 ~ 15:15 | ポスター会場 幕張メッセ国際展示場 8ホール_10

[M-TT46] 統合地球観測システムとしてのGPS/GNSSの新展開

コンビーナ:小司 禎教(気象研究所気象衛星・観測システム研究部第２研究室)、市川 香(九州大学応用力学研究所)、太田 雄策(東北大学大学院理学研究科附属地震・噴火予知研究観測センター)、津川 卓也(情報通信研究機構)

[MTT46-P01] 新たな海底地殻変動観測手法のためのGNSSブイからの連続音響測距

*田所 敬一[1]、衣笠 菜月[1]、加藤 照之[2]、寺田 幸博[3]、二村 彰[4]、松廣 健二郎[1] (1.名古屋大学地震火山研究センター、2.神奈川県温泉地学研究所、3.高知工業高等専門学校、4.弓削商船高等専門学校)

[MTT46-P02] Accuracy and precision assessment of the real-time kinematic GNSS time series for moored buoy using three-axis programable moving table

*太田 雄策[1]、今野 美冴[1]、木戸 元之[2] (1.東北大学大学院理学研究科附属地震・噴火予知研究観測センター、2.東北大学災害科学国際研究所)

[MTT46-P03] 静止衛星によるGNSS-R海面高度計測

*市川 香[1]、奥村 立樹[2]、根田 昌典[3]、馬場 康之[4] (1.九州大学応用力学研究所、2.九州大学総合理工学府大気海洋環境システム学専攻、3.京都大学大学院理学研究科、4.京都大学防災研究所)

[MTT46-P04] **Estimation of typhoon wind speed using CYGNSS observations: A case study of Typhoon Lan in 2017**

*加古 真一郎[1]、富田 裕之[2]、市川 香[3] (1.鹿児島大学大学院理工学研究科、2.名古屋大学 宇宙地球環境研究所、3.九州大学応用力学研究所)

[MTT46-P05] Ionospheric and seismic effects caused by the North Korea nuclear tests realized on 2006-2017

Nataliia Perevalova[2]、*Nikolai Shestakov[1]、Anna Dobrynina[3,4]、Dmitry Kostylev[7]、Meng Guojie[5]、Wei-Wei Wu[5,6] (1.Institute for Applied Mathematics FEB RAS, Vladivostok, Russia; Far Eastern Federal University, Vladivostok, Russia、2.Institute of Solar-Terrestrial Physics SB RAS, Irkutsk, Russia、3.Institute of the Earth's Crust SB RAS, Irkutsk, Russia 、4.Geological institute SB RAS, Ulan-Ude, Russia 、5.Institute of Earthquake Forecasting, China Earthquake Administration, Beijing, China、6.College of Surveying and Geo-informatics, Tongji University, Shanghai, China、7.Sakhalin Branch of Federal Research Center Geophysical Survey RAS, Yuzhno_Sakhalinsk, Russia)

[MTT46-P06] Relationships between Water Vapor Concentration Index derived from GNSS and Surface Wind Convergence during Localized Heavy Rainfall in Tokyo in Summer

*瀬戸 芳一[1]、小司 禎教[2]、常松 展充[3]、高橋 日出男[1] (1.首都大学東京大学院都市環境科学研究科地理環境学域、2.気象庁気象研究所、3.東京都環境科学研究所)

[MTT46-P07] 次世代高感度マイクロ波放射計の開発-序報-

*市川 隆一[1]、氏原 秀樹[1]、佐藤 晋介[1]、雨谷 純[1]、太田 雄策[2]、宮原 伐折羅[3]、宗包 浩志[3]、長崎 岳人[4]、田島 治[5]、荒木 健太郎[6]、田尻 拓也[6]、瀧口 博士[7]、松島 健[8]、松島 喜雄[9]、桃谷 辰也[10]、宇都宮 健志[10] (1.情報通信研究機構、2.東北大学、3.国土地理院、4.高エネルギー加速器研究機構、5.京都大学、6.気象研究所、7.宇宙航空研究開発機構、8.九州大学、9.産業技術総合研究所、10.日本気象協会)

[MTT46-P08] Refractivity Distributions over the Kanto Plain Obtained by Dual-polarization Radar

*瀬古 弘[1]、佐藤 英一[1]、山内 洋[2] (1.気象研究所、2.気象庁)

[MTT46-P09] Spatial and temporal distribution of tropospheric water vapor observed by a Raman lidar and a GNSS receiver network over Shigaraki, Japan

*矢吹 正教[1]、津田 敏隆[1]、河野 邑弥[2]、鳥取 裕作[2]、塚本 誠[2]、竹内 栄治[2] (1.京都大学生存圏研究所、2.英弘精機株式会社)

[MTT46-P10] **Study of the Mechanisms of Severe Thunderstorm in Tokyo Metropolitan Area using High Frequent Assimilation of GNSS and Other Ground-based Observations**

*小司 禎教[1]、酒井 哲[2]、足立 アホロ[1]、吉田 智[2]、永井 智広[2] (1.気象研究所気象衛星・観測システム研究部第２研究室、2.気象研究所気象衛星・観測システム研究部第３研究室)

[E] ポスター発表 | セッション記号 M (領域外・複数領域)：M-TT 計測技術・研究手法

17:15 ~ 18:30 | ポスター会場 幕張メッセ国際展示場 8ホール_43

[M-TT46] 統合地球観測システムとしてのGPS/GNSSの新展開

コンビーナ:小司 禎教(気象研究所気象衛星・観測システム研究部第２研究室)、市川 香(九州大学応用力学研究所)、太田 雄策(東北大学大学院理学研究科附属地震・噴火予知研究観測センター)、津川 卓也(情報通信研究機構)

[MTT46-P01] 新たな海底地殻変動観測手法のためのGNSSブイからの連続音響測距

*田所 敬一[1]、衣笠 菜月[1]、加藤 照之[2]、寺田 幸博[3]、二村 彰[4]、松廣 健二郎[1] (1.名古屋大学地震火山研究センター、2.神奈川県温泉地学研究所、3.高知工業高等専門学校、4.弓削商船高等専門学校)

[MTT46-P02] Accuracy and precision assessment of the real-time kinematic GNSS time series for moored buoy using three-axis programable moving table

*太田 雄策[1]、今野 美冴[1]、木戸 元之[2] (1.東北大学大学院理学研究科附属地震・噴火予知研究観測センター、2.東北大学災害科学国際研究所)

[MTT46-P03] 静止衛星によるGNSS-R海面高度計測

*市川 香[1]、奥村 立樹[2]、根田 昌典[3]、馬場 康之[4] (1.九州大学応用力学研究所、2.九州大学総合理工学府大気海洋環境システム学専攻、3.京都大学大学院理学研究科、4.京都大学防災研究所)

[MTT46-P04] **Estimation of typhoon wind speed using CYGNSS observations: A case study of Typhoon Lan in 2017**

*加古 真一郎[1]、富田 裕之[2]、市川 香[3] (1.鹿児島大学大学院理工学研究科、2.名古屋大学 宇宙地球環境研究所、3.九州大学応用力学研究所)

[MTT46-P05] Ionospheric and seismic effects caused by the North Korea nuclear tests realized on 2006-2017

Nataliia Perevalova[2]、*Nikolai Shestakov[1]、Anna Dobrynina[3,4]、Dmitry Kostylev[7]、Meng Guojie[5]、Wei-Wei Wu[5,6] (1.Institute for Applied Mathematics FEB RAS, Vladivostok, Russia; Far Eastern Federal University, Vladivostok, Russia、2.Institute of Solar-Terrestrial Physics SB RAS, Irkutsk, Russia、3.Institute of the Earth's Crust SB RAS, Irkutsk, Russia 、4.Geological institute SB RAS, Ulan-Ude, Russia 、5.Institute of Earthquake Forecasting, China Earthquake Administration, Beijing, China、6.College of Surveying and Geo-informatics, Tongji University, Shanghai, China、7.Sakhalin Branch of Federal Research Center Geophysical Survey RAS, Yuzhno_Sakhalinsk, Russia)

[MTT46-P06] Relationships between Water Vapor Concentration Index derived from GNSS and Surface Wind Convergence during Localized Heavy Rainfall in Tokyo in Summer

*瀬戸 芳一[1]、小司 禎教[2]、常松 展充[3]、高橋 日出男[1] (1.首都大学東京大学院都市環境科学研究科地理環境学域、2.気象庁気象研究所、3.東京都環境科学研究所)

[MTT46-P07] 次世代高感度マイクロ波放射計の開発-序報-

*市川 隆一[1]、氏原 秀樹[1]、佐藤 晋介[1]、雨谷 純[1]、太田 雄策[2]、宮原 伐折羅[3]、宗包 浩志[3]、長崎 岳人[4]、田島 治[5]、荒木 健太郎[6]、田尻 拓也[6]、瀧口 博士[7]、松島 健[8]、松島 喜雄[9]、桃谷 辰也[10]、宇都宮 健志[10] (1.情報通信研究機構、2.東北大学、3.国土地理院、4.高エネルギー加速器研究機構、5.京都大学、6.気象研究所、7.宇宙航空研究開発機構、8.九州大学、9.産業技術総合研究所、10.日本気象協会)

[MTT46-P08] Refractivity Distributions over the Kanto Plain Obtained by Dual-polarization Radar

*瀬古 弘[1]、佐藤 英一[1]、山内 洋[2] (1.気象研究所、2.気象庁)

[MTT46-P09] Spatial and temporal distribution of tropospheric water vapor observed by a Raman lidar and a GNSS receiver network over Shigaraki, Japan

*矢吹 正教[1]、津田 敏隆[1]、河野 邑弥[2]、鳥取 裕作[2]、塚本 誠[2]、竹内 栄治[2] (1.京都大学生存圏研究所、2.英弘精機株式会社)

[MTT46-P10] **Study of the Mechanisms of Severe Thunderstorm in Tokyo Metropolitan Area using High Frequent Assimilation of GNSS and Other Ground-based Observations**

*小司 禎教[1]、酒井 哲[2]、足立 アホロ[1]、吉田 智[2]、永井 智広[2] (1.気象研究所気象衛星・観測システム研究部第２研究室、2.気象研究所気象衛星・観測システム研究部第３研究室)

[E] ポスター発表 | セッション記号 M (領域外・複数領域)：M-TT 計測技術・研究手法

13:45 ~ 15:15 | ポスター会場 幕張メッセ国際展示場 8ホール_11

[M-TT47] 人新世における高精細地形・地球物理データの活用

コンビーナ:早川 裕弋(北海道大学地球環境科学研究院)、楠本 成寿(富山大学大学院理工学研究部(都市デザイン学))、Gomez Christopher(神戸大学 海事科学部 海域火山リスク科学研究室)

[MTT47-P01] High-definition topography monitoring after riverbed cultivation in the Echi River, central Japan

*小倉 拓郎[1,2]、淺野 悟史[3]、水野 敏明[3]、東 善広[3]、北井 剛[4]、早川 裕弋[5,6]、飯塚 浩太郎[6] (1.東京大学大学院新領域創成科学研究科、2.北海道大学大学院環境科学院、3.滋賀県琵琶湖環境科学研究センター、4.滋賀県立琵琶湖博物館、5.北海道大学地球環境研究院、6.東京大学空間情報科学研究センター)

[MTT47-P02] **Spatial distribution of land surface displacements in the crater of Tateyama Midagahara Volcano using high-definition topographic data**

*早川 裕弋[1]、楠本 成寿[2]、小倉 拓郎[3,4] (1.北海道大学地球環境科学研究院、2.富山大学大学院理工学研究部、3.東京大学新領域創成科学研究科、4.北海道大学大学院環境科学院)

[MTT47-P03] SfM/MVSを用いた簡易的な河床形状復元および水深評価に関する検討

*大澤 幸太[1]、新里 忠史[2]、三田地 勝昭[3]、川村 淳[1]、大川 真弘[1] (1.三菱マテリアルテクノ株式会社、2.日本原子力研究開発機構、3.エイ・ティ・エス株式会社)

[MTT47-P04] Ground Penetrating Radar Imaging of Moisture and Water movement in volcanic soil

*Christopher A Gomez[1] (1.Kobe University Faculty of Maritime Sciences Volcanic Risk at Sea Research Group)

[MTT47-P05] **Estimating Eruptive Volumes of Mud Volcano Southwestern Taiwan by Using UAV and SfM-MVS Photogrammetry**

*CHIA-YING LIU[1]、Ray Y Chuang[1]、Horng-Yue Chen[2] (1.Department of Geography, National Taiwan University、2.Academia Sinica, Institute of Earth Sciences)

[MTT47-P06] Increasing temporal depth of urban Land-Use Regression Models by wind-data driven dynamic buffer generation

*Tilman Leo Hohenberger[1]、King Wai Leung[1] (1.Division of Environment and Sustainability, Hong Kong University of Science and Technology)

[E] ポスター発表 | セッション記号 M (領域外・複数領域)：M-TT 計測技術・研究手法

17:15 ~ 18:30 | ポスター会場 幕張メッセ国際展示場 8ホール_44

[M-TT47] 人新世における高精細地形・地球物理データの活用

コンビーナ:早川 裕弋(北海道大学地球環境科学研究院)、楠本 成寿(富山大学大学院理工学研究部(都市デザイン学))、Gomez Christopher(神戸大学 海事科学部 海域火山リスク科学研究室)

[MTT47-P01] High-definition topography monitoring after riverbed cultivation in the Echi River, central Japan

*小倉 拓郎[1,2]、淺野 悟史[3]、水野 敏明[3]、東 善広[3]、北井 剛[4]、早川 裕弋[5,6]、飯塚 浩太郎[6] (1.東京大学大学院新領域創成科学研究科、2.北海道大学大学院環境科学院、3.滋賀県琵琶湖環境科学研究センター、4.滋賀県立琵琶湖博物館、5.北海道大学地球環境研究院、6.東京大学空間情報科学研究センター)

[MTT47-P02] **Spatial distribution of land surface displacements in the crater of Tateyama Midagahara Volcano using high-definition topographic data**

*早川 裕弋[1]、楠本 成寿[2]、小倉 拓郎[3,4] (1.北海道大学地球環境科学研究院、2.富山大学大学院理工学研究部、3.東京大学新領域創成科学研究科、4.北海道大学大学院環境科学院)

[MTT47-P03] SfM/MVSを用いた簡易的な河床形状復元および水深評価に関する検討

*大澤 幸太[1]、新里 忠史[2]、三田地 勝昭[3]、川村 淳[1]、大川 真弘[1] (1.三菱マテリアルテクノ株式会社、2.日本原子力研究開発機構、3.エイ・ティ・エス株式会社)

[MTT47-P04] Ground Penetrating Radar Imaging of Moisture and Water movement in volcanic soil

*Christopher A Gomez[1] (1.Kobe University Faculty of Maritime Sciences Volcanic Risk at Sea Research Group)

[MTT47-P05] **Estimating Eruptive Volumes of Mud Volcano Southwestern Taiwan by Using UAV and SfM-MVS Photogrammetry**

*CHIA-YING LIU[1]、Ray Y Chuang[1]、Horng-Yue Chen[2] (1.Department of Geography, National Taiwan University、2.Academia Sinica, Institute of Earth Sciences)

[MTT47-P06] Increasing temporal depth of urban Land-Use Regression Models by wind-data driven dynamic buffer generation

*Tilman Leo Hohenberger[1]、King Wai Leung[1] (1.Division of Environment and Sustainability, Hong Kong University of Science and Technology)

[E] ポスター発表 | セッション記号 P (宇宙惑星科学)：P-PS 惑星科学

2019年5月27日(月) 15:30 ~ 17:00 | ポスター会場 幕張メッセ国際展示場 8ホール_1

[P-PS05] Recent advances of Venus science

コンビーナ:佐藤 毅彦(宇宙航空研究開発機構・宇宙科学研究本部)、堀之内 武(北海道大学地球環境科学研究院)、山本 勝(九州大学応用力学研究所)、Kevin McGouldrick(University of Colorado Boulder)

Akatsuki, being in Venus orbit since December 2015, has acquired a volume of high-quality data, unveiled many new phenomena and is allowing researchers to investigate the underlying mechanisms. As the data accumulate, numerical models and theories are being advanced as well. We are no doubt living in the new golden era of Venus studies. This session invites papers of the new scientific results with Akatsuki data and the latest results of theoretical and numerical works. We expect participants of this session share the latest research results through presentations and discussion.

[PPS05-P01] New thermal infrared camera for fine horizontal brightness temperature structures at the cloud-top level of Venus

*Tetsuya Fukuhara[1]、Makoto Taguchi[1]、Takeshi Imamura[2]、Sanjay S Limaye[3] (1.Rikkyo University、2.The University of Tokyo、3.University of Wisconsin)

[PPS05-P02] Temperature and wind variations in Venusian mesosphere and lower thermosphere by mid-infrared heterodyne spectrometer in 2018

*高見 康介[1]、中川 広務[1]、佐川 英夫[2]、村田 功[1]、笠羽 康正[1] (1.東北大学大学院理学研究科地球物理学専攻惑星大気物理学分野、2.京都産業大学大学院理学研究科物理学専攻)

[PPS05-P03] Local time dependence of limb darkening seen in the thermal infrared Venus disk

*秋場 聖浩[1] (1.立教大学院理学研究所物理学専攻)

[PPS05-P04] あかつき中間赤外画像の積算による金星雲頂の定在構造と帯状構造の抽出

*福谷 貴一[1]、今村 剛[1]、田口 真[2]、福原 哲哉[2]、神山 徹[3] (1.東京大学、2.立教大学、3.産総研)

[PPS05-P05] Akatsuki's IR2 Nightside Photometry Restoration by Deconvolution

*Choon Wei Vun[1]、Takehiko Satoh[2,1]、Kevin McGouldrick[3]、Takeshi Horinouchi[4]、Takao M. Sato[5] (1.SOKENDAI、2.ISAS/JAXA、3.University of Colorado Boulder、4.Hokkaido University、5.Hokkaido Information University)

[PPS05-P06] Enormous cloud cover as seen by Akatsuki/IR2 on the night-side disk of Venus

*佐藤 毅彦[1,2]、Vun Choon Wei[2]、佐藤 隆雄[3]、堀之内 武[4]、はしもと じょーじ[5]、McGouldrick Kevin[6] (1.宇宙航空研究開発機構・宇宙科学研究所、2.総合研究大学院大学・宇宙科学専攻、3.北海道情報大学・経営情報学部、4.北海道大学・地球環境科学研究院 、5.岡山大学・理学部地球科学科、6.LASP, University of Colorado Boulder)

[PPS05-P07] あかつき搭載IR1から明らかにする金星雲の全球変動

*高木 聖子[1]、岩上 直幹、高橋 幸弘[1]、佐藤 光輝[1] (1.北海道大学大学院理学研究院)

[PPS05-P08] 対流モデルに向けた金星雲計算スキームの開発

*杉山 耕一朗[1]、福原 望[1]、小高 正嗣[2]、中島 健介[3]、石渡 正樹[2]、今村 剛[4]、林 祥介[5] (1.松江高専・情報、2.北大・理・宇宙、3.九大・理・地惑、4.東大・新領域創成科学、5.神戸大・理・地惑)

[PPS05-P09] 放射伝達を陽に考慮した金星大気大循環モデルで見られる東西平均構造
★招待講演

*林 祥介[1]、塩尻 千里[1]、樫村 博基[1]、高橋 芳幸[1] (1.神戸大学・大学院理学研究科 惑星学専攻/惑星科学研究センター（CPS）)

[PPS05-P10] 電波掩蔽による金星大気温度データからの重力波の波束の抽出

*森 亮太[1]、今村 剛[1]、Javier Peralta[2] (1.東京大学、2.宇宙航空研究開発機構)

[PPS05-P11] **Status of lightning hunt in Venus with Akatsuki/LAC and Pirka telescope**

*高橋 幸弘[1,2]、佐藤 光輝[1,2]、今井 正尭[3]、Lorenz Ralph[4]、高木 聖子[1,2]、大野 辰遼[1] (1.北海道大学・大学院理学院・宇宙理学専攻、2.北海道大学・大学院理学研究院、3.産業技術総合研究所、4.ジョンズホプキンズ大学応用物理研究所)

[PPS05-P12] **Possibility of electric discharge in the Venusian atmosphere due to the super-rotation of clouds**

*Adhithiyan Neduncheran[1]、Ugur Guven[1,2]、Ananyo Bhattacharya[3] (1.University of Petroleum and Energy Studies, India、2.United Nations Centre for Space Science and Technology Education in Asia and the Pacific、3.Sardar Vallabhbhai National Institute of Technology,India)

New thermal infrared camera for fine horizontal brightness temperature structures at the cloud-top level of Venus

*Tetsuya Fukuhara[1], Makoto Taguchi[1], Takeshi Imamura[2], Sanjay S Limaye[3]

1. Rikkyo University, 2. The University of Tokyo, 3. University of Wisconsin

The Longwave Infrared Camera (LIR), which is an uncooled microbolometer camera, is currently acquiring thermal infrared images (8-12 μm) of Venus and depicting the cloud-top brightness temperatures from Akatsuki orbiter around Venus since December 2015. The outstanding result of LIR has been the discovery of an interhemispheric bow-shaped structure meridionally stretching 10,000 km across the equator at the Venus cloud-top. Over several days of observations, the bow-shaped structure remains relatively fixed in position above the highland on the slowly rotating surface, despite the background atmospheric super rotation at ~100 m/s. We infer that the bow-shaped structure is the result of an atmospheric gravity wave generated in the lower atmosphere by mountain topography that then propagated upwards [1]. This indicates that the horizontal temperature distribution seen at the cloud-top level represents not only direct physical property at the cloud-top but also influence of dynamics in the lower atmosphere. In fact, preliminary observation of LIR has detected fine structure (~100 km) in temperature distribution from close-up observations near the periapsis. We suggest that this may be caused by the upward propagation of a gravity wave, which is generated by the convection layer at ~40 km altitude. However, the spatial resolution of LIR seems insufficient to understand the origins of such a fine structure. We need better observations at higher spatial resolution than possible from LIR in Akatsuki’s orbit.

We propose that a future Venus orbiter carries an updated version of the uncooled microbolometer camera (BOL) with 1024x768 pixels and angular resolution of ~0.01 deg/pixel to detect fine temperature structure on the cloud-tops. When the orbiter is typically injected to a high-inclined elliptical orbit with altitude of 500-50,000 km, BOL provides a spatial resolution of 8.5 km at apoapsis and 0.08 km at periapsis, respectively. It will be enough to observe the fine temperature structure at the cloud-top. Further, BOL will capture the fine temperature structure at polar region near the “eye” of the hemispheric vortex situated over the poles, where the horizontal temperature varies drastically near the Venus cloud-tops. VIRTIS instrument on Venus Express orbiter showed complex structures at near infrared wavelengths [2]. Akatsuki from its near equatorial elliptical orbit cannot observe the fine structure in polar regions.

During 2012-2014, we developed an uncooled micro-bolometer array (UMBA) camera for the 50 kg class Earth observing satellite based on the experience of LIR development [3]. The camera with the pixel size of 640 ×480 was launched in 2014 and successfully detect a small wildfire which was main observation target for the mission. The results showed that its performance was better than expected. Furthermore, the newest UMBA camera with the pixel size increased to 1024 ×768 has been developed for the next wildfire mission to take finer spatial resolution image with ~0.01 deg/pixel. Unfortunately, this camera has lost the launch opportunity. However, the flight-model has been assembled and has passed function tests. Since BOL does not need heavy cryogenic systems, its mass and size are less than ~1 kg and 100 mm x 100 mm x 120 mm, respectively; it would be a relatively small mass increment for the future Venus mission.

References

[1] Fukuhara, T., et al., 2017, Large stationary gravity wave in the atmosphere of Venus, Nature Geoscience, Vol. 10, 85–88.

©2019. Japan Geoscience Union. All Right Reserved.

[2] Garate-Lopez, I., et al., 2015, Atmospheric dynamics at the southern pole of Venus: Three-dimensional winds, temperature and vorticity, AGU Fall Meeting Abstracts, 23.
[3] Fukuhara, T., et al., 2017, Detection of small wildfire by thermal infrared camera with the uncooled microbolometer array for 50 kg class satellite, IEEE Transactions on Geoscience and Remote Sensing, 2017, Vol. 55, No. 8, 4314-4324

Keywords: Venus, atmosphere, Akatsuki

©2019. Japan Geoscience Union. All Right Reserved.

Temperature and wind variations in Venusian mesosphere and lower thermosphere by mid-infrared heterodyne spectrometer in 2018

*高見 康介[1]、中川 広務[1]、佐川 英夫[2]、村田 功[1]、笠羽 康正[1]
*Kosuke Takami[1], Hiromu Nakagawa[1], Hideo Sagawa[2], Isao Murata[1], Yasumasa Kasaba[1]

1. 東北大学大学院理学研究科地球物理学専攻惑星大気物理学分野、2. 京都産業大学大学院理学研究科物理学専攻
1. Graduate School of Science, Tohoku University, 2. Division of Science, Kyoto Sangyo University

The most extensive observations of Venusian mesosphere have been performed by Venus Express (VEX) up to 2014 (e.g., Patzold et al., 2007; Mahieux et al., 2015). These observations have found the highly spatial and temporal variations in the thermal structure. The temperature discrepancies between observations by VEX/SOIR and general circulation models in the altitude of 80 - 100 km have not been properly interpreted (Bougher et al., 2015; Gilli et al., 2017). In addition, the mesospheric dynamics located between retrograde superrotational zonal wind (cloud deck) and subsolar-to-antisolar flow (above 120 km altitude) have not been well understood due to lack of observations. On the other hand, the lower thermosphere has been observed by mid-infrared heterodyne spectrometer (MIR-HS). Temperature in this region varied extensively between 140 K and 240 K, and wind velocity changed intensely from 130 m/s to 190 m/s for a terrestrial day (Sornig et al., 2013; Krause et al., 2018). Temperature and wind variations such as periodicity and locality in Venusian mesosphere and lower thermosphere have not been comprehended. The purpose of our observations is to solve it with continuous observations by MIR-HS.
Our Mid-Infrared Laser Heterodyne Instrument (MILAHI) have been inserted to Tohoku 60 cm telescope located the summit of Mt. Haleakala in Maui, Hawaii (Nakagawa et al., 2016). MILAHI has 10 um CO_2 laser as local oscillator. The field of view is 4 arcsec with 60 cm telescope and in the wavelength of 10 um. MIR-HS can retrieve temperature and wind in different altitude between dayside observations and nightside observations. CO_2 emerge non-local thermodynamic equilibrium emission from 100 –120 km altitude in dayside (Lopez-Valverde et al., 2011). Temperature and wind are derived from Doppler width and Doppler shift of the emission spectra, respectively. In nightside, CO_2 in the mesosphere absorbs background radiation from the cloud deck. Temperature profile and wind are retrieved from this absorption spectra with radiative transfer equation and inverse method of AMATERASU developed in National Institute of Information and Communications Technology.
Dayside observations were conducted between 24th and 27th in June, 2018. Apparent diameter was 15 arcsec and apparent dayside was half of the disk in this term. Observed points were North, South, disk center, and equator with integration times of 30 - 55 minutes. Each observed point gave different temperature variation feature. Temperature variation range was 170 - 220 K in agreement with Sonnabend et al. (2010). Temperature distribution showed both latitudinal dependence in 25th and convergence at 200 K in 26th.
Nightside observations were conducted from 11th to 13th, 19th, and 20th in November, 2018. Apparent diameter of Venus changed between 55.4 and 49.4 arcsec after inferior conjunction. We observed equator with three days, north 33 degree and south 33 degree for diurnal and latitudinal variations with integration times of 80 - 130 minutes. The observed spectra in the unit of relative intensity are under conversion because the retrieval with AMATERASU is necessary to use absolute radiation. We will show retrieved temperature profile and wind velocity at this presentation.

キーワード：金星、中間圏、中間赤外分光
Keywords: Venus, Mesosphere, mid-infrared spectroscopy

©2019. Japan Geoscience Union. All Right Reserved.

©2019. Japan Geoscience Union. All Right Reserved.

Local time dependence of limb darkening seen in the thermal infrared Venus disk

*秋場 聖浩[1]
*Masahiro Akiba[1]

1. 立教大学院理学研究所物理学専攻
1. Rikkyo University

Brightness temperature of the Venus disk obtained by Longwave Infrared Camera (LIR) onboard Akatuski shows clear limb darkening in the low and middle latitudes. Limb darkening is an apparent temperature decrease from the center to the limb of the Venus disk. It is caused by thermal and radiative characteristics that the sensing altitude of LIR increases as an emission angle, which is a zenith angle of direction of emission from the Venus atmosphere to the sensor, increases and that the atmospheric temperature monotonically decreases with altitude. In higher latitudes limb brightening is observed, because an inversion layer exists at the cloud-top altitudes in higher latitudes. In other word a profile of the limb darkening reflects vertical distributions of atmospheric temperature and optical thickness of cloud particles. Taylor et al. [1980] presented local time dependence of limb darkening using brightness temperature data obtained by the Pioneer Venus orbiter, but did not mention its physical mechanism. In this study brightness temperature distributions obtained by LIR when Akatsuki was in the altitude range from 60,000 to 100,000 km during the period from October 19, 2016 to July 17, 2018 were analyzed to investigate temperature and cloud particle property at the cloud-tops. Each brightness temperature image with 328 x 248 pixels was divided into 3280 x 2480 sub-pixels, and 32 successive images were accumulated after precise adjustment of the Venus disk position to improve S/N. Brightness temperature profiles as a function of the emission angle were derived for 24 local time zones and 9 zonal belts with a latitudinal width of 10˚ within ±45˚. A degree of limb darkening and a brightness temperature at the disk center were determined by least-square function fitting. As a result, the degree of limb darkening shows a clear semi-diurnal variation, and is the strongest at 11h and 22h and the weakest at 7h and 18h in local time. The amplitude of semi-diurnal variation peaks at the equator, whereas its phase seems constant in all latitudes. The temperature at the disk center also shows a semi-diurnal variation with a phase shift of approximately two hours earlier than the phase of the degree of limb darkening and a slight diurnal variation in higher latitudes. These semi-diurnal and diurnal components observed by LIR are consistent with the past observation of thermal tides in the Venus atmosphere by VENERA 15 [Zasova et al., 2007]. The physical mechanism of the semi-diurnal and diurnal thermal tide components seen in the degree of limb darkening and cloud-top temperature will be discussed.

©2019. Japan Geoscience Union. All Right Reserved.

Local time dependence of limb darkening seen in the thermal infrared Venus disk

Masahiro Akiba, Tetsuya Fukuhara, and Makoto Taguchi
Rikkyo University

Brightness temperature of the Venus disk obtained by Longwave Infrared Camera (LIR) onboard Akatuski shows clear limb darkening in the low and middle latitudes. Limb darkening is an apparent temperature decrease from the center to the limb of the Venus disk. It is caused by thermal and radiative characteristics that the sensing altitude of LIR increases as an emission angle, which is a zenith angle of direction of emission from the Venus atmosphere to the sensor, increases and that the atmospheric temperature monotonically decreases with altitude. In higher latitudes limb brightening is observed, because an inversion layer exists at the cloud-top altitudes in higher latitudes. In other word a profile of the limb darkening reflects vertical distributions of atmospheric temperature and optical thickness of cloud particles. Taylor et al. [1980] presented local time dependence of limb darkening using brightness temperature data obtained by the Pioneer Venus orbiter, but did not mention its physical mechanism. In this study brightness temperature distributions obtained by LIR when Akatsuki was in the altitude range from 60,000 to 100,000 km during the period from October 19, 2016 to July 17, 2018 were analyzed to investigate temperature and cloud particle property at the cloud-tops. Each brightness temperature image with 328 x 248 pixels was divided into 3280 x 2480 sub-pixels, and 32 successive images were accumulated after precise adjustment of the Venus disk position to improve S/N. Brightness temperature profiles as a function of the emission angle were derived for 24 local time zones and 9 zonal belts with a latitudinal width of 10° within ±45°. A degree of limb darkening and a brightness temperature at the disk center were determined by least-square function fitting. As a result, the degree of limb darkening shows a clear semi-diurnal variation, and is the strongest at 11h and 22h and the weakest at 7h and 18h in local time. The amplitude of semi-diurnal variation peaks at the equator, whereas its phase seems constant in all latitudes. The temperature at the disk center also shows a semi-diurnal variation with a phase shift of approximately two hours earlier than the phase of the degree of limb darkening and a slight diurnal variation in higher latitudes. These semi-diurnal and diurnal components observed by LIR are consistent with the past observation of thermal tides in the Venus atmosphere by VENERA 15 [Zasova et al., 2007]. The physical mechanism of the semi-diurnal and diurnal thermal tide components seen in the degree of limb darkening and cloud-top temperature will be discussed.

©2019. Japan Geoscience Union. All Right Reserved.

あかつき中間赤外画像の積算による金星雲頂の定在構造と帯状構造の抽出
Stationary wavy features and Banded structures at Venusian cloud top extracted by averaging multiple LIR images

*福谷 貴一[1]、今村 剛[1]、田口 真[2]、福原 哲哉[2]、神山 徹[3]
*Kiichi Fukuya[1], Takeshi Imamura[1], Makoto Taguchi[2], Tetsuya Fukuhara[2], Toru Kouyama[3]

1. 東京大学、2. 立教大学、3. 産総研
1. Univ. of Tokyo, 2. Rikkyo Univ., 3. AIST

Venus’ cloud-top temperature distribution is now continuously mapped by LIR (Long-wave Infrared camera) mounted on the Venus orbiter Akatsuki. Fukuhara et al. (2017) analyzed LIR data and reported the existence of bow-shaped structures extending over 10,000 km in the north-south direction. The features are fixed in position without flowing with the super-rotation and appear above highlands with altitudes higher than 3 km. It was suggested based on a comparison with numerical simulations that the features are gravity waves generated by near-surface flows impinging on mountains. Kouyama et al. (2017) observed stationary features over 4 Venus days and revealed that the features tend to occur in the local afternoon. Gravity waves, whose restoring force is buoyancy, transport horizontal momentum in the vertical direction and accelerate or decelerate the background wind when they dissipate. Therefore, stationary gravity waves influence the general circulation of the atmosphere. In order to estimate the influence, it is essential to reveal the spatial and temporal distributions of gravity waves.
In the previous studies using LIR data, only planetary-scale stationary features have been investigated. On the other hand, Peralta et al. (2017) analyzed the data taken by VIRTIS onboard Venus Express, and reported the existence of many small-scale stationary features; however, VIRTIS can observe the night side only, and the observations were confined to the high latitude of the southern hemisphere because of the geometry of the orbit. Therefore, we intend to investigate with a new analysis method the topographical and local time dependency of small-scale, weak stationary features by using LIR data, which can observe all latitude regions at any local time. Though the S/N ratio of LIR is lower than VIRTIS, averaging of multiple images can suppress noises and at the same time emphasize stationary patterns. By using this method, small-scale, stationary wave trains were newly found above relatively-low topographic rises with altitudes of 1-3 km. In addition to stationary features, zonally-elongated banded structures were also found in averaged LIR images. Such structures have once been detected in LIR images taken during Akatsuki’s Venus flyby in 2010 (Taguchi et al., 2012); the new analysis confirmed that banded structures are ubiquitous at the cloud top. The orientations of the banded structures are different from those of dark streaks found in ultraviolet images.

キーワード：地形性重力波、金星、あかつき
Keywords: Stationary gravity waves, Venus, Akatsuki

©2019. Japan Geoscience Union. All Right Reserved.

Akatsuki's IR2 Nightside Photometry Restoration by Deconvolution

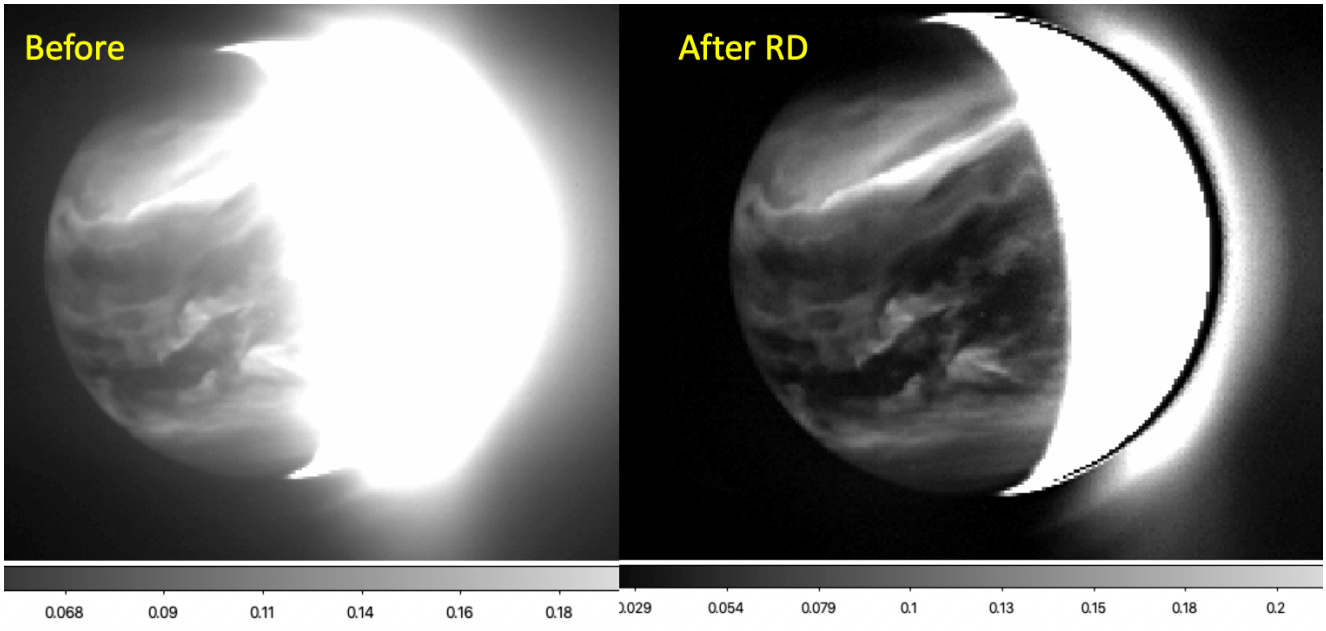
*Choon Wei Vun[1], Takehiko Satoh[2,1], Kevin McGouldrick[3], Takeshi Horinouchi[4], Takao M. Sato[5]

1. SOKENDAI, 2. ISAS/JAXA, 3. University of Colorado Boulder, 4. Hokkaido University, 5. Hokkaido Information University

Akatsuki’ s IR2 camera captures images of Venus at different filters: 1.735um, 2.26um, and 2.32um. At near-dawn/dusk views (phase angles ~90 to 115 degree) of these images, the nightside photometry is contaminated by the intense dayside reflectance. As the potential well of a pixel is overfilled with incoming generated photoelectrons, the pixel is saturated and hence no longer contain information. This saturation can occur in the dayside and nightside near the terminator.
Owing to the saturation problem, main task of the restoration process is thus to simulate both day and night sides to replace the information loss in saturation. Point spread function (PSF) of the IR2 camera was modeled using Moffat function with observation of experimental image taken of point source street light before launch. Then, deconvolution by model-PSF can restore the nightside photometry of unsaturated pixels. Dayside reflectance was modeled with Lambert’ s law, where its distribution is multiplied by an F factor (W m^{-2} sr^{-1} um^{-1}). Methods of finding the F factor will be shown.
We present our Restoration by Deconvolution (RD) results of the selected dates. The restored images were limb darkening corrected. Efficiency of RD can be restored to ~0.005 sigma in standard deviation accuracy when performed on synthetic image with known answer image.
Correlation plot of unsaturated nightside radiances between two filters (2.26mm and 1.735mm) were produced to extract possible ‘branch’ phenomena. The branching in the correlation plot indicates the differences in optical depths of different particle size modes [1].
Restoration of nightside pixels also opens up the opportunity to study the cloud dynamics transiting from the dayside into the nightside. Moreover, interesting cloud features such as vortices, instabilities, and streaks are more distinct in recovered images. This in overall opens up new window to understanding the evolution of cloud motion in the middle layer.
References: [1] Carlson R.W. et al. (1993) *Planet. Space Sci., 41,* No. 7, 477-485. [2] Grinspoon D.H. et al. (1993) *Planet. Spce Sci, 41,* No. 7, 515-542. [3] Nakamura M. et al. (2011)*Earth, Planets and Space, 63,* 443-457. [4] Satoh T. et al. (2016) *Earth, Planets and Space 68:74*. [5] Satoh T. et al. (2017) *Earth, Planets and Space 69:154.* [6] Wilson C.F. et al. (2008) *JGR, 113,* E00B13

Keywords: Venus, atmosphere, image restoration, infrared

©2019. Japan Geoscience Union. All Right Reserved.



©2019. Japan Geoscience Union. All Right Reserved.

Enormous cloud cover as seen by Akatsuki/IR2 on the night-side disk of Venus

Enormous cloud cover as seen by Akatsuki/IR2 on the night-side disk of Venus

*佐藤 毅彦[1,2]、Vun Choon Wei[2]、佐藤 隆雄[3]、堀之内 武[4]、はしもと じょーじ[5]、McGouldrick Kevin[6]
*Takehiko Satoh[1,2], Choon Wei Vun[2], Takao M. Sato[3], Takeshi Horinouchi[4], George HASHIMOTO[5], Kevin McGouldrick[6]

1. 宇宙航空研究開発機構・宇宙科学研究所、2. 総合研究大学院大学・宇宙科学専攻、3. 北海道情報大学・経営情報学部、4. 北海道大学・地球環境科学研究院 、5. 岡山大学・理学部地球科学科、6. LASP, University of Colorado Boulder
1. Institute of Space and Astronautical Science, Japan Aerospace Exploration Agency, 2. Department of Space Science, SOKENDAI, 3. Department of Business and Information Systems, Hokkaido Information University, 4. Faculty of Environmental Earth Science, Hokkaido University, 5. Department of Earth Science, Okayama University, 6. LASP, University of Colorado Boulder

Night-side observations in transparency windows of CO_2 atmosphere of Venus allow visualizing inhomogeneous clouds in ~50 to ~60 km altitudes. The IR2 camera on board Akatsuki captured such images at 1.735, 2.26, and 2.32 um wavelengths. In the IR2 night-side data, an enormous cloud of greater opacity and very sharp edge in the front (western end) is seen repeatedly. This feature seems to encircle the planet with a period of ~4.5 days (Peralta).

Although interesting, property of particles in this feature was not studied before due to difficulty of photometric measurements in IR2 night-side data. This difficulty comes from a combination of the intense day crescent and extended tail of IR2 point-spread function (multiple reflection in the detector is the cause). We have developed a technique to restore the contrast of the night-side data by deconvolution so that the photometric studies can be done with IR2 night-side data.

The data acquired on 18th and 27th August 2016 are analyzed. We have performed a series of radiative transfer computations to reproduce both 1.735- and 2.26-um opacities in this enormous cloud. Properties of the cloud partices will be presented and possible mechanism of this remarkable phenomenon will be discussed.

キーワード：あかつきIR2、金星夜面、雲濃度
Keywords: Akatsuki IR2, Venus night-side, Cloud opacity

©2019. Japan Geoscience Union. All Right Reserved.

あかつき搭載IR1から明らかにする金星雲の全球変動
The global variation of Venus cloud obtained from IR1 camera onboard AKATSUKI

*高木 聖子[1]、岩上 直幹、高橋 幸弘[1]、佐藤 光輝[1]
*Seiko Takagi[1], Naomoto Iwagami, Yukihiro Takahashi[1], Mitsuteru Sato[1]

1. 北海道大学大学院理学研究院
1. Hokkaido University, Graduate School of Science

金星は地球とほぼ同じ大きさ・密度を持ち、太陽系形成時には互いに似た惑星として誕生したと考えられているが、90気圧もの二酸化炭素大気や全球を一様に覆う硫酸雲の存在など地球とは全く異なる様相を見せる。
金星探査機あかつき(JAXA)は、2015年12月に金星周回軌道投入に成功した。あかつきは複数波長による撮像観測を行い、金星気象の3次元的理解を目指す。搭載された近赤外カメラIR1は、軌道投入後約1年間、近赤外波長0.90 umにおける金星昼面撮像を行った。大気の窓領域である近赤外波長を用いた金星昼面撮像観測では、雲の光学的厚さの増減を金星表面のコントラストとしてとらえることができる[Takagi and Iwagami. 2011]。木星探査機Galileo/SSI (NASA)により得られた金星昼面近赤外画像(0.986 um)では、金星表面のコントラストはわずか3 %と示されている[Belton et al., 1991]が、IR1はかつて木星探査機Galileo/SSIが得たものと整合的な昼面画像を多数取得している。本研究では、IR1が取得した0.90 um昼面画像から雲の変動傾向を全球的に知る。合わせてVenus Express(ESA)搭載赤外分光計SOIRから得られた金星高高度の雲情報[Takagi et al. in rev.]を反映した放射輸送計算を近赤外波長において実行し、雲変動に寄与する金星の気象変化について考察する。さらに北海道大学が所有するピリカ望遠鏡を用いた同波長領域における観測計画を紹介する。

キーワード：金星、雲、近赤外
Keywords: Venus, cloud, near infrared

©2019. Japan Geoscience Union. All Right Reserved.

対流モデルに向けた金星雲計算スキームの開発
Development of a Venus' cloud formation scheme for a convection resolving model

*杉山 耕一朗[1]、福原 望[1]、小高 正嗣[2]、中島 健介[3]、石渡 正樹[2]、今村 剛[4]、林 祥介[5]
*Ko-ichiro SUGIYAMA[1], Nozomu Fukuhara[1], Masatsugu Odaka[2], Kensuke Nakajima[3], Masaki Ishiwatari[2], Takeshi Imamura[4], Yoshi-Yuki Hayashi[5]

1. 松江高専・情報、2. 北大・理・宇宙、3. 九大・理・地惑、4. 東大・新領域創成科学、5. 神戸大・理・地惑
1. National Institute of Technology, Matsue College, 2. Department of Cosmoscience, Graduate School of Science, Hokkaido University, 3. Department of Earth and Planetary Sciences,Flculty of Sciences,Kyushu University, 4. Graduate School of Frontier Sciences, The University of Tokyo, 5. Department of Planetology, Graduate School of Science, Kobe University / Center for Planetary Science (CPS)

Although convection has been suggested to occur in the lower part of Venus' cloud layer by some observational evidences, its structure remains to be clarified. In the previous studies, Baker et al. (1998, 2000), Imamura et al. (2014), and Lefevre et al. (2017) try to simulate Venus' cloud-level convection, but their models they utilized do not consider cloud formation process. Our purpose is to develop new cloud formation scheme and to perform numerical simulation using the scheme in order to investigate a possible structure of Venus' cloud-level convection and clouds distribution.

Our cloud formation scheme is based on Imamura and Hashimoto (1998). The number densities of sulfuric acid (H2SO4) and water (H2O) in the gas and liquid phases are calculated. Sedimentation of H2SO4-H2O solution droplets and chemical reactions of sulfuric acid are also considered. The scheme is implemented into our convection resolving model developed by Sugiyama et al. (2009). The model is based on the quasi-compressible system (Klemp and Wilhelmson, 1978), and is used in the simulations of the atmospheric convections of Jupiter (Sugiyama et al., 2011, 2014) and Mars (Yamashita et al. 2017).

In our poster, we will show the details of our cloud formation scheme and demonstrate some results of our calculation using similar settings of Imamura et al. (2014).

キーワード：金星大気、対流、雲形成、数値計算
Keywords: Venus atmosphere, convection, cloud formation, numerical modeling

©2019. Japan Geoscience Union. All Right Reserved.

放射伝達を陽に考慮した金星大気大循環モデルで見られる東西平均構造
Zonal mean structure of Venus atmosphere observed in a Venus general circulation model with explicit radiative transfer

*林 祥介[1]、塩尻 千里[1]、樫村 博基[1]、高橋 芳幸[1]
*Yoshi-Yuki Hayashi[1], Chisato Shiojiri[1], Hiroki Kashimura[1], Yoshiyuki O. Takahashi[1]

1. 神戸大学・大学院理学研究科 惑星学専攻/惑星科学研究センター（CPS）
1. Department of Planetology/CPS, Graduate School of Science, Kobe University

金星大気の東西平均東西風は他の惑星大気にはない特徴を示している。ほぼすべての緯度において超回転状態にあり、スーパーローテーションと呼ばれる。数値計算や地上観測による数多くの研究がこの特徴を説明するべく試みられてきたが、2010年代になって遂に、Lebonnois et al. (2010) や Ikeda (2010) は、放射伝達を陽に計算することによりスーパーローテーションを表現することに成功した。これらは、放射過程をニュートン冷却によって代替えさせていたそれ以前の数値モデルとは一線を画すモデルである。

一方、我々は多様な惑星大気を包括的に扱うことのできる大気大循環モデルの開発を進めてきており、その一環として、今回、分厚いCO_2大気を持つ大気のための大循環放射伝達計算を実現するパラメタを用意した。ここでは, 我々が決めた放射パラメタを金星大気の場合に応用してその大循環を計算し、放射伝達を陽に計算した先行研究との比較を行う。

我々が用いる大気大循環モデルは DCPAM (http://www.gfd-dennou.org/library/dcpam/) である。DCPAMはプリミティブ方程式系を力学モデルとして用いており、これをスペクトル法によって解いている。物理過程としては放射過程、乱流混合過程を含み、地表面温度の計算においては地中熱伝導も計算する。放射パラメタは相関k-分布法を用いて導出、計算された放射フラックスは観測された放射フラックスとよく一致することを確認している。大気大循環計算においては、表面地形の有り無しの二種類の数値実験を行った。用いた分解能は T15L52, 格子点でいえば 48 x 24 であり、鉛直 52 層を有している。初期条件はどちらの実験も静止、温度分布は水平一様の VIRA 鉛直温度分布とした。金星の日変化は考慮したが、年変化は考慮していない（自転軸傾斜角はゼロ）。数値積分は 150000 地球日実行した。

100000地球日程度の積分によりエネルギーの時間変化で見るとほぼ統計的に平衡な状態に達する。この統計的な定常状態では , 地形有り無しどちらの実験でも、現実の金星大気東西風速強度の約半分、およそ 50 m/s 程度の超回転風速が雲層の中低緯度領域に見られた。

平均子午面循環は両半球にわたる大きな直接循環で構成されていた。地表面地形無し実験では、この子午面直接循環は、低緯度地表面付近に見られる逆循環を除き、地表面からモデルトップまで覆っていた。一方、地表面有り実験では雲層下部付近に逆循環が存在し、子午面循環は上下に分断される構造をなしていた。その他の逆循環としては、高緯度雲層付近の逆循環と、地形無し実験で見られた赤道域雲層以下の複数の高度領域に見らえる逆循環群である。

発表では、モデルで得られた東西平均構造と東西角運動流収支の解析結果を示す予定である。

キーワード：金星、惑星大気、大気大循環モデル、放射伝達計算
Keywords: Venus, planetary atmosphere, general circulation model, explicit calculation of radiative transfer

©2019. Japan Geoscience Union. All Right Reserved.

©2019. Japan Geoscience Union. All Right Reserved.

電波掩蔽による金星大気温度データからの重力波の波束の抽出
Gravity wave packets detected in radio occultation temperature profiles of the Venus atmosphere

*森 亮太[1]、今村 剛[1]、Javier Peralta[2]
*Ryota Mori[1], Takeshi Imamura[1], Javier Peralta[2]

1. 東京大学、2. 宇宙航空研究開発機構
1. The University of Tokyo, 2. Japan Aerospace Exploration Agency

金星探査機「あかつき」の電波掩蔽観測により2016年から現在に至るまで大気温度の高度分布が得られている。電波掩蔽観測は、探査機から送信される電波が惑星大気を通過して屈折したのち地球の受信局に届く機会を利用して、大気の屈折率の変化を地上での受信周波数の変化として捉える手法であり、屈折率の高度分布から気圧や気温を導出することが出来る。こうして得られる気温分布には様々な大気擾乱に起因する変動が観測される。ここでは、大気大循環の駆動において重要な役割を持つと考えられる大気重力波に注目する。

重力波は大気中の浮力を復元力とする小規模な波動である。重力波は運動量を鉛直方向に運ぶ働きがあり、散逸に際して背景大気に運動量を受け渡すことにより、平均風の加減速をもたらす。金星においては高速帯状風の全球的な構造に影響を与えていることが予想されている。しかし、重力波は空間スケールが小さく、周期が比較的短いという性質があるために、その空間構造を観測で捉えることが難しい。これまでに、重力波に伴うと考えられる短鉛直波長の温度擾乱の振幅の緯度-高度分布などが調べられてきたが、卓越する波長や高度方向の拡がりについては分かっていなかった。

そこで、本研究では、ウェーブレット解析を鉛直温度分布に適用し、空間的に局在した温度擾乱を抽出する。今までは、温度データにフーリエ変換を適用した研究はあるが、フーリエ変換は無限に続く波を仮定としており、空間的に局在した波束の特徴を取り出すのには適切ではない。ウェーブレット解析はそのような有限区間の波に関して周期や振幅を得たい時に有効である。本発表では電波ホログラフィという方法で従来より高い高度分解能で得られた温度データに対してウェーブレット解析を適用した結果を報告する。また、得られた結果から、大気重力波の波束の長さや高度分布などに関係も報告する。

キーワード：あかつき、大気重力波、電波掩蔽観測
Keywords: Akatsuki, Gravity wave in the atmosphere, The radio occultation experiment

©2019. Japan Geoscience Union. All Right Reserved.

Status of lightning hunt in Venus with Akatsuki/LAC and Pirka telescope

*高橋 幸弘[1,2]、佐藤 光輝[1,2]、今井 正尭[3]、Lorenz Ralph[4]、高木 聖子[1,2]、大野 辰遼[1]
*Yukihiro Takahashi[1,2], Mitsuteru Sato[1,2], Masataka Imai[3], Ralph Lorenz[4], Seiko Takagi[1,2], Ono Tatsuharu[1]

1. 北海道大学・大学院理学院・宇宙理学専攻、2. 北海道大学・大学院理学研究院、3. 産業技術総合研究所、4. ジョンズホプキンズ大学応用物理研究所
1. Graduate School of Science, Hokkaido University, 2. Faculty of Science, Hokkaido University, 3. National Institute of Advanced Industrial Science and Technology,, 4. Applied Physics Laboratory, Johns Hopkins University

The existence of lightning discharge in Venus has been controversial for three decades, which might be attributed to the luck of conclusive observational evidence. There had been no satellite payload intentionally designed for the detection of lightning phenomena using radio wave or optical sensor. LAC, lightning and airglow camera, on board Akatsuki spacecraft, is the first sensor optimized for the lightning optical flash measurement in planets other than the Earth. It is expected that LAC could conclude this 30-year discussion on the existence of lightning in Venus. Unique performance of LAC compared to other equipment used in the previous exploration of Venus is the high-speed sampling rate at 20 kHz with 32 pixels of Avalanche Photo Diode (APD) matrix, enabling us to distinguish the natural optical lightning flash from other pulsing noises, including artificial electrical noise and cosmic rays. We selected OI 777 nm line for lightning detection, which is expected to be the most prominent emission in CO2-dominant atmosphere based on the laboratory experiments.

The triggering parameter was set so as to optimize for the light curve similar to the normal lightning in the Earth and data obtained totally for about 4 hours were examined. However, we couldn’t find any lightning signals. Adding to this triggering parameter set, we added one more parameter set, optimized for sprite type emission with duration of up to 10s of ms. Furthermore, in order to investigate fainter emissions, we are now conducting successive force triggering recordings without any threshold, achieving 5 times better sensitivity than the intensity of 1 digital unit at best.

The total coverage of the LAC lightning hunt became 81.6 [million km2-hr], meaning 81 percent detectability of previous results with ground-based telescope by Hansell et al. (1995). Here we report the detailed strategy and the latest status of the LAC observation in 2018, and discuss the future observation plan.

Also we will make ground observation with a high-speed photometer installed at Pirka telescope, a 1.6-m reflector deployed by Hokkaido University. Here we report the initial results of lightning flash observation with it.

キーワード：雷、金星、あかつき、ピリカ望遠鏡
Keywords: lightning, Venus, Akatsuki, Pirka telescope

©2019. Japan Geoscience Union. All Right Reserved.

Possibility of electric discharge in the Venusian atmosphere due to the super-rotation of clouds

*Adhithiyan Neduncheran[1], Ugur Guven[1,2], Ananyo Bhattacharya[3]

1. University of Petroleum and Energy Studies, India, 2. United Nations Centre for Space Science and Technology Education in Asia and the Pacific, 3. Sardar Vallabhbhai National Institute of Technology,India

Several evidences of electromagnetic bursts were measured by various landers and orbiters studying Venus atmosphere (Venera landers, Venus Express and the Pioneer Venus Orbiter). The electromagnetic bursts that are taking place in the cloud region in the form of lightning or fluorescence might be a result of momentum transfer, solar convection and charge dispersion in the clouds of Venus. While the lightning in Earth takes place mostly in the equatorial region, in case of Venus it is possible for lightning to occur in the polar regions, considering the kinetic energy transfer and the formation of dipoles in both hemispheres of Venus. The meridional and zonal flows can interact and cause the charge separation which possibly lead to electromagnetic bursts in different spectrum and in different regions in Venus. In labs, it is observed that SO2 emissions in UV region cause fluorescence which is one of the major phenomena taking place in the cloud tops. Based on the photochemical model published by *Krasnopolsky 2011(*doi:10.1016/j.icarus.2011.11.012) and the principle of refraction, we present the possibility of lightning/fluorescence phenomena being caused by the super-rotation of the clouds in the Venusian atmosphere.

Keywords: Venus , Super-rotation, lightning, electric discharge, atmosphere

©2019. Japan Geoscience Union. All Right Reserved.

[E] ポスター発表 | セッション記号 P (宇宙惑星科学)：P-PS 惑星科学

2019年5月27日(月) 17:15 ~ 18:30 | ポスター会場 幕張メッセ国際展示場 8ホール_2

[P-PS05] Recent advances of Venus science

コンビーナ:佐藤 毅彦(宇宙航空研究開発機構・宇宙科学研究本部)、堀之内 武(北海道大学地球環境科学研究院)、山本 勝(九州大学応用力学研究所)、Kevin McGouldrick(University of Colorado Boulder)

Akatsuki, being in Venus orbit since December 2015, has acquired a volume of high-quality data, unveiled many new phenomena and is allowing researchers to investigate the underlying mechanisms. As the data accumulate, numerical models and theories are being advanced as well. We are no doubt living in the new golden era of Venus studies. This session invites papers of the new scientific results with Akatsuki data and the latest results of theoretical and numerical works. We expect participants of this session share the latest research results through presentations and discussion.

[PPS05-P01] New thermal infrared camera for fine horizontal brightness temperature structures at the cloud-top level of Venus

*Tetsuya Fukuhara[1]、Makoto Taguchi[1]、Takeshi Imamura[2]、Sanjay S Limaye[3] (1.Rikkyo University、2.The University of Tokyo、3.University of Wisconsin)

[PPS05-P02] Temperature and wind variations in Venusian mesosphere and lower thermosphere by mid-infrared heterodyne spectrometer in 2018

*高見 康介[1]、中川 広務[1]、佐川 英夫[2]、村田 功[1]、笠羽 康正[1] (1.東北大学大学院理学研究科地球物理学専攻惑星大気物理学分野、2.京都産業大学大学院理学研究科物理学専攻)

[PPS05-P03] Local time dependence of limb darkening seen in the thermal infrared Venus disk

*秋場 聖浩[1] (1.立教大学院理学研究所物理学専攻)

[PPS05-P04] あかつき中間赤外画像の積算による金星雲頂の定在構造と帯状構造の抽出

*福谷 貴一[1]、今村 剛[1]、田口 真[2]、福原 哲哉[2]、神山 徹[3] (1.東京大学、2.立教大学、3.産総研)

[PPS05-P05] Akatsuki's IR2 Nightside Photometry Restoration by Deconvolution

*Choon Wei Vun[1]、Takehiko Satoh[2,1]、Kevin McGouldrick[3]、Takeshi Horinouchi[4]、Takao M. Sato[5] (1.SOKENDAI、2.ISAS/JAXA、3.University of Colorado Boulder、4.Hokkaido University、5.Hokkaido Information University)

[PPS05-P06] Enormous cloud cover as seen by Akatsuki/IR2 on the night-side disk of Venus

*佐藤 毅彦[1,2]、Vun Choon Wei[2]、佐藤 隆雄[3]、堀之内 武[4]、はしもと じょーじ[5]、McGouldrick Kevin[6] (1.宇宙航空研究開発機構・宇宙科学研究所、2.総合研究大学院大学・宇宙科学専攻、3.北海道情報大学・経営情報学部、4.北海道大学・地球環境科学研究院 、5.岡山大学・理学部地球科学科、6.LASP, University of Colorado Boulder)

[PPS05-P07] あかつき搭載IR1から明らかにする金星雲の全球変動

*高木 聖子[1]、岩上 直幹、高橋 幸弘[1]、佐藤 光輝[1] (1.北海道大学大学院理学研究院)

[PPS05-P08] 対流モデルに向けた金星雲計算スキームの開発

*杉山 耕一朗[1]、福原 望[1]、小高 正嗣[2]、中島 健介[3]、石渡 正樹[2]、今村 剛[4]、林 祥介[5] (1.松江高専・情報、2.北大・理・宇宙、3.九大・理・地惑、4.東大・新領域創成科学、5.神戸大・理・地惑)

[PPS05-P09] 放射伝達を陽に考慮した金星大気大循環モデルで見られる東西平均構造
★招待講演

*林 祥介[1]、塩尻 千里[1]、樫村 博基[1]、高橋 芳幸[1] (1.神戸大学・大学院理学研究科 惑星学専攻/惑星科学研究センター（CPS）)

[PPS05-P10] 電波掩蔽による金星大気温度データからの重力波の波束の抽出

*森 亮太[1]、今村 剛[1]、Javier Peralta[2] (1.東京大学、2.宇宙航空研究開発機構)

[PPS05-P11] **Status of lightning hunt in Venus with Akatsuki/LAC and Pirka telescope**

*高橋 幸弘[1,2]、佐藤 光輝[1,2]、今井 正尭[3]、Lorenz Ralph[4]、高木 聖子[1,2]、大野 辰遼[1] (1.北海道大学・大学院理学院・宇宙理学専攻、2.北海道大学・大学院理学研究院、3.産業技術総合研究所、4.ジョンズホプキンズ大学応用物理研究所)

[PPS05-P12] **Possibility of electric discharge in the Venusian atmosphere due to the super-rotation of clouds**

*Adhithiyan Neduncheran[1]、Ugur Guven[1,2]、Ananyo Bhattacharya[3] (1.University of Petroleum and Energy Studies, India、2.United Nations Centre for Space Science and Technology Education in Asia and the Pacific、3.Sardar Vallabhbhai National Institute of Technology,India)

New thermal infrared camera for fine horizontal brightness temperature structures at the cloud-top level of Venus

*Tetsuya Fukuhara[1], Makoto Taguchi[1], Takeshi Imamura[2], Sanjay S Limaye[3]

1. Rikkyo University, 2. The University of Tokyo, 3. University of Wisconsin

The Longwave Infrared Camera (LIR), which is an uncooled microbolometer camera, is currently acquiring thermal infrared images (8-12 μm) of Venus and depicting the cloud-top brightness temperatures from Akatsuki orbiter around Venus since December 2015. The outstanding result of LIR has been the discovery of an interhemispheric bow-shaped structure meridionally stretching 10,000 km across the equator at the Venus cloud-top. Over several days of observations, the bow-shaped structure remains relatively fixed in position above the highland on the slowly rotating surface, despite the background atmospheric super rotation at ~100 m/s. We infer that the bow-shaped structure is the result of an atmospheric gravity wave generated in the lower atmosphere by mountain topography that then propagated upwards [1]. This indicates that the horizontal temperature distribution seen at the cloud-top level represents not only direct physical property at the cloud-top but also influence of dynamics in the lower atmosphere. In fact, preliminary observation of LIR has detected fine structure (~100 km) in temperature distribution from close-up observations near the periapsis. We suggest that this may be caused by the upward propagation of a gravity wave, which is generated by the convection layer at ~40 km altitude. However, the spatial resolution of LIR seems insufficient to understand the origins of such a fine structure. We need better observations at higher spatial resolution than possible from LIR in Akatsuki’s orbit.

We propose that a future Venus orbiter carries an updated version of the uncooled microbolometer camera (BOL) with 1024x768 pixels and angular resolution of ~0.01 deg/pixel to detect fine temperature structure on the cloud-tops. When the orbiter is typically injected to a high-inclined elliptical orbit with altitude of 500-50,000 km, BOL provides a spatial resolution of 8.5 km at apoapsis and 0.08 km at periapsis, respectively. It will be enough to observe the fine temperature structure at the cloud-top. Further, BOL will capture the fine temperature structure at polar region near the “eye” of the hemispheric vortex situated over the poles, where the horizontal temperature varies drastically near the Venus cloud-tops. VIRTIS instrument on Venus Express orbiter showed complex structures at near infrared wavelengths [2]. Akatsuki from its near equatorial elliptical orbit cannot observe the fine structure in polar regions.

During 2012-2014, we developed an uncooled micro-bolometer array (UMBA) camera for the 50 kg class Earth observing satellite based on the experience of LIR development [3]. The camera with the pixel size of 640 ×480 was launched in 2014 and successfully detect a small wildfire which was main observation target for the mission. The results showed that its performance was better than expected. Furthermore, the newest UMBA camera with the pixel size increased to 1024 ×768 has been developed for the next wildfire mission to take finer spatial resolution image with ~0.01 deg/pixel. Unfortunately, this camera has lost the launch opportunity. However, the flight-model has been assembled and has passed function tests. Since BOL does not need heavy cryogenic systems, its mass and size are less than ~1 kg and 100 mm x 100 mm x 120 mm, respectively; it would be a relatively small mass increment for the future Venus mission.

References

[1] Fukuhara, T., et al., 2017, Large stationary gravity wave in the atmosphere of Venus, Nature Geoscience, Vol. 10, 85–88.

©2019. Japan Geoscience Union. All Right Reserved.

[2] Garate-Lopez, I., et al., 2015, Atmospheric dynamics at the southern pole of Venus: Three-dimensional winds, temperature and vorticity, AGU Fall Meeting Abstracts, 23.
[3] Fukuhara, T., et al., 2017, Detection of small wildfire by thermal infrared camera with the uncooled microbolometer array for 50 kg class satellite, IEEE Transactions on Geoscience and Remote Sensing, 2017, Vol. 55, No. 8, 4314-4324

Keywords: Venus, atmosphere, Akatsuki

©2019. Japan Geoscience Union. All Right Reserved.

Temperature and wind variations in Venusian mesosphere and lower thermosphere by mid-infrared heterodyne spectrometer in 2018

*高見 康介[1]、中川 広務[1]、佐川 英夫[2]、村田 功[1]、笠羽 康正[1]
*Kosuke Takami[1], Hiromu Nakagawa[1], Hideo Sagawa[2], Isao Murata[1], Yasumasa Kasaba[1]

1. 東北大学大学院理学研究科地球物理学専攻惑星大気物理学分野、2. 京都産業大学大学院理学研究科物理学専攻
1. Graduate School of Science, Tohoku University, 2. Division of Science, Kyoto Sangyo University

The most extensive observations of Venusian mesosphere have been performed by Venus Express (VEX) up to 2014 (e.g., Patzold et al., 2007; Mahieux et al., 2015). These observations have found the highly spatial and temporal variations in the thermal structure. The temperature discrepancies between observations by VEX/SOIR and general circulation models in the altitude of 80 - 100 km have not been properly interpreted (Bougher et al., 2015; Gilli et al., 2017). In addition, the mesospheric dynamics located between retrograde superrotational zonal wind (cloud deck) and subsolar-to-antisolar flow (above 120 km altitude) have not been well understood due to lack of observations. On the other hand, the lower thermosphere has been observed by mid-infrared heterodyne spectrometer (MIR-HS). Temperature in this region varied extensively between 140 K and 240 K, and wind velocity changed intensely from 130 m/s to 190 m/s for a terrestrial day (Sornig et al., 2013; Krause et al., 2018). Temperature and wind variations such as periodicity and locality in Venusian mesosphere and lower thermosphere have not been comprehended. The purpose of our observations is to solve it with continuous observations by MIR-HS.
Our Mid-Infrared Laser Heterodyne Instrument (MILAHI) have been inserted to Tohoku 60 cm telescope located the summit of Mt. Haleakala in Maui, Hawaii (Nakagawa et al., 2016). MILAHI has 10 um CO_2 laser as local oscillator. The field of view is 4 arcsec with 60 cm telescope and in the wavelength of 10 um. MIR-HS can retrieve temperature and wind in different altitude between dayside observations and nightside observations. CO_2 emerge non-local thermodynamic equilibrium emission from 100 –120 km altitude in dayside (Lopez-Valverde et al., 2011). Temperature and wind are derived from Doppler width and Doppler shift of the emission spectra, respectively. In nightside, CO_2 in the mesosphere absorbs background radiation from the cloud deck. Temperature profile and wind are retrieved from this absorption spectra with radiative transfer equation and inverse method of AMATERASU developed in National Institute of Information and Communications Technology.
Dayside observations were conducted between 24th and 27th in June, 2018. Apparent diameter was 15 arcsec and apparent dayside was half of the disk in this term. Observed points were North, South, disk center, and equator with integration times of 30 - 55 minutes. Each observed point gave different temperature variation feature. Temperature variation range was 170 - 220 K in agreement with Sonnabend et al. (2010). Temperature distribution showed both latitudinal dependence in 25th and convergence at 200 K in 26th.
Nightside observations were conducted from 11th to 13th, 19th, and 20th in November, 2018. Apparent diameter of Venus changed between 55.4 and 49.4 arcsec after inferior conjunction. We observed equator with three days, north 33 degree and south 33 degree for diurnal and latitudinal variations with integration times of 80 - 130 minutes. The observed spectra in the unit of relative intensity are under conversion because the retrieval with AMATERASU is necessary to use absolute radiation. We will show retrieved temperature profile and wind velocity at this presentation.

キーワード：金星、中間圏、中間赤外分光
Keywords: Venus, Mesosphere, mid-infrared spectroscopy

©2019. Japan Geoscience Union. All Right Reserved.

©2019. Japan Geoscience Union. All Right Reserved.

Local time dependence of limb darkening seen in the thermal infrared Venus disk

*秋場 聖浩[1]
*Masahiro Akiba[1]

1. 立教大学院理学研究所物理学専攻
1. Rikkyo University

Brightness temperature of the Venus disk obtained by Longwave Infrared Camera (LIR) onboard Akatuski shows clear limb darkening in the low and middle latitudes. Limb darkening is an apparent temperature decrease from the center to the limb of the Venus disk. It is caused by thermal and radiative characteristics that the sensing altitude of LIR increases as an emission angle, which is a zenith angle of direction of emission from the Venus atmosphere to the sensor, increases and that the atmospheric temperature monotonically decreases with altitude. In higher latitudes limb brightening is observed, because an inversion layer exists at the cloud-top altitudes in higher latitudes. In other word a profile of the limb darkening reflects vertical distributions of atmospheric temperature and optical thickness of cloud particles. Taylor et al. [1980] presented local time dependence of limb darkening using brightness temperature data obtained by the Pioneer Venus orbiter, but did not mention its physical mechanism. In this study brightness temperature distributions obtained by LIR when Akatsuki was in the altitude range from 60,000 to 100,000 km during the period from October 19, 2016 to July 17, 2018 were analyzed to investigate temperature and cloud particle property at the cloud-tops. Each brightness temperature image with 328 x 248 pixels was divided into 3280 x 2480 sub-pixels, and 32 successive images were accumulated after precise adjustment of the Venus disk position to improve S/N. Brightness temperature profiles as a function of the emission angle were derived for 24 local time zones and 9 zonal belts with a latitudinal width of 10˚ within ±45˚. A degree of limb darkening and a brightness temperature at the disk center were determined by least-square function fitting. As a result, the degree of limb darkening shows a clear semi-diurnal variation, and is the strongest at 11h and 22h and the weakest at 7h and 18h in local time. The amplitude of semi-diurnal variation peaks at the equator, whereas its phase seems constant in all latitudes. The temperature at the disk center also shows a semi-diurnal variation with a phase shift of approximately two hours earlier than the phase of the degree of limb darkening and a slight diurnal variation in higher latitudes. These semi-diurnal and diurnal components observed by LIR are consistent with the past observation of thermal tides in the Venus atmosphere by VENERA 15 [Zasova et al., 2007]. The physical mechanism of the semi-diurnal and diurnal thermal tide components seen in the degree of limb darkening and cloud-top temperature will be discussed.

©2019. Japan Geoscience Union. All Right Reserved.

Local time dependence of limb darkening seen in the thermal infrared Venus disk

Masahiro Akiba, Tetsuya Fukuhara, and Makoto Taguchi
Rikkyo University

Brightness temperature of the Venus disk obtained by Longwave Infrared Camera (LIR) onboard Akatuski shows clear limb darkening in the low and middle latitudes. Limb darkening is an apparent temperature decrease from the center to the limb of the Venus disk. It is caused by thermal and radiative characteristics that the sensing altitude of LIR increases as an emission angle, which is a zenith angle of direction of emission from the Venus atmosphere to the sensor, increases and that the atmospheric temperature monotonically decreases with altitude. In higher latitudes limb brightening is observed, because an inversion layer exists at the cloud-top altitudes in higher latitudes. In other word a profile of the limb darkening reflects vertical distributions of atmospheric temperature and optical thickness of cloud particles. Taylor et al. [1980] presented local time dependence of limb darkening using brightness temperature data obtained by the Pioneer Venus orbiter, but did not mention its physical mechanism. In this study brightness temperature distributions obtained by LIR when Akatsuki was in the altitude range from 60,000 to 100,000 km during the period from October 19, 2016 to July 17, 2018 were analyzed to investigate temperature and cloud particle property at the cloud-tops. Each brightness temperature image with 328 x 248 pixels was divided into 3280 x 2480 sub-pixels, and 32 successive images were accumulated after precise adjustment of the Venus disk position to improve S/N. Brightness temperature profiles as a function of the emission angle were derived for 24 local time zones and 9 zonal belts with a latitudinal width of 10° within ±45°. A degree of limb darkening and a brightness temperature at the disk center were determined by least-square function fitting. As a result, the degree of limb darkening shows a clear semi-diurnal variation, and is the strongest at 11h and 22h and the weakest at 7h and 18h in local time. The amplitude of semi-diurnal variation peaks at the equator, whereas its phase seems constant in all latitudes. The temperature at the disk center also shows a semi-diurnal variation with a phase shift of approximately two hours earlier than the phase of the degree of limb darkening and a slight diurnal variation in higher latitudes. These semi-diurnal and diurnal components observed by LIR are consistent with the past observation of thermal tides in the Venus atmosphere by VENERA 15 [Zasova et al., 2007]. The physical mechanism of the semi-diurnal and diurnal thermal tide components seen in the degree of limb darkening and cloud-top temperature will be discussed.

©2019. Japan Geoscience Union. All Right Reserved.

あかつき中間赤外画像の積算による金星雲頂の定在構造と帯状構造の抽出
Stationary wavy features and Banded structures at Venusian cloud top extracted by averaging multiple LIR images

*福谷 貴一[1]、今村 剛[1]、田口 真[2]、福原 哲哉[2]、神山 徹[3]
*Kiichi Fukuya[1], Takeshi Imamura[1], Makoto Taguchi[2], Tetsuya Fukuhara[2], Toru Kouyama[3]

1. 東京大学、2. 立教大学、3. 産総研
1. Univ. of Tokyo, 2. Rikkyo Univ., 3. AIST

Venus’ cloud-top temperature distribution is now continuously mapped by LIR (Long-wave Infrared camera) mounted on the Venus orbiter Akatsuki. Fukuhara et al. (2017) analyzed LIR data and reported the existence of bow-shaped structures extending over 10,000 km in the north-south direction. The features are fixed in position without flowing with the super-rotation and appear above highlands with altitudes higher than 3 km. It was suggested based on a comparison with numerical simulations that the features are gravity waves generated by near-surface flows impinging on mountains. Kouyama et al. (2017) observed stationary features over 4 Venus days and revealed that the features tend to occur in the local afternoon. Gravity waves, whose restoring force is buoyancy, transport horizontal momentum in the vertical direction and accelerate or decelerate the background wind when they dissipate. Therefore, stationary gravity waves influence the general circulation of the atmosphere. In order to estimate the influence, it is essential to reveal the spatial and temporal distributions of gravity waves.
In the previous studies using LIR data, only planetary-scale stationary features have been investigated. On the other hand, Peralta et al. (2017) analyzed the data taken by VIRTIS onboard Venus Express, and reported the existence of many small-scale stationary features; however, VIRTIS can observe the night side only, and the observations were confined to the high latitude of the southern hemisphere because of the geometry of the orbit. Therefore, we intend to investigate with a new analysis method the topographical and local time dependency of small-scale, weak stationary features by using LIR data, which can observe all latitude regions at any local time. Though the S/N ratio of LIR is lower than VIRTIS, averaging of multiple images can suppress noises and at the same time emphasize stationary patterns. By using this method, small-scale, stationary wave trains were newly found above relatively-low topographic rises with altitudes of 1-3 km. In addition to stationary features, zonally-elongated banded structures were also found in averaged LIR images. Such structures have once been detected in LIR images taken during Akatsuki’s Venus flyby in 2010 (Taguchi et al., 2012); the new analysis confirmed that banded structures are ubiquitous at the cloud top. The orientations of the banded structures are different from those of dark streaks found in ultraviolet images.

キーワード：地形性重力波、金星、あかつき
Keywords: Stationary gravity waves, Venus, Akatsuki

©2019. Japan Geoscience Union. All Right Reserved.

Akatsuki's IR2 Nightside Photometry Restoration by Deconvolution

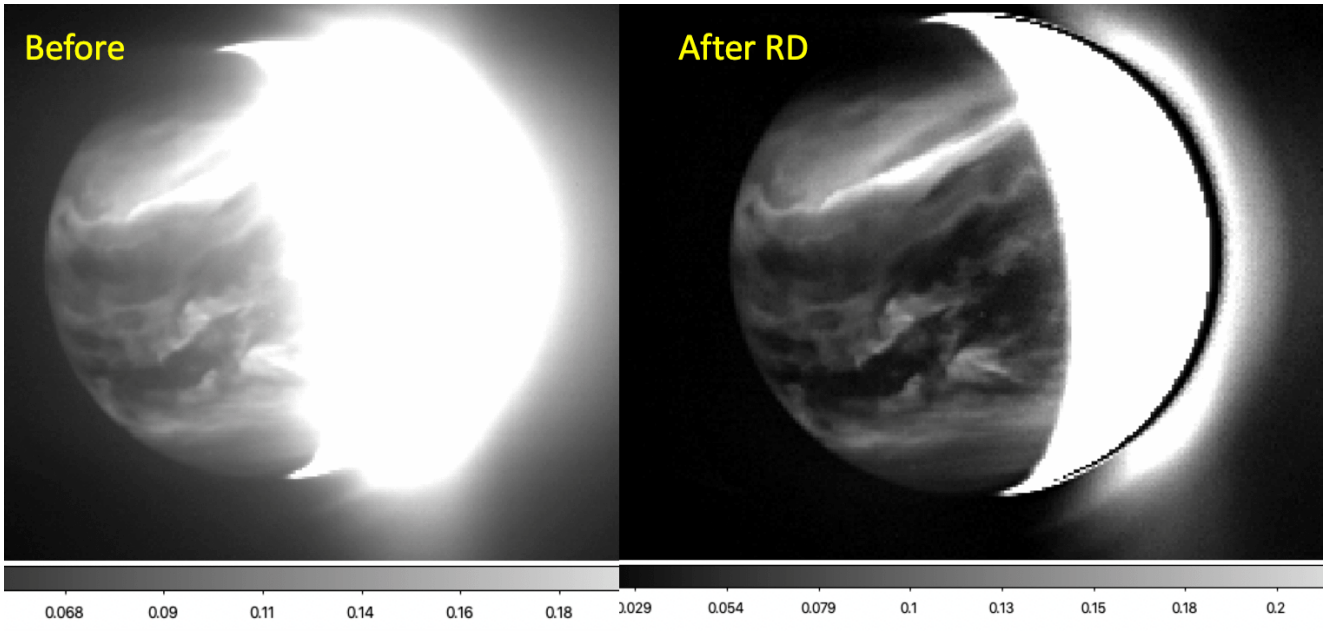
*Choon Wei Vun[1], Takehiko Satoh[2,1], Kevin McGouldrick[3], Takeshi Horinouchi[4], Takao M. Sato[5]

1. SOKENDAI, 2. ISAS/JAXA, 3. University of Colorado Boulder, 4. Hokkaido University, 5. Hokkaido Information University

Akatsuki’ s IR2 camera captures images of Venus at different filters: 1.735um, 2.26um, and 2.32um. At near-dawn/dusk views (phase angles ~90 to 115 degree) of these images, the nightside photometry is contaminated by the intense dayside reflectance. As the potential well of a pixel is overfilled with incoming generated photoelectrons, the pixel is saturated and hence no longer contain information. This saturation can occur in the dayside and nightside near the terminator.
Owing to the saturation problem, main task of the restoration process is thus to simulate both day and night sides to replace the information loss in saturation. Point spread function (PSF) of the IR2 camera was modeled using Moffat function with observation of experimental image taken of point source street light before launch. Then, deconvolution by model-PSF can restore the nightside photometry of unsaturated pixels. Dayside reflectance was modeled with Lambert’ s law, where its distribution is multiplied by an F factor (W m^{-2} sr^{-1} um^{-1}). Methods of finding the F factor will be shown.
We present our Restoration by Deconvolution (RD) results of the selected dates. The restored images were limb darkening corrected. Efficiency of RD can be restored to ~0.005 sigma in standard deviation accuracy when performed on synthetic image with known answer image.
Correlation plot of unsaturated nightside radiances between two filters (2.26mm and 1.735mm) were produced to extract possible ‘branch’ phenomena. The branching in the correlation plot indicates the differences in optical depths of different particle size modes [1].
Restoration of nightside pixels also opens up the opportunity to study the cloud dynamics transiting from the dayside into the nightside. Moreover, interesting cloud features such as vortices, instabilities, and streaks are more distinct in recovered images. This in overall opens up new window to understanding the evolution of cloud motion in the middle layer.
References: [1] Carlson R.W. et al. (1993) *Planet. Space Sci., 41,* No. 7, 477-485. [2] Grinspoon D.H. et al. (1993) *Planet. Spce Sci, 41,* No. 7, 515-542. [3] Nakamura M. et al. (2011)*Earth, Planets and Space, 63,* 443-457. [4] Satoh T. et al. (2016) *Earth, Planets and Space 68:74*. [5] Satoh T. et al. (2017) *Earth, Planets and Space 69:154.* [6] Wilson C.F. et al. (2008) *JGR, 113,* E00B13

Keywords: Venus, atmosphere, image restoration, infrared

©2019. Japan Geoscience Union. All Right Reserved.



©2019. Japan Geoscience Union. All Right Reserved.

Enormous cloud cover as seen by Akatsuki/IR2 on the night-side disk of Venus

Enormous cloud cover as seen by Akatsuki/IR2 on the night-side disk of Venus

*佐藤 毅彦[1,2]、Vun Choon Wei[2]、佐藤 隆雄[3]、堀之内 武[4]、はしもと じょーじ[5]、McGouldrick Kevin[6]
*Takehiko Satoh[1,2], Choon Wei Vun[2], Takao M. Sato[3], Takeshi Horinouchi[4], George HASHIMOTO[5], Kevin McGouldrick[6]

1. 宇宙航空研究開発機構・宇宙科学研究所、2. 総合研究大学院大学・宇宙科学専攻、3. 北海道情報大学・経営情報学部、4. 北海道大学・地球環境科学研究院 、5. 岡山大学・理学部地球科学科、6. LASP, University of Colorado Boulder
1. Institute of Space and Astronautical Science, Japan Aerospace Exploration Agency, 2. Department of Space Science, SOKENDAI, 3. Department of Business and Information Systems, Hokkaido Information University, 4. Faculty of Environmental Earth Science, Hokkaido University, 5. Department of Earth Science, Okayama University, 6. LASP, University of Colorado Boulder

Night-side observations in transparency windows of CO_2 atmosphere of Venus allow visualizing inhomogeneous clouds in ~50 to ~60 km altitudes. The IR2 camera on board Akatsuki captured such images at 1.735, 2.26, and 2.32 um wavelengths. In the IR2 night-side data, an enormous cloud of greater opacity and very sharp edge in the front (western end) is seen repeatedly. This feature seems to encircle the planet with a period of ~4.5 days (Peralta).

Although interesting, property of particles in this feature was not studied before due to difficulty of photometric measurements in IR2 night-side data. This difficulty comes from a combination of the intense day crescent and extended tail of IR2 point-spread function (multiple reflection in the detector is the cause). We have developed a technique to restore the contrast of the night-side data by deconvolution so that the photometric studies can be done with IR2 night-side data.

The data acquired on 18th and 27th August 2016 are analyzed. We have performed a series of radiative transfer computations to reproduce both 1.735- and 2.26-um opacities in this enormous cloud. Properties of the cloud partices will be presented and possible mechanism of this remarkable phenomenon will be discussed.

キーワード：あかつきIR2、金星夜面、雲濃度
Keywords: Akatsuki IR2, Venus night-side, Cloud opacity

©2019. Japan Geoscience Union. All Right Reserved.

あかつき搭載IR1から明らかにする金星雲の全球変動
The global variation of Venus cloud obtained from IR1 camera onboard AKATSUKI

*高木 聖子[1]、岩上 直幹、高橋 幸弘[1]、佐藤 光輝[1]
*Seiko Takagi[1], Naomoto Iwagami, Yukihiro Takahashi[1], Mitsuteru Sato[1]

1. 北海道大学大学院理学研究院
1. Hokkaido University, Graduate School of Science

金星は地球とほぼ同じ大きさ・密度を持ち、太陽系形成時には互いに似た惑星として誕生したと考えられているが、90気圧もの二酸化炭素大気や全球を一様に覆う硫酸雲の存在など地球とは全く異なる様相を見せる。
金星探査機あかつき(JAXA)は、2015年12月に金星周回軌道投入に成功した。あかつきは複数波長による撮像観測を行い、金星気象の3次元的理解を目指す。搭載された近赤外カメラIR1は、軌道投入後約1年間、近赤外波長0.90 umにおける金星昼面撮像を行った。大気の窓領域である近赤外波長を用いた金星昼面撮像観測では、雲の光学的厚さの増減を金星表面のコントラストとしてとらえることができる[Takagi and Iwagami. 2011]。木星探査機Galileo/SSI (NASA)により得られた金星昼面近赤外画像(0.986 um)では、金星表面のコントラストはわずか3 %と示されている[Belton et al., 1991]が、IR1はかつて木星探査機Galileo/SSIが得たものと整合的な昼面画像を多数取得している。本研究では、IR1が取得した0.90 um昼面画像から雲の変動傾向を全球的に知る。合わせてVenus Express(ESA)搭載赤外分光計SOIRから得られた金星高高度の雲情報[Takagi et al. in rev.]を反映した放射輸送計算を近赤外波長において実行し、雲変動に寄与する金星の気象変化について考察する。さらに北海道大学が所有するピリカ望遠鏡を用いた同波長領域における観測計画を紹介する。

キーワード：金星、雲、近赤外
Keywords: Venus, cloud, near infrared

©2019. Japan Geoscience Union. All Right Reserved.

対流モデルに向けた金星雲計算スキームの開発
Development of a Venus' cloud formation scheme for a convection resolving model

*杉山 耕一朗[1]、福原 望[1]、小高 正嗣[2]、中島 健介[3]、石渡 正樹[2]、今村 剛[4]、林 祥介[5]
*Ko-ichiro SUGIYAMA[1], Nozomu Fukuhara[1], Masatsugu Odaka[2], Kensuke Nakajima[3], Masaki Ishiwatari[2], Takeshi Imamura[4], Yoshi-Yuki Hayashi[5]

1. 松江高専・情報、2. 北大・理・宇宙、3. 九大・理・地惑、4. 東大・新領域創成科学、5. 神戸大・理・地惑
1. National Institute of Technology, Matsue College, 2. Department of Cosmoscience, Graduate School of Science, Hokkaido University, 3. Department of Earth and Planetary Sciences,Flculty of Sciences,Kyushu University, 4. Graduate School of Frontier Sciences, The University of Tokyo, 5. Department of Planetology, Graduate School of Science, Kobe University / Center for Planetary Science (CPS)

Although convection has been suggested to occur in the lower part of Venus' cloud layer by some observational evidences, its structure remains to be clarified. In the previous studies, Baker et al. (1998, 2000), Imamura et al. (2014), and Lefevre et al. (2017) try to simulate Venus' cloud-level convection, but their models they utilized do not consider cloud formation process. Our purpose is to develop new cloud formation scheme and to perform numerical simulation using the scheme in order to investigate a possible structure of Venus' cloud-level convection and clouds distribution.

Our cloud formation scheme is based on Imamura and Hashimoto (1998). The number densities of sulfuric acid (H2SO4) and water (H2O) in the gas and liquid phases are calculated. Sedimentation of H2SO4-H2O solution droplets and chemical reactions of sulfuric acid are also considered. The scheme is implemented into our convection resolving model developed by Sugiyama et al. (2009). The model is based on the quasi-compressible system (Klemp and Wilhelmson, 1978), and is used in the simulations of the atmospheric convections of Jupiter (Sugiyama et al., 2011, 2014) and Mars (Yamashita et al. 2017).

In our poster, we will show the details of our cloud formation scheme and demonstrate some results of our calculation using similar settings of Imamura et al. (2014).

キーワード：金星大気、対流、雲形成、数値計算
Keywords: Venus atmosphere, convection, cloud formation, numerical modeling

©2019. Japan Geoscience Union. All Right Reserved.

放射伝達を陽に考慮した金星大気大循環モデルで見られる東西平均構造
Zonal mean structure of Venus atmosphere observed in a Venus general circulation model with explicit radiative transfer

*林 祥介[1]、塩尻 千里[1]、樫村 博基[1]、高橋 芳幸[1]
*Yoshi-Yuki Hayashi[1], Chisato Shiojiri[1], Hiroki Kashimura[1], Yoshiyuki O. Takahashi[1]

1. 神戸大学・大学院理学研究科 惑星学専攻/惑星科学研究センター（CPS）
1. Department of Planetology/CPS, Graduate School of Science, Kobe University

金星大気の東西平均東西風は他の惑星大気にはない特徴を示している。ほぼすべての緯度において超回転状態にあり、スーパーローテーションと呼ばれる。数値計算や地上観測による数多くの研究がこの特徴を説明するべく試みられてきたが、2010年代になって遂に、Lebonnois et al. (2010) や Ikeda (2010) は、放射伝達を陽に計算することによりスーパーローテーションを表現することに成功した。これらは、放射過程をニュートン冷却によって代替えさせていたそれ以前の数値モデルとは一線を画すモデルである。

一方、我々は多様な惑星大気を包括的に扱うことのできる大気大循環モデルの開発を進めてきており、その一環として、今回、分厚いCO_2大気を持つ大気のための大循環放射伝達計算を実現するパラメタを用意した。ここでは, 我々が決めた放射パラメタを金星大気の場合に応用してその大循環を計算し、放射伝達を陽に計算した先行研究との比較を行う。

我々が用いる大気大循環モデルは DCPAM (http://www.gfd-dennou.org/library/dcpam/) である。DCPAMはプリミティブ方程式系を力学モデルとして用いており、これをスペクトル法によって解いている。物理過程としては放射過程、乱流混合過程を含み、地表面温度の計算においては地中熱伝導も計算する。放射パラメタは相関k-分布法を用いて導出、計算された放射フラックスは観測された放射フラックスとよく一致することを確認している。大気大循環計算においては、表面地形の有り無しの二種類の数値実験を行った。用いた分解能は T15L52, 格子点でいえば 48 x 24 であり、鉛直 52 層を有している。初期条件はどちらの実験も静止、温度分布は水平一様の VIRA 鉛直温度分布とした。金星の日変化は考慮したが、年変化は考慮していない（自転軸傾斜角はゼロ）。数値積分は 150000 地球日実行した。

100000地球日程度の積分によりエネルギーの時間変化で見るとほぼ統計的に平衡な状態に達する。この統計的な定常状態では , 地形有り無しどちらの実験でも、現実の金星大気東西風速強度の約半分、およそ 50 m/s 程度の超回転風速が雲層の中低緯度領域に見られた。

平均子午面循環は両半球にわたる大きな直接循環で構成されていた。地表面地形無し実験では、この子午面直接循環は、低緯度地表面付近に見られる逆循環を除き、地表面からモデルトップまで覆っていた。一方、地表面有り実験では雲層下部付近に逆循環が存在し、子午面循環は上下に分断される構造をなしていた。その他の逆循環としては、高緯度雲層付近の逆循環と、地形無し実験で見られた赤道域雲層以下の複数の高度領域に見らえる逆循環群である。

発表では、モデルで得られた東西平均構造と東西角運動流収支の解析結果を示す予定である。

キーワード：金星、惑星大気、大気大循環モデル、放射伝達計算
Keywords: Venus, planetary atmosphere, general circulation model, explicit calculation of radiative transfer

©2019. Japan Geoscience Union. All Right Reserved.

©2019. Japan Geoscience Union. All Right Reserved.

電波掩蔽による金星大気温度データからの重力波の波束の抽出
Gravity wave packets detected in radio occultation temperature profiles of the Venus atmosphere

*森 亮太[1]、今村 剛[1]、Javier Peralta[2]
*Ryota Mori[1], Takeshi Imamura[1], Javier Peralta[2]

1. 東京大学、2. 宇宙航空研究開発機構
1. The University of Tokyo, 2. Japan Aerospace Exploration Agency

金星探査機「あかつき」の電波掩蔽観測により2016年から現在に至るまで大気温度の高度分布が得られている。電波掩蔽観測は、探査機から送信される電波が惑星大気を通過して屈折したのち地球の受信局に届く機会を利用して、大気の屈折率の変化を地上での受信周波数の変化として捉える手法であり、屈折率の高度分布から気圧や気温を導出することが出来る。こうして得られる気温分布には様々な大気擾乱に起因する変動が観測される。ここでは、大気大循環の駆動において重要な役割を持つと考えられる大気重力波に注目する。

重力波は大気中の浮力を復元力とする小規模な波動である。重力波は運動量を鉛直方向に運ぶ働きがあり、散逸に際して背景大気に運動量を受け渡すことにより、平均風の加減速をもたらす。金星においては高速帯状風の全球的な構造に影響を与えていることが予想されている。しかし、重力波は空間スケールが小さく、周期が比較的短いという性質があるために、その空間構造を観測で捉えることが難しい。これまでに、重力波に伴うと考えられる短鉛直波長の温度擾乱の振幅の緯度-高度分布などが調べられてきたが、卓越する波長や高度方向の拡がりについては分かっていなかった。

そこで、本研究では、ウェーブレット解析を鉛直温度分布に適用し、空間的に局在した温度擾乱を抽出する。今までは、温度データにフーリエ変換を適用した研究はあるが、フーリエ変換は無限に続く波を仮定としており、空間的に局在した波束の特徴を取り出すのには適切ではない。ウェーブレット解析はそのような有限区間の波に関して周期や振幅を得たい時に有効である。本発表では電波ホログラフィという方法で従来より高い高度分解能で得られた温度データに対してウェーブレット解析を適用した結果を報告する。また、得られた結果から、大気重力波の波束の長さや高度分布などに関係も報告する。

キーワード：あかつき、大気重力波、電波掩蔽観測
Keywords: Akatsuki, Gravity wave in the atmosphere, The radio occultation experiment

©2019. Japan Geoscience Union. All Right Reserved.

Status of lightning hunt in Venus with Akatsuki/LAC and Pirka telescope

*高橋 幸弘[1,2]、佐藤 光輝[1,2]、今井 正尭[3]、Lorenz Ralph[4]、高木 聖子[1,2]、大野 辰遼[1]
*Yukihiro Takahashi[1,2], Mitsuteru Sato[1,2], Masataka Imai[3], Ralph Lorenz[4], Seiko Takagi[1,2], Ono Tatsuharu[1]

1. 北海道大学・大学院理学院・宇宙理学専攻、2. 北海道大学・大学院理学研究院、3. 産業技術総合研究所、4. ジョンズホプキンズ大学応用物理研究所
1. Graduate School of Science, Hokkaido University, 2. Faculty of Science, Hokkaido University, 3. National Institute of Advanced Industrial Science and Technology,, 4. Applied Physics Laboratory, Johns Hopkins University

The existence of lightning discharge in Venus has been controversial for three decades, which might be attributed to the luck of conclusive observational evidence. There had been no satellite payload intentionally designed for the detection of lightning phenomena using radio wave or optical sensor. LAC, lightning and airglow camera, on board Akatsuki spacecraft, is the first sensor optimized for the lightning optical flash measurement in planets other than the Earth. It is expected that LAC could conclude this 30-year discussion on the existence of lightning in Venus. Unique performance of LAC compared to other equipment used in the previous exploration of Venus is the high-speed sampling rate at 20 kHz with 32 pixels of Avalanche Photo Diode (APD) matrix, enabling us to distinguish the natural optical lightning flash from other pulsing noises, including artificial electrical noise and cosmic rays. We selected OI 777 nm line for lightning detection, which is expected to be the most prominent emission in CO2-dominant atmosphere based on the laboratory experiments.

The triggering parameter was set so as to optimize for the light curve similar to the normal lightning in the Earth and data obtained totally for about 4 hours were examined. However, we couldn’t find any lightning signals. Adding to this triggering parameter set, we added one more parameter set, optimized for sprite type emission with duration of up to 10s of ms. Furthermore, in order to investigate fainter emissions, we are now conducting successive force triggering recordings without any threshold, achieving 5 times better sensitivity than the intensity of 1 digital unit at best.

The total coverage of the LAC lightning hunt became 81.6 [million km2-hr], meaning 81 percent detectability of previous results with ground-based telescope by Hansell et al. (1995). Here we report the detailed strategy and the latest status of the LAC observation in 2018, and discuss the future observation plan.

Also we will make ground observation with a high-speed photometer installed at Pirka telescope, a 1.6-m reflector deployed by Hokkaido University. Here we report the initial results of lightning flash observation with it.

キーワード：雷、金星、あかつき、ピリカ望遠鏡
Keywords: lightning, Venus, Akatsuki, Pirka telescope

©2019. Japan Geoscience Union. All Right Reserved.

Possibility of electric discharge in the Venusian atmosphere due to the super-rotation of clouds

*Adhithiyan Neduncheran[1], Ugur Guven[1,2], Ananyo Bhattacharya[3]

1. University of Petroleum and Energy Studies, India, 2. United Nations Centre for Space Science and Technology Education in Asia and the Pacific, 3. Sardar Vallabhbhai National Institute of Technology,India

Several evidences of electromagnetic bursts were measured by various landers and orbiters studying Venus atmosphere (Venera landers, Venus Express and the Pioneer Venus Orbiter). The electromagnetic bursts that are taking place in the cloud region in the form of lightning or fluorescence might be a result of momentum transfer, solar convection and charge dispersion in the clouds of Venus. While the lightning in Earth takes place mostly in the equatorial region, in case of Venus it is possible for lightning to occur in the polar regions, considering the kinetic energy transfer and the formation of dipoles in both hemispheres of Venus. The meridional and zonal flows can interact and cause the charge separation which possibly lead to electromagnetic bursts in different spectrum and in different regions in Venus. In labs, it is observed that SO2 emissions in UV region cause fluorescence which is one of the major phenomena taking place in the cloud tops. Based on the photochemical model published by *Krasnopolsky 2011(*doi:10.1016/j.icarus.2011.11.012) and the principle of refraction, we present the possibility of lightning/fluorescence phenomena being caused by the super-rotation of the clouds in the Venusian atmosphere.

Keywords: Venus , Super-rotation, lightning, electric discharge, atmosphere

©2019. Japan Geoscience Union. All Right Reserved.

[E] ポスター発表 | セッション記号 P (宇宙惑星科学)：P-EM 太陽地球系科学・宇宙電磁気学・宇宙環境

2019年5月27日(月) 13:45 ~ 15:15 | ポスター会場 幕張メッセ国際展示場 8ホール_1

[P-EM10] Multi-scale Coupling in the Magnetosphere-Ionosphere-Thermosphere System

コンビーナ:Yue Deng(University of Texas at Arlington)、Toshi Nishimura(Boston University)、Liu Huixin(九州大学理学研究院地球惑星科学専攻 九州大学宙空環境研究センター)、Yanshi Huang(Harbin Institute of Technology, Shenzhen)

Determining the effects of energy deposition and transport, and momentum exchange across different spatial and temporal scales is an important objective in the M-I-T system, due to the clear evidence of multi-scale forcing. Coupling over multiple scales is also a critical challenge since observational and modeling methodologies for bridging different scales do not presently exist. This session solicits presentations on a wide range of coupling processes in the high-latitude M-I-T system from global to small-scale processes and related solar wind forcing. Relevant topics include (but are not limited to) (1) density structures and temperature gradients (polar cap, cusp, plume, trough, irregularities); (2) convection (flow channels, SAPS) and FAC; (3) energy transfer and deposition by precipitation and ULF waves, conductivity, aurora, and heating; and (4) coupling and feedback into the magnetosphere. Discussions of relevant multi-scale observations by means of multiple instruments, including space and ground-based, modeling and data science are encouraged.

[PEM10-P01] 相対論的電子降り込みに対する南北両半球大気のレスポンス

*田中 良昌[1,13,14]、西山 尚典[1,14]、門倉 昭[1,13,14]、尾崎 光紀[2]、三好 由純[3]、大山 伸一郎[3,15]、片岡 龍峰[1,14]、堤 雅基[1,14]、西村 耕司[1,13,14]、佐藤 薫[4]、笠原 禎也[2]、熊本 篤志[5]、土屋 史紀[5]、吹澤 瑞貴[5]、疋島 充[6]、松田 昇也[6]、松岡 彩子[6]、篠原 育[6]、能勢 正仁[3]、長妻 努[7]、篠原 学[8]、藤本 晶子[9]、寺本 万里子[3]、野村 麗子[10]、行松 彰[1,14]、細川 敬祐[11]、小路 真史[3]、Ralph Latteck[12] (1.国立極地研究所、2.金沢大学理工研究域、3.名古屋大学宇宙地球環境研究所、4.東京大学大学院理学系研究科、5.東北大学大学院理学研究科、6.宇宙航空研究開発機構宇宙科学研究所、7.情報通信研究機構、8.鹿児島工業高等専門学校、9.九州工業大学、10.国立天文台、11.電気通信大学大学院情報理工学研究科、12.Leibniz-Institute of Atmospheric Physics e.V. at the University Rostock, Germany、13.情報・システム研究機構 データサイエンス共同利用基盤施設 極域環境データサイエンスセンター、14.総合研究大学院大学、15.University of Oulu, Finland)

[PEM10-P02] Comparison of precipitating particle energy of proton aurora at geomagnetic conjugate points

*田口 真[1]、西島 樹[1]、門倉 昭[2] (1.立教大学、2.情報・システム研究機構)

[PEM10-P03] A regularized deep convolutional general adversarial network (R-DCGAN) for total electron content map completion

*Mingwu Jin[1]、Zhou Chen[2,3]、Yue Deng[1]、Yang Pan[1]、Jin-Song Wang[2] (1.University of Texas at Arlington、2.Institute of Space Science and Technology, Nanchang University, Nanchang, China、3.Key Laboratory of Space Weather, National Center for Space Weather, China Meteorological Administration, Beijing, China)

[PEM10-P04] A long-lasting auroral bright spot around magnetic north pole: Is it the evidence of stable magnetic reconnection?

*Qing-He Zhang[1]、Guo-Cheng Shen[1]、Yong-Liang Zhang[2]、Kjellmar Oksavik[3]、Michael Lockwood[4]、Zan-Yang Xing[1]、Yu-Zhang Ma[1] (1.Institute of Space Sciences, Shandong University, Weihai, China、2.The Johns Hopkins University Applied Physics Laboratory, Laurel, Maryland, USA、3.Birkeland Centre for Space Science, University of Bergen, Bergen, Norway、4.Department of Meteorology, University of Reading, Earley Gate, Post Office Box 243, RG6 6BB, UK.)

[PEM10-P05] Statistical study of the relationship between ion upflow and field-aligned current in the topside ionosphere for both hemispheres during disturbed and quiet times

Shan-Yu Zhou[1]、*Qing-He Zhang[1]、P. T. Jayachandran[2]、Kjellmar Oksavik[3]、Larry Lyons[4]、Zan-Yang Xing[1]、Yu-Zhang Ma[1]、Marc Hairston[5]、Yong Wang[1] (1.Institute of Space Sciences, Shandong University, Weihai, China、2.Physics Department, University of New Brunswick, Fredericton, New Brunswick,

Canada、3.Birkeland Centre for Space Science, University of Bergen, Bergen, Norway、4.Department of Atmospheric and Oceanic Sciences, University of California, Los Angeles, California, USA、5.William B. Hanson Center for Space Sciences, University of Texas at Dallas, Richardson, Texas, USA)

[PEM10-P06] SAPS in the 2013 March 17 Storm Event: Initial Results from the Coupled Magnetosphere-Ionosphere-Thermosphere Model

*Dong Lin[1,2]、Wenbin Wang[2]、Wayne Scales[1]、Kevin Pham[2]、Jing Liu[2]、Binzheng Zhang[2]、Viacheslav Merkin[3]、Xueling Shi[1] (1.Virginia Tech、2.High Altitude Observatory, NCAR、3.APL, John Hopkins Univ.)

[PEM10-P07] **Westward turning motions of nighttime medium-scale traveling ionospheric disturbances (MSTIDs) at the equatorward side of the dusk side auroral oval associated with auroral brightening**

*Sneha Yadav[1,2]、Kazuo Shiokawa[1]、Shin-ichiro Oyama[1,3,4]、Yuichi Otsuka[1] (1.ISEE, Nagoya University, Nagoya, Japan、2.SPL, VSSC, India、3.Ionosphere Research Unit, University of Oulu, Oulu, Finland、4.NIPR, Tachikawa, Japan)

相対論的電子降り込みに対する南北両半球大気のレスポンス
Atmospheric responses in both hemispheres to relativistic electron precipitation

*田中 良昌[1,13,14]、西山 尚典[1,14]、門倉 昭[1,13,14]、尾崎 光紀[2]、三好 由純[3]、大山 伸一郎[3,15]、片岡 龍峰[1,14]、堤 雅基[1,14]、西村 耕司[1,13,14]、佐藤 薫[4]、笠原 禎也[2]、熊本 篤志[5]、土屋 史紀[5]、吹澤 瑞貴[5]、疋島 充[6]、松田 昇也[6]、松岡 彩子[6]、篠原 育[6]、能勢 正仁[3]、長妻 努[7]、篠原 学[8]、藤本 晶子[9]、寺本 万里子[3]、野村 麗子[10]、行松 彰[1,14]、細川 敬祐[11]、小路 真史[3]、Ralph Latteck[12]
*Yoshimasa Tanaka[1,13,14], Takanori Nishiyama[1,14], Akira Kadokura[1,13,14], Mitsunori Ozaki[2], Yoshizumi Miyoshi[3], Shin-ichiro Oyama[3,15], Ryuho Kataoka[1,14], Masaki Tsutsumi[1,14], Koji Nishimura[1,13,14], Kaoru Sato[4], Yoshiya Kasahara[2], Atsushi Kumamoto[5], Fuminori Tsuchiya[5], Mizuki Fukizawa[5], Mitsuru Hikishima[6], Shoya Matsuda[6], Ayako Matsuoka[6], Iku Shinohara[6], Masahito Nose[3], Tsutomu Nagatsuma[7], Manabu Shinohara[8], Akiko Fujimoto[9], Mariko Teramoto[3], Reiko Nomura[10], Akira Sessai Yukimatu[1,14], Keisuke Hosokawa[11], Masafumi Shoji[3], Ralph Latteck[12]

1. 国立極地研究所、2. 金沢大学理工研究域、3. 名古屋大学宇宙地球環境研究所、4. 東京大学大学院理学系研究科、5. 東北大学大学院理学研究科、6. 宇宙航空研究開発機構宇宙科学研究所、7. 情報通信研究機構、8. 鹿児島工業高等専門学校、9. 九州工業大学、10. 国立天文台、11. 電気通信大学大学院情報理工学研究科、12. Leibniz-Institute of Atmospheric Physics e.V. at the University Rostock, Germany、13. 情報・システム研究機構 データサイエンス共同利用基盤施設 極域環境データサイエンスセンター、14. 総合研究大学院大学、15. University of Oulu, Finland
1. National Institute of Polar Research, 2. Institute of Science and Engineering, Kanazawa University, 3. Institute for Space-Earth Environmental Research, Nagoya University, 4. Graduate School of Science, The University of Tokyo, 5. Graduate School of Science, Tohoku University, 6. Japan aerospace exploration agency, Institute of space and astronautical science, 7. National Institute of Information and Communications Technology, 8. Kagoshima National College of Technology, 9. Kyushu Institute of Technology, 10. National Observatory of Japan, 11. Department of Communication Engineering and Informatics, University of Electro-Communications, 12. Leibniz-Institute of Atmospheric Physics e.V. at the University Rostock, Germany, 13. Polar Environment Data Science Center, Joint-Support Center for Data Science Research, Research Organization of Information and Systems, 14. The Graduate University for Advanced Studies (SOKENDAI), 15. University of Oulu, Finland

Relativistic electron precipitation (REP) in the polar atmosphere has been paid attention to because it changes atmospheric composition, causing ozone depletion after migrating to the lower altitude during polar winter. A plausible mechanism for REP is the interaction with magnetospheric plasma waves, such as electromagnetic ion cyclotron (EMIC) waves and whistler-mode chorus waves. Previous studies have already shown that EMIC waves can effectively drive REP, however, observational evidence that chorus waves can drive REP was lacking. In this study we present direct comparison between magnetospheric plasma waves and polar mesosphere winter echoes (PMWE) simultaneously observed with the Arase satellite and high-power Mesosphere, Stratosphere and Troposphere (MST) radars in both hemispheres, PANSY and MAARSY. PMWE can be related to the ionization in the mesosphere due to REP. The PMWE were observed at 03-07 UT on March 21, 2017 during the passage of corotating interaction region (CIR), during which the Arase footprints were close to Syowa Station (SYO; −69.00S, 39.58E), Antarctica, and Husafell (HUS; 65.67N, −21.03E), Iceland.
The observational results are summarized as follows. (1) EMIC waves and whistler-mode chorus waves were observed by Arase near the equatorial magnetosphere during 02:30-04:45 UT and 04:45-07:00 UT, respectively. (2) PMWE were detected with both the MAARSY radar at Andøya (AND; 69.30N, 16.04E), Norway, and the PANSY radar at SYO, Antarctica, during 04:45-07:00 UT, which was the recovery phase of an isolated substorm. We believe this is the first time PMWE have been observed in both hemispheres

©2019. Japan Geoscience Union. All Right Reserved.

at exactly the same time. (3) During 04:45-07:00 UT, the temporal variation of the chorus wave power was similar to those of the PMWE power in the both hemispheres. (4) The PMWE observed at SYO during 03:00-04:00 UT before the substorm onset was consistent with the occurrence of the EMIC waves. The item (2) shows direct evidence that chorus waves during the substorm recovery phase cause REP. We estimated the resonance energy of electrons interacting with the observed LBC waves, however, the estimated energy was too low to cause PMWE at an altitude lower than 70 km. However, we found that the resonance energy becomes greater than 1 MeV, if LBC waves propagate to the magnetic latitude greater than 30 degrees and resonate with energetic electrons there. As for item (4), the PMWE observed at SYO during 03:00-04:00 can be related to wave-particle interaction with EMIC waves, which may be generated inside the plasmapause by ring-current hot ions with temperature anisotropy. This anisotropy was caused by magnetospheric compression due to increasing solar wind dynamic pressure during 01:00–06:00 UT just after the arrival of the CIR. Since CIRs are main sources of geomagnetic disturbances during the declining phase of the solar cycle and solar minimum, this event is not rare but rather a common atmospheric response caused by interaction between recurrent large-scale solar wind structures and geospace.

キーワード：極域中間圏冬季エコー、あらせ衛星、PANSYレーダー、MAARSYレーダー、相対論的電子降り込み、磁気圏プラズマ波動
Keywords: Polar Mesosphere Winter Echoes, Arase satellite, PANSY radar, MAARSY radar, relativistic electron precipitation, magnetospheric plasma waves

©2019. Japan Geoscience Union. All Right Reserved.

Comparison of precipitating particle energy of proton aurora at geomagnetic conjugate points

*田口 真[1]、西島 樹[1]、門倉 昭[2]
*Makoto Taguchi[1], Tatsuki Nishijima[1], Akira Kadokura[2]

1. 立教大学、2. 情報・システム研究機構
1. Rikkyo University, 2. Research Organization of Information and Systems

It is expected that mirror images of aurora are observed at geomagnetic conjugate points in the northern and southern auroral zones connected by a geomagnetic field line. However, geomagnetic conjugate auroras often show non-conjugacy, which reflects north-south asymmetry of the solar wind, the magnetosphere and the ionospheres. In other words acceleration mechanism of auroral particles may be studied by comparing aurora simultaneously occurring at geomagnetic conjugate points. A hydrogen Balmer beta emission at the wavelength of 486.1 nm which is the brightest among the proton auroral lines was observed at a pair of geomagnetic conjugate points to compare precipitating particle energy. Two identical Proton Auroral Specrographs (PASs) which obtain auroral spectra along a geomagnetic meridian at a rate of 1 image/min were installed at Tjornes in Iceland and Syowa Station in Antarctica. Data obtained during a period from September 4, 2018 to October 9, 2018 were analyzed to derive an average kinetic energy of precipitating protons along a local geomagnetic field line from a Doppler shift of the H beta line. As a result we are succeeded in simultaneous observations of proton auroras at both conjugate points in 5 nights on September 4, 5, 6, 7 , and 10. The average energies of precipitating protons range from 0 keV to 7 keV, and sometimes show a periodical variation with a period of 4 - 5 min. Conjugacy of precipitating particle energy will be discussed in the presentation.

©2019. Japan Geoscience Union. All Right Reserved.

A regularized deep convolutional general adversarial network (R-DCGAN) for total electron content map completion

*Mingwu Jin[1], Zhou Chen[2,3], Yue Deng[1], Yang Pan[1], Jin-Song Wang[2]

1. University of Texas at Arlington, 2. Institute of Space Science and Technology, Nanchang University, Nanchang, China, 3. Key Laboratory of Space Weather, National Center for Space Weather, China Meteorological Administration, Beijing, China

Observations with a complete global coverage are important for space physics research and applications. However, due to the technical limitations and costs, such a complete global coverage is often unavailable. Thus, data filling algorithms are often pursued to fill missing data gaps to create a global map from the incomplete data. In this work, a novel deep learning algorithm, regularized deep convolutional generative adversarial network (R-DCGAN), is developed by adding an extra discriminator to the conventional DCGAN to fill the missing data of total electron content (TEC) map images. R-DCGAN incorporates the knowledge from reference TEC maps of the International Global Navigation Satellite Systems Service Ionosphere Working Group to achieve much better TEC map completion performance than the conventional DCGAN as demonstrated by both synthetic and real data. The R-DCGAN framework can be extended to other fields of space sciences to address the missing observation data issues.

Keywords: Deep learning method, TEC , map completion

©2019. Japan Geoscience Union. All Right Reserved.

A long-lasting auroral bright spot around magnetic north pole: Is it the evidence of stable magnetic reconnection?

*Qing-He Zhang[1], Guo-Cheng Shen[1], Yong-Liang Zhang[2], Kjellmar Oksavik[3], Michael Lockwood[4], Zan-Yang Xing[1], Yu-Zhang Ma[1]

1. Institute of Space Sciences, Shandong University, Weihai, China, 2. The Johns Hopkins University Applied Physics Laboratory, Laurel, Maryland, USA, 3. Birkeland Centre for Space Science, University of Bergen, Bergen, Norway, 4. Department of Meteorology, University of Reading, Earley Gate, Post Office Box 243, RG6 6BB, UK.

An intense and large auroral bright spot appears around the magnetic north pole observed by the Special Sensor Ultraviolet Spectrographic Imager (SSUSI) on board four different Defense Meteorological Satellite Program (DMSP) satellites during long time northward IMF conditions. The bright spot is even brighter than aurora in the auroral oval which is about 5-10° magnetic latitude equatorward of the bright spot. The bright spot is lasting about 8 hours, and sometimes appears as a cyclone-shape with a clockwise rotation. The DMSP in situ plasma observations suggest that the bright spot is clear associated with electron invert-V acceleration with 10s keV energy electron precipitations around the center regions and 1s keV energy electron precipitations around the egde regions. There are also strong flow shears between the two sides of the bright spot: strong sunward flows on the duskside and antisunward flows on the dawnside. These types of plasma should come from the high-latitude lobe region of the magnetotail due to the high-latitude lobe magnetic reconnections. Is it the evidence of stable lobe reconnection during long time northward IMF conditions? The detail and further analysis should be pursued in the following studies.

Keywords: Auroral bright spot, Magnetosphere-ionosphere coupling, High-latitude lobe magnetic reconnection, Stable reconnection

©2019. Japan Geoscience Union. All Right Reserved.

Statistical study of the relationship between ion upflow and field-aligned current in the topside ionosphere for both hemispheres during disturbed and quiet times

Shan-Yu Zhou[1], *Qing-He Zhang[1], P. T. Jayachandran[2], Kjellmar Oksavik[3], Larry Lyons[4], Zan-Yang Xing[1], Yu-Zhang Ma[1], Marc Hairston[5], Yong Wang[1]

1. Institute of Space Sciences, Shandong University, Weihai, China, 2. Physics Department, University of New Brunswick, Fredericton, New Brunswick, Canada, 3. Birkeland Centre for Space Science, University of Bergen, Bergen, Norway, 4. Department of Atmospheric and Oceanic Sciences, University of California, Los Angeles, California, USA, 5. William B. Hanson Center for Space Sciences, University of Texas at Dallas, Richardson, Texas, USA

A statistical study of ion upflow and field-aligned currents (FACs) has been performed in the topside ionosphere of both hemispheres for magnetic quiet and disturbed times by using DMSP satellite observations from 2010-2013. Distributions in MLT/MLAT reveal that ion upflow shows a dawn-dusk asymmetry distribution that corresponds well with the region 1 field-aligned currents. In addition, there are highest occurrence regions near noon and within the near midnight auroral disturbance area. These correspond to cusp and nightside dynamical processes, respectively. Both the ion upflow occurrence and FAC regions expand equatorward to a wider area during disturbed times.

Keywords: Ion upflows, Field-aligned current, Magnetosphere-ionosphere coupling

©2019. Japan Geoscience Union. All Right Reserved.

SAPS in the 2013 March 17 Storm Event: Initial Results from the Coupled Magnetosphere-Ionosphere-Thermosphere Model

*Dong Lin[1,2], Wenbin Wang[2], Wayne Scales[1], Kevin Pham[2], Jing Liu[2], Binzheng Zhang[2], Viacheslav Merkin[3], Xueling Shi[1]

1. Virginia Tech, 2. High Altitude Observatory, NCAR, 3. APL, John Hopkins Univ.

Subauroral polarization stream (SAPS) are latitudinally narrow flow channels of large westward plasma drifts in the subauroral ionosphere. In this study, the global structure and dynamic evolution of SAPS are investigated by using the National Center for Atmospheric Research (NCAR) Coupled Magnetosphere-Ionosphere-Thermosphere (CMIT) model with Ring Current extension, namely the LFM-TIEGCM-RCM (LTR) model, to simulate the 2013 St. Patrick's Day storm event. This is the first time that the global distribution and temporal evolution of SAPS are investigated using first-principle models. The model shows a strong westward ion drift channel formed equatorward of the auroral electron precipitation boundary on the duskside, which is identified as the SAPS structure. The simulated ion drift velocity and auroral electron precipitation sampled along the trajectory of the DMSP F18 satellite are in good agreement with the satellite measurements. SAPS initiate in the pre-dusk sector when the interplanetary magnetic field (IMF) turns southward. SAPS latitude generally decreases with magnetic local time (MLT) from dusk to midnight. The SAPS channel shows wedge, inverse wedge, and crescent morphologies during the storm, and becomes discontinuous when the IMF is weakly southward. The SAPS mean latitude has a correlation coefficient of 0.77 with the Dst index. The mean latitude moves equatorward and the flow channel broadens in the storm main phase. The simulation results are consistent with observational studies. They also illustrate the global distributions and highly dynamic behaviors of SAPS that are not readily apparent from observation data.

Keywords: SAPS, Magnetosphere-Ionosphere-Thermosphere coupling, LFM-TIEGCM-RCM

©2019. Japan Geoscience Union. All Right Reserved.

Westward turning motions of nighttime medium-scale traveling ionospheric disturbances (MSTIDs) at the equatorward side of the dusk side auroral oval associated with auroral brightening

*Sneha Yadav[1,2], Kazuo Shiokawa[1], Shin-ichiro Oyama[1,3,4], Yuichi Otsuka[1]

1. ISEE, Nagoya University, Nagoya, Japan, 2. SPL, VSSC, India, 3. Ionosphere Research Unit, University of Oulu, Oulu, Finland, 4. NIPR, Tachikawa, Japan

The characteristics of high-latitude nighttime medium-scale traveling ionospheric disturbances (MSTIDs) have not been well investigated using all-sky imagers because of the hindrance caused by the bright aurora. The limited results on the propagation characteristics of MSTIDs over high-latitudes hindered the progress in our understanding on these dynamical structure. In a case study carried out by Shiokawa et al. (JGR, 2012), an event of oscillating MSTIDs was reported over Tromsø (69.6˚N, 19.2˚E; corrected geomagnetic latitude: 66.6˚N), which was observed to be associated with auroral brightening. However, after this case study, which comprised of only one event, no observations showing oscillating motion of MSTIDs have been reported till date. In this study, for the first time, the comprehensive investigation on the westward turning of the MSTIDs in the equatorward side of the dusk side auroral oval has been performed. The all-sky imaging data of 630.0 nm airglow emissions during 2010-2018 are used to study the motions of MSTIDs over Tromsø. The results indicate that the nighttime MSTIDs primarily exhibit eastward motion under quiet magnetic conditions but turned in the westward direction during the active geomagnetic conditions. The turning of MSTIDs in the westward direction were invariably associated with the auroral brightening observed at the poleward edge of the all-sky image and localized magnetic field perturbations observed by ground-based magnetometers at Tromsø. The interesting aspect of the observations is the fact that these westward moving MSTIDs again turned in the eastward direction when the geomagnetic disturbance ceases. The SuperDARN (Super Dual Auroral Radar Network) convection maps revealed that the location of Tromsø was inside/outside the convection cell region during the time of appearance of westward/eastward moving MSTIDs. The Doppler shift measurement of the 630-nm airglow by a Fabry-Perot interferometer at Tromsø showed that northeastward winds were predominant during the appearance of eastward moving MSTIDs. The cause of the observed MSTIDs remains in question as they might either be triggered by atmospheric gravity waves or by Perkins instability. These experimental evidences suggest that the MSTIDs tend to move eastward in accordance with the background F-region dynamo electric field, but show westward motion under the influence of electric field associated with auroral activities in the dusk side of two-cell convection pattern.

Keywords: MSTIDs, Auroral oval, Airglow

©2019. Japan Geoscience Union. All Right Reserved.

[E] ポスター発表 | セッション記号 P (宇宙惑星科学)：P-EM 太陽地球系科学・宇宙電磁気学・宇宙環境

2019年5月27日(月) 17:15 ~ 18:30 | ポスター会場 幕張メッセ国際展示場 8ホール_4

[P-EM10] Multi-scale Coupling in the Magnetosphere-Ionosphere-Thermosphere System

コンビーナ:Yue Deng(University of Texas at Arlington)、Toshi Nishimura(Boston University)、Liu Huixin(九州大学理学研究院地球惑星科学専攻 九州大学宙空環境研究センター)、Yanshi Huang(Harbin Institute of Technology, Shenzhen)

Determining the effects of energy deposition and transport, and momentum exchange across different spatial and temporal scales is an important objective in the M-I-T system, due to the clear evidence of multi-scale forcing. Coupling over multiple scales is also a critical challenge since observational and modeling methodologies for bridging different scales do not presently exist. This session solicits presentations on a wide range of coupling processes in the high-latitude M-I-T system from global to small-scale processes and related solar wind forcing. Relevant topics include (but are not limited to) (1) density structures and temperature gradients (polar cap, cusp, plume, trough, irregularities); (2) convection (flow channels, SAPS) and FAC; (3) energy transfer and deposition by precipitation and ULF waves, conductivity, aurora, and heating; and (4) coupling and feedback into the magnetosphere. Discussions of relevant multi-scale observations by means of multiple instruments, including space and ground-based, modeling and data science are encouraged.

[PEM10-P01] 相対論的電子降り込みに対する南北両半球大気のレスポンス

*田中 良昌[1,13,14]、西山 尚典[1,14]、門倉 昭[1,13,14]、尾崎 光紀[2]、三好 由純[3]、大山 伸一郎[3,15]、片岡 龍峰[1,14]、堤 雅基[1,14]、西村 耕司[1,13,14]、佐藤 薫[4]、笠原 禎也[2]、熊本 篤志[5]、土屋 史紀[5]、吹澤 瑞貴[5]、疋島 充[6]、松田 昇也[6]、松岡 彩子[6]、篠原 育[6]、能勢 正仁[3]、長妻 努[7]、篠原 学[8]、藤本 晶子[9]、寺本 万里子[3]、野村 麗子[10]、行松 彰[1,14]、細川 敬祐[11]、小路 真史[3]、Ralph Latteck[12] (1.国立極地研究所、2.金沢大学理工研究域、3.名古屋大学宇宙地球環境研究所、4.東京大学大学院理学系研究科、5.東北大学大学院理学研究科、6.宇宙航空研究開発機構宇宙科学研究所、7.情報通信研究機構、8.鹿児島工業高等専門学校、9.九州工業大学、10.国立天文台、11.電気通信大学大学院情報理工学研究科、12.Leibniz-Institute of Atmospheric Physics e.V. at the University Rostock, Germany、13.情報・システム研究機構 データサイエンス共同利用基盤施設 極域環境データサイエンスセンター、14.総合研究大学院大学、15.University of Oulu, Finland)

[PEM10-P02] Comparison of precipitating particle energy of proton aurora at geomagnetic conjugate points

*田口 真[1]、西島 樹[1]、門倉 昭[2] (1.立教大学、2.情報・システム研究機構)

[PEM10-P03] A regularized deep convolutional general adversarial network (R-DCGAN) for total electron content map completion

*Mingwu Jin[1]、Zhou Chen[2,3]、Yue Deng[1]、Yang Pan[1]、Jin-Song Wang[2] (1.University of Texas at Arlington、2.Institute of Space Science and Technology, Nanchang University, Nanchang, China、3.Key Laboratory of Space Weather, National Center for Space Weather, China Meteorological Administration, Beijing, China)

[PEM10-P04] A long-lasting auroral bright spot around magnetic north pole: Is it the evidence of stable magnetic reconnection?

*Qing-He Zhang[1]、Guo-Cheng Shen[1]、Yong-Liang Zhang[2]、Kjellmar Oksavik[3]、Michael Lockwood[4]、Zan-Yang Xing[1]、Yu-Zhang Ma[1] (1.Institute of Space Sciences, Shandong University, Weihai, China、2.The Johns Hopkins University Applied Physics Laboratory, Laurel, Maryland, USA、3.Birkeland Centre for Space Science, University of Bergen, Bergen, Norway、4.Department of Meteorology, University of Reading, Earley Gate, Post Office Box 243, RG6 6BB, UK.)

[PEM10-P05] Statistical study of the relationship between ion upflow and field-aligned current in the topside ionosphere for both hemispheres during disturbed and quiet times

Shan-Yu Zhou[1]、*Qing-He Zhang[1]、P. T. Jayachandran[2]、Kjellmar Oksavik[3]、Larry Lyons[4]、Zan-Yang Xing[1]、Yu-Zhang Ma[1]、Marc Hairston[5]、Yong Wang[1] (1.Institute of Space Sciences, Shandong University, Weihai, China、2.Physics Department, University of New Brunswick, Fredericton, New Brunswick,

Canada、3.Birkeland Centre for Space Science, University of Bergen, Bergen, Norway、4.Department of Atmospheric and Oceanic Sciences, University of California, Los Angeles, California, USA、5.William B. Hanson Center for Space Sciences, University of Texas at Dallas, Richardson, Texas, USA)

[PEM10-P06] SAPS in the 2013 March 17 Storm Event: Initial Results from the Coupled Magnetosphere-Ionosphere-Thermosphere Model

*Dong Lin[1,2]、Wenbin Wang[2]、Wayne Scales[1]、Kevin Pham[2]、Jing Liu[2]、Binzheng Zhang[2]、Viacheslav Merkin[3]、Xueling Shi[1] (1.Virginia Tech、2.High Altitude Observatory, NCAR、3.APL, John Hopkins Univ.)

[PEM10-P07] **Westward turning motions of nighttime medium-scale traveling ionospheric disturbances (MSTIDs) at the equatorward side of the dusk side auroral oval associated with auroral brightening**

*Sneha Yadav[1,2]、Kazuo Shiokawa[1]、Shin-ichiro Oyama[1,3,4]、Yuichi Otsuka[1] (1.ISEE, Nagoya University, Nagoya, Japan、2.SPL, VSSC, India、3.Ionosphere Research Unit, University of Oulu, Oulu, Finland、4.NIPR, Tachikawa, Japan)

相対論的電子降り込みに対する南北両半球大気のレスポンス
Atmospheric responses in both hemispheres to relativistic electron precipitation

*田中 良昌[1,13,14]、西山 尚典[1,14]、門倉 昭[1,13,14]、尾崎 光紀[2]、三好 由純[3]、大山 伸一郎[3,15]、片岡 龍峰[1,14]、堤 雅基[1,14]、西村 耕司[1,13,14]、佐藤 薫[4]、笠原 禎也[2]、熊本 篤志[5]、土屋 史紀[5]、吹澤 瑞貴[5]、疋島 充[6]、松田 昇也[6]、松岡 彩子[6]、篠原 育[6]、能勢 正仁[3]、長妻 努[7]、篠原 学[8]、藤本 晶子[9]、寺本 万里子[3]、野村 麗子[10]、行松 彰[1,14]、細川 敬祐[11]、小路 真史[3]、Ralph Latteck[12]
*Yoshimasa Tanaka[1,13,14], Takanori Nishiyama[1,14], Akira Kadokura[1,13,14], Mitsunori Ozaki[2], Yoshizumi Miyoshi[3], Shin-ichiro Oyama[3,15], Ryuho Kataoka[1,14], Masaki Tsutsumi[1,14], Koji Nishimura[1,13,14], Kaoru Sato[4], Yoshiya Kasahara[2], Atsushi Kumamoto[5], Fuminori Tsuchiya[5], Mizuki Fukizawa[5], Mitsuru Hikishima[6], Shoya Matsuda[6], Ayako Matsuoka[6], Iku Shinohara[6], Masahito Nose[3], Tsutomu Nagatsuma[7], Manabu Shinohara[8], Akiko Fujimoto[9], Mariko Teramoto[3], Reiko Nomura[10], Akira Sessai Yukimatu[1,14], Keisuke Hosokawa[11], Masafumi Shoji[3], Ralph Latteck[12]

1. 国立極地研究所、2. 金沢大学理工研究域、3. 名古屋大学宇宙地球環境研究所、4. 東京大学大学院理学系研究科、5. 東北大学大学院理学研究科、6. 宇宙航空研究開発機構宇宙科学研究所、7. 情報通信研究機構、8. 鹿児島工業高等専門学校、9. 九州工業大学、10. 国立天文台、11. 電気通信大学大学院情報理工学研究科、12. Leibniz-Institute of Atmospheric Physics e.V. at the University Rostock, Germany、13. 情報・システム研究機構 データサイエンス共同利用基盤施設 極域環境データサイエンスセンター、14. 総合研究大学院大学、15. University of Oulu, Finland
1. National Institute of Polar Research, 2. Institute of Science and Engineering, Kanazawa University, 3. Institute for Space-Earth Environmental Research, Nagoya University, 4. Graduate School of Science, The University of Tokyo, 5. Graduate School of Science, Tohoku University, 6. Japan aerospace exploration agency, Institute of space and astronautical science, 7. National Institute of Information and Communications Technology, 8. Kagoshima National College of Technology, 9. Kyushu Institute of Technology, 10. National Observatory of Japan, 11. Department of Communication Engineering and Informatics, University of Electro-Communications, 12. Leibniz-Institute of Atmospheric Physics e.V. at the University Rostock, Germany, 13. Polar Environment Data Science Center, Joint-Support Center for Data Science Research, Research Organization of Information and Systems, 14. The Graduate University for Advanced Studies (SOKENDAI), 15. University of Oulu, Finland

Relativistic electron precipitation (REP) in the polar atmosphere has been paid attention to because it changes atmospheric composition, causing ozone depletion after migrating to the lower altitude during polar winter. A plausible mechanism for REP is the interaction with magnetospheric plasma waves, such as electromagnetic ion cyclotron (EMIC) waves and whistler-mode chorus waves. Previous studies have already shown that EMIC waves can effectively drive REP, however, observational evidence that chorus waves can drive REP was lacking. In this study we present direct comparison between magnetospheric plasma waves and polar mesosphere winter echoes (PMWE) simultaneously observed with the Arase satellite and high-power Mesosphere, Stratosphere and Troposphere (MST) radars in both hemispheres, PANSY and MAARSY. PMWE can be related to the ionization in the mesosphere due to REP. The PMWE were observed at 03-07 UT on March 21, 2017 during the passage of corotating interaction region (CIR), during which the Arase footprints were close to Syowa Station (SYO; −69.00S, 39.58E), Antarctica, and Husafell (HUS; 65.67N, −21.03E), Iceland.
The observational results are summarized as follows. (1) EMIC waves and whistler-mode chorus waves were observed by Arase near the equatorial magnetosphere during 02:30-04:45 UT and 04:45-07:00 UT, respectively. (2) PMWE were detected with both the MAARSY radar at Andøya (AND; 69.30N, 16.04E), Norway, and the PANSY radar at SYO, Antarctica, during 04:45-07:00 UT, which was the recovery phase of an isolated substorm. We believe this is the first time PMWE have been observed in both hemispheres

©2019. Japan Geoscience Union. All Right Reserved.

at exactly the same time. (3) During 04:45-07:00 UT, the temporal variation of the chorus wave power was similar to those of the PMWE power in the both hemispheres. (4) The PMWE observed at SYO during 03:00-04:00 UT before the substorm onset was consistent with the occurrence of the EMIC waves. The item (2) shows direct evidence that chorus waves during the substorm recovery phase cause REP. We estimated the resonance energy of electrons interacting with the observed LBC waves, however, the estimated energy was too low to cause PMWE at an altitude lower than 70 km. However, we found that the resonance energy becomes greater than 1 MeV, if LBC waves propagate to the magnetic latitude greater than 30 degrees and resonate with energetic electrons there. As for item (4), the PMWE observed at SYO during 03:00-04:00 can be related to wave-particle interaction with EMIC waves, which may be generated inside the plasmapause by ring-current hot ions with temperature anisotropy. This anisotropy was caused by magnetospheric compression due to increasing solar wind dynamic pressure during 01:00–06:00 UT just after the arrival of the CIR. Since CIRs are main sources of geomagnetic disturbances during the declining phase of the solar cycle and solar minimum, this event is not rare but rather a common atmospheric response caused by interaction between recurrent large-scale solar wind structures and geospace.

キーワード：極域中間圏冬季エコー、あらせ衛星、PANSYレーダー、MAARSYレーダー、相対論的電子降り込み、磁気圏プラズマ波動
Keywords: Polar Mesosphere Winter Echoes, Arase satellite, PANSY radar, MAARSY radar, relativistic electron precipitation, magnetospheric plasma waves

©2019. Japan Geoscience Union. All Right Reserved.

Comparison of precipitating particle energy of proton aurora at geomagnetic conjugate points

*田口 真[1]、西島 樹[1]、門倉 昭[2]
*Makoto Taguchi[1], Tatsuki Nishijima[1], Akira Kadokura[2]

1. 立教大学、2. 情報・システム研究機構
1. Rikkyo University, 2. Research Organization of Information and Systems

It is expected that mirror images of aurora are observed at geomagnetic conjugate points in the northern and southern auroral zones connected by a geomagnetic field line. However, geomagnetic conjugate auroras often show non-conjugacy, which reflects north-south asymmetry of the solar wind, the magnetosphere and the ionospheres. In other words acceleration mechanism of auroral particles may be studied by comparing aurora simultaneously occurring at geomagnetic conjugate points. A hydrogen Balmer beta emission at the wavelength of 486.1 nm which is the brightest among the proton auroral lines was observed at a pair of geomagnetic conjugate points to compare precipitating particle energy. Two identical Proton Auroral Specrographs (PASs) which obtain auroral spectra along a geomagnetic meridian at a rate of 1 image/min were installed at Tjornes in Iceland and Syowa Station in Antarctica. Data obtained during a period from September 4, 2018 to October 9, 2018 were analyzed to derive an average kinetic energy of precipitating protons along a local geomagnetic field line from a Doppler shift of the H beta line. As a result we are succeeded in simultaneous observations of proton auroras at both conjugate points in 5 nights on September 4, 5, 6, 7 , and 10. The average energies of precipitating protons range from 0 keV to 7 keV, and sometimes show a periodical variation with a period of 4 - 5 min. Conjugacy of precipitating particle energy will be discussed in the presentation.

©2019. Japan Geoscience Union. All Right Reserved.

A regularized deep convolutional general adversarial network (R-DCGAN) for total electron content map completion

*Mingwu Jin[1], Zhou Chen[2,3], Yue Deng[1], Yang Pan[1], Jin-Song Wang[2]

1. University of Texas at Arlington, 2. Institute of Space Science and Technology, Nanchang University, Nanchang, China, 3. Key Laboratory of Space Weather, National Center for Space Weather, China Meteorological Administration, Beijing, China

Observations with a complete global coverage are important for space physics research and applications. However, due to the technical limitations and costs, such a complete global coverage is often unavailable. Thus, data filling algorithms are often pursued to fill missing data gaps to create a global map from the incomplete data. In this work, a novel deep learning algorithm, regularized deep convolutional generative adversarial network (R-DCGAN), is developed by adding an extra discriminator to the conventional DCGAN to fill the missing data of total electron content (TEC) map images. R-DCGAN incorporates the knowledge from reference TEC maps of the International Global Navigation Satellite Systems Service Ionosphere Working Group to achieve much better TEC map completion performance than the conventional DCGAN as demonstrated by both synthetic and real data. The R-DCGAN framework can be extended to other fields of space sciences to address the missing observation data issues.

Keywords: Deep learning method, TEC , map completion

©2019. Japan Geoscience Union. All Right Reserved.

A long-lasting auroral bright spot around magnetic north pole: Is it the evidence of stable magnetic reconnection?

*Qing-He Zhang[1], Guo-Cheng Shen[1], Yong-Liang Zhang[2], Kjellmar Oksavik[3], Michael Lockwood[4], Zan-Yang Xing[1], Yu-Zhang Ma[1]

1. Institute of Space Sciences, Shandong University, Weihai, China, 2. The Johns Hopkins University Applied Physics Laboratory, Laurel, Maryland, USA, 3. Birkeland Centre for Space Science, University of Bergen, Bergen, Norway, 4. Department of Meteorology, University of Reading, Earley Gate, Post Office Box 243, RG6 6BB, UK.

An intense and large auroral bright spot appears around the magnetic north pole observed by the Special Sensor Ultraviolet Spectrographic Imager (SSUSI) on board four different Defense Meteorological Satellite Program (DMSP) satellites during long time northward IMF conditions. The bright spot is even brighter than aurora in the auroral oval which is about 5-10° magnetic latitude equatorward of the bright spot. The bright spot is lasting about 8 hours, and sometimes appears as a cyclone-shape with a clockwise rotation. The DMSP in situ plasma observations suggest that the bright spot is clear associated with electron invert-V acceleration with 10s keV energy electron precipitations around the center regions and 1s keV energy electron precipitations around the egde regions. There are also strong flow shears between the two sides of the bright spot: strong sunward flows on the duskside and antisunward flows on the dawnside. These types of plasma should come from the high-latitude lobe region of the magnetotail due to the high-latitude lobe magnetic reconnections. Is it the evidence of stable lobe reconnection during long time northward IMF conditions? The detail and further analysis should be pursued in the following studies.

Keywords: Auroral bright spot, Magnetosphere-ionosphere coupling, High-latitude lobe magnetic reconnection, Stable reconnection

©2019. Japan Geoscience Union. All Right Reserved.

Statistical study of the relationship between ion upflow and field-aligned current in the topside ionosphere for both hemispheres during disturbed and quiet times

Shan-Yu Zhou[1], *Qing-He Zhang[1], P. T. Jayachandran[2], Kjellmar Oksavik[3], Larry Lyons[4], Zan-Yang Xing[1], Yu-Zhang Ma[1], Marc Hairston[5], Yong Wang[1]

1. Institute of Space Sciences, Shandong University, Weihai, China, 2. Physics Department, University of New Brunswick, Fredericton, New Brunswick, Canada, 3. Birkeland Centre for Space Science, University of Bergen, Bergen, Norway, 4. Department of Atmospheric and Oceanic Sciences, University of California, Los Angeles, California, USA, 5. William B. Hanson Center for Space Sciences, University of Texas at Dallas, Richardson, Texas, USA

A statistical study of ion upflow and field-aligned currents (FACs) has been performed in the topside ionosphere of both hemispheres for magnetic quiet and disturbed times by using DMSP satellite observations from 2010-2013. Distributions in MLT/MLAT reveal that ion upflow shows a dawn-dusk asymmetry distribution that corresponds well with the region 1 field-aligned currents. In addition, there are highest occurrence regions near noon and within the near midnight auroral disturbance area. These correspond to cusp and nightside dynamical processes, respectively. Both the ion upflow occurrence and FAC regions expand equatorward to a wider area during disturbed times.

Keywords: Ion upflows, Field-aligned current, Magnetosphere-ionosphere coupling

©2019. Japan Geoscience Union. All Right Reserved.

SAPS in the 2013 March 17 Storm Event: Initial Results from the Coupled Magnetosphere-Ionosphere-Thermosphere Model

*Dong Lin[1,2], Wenbin Wang[2], Wayne Scales[1], Kevin Pham[2], Jing Liu[2], Binzheng Zhang[2], Viacheslav Merkin[3], Xueling Shi[1]

1. Virginia Tech, 2. High Altitude Observatory, NCAR, 3. APL, John Hopkins Univ.

Subauroral polarization stream (SAPS) are latitudinally narrow flow channels of large westward plasma drifts in the subauroral ionosphere. In this study, the global structure and dynamic evolution of SAPS are investigated by using the National Center for Atmospheric Research (NCAR) Coupled Magnetosphere-Ionosphere-Thermosphere (CMIT) model with Ring Current extension, namely the LFM-TIEGCM-RCM (LTR) model, to simulate the 2013 St. Patrick's Day storm event. This is the first time that the global distribution and temporal evolution of SAPS are investigated using first-principle models. The model shows a strong westward ion drift channel formed equatorward of the auroral electron precipitation boundary on the duskside, which is identified as the SAPS structure. The simulated ion drift velocity and auroral electron precipitation sampled along the trajectory of the DMSP F18 satellite are in good agreement with the satellite measurements. SAPS initiate in the pre-dusk sector when the interplanetary magnetic field (IMF) turns southward. SAPS latitude generally decreases with magnetic local time (MLT) from dusk to midnight. The SAPS channel shows wedge, inverse wedge, and crescent morphologies during the storm, and becomes discontinuous when the IMF is weakly southward. The SAPS mean latitude has a correlation coefficient of 0.77 with the Dst index. The mean latitude moves equatorward and the flow channel broadens in the storm main phase. The simulation results are consistent with observational studies. They also illustrate the global distributions and highly dynamic behaviors of SAPS that are not readily apparent from observation data.

Keywords: SAPS, Magnetosphere-Ionosphere-Thermosphere coupling, LFM-TIEGCM-RCM

©2019. Japan Geoscience Union. All Right Reserved.

Westward turning motions of nighttime medium-scale traveling ionospheric disturbances (MSTIDs) at the equatorward side of the dusk side auroral oval associated with auroral brightening

*Sneha Yadav[1,2], Kazuo Shiokawa[1], Shin-ichiro Oyama[1,3,4], Yuichi Otsuka[1]

1. ISEE, Nagoya University, Nagoya, Japan, 2. SPL, VSSC, India, 3. Ionosphere Research Unit, University of Oulu, Oulu, Finland, 4. NIPR, Tachikawa, Japan

The characteristics of high-latitude nighttime medium-scale traveling ionospheric disturbances (MSTIDs) have not been well investigated using all-sky imagers because of the hindrance caused by the bright aurora. The limited results on the propagation characteristics of MSTIDs over high-latitudes hindered the progress in our understanding on these dynamical structure. In a case study carried out by Shiokawa et al. (JGR, 2012), an event of oscillating MSTIDs was reported over Tromsø (69.6˚N, 19.2˚E; corrected geomagnetic latitude: 66.6˚N), which was observed to be associated with auroral brightening. However, after this case study, which comprised of only one event, no observations showing oscillating motion of MSTIDs have been reported till date. In this study, for the first time, the comprehensive investigation on the westward turning of the MSTIDs in the equatorward side of the dusk side auroral oval has been performed. The all-sky imaging data of 630.0 nm airglow emissions during 2010-2018 are used to study the motions of MSTIDs over Tromsø. The results indicate that the nighttime MSTIDs primarily exhibit eastward motion under quiet magnetic conditions but turned in the westward direction during the active geomagnetic conditions. The turning of MSTIDs in the westward direction were invariably associated with the auroral brightening observed at the poleward edge of the all-sky image and localized magnetic field perturbations observed by ground-based magnetometers at Tromsø. The interesting aspect of the observations is the fact that these westward moving MSTIDs again turned in the eastward direction when the geomagnetic disturbance ceases. The SuperDARN (Super Dual Auroral Radar Network) convection maps revealed that the location of Tromsø was inside/outside the convection cell region during the time of appearance of westward/eastward moving MSTIDs. The Doppler shift measurement of the 630-nm airglow by a Fabry-Perot interferometer at Tromsø showed that northeastward winds were predominant during the appearance of eastward moving MSTIDs. The cause of the observed MSTIDs remains in question as they might either be triggered by atmospheric gravity waves or by Perkins instability. These experimental evidences suggest that the MSTIDs tend to move eastward in accordance with the background F-region dynamo electric field, but show westward motion under the influence of electric field associated with auroral activities in the dusk side of two-cell convection pattern.

Keywords: MSTIDs, Auroral oval, Airglow

©2019. Japan Geoscience Union. All Right Reserved.

[E] ポスター発表 | セッション記号 A (大気水圏科学)：A-OS 海洋科学・海洋環境

2019年5月27日(月) 15:30 ~ 17:00 | ポスター会場 幕張メッセ国際展示場 8ホール_3

[A-OS12] Marine ecosystems and biogeochemical cycles: theory, observation and modeling

コンビーナ:伊藤 進一(東京大学大気海洋研究所)、平田 貴文(北海道大学地球環境科学研究院)、Enrique N Curchitser(Rutgers University New Brunswick)、Eileen E Hofmann(Old Dominion University)

The ocean accounts for about 50% of global net primary production. This production is significant for carbon cycling and ecosystem functioning, and is related directly or indirectly to a variety of climatic and ecological phenomena. The responses to natural and anthropogenic environmental stressors that influence marine production and diversity can cause perturbations to marine ecosystems that alter trophic dependencies and interactions among organisms at a range of space and time scales. Quantification of the principal mechanisms driving spatio-temporal variability of marine ecosystem remains to be done, especially in terms of evaluation of uncertainty in responses. As a result, evaluating vulnerability of marine ecosystems to environmental change requires systematic and holistic approaches that integrate physics to ecology and are based in observations and modelling. In addition, expectations to deliver these science to public society is raising. This session aims to provide a venue for not only discussing recent advances in understanding marine biogeochemical cycles, ecosystems and their interactions, but also networking with a variety of people to seed new ideas in marine ecological research. Observational, modeling and conceptual studies, including technological development and operational applications, that consider linkages among biogeochemical and ecosystem processes, biodiversity, and the effects of multiple stressors from molecular to planetary scales are encouraged.

[AOS12-P01] 日本海の生態系に対する対馬海峡を経由する栄養塩輸送の影響

*柴野 良太[1]、森本 昭彦[1]、髙山 勝巳[2]、滝川 哲太郎[3]、伊藤 雅[4] (1.愛媛大学沿岸環境科学研究センター、2.九州大学応用力学研究所、3.長崎大学大学院水産・環境科学総合研究科、4.水産研究・教育機構日本海区水産研究所)

[AOS12-P02] Revisiting vertical variations in stoichiometry during oceanic organic matter decomposition

*重光 雅仁[1]、青山 道夫[1]、土居 知将[1]、横川 太一[1]、村田 昌彦[1] (1.国立研究開発法人　海洋研究開発機構)

[AOS12-P03] Reproduction of iron-rich intermediate water in the Sea of Okhotsk by high resolution biogeochemical model.

*西川 はつみ[1]、三寺 史夫[1]、浩志 吉成[2]、拓也 中野渡[3]、中村 知裕[1]、内本 圭亮[4]、羽角 博康[5] (1.北海道大学低温科学研究所、2.国立環境研究所、3.北海道区水産研究所、4.地球環境産業技術研究機構、5.東京大学　大気海洋研究所)

[AOS12-P04] The global oceanic iron distribution estimated by data assimilation approach

*土居 知将[1]、長船 哲史[1]、増田 周平[1]、小畑 元[2]、三角 和弘[3]、西岡 純[4] (1.海洋研究開発機構、2.東京大学、3.電力中央研究所、4.北海道大学)

[AOS12-P05] A high-resolution multi-purpose particle tracking framework for coastal areas near Japan

*松村 義正[1]、桂 将太[1]、黒木 聖夫[2]、中野 英之[3]、山岸 孝輝[4] (1.東京大学 大気海洋研究所、2.海洋研究開発機構、3.気象庁気象研究所、4.高度情報科学技術研究機構)

[AOS12-P06] Numerical study on seasonality of ocean litters collected at the Dongsha Island in the northern South China Sea

*Yi-Chia Hsin[1]、Chia-Ying Ko[2]、Ming-Shiou Jeng[3] (1.Research Center for Environmental Changes, Academia Sinica、2.Institute of Fisheries Science, National Taiwan University、3.Biodiversity Research Center, Academia Sinica)

[AOS12-P07] A key spot and timing to monitor chlorophyll-a in the Kuroshio western boundary current

*平田 貴文[1] (1.北海道大学地球環境科学研究院)

[AOS12-P08] **Impacts of cyclonic eddies on phytoplankton biomass and phenology in the Kuroshio Extension region**

*Eko Siswanto[1]、Yoshikazu Sasai[1] (1.Japan Agency for Marine-Earth Science and Technology)

[AOS12-P09] Diagnostic estimation and uncertainties of nutrient limitation of phytoplankton growth in Michaelis-Menten functional form

*橋岡 豪人[1]、相田 真希[1] (1.国立研究開発法人 海洋研究開発機構)

[AOS12-P10] Modeling productivity in lower trophic levels in Otsuchi Bay, northeast of Japan, using a nested OGCM with a biogeochemical component

*坂本 天[1]、浦川 昇吾[2]、伊藤 幸彦[1]、羽角 博康[1]、田中 潔[1] (1.東京大学大気海洋研究所、2.気象庁気象研究所)

[AOS12-P11] Change in lower trophic level ecosystems to decadal scale variation of climate system in the North Pacific Ocean

*相田 真希[1]、田所 和明[2]、小室 芳樹[3]、橋岡 豪人[1]、原田 尚美[1] (1.国立研究開発法人 海洋研究開発機構 地球環境観測研究開発センター、2.国立研究開発法人 水産研究・教育機構　東北区水産研究所、3.国立研究開発法人 海洋研究開発機構　北極環境変動総合研究センター)

[AOS12-P12] Estimation of experienced environment of jack mackerel in the East China Sea

*樋口 富彦[1]、高橋 素光[2]、白井 厚太朗[1]、伊藤 進一[1] (1.東京大学大気海洋研究所、2.国立研究開発法人 水産研究・教育機構 西海区水産研究所)

日本海の生態系に対する対馬海峡を経由する栄養塩輸送の影響
Impact of the nutrient transport through the Tsushima Strait on the ecosystem in the Japan Sea

*柴野 良太[1]、森本 昭彦[1]、髙山 勝巳[2]、滝川 哲太郎[3]、伊藤 雅[4]
*Ryota Shibano[1], Akihiko Morimoto[1], Katsumi Takayama[2], Tetsutaro Takikawa[3], Masashi Ito[4]

1. 愛媛大学沿岸環境科学研究センター、2. 九州大学応用力学研究所、3. 長崎大学大学院水産・環境科学総合研究科、4. 水産研究・教育機構日本海区水産研究所
1. Center for Marine Environmental Studies, Ehime University, 2. Research Institute for Applied Mechanics, Kyushu University, 3. Graduate School of Fisheries and Environmental Sciences, Nagasaki University, 4. Fisheries Oceanography Department, Japan Sea National Fisheries Research Institute

日本海は対馬海峡をはじめとする狭く浅いいくつかの海峡でのみ外海と接続する半閉鎖海域である。対馬海峡を介し供給される栄養塩は東シナ海を介して供給され、それらは日本海沿岸部などの生態系に対し強い影響力をもつ。その起源は海洋からの供給源としては黒潮・台湾海峡・黄海からもたらされるものが多くあり、海洋外からの供給源としては長江・黄河・ダストによるものがある。我々は2005年から2017年までの対馬海峡における船舶観測データから、同海域における流量変動・栄養塩濃度などの経年変動を調べた。その結果、対馬海峡を通過する栄養塩輸送量は±50%程度増減していることがわかった。近年の報告から、経年変動で栄養塩輸送量が変動している時、前述の起源の寄与率も変動していることが指摘されている(Morimoto et al., 2012)。

我々は観測事実に基づいた領域海洋モデルに生態系モデルを統合した数値モデルを開発し、日本海および東シナ海におけるこれらの栄養塩動態について定量的に評価した。また黒潮・台湾海峡・長江・黄河・ダスト・底層(黄海)由来の各起源についても各輸送量と寄与率について定量的に評価することで、経年変動に伴いどのような時空間変動があらわれるかについて評価した。

キーワード：対馬暖流、栄養塩輸送、日本海
Keywords: Tsushima Warm Current, nutrient transport, the Sea of Japan

©2019. Japan Geoscience Union. All Right Reserved.

Revisiting vertical variations in stoichiometry during oceanic organic matter decomposition

Revisiting vertical variations in stoichiometry during oceanic organic matter decomposition

*重光 雅仁[1]、青山 道夫[1]、土居 知将[1]、横川 太一[1]、村田 昌彦[1]
*Masahito Shigemitsu[1], Michio Aoyama[1], Toshimasa Doi[1], Taichi Yokokawa[1], Akihiko Murata[1]

1. 国立研究開発法人　海洋研究開発機構
1. Japan Agency for Marine-Earth Science and Technology

Using the new global nutrient data set, we re-evaluate basin-wide stoichiometric ratios of remineralization estimated by Anderson and Sarmiento (1994) (hereinafter, AS94). For the same latitudinal ranges of the Atlantic, Indian and Pacific Oceans as in AS94, we construct one or two end-member mixing models on 14 neutral surfaces and estimate the stoichiometric ratios with a probabilistic approach. Unlike the results of AS94, significant vertical variations in the stoichiometry are found in the Atlantic and Pacific, while relatively constant stoichiometry with depth is found in the Indian Ocean, similar to AS94. The decreases in the C/P and $-O_2$/P ratios with depth in the Atlantic could be caused via dark DIC fixation by chemoautotrophs in the deep waters. In the Pacific, changes in organic matter composition with depth would be the most important factor in the increases in stoichiometry with depth. In all the basins, the N/P ratios are probably affected by benthic denitrification, as in AS94. The P/C/-O_2ratios (mean and $5^{th}$to 95^{th}percentile) are estimated to be 1/111(97 to 129)/155(149 to 163) in the depths below 2000 m of the Indian and Pacific Oceans, where DIC fixation and vertical change in organic matter composition have little influence on the stoichiometry estimates. We suggest that chemoautotrophic DIC fixation and the effect of change in organic matter composition with depth on the stoichiometry in waters above 2000 m should be considered for large-scale biogeochemical modeling and estimation of oceanic uptake of anthropogenic carbon from observational data.

キーワード：栄養塩、化学量論比、有機物分解
Keywords: nutrients, stoichiometric ratios, remineralization of organic matter

©2019. Japan Geoscience Union. All Right Reserved.

Reproduction of iron-rich intermediate water in the Sea of Okhotsk by high resolution biogeochemical model.

*西川 はつみ[1]、三寺 史夫[1]、浩志 吉成[2]、拓也 中野渡[3]、中村 知裕[1]、内本 圭亮[4]、羽角 博康[5]
*Hatsumi Nishikawa[1], Humio Mitsudera[1], Hiroshi Yoshinari[2], Takuya Nakanowatari[3], Tomohiro Nakamura[1], Keisuke Uchimoto[4], Hiroyasu Hasumi[5]

1. 北海道大学　低温科学研究所、2. 国立環境研究所、3. 北海道区水産研究所、4. 地球環境産業技術研究機構、5. 東京大学大気海洋研究所
1. Institute of Low Temperature Science, Hokkaido University, 2. National Institute for Environmental Studies, 3. Tohoku National Fisheries Research Institute, Japan Fisheries Research and Education Agency, 4. Research Institute of Innovative Technology for the Earth, 5. Atmosphere and Ocean Research Institute, University of Tokyo

Recent observation studies suggest that iron supply from sediment on the northwest continental shelf the Okhotsk Sea plays an important role for the subarctic primary production (e.g. Nishioka et al., 2013). Dense shelf water (DSW) takes up iron from sediment, thereby transporting iron into the Okhotsk Sea intermediate water. However, observational data is still limited.

To clarify detailed structure of iron circulation in the North Pacific, we develop the high-resolution biogeochemical model. However, our model did not reproduce high iron concentration in the intermediate water the Sea of Okhotsk. We use biogeochemical model developed by Parekh et al. (2005). They set the value of total ligand concentration to constant value in all place. Recent observations, however, suggest that ligand concentration varies with sea area and depth. Then, we conducted a new experiment with the ligand concentration changed in the vertical direction. The iron concentration intermediate water of the new experiment becaame higher than before.

キーワード：高解像度モデル、中層水鉄、リガンド濃度
Keywords: High-resolution modeling, Iron-rich intermediate water, Ligand concentration

©2019. Japan Geoscience Union. All Right Reserved.

The global oceanic iron distribution estimated by data assimilation approach

*土居 知将[1]、長船 哲史[1]、増田 周平[1]、小畑 元[2]、三角 和弘[3]、西岡 純[4]
*Doi Toshimasa[1], Satoshi Osafune[1], Shuhei Masuda[1], Hajime Obata[2], Kazuhiro Misumi[3], Jun Nishioka[4]

1. 海洋研究開発機構、2. 東京大学、3. 電力中央研究所、4. 北海道大学
1. Japan Agency for Marine-Earth Science and Technology, 2. The University of Tokyo, 3. Central Research Institute of Electric Power Industry, 4. Hokkaido University

Since distribution of oceanic iron is considered as one of the restriction factors of phytoplankton activity, it is necessary for a pelagic lower trophic level ecosystem model to take into account the effect of iron. In this study, we constructed a three dimensional gridded data of oceanic iron concentration by using both available in situ observation and simple iron cycle model. For the physical process of iron transport, the advection/diffusion model was used along with the flow field of ESTOC (Estimated State of Global Ocean for Climate Research). The falling atmospheric dust in the sea-surface and flux from the sediment at sea floor of the coast were set as the input of the iron. The scavenging or desorption by particulate matter in the water column were employed as the control variables and we constructed the simple iron cycle model. The optimized set of control parameters was obtained based on a Green's function approach by using available in situ iron concentration observations. The results showed that the iron concentration in the southern hemisphere is lower than northern hemisphere, and the low iron regions were well reproduced around the regions of high nutrient / low chlorophyll. Moreover, it is suggested that the Atlantic Ocean is more affected by the atmospheric dust compared with the Pacific Ocean.

キーワード：海洋溶存鉄、データ同化
Keywords: oceanic iron, data assimilation

©2019. Japan Geoscience Union. All Right Reserved.

A high-resolution multi-purpose particle tracking framework for coastal areas near Japan

*松村 義正[1]、桂 将太[1]、黒木 聖夫[2]、中野 英之[3]、山岸 孝輝[4]
*Yoshimasa Matsumura[1], Shota Katsura[1], Masao Kurogi[2], Hideyuki Nakano[3], Takateru Yamagishi[4]

1. 東京大学 大気海洋研究所、2. 海洋研究開発機構、3. 気象庁気象研究所、4. 高度情報科学技術研究機構
1. Atmosphere and Ocean Research Institute, University of Tokyo, 2. Japan Agency for Marine-Earth Science and Technology, 3. Meteorological Research Institute, Japan Meteorological Agency , 4. Research organization for Information Science and Technology

A comprehensive and multi-purpose particle tracking framework using latest high resolution velocity field in the coastal regions near Japan is developed.
The particle tracking system uses accurate fourth order Runge-Kutta method and implements random-walk based diffusivity, and is built-in the recent versions of MRI.com (an OGCM developed in Meteorological Research Institute, Japan Meteorological Agency) and kinaco (a non-hydrostatic ocean model developed in Atmosphere and Ocean Research Institute, University of Tokyo) for *on-line* use. Each particle is able to store up to seven arbitrary properties (such as size, age, exposed temperature, orientation, mass and buoyancy, etc.) and record the history of them.

The code is effectively parallelized (using MPI and OpenMP hybrid technique) and allows ~O(10^{10}) particles on modern massive-parallel supercomputers, and is also ported to GPU architecture using CUDA language.

This particle tracking framework has no particular target in a priori, and can be applied to various purposes for both physical oceanography (from large scale tracking of water masses to small scale modeling of suspended sediment matter or frazil ice crystals) and ocean biogeochemistry (tracking of trace elements, Laglangian modeling of plankton and detritus, individual based modeling of fishes and marine resources), only by defining appropriate properties and inserting a few lines of code that manipulats them corresponding to the particular target use.

In the presentation, we will introduce an application of this framework to the tracking of passive particles scattered in the coastal areas near Japan using velocity field provided by the latest very high resolution ocean modeling (~300 m mesh). Each model particle records its trajectory and the history of exposed environment, and can be interpreted as eggs or larvae (before acquiring swimming ability) of species of corresponding spawning areas and seasons as well as the tracers for small scale water mass exchanges.

キーワード：粒子追跡法
Keywords: Particle tracking system

©2019. Japan Geoscience Union. All Right Reserved.

Numerical study on seasonality of ocean litters collected at the Dongsha Island in the northern South China Sea

*Yi-Chia Hsin[1], Chia-Ying Ko[2], Ming-Shiou Jeng[3]

1. Research Center for Environmental Changes, Academia Sinica, 2. Institute of Fisheries Science, National Taiwan University, 3. Biodiversity Research Center, Academia Sinica

Distribution of ocean litters collected at the Dongsha Island, an isolated island in the northern South China Sea, shows a significant seasonal change. More litters were accumulated in the northern (southern) part of the island in winter (summer). By means of backward-tracking simulation by considering the effect of both ocean currents and winds (i.e., windage), a series of numerical experiments are carried out to clarify the possible source and mechanisms for the observational seasonal change of litters. Results exhibit that, in winter, low-windage litters are mainly from the western Philippine Sea via the Luzon Strait while the high-windage ones are contributed from the Taiwan Strait. In summer, litters from the southwestern South China Sea, i.e. east of Vietnam, could be a major origin.

Keywords: ocean litters, numercial study, South China Sea

©2019. Japan Geoscience Union. All Right Reserved.

A key spot and timing to monitor chlorophyll-a in the Kuroshio western boundary current

*平田 貴文[1]
*Takafumi Hirata[1]

1. 北海道大学地球環境科学研究院
1. Faculty of Environmental Earth Science, Hokkaido University

The Kuroshio western boundary current originates from the subtropics in the Western Pacific and carries a thermal energy and oceanic water mass towards the north, including the south coasts and offshore islands of Japan. In spite of the oligotrophy of the origin water that the Kuroshio carries, the Kuroshio water is known for spawning and feeding grounds of commercial/non-commercial fish larvae, explaining a higher fisheries production in the region. Thus, it puzzles an oceanographic and ecological relationships among nutrient fields, standing stock and productivity of organisms. In order to understand the complex Kuroshio ecosystems, phytoplankton dynamics is investigated using remote sensing data, namely phytoplankton pigment or chlorophyll-a observed by Advanced Himawari Imager (AHI) onboard Himawari-8. The area-integrated, and the area average of, Kuroshio chlorophyll-a was found predictable from a chlorophyll-a measurement in the 134-136 ˚E, where the Kuroshio current direction is most stable between 130-150 ˚E . An analysis of short term variability (< 1 year) of the Kuroshio chlorophyll-a concentration revealed that a cumulative, and monthly average of, chlorophyll-a over a month in the Kuroshio surface water could be estimated from a chlorophyll-a measurement at a single day in the month. These results suggest that there is a key spot and timing to monitor the phytoplankton activities in the Kuroshio current.

キーワード：黒潮、クロロフィル、リモートセンシング
Keywords: Kuroshio, Chlorophyll, Remote Sensing

©2019. Japan Geoscience Union. All Right Reserved.

Impacts of cyclonic eddies on phytoplankton biomass and phenology in the Kuroshio Extension region

*Eko Siswanto[1], Yoshikazu Sasai[1]

1. Japan Agency for Marine-Earth Science and Technology

Two-decade ocean color chlorophyll-a concentration (CHL, a metric of phytoplankton biomass) data from 1997 to 2017 were used to comprehend the impact of cyclonic eddies on phytoplankton biomass and phenology in the Kuroshio Extension region (KE) of the western North Pacific Ocean. The CHL data have 4-km and 8-day spatiotemporal resolution and were acquired from the ESA Ocean Colour-Climate Change Initiative (http://www.esa-oceancolour-cci.org/). Prior to defining spring bloom onset, spatiotemporal gaps in CHL data were filled by applying empirical orthogonal function-based interpolation. The analysis was mainly focused on the winter season (January-March) as oceanographic conditions during the winter largely control phytoplankton spring bloom in terms of both magnitude and onset. Based on winter sea surface height anomaly (SSHa), cyclonic eddies (negative SSHa) were dominant mainly within the periods from 1998 to 2001 and from 2005 to 2009, whereas anti-cyclonic eddies (positive SSHa) were dominant mainly within the periods from 2002 to 2004 and from 2011 to 2015. Based on datasets from all seasons, the concurrences of negative SSHa and positive phytoplankton chlorophyll anomaly (CHLa) were observed, albeit not always. This indicates an eddy-induced upwelling supplies nutrients to the near-surface layer. Upwelled nutrients eventually promote phytoplankton growth. Such a concurrence of low SSHa and high CHLa was less obvious during the winter indicating that another factor (such as intense winter vertical mixing) also non-trivially controlled nutrient input to the surface layer, and hence CHLa variability. Overall temporal mean indeed showed that the active cyclonic eddy area (approximately south of the Kuroshio Current main axis) was characterized by high CHLa, low SSHa, and shoaled mixed layer. In this study, a Cumulative Sum method was applied to find phytoplankton spring bloom onset. Correlation between SSHa and spring bloom onset time was investigated, and it was found that approximately over the active cyclonic eddy area, positive correlation between winter/late winter SSHa and time of spring bloom onset was observed. Such a positive correlation indicates that cyclonic eddies during the winter likely tended to advance phytoplankton spring bloom onset.

Keywords: Ocean color, Phytoplankton, Bloom onset, Upwelling

©2019. Japan Geoscience Union. All Right Reserved.

Diagnostic estimation and uncertainties of nutrient limitation of phytoplankton growth in Michaelis-Menten functional form

*橋岡 豪人[1]、相田 真希[1]
*Taketo Hashioka[1], Maki Noguchi Aita[1]

1. 国立研究開発法人 海洋研究開発機構
1. Japan Agency for Marine-Science and Technology

Michaelis-Menten functional form (MM) is most widely used relationship of nutrient limitation of phytoplankton growth in large-scale ecosystem models. In MM functional form, the choice of parameter value of a half-saturation constant is a key point for controlling the strength of nutrient limitation. In general, the half-saturation constant increase with the size of the phytoplankton cell depending on the surface-to-volume ratio by diffusive hypothesis, and wide ranges of values are reported from observational studies. On the other hand, the most of Plankton Functional Types (PFT) models represent a phytoplankton type as one representative PFT with one global parameter. The parameter value is chosen in the observed range as a most reasonable value that could reproduce observed chl-a or nutrient concentration in each model. As a result, there are uncertainties of the global pattern of nutrient limitation among models. In this study, we diagnostically estimated the nutrient limitation using various parameter set of different global PFT models form CMIP5 together with the observation based nutrient concentrations (World Ocean Atlas for macro nutrient and multi-model median for dissolved iron and ammonium concentration). Then we show uncertainties and robustness of estimation of nutrient limitation in the current PFT models with MM functional form.

キーワード：プランクトン機能タイプモデル、ミカエリスメンテン式
Keywords: Plankton Functional Types model, Michaelis-Menten functional form

©2019. Japan Geoscience Union. All Right Reserved.

Modeling productivity in lower trophic levels in Otsuchi Bay, northeast of Japan, using a nested OGCM with a biogeochemical component

*坂本 天[1]、浦川 昇吾[2]、伊藤 幸彦[1]、羽角 博康[1]、田中 潔[1]
*Takashi T Sakamoto[1], L. Shogo Urakawa[2], Sachihiko Itoh[1], Hiroyasu Hasumi[1], Kiyoshi Tanaka[1]

1. 東京大学大気海洋研究所、2. 気象庁気象研究所
1. Atmosphere and Ocean Research Institute, the University of Tokyo, 2. Meteorological Research Institute, Japan Meteorologica Agancy

Otsuchi Bay is located on the northeast coast of Honshu Island, Japan, where was extensively damaged by the huge tsunamis caused by the 2011 off the Pacific coast of Tohoku Earthquake. Motivated by how the biogeochemical circumstance and fishery resource recover, some observations have been conducted in the bay, but those have not been enough because of several restrictions and human resources. Aimed at filling the observational shortage and the acquirement of some information about physical and low trophic fields, a modeling approach has been discussed. Using a triply-nested OGCM and a downscaling method, the authors succeeded to reproduce seasonal variability of the circulation in the bay, and also showed a seasonality of the water exchange mechanism between the bay and the open ocean (Sakamoto et al. 2017). In order to know the low trophic processes in the bay, a numerical simulation using a nested OGCM with a NPZD model is conducted. The OGCM is an improved version of Sakamoto et al’ s (2017) model, and the NPZD one is based on Nagata and Hasumi (2014). In this poster, our modeling strategy and some results will be presented. The final goal of this study is to perform hindcasting simulations of the bay with realistic boundary conditions, that are the river runoff, the atmospheric forcings, and the open ocean states.

キーワード：ダウンスケーリング、ネストモデル、NPZDモデル
Keywords: downscaling, nest-modeling, NPZD model

©2019. Japan Geoscience Union. All Right Reserved.

Change in lower trophic level ecosystems to decadal scale variation of climate system in the North Pacific Ocean

*相田 真希[1]、田所 和明[2]、小室 芳樹[3]、橋岡 豪人[1]、原田 尚美[1]
*Maki Noguchi Aita[1], Kazuaki Tadokoro[2], Yoshiki Komuro[3], Taketo Hashioka[1], Naomi Harada[1]

1. 国立研究開発法人 海洋研究開発機構 地球環境観測研究開発センター、2. 国立研究開発法人 水産研究・教育機構　東北区水産研究所、3. 国立研究開発法人 海洋研究開発機構　北極環境変動総合研究センター
1. Research and Development Center for Global Change, Japan Agency for Marine-Earth Science and Technology, 2. Tohoku National Fisheries Research Institute, Japan Fisheries Research and Education Agency, 3. Institute of Arctic Climate and Environment Research, Japan Agency for Marine-Earth Science and Technology

The changes related to interdecadal climate variations, such as the Pacific Decadal Oscillation and the 18.6-y tidal cycle, have been discussed in many marine ecosystem studies. By analyzing data from observation of nutrient concentrations, decreasing and increasing trends of nutrients in the surface and subsurface layers, have been reported in many studies. Changes have also been observed in the biomass of phytoplankton and zooplankton. To clarify variability of lower trophic level productivity and its controlling factor, we simulated changes in the marine ecosystem caused by interdecadal climate variability, using the JRA55-do (Japanese 55-year atmospheric reanalysis) dataset from 1958 to 2017 to drive an ecosystem model, NEMURO, embedded in a global three-dimensional physical-biological coupled model, ‘COCO-NEMURO’. We compared and verified ecosystem model results with observations of phytoplankton and zooplankton species composition data collected by the Tohoku National Fisheries Research Institute, Japan Fisheries Research and Education Agency (FRA). Our model results showed that changes in biomass and nutrient concentration greatly differ depending on the region. According to our model results, sea surface temperature (SST) was very low during mid 1960s to mid 1970s, then SST increased after the mid 1970s to the end of 1990s in the western subarctic North Pacific. Changes in phytoplankton biomass was follow to this. However, the change in SST and phytoplankton and zooplankton biomass were contrary to this in the western subtropical North Pacific. We also checked decadal time series of annual mean sea ice concentration, SST, and phytoplankton biomass in the eastern Bering Sea and the western Arctic. The simulated sea ice concentration in the eastern Bering Sea decreased from the late 1970s to the early 1980s, while it was higher in the early 1990s and the late 2000s. The SST had its peaks in the late 1970s and the early 2000s. The phytoplankton biomass was inversely correlated with the sea ice concentration. In the western Arctic, the simulated sea ice concentration (SST) showed negative (positive) trends on the decadal timescale. The phytoplankton biomass has also been increasing, but its trend was not so simple. To elucidate the mechanism that sustains marine ecosystems, we will also analyze focusing on primary producers and zooplankton to key link to higher trophic levels.

キーワード：気候変化、10年規模変動、海洋低次生態系、海洋生態系モデル’NEMURO’
Keywords: Climate change, decadal change, lower trophic marine ecosystem, marine ecosystem model 'NEMURO'

©2019. Japan Geoscience Union. All Right Reserved.

Estimation of experienced environment of jack mackerel in the East China Sea

*樋口 富彦[1]、高橋 素光[2]、白井 厚太朗[1]、伊藤 進一[1]
*Tomihiko Higuchi[1], Motomitsu Takahashi[2], Kotaro Shirai[1], Shin-ichi Ito[1]

1. 東京大学大気海洋研究所、2. 国立研究開発法人 水産研究・教育機構 西海区水産研究所
1. Atmosphere and Ocean Research Institute, The University of Tokyo, 2. Seikai National Fisheries Research Institute,FRA

Jack mackerel *Trachurus japonicus* is distributed on the continental shelf waters along the subtropical Kuroshio Current and the Tsushima Warm Current in the western North Pacific. The East China Sea (ECS) is one of major region for jack mackerel and understanding the recruitment processes of jack mackerel into the fishing grounds in the ECS is important. However, marine environment such as water temperature that jack mackerel actually experiences is not directly observed yet. In this study, oxygen ($\delta^{18}O$) and carbon ($\delta^{13}C$) stable isotope of jack mackerel otolith were analyzed and the experienced environment was estimated. When we compared $\delta^{18}O$ of otolith caught in between three different station with different temperature, average of $\delta^{18}O$ varied and was negatively correlated with water temperature of sampling station. Most of individual indicated that $\delta^{13}C$ relatively increased from core part to edge in otolith. Thus, these results suggest that otolith of jack mackerel recorded experienced environment. However, because jack mackerel migrate vertically, it needs to consider vertical profile of seawater temperature and other parameters such as salinity and prey availability. A combination with fish distribution information and ecological modeling may help the improvement of estimation for detail experienced environment.

キーワード：fish otolith、isotope analysis、experienced environment、fish migration
Keywords: fish otolith, isotope analysis, experienced environment, fish migration

©2019. Japan Geoscience Union. All Right Reserved.

[E] ポスター発表 | セッション記号 A (大気水圏科学)：A-OS 海洋科学・海洋環境

2019年5月27日(月) 17:15 ~ 18:30 | ポスター会場 幕張メッセ国際展示場 8ホール_5

[A-OS12] Marine ecosystems and biogeochemical cycles: theory, observation and modeling

コンビーナ:伊藤 進一(東京大学大気海洋研究所)、平田 貴文(北海道大学地球環境科学研究院)、Enrique N Curchitser(Rutgers University New Brunswick)、Eileen E Hofmann(Old Dominion University)

The ocean accounts for about 50% of global net primary production. This production is significant for carbon cycling and ecosystem functioning, and is related directly or indirectly to a variety of climatic and ecological phenomena. The responses to natural and anthropogenic environmental stressors that influence marine production and diversity can cause perturbations to marine ecosystems that alter trophic dependencies and interactions among organisms at a range of space and time scales. Quantification of the principal mechanisms driving spatio-temporal variability of marine ecosystem remains to be done, especially in terms of evaluation of uncertainty in responses. As a result, evaluating vulnerability of marine ecosystems to environmental change requires systematic and holistic approaches that integrate physics to ecology and are based in observations and modelling. In addition, expectations to deliver these science to public society is raising. This session aims to provide a venue for not only discussing recent advances in understanding marine biogeochemical cycles, ecosystems and their interactions, but also networking with a variety of people to seed new ideas in marine ecological research. Observational, modeling and conceptual studies, including technological development and operational applications, that consider linkages among biogeochemical and ecosystem processes, biodiversity, and the effects of multiple stressors from molecular to planetary scales are encouraged.

[AOS12-P01] 日本海の生態系に対する対馬海峡を経由する栄養塩輸送の影響

*柴野 良太[1]、森本 昭彦[1]、髙山 勝巳[2]、滝川 哲太郎[3]、伊藤 雅[4] (1.愛媛大学沿岸環境科学研究センター、2.九州大学応用力学研究所、3.長崎大学大学院水産・環境科学総合研究科、4.水産研究・教育機構日本海区水産研究所)

[AOS12-P02] Revisiting vertical variations in stoichiometry during oceanic organic matter decomposition

*重光 雅仁[1]、青山 道夫[1]、土居 知将[1]、横川 太一[1]、村田 昌彦[1] (1.国立研究開発法人　海洋研究開発機構)

[AOS12-P03] Reproduction of iron-rich intermediate water in the Sea of Okhotsk by high resolution biogeochemical model.

*西川 はつみ[1]、三寺 史夫[1]、浩志 吉成[2]、拓也 中野渡[3]、中村 知裕[1]、内本 圭亮[4]、羽角 博康[5] (1.北海道大学低温科学研究所、2.国立環境研究所、3.北海道区水産研究所、4.地球環境産業技術研究機構、5.東京大学　大気海洋研究所)

[AOS12-P04] The global oceanic iron distribution estimated by data assimilation approach

*土居 知将[1]、長船 哲史[1]、増田 周平[1]、小畑 元[2]、三角 和弘[3]、西岡 純[4] (1.海洋研究開発機構、2.東京大学、3.電力中央研究所、4.北海道大学)

[AOS12-P05] A high-resolution multi-purpose particle tracking framework for coastal areas near Japan

*松村 義正[1]、桂 将太[1]、黒木 聖夫[2]、中野 英之[3]、山岸 孝輝[4] (1.東京大学 大気海洋研究所、2.海洋研究開発機構、3.気象庁気象研究所、4.高度情報科学技術研究機構)

[AOS12-P06] Numerical study on seasonality of ocean litters collected at the Dongsha Island in the northern South China Sea

*Yi-Chia Hsin[1]、Chia-Ying Ko[2]、Ming-Shiou Jeng[3] (1.Research Center for Environmental Changes, Academia Sinica、2.Institute of Fisheries Science, National Taiwan University、3.Biodiversity Research Center, Academia Sinica)

[AOS12-P07] A key spot and timing to monitor chlorophyll-a in the Kuroshio western boundary current

*平田 貴文[1] (1.北海道大学地球環境科学研究院)

[AOS12-P08] **Impacts of cyclonic eddies on phytoplankton biomass and phenology in the Kuroshio Extension region**

*Eko Siswanto[1]、Yoshikazu Sasai[1] (1.Japan Agency for Marine-Earth Science and Technology)

[AOS12-P09] Diagnostic estimation and uncertainties of nutrient limitation of phytoplankton growth in Michaelis-Menten functional form

*橋岡 豪人[1]、相田 真希[1] (1.国立研究開発法人 海洋研究開発機構)

[AOS12-P10] Modeling productivity in lower trophic levels in Otsuchi Bay, northeast of Japan, using a nested OGCM with a biogeochemical component

*坂本 天[1]、浦川 昇吾[2]、伊藤 幸彦[1]、羽角 博康[1]、田中 潔[1] (1.東京大学大気海洋研究所、2.気象庁気象研究所)

[AOS12-P11] Change in lower trophic level ecosystems to decadal scale variation of climate system in the North Pacific Ocean

*相田 真希[1]、田所 和明[2]、小室 芳樹[3]、橋岡 豪人[1]、原田 尚美[1] (1.国立研究開発法人 海洋研究開発機構 地球環境観測研究開発センター、2.国立研究開発法人 水産研究・教育機構　東北区水産研究所、3.国立研究開発法人 海洋研究開発機構　北極環境変動総合研究センター)

[AOS12-P12] Estimation of experienced environment of jack mackerel in the East China Sea

*樋口 富彦[1]、高橋 素光[2]、白井 厚太朗[1]、伊藤 進一[1] (1.東京大学大気海洋研究所、2.国立研究開発法人 水産研究・教育機構 西海区水産研究所)

日本海の生態系に対する対馬海峡を経由する栄養塩輸送の影響
Impact of the nutrient transport through the Tsushima Strait on the ecosystem in the Japan Sea

*柴野 良太[1]、森本 昭彦[1]、髙山 勝巳[2]、滝川 哲太郎[3]、伊藤 雅[4]
*Ryota Shibano[1], Akihiko Morimoto[1], Katsumi Takayama[2], Tetsutaro Takikawa[3], Masashi Ito[4]

1. 愛媛大学沿岸環境科学研究センター、2. 九州大学応用力学研究所、3. 長崎大学大学院水産・環境科学総合研究科、4. 水産研究・教育機構日本海区水産研究所
1. Center for Marine Environmental Studies, Ehime University, 2. Research Institute for Applied Mechanics, Kyushu University, 3. Graduate School of Fisheries and Environmental Sciences, Nagasaki University, 4. Fisheries Oceanography Department, Japan Sea National Fisheries Research Institute

日本海は対馬海峡をはじめとする狭く浅いいくつかの海峡でのみ外海と接続する半閉鎖海域である。対馬海峡を介し供給される栄養塩は東シナ海を介して供給され、それらは日本海沿岸部などの生態系に対し強い影響力をもつ。その起源は海洋からの供給源としては黒潮・台湾海峡・黄海からもたらされるものが多くあり、海洋外からの供給源としては長江・黄河・ダストによるものがある。我々は2005年から2017年までの対馬海峡における船舶観測データから、同海域における流量変動・栄養塩濃度などの経年変動を調べた。その結果、対馬海峡を通過する栄養塩輸送量は±50%程度増減していることがわかった。近年の報告から、経年変動で栄養塩輸送量が変動している時、前述の起源の寄与率も変動していることが指摘されている(Morimoto et al., 2012)。

我々は観測事実に基づいた領域海洋モデルに生態系モデルを統合した数値モデルを開発し、日本海および東シナ海におけるこれらの栄養塩動態について定量的に評価した。また黒潮・台湾海峡・長江・黄河・ダスト・底層(黄海)由来の各起源についても各輸送量と寄与率について定量的に評価することで、経年変動に伴いどのような時空間変動があらわれるかについて評価した。

キーワード：対馬暖流、栄養塩輸送、日本海
Keywords: Tsushima Warm Current, nutrient transport, the Sea of Japan

©2019. Japan Geoscience Union. All Right Reserved.

Revisiting vertical variations in stoichiometry during oceanic organic matter decomposition

Revisiting vertical variations in stoichiometry during oceanic organic matter decomposition

*重光 雅仁[1]、青山 道夫[1]、土居 知将[1]、横川 太一[1]、村田 昌彦[1]
*Masahito Shigemitsu[1], Michio Aoyama[1], Toshimasa Doi[1], Taichi Yokokawa[1], Akihiko Murata[1]

1. 国立研究開発法人　海洋研究開発機構
1. Japan Agency for Marine-Earth Science and Technology

Using the new global nutrient data set, we re-evaluate basin-wide stoichiometric ratios of remineralization estimated by Anderson and Sarmiento (1994) (hereinafter, AS94). For the same latitudinal ranges of the Atlantic, Indian and Pacific Oceans as in AS94, we construct one or two end-member mixing models on 14 neutral surfaces and estimate the stoichiometric ratios with a probabilistic approach. Unlike the results of AS94, significant vertical variations in the stoichiometry are found in the Atlantic and Pacific, while relatively constant stoichiometry with depth is found in the Indian Ocean, similar to AS94. The decreases in the C/P and $-O_2$/P ratios with depth in the Atlantic could be caused via dark DIC fixation by chemoautotrophs in the deep waters. In the Pacific, changes in organic matter composition with depth would be the most important factor in the increases in stoichiometry with depth. In all the basins, the N/P ratios are probably affected by benthic denitrification, as in AS94. The P/C/-O_2ratios (mean and $5^{th}$to 95^{th}percentile) are estimated to be 1/111(97 to 129)/155(149 to 163) in the depths below 2000 m of the Indian and Pacific Oceans, where DIC fixation and vertical change in organic matter composition have little influence on the stoichiometry estimates. We suggest that chemoautotrophic DIC fixation and the effect of change in organic matter composition with depth on the stoichiometry in waters above 2000 m should be considered for large-scale biogeochemical modeling and estimation of oceanic uptake of anthropogenic carbon from observational data.

キーワード：栄養塩、化学量論比、有機物分解
Keywords: nutrients, stoichiometric ratios, remineralization of organic matter

©2019. Japan Geoscience Union. All Right Reserved.

Reproduction of iron-rich intermediate water in the Sea of Okhotsk by high resolution biogeochemical model.

*西川 はつみ[1]、三寺 史夫[1]、浩志 吉成[2]、拓也 中野渡[3]、中村 知裕[1]、内本 圭亮[4]、羽角 博康[5]
*Hatsumi Nishikawa[1], Humio Mitsudera[1], Hiroshi Yoshinari[2], Takuya Nakanowatari[3], Tomohiro Nakamura[1], Keisuke Uchimoto[4], Hiroyasu Hasumi[5]

1. 北海道大学　低温科学研究所、2. 国立環境研究所、3. 北海道区水産研究所、4. 地球環境産業技術研究機構、5. 東京大学大気海洋研究所
1. Institute of Low Temperature Science, Hokkaido University, 2. National Institute for Environmental Studies, 3. Tohoku National Fisheries Research Institute, Japan Fisheries Research and Education Agency, 4. Research Institute of Innovative Technology for the Earth, 5. Atmosphere and Ocean Research Institute, University of Tokyo

Recent observation studies suggest that iron supply from sediment on the northwest continental shelf the Okhotsk Sea plays an important role for the subarctic primary production (e.g. Nishioka et al., 2013). Dense shelf water (DSW) takes up iron from sediment, thereby transporting iron into the Okhotsk Sea intermediate water. However, observational data is still limited.

To clarify detailed structure of iron circulation in the North Pacific, we develop the high-resolution biogeochemical model. However, our model did not reproduce high iron concentration in the intermediate water the Sea of Okhotsk. We use biogeochemical model developed by Parekh et al. (2005). They set the value of total ligand concentration to constant value in all place. Recent observations, however, suggest that ligand concentration varies with sea area and depth. Then, we conducted a new experiment with the ligand concentration changed in the vertical direction. The iron concentration intermediate water of the new experiment becaame higher than before.

キーワード：高解像度モデル、中層水鉄、リガンド濃度
Keywords: High-resolution modeling, Iron-rich intermediate water, Ligand concentration

©2019. Japan Geoscience Union. All Right Reserved.

The global oceanic iron distribution estimated by data assimilation approach

*土居 知将[1]、長船 哲史[1]、増田 周平[1]、小畑 元[2]、三角 和弘[3]、西岡 純[4]
*Doi Toshimasa[1], Satoshi Osafune[1], Shuhei Masuda[1], Hajime Obata[2], Kazuhiro Misumi[3], Jun Nishioka[4]

1. 海洋研究開発機構、2. 東京大学、3. 電力中央研究所、4. 北海道大学
1. Japan Agency for Marine-Earth Science and Technology, 2. The University of Tokyo, 3. Central Research Institute of Electric Power Industry, 4. Hokkaido University

Since distribution of oceanic iron is considered as one of the restriction factors of phytoplankton activity, it is necessary for a pelagic lower trophic level ecosystem model to take into account the effect of iron. In this study, we constructed a three dimensional gridded data of oceanic iron concentration by using both available in situ observation and simple iron cycle model. For the physical process of iron transport, the advection/diffusion model was used along with the flow field of ESTOC (Estimated State of Global Ocean for Climate Research). The falling atmospheric dust in the sea-surface and flux from the sediment at sea floor of the coast were set as the input of the iron. The scavenging or desorption by particulate matter in the water column were employed as the control variables and we constructed the simple iron cycle model. The optimized set of control parameters was obtained based on a Green's function approach by using available in situ iron concentration observations. The results showed that the iron concentration in the southern hemisphere is lower than northern hemisphere, and the low iron regions were well reproduced around the regions of high nutrient / low chlorophyll. Moreover, it is suggested that the Atlantic Ocean is more affected by the atmospheric dust compared with the Pacific Ocean.

キーワード：海洋溶存鉄、データ同化
Keywords: oceanic iron, data assimilation

©2019. Japan Geoscience Union. All Right Reserved.

A high-resolution multi-purpose particle tracking framework for coastal areas near Japan

*松村 義正[1]、桂 将太[1]、黒木 聖夫[2]、中野 英之[3]、山岸 孝輝[4]
*Yoshimasa Matsumura[1], Shota Katsura[1], Masao Kurogi[2], Hideyuki Nakano[3], Takateru Yamagishi[4]

1. 東京大学 大気海洋研究所、2. 海洋研究開発機構、3. 気象庁気象研究所、4. 高度情報科学技術研究機構
1. Atmosphere and Ocean Research Institute, University of Tokyo, 2. Japan Agency for Marine-Earth Science and Technology, 3. Meteorological Research Institute, Japan Meteorological Agency , 4. Research organization for Information Science and Technology

A comprehensive and multi-purpose particle tracking framework using latest high resolution velocity field in the coastal regions near Japan is developed.
The particle tracking system uses accurate fourth order Runge-Kutta method and implements random-walk based diffusivity, and is built-in the recent versions of MRI.com (an OGCM developed in Meteorological Research Institute, Japan Meteorological Agency) and kinaco (a non-hydrostatic ocean model developed in Atmosphere and Ocean Research Institute, University of Tokyo) for *on-line* use. Each particle is able to store up to seven arbitrary properties (such as size, age, exposed temperature, orientation, mass and buoyancy, etc.) and record the history of them.

The code is effectively parallelized (using MPI and OpenMP hybrid technique) and allows ~O(10^{10}) particles on modern massive-parallel supercomputers, and is also ported to GPU architecture using CUDA language.

This particle tracking framework has no particular target in a priori, and can be applied to various purposes for both physical oceanography (from large scale tracking of water masses to small scale modeling of suspended sediment matter or frazil ice crystals) and ocean biogeochemistry (tracking of trace elements, Laglangian modeling of plankton and detritus, individual based modeling of fishes and marine resources), only by defining appropriate properties and inserting a few lines of code that manipulats them corresponding to the particular target use.

In the presentation, we will introduce an application of this framework to the tracking of passive particles scattered in the coastal areas near Japan using velocity field provided by the latest very high resolution ocean modeling (~300 m mesh). Each model particle records its trajectory and the history of exposed environment, and can be interpreted as eggs or larvae (before acquiring swimming ability) of species of corresponding spawning areas and seasons as well as the tracers for small scale water mass exchanges.

キーワード：粒子追跡法
Keywords: Particle tracking system

©2019. Japan Geoscience Union. All Right Reserved.

Numerical study on seasonality of ocean litters collected at the Dongsha Island in the northern South China Sea

*Yi-Chia Hsin[1], Chia-Ying Ko[2], Ming-Shiou Jeng[3]

1. Research Center for Environmental Changes, Academia Sinica, 2. Institute of Fisheries Science, National Taiwan University, 3. Biodiversity Research Center, Academia Sinica

Distribution of ocean litters collected at the Dongsha Island, an isolated island in the northern South China Sea, shows a significant seasonal change. More litters were accumulated in the northern (southern) part of the island in winter (summer). By means of backward-tracking simulation by considering the effect of both ocean currents and winds (i.e., windage), a series of numerical experiments are carried out to clarify the possible source and mechanisms for the observational seasonal change of litters. Results exhibit that, in winter, low-windage litters are mainly from the western Philippine Sea via the Luzon Strait while the high-windage ones are contributed from the Taiwan Strait. In summer, litters from the southwestern South China Sea, i.e. east of Vietnam, could be a major origin.

Keywords: ocean litters, numercial study, South China Sea

©2019. Japan Geoscience Union. All Right Reserved.

A key spot and timing to monitor chlorophyll-a in the Kuroshio western boundary current

*平田 貴文[1]
*Takafumi Hirata[1]

1. 北海道大学地球環境科学研究院
1. Faculty of Environmental Earth Science, Hokkaido University

The Kuroshio western boundary current originates from the subtropics in the Western Pacific and carries a thermal energy and oceanic water mass towards the north, including the south coasts and offshore islands of Japan. In spite of the oligotrophy of the origin water that the Kuroshio carries, the Kuroshio water is known for spawning and feeding grounds of commercial/non-commercial fish larvae, explaining a higher fisheries production in the region. Thus, it puzzles an oceanographic and ecological relationships among nutrient fields, standing stock and productivity of organisms. In order to understand the complex Kuroshio ecosystems, phytoplankton dynamics is investigated using remote sensing data, namely phytoplankton pigment or chlorophyll-a observed by Advanced Himawari Imager (AHI) onboard Himawari-8. The area-integrated, and the area average of, Kuroshio chlorophyll-a was found predictable from a chlorophyll-a measurement in the 134-136 ˚E, where the Kuroshio current direction is most stable between 130-150 ˚E . An analysis of short term variability (< 1 year) of the Kuroshio chlorophyll-a concentration revealed that a cumulative, and monthly average of, chlorophyll-a over a month in the Kuroshio surface water could be estimated from a chlorophyll-a measurement at a single day in the month. These results suggest that there is a key spot and timing to monitor the phytoplankton activities in the Kuroshio current.

キーワード：黒潮、クロロフィル、リモートセンシング
Keywords: Kuroshio, Chlorophyll, Remote Sensing

©2019. Japan Geoscience Union. All Right Reserved.

Impacts of cyclonic eddies on phytoplankton biomass and phenology in the Kuroshio Extension region

*Eko Siswanto[1], Yoshikazu Sasai[1]

1. Japan Agency for Marine-Earth Science and Technology

Two-decade ocean color chlorophyll-a concentration (CHL, a metric of phytoplankton biomass) data from 1997 to 2017 were used to comprehend the impact of cyclonic eddies on phytoplankton biomass and phenology in the Kuroshio Extension region (KE) of the western North Pacific Ocean. The CHL data have 4-km and 8-day spatiotemporal resolution and were acquired from the ESA Ocean Colour-Climate Change Initiative (http://www.esa-oceancolour-cci.org/). Prior to defining spring bloom onset, spatiotemporal gaps in CHL data were filled by applying empirical orthogonal function-based interpolation. The analysis was mainly focused on the winter season (January-March) as oceanographic conditions during the winter largely control phytoplankton spring bloom in terms of both magnitude and onset. Based on winter sea surface height anomaly (SSHa), cyclonic eddies (negative SSHa) were dominant mainly within the periods from 1998 to 2001 and from 2005 to 2009, whereas anti-cyclonic eddies (positive SSHa) were dominant mainly within the periods from 2002 to 2004 and from 2011 to 2015. Based on datasets from all seasons, the concurrences of negative SSHa and positive phytoplankton chlorophyll anomaly (CHLa) were observed, albeit not always. This indicates an eddy-induced upwelling supplies nutrients to the near-surface layer. Upwelled nutrients eventually promote phytoplankton growth. Such a concurrence of low SSHa and high CHLa was less obvious during the winter indicating that another factor (such as intense winter vertical mixing) also non-trivially controlled nutrient input to the surface layer, and hence CHLa variability. Overall temporal mean indeed showed that the active cyclonic eddy area (approximately south of the Kuroshio Current main axis) was characterized by high CHLa, low SSHa, and shoaled mixed layer. In this study, a Cumulative Sum method was applied to find phytoplankton spring bloom onset. Correlation between SSHa and spring bloom onset time was investigated, and it was found that approximately over the active cyclonic eddy area, positive correlation between winter/late winter SSHa and time of spring bloom onset was observed. Such a positive correlation indicates that cyclonic eddies during the winter likely tended to advance phytoplankton spring bloom onset.

Keywords: Ocean color, Phytoplankton, Bloom onset, Upwelling

©2019. Japan Geoscience Union. All Right Reserved.

Diagnostic estimation and uncertainties of nutrient limitation of phytoplankton growth in Michaelis-Menten functional form

*橋岡 豪人[1]、相田 真希[1]
*Taketo Hashioka[1], Maki Noguchi Aita[1]

1. 国立研究開発法人 海洋研究開発機構
1. Japan Agency for Marine-Science and Technology

Michaelis-Menten functional form (MM) is most widely used relationship of nutrient limitation of phytoplankton growth in large-scale ecosystem models. In MM functional form, the choice of parameter value of a half-saturation constant is a key point for controlling the strength of nutrient limitation. In general, the half-saturation constant increase with the size of the phytoplankton cell depending on the surface-to-volume ratio by diffusive hypothesis, and wide ranges of values are reported from observational studies. On the other hand, the most of Plankton Functional Types (PFT) models represent a phytoplankton type as one representative PFT with one global parameter. The parameter value is chosen in the observed range as a most reasonable value that could reproduce observed chl-a or nutrient concentration in each model. As a result, there are uncertainties of the global pattern of nutrient limitation among models. In this study, we diagnostically estimated the nutrient limitation using various parameter set of different global PFT models form CMIP5 together with the observation based nutrient concentrations (World Ocean Atlas for macro nutrient and multi-model median for dissolved iron and ammonium concentration). Then we show uncertainties and robustness of estimation of nutrient limitation in the current PFT models with MM functional form.

キーワード：プランクトン機能タイプモデル、ミカエリスメンテン式
Keywords: Plankton Functional Types model, Michaelis-Menten functional form

©2019. Japan Geoscience Union. All Right Reserved.

Modeling productivity in lower trophic levels in Otsuchi Bay, northeast of Japan, using a nested OGCM with a biogeochemical component

*坂本 天[1]、浦川 昇吾[2]、伊藤 幸彦[1]、羽角 博康[1]、田中 潔[1]
*Takashi T Sakamoto[1], L. Shogo Urakawa[2], Sachihiko Itoh[1], Hiroyasu Hasumi[1], Kiyoshi Tanaka[1]

1. 東京大学大気海洋研究所、2. 気象庁気象研究所
1. Atmosphere and Ocean Research Institute, the University of Tokyo, 2. Meteorological Research Institute, Japan Meteorologica Agancy

Otsuchi Bay is located on the northeast coast of Honshu Island, Japan, where was extensively damaged by the huge tsunamis caused by the 2011 off the Pacific coast of Tohoku Earthquake. Motivated by how the biogeochemical circumstance and fishery resource recover, some observations have been conducted in the bay, but those have not been enough because of several restrictions and human resources. Aimed at filling the observational shortage and the acquirement of some information about physical and low trophic fields, a modeling approach has been discussed. Using a triply-nested OGCM and a downscaling method, the authors succeeded to reproduce seasonal variability of the circulation in the bay, and also showed a seasonality of the water exchange mechanism between the bay and the open ocean (Sakamoto et al. 2017). In order to know the low trophic processes in the bay, a numerical simulation using a nested OGCM with a NPZD model is conducted. The OGCM is an improved version of Sakamoto et al’ s (2017) model, and the NPZD one is based on Nagata and Hasumi (2014). In this poster, our modeling strategy and some results will be presented. The final goal of this study is to perform hindcasting simulations of the bay with realistic boundary conditions, that are the river runoff, the atmospheric forcings, and the open ocean states.

キーワード：ダウンスケーリング、ネストモデル、NPZDモデル
Keywords: downscaling, nest-modeling, NPZD model

©2019. Japan Geoscience Union. All Right Reserved.

Change in lower trophic level ecosystems to decadal scale variation of climate system in the North Pacific Ocean

*相田 真希[1]、田所 和明[2]、小室 芳樹[3]、橋岡 豪人[1]、原田 尚美[1]
*Maki Noguchi Aita[1], Kazuaki Tadokoro[2], Yoshiki Komuro[3], Taketo Hashioka[1], Naomi Harada[1]

1. 国立研究開発法人 海洋研究開発機構 地球環境観測研究開発センター、2. 国立研究開発法人 水産研究・教育機構　東北区水産研究所、3. 国立研究開発法人 海洋研究開発機構　北極環境変動総合研究センター
1. Research and Development Center for Global Change, Japan Agency for Marine-Earth Science and Technology, 2. Tohoku National Fisheries Research Institute, Japan Fisheries Research and Education Agency, 3. Institute of Arctic Climate and Environment Research, Japan Agency for Marine-Earth Science and Technology

The changes related to interdecadal climate variations, such as the Pacific Decadal Oscillation and the 18.6-y tidal cycle, have been discussed in many marine ecosystem studies. By analyzing data from observation of nutrient concentrations, decreasing and increasing trends of nutrients in the surface and subsurface layers, have been reported in many studies. Changes have also been observed in the biomass of phytoplankton and zooplankton. To clarify variability of lower trophic level productivity and its controlling factor, we simulated changes in the marine ecosystem caused by interdecadal climate variability, using the JRA55-do (Japanese 55-year atmospheric reanalysis) dataset from 1958 to 2017 to drive an ecosystem model, NEMURO, embedded in a global three-dimensional physical-biological coupled model, ‘COCO-NEMURO’. We compared and verified ecosystem model results with observations of phytoplankton and zooplankton species composition data collected by the Tohoku National Fisheries Research Institute, Japan Fisheries Research and Education Agency (FRA). Our model results showed that changes in biomass and nutrient concentration greatly differ depending on the region. According to our model results, sea surface temperature (SST) was very low during mid 1960s to mid 1970s, then SST increased after the mid 1970s to the end of 1990s in the western subarctic North Pacific. Changes in phytoplankton biomass was follow to this. However, the change in SST and phytoplankton and zooplankton biomass were contrary to this in the western subtropical North Pacific. We also checked decadal time series of annual mean sea ice concentration, SST, and phytoplankton biomass in the eastern Bering Sea and the western Arctic. The simulated sea ice concentration in the eastern Bering Sea decreased from the late 1970s to the early 1980s, while it was higher in the early 1990s and the late 2000s. The SST had its peaks in the late 1970s and the early 2000s. The phytoplankton biomass was inversely correlated with the sea ice concentration. In the western Arctic, the simulated sea ice concentration (SST) showed negative (positive) trends on the decadal timescale. The phytoplankton biomass has also been increasing, but its trend was not so simple. To elucidate the mechanism that sustains marine ecosystems, we will also analyze focusing on primary producers and zooplankton to key link to higher trophic levels.

キーワード：気候変化、10年規模変動、海洋低次生態系、海洋生態系モデル’NEMURO’
Keywords: Climate change, decadal change, lower trophic marine ecosystem, marine ecosystem model 'NEMURO'

©2019. Japan Geoscience Union. All Right Reserved.

Estimation of experienced environment of jack mackerel in the East China Sea

*樋口 富彦[1]、高橋 素光[2]、白井 厚太朗[1]、伊藤 進一[1]
*Tomihiko Higuchi[1], Motomitsu Takahashi[2], Kotaro Shirai[1], Shin-ichi Ito[1]

1. 東京大学大気海洋研究所、2. 国立研究開発法人 水産研究・教育機構 西海区水産研究所
1. Atmosphere and Ocean Research Institute, The University of Tokyo, 2. Seikai National Fisheries Research Institute,FRA

Jack mackerel *Trachurus japonicus* is distributed on the continental shelf waters along the subtropical Kuroshio Current and the Tsushima Warm Current in the western North Pacific. The East China Sea (ECS) is one of major region for jack mackerel and understanding the recruitment processes of jack mackerel into the fishing grounds in the ECS is important. However, marine environment such as water temperature that jack mackerel actually experiences is not directly observed yet. In this study, oxygen ($\delta^{18}O$) and carbon ($\delta^{13}C$) stable isotope of jack mackerel otolith were analyzed and the experienced environment was estimated. When we compared $\delta^{18}O$ of otolith caught in between three different station with different temperature, average of $\delta^{18}O$ varied and was negatively correlated with water temperature of sampling station. Most of individual indicated that $\delta^{13}C$ relatively increased from core part to edge in otolith. Thus, these results suggest that otolith of jack mackerel recorded experienced environment. However, because jack mackerel migrate vertically, it needs to consider vertical profile of seawater temperature and other parameters such as salinity and prey availability. A combination with fish distribution information and ecological modeling may help the improvement of estimation for detail experienced environment.

キーワード：fish otolith、isotope analysis、experienced environment、fish migration
Keywords: fish otolith, isotope analysis, experienced environment, fish migration

©2019. Japan Geoscience Union. All Right Reserved.

[E] ポスター発表 | セッション記号 H (地球人間圏科学)：H-DS 防災地球科学

2019年5月27日(月) 13:45 ~ 15:15 | ポスター会場 幕張メッセ国際展示場 8ホール_3

[H-DS11] Subaqueous Landslides and Their Anthropogenic Impact for Coastal Regions

コンビーナ:北村 有迅(鹿児島大学大学院理工学研究科地球環境科学専攻)、山田 泰広(海洋研究開発機構　海洋掘削科学研究開発センター)

A large number of people inhabit coastal areas around the world that are susceptible to natural catastrophes and subaqueous landslides are one of such hazards as demostrated recently. The risk associated with the occurrence of subaqueous landslides is not only constrained to passive margins or subduction zones but any of water areas is also susceptible to their occurrence since subaqueous failures can be triggered at very low slope angles. This realization poses a significant challenge that requires the collection of vast amounts of information and data to unravel the true nature of these events and their potential risk to coastal communities. Despite these challenges, recent technical and engineering advances in the acquisition and processing of sea floor and shallow subsurface data are encouraging. There has also been a concerted effort by scientists from different earth-science disciplines to increase interdisciplinary cooperation at an international level to advance our collective understanding of subaqueous landslides and their consequences.
This session calls for technical contributions covering all aspects of subaqueous landslide research including but not limited to: physical properties of deformed sediments (pre- and post- deformation), role of interstitial fluids in subaqueous landslide development, slope stability and risk assessments, geomorphological and sedimentological/stratigraphic descriptions, tsunamigenic risk and modeling, description of ancient subaqueous landslides, sand-box models and numerical simulations of subaqueous landslides. Case studies from lacustrine landslides and subaerial coastal landslides transitioning into the marine realm are also welcome. Case studies associated with the broader topic of subaqueous gravity-driven flows (e.g.: turbidites and transitional flows) and their relationship with seafloor faulting are also of interest to this session. Participants of IUGS project S4SLIDE IGCP-640 sponsor this session.

[HDS11-P01] Deformed sediment gravity flow deposits associated with bypassing slides:an example from the Miocene Ushikiri Formation, Southwest Japan

*小林 未季[1]、酒井 哲弥[2] (1.日本工営株式会社、2.島根大学総合理工学部)

[HDS11-P02] 四国沖大陸棚斜面の海底地すべり調査と津波計算

*権 容大[1]、馬場 俊孝[1]、松野 哲男、林 美鶴、市原 寛 (1.徳島大学大学院)

[HDS11-P03] 八代海南部における白鳳丸KH-18-3次研究航海で採取された堆積物コアの物性から推定される堆積環境

*堀 航喜[1]、北村 有迅[2]、白鳳丸K-18-3次研究航海 乗船研究者一同 (1.九州大学大学院理学府地球惑星科学専攻、2.鹿児島大学大学院理工学研究科地球環境科学専攻)

[HDS11-P04] 「白鳳丸」KH-18-3次研究航海で採取された八代海の堆積物コア試料のベーンせん断強さと帯磁率

*北村 有迅[1]、影山 遼[2]、山﨑 楓[2]、後藤 滝弥[2]、堀 航喜[2]、池端 雄太[2]、川端 訓代[1]、小山 大輝[2]、白鳳丸KH-18-3 乗船研究者 (1.鹿児島大学大学院理工学研究科地球環境科学専攻、2.鹿児島大学理学部地球環境科学科)

[HDS11-P05] Identification of turbidites in the Yatsushiro Sea surface sediment core samples from non-destructive measurements: Hakuho-maru KH-18-3 Cruise, Yatsushiro Sea, Western Kyushu, Japan

*後藤 滝弥[1]、北村 有迅[2]、白鳳丸KH-18-3次研究航海 乗船研究者一同 (1.東京大学大気海洋研究所、2.鹿児島大学大学院理工学研究科地球環境科学専攻)

[HDS11-P06] Revised columnar section based on grain size distribution analysis of samples from Hakuho-maru KH-18-3 in Yatsushiro sea

*池端 雄太[1]、北村 有迅[2]、白鳳丸KH-18-3次研究航海乗船研究者 Family (1.九州大学大学院理学府地球惑星科学専攻、2.鹿児島大学大学院理工学研究科地球環境科学専攻)

Deformed sediment gravity flow deposits associated with bypassing slides: an example from the Miocene Ushikiri Formation, Southwest Japan

*小林 未季[1]、酒井 哲弥[2]
*Miki Kobayashi[1], Tetsuya Sakai[2]

1. 日本工営株式会社、2. 島根大学総合理工学部
1. Nippon Koei, 2. Shimane University

The Middle Miocene Ushikiri Formation in Shimane Peninsula, southwest Japan, is interpreted to have been deposited on the shelf margin to the middle continental shelf, and is known to contain unique sediment gravity flow deposits, similar to hybrid sediment gravity flow deposits (turbidite + debrite). Intensely deformed mud clasts have been described from this formation. However, their formation has not been focused on previous studies. The present study aims to characterize the deformation of sandstone beds and mud clasts contained within the sediment gravity flow deposits and to discuss of the deformation process of the sediments.

Many of the sandstone beds in the upper Ushikiri Formation (averaging 0.6 m thick) are bipartite, with lower parts showing characteristics similar to Ta or Ta-b turbidites with rich mud clasts. The upper parts of the sandstone beds are represented by poorly-sorted muddy sand with scattered mud clasts having debrite-like features. The small mud clasts in the lower part show features different from those in ordinary turbidites: some are subject to injection of surrounding sand and some scattered in sands show jigsaw-puzzle patterns, suggesting in situ mud clast fragmentation. Some mud clasts are intensely stretched. The beds also host large mud clasts (maximum length: ca 3 m), in which deformation structures, such as slump folds, are well developed. Mud clast shapes are not consistent with internal deformation structures and the most of them have sharp margins. The sand around some large mud clasts shows local liquefaction. Local grading is also found above the large mud clasts and does not continue beyond the edge of the mud clasts.

The injection of sand into mud clasts and their in situ fragmentation into jigsaw-puzzle patterns can be explained by liquefaction of beds with overburden pressure. A possible pressure source is slides that passed over a freshly deposited turbidite bed. When a slide bypassed the sand bed, the bed once deposited as turbidite easily liquefied under the moving slide mass, having led overburden pressure in the bed that caused injection and in situ fragmentation. On the contrary, the large mud clasts may have been fragments ripped from a major sliding body that bypassed the studied locality. Local liquefaction around large mud clasts indicates they sank or were forced into the bed from above. The presence of local grading above the mud clasts can be explained by local resuspension of sand around the mud clasts when they sank into the sand. The above mentioned sediment deformation process is supported by beds with a slide deposit above a sandy part having similar mud clast deformation.
The bypassing of the slide may have been due to hydroplaning of the slide mass. The slide deposits are represented by up to 2 m thick of large mud block rich sediments with variety of deformation structures, which grades from an underlying debrite-like bed that consists of poorly-sorted muddy sand with rich mud clasts with injection of surrounding muddy sand. Some mud clasts in the muddy sandstone beds are intensely stretched, implying that shear stress exerted within the beds. The poorly-sorted muddy sand is thus interpreted as a fluid layer, which has been existed below the moving landslide mass, having

©2019. Japan Geoscience Union. All Right Reserved.

triggered the hydroplaning.

キーワード：海底地すべり堆積物、地すべり土塊のバイパス、島根
Keywords: submarine landslide deposit, bypassing of landslide mass, Shamane

©2019. Japan Geoscience Union. All Right Reserved.

四国沖大陸棚斜面の海底地すべり調査と津波計算
Submarine Landslide and Resulting Tsunami on the Continental Shelf Slope off Shikoku

*権 容大[1]、馬場 俊孝[1]、松野 哲男、林 美鶴、市原 寛
*Youdai Gon[1], Toshitaka Baba[1], Tetsuo Matsuno, Mitsuru Hayashi, Hiroshi Ichihara

1. 徳島大学大学院
1. Tokushima University graduate school

海底地すべりは，主に地震の揺れが原因となって発生し，海底通信ケーブル等の海域インフラに被害を与えるとともに津波を発生させる．南海トラフには多数の海底地すべりの痕跡があり，四国沖およそ24kmの海底の大陸棚斜面にも海底地すべり地形（以降，四国沖海底地すべりと呼ぶ）が存在する．この海域で同様な海底地すべりが発生した場合，津波が発生すると予想される．そこで，本研究では四国沖海底地すべりマルチナロービーム音響測深を実施するとともに，この海底地すべりによって励起される津波のシミュレーションを行った。

マルチナロービーム音響測深は神戸大学大学院海事科学研究科附属練習船深江丸で，平成29年度に1回，平成30年度に2回実施された．得られた海底地形データから，四国沖海底地すべりは４つの馬蹄形の崩壊跡（西からA,B,C,Dとする）からなる。最も西側の崩壊（以降，A崩壊と呼ぶ）には斜面下方に崩壊土砂の堆積も確認された。地形的特徴からA崩壊の時代が新しいとみられる．また，隣接して複数の崩壊跡が存在するため，今後も同様な海底地すべりが発生する可能性がある。

津波計算では，A崩壊，地形的特徴から同時期に崩壊したと思われるBとCの同時崩壊（以降，B・C崩壊と呼ぶ），またDより東側である未崩壊部分にてA崩壊と同じ規模の崩壊を想定し（以降，E崩壊,F崩壊と呼ぶ），計算を行った．四国の南東部にある海岸沿いでは最大波高がA崩壊,B・C崩壊によって約15分後にそれぞれ約2m，約10m，E崩壊，F崩壊によって約20分後にそれぞれ約4.5m，約5mという結果となった．さらに，他の未崩壊箇所にて海底地すべり発生を想定し津波シミュレーションを実施するとともに，過去の津波記録との比較を行う．

キーワード：四国沖海底地すべり、津波シミュレーション
Keywords: The submarine landslide off Shikoku, Tsunami simulation

©2019. Japan Geoscience Union. All Right Reserved.

八代海南部における白鳳丸KH-18-3次研究航海で採取された堆積物コアの物性から推定される堆積環境

Sedimentary environment estimated from physical properties of sediment core collected during the cruise of Hakuho-maru KH-18-3 in the South Yatsushiro sea, western Kyushu.

*堀 航喜[1]、北村 有迅[2]、白鳳丸K-18-3次研究航海 乗船研究者一同
*Koki Hori[1], Yujin Kitamura[2], Hakuho-maru KH-18-3 Scientists

1. 九州大学大学院理学府地球惑星科学専攻、2. 鹿児島大学大学院理工学研究科地球環境科学専攻
1. Department of Earth and Planetary Sciences, Graduate School of Science, Kyushu University , 2. Department of Earth and Environmental Sciences, Graduate School of Science and Engineering , Kagoshima University

The research cruise KH-18-3 was carried out in the South Yatsushiro sea from 27th to 30th July 2018. The purpose of this cruise is to clarify the occurrence history of the submarine landslides in the Yatsushiro sea. In this survey, bottom surface sediment samples were collected by using Piston corer which is 6 meters long.
The study on physical properties of event sediment using core samples are conducted in ocean areas around the world. For example, Prior et al. (1984) reported that Mass transport deposits (MTD) commonly have a higher density than surrounding, sediments that are not submarine landslide origin. Therefore, in this study, the physical properties that serve as the basic information of the core samples were measured. In addition, we estimated the sedimentary environment in the survey area by applying tidal current, sedimentation rate, and bottom surface muddy rate in the south Yatsushiro sea (Rifardi et al.,1998) and conventional radiocarbon ages of piston core samples recovered in the same area reported by Inoue et al. (2011).

Core samples were collected from 11 sites (core name:PC01 to PC11) in the south Yatsushiro sea where the Taura-Tsunagi Oki fault group and Minamata Oki fault group are distributed.
All analyses other than the grain size distribution analysis were conducted at the Center for Advanced Marine Core Research, Kochi University. Initially, GRA density, Magnetic susceptibility and fractional porosity were measured using Whole round multi sensor core logger (MSCL-W). After the analysis, core samples were divided vertically and visual observation and color measurement of them were performed. Subsequently, a vane shear test and sub-samples which were used for MAD measurements and grain size distribution analysis collecting were performed at approximately 50 cm intervals, respectively, and the test and two sampling location were the same points.

Area 1 is under condition of rather stagnant water masses or rather weak tidal current system and is characterized fine-grained sediments. We estimated age of core samples by comparing physical properties reported by Inoue et al. (2011) because sampling point in this area matched with piston coring points of Inoue et al. (2011) and the behaviors of both physical properties were similar. As a result, a gap of more than 7000 years of sediment age is estimated at depth of 2 to 3 meters in area 1a (PC01 to PC03) and it is presumed that sediments indicating the age of about 10,000 years BP exist at depth of several tens of centimeters from the seabed surface in area 1b (PC06, PC07). In addition, K-Ah volcanic ash layer (7.3ka) could not be confirmed from sediments in both sea areas. From this, it is assumed that there was an event such as a submarine landslide or erosion with the lower part of the tephra as a sliding or eroding

©2019. Japan Geoscience Union. All Right Reserved.

surface.
Since we could not obtain an index to estimate the age of the PC 08 to PC 11, we estimated the sedimentary environment using only the physical properties of sediments. PC08 and PC10 (Area 2) is located near the strait of Goshoura-jima and sisi-jima island, under influence of strong tidal and bottom currents, and is characterized by coarse sediments. Especially, upward grain refinement was observed and the tendency that the porosity decreases within each monolayer is repeated in PC10. From this, it is assumed that the upper sediment functions as an impermeable layer against the lower sediment, and the drainage is difficult to proceed. PC 09 and PC 11 (Area 3) are relatively close to supply sources such as Minamata River and Komenotsu River, and are characterized as relatively coarse sediments. From the depth of 60 cm of PC09, and from the outermost surface layer in PC 11, the porosity does not decrease almost from around 60%. From this, it is estimated that the new sediment has been recently cleared recently.

キーワード：ピストンコアリング、八代海
Keywords: Piston coring, Yatsushiro sea

©2019. Japan Geoscience Union. All Right Reserved.

「白鳳丸」KH-18-3次研究航海で採取された八代海の堆積物コア試料のベーンせん断強さと帯磁率

Variation in vane shear strength and magnetic susceptibility in the cores recovered by Hakuho-maru KH-18-3 cruise in Yatsushiro sea

*北村 有迅[1]、影山 遼[2]、山﨑 楓[2]、後藤 滝弥[2]、堀 航喜[2]、池端 雄太[2]、川端 訓代[1]、小山 大輝[2]、白鳳丸KH-18-3 乗船研究者
*Yujin Kitamura[1], Haruka Kageyama[2], Kaede Yamasaki[2], Ryoya Goto[2], Koki Hori[2], Yuta Ikebata[2], Kuniyo Kawabata[1], Daiki Oyama[2], Hakuho-maru KH-18-3 Scientists

1. 鹿児島大学大学院理工学研究科地球環境科学専攻、2. 鹿児島大学理学部地球環境科学科
1. Department of Earth and Environmental Sciences, Graduate School of Science and Engineering, Kagoshima University, 2. Department of Earth and Environmental Sciences, Faculty of Science, Kagoshima University

1. はじめに

2016年4月に起きた熊本地震は，布田川断層帯・日奈久断層帯における一連の地震である．このうち，日奈久断層帯の南西部は「八代海区間」を構成している．地震は海底地すべり発生の引き金となるが，熊本地震発生後，海域での調査はほとんど行われていない．そこで，「白鳳丸」KH-18-3次研究航海において八代海で11本のピストンコア試料（PC01~PC11）を採泥した．また，海底地すべり堆積物の下層ではせん断強さが小さくなる（Flemings et al., 2012）ことから，せん断強さは海底地すべりの評価において重要な役割を果たす．本研究では，海底地すべりが発生した可能性の高い八代海のコア試料において，ベーンせん断試験でせん断強さを算出し，八代海の堆積物分布を考察した．

2. 手法

航海は2018年7月27日から7月30日の期間に八代海において学術研究船「白鳳丸」を利用して行われた．長さ6 m，直径7.5 cmの塩ビ管を用いてピストンコアラーによる11地点の採泥を行い，船上において6つのセクションに切り分けた．採取したコアは高知コアセンターに持ち込み物性測定を行った．CTスキャナとマルチセンサーコアロガー(MSCL)を用いた非破壊計測を行い，それぞれ内部構造の計測とγ線密度・帯磁率を測定した．CTスキャンの結果からはCT値を抽出した．その後肉眼記載を行い，非破壊計測のデータとあわせて柱状図を作成した．その後，1本のコアをアーカイブ（保存用）コアとワーキング（作業用）コアに半裁した．ベーンせん断試験は，肉眼記載後のワーキングコアにおいておよそ50 cm間隔で実施した．試験にはトルクメーターに取り付けた十字型のベーン（羽根）を使用した．ベーンを試料に押し込み，軸を水平に回転させて，試料を破断するのに要する最大モーメントからせん断強さを算出した．また，蛍光X線分析を行い，主要元素濃度を測定した．

3. 結果と考察

帯磁率

採取されたコアは主にオリーブ灰や黒の砂泥を基質とする．CT値と帯磁率，γ線密度は深さに伴って増加傾向にあった．しかし，帯磁率は周期的にピークを繰り返していることが結果からわかったため，ピークを一つのユニットとして層区分を行った．区分した層は八木ほか(2016)による高分解能地層探査断面図と井上ほか(2011)で採取されたピストンコアを用いて比較した．

©2019. Japan Geoscience Union. All Right Reserved.

地層探査断面図では，帯磁率によって区分した層と音波探査による層を対比させることが可能であった．八木ほか(2016)による解釈から，白神岩付近で採取したコアは最終氷期極相期~縄文海進時の堆積物を含むことがわかった．このように，本コアにおいて帯磁率の周期的なピークは堆積時の環境・堆積層を反映していることがわかった．

帯磁率を用いた井上ほか(2011)とのコア対比は概ね帯磁率が一致しており， PC02とPC06ではイベント層の推定が可能であった．推定されたイベント層では帯磁率が極大を示す傾向がある．鉄濃度はイベント層の前後で相対的に高くなる傾向がみられたことから，鉄の濃度を用いたイベント層の推定が可能であると考えられる．鉄の濃度がイベント層で変化する要因として，タービダイトの発生後は重い粒子が先に沈殿すると考えられ，重金属である鉄も早くに沈殿するためであると考えられる．

ベーンせん断強さ

そして，田浦-津奈木沖断層群の北東部に位置するPC01･PC02･PC07は深度に伴ってせん断強さが増加している．そのため，埋没による圧密が堆積物の強度増加の主要因であると考えられる．また，井上ほか（2011）の年代測定結果と比較したところ，年代のギャップがある部分でせん断強さの増加率が変化している．このことから，年代の違いによる圧密の影響を受けた堆積物であると考えられる．PC03については，下部の火山灰層が特異的なせん断強さを示すが，その他の層については深度に伴ってせん断強さが大きくなっている．PC04･PC05･PC06については，最上部のみせん断強さが小さいことから，上部の堆積物は削剥された可能性がある．田浦-津奈木沖断層群西部に位置するPC10には砂や礫といった粗粒分が堆積している．また，水俣沖断層群に位置するPC09･PC11はせん断強さと間隙率に相関関係がなく，せん断強さが深度に伴って増加するという傾向はみられない．PC11については，最上部に堆積した泥が削剥されて欠落していると考えられる．

キーワード：タービダイト、浅海堆積物、平成28年熊本地震
Keywords: turbidites, shallow marine deposits, 2016 Kumamoto earthquake

©2019. Japan Geoscience Union. All Right Reserved.

Identification of turbidites in the Yatsushiro Sea surface sediment core samples from non-destructive measurements: Hakuho-maru KH-18-3 Cruise, Yatsushiro Sea, Western Kyushu, Japan

*後藤 滝弥[1]、北村 有迅[2]、白鳳丸KH-18-3次研究航海 乗船研究者一同
*Ryoya Goto[1], Yujin Kitamura[2], Hakuho-maru KH-18-3 Cruise Scientist

1. 東京大学大気海洋研究所、2. 鹿児島大学大学院理工学研究科地球環境科学専攻
1. Atmosphere and Ocean Research Institute, The University of Tokyo, 2. Department of Earth and Environmental Sciences, Graduate School of Science, Kagoshima University

Submarine active faults in Yatsusiro Sea, western Kyushu, Japan, constitute the Yatsushiro section of Hinagu fault zone in its southwest end (AIST et al., 2011). The 2016 Kumamoto Earthquake was sourced from a part of active faults of the Futagawa-Hinagu fault zones (JMA, 2018), and survey has hardly conducted in the sea area after the earthquake occurrence. Earthquake shaking occasionally triggers turbidity currents by submarine landslides and resuspension of unconsolidated sediments on the seafloor (Ikehara et al., 2018). In recent years, the study of earthquake occurrence history using earthquake turbidites formed by turbidity currents is being conducted throughout the world. As earthquake-origin turbidity currents can take place in very gentle slope (e.g. the Mississippi-Delta 0.01°: D. B. Prior et al., 1978), its occurrence is sufficiently thought even in Yatsushiro Sea. However, any record of earthquake turbidites in this area has not been reported. In this study, identification of turbidites in the Yatsushiro Sea surface sediment core samples from non-destructive measurements.

Here we conducted four-days research cruise Hakuho-maru KH-18-3 in July, 2018. We conducted sub-bottom profiling on eight lines, piston coring at 11 sites in Yatsushiro Sea, western Kyushu, Japan. Recovered cores are analyzed by X-ray CT scanner, multi-sensor core logger, core imaging apparatus, visual core description, color spectroscope and X-ray fluorescence core scanner (Itrax) in the Center for Advanced Marine Core Research, Kochi University. With reference to the previous studies (Iwai et al., 2014, JGS abstract; Isabel Rodríguez-Germade et al, 2015; Okutsu et al., 2017, JGS abstract), the behavior of Ca/Ti and Fe/Ti where the peak was observed at the base of turbidites, and the behavior of Fe/Ti and Zr/Ti where the peak was observed at the base of volcaniclastics turbidites.

Our results revealed turbidites and volcaniclastics turbidites in six piston coring sites (PC01 to PC06). As all of sites are located in the Taura-Tsunagioki fault group or Minamataoki fault group, turbidites were considered to be present in all of sites. However, turbidites were identified from PC01 to PC06, but not identified from PC07 to PC11. According to Rifardi et al. (1998), PC01 to PC06 are located in the sea area where the deposition rate is high, and PC07 to PC11 are located in the sea area where the deposition rate is slow.

As turbidite is formed by various factors besides earthquakes, it is necessary to consider whether the turbidites identified in this study are earthquake turbidites. In addition, to investigate the history of earthquakes, it is also a future task to conduct individual sample measurements (such as grain size distribution analysis) and dating.

Hakuho-maru KH-18-3 Cruise Scientists: Takashi Tomiyasu, Hitoshi Kodamatani, Kuniyo Kawabata, Daiki

©2019. Japan Geoscience Union. All Right Reserved.

Oyama, Haruka Kageyama, Kaede Yamasaki (Kagoshima Univ.), Yuta Ikebata, Koki Hori (Kyushu Univ.), Asuka Yamaguchi, Fumiaki Tsunomori, Kameo Katsura, Tsubasa Miki, Natsumi Okutsu, Hiroaki Koge, Kotaro Fujita, Ayaka Nakazawa, Yuichi Okuma, Genki Kobayashi, Rina Fukuchi (Tokyo Univ.), Jun Kameda, Tomonori Morisaki (Hokkaido Univ.)

キーワード：海底地すべり、タービダイト、浅海堆積物、八代海、2016年熊本地震
Keywords: submarine landslides, turbidites, shallow sea deposits, Yatsushiro Sea, 2016 Kumamoto Earthquake

©2019. Japan Geoscience Union. All Right Reserved.

Revised columnar section based on grain size distribution analysis of samples from Hakuho-maru KH-18-3 in Yatsushiro sea

*池端 雄太[1]、北村 有迅[2]、白鳳丸KH-18-3次研究航海乗船研究者 Family
*Yuta Ikebata[1], Yujin Kitamura[2], Hakuho-maru KH-18-3 Scientists Family

1. 九州大学大学院理学府地球惑星科学専攻、2. 鹿児島大学大学院理工学研究科地球環境科学専攻
1. Kyusyu University Graduate School Of Science Earth and Planetary Science, 2. Graduate school of science, Kagoshima University

Hakuho-maru KH-18-3 was held in the Yatsushiro Sea from 27th to 30th July 2018 for clarifying history of occurrence of submarine landslides. Earthquake is a one of big trigger of submarine landslides, and submarine landslides occurs in an very easy slope. Kumamoto earthquake occurred at April, 2016 and a lot of surveys in the land area were conducted but survey in the sea area weren’ t conducted much. In the Yatsushiro sea, the occurrence of submarine landslides caused by earthquake of the Futagawa-Hinagu fault zones can be considered sufficiently. Therefore, in this study, the creation of the columnar section which is the basic information of the submarine landslide accreditation was made based on the grain size distribution analysis.

In the Expedition, eleven piston cores(6m) from PC01 to PC11 were collected in the southern part of Yatsushiro sea, and the obtained core was subjected to non-destructive measurement and individual sample measurement at the Kochi Core Center. For non-destructive measurement, CT images and core continuous images were taken, and for individual sample measurement, Density, Magnetic susceptibility, porosity, vane shear strength, color, concentration change of major elements were examined. Grain size distribution analysis was conducted at Kagoshima University. Samples used for grain size distribution analysis were collected every 50 cm and analyzed with a laser diffraction type grain size distribution analyzer. Since it is difficult to judge the stratum boundary only with the result of grain size distribution measurement at intervals of 50 cm, it was judged by using γ ray density, magnetic susceptibility and color measurement result which are continuous data.

Grain size distribution analysis revealed PC01 to PC07 are muddy cores and PC08 to PC11 contains much sand. Grain size of PC01, PC04, PC06, PC07, PC09, PC11 are very different in Grain size distribution analysis and visual core description. Based on the results of the grain size distribution analysis, the stratum boundary was determined from the change commonly seen in the γ ray density, magnetic susceptibility and color, and a columnar section was prepared. In Rifardi et al.(1998), the distribution of mud content in the Yatsushiro Sea has been surveyed. As a result of comparing the columnar map of this study with its distribution for each sampling point, cores excluding PC08 corresponded well. It is thought that it is influenced by the supply of sediment by river and stagnant water mass, tide current as in previous research. Also, in Inoue et al.(2011), which was a reference for determining the core harvest point, dating is done in the same area. At Hori(2019MS), we compare the data with Inoue et al.(2011) and estimate the core age of this research. We also compare the columnar section made in this study with the columnar section of Inoue et al.(2011), using the comparative categories determined at the time of estimating the age. As a result, PC01 and PC02 were in good agreement, PC06 and PC07 had different stratum in the surface layer. This is probably because the sampling site of PC06 is actually about 150 m far from Inoue et al.(2011) and the sampling site of PC07 is actually about 111 m far from Inoue et al.(2011), and the sedimentary environment is slightly different. Also, in the grain size distribution analysis of this study, there is a possibility that coarse grains may be

©2019. Japan Geoscience Union. All Right Reserved.

selectively left out when putting the sample into the machine, and it may be doubtful in accuracy.

キーワード：海底地すべり
Keywords: Submarine landslide

©2019. Japan Geoscience Union. All Right Reserved.

[E] ポスター発表 | セッション記号 H (地球人間圏科学)：H-DS 防災地球科学

2019年5月27日(月) 17:15 ~ 18:30 | ポスター会場 幕張メッセ国際展示場 8ホール_13

[H-DS11] Subaqueous Landslides and Their Anthropogenic Impact for Coastal Regions

コンビーナ:北村 有迅(鹿児島大学大学院理工学研究科地球環境科学専攻)、山田 泰広(海洋研究開発機構　海洋掘削科学研究開発センター)

A large number of people inhabit coastal areas around the world that are susceptible to natural catastrophes and subaqueous landslides are one of such hazards as demostrated recently. The risk associated with the occurrence of subaqueous landslides is not only constrained to passive margins or subduction zones but any of water areas is also susceptible to their occurrence since subaqueous failures can be triggered at very low slope angles. This realization poses a significant challenge that requires the collection of vast amounts of information and data to unravel the true nature of these events and their potential risk to coastal communities. Despite these challenges, recent technical and engineering advances in the acquisition and processing of sea floor and shallow subsurface data are encouraging. There has also been a concerted effort by scientists from different earth-science disciplines to increase interdisciplinary cooperation at an international level to advance our collective understanding of subaqueous landslides and their consequences.
This session calls for technical contributions covering all aspects of subaqueous landslide research including but not limited to: physical properties of deformed sediments (pre- and post- deformation), role of interstitial fluids in subaqueous landslide development, slope stability and risk assessments, geomorphological and sedimentological/stratigraphic descriptions, tsunamigenic risk and modeling, description of ancient subaqueous landslides, sand-box models and numerical simulations of subaqueous landslides. Case studies from lacustrine landslides and subaerial coastal landslides transitioning into the marine realm are also welcome. Case studies associated with the broader topic of subaqueous gravity-driven flows (e.g.: turbidites and transitional flows) and their relationship with seafloor faulting are also of interest to this session. Participants of IUGS project S4SLIDE IGCP-640 sponsor this session.

[HDS11-P01] Deformed sediment gravity flow deposits associated with bypassing slides:an example from the Miocene Ushikiri Formation, Southwest Japan

*小林 未季[1]、酒井 哲弥[2] (1.日本工営株式会社、2.島根大学総合理工学部)

[HDS11-P02] 四国沖大陸棚斜面の海底地すべり調査と津波計算

*権 容大[1]、馬場 俊孝[1]、松野 哲男、林 美鶴、市原 寛 (1.徳島大学大学院)

[HDS11-P03] 八代海南部における白鳳丸KH-18-3次研究航海で採取された堆積物コアの物性から推定される堆積環境

*堀 航喜[1]、北村 有迅[2]、白鳳丸K-18-3次研究航海 乗船研究者一同 (1.九州大学大学院理学府地球惑星科学専攻、2.鹿児島大学大学院理工学研究科地球環境科学専攻)

[HDS11-P04] 「白鳳丸」KH-18-3次研究航海で採取された八代海の堆積物コア試料のベーンせん断強さと帯磁率

*北村 有迅[1]、影山 遼[2]、山﨑 楓[2]、後藤 滝弥[2]、堀 航喜[2]、池端 雄太[2]、川端 訓代[1]、小山 大輝[2]、白鳳丸KH-18-3 乗船研究者 (1.鹿児島大学大学院理工学研究科地球環境科学専攻、2.鹿児島大学理学部地球環境科学科)

[HDS11-P05] Identification of turbidites in the Yatsushiro Sea surface sediment core samples from non-destructive measurements: Hakuho-maru KH-18-3 Cruise, Yatsushiro Sea, Western Kyushu, Japan

*後藤 滝弥[1]、北村 有迅[2]、白鳳丸KH-18-3次研究航海 乗船研究者一同 (1.東京大学大気海洋研究所、2.鹿児島大学大学院理工学研究科地球環境科学専攻)

[HDS11-P06] Revised columnar section based on grain size distribution analysis of samples from Hakuho-maru KH-18-3 in Yatsushiro sea

*池端 雄太[1]、北村 有迅[2]、白鳳丸KH-18-3次研究航海乗船研究者 Family (1.九州大学大学院理学府地球惑星科学専攻、2.鹿児島大学大学院理工学研究科地球環境科学専攻)

Deformed sediment gravity flow deposits associated with bypassing slides: an example from the Miocene Ushikiri Formation, Southwest Japan

*小林 未季[1]、酒井 哲弥[2]
*Miki Kobayashi[1], Tetsuya Sakai[2]

1. 日本工営株式会社、2. 島根大学総合理工学部
1. Nippon Koei, 2. Shimane University

The Middle Miocene Ushikiri Formation in Shimane Peninsula, southwest Japan, is interpreted to have been deposited on the shelf margin to the middle continental shelf, and is known to contain unique sediment gravity flow deposits, similar to hybrid sediment gravity flow deposits (turbidite + debrite). Intensely deformed mud clasts have been described from this formation. However, their formation has not been focused on previous studies. The present study aims to characterize the deformation of sandstone beds and mud clasts contained within the sediment gravity flow deposits and to discuss of the deformation process of the sediments.

Many of the sandstone beds in the upper Ushikiri Formation (averaging 0.6 m thick) are bipartite, with lower parts showing characteristics similar to Ta or Ta-b turbidites with rich mud clasts. The upper parts of the sandstone beds are represented by poorly-sorted muddy sand with scattered mud clasts having debrite-like features. The small mud clasts in the lower part show features different from those in ordinary turbidites: some are subject to injection of surrounding sand and some scattered in sands show jigsaw-puzzle patterns, suggesting in situ mud clast fragmentation. Some mud clasts are intensely stretched. The beds also host large mud clasts (maximum length: ca 3 m), in which deformation structures, such as slump folds, are well developed. Mud clast shapes are not consistent with internal deformation structures and the most of them have sharp margins. The sand around some large mud clasts shows local liquefaction. Local grading is also found above the large mud clasts and does not continue beyond the edge of the mud clasts.

The injection of sand into mud clasts and their in situ fragmentation into jigsaw-puzzle patterns can be explained by liquefaction of beds with overburden pressure. A possible pressure source is slides that passed over a freshly deposited turbidite bed. When a slide bypassed the sand bed, the bed once deposited as turbidite easily liquefied under the moving slide mass, having led overburden pressure in the bed that caused injection and in situ fragmentation. On the contrary, the large mud clasts may have been fragments ripped from a major sliding body that bypassed the studied locality. Local liquefaction around large mud clasts indicates they sank or were forced into the bed from above. The presence of local grading above the mud clasts can be explained by local resuspension of sand around the mud clasts when they sank into the sand. The above mentioned sediment deformation process is supported by beds with a slide deposit above a sandy part having similar mud clast deformation.
The bypassing of the slide may have been due to hydroplaning of the slide mass. The slide deposits are represented by up to 2 m thick of large mud block rich sediments with variety of deformation structures, which grades from an underlying debrite-like bed that consists of poorly-sorted muddy sand with rich mud clasts with injection of surrounding muddy sand. Some mud clasts in the muddy sandstone beds are intensely stretched, implying that shear stress exerted within the beds. The poorly-sorted muddy sand is thus interpreted as a fluid layer, which has been existed below the moving landslide mass, having

©2019. Japan Geoscience Union. All Right Reserved.

triggered the hydroplaning.

キーワード：海底地すべり堆積物、地すべり土塊のバイパス、島根
Keywords: submarine landslide deposit, bypassing of landslide mass, Shamane

©2019. Japan Geoscience Union. All Right Reserved.

四国沖大陸棚斜面の海底地すべり調査と津波計算
Submarine Landslide and Resulting Tsunami on the Continental Shelf Slope off Shikoku

*権 容大[1]、馬場 俊孝[1]、松野 哲男、林 美鶴、市原 寛
*Youdai Gon[1], Toshitaka Baba[1], Tetsuo Matsuno, Mitsuru Hayashi, Hiroshi Ichihara

1. 徳島大学大学院
1. Tokushima University graduate school

海底地すべりは，主に地震の揺れが原因となって発生し，海底通信ケーブル等の海域インフラに被害を与えるとともに津波を発生させる．南海トラフには多数の海底地すべりの痕跡があり，四国沖およそ24kmの海底の大陸棚斜面にも海底地すべり地形（以降，四国沖海底地すべりと呼ぶ）が存在する．この海域で同様な海底地すべりが発生した場合，津波が発生すると予想される．そこで，本研究では四国沖海底地すべりマルチナロービーム音響測深を実施するとともに，この海底地すべりによって励起される津波のシミュレーションを行った。

マルチナロービーム音響測深は神戸大学大学院海事科学研究科附属練習船深江丸で，平成29年度に1回，平成30年度に2回実施された．得られた海底地形データから，四国沖海底地すべりは４つの馬蹄形の崩壊跡（西からA,B,C,Dとする）からなる。最も西側の崩壊（以降，A崩壊と呼ぶ）には斜面下方に崩壊土砂の堆積も確認された。地形的特徴からA崩壊の時代が新しいとみられる．また，隣接して複数の崩壊跡が存在するため，今後も同様な海底地すべりが発生する可能性がある。

津波計算では，A崩壊，地形的特徴から同時期に崩壊したと思われるBとCの同時崩壊（以降，B・C崩壊と呼ぶ），またDより東側である未崩壊部分にてA崩壊と同じ規模の崩壊を想定し（以降，E崩壊,F崩壊と呼ぶ），計算を行った．四国の南東部にある海岸沿いでは最大波高がA崩壊,B・C崩壊によって約15分後にそれぞれ約2m，約10m，E崩壊，F崩壊によって約20分後にそれぞれ約4.5m，約5mという結果となった．さらに，他の未崩壊箇所にて海底地すべり発生を想定し津波シミュレーションを実施するとともに，過去の津波記録との比較を行う．

キーワード：四国沖海底地すべり、津波シミュレーション
Keywords: The submarine landslide off Shikoku, Tsunami simulation

©2019. Japan Geoscience Union. All Right Reserved.

八代海南部における白鳳丸KH-18-3次研究航海で採取された堆積物コアの物性から推定される堆積環境

Sedimentary environment estimated from physical properties of sediment core collected during the cruise of Hakuho-maru KH-18-3 in the South Yatsushiro sea, western Kyushu.

*堀 航喜[1]、北村 有迅[2]、白鳳丸K-18-3次研究航海 乗船研究者一同
*Koki Hori[1], Yujin Kitamura[2], Hakuho-maru KH-18-3 Scientists

1. 九州大学大学院理学府地球惑星科学専攻、2. 鹿児島大学大学院理工学研究科地球環境科学専攻
1. Department of Earth and Planetary Sciences, Graduate School of Science, Kyushu University , 2. Department of Earth and Environmental Sciences, Graduate School of Science and Engineering , Kagoshima University

The research cruise KH-18-3 was carried out in the South Yatsushiro sea from 27th to 30th July 2018. The purpose of this cruise is to clarify the occurrence history of the submarine landslides in the Yatsushiro sea. In this survey, bottom surface sediment samples were collected by using Piston corer which is 6 meters long.
The study on physical properties of event sediment using core samples are conducted in ocean areas around the world. For example, Prior et al. (1984) reported that Mass transport deposits (MTD) commonly have a higher density than surrounding, sediments that are not submarine landslide origin. Therefore, in this study, the physical properties that serve as the basic information of the core samples were measured. In addition, we estimated the sedimentary environment in the survey area by applying tidal current, sedimentation rate, and bottom surface muddy rate in the south Yatsushiro sea (Rifardi et al.,1998) and conventional radiocarbon ages of piston core samples recovered in the same area reported by Inoue et al. (2011).

Core samples were collected from 11 sites (core name:PC01 to PC11) in the south Yatsushiro sea where the Taura-Tsunagi Oki fault group and Minamata Oki fault group are distributed.
All analyses other than the grain size distribution analysis were conducted at the Center for Advanced Marine Core Research, Kochi University. Initially, GRA density, Magnetic susceptibility and fractional porosity were measured using Whole round multi sensor core logger (MSCL-W). After the analysis, core samples were divided vertically and visual observation and color measurement of them were performed. Subsequently, a vane shear test and sub-samples which were used for MAD measurements and grain size distribution analysis collecting were performed at approximately 50 cm intervals, respectively, and the test and two sampling location were the same points.

Area 1 is under condition of rather stagnant water masses or rather weak tidal current system and is characterized fine-grained sediments. We estimated age of core samples by comparing physical properties reported by Inoue et al. (2011) because sampling point in this area matched with piston coring points of Inoue et al. (2011) and the behaviors of both physical properties were similar. As a result, a gap of more than 7000 years of sediment age is estimated at depth of 2 to 3 meters in area 1a (PC01 to PC03) and it is presumed that sediments indicating the age of about 10,000 years BP exist at depth of several tens of centimeters from the seabed surface in area 1b (PC06, PC07). In addition, K-Ah volcanic ash layer (7.3ka) could not be confirmed from sediments in both sea areas. From this, it is assumed that there was an event such as a submarine landslide or erosion with the lower part of the tephra as a sliding or eroding

©2019. Japan Geoscience Union. All Right Reserved.

surface.
Since we could not obtain an index to estimate the age of the PC 08 to PC 11, we estimated the sedimentary environment using only the physical properties of sediments. PC08 and PC10 (Area 2) is located near the strait of Goshoura-jima and sisi-jima island, under influence of strong tidal and bottom currents, and is characterized by coarse sediments. Especially, upward grain refinement was observed and the tendency that the porosity decreases within each monolayer is repeated in PC10. From this, it is assumed that the upper sediment functions as an impermeable layer against the lower sediment, and the drainage is difficult to proceed. PC 09 and PC 11 (Area 3) are relatively close to supply sources such as Minamata River and Komenotsu River, and are characterized as relatively coarse sediments. From the depth of 60 cm of PC09, and from the outermost surface layer in PC 11, the porosity does not decrease almost from around 60%. From this, it is estimated that the new sediment has been recently cleared recently.

キーワード：ピストンコアリング、八代海
Keywords: Piston coring, Yatsushiro sea

©2019. Japan Geoscience Union. All Right Reserved.

「白鳳丸」KH-18-3次研究航海で採取された八代海の堆積物コア試料のベーンせん断強さと帯磁率

Variation in vane shear strength and magnetic susceptibility in the cores recovered by Hakuho-maru KH-18-3 cruise in Yatsushiro sea

*北村 有迅[1]、影山 遼[2]、山﨑 楓[2]、後藤 滝弥[2]、堀 航喜[2]、池端 雄太[2]、川端 訓代[1]、小山 大輝[2]、白鳳丸KH-18-3 乗船研究者
*Yujin Kitamura[1], Haruka Kageyama[2], Kaede Yamasaki[2], Ryoya Goto[2], Koki Hori[2], Yuta Ikebata[2], Kuniyo Kawabata[1], Daiki Oyama[2], Hakuho-maru KH-18-3 Scientists

1. 鹿児島大学大学院理工学研究科地球環境科学専攻、2. 鹿児島大学理学部地球環境科学科
1. Department of Earth and Environmental Sciences, Graduate School of Science and Engineering, Kagoshima University, 2. Department of Earth and Environmental Sciences, Faculty of Science, Kagoshima University

1. はじめに

2016年4月に起きた熊本地震は，布田川断層帯・日奈久断層帯における一連の地震である．このうち，日奈久断層帯の南西部は「八代海区間」を構成している．地震は海底地すべり発生の引き金となるが，熊本地震発生後，海域での調査はほとんど行われていない．そこで，「白鳳丸」KH-18-3次研究航海において八代海で11本のピストンコア試料（PC01~PC11）を採泥した．また，海底地すべり堆積物の下層ではせん断強さが小さくなる（Flemings et al., 2012）ことから，せん断強さは海底地すべりの評価において重要な役割を果たす．本研究では，海底地すべりが発生した可能性の高い八代海のコア試料において，ベーンせん断試験でせん断強さを算出し，八代海の堆積物分布を考察した．

2. 手法

航海は2018年7月27日から7月30日の期間に八代海において学術研究船「白鳳丸」を利用して行われた．長さ6 m，直径7.5 cmの塩ビ管を用いてピストンコアラーによる11地点の採泥を行い，船上において6つのセクションに切り分けた．採取したコアは高知コアセンターに持ち込み物性測定を行った．CTスキャナとマルチセンサーコアロガー(MSCL)を用いた非破壊計測を行い，それぞれ内部構造の計測とγ線密度・帯磁率を測定した．CTスキャンの結果からはCT値を抽出した．その後肉眼記載を行い，非破壊計測のデータとあわせて柱状図を作成した．その後，1本のコアをアーカイブ（保存用）コアとワーキング（作業用）コアに半裁した．ベーンせん断試験は，肉眼記載後のワーキングコアにおいておよそ50 cm間隔で実施した．試験にはトルクメーターに取り付けた十字型のベーン（羽根）を使用した．ベーンを試料に押し込み，軸を水平に回転させて，試料を破断するのに要する最大モーメントからせん断強さを算出した．また，蛍光X線分析を行い，主要元素濃度を測定した．

3. 結果と考察

帯磁率

採取されたコアは主にオリーブ灰や黒の砂泥を基質とする．CT値と帯磁率，γ線密度は深さに伴って増加傾向にあった．しかし，帯磁率は周期的にピークを繰り返していることが結果からわかったため，ピークを一つのユニットとして層区分を行った．区分した層は八木ほか(2016)による高分解能地層探査断面図と井上ほか(2011)で採取されたピストンコアを用いて比較した．

©2019. Japan Geoscience Union. All Right Reserved.

地層探査断面図では，帯磁率によって区分した層と音波探査による層を対比させることが可能であった．八木ほか(2016)による解釈から，白神岩付近で採取したコアは最終氷期極相期~縄文海進時の堆積物を含むことがわかった．このように，本コアにおいて帯磁率の周期的なピークは堆積時の環境・堆積層を反映していることがわかった．

帯磁率を用いた井上ほか(2011)とのコア対比は概ね帯磁率が一致しており， PC02とPC06ではイベント層の推定が可能であった．推定されたイベント層では帯磁率が極大を示す傾向がある．鉄濃度はイベント層の前後で相対的に高くなる傾向がみられたことから，鉄の濃度を用いたイベント層の推定が可能であると考えられる．鉄の濃度がイベント層で変化する要因として，タービダイトの発生後は重い粒子が先に沈殿すると考えられ，重金属である鉄も早くに沈殿するためであると考えられる．

ベーンせん断強さ

そして，田浦-津奈木沖断層群の北東部に位置するPC01･PC02･PC07は深度に伴ってせん断強さが増加している．そのため，埋没による圧密が堆積物の強度増加の主要因であると考えられる．また，井上ほか（2011）の年代測定結果と比較したところ，年代のギャップがある部分でせん断強さの増加率が変化している．このことから，年代の違いによる圧密の影響を受けた堆積物であると考えられる．PC03については，下部の火山灰層が特異的なせん断強さを示すが，その他の層については深度に伴ってせん断強さが大きくなっている．PC04･PC05･PC06については，最上部のみせん断強さが小さいことから，上部の堆積物は削剥された可能性がある．田浦-津奈木沖断層群西部に位置するPC10には砂や礫といった粗粒分が堆積している．また，水俣沖断層群に位置するPC09･PC11はせん断強さと間隙率に相関関係がなく，せん断強さが深度に伴って増加するという傾向はみられない．PC11については，最上部に堆積した泥が削剥されて欠落していると考えられる．

キーワード：タービダイト、浅海堆積物、平成28年熊本地震
Keywords: turbidites, shallow marine deposits, 2016 Kumamoto earthquake

©2019. Japan Geoscience Union. All Right Reserved.

Identification of turbidites in the Yatsushiro Sea surface sediment core samples from non-destructive measurements: Hakuho-maru KH-18-3 Cruise, Yatsushiro Sea, Western Kyushu, Japan

*後藤 滝弥[1]、北村 有迅[2]、白鳳丸KH-18-3次研究航海 乗船研究者一同
*Ryoya Goto[1], Yujin Kitamura[2], Hakuho-maru KH-18-3 Cruise Scientist

1. 東京大学大気海洋研究所、2. 鹿児島大学大学院理工学研究科地球環境科学専攻
1. Atmosphere and Ocean Research Institute, The University of Tokyo, 2. Department of Earth and Environmental Sciences, Graduate School of Science, Kagoshima University

Submarine active faults in Yatsusiro Sea, western Kyushu, Japan, constitute the Yatsushiro section of Hinagu fault zone in its southwest end (AIST et al., 2011). The 2016 Kumamoto Earthquake was sourced from a part of active faults of the Futagawa-Hinagu fault zones (JMA, 2018), and survey has hardly conducted in the sea area after the earthquake occurrence. Earthquake shaking occasionally triggers turbidity currents by submarine landslides and resuspension of unconsolidated sediments on the seafloor (Ikehara et al., 2018). In recent years, the study of earthquake occurrence history using earthquake turbidites formed by turbidity currents is being conducted throughout the world. As earthquake-origin turbidity currents can take place in very gentle slope (e.g. the Mississippi-Delta 0.01°: D. B. Prior et al., 1978), its occurrence is sufficiently thought even in Yatsushiro Sea. However, any record of earthquake turbidites in this area has not been reported. In this study, identification of turbidites in the Yatsushiro Sea surface sediment core samples from non-destructive measurements.

Here we conducted four-days research cruise Hakuho-maru KH-18-3 in July, 2018. We conducted sub-bottom profiling on eight lines, piston coring at 11 sites in Yatsushiro Sea, western Kyushu, Japan. Recovered cores are analyzed by X-ray CT scanner, multi-sensor core logger, core imaging apparatus, visual core description, color spectroscope and X-ray fluorescence core scanner (Itrax) in the Center for Advanced Marine Core Research, Kochi University. With reference to the previous studies (Iwai et al., 2014, JGS abstract; Isabel Rodríguez-Germade et al, 2015; Okutsu et al., 2017, JGS abstract), the behavior of Ca/Ti and Fe/Ti where the peak was observed at the base of turbidites, and the behavior of Fe/Ti and Zr/Ti where the peak was observed at the base of volcaniclastics turbidites.

Our results revealed turbidites and volcaniclastics turbidites in six piston coring sites (PC01 to PC06). As all of sites are located in the Taura-Tsunagioki fault group or Minamataoki fault group, turbidites were considered to be present in all of sites. However, turbidites were identified from PC01 to PC06, but not identified from PC07 to PC11. According to Rifardi et al. (1998), PC01 to PC06 are located in the sea area where the deposition rate is high, and PC07 to PC11 are located in the sea area where the deposition rate is slow.

As turbidite is formed by various factors besides earthquakes, it is necessary to consider whether the turbidites identified in this study are earthquake turbidites. In addition, to investigate the history of earthquakes, it is also a future task to conduct individual sample measurements (such as grain size distribution analysis) and dating.

Hakuho-maru KH-18-3 Cruise Scientists: Takashi Tomiyasu, Hitoshi Kodamatani, Kuniyo Kawabata, Daiki

©2019. Japan Geoscience Union. All Right Reserved.

Oyama, Haruka Kageyama, Kaede Yamasaki (Kagoshima Univ.), Yuta Ikebata, Koki Hori (Kyushu Univ.), Asuka Yamaguchi, Fumiaki Tsunomori, Kameo Katsura, Tsubasa Miki, Natsumi Okutsu, Hiroaki Koge, Kotaro Fujita, Ayaka Nakazawa, Yuichi Okuma, Genki Kobayashi, Rina Fukuchi (Tokyo Univ.), Jun Kameda, Tomonori Morisaki (Hokkaido Univ.)

キーワード：海底地すべり、タービダイト、浅海堆積物、八代海、2016年熊本地震
Keywords: submarine landslides, turbidites, shallow sea deposits, Yatsushiro Sea, 2016 Kumamoto Earthquake

©2019. Japan Geoscience Union. All Right Reserved.

Revised columnar section based on grain size distribution analysis of samples from Hakuho-maru KH-18-3 in Yatsushiro sea

*池端 雄太[1]、北村 有迅[2]、白鳳丸KH-18-3次研究航海乗船研究者 Family
*Yuta Ikebata[1], Yujin Kitamura[2], Hakuho-maru KH-18-3 Scientists Family

1. 九州大学大学院理学府地球惑星科学専攻、2. 鹿児島大学大学院理工学研究科地球環境科学専攻
1. Kyusyu University Graduate School Of Science Earth and Planetary Science, 2. Graduate school of science, Kagoshima University

Hakuho-maru KH-18-3 was held in the Yatsushiro Sea from 27th to 30th July 2018 for clarifying history of occurrence of submarine landslides. Earthquake is a one of big trigger of submarine landslides, and submarine landslides occurs in an very easy slope. Kumamoto earthquake occurred at April, 2016 and a lot of surveys in the land area were conducted but survey in the sea area weren’ t conducted much. In the Yatsushiro sea, the occurrence of submarine landslides caused by earthquake of the Futagawa-Hinagu fault zones can be considered sufficiently. Therefore, in this study, the creation of the columnar section which is the basic information of the submarine landslide accreditation was made based on the grain size distribution analysis.

In the Expedition, eleven piston cores(6m) from PC01 to PC11 were collected in the southern part of Yatsushiro sea, and the obtained core was subjected to non-destructive measurement and individual sample measurement at the Kochi Core Center. For non-destructive measurement, CT images and core continuous images were taken, and for individual sample measurement, Density, Magnetic susceptibility, porosity, vane shear strength, color, concentration change of major elements were examined. Grain size distribution analysis was conducted at Kagoshima University. Samples used for grain size distribution analysis were collected every 50 cm and analyzed with a laser diffraction type grain size distribution analyzer. Since it is difficult to judge the stratum boundary only with the result of grain size distribution measurement at intervals of 50 cm, it was judged by using γ ray density, magnetic susceptibility and color measurement result which are continuous data.

Grain size distribution analysis revealed PC01 to PC07 are muddy cores and PC08 to PC11 contains much sand. Grain size of PC01, PC04, PC06, PC07, PC09, PC11 are very different in Grain size distribution analysis and visual core description. Based on the results of the grain size distribution analysis, the stratum boundary was determined from the change commonly seen in the γ ray density, magnetic susceptibility and color, and a columnar section was prepared. In Rifardi et al.(1998), the distribution of mud content in the Yatsushiro Sea has been surveyed. As a result of comparing the columnar map of this study with its distribution for each sampling point, cores excluding PC08 corresponded well. It is thought that it is influenced by the supply of sediment by river and stagnant water mass, tide current as in previous research. Also, in Inoue et al.(2011), which was a reference for determining the core harvest point, dating is done in the same area. At Hori(2019MS), we compare the data with Inoue et al.(2011) and estimate the core age of this research. We also compare the columnar section made in this study with the columnar section of Inoue et al.(2011), using the comparative categories determined at the time of estimating the age. As a result, PC01 and PC02 were in good agreement, PC06 and PC07 had different stratum in the surface layer. This is probably because the sampling site of PC06 is actually about 150 m far from Inoue et al.(2011) and the sampling site of PC07 is actually about 111 m far from Inoue et al.(2011), and the sedimentary environment is slightly different. Also, in the grain size distribution analysis of this study, there is a possibility that coarse grains may be

©2019. Japan Geoscience Union. All Right Reserved.

selectively left out when putting the sample into the machine, and it may be doubtful in accuracy.

キーワード：海底地すべり
Keywords: Submarine landslide

©2019. Japan Geoscience Union. All Right Reserved.

[E] ポスター発表 | セッション記号 H (地球人間圏科学)：H-DS 防災地球科学

2019年5月27日(月) 13:45 ~ 15:15 | ポスター会場 幕張メッセ国際展示場 8ホール_4

[H-DS12] Advanced Remote Sensing toward Mega-Disaster Response

コンビーナ:栄珠 郭(水災害リスクマネジメント国際センター)、竹内 渉(東京大学生産技術研究所)

Natural disaster under climate change is a serious threat to sustainable development, and in recent years natural disasters, i.e., hydro-geo-meteorological hazards and risks, have been frequently experienced in many countries by both developing and developed countries.
To achieve Sustainable Development Goals (SDGs), this session introduces papers focused on both principles and applications of remote sensing to promote investment in disaster risk reduction using integrated GIS and space infra data. Advanced remote sensing with Earth observation (EO) data appears to be the way forward in reducing damages and the death toll or affected people at local, national, regional and global levels.
We encourage the presentation of new research findings and novel approaches on land surface dynamics due to mega disasters between near-real time observation and long-term trends with water/hydrological cycle, such as floods, tropical cyclones (typhoons), storm surges, earthquakes, tsunamis, landslides, and wildfires.

[HDS12-P01] Satellite-based assessment of electricity restoration efforts in Puerto Rico after Hurricane Maria

*Miguel O Roman[1]、Eleanor Stokes[2,3]、Zhuosen Wang[2,3]、Virginia Kalb[3]、Ranjay Shrestha[4,3] (1.Earth from Space Institute, Universities Space Research Association、2.Earth System Science Interdisciplinary Center, University of Maryland、3.NASA Goddard Space Flight Center、4.Science Systems and Applications, Inc)

[HDS12-P02] **Flood inundation forecasting coupled with in-situ water level and satellite data**

*Young-Joo Kwak[1]、Jonggeol Park[2]、Wataru Takeuchi[3] (1.ICHARM-UNESCO: International Centre for Water Hazard And Risk Management、2.Tokyo University of Information and Sciences、3.University of Tokyo)

[HDS12-P03] バングラデッシュ海岸域における水害長期モニタリング
★招待講演

*朴 鍾杰[1]、栄珠 郭[2] (1.東京情報大学、2.土木研究所)

[HDS12-P04] Automatic shoreline detection and coastal change detection using multiple satellite data in Bangladesh

*Young-Joo Kwak[1] (1.ICHARM-UNESCO: International Centre for Water Hazard And Risk Management)

Satellite-based assessment of electricity restoration efforts in Puerto Rico after Hurricane Maria

*Miguel O Roman[1], Eleanor Stokes[2,3], Zhuosen Wang[2,3], Virginia Kalb[3], Ranjay Shrestha[4,3]

1. Earth from Space Institute, Universities Space Research Association, 2. Earth System Science Interdisciplinary Center, University of Maryland, 3. NASA Goddard Space Flight Center, 4. Science Systems and Applications, Inc

Understanding the distribution and duration of power outages after a disaster is a precursor to minimizing their harmful consequences, especially to vulnerable communities. Here, we use satellite-derived daily estimates of lights to monitor electricity restoration efforts in Puerto Rico following Hurricane Maria, which caused the longest blackout in US history. Within all settlements, we track how long it took to restore electricity, and assess the characteristics of communities that shouldered the most extended outages. Our results show an 80% decrease in lights, in total, immediately after Hurricane Maria. During the recovery, a disproportionate share of long-duration power failures (> 120 days) occurred in rural municipalities (41% of rural municipalities vs. 29% of urban municipalities), and in the northern and eastern districts. Unexpectedly, we also identify significant disparities in electricity recovery within municipalities. Land use, proximity to highways, and the structure and density of the built environment were all factors that influenced restoration times. For many urban municipalities, poor residents lived in less dense, detached housing—where power restoration lagged. The results demonstrate the capability of nighttime satellite imagery to monitor power availability at a high spatial resolution, linking monitoring efforts to neighborhood-scale demographic data. They also identify the unintended consequences of current density-based power restoration protocols. Through the integration of in-situ, satellite, and socioeconomic data products, disaster responses to long-term events can become more strategic to minimize harm, incorporating adaptive community capacity as an additional variable to determine where power should be restored.

Keywords: VIIRS DNB, Black Marble, nighttime lights, power outage detection, energy access, disaster risk reduction

©2019. Japan Geoscience Union. All Right Reserved.

Flood inundation forecasting coupled with in-situ water level and satellite data

*Young-Joo Kwak[1], Jonggeol Park[2], Wataru Takeuchi[3]

1. ICHARM-UNESCO: International Centre for Water Hazard And Risk Management, 2. Tokyo University of Information and Sciences, 3. University of Tokyo

With extreme weather events, catastrophic floods occur as one of the major disasters in the world. With the development of spaceborne optical and SAR (synthetic aperture radar) sensors, flood detection algorithms should be progressively developed to produce more accurate flood maps

Despite very limited satellite-based data, this study introduces good examples of snapshot flood detection and flood inundation forecasting focusing on short-term flood extent change using a new index-based flood algorithm with a synchronized floodwater index ($SfWI^2$). MODIS (MODerate resolution Imaging Spectroradiometer, NASA-USGS) time series data were mainly employed to detect the annual and potential flood extent of 2017. The pilot study was selected in the mega deltas over vast low-lying areas of Bangladesh and India (i.e., the 2017 flood in the basins of the Ganges, Brahmaputra and Magna rivers) As preliminary results, the resultant maps represented the dynamics of flood extent and flood propagation process. This approach shows a methodological possibility for instant and comprehensive flood mapping at the international river-basin level. For application to a global flood mapping, reliable satellite-derived flood maps will contribute flood risk management. In order to improve the accuracy of rapid flood mapping, we should solve many ambiguities in particular, surface complexity, i.e., urbanized mega-delta floodplains.

Keywords: Flood detection, Inundation forecasting, MODIS

©2019. Japan Geoscience Union. All Right Reserved.

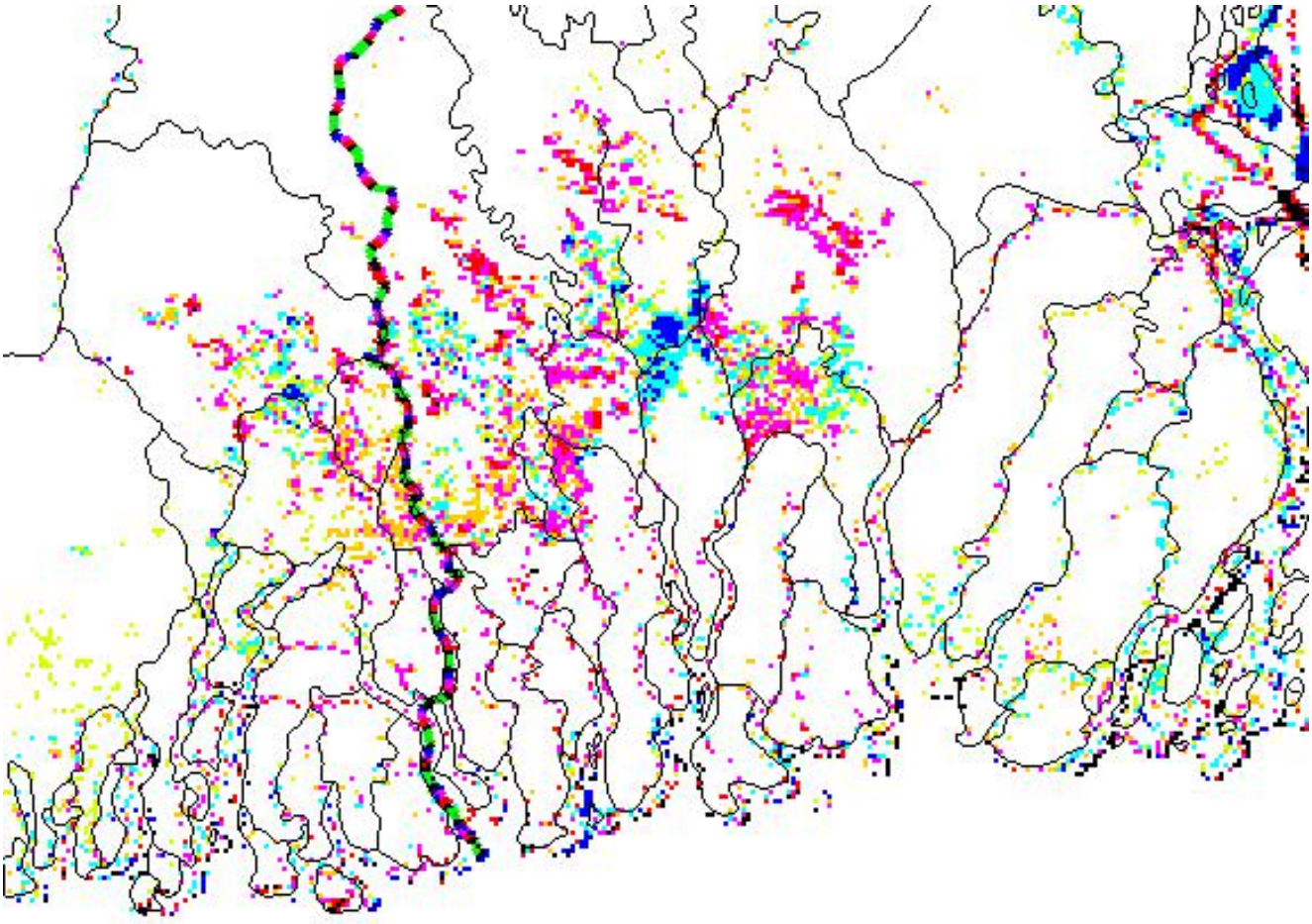
バングラデッシュ海岸域における水害長期モニタリング
Long term monitoring of flood damage in the coastal area of Bangladesh

*朴 鍾杰[1]、栄珠 郭[2]
*Park Jonggeol[1], Young-Joo Kwak[2]

1. 東京情報大学、2. 土木研究所
1. Tokyo University of Information Sciences, 2. ICHARM-UNESCO

本研究は15年間（2001年から2015年まで）のMOD13A2データを用いてバングラデシュの海岸域における洪水域変化傾向について調べた。MOD13A2データセットからNDVIとNDWIを計算し、さらに雲の影響を取り除くためにカルマンフィルタを用いた。水域検出はNDVIとNDWIを用いた判別分析によって求めた。年間水域検出データ（23旬）を用いて最大連続浸水期間を求め、最小二乗法による1次線形勾配を求めた。その結果、クルナ管区では増加傾向であることが分かった。

キーワード：洪水、MODISデータ、NDWI
Keywords: Flood, MODIS, NDWI



©2019. Japan Geoscience Union. All Right Reserved.

Automatic shoreline detection and coastal change detection using multiple satellite data in Bangladesh

*Young-Joo Kwak[1]

1. ICHARM-UNESCO: International Centre for Water Hazard And Risk Management

The Bangladesh government has been faced with the risk of coastal erosion as one of the urgent issues in land use planning and coastal management. As a preliminary investigation, an automated algorithm was proposed focusing on shoreline detection using multiple satellite data. The selected study site is located in the estuary of the Meghna River around the Gulf of Bengal in Bangladesh.

We employed Landsat-7, -8 data (90m and 30m spatial resolution, respectively) and ALOS, ALOS-2 (12.5m and 25m spatial resolution, respectively) to detect accurate coastal lines during the similar snapshot period.

As a result of automatic shoreline detection and coastal change detection by the interpretation and classification, the average rate of coastal line change was 0.5km (eroded) per year for the period between 2010 and 2019 in case of Meghna River along Noahkali (Noler Char). In addition, the resultant coastal change line was also verified by ground truth and field survey data using a small unmanned aerial vehicle (sUAV: Quadcopter with a flight control system, ©DJI Technology Co. Ltd., China) for comprehensive validation.

This feasibility study will continually investigate the characteristics of short-term and long-term changes with the relationship between hydrological parameters such as precipitation, river discharge, wave, and tidal effect.

Keywords: Shoreline detection, Coastal change

©2019. Japan Geoscience Union. All Right Reserved.

[E] ポスター発表 | セッション記号 H (地球人間圏科学)：H-DS 防災地球科学

2019年5月27日(月) 17:15 ~ 18:30 | ポスター会場 幕張メッセ国際展示場 8ホール_14

[H-DS12] Advanced Remote Sensing toward Mega-Disaster Response

コンビーナ:栄珠 郭(水災害リスクマネジメント国際センター)、竹内 渉(東京大学生産技術研究所)

Natural disaster under climate change is a serious threat to sustainable development, and in recent years natural disasters, i.e., hydro-geo-meteorological hazards and risks, have been frequently experienced in many countries by both developing and developed countries.
To achieve Sustainable Development Goals (SDGs), this session introduces papers focused on both principles and applications of remote sensing to promote investment in disaster risk reduction using integrated GIS and space infra data. Advanced remote sensing with Earth observation (EO) data appears to be the way forward in reducing damages and the death toll or affected people at local, national, regional and global levels.
We encourage the presentation of new research findings and novel approaches on land surface dynamics due to mega disasters between near-real time observation and long-term trends with water/hydrological cycle, such as floods, tropical cyclones (typhoons), storm surges, earthquakes, tsunamis, landslides, and wildfires.

[HDS12-P01] Satellite-based assessment of electricity restoration efforts in Puerto Rico after Hurricane Maria

*Miguel O Roman[1]、Eleanor Stokes[2,3]、Zhuosen Wang[2,3]、Virginia Kalb[3]、Ranjay Shrestha[4,3] (1.Earth from Space Institute, Universities Space Research Association、2.Earth System Science Interdisciplinary Center, University of Maryland、3.NASA Goddard Space Flight Center、4.Science Systems and Applications, Inc)

[HDS12-P02] **Flood inundation forecasting coupled with in-situ water level and satellite data**

*Young-Joo Kwak[1]、Jonggeol Park[2]、Wataru Takeuchi[3] (1.ICHARM-UNESCO: International Centre for Water Hazard And Risk Management、2.Tokyo University of Information and Sciences、3.University of Tokyo)

[HDS12-P03] バングラデッシュ海岸域における水害長期モニタリング
★招待講演

*朴 鍾杰[1]、栄珠 郭[2] (1.東京情報大学、2.土木研究所)

[HDS12-P04] Automatic shoreline detection and coastal change detection using multiple satellite data in Bangladesh

*Young-Joo Kwak[1] (1.ICHARM-UNESCO: International Centre for Water Hazard And Risk Management)

Satellite-based assessment of electricity restoration efforts in Puerto Rico after Hurricane Maria

*Miguel O Roman[1], Eleanor Stokes[2,3], Zhuosen Wang[2,3], Virginia Kalb[3], Ranjay Shrestha[4,3]

1. Earth from Space Institute, Universities Space Research Association, 2. Earth System Science Interdisciplinary Center, University of Maryland, 3. NASA Goddard Space Flight Center, 4. Science Systems and Applications, Inc

Understanding the distribution and duration of power outages after a disaster is a precursor to minimizing their harmful consequences, especially to vulnerable communities. Here, we use satellite-derived daily estimates of lights to monitor electricity restoration efforts in Puerto Rico following Hurricane Maria, which caused the longest blackout in US history. Within all settlements, we track how long it took to restore electricity, and assess the characteristics of communities that shouldered the most extended outages. Our results show an 80% decrease in lights, in total, immediately after Hurricane Maria. During the recovery, a disproportionate share of long-duration power failures (> 120 days) occurred in rural municipalities (41% of rural municipalities vs. 29% of urban municipalities), and in the northern and eastern districts. Unexpectedly, we also identify significant disparities in electricity recovery within municipalities. Land use, proximity to highways, and the structure and density of the built environment were all factors that influenced restoration times. For many urban municipalities, poor residents lived in less dense, detached housing—where power restoration lagged. The results demonstrate the capability of nighttime satellite imagery to monitor power availability at a high spatial resolution, linking monitoring efforts to neighborhood-scale demographic data. They also identify the unintended consequences of current density-based power restoration protocols. Through the integration of in-situ, satellite, and socioeconomic data products, disaster responses to long-term events can become more strategic to minimize harm, incorporating adaptive community capacity as an additional variable to determine where power should be restored.

Keywords: VIIRS DNB, Black Marble, nighttime lights, power outage detection, energy access, disaster risk reduction

©2019. Japan Geoscience Union. All Right Reserved.

Flood inundation forecasting coupled with in-situ water level and satellite data

*Young-Joo Kwak[1], Jonggeol Park[2], Wataru Takeuchi[3]

1. ICHARM-UNESCO: International Centre for Water Hazard And Risk Management, 2. Tokyo University of Information and Sciences, 3. University of Tokyo

With extreme weather events, catastrophic floods occur as one of the major disasters in the world. With the development of spaceborne optical and SAR (synthetic aperture radar) sensors, flood detection algorithms should be progressively developed to produce more accurate flood maps

Despite very limited satellite-based data, this study introduces good examples of snapshot flood detection and flood inundation forecasting focusing on short-term flood extent change using a new index-based flood algorithm with a synchronized floodwater index ($SfWI^2$). MODIS (MODerate resolution Imaging Spectroradiometer, NASA-USGS) time series data were mainly employed to detect the annual and potential flood extent of 2017. The pilot study was selected in the mega deltas over vast low-lying areas of Bangladesh and India (i.e., the 2017 flood in the basins of the Ganges, Brahmaputra and Magna rivers) As preliminary results, the resultant maps represented the dynamics of flood extent and flood propagation process. This approach shows a methodological possibility for instant and comprehensive flood mapping at the international river-basin level. For application to a global flood mapping, reliable satellite-derived flood maps will contribute flood risk management. In order to improve the accuracy of rapid flood mapping, we should solve many ambiguities in particular, surface complexity, i.e., urbanized mega-delta floodplains.

Keywords: Flood detection, Inundation forecasting, MODIS

©2019. Japan Geoscience Union. All Right Reserved.

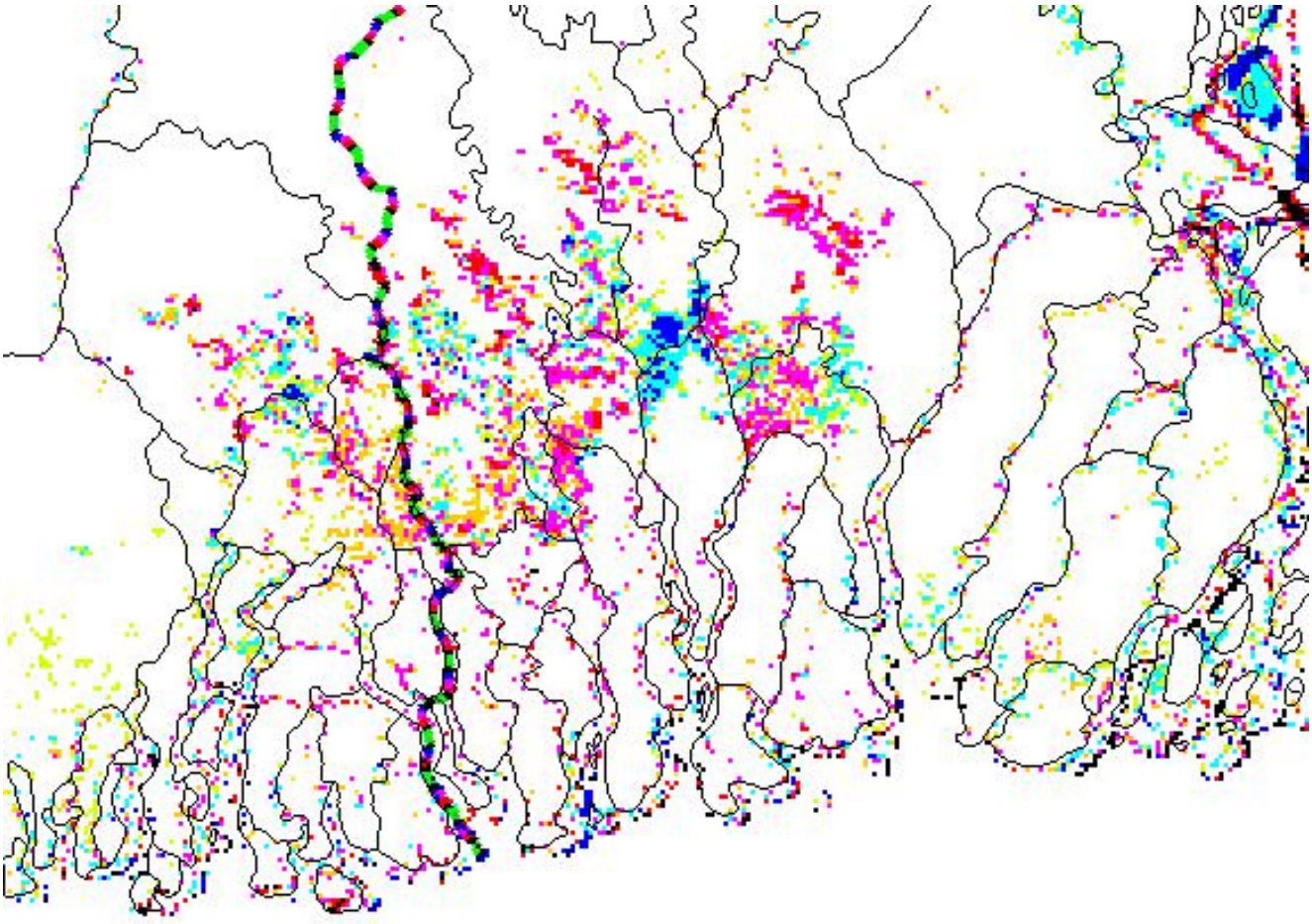
バングラデッシュ海岸域における水害長期モニタリング
Long term monitoring of flood damage in the coastal area of Bangladesh

*朴 鍾杰[1]、栄珠 郭[2]
*Park Jonggeol[1], Young-Joo Kwak[2]

1. 東京情報大学、2. 土木研究所
1. Tokyo University of Information Sciences, 2. ICHARM-UNESCO

本研究は15年間（2001年から2015年まで）のMOD13A2データを用いてバングラデシュの海岸域における洪水域変化傾向について調べた。MOD13A2データセットからNDVIとNDWIを計算し、さらに雲の影響を取り除くためにカルマンフィルタを用いた。水域検出はNDVIとNDWIを用いた判別分析によって求めた。年間水域検出データ（23旬）を用いて最大連続浸水期間を求め、最小二乗法による1次線形勾配を求めた。その結果、クルナ管区では増加傾向であることが分かった。

キーワード：洪水、MODISデータ、NDWI
Keywords: Flood, MODIS, NDWI



©2019. Japan Geoscience Union. All Right Reserved.

Automatic shoreline detection and coastal change detection using multiple satellite data in Bangladesh

*Young-Joo Kwak[1]

1. ICHARM-UNESCO: International Centre for Water Hazard And Risk Management

The Bangladesh government has been faced with the risk of coastal erosion as one of the urgent issues in land use planning and coastal management. As a preliminary investigation, an automated algorithm was proposed focusing on shoreline detection using multiple satellite data. The selected study site is located in the estuary of the Meghna River around the Gulf of Bengal in Bangladesh.

We employed Landsat-7, -8 data (90m and 30m spatial resolution, respectively) and ALOS, ALOS-2 (12.5m and 25m spatial resolution, respectively) to detect accurate coastal lines during the similar snapshot period.

As a result of automatic shoreline detection and coastal change detection by the interpretation and classification, the average rate of coastal line change was 0.5km (eroded) per year for the period between 2010 and 2019 in case of Meghna River along Noahkali (Noler Char). In addition, the resultant coastal change line was also verified by ground truth and field survey data using a small unmanned aerial vehicle (sUAV: Quadcopter with a flight control system, ©DJI Technology Co. Ltd., China) for comprehensive validation.

This feasibility study will continually investigate the characteristics of short-term and long-term changes with the relationship between hydrological parameters such as precipitation, river discharge, wave, and tidal effect.

Keywords: Shoreline detection, Coastal change

©2019. Japan Geoscience Union. All Right Reserved.

[E] ポスター発表 | セッション記号 H (地球人間圏科学)：H-CG 地球人間圏科学複合領域・一般

2019年5月27日(月) 15:30 ~ 17:00 | ポスター会場 幕張メッセ国際展示場 8ホール_9

[H-CG26] デルタとエスチュアリー：複雑な河口システムへの学際的取り組み

コンビーナ:齋藤 文紀(島根大学エスチュアリー研究センター)、Guan-Hong Lee(Inha University)、David L Dettman(University of Arizona)、堀 和明(名古屋大学環境学研究科地理学講座)

This session has foci on morphodynamics, material cycling, and sustainability in deltas and estuaries. We invite contributions that advance research on deltas and estuaries as complex river-mouth systems from modern and ancient examples, and that develop integrated frameworks for delta & estuary dynamics modeling on a broad range of temporal and spatial scales: from studies of coastal evolution over the Quaternary to small-scale sediment/material transport processes. We also invite physical processes studies based on field observations, numerical simulation and flume experiments. Finally, the conveners encourage contributions that promote data collection and sharing for both advancing science and local problem solving, that consider policy and governance issues linked to the sustainable development of deltas and estuaries, and that use in-situ and satellite data for modeling and risk assessment.

[HCG26-P01] Deltafront Clinoform of Abandoned Yellow River Delta in Jiangsu Province, China

*LIANGYONG ZHOU[1] (1.Qingdao Institute of Marine Geology China Geological Survey)

[HCG26-P02] Holocene evolution and Anthropocene destruction of the Krishna delta, east coast of India: delta lobe shifts, human impact, and sea-level history

Kakani Nageswara Rao[2]、*Yoshiki Saito[1]、K.Ch.V. Nagakumar[4]、Sumiko Kubo[3]、Shilpa Pandey[5]、 Zhen Li[6]、G. Demudu[2]、A.S. Rajawat[7] (1.Estuary Research Center, Shimane University、2.Andhra University、3.Waseda University、4.Centre for Water Resources and Management、5.Birbal Sahni Institute of Palaeosciences、6.University of Victoria、7.Space Applications Centre)

[HCG26-P03] 日本周辺の完新統中の海生生物遺体と陸生植物の放射性炭素年代値の差異

*中西 利典[1,2]、七山 太[3,4]、卜部 厚志[5]、堀 和明[6]、ホン ワン[7] (1.京都大学、2.日本原子力研究開発機構、3.産業技術総合研究所、4.熊本大学、5.新潟大学、6.名古屋大学、7.KIGAM)

[HCG26-P04] Assessment of MEIS for Marine Spatial Planning in the Nakdong River Estuary, Busan Metropolitan City, South Korea

*Jun-Ho Lee[1]、Han Jun Woo[1]、Hoi-Soo Jung[1]、Chan Mi Park[1] (1.Korea Institute of Ocean Science and Technology)

[HCG26-P05] Tidal changes at Asian deltas in response to future sea-level rise

*上原 克人[1] (1.九州大学)

[HCG26-P06] A governing equation of non-deltaic transgressive profile: 2D numerical simulation and flume experiments

*Junhui Wang[1,2,3]、Tetsuji Muto[3] (1.China University of Petroleum (Beijing)、2.State Key Laboratory of Petroleum Resources and Prospecting, China、3.Nagasaki University)

Deltafront Clinoform of Abandoned Yellow River Delta in Jiangsu Province, China

*LIANGYONG ZHOU[1]

1. Qingdao Institute of Marine Geology China Geological Survey

The abandoned Yellow River delta in Jiangsu province is a major sediment supplier to the South Yellow Sea and East China Sea. In this study, comparison of historical maps, two cores and three seismic profiles were used to examine its deltafront clinoform (nearshore clinoform). The original historical maps and nautical charts since AD 1750s were collected and compared after calibration, showing the accretion of the shoreline before 1855, when the Yellow River shifted to the Bohai Sea. Near Sheyang River mouth, two 20m-long cores onshore (1 m above present sea level) and offshore (6 m bellow present sea level) were on a line normal to the shoreline. Samples og both cores were dated using AMS ^{14}C and OSL(Optical Stimulated Luminescence) dating technologies. Ages in bottoms of the cores are 43000 to 44000 cal yr BP. At approximate 17.5m bellow present sea level in both cores, yellow and younger (younger than 5000 yr BP) silt sediment occurs. Several young ages in upper part of two cores were obtained, and these show a clear clinoform pattern. Furthermore, seismic profiles across the offshore core show the deltafront clinoform. The upper part weak reflector or transparent part in seismic profiles become thinner seaward and the lower part is strong reflectors. Sea bottom nearshore show a convex shape, but the seaward low gradient part show erosional gullies. The evolution of the deltafront clinoform was revealed in profiles and in plan view.

Keywords: Abandoned Yellow River Delta, Deltafront clinoform, C-14 ages, OSL ages

©2019. Japan Geoscience Union. All Right Reserved.

Holocene evolution and Anthropocene destruction of the Krishna delta, east coast of India: delta lobe shifts, human impact, and sea-level history

Kakani Nageswara Rao[2], *Yoshiki Saito[1], K.Ch.V. Nagakumar[4], Sumiko Kubo[3], Shilpa Pandey[5], Zhen Li[6], G. Demudu[2], A.S. Rajawat[7]

1. Estuary Research Center, Shimane University, 2. Andhra University, 3. Waseda University, 4. Centre for Water Resources and Management, 5. Birbal Sahni Institute of Palaeosciences, 6. University of Victoria, 7. Space Applications Centre

Holocene evolution of the Krishna delta was inferred using landform characteristics and 11 sediment cores with 59 Accelerator Mass Spectrometry ^{14}C dates. Landform assemblage in 5880 km^2area of the Krishna delta indicated the upper river-built fluvial plain and the lower marine-built beach-ridge delta plain with the maximum landwardbeach ridge located at~30 km from the shoreline separating the two plains. Sedimentary facies and their ages showed the Holocene marine sediment overlying the Pleistocene basement and progressively thickened seaward from <10 m to 25 m below the present sea level. The basal mangrove peat layers indicated that the sea level rose from −9 m to −3 m during 8.3–6.3 cal ky BP before stabilizing at the present level around 5 cal ky BP.
Considering the spatiotemporal variations of sediment facies and sediment accumulation rates and the configuration of the palaeo beach ridges (former shorelines), we surmised five major stages in the growth of 3539 km^2area of the Krishna delta beach-ridge plain during the last 6 cal ky BP with distinct lateral and seaward migration of delta lobes (depocentre shifts). Delta progradation was accelerated in the last 500 years, forming an out-building lobate delta. However, predominant erosion along the sediment-starved Krishna delta front coast during the past 50 years, due to impoundment of the riverine inputs at the burgeoning upstream dams pushed the Krishna delta into a persistent a destruction phase after ~6,000 years of delta progradation.

Keywords: Beach-ridge plain, Sedimentary facies, Delta lobes, Coastal erosion

©2019. Japan Geoscience Union. All Right Reserved.

日本周辺の完新統中の海生生物遺体と陸生植物の放射性炭素年代値の差異
Offset in radiocarbon ages between marine bioclast and terrestrial plant pairs in the Holocene sediments around Japan

*中西 利典[1,2]、七山 太[3,4]、卜部 厚志[5]、堀 和明[6]、ホン ワン[7]
*Nakanishi Toshimichi[1,2], Futoshi Nanayama[3,4], Atsushi Urabe[5], Kazuaki Hori[6], Wan Hong[7]

1. 京都大学、2. 日本原子力研究開発機構、3. 産業技術総合研究所、4. 熊本大学、5. 新潟大学、6. 名古屋大学、7. KIGAM
1. Kyoto Univ., 2. JAEA, 3. AIST, 4. Kumamoto Univ., 5. Niigata Univ., 6. Nagoya Univ., 7. KIGAM

放射性炭素（^{14}C）の海洋リザーバー効果の時空間変化を評価するために，日本周辺の完新統で同層準から採取した植物片と海生生物遺体の^{14}C年代値を比較検討する研究を進めてきた（Nakanishi et al. 2013, 2015, 2017abc）．これまで得られた100～10,200 cal BPのリザーバー年代は60～1100年であり，核実験以前に生成された試料から得られた値よりも明らかに大きなバラツキを持つことが示された．このことは地質や考古の海成試料の^{14}C年代値を編年する際には，現世の海洋リザーバー効果の補正だけでは不十分なことを示している．また，海洋リザーバー効果は，デルタやエスチュアリーといった複雑な河口システムの影響も反映していると考えられる．黒潮と対馬海流の影響する地域の間の海洋リザーバー効果の時間変化を直接的に捉えるために，宿毛平野，宮崎平野および隠岐諸島において採取した試料を検討した．それらの結果を大分平野，博多湾および韓国沿岸における既存研究の結果（Nakanishi et al. 2013, 2015, 2017abc）と比較する．この研究の一部に日本学術振興会の科学研究費補助金，基盤研究（B）18H01310を使用いたしました．

引用文献

Nakanishi T, Hong W, Sung KS, Lim J. 2013. Radiocarbon reservoir effect from shell and plant pair in Holocene sediments around the Yeongsan River in Korea. *Nuclear Instruments and Methods in Physics Research B* 294: 444–51.

Nakanishi T, Hong W, Sung KS, Sung KH, Nakashima R. 2015. Offsets in radiocarbon ages between plants and shells from same horizons of coastal sediments in Korea. *Nuclear Instruments and Methods in Physics Research B* 361: 670–9.

Nakanishi T, Hong W, Shimoyama S, Sato S, Park G, Lee JG. 2017a. Radiocarbon age offset between shell and plant pairs in the Holocene sediments under the Hakata Bay, western Japan. *Radiocarbon* 59 (2): 423–34.

Nakanishi T, Hong W, Sung KS, Nakashima R, Nahm WH, Lim J, Katsuki K. 2017b. Offset in radiocarbon age between plant and shell pairs in Holocene sediment around the Mae-ho Lagoon on the eastern coast of Korea. *Quaternary International* 447: 3–12.

Nakanishi T, Takemura K, Matsuyama H, Shimoyama S, Hong W, Okuno M. 2017c. Activity of the Funai fault and radiocarbon age offsets of shell and plant pairs from the latest Pleistocene to Holocene sediments beneath the Oita Plain, western Japan. *Radiocarbon* 59(6): 1737–48.

キーワード：放射性炭素年代、海洋リザーバー効果、完新世、黒潮
Keywords: Radiocarbon age, Marine reservoir effect, Holocene, Kuroshio Current

©2019. Japan Geoscience Union. All Right Reserved.

Assessment of MEIS for Marine Spatial Planning in the Nakdong River Estuary, Busan Metropolitan City, South Korea

*Jun-Ho Lee[1], Han Jun Woo[1], Hoi-Soo Jung[1], Chan Mi Park[1]

1. Korea Institute of Ocean Science and Technology

The Nakdong River has a length of nearly 510 km, with a drainage basin of around 23,400 km^2 in South Korea. The Nakdong River Estuary (NRE) in Busan city is a typical example of an estuary in which the throughput is manipulated artificially. The Noksan barrage, built in 1934, blocks the flow of the West Nakdong River, and the NRE barrage was completed between 1983 and 1987 to regulate the flow of the East Nakdong River. With the construction of several huge industrial complexes on reclaimed land near the NRE barrage in the last 65 years, the hydraulic circulation in the NRE has undergone dramatic changes in river discharge and geomorphic configuration, such as the formation of a series of barrier islands. In this study, marine environmental information system (MEIS) data collected after May 2015 were applied to support marine spatial planning (MSP) in the brackish water zone of NRE. The MEIS data in NRE consists of landscape classification of sub-environments, surface sediment distributions, characteristics of suspended sediment, short-term sedimentation, stratification index analysis in channels, closed circuit television (CCTV) using 4G long term evolution (LTE), automatic weather stations (AWS) in real time, calculated residual flow (R_f), net suspended sediment loads (Q_S), and net suspended sediment flux (F_S) in main stream inlet using mooring station, *etc*. The NRE could be divided into areas continuously managed by government, marine protected areas, areas for the development of marine attractions, areas conserved for research education, and coastal areas subject to safety management, e*tc*. For MSP, it was possible to use comparative data of the characteristics of environmental changes in the estuarine watershed to prepare the NRE for the partial opening or drainage extension in 2019 to 2021. This study aims to discuss how to predict environmental change after partial or full opening in NRE barrage and use ecological-based environmental maps in the process of MSP. The development of marine spatial planning mapping in NRE is much necessary for the nation at a time when the diversity of marine use and the demand for policies regarding marine space rapidly increase.

Keywords: Barrage, Busan, Estuary, Marine Environmental Information System, Marine Spatial Planning, Nakdong River Estuary

©2019. Japan Geoscience Union. All Right Reserved.

Assessment of MEIS for Marine Spatial Planning in the Nakdong River Estuary, Busan Metropolitan City, South Korea

Jun-Ho Lee[1] · Han Jun Woo[1] · Hoi-Soo Jung[1] · Chan Mi Park[1]

[1]Korean Seas Geosystem Research Unit, Korea Institute of Ocean Science & Technology, 385 Yeongdo, Busan 49111, Republic of Korea

The Nakdong River has a length of nearly 510 km, with a drainage basin of around 23,400 km^2 in South Korea. The Nakdong River Estuary (NRE) in Busan city is a typical example of an estuary in which the throughput is manipulated artificially. The Noksan barrage, built in 1934, blocks the flow of the West Nakdong River, and the NRE barrage was completed between 1983 and 1987 to regulate the flow of the East Nakdong River. With the construction of several huge industrial complexes on reclaimed land near the NRE barrage in the last 65 years, the hydraulic circulation in the NRE has undergone dramatic changes in river discharge and geomorphic configuration, such as the formation of a series of barrier islands. In this study, marine environmental information system (MEIS) data collected after May 2015 were applied to support marine spatial planning (MSP) in the brackish water zone of NRE. The MEIS data in NRE consists of landscape classification of sub-environments, surface sediment distributions, characteristics of suspended sediment, short-term sedimentation, stratification index analysis in channels, closed circuit television (CCTV) using 4G long term evolution (LTE), automatic weather stations (AWS) in real time, calculated residual flow (R_f), net suspended sediment loads (Q_S), and net suspended sediment flux (F_S) in main stream inlet using mooring station, *etc*. The NRE could be divided into areas continuously managed by government, marine protected areas, areas for the development of marine attractions, areas conserved for research education, and coastal areas subject to safety management, *etc*. For MSP, it was possible to use comparative data of the characteristics of environmental changes in the estuarine watershed to prepare the NRE for the partial opening or drainage extension in 2019 to 2021. This study aims to discuss how to predict environmental change after partial or full opening in NRE barrage and use ecological-based environmental maps in the process of MSP. The development of marine spatial planning mapping in NRE is much necessary for the nation at a time when the diversity of marine use and the demand for policies regarding marine space rapidly increase.

©2019. Japan Geoscience Union. All Right Reserved.

Tidal changes at Asian deltas in response to future sea-level rise

*上原 克人[1]
*Katsuto Uehara[1]

1. 九州大学
1. Kyushu University

A numerical model has been employed to assess the impact of sea level rise on tidal regimes in the East China Sea and the South China Sea with a special interest on tidal changes at around the deltaic region where the elevation is low and coasts are vulnerable to changes in water levels. The model covers the East and South China seas as a whole with a spatial resolution of 2 minutes (approx. 3 km). A preliminary result for the East China Sea suggests recognizable changes in the amplitude of M2 tides and M2 tidal currents at region such as Hangzhou Bay, the Changjiang Estuary and Haizhou Bay when the sea-level was raised by 1 m. Off the Changjiang Estuary, for example, tidal velocity increased for more than 10 cm/s at deep channels while decreased by about 5 cm/s on shoals. These results indicate that the sea-level rise may alter equilibrium among water currents and seafloor and modify the bottom topography of large estuaries and subaquatic deltas through the induced changes in tides and tidal currents.

キーワード：潮汐、中国海、海面上昇
Keywords: tides, china sea, sea level rise

©2019. Japan Geoscience Union. All Right Reserved.

A governing equation of non-deltaic transgressive profile: 2D numerical simulation and flume experiments

*Junhui Wang[1,2,3], Tetsuji Muto[3]

1. China University of Petroleum (Beijing), 2. State Key Laboratory of Petroleum Resources and Prospecting, China, 3. Nagasaki University

An alluvial river subject to relative sea level rise has a critical length (L_{crt}), beyond which the river can no longer sustain deltaic sedimentation but behaves to develop an estuarine environment. In such cases, there occurs non-deltaic rapid transgression. It is not difficult to imagine that non-deltaic transgression is pervasive in geological records, since most of the world large rivers would have “over-extended” to as far as the shelf edges during glacial or lowstand sea level periods. The configuration of non-deltaic transgressive profiles deserves a study because (1) it would provide a criterion for identifying non-deltaic transgression in the past and thus the fact of over-extension of the feeder alluvial river, and (2) it would constrain arguments on sediment transportation to the deep-water depositional systems.

Suppose that a river has an over-extended alluvial length of L ($>>L_{crt}$). During non-deltaic transgression, all the sediment fed by the river is consumed for alluvial aggradation and thus allocated in the subaerial realm. On the assumption that the supplied sediment is evenly distributed along the river profile which is approximately regarded as linear and has an averaged slope of α, the local transgressive slope Ψcan be expressed as:

$$\Psi = \alpha L / [L - \Lambda_{2D}(1+\alpha^2)^{0.5}] \quad (1)$$

We set an x–z coordinate system (x: basinward horizontal, z: vertical) that originates from the intersection of the initial horizontal line and the hinterland profile. Let x to be positive downstream and z to be positive upward. Equation 1 can be rewritten as:

$$\Psi_{x,z} = \alpha(\gamma x+z) / [(\gamma x+z) - \Lambda_{2D}(\gamma-\alpha)] \quad (2)$$

where $\gamma$is the averaged hinterland slope.

Equation 2 can be regarded as the derivative function of the governing equation of the non-deltaic transgressive profile, which can be expressed as:

$$\partial \eta_{x,z} / \partial x = \alpha(\gamma x+z) / [(\gamma x+z) - \Lambda_{2D}(\gamma-\alpha)] \quad (3)$$

where $\eta_{x,z}$ denotes the non-deltaic transgressive profile expressed as the pathway of shoreline. Note that sediment compaction is not considered.

Equation 3 can hardly be solved analytically but by numerical simulation. The solutions that we have obtained indicate that $\eta_{x,z}$ takes a concave-upward geometry with upstream-increasing gradient.

To test our numerical model, a series of 2D physical experiments was performed at Nagasaki University. The experiments were conducted using a 4 m-long and 2.0 cm-wide, open flume, from the upstream end of which sediment and water were fed at constant rates. Before each experimental run, we built a sufficiently long river profile inside the flume, to model the initial over-extended alluvial river ($L >> L_{crt}$). The initial river lengths were different by runs (L_0, ranging from 120–350 cm) and were set to be within a range of 0.139–0.158 (α). The hinterland slope was set as a constant value of 0.612 (γ). In each run, there occurred non-deltaic transgression as soon as base level started to rise.

©2019. Japan Geoscience Union. All Right Reserved.

Any of the resulting profiles of non-deltaic transgression shows a concave-upward geometry. The downstream end of the profile was tangent to the initial river profile (thus $\alpha \sim \Psi$). To the upstream, Ψ gradually increased, and approached a value as large as γ when the alluvial river was sufficiently shortened. The non-deltaic transgressive profiles generated in the experiments match well with the numerical model, implying that equation 3 can account for the non-deltaic transgressive profile in nature.

Keywords: Autostratigraphy, Non-deltaic transgressive profile, Numerical simulation, Flume experiments

©2019. Japan Geoscience Union. All Right Reserved.

[E] ポスター発表 | セッション記号 H (地球人間圏科学)：H-CG 地球人間圏科学複合領域・一般

2019年5月27日(月) 17:15 ~ 18:30 | ポスター会場 幕張メッセ国際展示場 8ホール_16

[H-CG26] デルタとエスチュアリー：複雑な河口システムへの学際的取り組み

コンビーナ:齋藤 文紀(島根大学エスチュアリー研究センター)、Guan-Hong Lee(Inha University)、David L Dettman(University of Arizona)、堀 和明(名古屋大学環境学研究科地理学講座)

This session has foci on morphodynamics, material cycling, and sustainability in deltas and estuaries. We invite contributions that advance research on deltas and estuaries as complex river-mouth systems from modern and ancient examples, and that develop integrated frameworks for delta & estuary dynamics modeling on a broad range of temporal and spatial scales: from studies of coastal evolution over the Quaternary to small-scale sediment/material transport processes. We also invite physical processes studies based on field observations, numerical simulation and flume experiments. Finally, the conveners encourage contributions that promote data collection and sharing for both advancing science and local problem solving, that consider policy and governance issues linked to the sustainable development of deltas and estuaries, and that use in-situ and satellite data for modeling and risk assessment.

[HCG26-P01] Deltafront Clinoform of Abandoned Yellow River Delta in Jiangsu Province, China

*LIANGYONG ZHOU[1] (1.Qingdao Institute of Marine Geology China Geological Survey)

[HCG26-P02] Holocene evolution and Anthropocene destruction of the Krishna delta, east coast of India: delta lobe shifts, human impact, and sea-level history

Kakani Nageswara Rao[2]、*Yoshiki Saito[1]、K.Ch.V. Nagakumar[4]、Sumiko Kubo[3]、Shilpa Pandey[5]、 Zhen Li[6]、G. Demudu[2]、A.S. Rajawat[7] (1.Estuary Research Center, Shimane University、2.Andhra University、3.Waseda University、4.Centre for Water Resources and Management、5.Birbal Sahni Institute of Palaeosciences、6.University of Victoria、7.Space Applications Centre)

[HCG26-P03] 日本周辺の完新統中の海生生物遺体と陸生植物の放射性炭素年代値の差異

*中西 利典[1,2]、七山 太[3,4]、卜部 厚志[5]、堀 和明[6]、ホン ワン[7] (1.京都大学、2.日本原子力研究開発機構、3.産業技術総合研究所、4.熊本大学、5.新潟大学、6.名古屋大学、7.KIGAM)

[HCG26-P04] Assessment of MEIS for Marine Spatial Planning in the Nakdong River Estuary, Busan Metropolitan City, South Korea

*Jun-Ho Lee[1]、Han Jun Woo[1]、Hoi-Soo Jung[1]、Chan Mi Park[1] (1.Korea Institute of Ocean Science and Technology)

[HCG26-P05] Tidal changes at Asian deltas in response to future sea-level rise

*上原 克人[1] (1.九州大学)

[HCG26-P06] A governing equation of non-deltaic transgressive profile: 2D numerical simulation and flume experiments

*Junhui Wang[1,2,3]、Tetsuji Muto[3] (1.China University of Petroleum (Beijing)、2.State Key Laboratory of Petroleum Resources and Prospecting, China、3.Nagasaki University)

Deltafront Clinoform of Abandoned Yellow River Delta in Jiangsu Province, China

*LIANGYONG ZHOU[1]

1. Qingdao Institute of Marine Geology China Geological Survey

The abandoned Yellow River delta in Jiangsu province is a major sediment supplier to the South Yellow Sea and East China Sea. In this study, comparison of historical maps, two cores and three seismic profiles were used to examine its deltafront clinoform (nearshore clinoform). The original historical maps and nautical charts since AD 1750s were collected and compared after calibration, showing the accretion of the shoreline before 1855, when the Yellow River shifted to the Bohai Sea. Near Sheyang River mouth, two 20m-long cores onshore (1 m above present sea level) and offshore (6 m bellow present sea level) were on a line normal to the shoreline. Samples og both cores were dated using AMS ^{14}C and OSL(Optical Stimulated Luminescence) dating technologies. Ages in bottoms of the cores are 43000 to 44000 cal yr BP. At approximate 17.5m bellow present sea level in both cores, yellow and younger (younger than 5000 yr BP) silt sediment occurs. Several young ages in upper part of two cores were obtained, and these show a clear clinoform pattern. Furthermore, seismic profiles across the offshore core show the deltafront clinoform. The upper part weak reflector or transparent part in seismic profiles become thinner seaward and the lower part is strong reflectors. Sea bottom nearshore show a convex shape, but the seaward low gradient part show erosional gullies. The evolution of the deltafront clinoform was revealed in profiles and in plan view.

Keywords: Abandoned Yellow River Delta, Deltafront clinoform, C-14 ages, OSL ages

©2019. Japan Geoscience Union. All Right Reserved.

Holocene evolution and Anthropocene destruction of the Krishna delta, east coast of India: delta lobe shifts, human impact, and sea-level history

Kakani Nageswara Rao[2], *Yoshiki Saito[1], K.Ch.V. Nagakumar[4], Sumiko Kubo[3], Shilpa Pandey[5], Zhen Li[6], G. Demudu[2], A.S. Rajawat[7]

1. Estuary Research Center, Shimane University, 2. Andhra University, 3. Waseda University, 4. Centre for Water Resources and Management, 5. Birbal Sahni Institute of Palaeosciences, 6. University of Victoria, 7. Space Applications Centre

Holocene evolution of the Krishna delta was inferred using landform characteristics and 11 sediment cores with 59 Accelerator Mass Spectrometry ^{14}C dates. Landform assemblage in 5880 km^2area of the Krishna delta indicated the upper river-built fluvial plain and the lower marine-built beach-ridge delta plain with the maximum landwardbeach ridge located at~30 km from the shoreline separating the two plains. Sedimentary facies and their ages showed the Holocene marine sediment overlying the Pleistocene basement and progressively thickened seaward from <10 m to 25 m below the present sea level. The basal mangrove peat layers indicated that the sea level rose from −9 m to −3 m during 8.3–6.3 cal ky BP before stabilizing at the present level around 5 cal ky BP.
Considering the spatiotemporal variations of sediment facies and sediment accumulation rates and the configuration of the palaeo beach ridges (former shorelines), we surmised five major stages in the growth of 3539 km^2area of the Krishna delta beach-ridge plain during the last 6 cal ky BP with distinct lateral and seaward migration of delta lobes (depocentre shifts). Delta progradation was accelerated in the last 500 years, forming an out-building lobate delta. However, predominant erosion along the sediment-starved Krishna delta front coast during the past 50 years, due to impoundment of the riverine inputs at the burgeoning upstream dams pushed the Krishna delta into a persistent a destruction phase after ~6,000 years of delta progradation.

Keywords: Beach-ridge plain, Sedimentary facies, Delta lobes, Coastal erosion

©2019. Japan Geoscience Union. All Right Reserved.

日本周辺の完新統中の海生生物遺体と陸生植物の放射性炭素年代値の差異
Offset in radiocarbon ages between marine bioclast and terrestrial plant pairs in the Holocene sediments around Japan

*中西 利典[1,2]、七山 太[3,4]、卜部 厚志[5]、堀 和明[6]、ホン ワン[7]
*Nakanishi Toshimichi[1,2], Futoshi Nanayama[3,4], Atsushi Urabe[5], Kazuaki Hori[6], Wan Hong[7]

1. 京都大学、2. 日本原子力研究開発機構、3. 産業技術総合研究所、4. 熊本大学、5. 新潟大学、6. 名古屋大学、7. KIGAM
1. Kyoto Univ., 2. JAEA, 3. AIST, 4. Kumamoto Univ., 5. Niigata Univ., 6. Nagoya Univ., 7. KIGAM

放射性炭素（^{14}C）の海洋リザーバー効果の時空間変化を評価するために，日本周辺の完新統で同層準から採取した植物片と海生生物遺体の^{14}C年代値を比較検討する研究を進めてきた（Nakanishi et al. 2013, 2015, 2017abc）．これまで得られた100～10,200 cal BPのリザーバー年代は60～1100年であり，核実験以前に生成された試料から得られた値よりも明らかに大きなバラツキを持つことが示された．このことは地質や考古の海成試料の^{14}C年代値を編年する際には，現世の海洋リザーバー効果の補正だけでは不十分なことを示している．また，海洋リザーバー効果は，デルタやエスチュアリーといった複雑な河口システムの影響も反映していると考えられる．黒潮と対馬海流の影響する地域の間の海洋リザーバー効果の時間変化を直接的に捉えるために，宿毛平野，宮崎平野および隠岐諸島において採取した試料を検討した．それらの結果を大分平野，博多湾および韓国沿岸における既存研究の結果（Nakanishi et al. 2013, 2015, 2017abc）と比較する．この研究の一部に日本学術振興会の科学研究費補助金，基盤研究（B）18H01310を使用いたしました．

引用文献

Nakanishi T, Hong W, Sung KS, Lim J. 2013. Radiocarbon reservoir effect from shell and plant pair in Holocene sediments around the Yeongsan River in Korea. *Nuclear Instruments and Methods in Physics Research B* 294: 444–51.

Nakanishi T, Hong W, Sung KS, Sung KH, Nakashima R. 2015. Offsets in radiocarbon ages between plants and shells from same horizons of coastal sediments in Korea. *Nuclear Instruments and Methods in Physics Research B* 361: 670–9.

Nakanishi T, Hong W, Shimoyama S, Sato S, Park G, Lee JG. 2017a. Radiocarbon age offset between shell and plant pairs in the Holocene sediments under the Hakata Bay, western Japan. *Radiocarbon* 59 (2): 423–34.

Nakanishi T, Hong W, Sung KS, Nakashima R, Nahm WH, Lim J, Katsuki K. 2017b. Offset in radiocarbon age between plant and shell pairs in Holocene sediment around the Mae-ho Lagoon on the eastern coast of Korea. *Quaternary International* 447: 3–12.

Nakanishi T, Takemura K, Matsuyama H, Shimoyama S, Hong W, Okuno M. 2017c. Activity of the Funai fault and radiocarbon age offsets of shell and plant pairs from the latest Pleistocene to Holocene sediments beneath the Oita Plain, western Japan. *Radiocarbon* 59(6): 1737–48.

キーワード：放射性炭素年代、海洋リザーバー効果、完新世、黒潮
Keywords: Radiocarbon age, Marine reservoir effect, Holocene, Kuroshio Current

©2019. Japan Geoscience Union. All Right Reserved.

Assessment of MEIS for Marine Spatial Planning in the Nakdong River Estuary, Busan Metropolitan City, South Korea

*Jun-Ho Lee[1], Han Jun Woo[1], Hoi-Soo Jung[1], Chan Mi Park[1]

1. Korea Institute of Ocean Science and Technology

The Nakdong River has a length of nearly 510 km, with a drainage basin of around 23,400 km^2 in South Korea. The Nakdong River Estuary (NRE) in Busan city is a typical example of an estuary in which the throughput is manipulated artificially. The Noksan barrage, built in 1934, blocks the flow of the West Nakdong River, and the NRE barrage was completed between 1983 and 1987 to regulate the flow of the East Nakdong River. With the construction of several huge industrial complexes on reclaimed land near the NRE barrage in the last 65 years, the hydraulic circulation in the NRE has undergone dramatic changes in river discharge and geomorphic configuration, such as the formation of a series of barrier islands. In this study, marine environmental information system (MEIS) data collected after May 2015 were applied to support marine spatial planning (MSP) in the brackish water zone of NRE. The MEIS data in NRE consists of landscape classification of sub-environments, surface sediment distributions, characteristics of suspended sediment, short-term sedimentation, stratification index analysis in channels, closed circuit television (CCTV) using 4G long term evolution (LTE), automatic weather stations (AWS) in real time, calculated residual flow (R_f), net suspended sediment loads (Q_S), and net suspended sediment flux (F_S) in main stream inlet using mooring station, *etc*. The NRE could be divided into areas continuously managed by government, marine protected areas, areas for the development of marine attractions, areas conserved for research education, and coastal areas subject to safety management, e*tc*. For MSP, it was possible to use comparative data of the characteristics of environmental changes in the estuarine watershed to prepare the NRE for the partial opening or drainage extension in 2019 to 2021. This study aims to discuss how to predict environmental change after partial or full opening in NRE barrage and use ecological-based environmental maps in the process of MSP. The development of marine spatial planning mapping in NRE is much necessary for the nation at a time when the diversity of marine use and the demand for policies regarding marine space rapidly increase.

Keywords: Barrage, Busan, Estuary, Marine Environmental Information System, Marine Spatial Planning, Nakdong River Estuary

©2019. Japan Geoscience Union. All Right Reserved.

Assessment of MEIS for Marine Spatial Planning in the Nakdong River Estuary, Busan Metropolitan City, South Korea

Jun-Ho Lee[1] · Han Jun Woo[1] · Hoi-Soo Jung[1] · Chan Mi Park[1]

[1]Korean Seas Geosystem Research Unit, Korea Institute of Ocean Science & Technology, 385 Yeongdo, Busan 49111, Republic of Korea

The Nakdong River has a length of nearly 510 km, with a drainage basin of around 23,400 km^2 in South Korea. The Nakdong River Estuary (NRE) in Busan city is a typical example of an estuary in which the throughput is manipulated artificially. The Noksan barrage, built in 1934, blocks the flow of the West Nakdong River, and the NRE barrage was completed between 1983 and 1987 to regulate the flow of the East Nakdong River. With the construction of several huge industrial complexes on reclaimed land near the NRE barrage in the last 65 years, the hydraulic circulation in the NRE has undergone dramatic changes in river discharge and geomorphic configuration, such as the formation of a series of barrier islands. In this study, marine environmental information system (MEIS) data collected after May 2015 were applied to support marine spatial planning (MSP) in the brackish water zone of NRE. The MEIS data in NRE consists of landscape classification of sub-environments, surface sediment distributions, characteristics of suspended sediment, short-term sedimentation, stratification index analysis in channels, closed circuit television (CCTV) using 4G long term evolution (LTE), automatic weather stations (AWS) in real time, calculated residual flow (R_f), net suspended sediment loads (Q_S), and net suspended sediment flux (F_S) in main stream inlet using mooring station, *etc*. The NRE could be divided into areas continuously managed by government, marine protected areas, areas for the development of marine attractions, areas conserved for research education, and coastal areas subject to safety management, *etc*. For MSP, it was possible to use comparative data of the characteristics of environmental changes in the estuarine watershed to prepare the NRE for the partial opening or drainage extension in 2019 to 2021. This study aims to discuss how to predict environmental change after partial or full opening in NRE barrage and use ecological-based environmental maps in the process of MSP. The development of marine spatial planning mapping in NRE is much necessary for the nation at a time when the diversity of marine use and the demand for policies regarding marine space rapidly increase.

©2019. Japan Geoscience Union. All Right Reserved.

Tidal changes at Asian deltas in response to future sea-level rise

*上原 克人[1]
*Katsuto Uehara[1]

1. 九州大学
1. Kyushu University

A numerical model has been employed to assess the impact of sea level rise on tidal regimes in the East China Sea and the South China Sea with a special interest on tidal changes at around the deltaic region where the elevation is low and coasts are vulnerable to changes in water levels. The model covers the East and South China seas as a whole with a spatial resolution of 2 minutes (approx. 3 km). A preliminary result for the East China Sea suggests recognizable changes in the amplitude of M2 tides and M2 tidal currents at region such as Hangzhou Bay, the Changjiang Estuary and Haizhou Bay when the sea-level was raised by 1 m. Off the Changjiang Estuary, for example, tidal velocity increased for more than 10 cm/s at deep channels while decreased by about 5 cm/s on shoals. These results indicate that the sea-level rise may alter equilibrium among water currents and seafloor and modify the bottom topography of large estuaries and subaquatic deltas through the induced changes in tides and tidal currents.

キーワード：潮汐、中国海、海面上昇
Keywords: tides, china sea, sea level rise

©2019. Japan Geoscience Union. All Right Reserved.

A governing equation of non-deltaic transgressive profile: 2D numerical simulation and flume experiments

*Junhui Wang[1,2,3], Tetsuji Muto[3]

1. China University of Petroleum (Beijing), 2. State Key Laboratory of Petroleum Resources and Prospecting, China, 3. Nagasaki University

An alluvial river subject to relative sea level rise has a critical length (L_{crt}), beyond which the river can no longer sustain deltaic sedimentation but behaves to develop an estuarine environment. In such cases, there occurs non-deltaic rapid transgression. It is not difficult to imagine that non-deltaic transgression is pervasive in geological records, since most of the world large rivers would have “over-extended” to as far as the shelf edges during glacial or lowstand sea level periods. The configuration of non-deltaic transgressive profiles deserves a study because (1) it would provide a criterion for identifying non-deltaic transgression in the past and thus the fact of over-extension of the feeder alluvial river, and (2) it would constrain arguments on sediment transportation to the deep-water depositional systems.

Suppose that a river has an over-extended alluvial length of L ($>>L_{crt}$). During non-deltaic transgression, all the sediment fed by the river is consumed for alluvial aggradation and thus allocated in the subaerial realm. On the assumption that the supplied sediment is evenly distributed along the river profile which is approximately regarded as linear and has an averaged slope of α, the local transgressive slope Ψcan be expressed as:

$$\Psi = \alpha L / [L - \Lambda_{2D}(1+\alpha^2)^{0.5}] \quad (1)$$

We set an x–z coordinate system (x: basinward horizontal, z: vertical) that originates from the intersection of the initial horizontal line and the hinterland profile. Let x to be positive downstream and z to be positive upward. Equation 1 can be rewritten as:

$$\Psi_{x,z} = \alpha(\gamma x+z) / [(\gamma x+z) - \Lambda_{2D}(\gamma-\alpha)] \quad (2)$$

where $\gamma$is the averaged hinterland slope.

Equation 2 can be regarded as the derivative function of the governing equation of the non-deltaic transgressive profile, which can be expressed as:

$$\partial \eta_{x,z} / \partial x = \alpha(\gamma x+z) / [(\gamma x+z) - \Lambda_{2D}(\gamma-\alpha)] \quad (3)$$

where $\eta_{x,z}$ denotes the non-deltaic transgressive profile expressed as the pathway of shoreline. Note that sediment compaction is not considered.

Equation 3 can hardly be solved analytically but by numerical simulation. The solutions that we have obtained indicate that $\eta_{x,z}$ takes a concave-upward geometry with upstream-increasing gradient.

To test our numerical model, a series of 2D physical experiments was performed at Nagasaki University. The experiments were conducted using a 4 m-long and 2.0 cm-wide, open flume, from the upstream end of which sediment and water were fed at constant rates. Before each experimental run, we built a sufficiently long river profile inside the flume, to model the initial over-extended alluvial river ($L >> L_{crt}$). The initial river lengths were different by runs (L_0, ranging from 120–350 cm) and were set to be within a range of 0.139–0.158 (α). The hinterland slope was set as a constant value of 0.612 (γ). In each run, there occurred non-deltaic transgression as soon as base level started to rise.

©2019. Japan Geoscience Union. All Right Reserved.

Any of the resulting profiles of non-deltaic transgression shows a concave-upward geometry. The downstream end of the profile was tangent to the initial river profile (thus $\alpha \sim \Psi$). To the upstream, Ψ gradually increased, and approached a value as large as γ when the alluvial river was sufficiently shortened. The non-deltaic transgressive profiles generated in the experiments match well with the numerical model, implying that equation 3 can account for the non-deltaic transgressive profile in nature.

Keywords: Autostratigraphy, Non-deltaic transgressive profile, Numerical simulation, Flume experiments

©2019. Japan Geoscience Union. All Right Reserved.

[E] ポスター発表 | セッション記号 S (固体地球科学)：S-SS 地震学

2019年5月27日(月) 13:45 ~ 15:15 | ポスター会場 幕張メッセ国際展示場 8ホール_5

[S-SS07] Rigorous Seismicity Modelling and Hypothesis Testing

コンビーナ:庄 建倉(統計数理研究所)、Schorlemmer Danijel(GFZ German Research Centre for Geosciences)、Matt Gerstenberger(GNS Science)、鶴岡 弘(東京大学地震研究所)

Probabilistic models have been developed for describing, analyzing, and forecasting seismicity since more than 100 years and, with the advent of large-scale digital networks, in high resolution during the last 30 years. These models include recurrence and stress-release models for long-term earthquake hazard assessment, and short-term models describing earthquake clustering, e.g. the ETAS model. Some models have become standard tools in seismic hazard assessment. However, the overall probabilities remain on the low end and the uncertainties of the forecasts are not well described. Rigorous data-based development and testing of models will help further improving forecasting power and accuracy of these models. Similarly, new hypotheses shall be evaluated rigorously using some existing model as the null hypothesis model or in dedicated tests addressing the hypothesis directly. In this context, the Collaboratory for the Study of Earthquake Predictability and its Japan branch provides the necessary testing capabilities for rigorous and unbiased evaluation of models and hypotheses. This session focuses on research that increases information on seismicity, being with respect to a reference model or as an independent hypothesis. We solicit contributions of model developments and hypothesis formulation based on the increased understanding of the physical process of earthquakes, such as the preparation and rupture processes of the earthquake source and the interaction between earthquakes and tectonic environments. We also welcome development and implementation of improved statistical methods for testing and validating physical hypotheses based on observed data. In particular, we welcome contributions about model- or hypothesis-test experiments that could be implemented in the Japan testing center.

[SSS07-P01] Development of Physics-based Ground Motion Simulation in A Hybrid Approach and Applications to Seismic Hazard Assessment in Taiwan

*Hsieh Ming-Che[1]、Yen Yin-Tung[1]、Ma Kuo-Fong[2,3] (1.Disaster Prevention Technology Research Center, Sinotech Engineering Consultants (Inc.), Taiwan、2.Department of Earth Sciences, National Central University, Taiwan、3.Earthquake-Disaster & Risk Evaluation and Management Center, National Central University, Taiwan)

[SSS07-P02] Increasing Earthquake Forecast Testability - CSEP Future Developments

*Danijel Schorlemmer[1]、Naoshi Hirata[2]、Fabrice Cotton[1]、Matt Gerstenberger[3]、Thomas Jordan[7]、Warner Marzocchi[4]、William Savran[7]、Maximilian Werner[5]、Stefan Wiemer[6]、Thomas Beutin[1]、David D Jackson[8]、Philip Maechling[7]、Sum Mak[1]、Kazuyoshi Nanjo[9]、Yosihiko Ogata[10]、David Rhoades[3]、Hiroshi Tsuruoka[2]、Graeme Weatherill[1]、Jiancang Zhuang[10] (1.GFZ German Research Centre for Geosciences、2.Earthquake Research Institute, University of Tokyo, Japan、3.GNS Science, Lower Hutt, New Zealand、4.University of Naples, Naples, Italy、5.University of Bristol, Bristol, United Kingdom、6.ETH Zurich, Zurich, Switzerland、7.University of Southern California, Los Angeles, USA、8.University of California Los Angeles, Los Angeles, USA、9.University of Shizuoka, Shizuoka, Japan、10.Institute of Statistical Mathematics, Tachikawa, Japan)

[SSS07-P03] Precision versus uncertainty in regional seismic hazard mapping

*Gerstenberger Matt[1]、Schorlemmer Danijel[2] (1.GNS Science、2.GFZ-Potsdam)

[SSS07-P04] An extreme value analysis of seismograms designed for early forecast of aftershocks

*澤崎 郁[1] (1.防災科学技術研究所)

[SSS07-P05] Spatio-temporal clustering of successive earthquakes: data analyses of global data.

*THYSTERE MATONDO BANTIDI[1]、Takeshi Nishimura[1] (1.Tohoku University)

[SSS07-P06] CSEPJapanにおける関東3ヶ月予測結果

*鶴岡 弘[1]、平田 直[1] (1.東京大学地震研究所)

[SSS07-P07] Long-term earthquake risk in North China estimated from a modern catalogue

熊 子瑶[2]、*庄 建倉[1]、周 仕勇[2] (1.統計数理研究所、2.北京大学)

[SSS07-P08] **Distributions of focal mechanisms in background seismicity and earthquake clusters in Japan**

*庄 建倉[1,2]、蒔田 恵理[2] (1.統計数理研究所、2.総合大学院大学)

[SSS07-P09] New Ground Motion Prediction Equations for Western Saudi Arabia

*木内 亮太[1,2]、Walter Mooney[1]、Hani Zahran[3] (1.U.S. Geological Survey、2.京都大学防災研究所、3.Saudi Geological Survey)

[SSS07-P10] Study on the spatial and temporal change of velocity structure before and after 2003 Chengkung earthquake, Taiwan

*TING YA LIANG[1]、Wen-Yen Chang[1,2,3]、Strong Wen[4] (1.National DONG HWA University、2.Eastern Taiwan Earthquake Research Center、3.National Center for Research on Earthquake Engineering、4.National Chung Cheng University)

Development of Physics-based Ground Motion Simulation in A Hybrid Approach and Applications to Seismic Hazard Assessment in Taiwan

Development of Physics-based Ground Motion Simulation in A Hybrid Approach and Applications to Seismic Hazard Assessment in Taiwan

*Hsieh Ming-Che[1]、Yen Yin-Tung[1]、Ma Kuo-Fong[2,3]
*Ming-Che Hsieh[1], Yin-Tung Yen[1], Kuo-Fong Ma[2,3]

1. Disaster Prevention Technology Research Center, Sinotech Engineering Consultants (Inc.), Taiwan、2. Department of Earth Sciences, National Central University, Taiwan、3. Earthquake-Disaster & Risk Evaluation and Management Center, National Central University, Taiwan
1. Disaster Prevention Technology Research Center, Sinotech Engineering Consultants (Inc.), Taiwan, 2. Department of Earth Sciences, National Central University, Taiwan, 3. Earthquake-Disaster & Risk Evaluation and Management Center, National Central University, Taiwan

Damages to engineering structures by an earthquake depend on the entire time history of the ground motion, which is affected by a number of factors including source-rupture process, seismic-wave velocity structure, topographic relief, and local site condition. To quantitatively assess these effects to ground motion, physics-based ground motion simulation is a powerful tool which enables rigorous modeling of each effect and their coupling. In this study, we present a recent-developed physics-based ground motion simulator in generating broadband seismograms for seismic hazard assessment. The simulator is essentially based on a hybrid approach in which long-period synthetics are calculated by the efficient 3-D strain Green’s tensor (SGT) and short-period synthetics are modeled by the stochastic method. Physical effects of (1) source slip distribution, (2) seismic wave propagation, (3) surface topography and (4) site amplification are taken into account. This hybrid approach has been validated by the 2016 M_W6.6 Meinong earthquake in southern Taiwan and reveals good potential for engineering applications. We also carried out simulations to model rupture scenarios of seismogenic structure and subduction zone sources. Output full waveform and ground motion parameters, e.g. peak ground acceleration (PGA) and 1.0-s-period spectral acceleration (SA1.0), have been further implemented to risk estimation, and even earthquake drill. Our result shows the ground motion simulator has the potential for earthquake scenario modeling and hazard assessment.

キーワード：Ground motion simulation、Seismic hazard assessment、Strain Green’s tensor、Stochastic method
Keywords: Ground motion simulation, Seismic hazard assessment, Strain Green’s tensor, Stochastic method

©2019. Japan Geoscience Union. All Right Reserved.

Increasing Earthquake Forecast Testability - CSEP Future Developments

*Danijel Schorlemmer[1], Naoshi Hirata[2], Fabrice Cotton[1], Matt Gerstenberger[3], Thomas Jordan[7], Warner Marzocchi[4], William Savran[7], Maximilian Werner[5], Stefan Wiemer[6], Thomas Beutin[1], David D Jackson[8], Philip Maechling[7], Sum Mak[1], Kazuyoshi Nanjo[9], Yosihiko Ogata[10], David Rhoades[3], Hiroshi Tsuruoka[2], Graeme Weatherill[1], Jiancang Zhuang[10]

1. GFZ German Research Centre for Geosciences, 2. Earthquake Research Institute, University of Tokyo, Japan, 3. GNS Science, Lower Hutt, New Zealand, 4. University of Naples, Naples, Italy, 5. University of Bristol, Bristol, United Kingdom, 6. ETH Zurich, Zurich, Switzerland, 7. University of Southern California, Los Angeles, USA, 8. University of California Los Angeles, Los Angeles, USA, 9. University of Shizuoka, Shizuoka, Japan, 10. Institute of Statistical Mathematics, Tachikawa, Japan

The Collaboratory for the Study of Earthquake Predictability (CSEP) has expanded over the years to many different testing areas hosted at multiple testing centers. Hundreds of earthquake forecast models have been submitted to CSEP and are being tested. New testing metrics were developed and implemented and a lot of progress was made to establish CSEP as an institution that cannot be ignored when issuing earthquake forecasts. Its rigor and independence became the standard in evaluating earthquake forecasts and in reporting on the results.

In the framework of the testing activities of the Global Earthquake Model, one line of expanding the capabilities of CSEP was developed at GFZ Potsdam. The group there applied the mechanisms that CSEP introduced to earthquake forecast models to the area of intensity prediction equations (IPEs) and ground-motion prediction equations (GMPEs). The first truly prospective tests were carried out on IPEs for Italy and also on GMPEs for Japan and New Zealand. This new set of tests helped CSEP move into the hazard domain and increase the relevance of its results to the hazard community. Finally, the group at GFZ Potsdam has also conducted the first prospective test of the US national seismic hazard maps.

Although these tests have been successful and well-received, they have also shown the limitations of the CSEP approach. Many aspects of seismic hazard or earthquake forecasting remain inherently untestable if only the model forecasts are tested and not the model ingredients. We propose to continue along the lines of the GFZ Potsdam developments and create new areas of activity for CSEP, namely targeted experiments that cannot be conducted with the current CSEP software system. As part of the eGSIM (European Ground Shaking Intensity Models) service, we will introduce permanent testing of IPEs and GMPEs to the testing center to establish strong performance records to be used in hazard models. Further targeted experiments include the predictive power of b-values, discrimination of foreshocks for short-term forecasting, as well as a deeper look into precursory
phenomena applying CSEP-style rigorous testing. We support including testability in future hazard models or their components to move to better testable seismic hazard models. Finally, to expand into the risk domain, we will test exposure models against new and independent data.

Keywords: Seismicity, Forecasting, Testing

©2019. Japan Geoscience Union. All Right Reserved.

Precision versus uncertainty in regional seismic hazard mapping

Precision versus uncertainty in regional seismic hazard mapping

*Gerstenberger Matt[1]、Schorlemmer Danijel[2]
*Matt Gerstenberger[1], Danijel Schorlemmer[2]

1. GNS Science、2. GFZ-Potsdam
1. GNS Science, 2. GFZ-Potsdam

Regional and national seismic hazard mapping efforts have increasingly pursued more detailed and precise models and outputs, particularly in terms of source characterisation and modelling. With increasing precision comes increasing uncertainty. In recent years much attention has been paid to modelling uncertainty in ground-motion models and including this in seismic hazard modelling. However, much less effort has been made to quantify and model uncertainty in seismic source characterisation. This raises two questions: 1) is increasing precision appropriate when uncertainty remains poorly quantified? 2) what is the optimal balance between precision and uncertainty? Ultimately the answer to this depends on the end-uses of the models and the implications of increasing uncertainty with increasing precision. Here we explore some of the main sources of uncertainty in seismic source characterisation such as incomplete and limited records of earthquake occurrence in paleoseismic data and earthquake catalogues, non-stationarity of seismicity and the poisson assumption, fault source characterisation and so-called moment balancing. We pay particular focus to uncertainties in estimating hazard in less seismically active regions and the implications for building design guidance.

キーワード：Seismic hazard、PSHA、uncertainty
Keywords: Seismic hazard, PSHA, uncertainty

©2019. Japan Geoscience Union. All Right Reserved.

An extreme value analysis of seismograms designed for early forecast of aftershocks

*澤崎 郁[1]
*Kaoru Sawazaki[1]

1. 防災科学技術研究所
1. National Research Institute for Earth Science and Disaster Resilience

Conventional aftershock forecasting has been operated through applying the Gutenberg-Richter and Omori-Utsu laws to an earthquake catalog. However, catalog’ s quality is influenced by detectability of earthquake signals (P or S waves), which causes degradation of the catalog in the early stage after a large earthquake and at regions which are sparsely covered by seismograph network. This eventually causes the catalog’ s nonuniformity and limitation of the forecasting performance.

In this study, we propose a new approach designed for high-performance early aftershock forecasting without using earthquake catalog. Instead, we use a continuous seismogram recorded at each station. First, we pick the maximum amplitude of the seismogram obtained in every assigned time interval (e.g., 1 minute). This picking process can be completely automated and is rarely affected by overlap of multiple seismic signals occurring in approximately the same time. We empirically derive a probability distribution (PD) that accounts for the frequency of the maximum amplitudes. This PD is essentially a non-stationary extreme value distribution derived from the generalized Pareto distribution (GPD) and the Omori-Utsu type temporal decay. We optimize three parameters that control the PD shape (K_a: parameter that controls whole aftershock activity, p_a: parameter that controls temporal decay of the aftershock frequency, m: parameter that controls power-law decay of the maximum amplitude) by applying the maximum likelihood estimation to the observed maximum amplitudes. By extrapolating the optimized PD, we estimate the number of maximum amplitudes that will exceed a threshold value within arbitral time interval in the future. The proposed approach provides forecast of peak ground motion at each station rather than magnitude, which is directly desired for public use. Moreover, the forecasted peak ground motion may automatically incorporate many factors that cannot be described by a simple ground motion attenuation model (e.g., site amplification, radiation pattern, rupture directivity, and so on).

We apply the proposed method to 25 Hi-net seismograms recorded the 2016 Kumamoto earthquakes in Japan. We set the learning periods every one hour after the mainshock (Mj7.3), and set the forecasting period within 24 hours after the end of each learning period. We find that parameters K_a and m become temporally stable within a few hours after the mainshock at many stations. On the other hand, the parameter p_a temporally varies more probably because the induced seismicity at northeast area (Aso and Oita regions) strongly affects the apparent temporal decay rate of the amplitudes. Within 3 hours after the mainshock, the forecasted number of the maximum amplitudes exceeding 10^{-4} m/s is within 0.5 to 2.0 times the actual observation for about 80 % of the used stations. For the threshold amplitude of 10^{-3} m/s, on the other hand, the forecasted number tends to overestimate, probably due to saturation of seismograms by both artificial and physical reasons.

キーワード：極値解析、余震予測、最大地震動
Keywords: extreme value analysis, aftershock forecasting, peak ground motion

©2019. Japan Geoscience Union. All Right Reserved.

Spatio-temporal clustering of successive earthquakes: data analyses of global data.

*THYSTERE MATONDO BANTIDI[1], Takeshi Nishimura[1]

1. Tohoku University

Spatio-temporal clustering of seismicity is an interesting phenomenon in the earthquake generation process. We investigate the earthquakes closely occurring in space and time, which have been sometimes observed at various regions. A recent example is *Mw*6.5 earthquake at Hinagu active fault on April 14, 2016, followed by a *Mw*7.3 at Futagawa active fault on April 16. The present study analyzes moderate and large earthquakes to clarify characteristics of such successive occurrence of earthquakes.

We use the Global Centroid Moment Tensor catalog for the period from 1976 to 2016. Earthquakes with moment magnitudes (*Mw*) of larger or equal to 5.0 and with depths less than or equal to 70 km are analyzed. The earthquakes that occur within some horizontal distance ranges (Δd*:* from 10 to 500 km*)*, and lapse times (Δt=30, 180 and 365 days*)* from the occurrence of each target earthquake is grouped in a cluster, and the number of clusters are counted.

The results show that cumulative numbers of clusters almost constantly increase in the logarithmic scale with increasing Δt, and the number of clusters increases constantly in general with increasing Δd. For example, for the *Mw* 5.0 –5.5, the cumulative number of clusters at Δd*=100* km are 3177, 4525 and 4808, respectively, for Δt of 30, 180 and 365 days.

To examine whether or not these successive earthquakes occur randomly, in other words, whether or not these successive earthquakes occur under some physical conditions, we compare the observed results with simulations in which earthquakes are set to randomly occur in time. The results show that the observed cumulative numbers of clusters are larger than those of simulation in short distance ranges. The former gradually approach to the latter with increasing the horizontal distance, and merge into a same number at a distance, which is defined as “triggering distance” in the present study. As Δt increases, the occurrence probability decreases and approaches to the normal condition in which the occurrence time intervals of earthquakes obey a Poisson distribution. For example, the triggering distances of Mw5.0-5.5 are 420 km and 66 km, respectively, for Δt*=30* days and *365* days. The results obtained by changing the parameters related to the spatial and temporal distributions of aftershock show no significant difference in the number of clusters and triggering distances.

Keywords: Clustering, Successive earthquakes, Triggering distance

©2019. Japan Geoscience Union. All Right Reserved.

CSEPJapanにおける関東3ヶ月予測結果
Kanto 3 month testing class results of CSEP Japan

*鶴岡 弘[1]、平田 直[1]
*Hiroshi Tsuruoka[1], Naoshi Hirata[1]

1. 東京大学地震研究所
1. Earthquake Research Institute, Tokyo Univ.

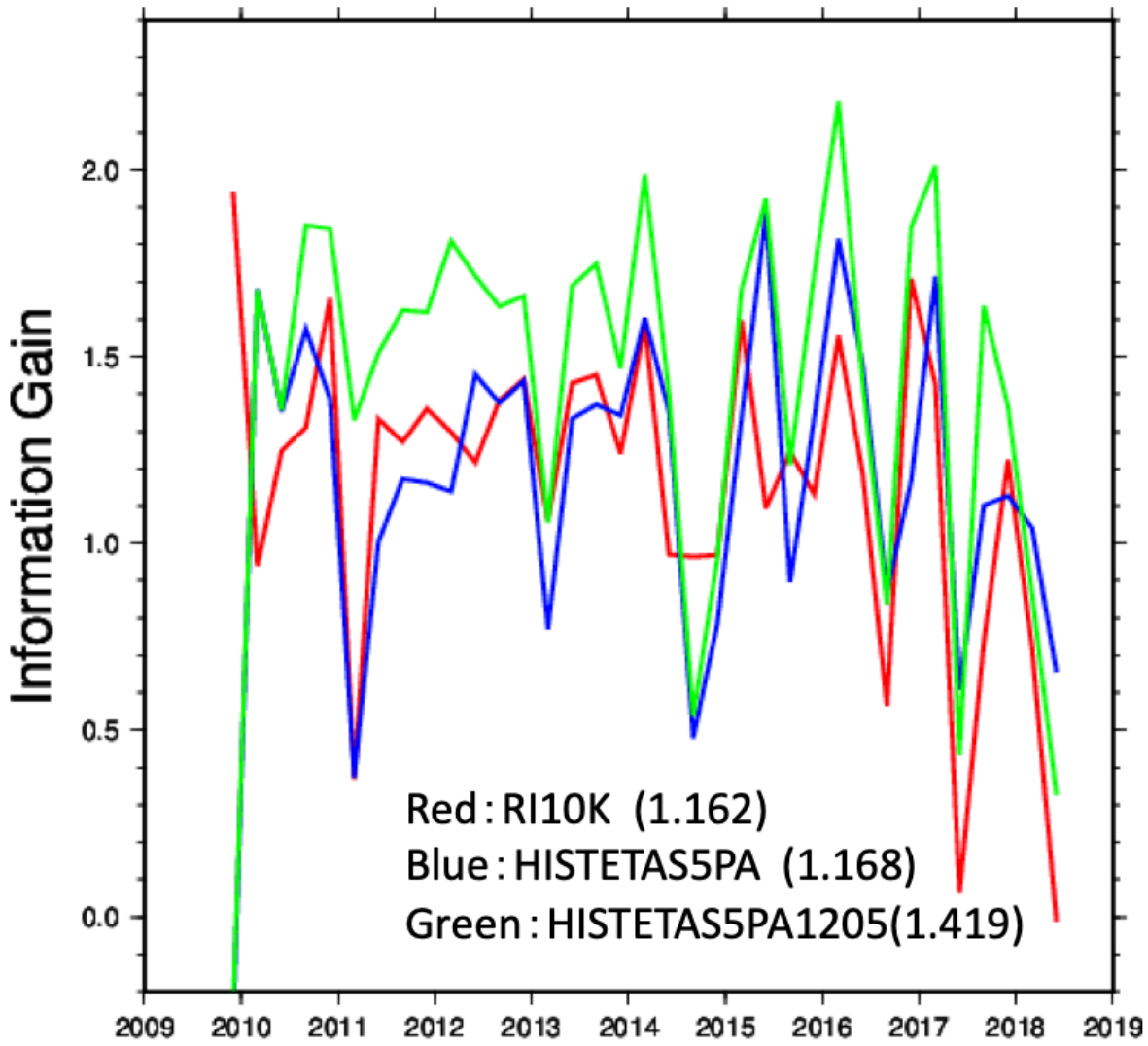
CSEP Japan における関東テスト領域の3ヶ月テスト結果を報告する．モデルは，RI10K，HISTETAS5PAおよびHISTETAS5PA1205である．HISTETAS5PA1205は東北地方太平洋沖地震後にテストセンターに投稿されたモデルとなる．テスト結果は，2009年11月1日からの約40ラウンド分である．

CSEPの標準テスト結果は，2017/5/1-8/1のラウンドにおいて，RI10KはS-testをパスしていなかった．また，観測地震数が少ない場合にすべてのモデルでN-Testをパスしていないラウンド等もあった．全ラウンドの各モデル毎の地震1個あたりの情報利得値の平均を計算するとHISTETAS5PA1205, HISTETAS5PA, RI10Kそれぞれ1.419, 1.168, 1.162であった．地震数の予測についてはHISTETA5PA1205は観測地震数をよく予測しているが，他のモデルは学習期間における平均発生数となるためあまりあっていないことがわかる．

複数ラウンドの結果から，地震数の予測についてモデル毎の対応が異なっておりこの精度向上は予測モデルの向上に直結する．また，モデルの評価は、空間予測性能と地震数の予測性能を評価することでよく把握できると思われる．

キーワード：地震予測可能性、CSEP
Keywords: Earthquake Predictability, CSEP

©2019. Japan Geoscience Union. All Right Reserved.



©2019. Japan Geoscience Union. All Right Reserved.

Long-term earthquake risk in North China estimated from a modern catalogue

Long-term earthquake risk in North China estimated from a modern catalogue

熊 子瑶[2]、*庄 建倉[1]、周 仕勇[2]
Ziyao Xiong[2], *Jiancang Zhuang[1], Shiyong Zhou[2]

1. 統計数理研究所、2. 北京大学
1. Institute of Statistical Mathematics, 2. Peking University

In this study, to obtain optimal estimates of the earthquake hazard in North China based on the modern earthquake catalogue, we used two variable kernel function estimation methods and two spatial tessellation methods to calculate the total and background seismic spatial occurrence rates for the study area.

The first problem of this study is to derive the best estimate of the long-term earthquake risk in North China. To address the first problem, we use the kernel function estimation methods of Stock and Smith (2002) and Zhuang et al. (2002), the Bayesian Delaunay-Tessellation Smoothing Method used by Ogata (ODTB) (2003, 2004), and ICVT to estimate the total earthquake hazard for North China. The results were compared and analyzed through the cross-validation method, to ensure accurate reflection of the seismic activity in North China. The sophisticated ODTB method is more stable than the others, but is relatively expensive, in terms of computation demands, while Zhuang et al.’s kernel estimate and the new ICVT method are able to provide reasonable estimates and easier to implement.

For the second problem, of b-value, we use Ogata’s method (2004, 2015) based on free nodes, to calculate the *b*-value spatial distribution. We expect that the obtained results of the spatial distribution of seismic risk and *b*-value provide a reference for the evaluation and prediction of large earthquakes and stress distribution in the study area.

For the third problem, we use two methods to estimate background seismic rates, and compare the results. The first method uses the result of the background seismic event probability, calculated by the epidemic-type aftershock sequence (ETAS) model (Zhuang et al., 2002; Zhuang, 2011), to simulate the background seismic risk distribution. The second method is to calculate the spatial distribution of earthquake hazard by using the HIST-ETAS model (Ogata, 2004).

Using comparative analyses and simulation experiments, we show that all of methods give similar spatial patterns of seismic occurrences.

キーワード：地震リスク、分割、常時地震活動、ETASモデル
Keywords: seismic risk, tessellation, background seismicity, ETAS model

©2019. Japan Geoscience Union. All Right Reserved.

Distributions of focal mechanisms in background seismicity and earthquake clusters in Japan

Distributions of focal mechanisms in background seismicity and earthquake clusters in Japan

*庄 建倉[1,2]、蒔田 恵理[2]
*Jiancang Zhuang[1,2], Eri Maita[2]

1. 統計数理研究所、2. 総合大学院大学
1. Institute of Statistical Mathematics, 2. Graduate University for Advanced Studies

This study tries to find the probability distributions of focal mechanisms in background seismicity and earthquake clusters in Japan by analyzing F-net data. To describe the probability distribution, each focal mechanism is discomposed as the result of a rotation about a particular pole starting from a reference focal mechanism. In this study, DC4 symmetry is considered, i.e., either nodal-plane can be the fault plane and the two sides of the fault plane are distinguishable.

To separate the background and clustering seismicity, we fit the space-time ETAS model (e.g., Zhuang et al, 2011) to the earthquakes with magnitude 4.2+ from 1997 to 2017 in the F-net catalog, and use the stochastic declustering method to estimate the background probabilities that each event is a background event and the triggered probabilities that each event is triggered by other events.

For the background events, the reference focal mechanism is taken as the average focal mechanism in each area, calculated by the method in Kagan (2014). The ration angles between a background event and the mean focal mechanisms at *(x, y)* is reconstructed by

$\zeta(\Delta) \propto \sum_j \phi_j I$(Rotation angle betwen j and the mean focal mechanism is within $(\Delta-\delta, \Delta+\delta)$),

where j runs over all background events near x,y, δ is a small number, and ϕj is the background probability estimated from fitting the space-time ETAS model. For the triggered events, the reference focal mechanism is naturally taken the focal mechanism of the event which triggers it. The rotation angles between the parent event and its direct offspring are reconstructed by

$\xi(\Delta) \propto \sum_{i,j} \rho_{i,j} I$(Rotation angle betwen i and j is within $(\Delta-\delta, \Delta+\delta)$) .

where i and j run over all the event pairs in the catalog, ρij is the probability that event j is triggered by event i estimated based on the ETAS model.

We find that the rotation poles are almost uniformly distributed. The reconstructed results for the rotation angles are shown in Figure 1.

Figure 1 (a) mean focal mechanisms of background seismicity in Japan. (b) Reconstructed distribution of rotation angles for focal mechanisms in the background seismicity and triggered seismicity.

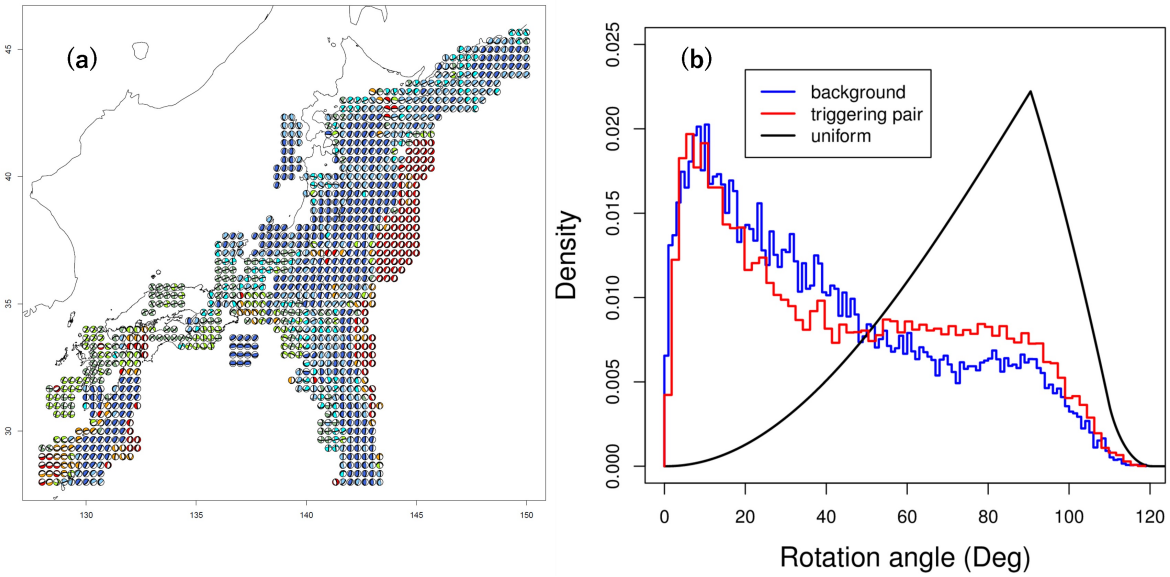
References:

Zhuang J., (2011) , *Next-day earthquake forecasts for the Japan region generated by the ETAS model.*

©2019. Japan Geoscience Union. All Right Reserved.

Earth Planets Space, 63, 207-216. doi:10.5047/eps.2010.12.010.
Kagan Y.Y. and Jackson D. D. (2014) Statistical earthquake focal mechanism forecasts. **Geophys. J. Int.** 197, 620–629. doi: 10.1093/gji/ggu015

キーワード：地震機構、確率分布、地震クラスター、常時地震、ETASモデル
Keywords: earthquake focal mechanism, probability distribution, earthquake cluster, background seismcity, ETAS model



©2019. Japan Geoscience Union. All Right Reserved.

New Ground Motion Prediction Equations for Western Saudi Arabia

*木内 亮太[1,2]、Walter Mooney[1]、Hani Zahran[3]
*Ryota Kiuchi[1,2], Walter Mooney[1], Hani Zahran[3]

1. U.S. Geological Survey、2. 京都大学防災研究所、3. Saudi Geological Survey
1. U.S. Geological Survey, 2. Disaster Prevenetion Research Institute, Kyoto University, 3. Saudi Geological Survey

We developed Ground Motion Prediction Equations (GMPEs) for western Saudi Arabia using 2770 selected records of PGA and PGV from 177 earthquakes of magnitude 3.0 –5.4, recorded at 58 stations in the distance range from 1 km to 400 km. Our GMPEs are developed based on one of the NGA-West2 Project GMPEs (Boore et al., 2014) by employing a mixed effects regression model.

Saudi Arabia is surrounded by several active tectonic regions, including an extension in the Red Sea and left-lateral strike-slip motion in the Gulf of Aqaba and along the Dead Sea Transform Fault (DSTF). In this area, multiple seismic swarms in and around volcanic fields, also known as harrats, have been detected over the past several decades (El-Isa and Shanti, 1989). The most recent large earthquake swarm in the region, which included more than 30,000 earthquakes, occurred from April to June 2009 beneath the volcanic field of Harrat Lunayyir in northwestern Saudi Arabia. The strongest seismic activity occurred May 13-19, 2009 and consisted of events M > 4 (Pallister et al., 2010). The largest earthquake occurred on May 19th, ML 5.4 as estimated by the SGS (Saudi Geological Survey) and Mw 5.7 by the USGS.

The NGA-West2 project used as a reference model mainly consists of shallow crustal earthquakes in active tectonic regions, rather than extensional earthquakes, such as those observed in Saudi Arabia. This deficiency is corrected by calculating a magnitude scaling of the new Saudi Arabia GMPEs compared to those of Boore et al. (2014). Furthermore, there is a clear difference in distance scaling for the Arabian GMPEs in comparison with the NGA-West2 GMPEs. This difference is especially significant at large distances and is mainly due to lower anelastic attenuation in the crystalline crust of western Saudi Arabia. Our empirical data demonstrate that the GMPEs presented here are in good agreement with observed earthquake ground motions in western Saudi Arabia.

キーワード：GMPE、Saudi Arabia、Seismic Hazard
Keywords: GMPE, Saudi Arabia, Seismic Hazard

©2019. Japan Geoscience Union. All Right Reserved.

Study on the spatial and temporal change of velocity structure before and after 2003 Chengkung earthquake, Taiwan

*TING YA LIANG[1], Wen-Yen Chang[1,2,3], Strong Wen[4]

1. National DONG HWA University, 2. Eastern Taiwan Earthquake Research Center, 3. National Center for Research on Earthquake Engineering, 4. National Chung Cheng University

Taiwan is located in the plate converge zone, in which the Longitudinal Valley(LV) is the suture zone between the Eurasian Plate and Philippine Sea Plate. The collision process yields two nearly parallel major fault systems: the Central Range fault (CRF) and the Longitudinal Valley fault(LVF). The Chihshang fault is a creeping thrust fault, which is located in the southern section of the LVF in eastern Taiwan. According to geodetic survey, this fault moves to northwest at a rate approximately 2–3 cm/yr. There were two significant earthquakes occurred nearby the Chihshang fault, the 1951 M7.1 Hualien-Taitung earthquake and the 2003 M6.4 Chengkung earthquake. In this study, the spatial and temporal variations of velocity structure before and after 2003 Chengkung earthquake were obtained through the tomography inversion beneath the southern segment of the Longitudinal Valley. The damping least-square technique and 3D ray tracing scheme were adopted to calculate the most appropriate solution and obtain the velocity structures. The results showed that the Vp values exhibit less significant variations than the parameters Vs and Vp/Vs ratio. But the Vs structures show larger variation after the 2003 mainshock. These results imply that Vp/Vs ratios began to increase before the mainshock, at the hanging wall of the Chihshang fault, which may be related to the increasing density of microcracks and fluid. Previous studies has shown that high Vp/Vs ratio may lead to cracks generating and fluid migration, which can result in changing rock volume and produce partial compensation. Therefore, our results not only give better understanding the seismogenic structures in the ES Taiwan, but also allow us to detect variations of physical parameters caused by crack propagating in stratum during the strong earthquake sequence. Hence, this study shows that the results from temporal and spatial variation of Vp/Vs values in the southern segment of the LVF could allow us to assess the seismic hazard potential in this area, and further explore the relationship between the seismicity and the rheology of fault plane. Finally, long-term monitoring of fault activities will contribute to the research of future earthquake early warning.

Keywords: spatial and temporal variations, Vp/Vs ratio

©2019. Japan Geoscience Union. All Right Reserved.

[E] ポスター発表 | セッション記号 S (固体地球科学)：S-SS 地震学

2019年5月27日(月) 17:15 ~ 18:30 | ポスター会場 幕張メッセ国際展示場 8ホール_19

[S-SS07] Rigorous Seismicity Modelling and Hypothesis Testing

コンビーナ:庄 建倉(統計数理研究所)、Schorlemmer Danijel(GFZ German Research Centre for Geosciences)、Matt Gerstenberger(GNS Science)、鶴岡 弘(東京大学地震研究所)

Probabilistic models have been developed for describing, analyzing, and forecasting seismicity since more than 100 years and, with the advent of large-scale digital networks, in high resolution during the last 30 years. These models include recurrence and stress-release models for long-term earthquake hazard assessment, and short-term models describing earthquake clustering, e.g. the ETAS model. Some models have become standard tools in seismic hazard assessment. However, the overall probabilities remain on the low end and the uncertainties of the forecasts are not well described. Rigorous data-based development and testing of models will help further improving forecasting power and accuracy of these models. Similarly, new hypotheses shall be evaluated rigorously using some existing model as the null hypothesis model or in dedicated tests addressing the hypothesis directly. In this context, the Collaboratory for the Study of Earthquake Predictability and its Japan branch provides the necessary testing capabilities for rigorous and unbiased evaluation of models and hypotheses. This session focuses on research that increases information on seismicity, being with respect to a reference model or as an independent hypothesis. We solicit contributions of model developments and hypothesis formulation based on the increased understanding of the physical process of earthquakes, such as the preparation and rupture processes of the earthquake source and the interaction between earthquakes and tectonic environments. We also welcome development and implementation of improved statistical methods for testing and validating physical hypotheses based on observed data. In particular, we welcome contributions about model- or hypothesis-test experiments that could be implemented in the Japan testing center.

[SSS07-P01] Development of Physics-based Ground Motion Simulation in A Hybrid Approach and Applications to Seismic Hazard Assessment in Taiwan

*Hsieh Ming-Che[1]、Yen Yin-Tung[1]、Ma Kuo-Fong[2,3] (1.Disaster Prevention Technology Research Center, Sinotech Engineering Consultants (Inc.), Taiwan、2.Department of Earth Sciences, National Central University, Taiwan、3.Earthquake-Disaster & Risk Evaluation and Management Center, National Central University, Taiwan)

[SSS07-P02] Increasing Earthquake Forecast Testability - CSEP Future Developments

*Danijel Schorlemmer[1]、Naoshi Hirata[2]、Fabrice Cotton[1]、Matt Gerstenberger[3]、Thomas Jordan[7]、Warner Marzocchi[4]、William Savran[7]、Maximilian Werner[5]、Stefan Wiemer[6]、Thomas Beutin[1]、David D Jackson[8]、Philip Maechling[7]、Sum Mak[1]、Kazuyoshi Nanjo[9]、Yosihiko Ogata[10]、David Rhoades[3]、Hiroshi Tsuruoka[2]、Graeme Weatherill[1]、Jiancang Zhuang[10] (1.GFZ German Research Centre for Geosciences、2.Earthquake Research Institute, University of Tokyo, Japan、3.GNS Science, Lower Hutt, New Zealand、4.University of Naples, Naples, Italy、5.University of Bristol, Bristol, United Kingdom、6.ETH Zurich, Zurich, Switzerland、7.University of Southern California, Los Angeles, USA、8.University of California Los Angeles, Los Angeles, USA、9.University of Shizuoka, Shizuoka, Japan、10.Institute of Statistical Mathematics, Tachikawa, Japan)

[SSS07-P03] Precision versus uncertainty in regional seismic hazard mapping

*Gerstenberger Matt[1]、Schorlemmer Danijel[2] (1.GNS Science、2.GFZ-Potsdam)

[SSS07-P04] An extreme value analysis of seismograms designed for early forecast of aftershocks

*澤崎 郁[1] (1.防災科学技術研究所)

[SSS07-P05] Spatio-temporal clustering of successive earthquakes: data analyses of global data.

*THYSTERE MATONDO BANTIDI[1]、Takeshi Nishimura[1] (1.Tohoku University)

[SSS07-P06] CSEPJapanにおける関東3ヶ月予測結果

*鶴岡 弘[1]、平田 直[1] (1.東京大学地震研究所)

[SSS07-P07] Long-term earthquake risk in North China estimated from a modern catalogue

熊 子瑶[2]、*庄 建倉[1]、周 仕勇[2] (1.統計数理研究所、2.北京大学)

[SSS07-P08] **Distributions of focal mechanisms in background seismicity and earthquake clusters in Japan**

*庄 建倉[1,2]、蒔田 恵理[2] (1.統計数理研究所、2.総合大学院大学)

[SSS07-P09] New Ground Motion Prediction Equations for Western Saudi Arabia

*木内 亮太[1,2]、Walter Mooney[1]、Hani Zahran[3] (1.U.S. Geological Survey、2.京都大学防災研究所、3.Saudi Geological Survey)

[SSS07-P10] Study on the spatial and temporal change of velocity structure before and after 2003 Chengkung earthquake, Taiwan

*TING YA LIANG[1]、Wen-Yen Chang[1,2,3]、Strong Wen[4] (1.National DONG HWA University、2.Eastern Taiwan Earthquake Research Center、3.National Center for Research on Earthquake Engineering、4.National Chung Cheng University)

Development of Physics-based Ground Motion Simulation in A Hybrid Approach and Applications to Seismic Hazard Assessment in Taiwan

Development of Physics-based Ground Motion Simulation in A Hybrid Approach and Applications to Seismic Hazard Assessment in Taiwan

*Hsieh Ming-Che[1]、Yen Yin-Tung[1]、Ma Kuo-Fong[2,3]
*Ming-Che Hsieh[1], Yin-Tung Yen[1], Kuo-Fong Ma[2,3]

1. Disaster Prevention Technology Research Center, Sinotech Engineering Consultants (Inc.), Taiwan、2. Department of Earth Sciences, National Central University, Taiwan、3. Earthquake-Disaster & Risk Evaluation and Management Center, National Central University, Taiwan
1. Disaster Prevention Technology Research Center, Sinotech Engineering Consultants (Inc.), Taiwan, 2. Department of Earth Sciences, National Central University, Taiwan, 3. Earthquake-Disaster & Risk Evaluation and Management Center, National Central University, Taiwan

Damages to engineering structures by an earthquake depend on the entire time history of the ground motion, which is affected by a number of factors including source-rupture process, seismic-wave velocity structure, topographic relief, and local site condition. To quantitatively assess these effects to ground motion, physics-based ground motion simulation is a powerful tool which enables rigorous modeling of each effect and their coupling. In this study, we present a recent-developed physics-based ground motion simulator in generating broadband seismograms for seismic hazard assessment. The simulator is essentially based on a hybrid approach in which long-period synthetics are calculated by the efficient 3-D strain Green’s tensor (SGT) and short-period synthetics are modeled by the stochastic method. Physical effects of (1) source slip distribution, (2) seismic wave propagation, (3) surface topography and (4) site amplification are taken into account. This hybrid approach has been validated by the 2016 M_W6.6 Meinong earthquake in southern Taiwan and reveals good potential for engineering applications. We also carried out simulations to model rupture scenarios of seismogenic structure and subduction zone sources. Output full waveform and ground motion parameters, e.g. peak ground acceleration (PGA) and 1.0-s-period spectral acceleration (SA1.0), have been further implemented to risk estimation, and even earthquake drill. Our result shows the ground motion simulator has the potential for earthquake scenario modeling and hazard assessment.

キーワード：Ground motion simulation、Seismic hazard assessment、Strain Green’s tensor、Stochastic method
Keywords: Ground motion simulation, Seismic hazard assessment, Strain Green’s tensor, Stochastic method

©2019. Japan Geoscience Union. All Right Reserved.

Increasing Earthquake Forecast Testability - CSEP Future Developments

*Danijel Schorlemmer[1], Naoshi Hirata[2], Fabrice Cotton[1], Matt Gerstenberger[3], Thomas Jordan[7], Warner Marzocchi[4], William Savran[7], Maximilian Werner[5], Stefan Wiemer[6], Thomas Beutin[1], David D Jackson[8], Philip Maechling[7], Sum Mak[1], Kazuyoshi Nanjo[9], Yosihiko Ogata[10], David Rhoades[3], Hiroshi Tsuruoka[2], Graeme Weatherill[1], Jiancang Zhuang[10]

1. GFZ German Research Centre for Geosciences, 2. Earthquake Research Institute, University of Tokyo, Japan, 3. GNS Science, Lower Hutt, New Zealand, 4. University of Naples, Naples, Italy, 5. University of Bristol, Bristol, United Kingdom, 6. ETH Zurich, Zurich, Switzerland, 7. University of Southern California, Los Angeles, USA, 8. University of California Los Angeles, Los Angeles, USA, 9. University of Shizuoka, Shizuoka, Japan, 10. Institute of Statistical Mathematics, Tachikawa, Japan

The Collaboratory for the Study of Earthquake Predictability (CSEP) has expanded over the years to many different testing areas hosted at multiple testing centers. Hundreds of earthquake forecast models have been submitted to CSEP and are being tested. New testing metrics were developed and implemented and a lot of progress was made to establish CSEP as an institution that cannot be ignored when issuing earthquake forecasts. Its rigor and independence became the standard in evaluating earthquake forecasts and in reporting on the results.

In the framework of the testing activities of the Global Earthquake Model, one line of expanding the capabilities of CSEP was developed at GFZ Potsdam. The group there applied the mechanisms that CSEP introduced to earthquake forecast models to the area of intensity prediction equations (IPEs) and ground-motion prediction equations (GMPEs). The first truly prospective tests were carried out on IPEs for Italy and also on GMPEs for Japan and New Zealand. This new set of tests helped CSEP move into the hazard domain and increase the relevance of its results to the hazard community. Finally, the group at GFZ Potsdam has also conducted the first prospective test of the US national seismic hazard maps.

Although these tests have been successful and well-received, they have also shown the limitations of the CSEP approach. Many aspects of seismic hazard or earthquake forecasting remain inherently untestable if only the model forecasts are tested and not the model ingredients. We propose to continue along the lines of the GFZ Potsdam developments and create new areas of activity for CSEP, namely targeted experiments that cannot be conducted with the current CSEP software system. As part of the eGSIM (European Ground Shaking Intensity Models) service, we will introduce permanent testing of IPEs and GMPEs to the testing center to establish strong performance records to be used in hazard models. Further targeted experiments include the predictive power of b-values, discrimination of foreshocks for short-term forecasting, as well as a deeper look into precursory
phenomena applying CSEP-style rigorous testing. We support including testability in future hazard models or their components to move to better testable seismic hazard models. Finally, to expand into the risk domain, we will test exposure models against new and independent data.

Keywords: Seismicity, Forecasting, Testing

©2019. Japan Geoscience Union. All Right Reserved.

Precision versus uncertainty in regional seismic hazard mapping

Precision versus uncertainty in regional seismic hazard mapping

*Gerstenberger Matt[1]、Schorlemmer Danijel[2]
*Matt Gerstenberger[1], Danijel Schorlemmer[2]

1. GNS Science、2. GFZ-Potsdam
1. GNS Science, 2. GFZ-Potsdam

Regional and national seismic hazard mapping efforts have increasingly pursued more detailed and precise models and outputs, particularly in terms of source characterisation and modelling. With increasing precision comes increasing uncertainty. In recent years much attention has been paid to modelling uncertainty in ground-motion models and including this in seismic hazard modelling. However, much less effort has been made to quantify and model uncertainty in seismic source characterisation. This raises two questions: 1) is increasing precision appropriate when uncertainty remains poorly quantified? 2) what is the optimal balance between precision and uncertainty? Ultimately the answer to this depends on the end-uses of the models and the implications of increasing uncertainty with increasing precision. Here we explore some of the main sources of uncertainty in seismic source characterisation such as incomplete and limited records of earthquake occurrence in paleoseismic data and earthquake catalogues, non-stationarity of seismicity and the poisson assumption, fault source characterisation and so-called moment balancing. We pay particular focus to uncertainties in estimating hazard in less seismically active regions and the implications for building design guidance.

キーワード：Seismic hazard、PSHA、uncertainty
Keywords: Seismic hazard, PSHA, uncertainty

©2019. Japan Geoscience Union. All Right Reserved.

An extreme value analysis of seismograms designed for early forecast of aftershocks

*澤崎 郁[1]
*Kaoru Sawazaki[1]

1. 防災科学技術研究所
1. National Research Institute for Earth Science and Disaster Resilience

Conventional aftershock forecasting has been operated through applying the Gutenberg-Richter and Omori-Utsu laws to an earthquake catalog. However, catalog’ s quality is influenced by detectability of earthquake signals (P or S waves), which causes degradation of the catalog in the early stage after a large earthquake and at regions which are sparsely covered by seismograph network. This eventually causes the catalog’ s nonuniformity and limitation of the forecasting performance.

In this study, we propose a new approach designed for high-performance early aftershock forecasting without using earthquake catalog. Instead, we use a continuous seismogram recorded at each station. First, we pick the maximum amplitude of the seismogram obtained in every assigned time interval (e.g., 1 minute). This picking process can be completely automated and is rarely affected by overlap of multiple seismic signals occurring in approximately the same time. We empirically derive a probability distribution (PD) that accounts for the frequency of the maximum amplitudes. This PD is essentially a non-stationary extreme value distribution derived from the generalized Pareto distribution (GPD) and the Omori-Utsu type temporal decay. We optimize three parameters that control the PD shape (K_a: parameter that controls whole aftershock activity, p_a: parameter that controls temporal decay of the aftershock frequency, m: parameter that controls power-law decay of the maximum amplitude) by applying the maximum likelihood estimation to the observed maximum amplitudes. By extrapolating the optimized PD, we estimate the number of maximum amplitudes that will exceed a threshold value within arbitral time interval in the future. The proposed approach provides forecast of peak ground motion at each station rather than magnitude, which is directly desired for public use. Moreover, the forecasted peak ground motion may automatically incorporate many factors that cannot be described by a simple ground motion attenuation model (e.g., site amplification, radiation pattern, rupture directivity, and so on).

We apply the proposed method to 25 Hi-net seismograms recorded the 2016 Kumamoto earthquakes in Japan. We set the learning periods every one hour after the mainshock (Mj7.3), and set the forecasting period within 24 hours after the end of each learning period. We find that parameters K_a and m become temporally stable within a few hours after the mainshock at many stations. On the other hand, the parameter p_a temporally varies more probably because the induced seismicity at northeast area (Aso and Oita regions) strongly affects the apparent temporal decay rate of the amplitudes. Within 3 hours after the mainshock, the forecasted number of the maximum amplitudes exceeding 10^{-4} m/s is within 0.5 to 2.0 times the actual observation for about 80 % of the used stations. For the threshold amplitude of 10^{-3} m/s, on the other hand, the forecasted number tends to overestimate, probably due to saturation of seismograms by both artificial and physical reasons.

キーワード：極値解析、余震予測、最大地震動
Keywords: extreme value analysis, aftershock forecasting, peak ground motion

©2019. Japan Geoscience Union. All Right Reserved.

Spatio-temporal clustering of successive earthquakes: data analyses of global data.

*THYSTERE MATONDO BANTIDI[1], Takeshi Nishimura[1]

1. Tohoku University

Spatio-temporal clustering of seismicity is an interesting phenomenon in the earthquake generation process. We investigate the earthquakes closely occurring in space and time, which have been sometimes observed at various regions. A recent example is *Mw*6.5 earthquake at Hinagu active fault on April 14, 2016, followed by a *Mw*7.3 at Futagawa active fault on April 16. The present study analyzes moderate and large earthquakes to clarify characteristics of such successive occurrence of earthquakes.

We use the Global Centroid Moment Tensor catalog for the period from 1976 to 2016. Earthquakes with moment magnitudes (*Mw*) of larger or equal to 5.0 and with depths less than or equal to 70 km are analyzed. The earthquakes that occur within some horizontal distance ranges (Δd*:* from 10 to 500 km*)*, and lapse times (Δt=30, 180 and 365 days*)* from the occurrence of each target earthquake is grouped in a cluster, and the number of clusters are counted.

The results show that cumulative numbers of clusters almost constantly increase in the logarithmic scale with increasing Δt, and the number of clusters increases constantly in general with increasing Δd. For example, for the *Mw* 5.0 –5.5, the cumulative number of clusters at Δd*=100* km are 3177, 4525 and 4808, respectively, for Δt of 30, 180 and 365 days.

To examine whether or not these successive earthquakes occur randomly, in other words, whether or not these successive earthquakes occur under some physical conditions, we compare the observed results with simulations in which earthquakes are set to randomly occur in time. The results show that the observed cumulative numbers of clusters are larger than those of simulation in short distance ranges. The former gradually approach to the latter with increasing the horizontal distance, and merge into a same number at a distance, which is defined as “triggering distance” in the present study. As Δt increases, the occurrence probability decreases and approaches to the normal condition in which the occurrence time intervals of earthquakes obey a Poisson distribution. For example, the triggering distances of Mw5.0-5.5 are 420 km and 66 km, respectively, for Δt*=30* days and *365* days. The results obtained by changing the parameters related to the spatial and temporal distributions of aftershock show no significant difference in the number of clusters and triggering distances.

Keywords: Clustering, Successive earthquakes, Triggering distance

©2019. Japan Geoscience Union. All Right Reserved.

CSEPJapanにおける関東3ヶ月予測結果
Kanto 3 month testing class results of CSEP Japan

*鶴岡 弘[1]、平田 直[1]
*Hiroshi Tsuruoka[1], Naoshi Hirata[1]

1. 東京大学地震研究所
1. Earthquake Research Institute, Tokyo Univ.

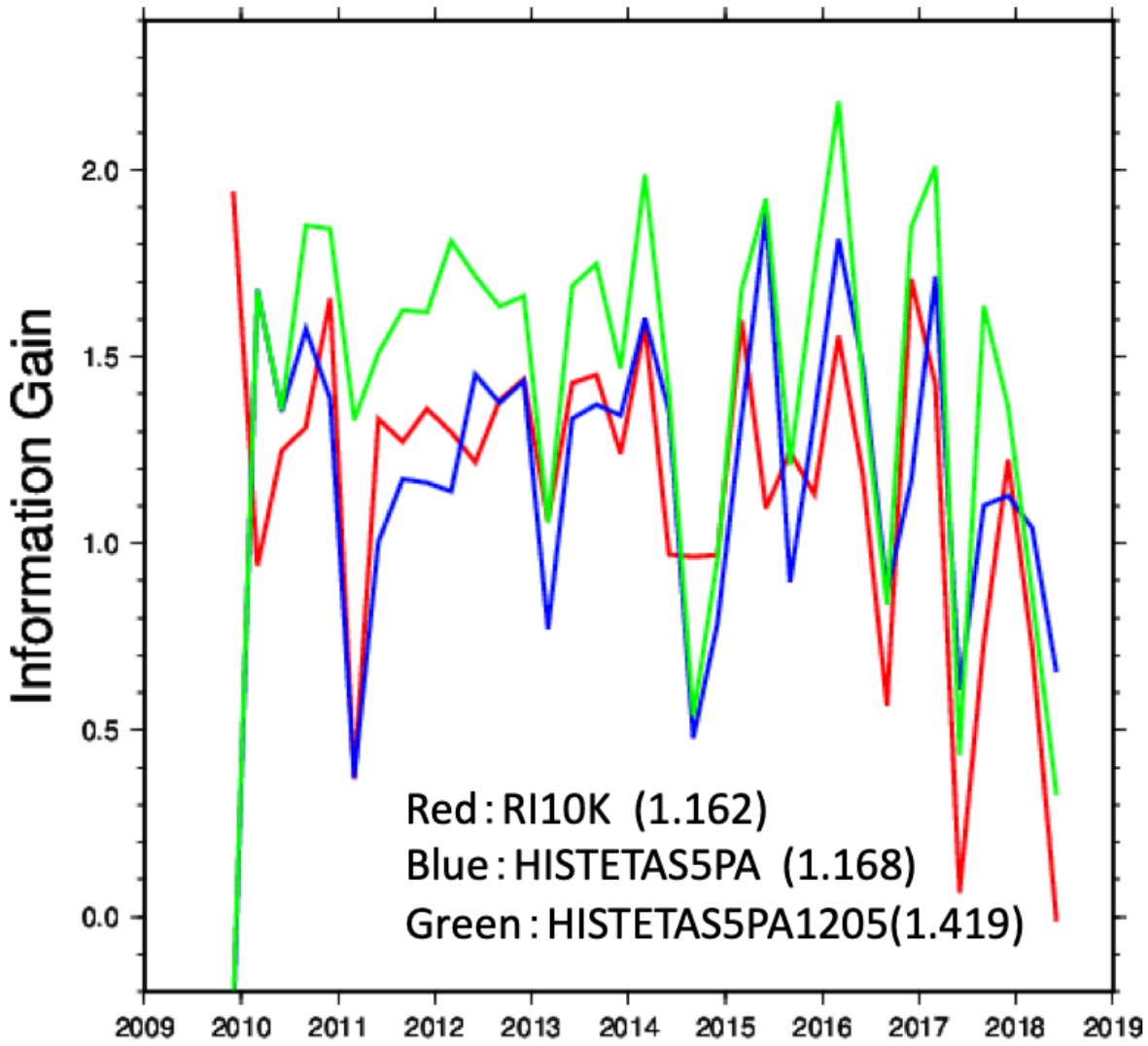
CSEP Japan における関東テスト領域の3ヶ月テスト結果を報告する．モデルは，RI10K，HISTETAS5PAおよびHISTETAS5PA1205である．HISTETAS5PA1205は東北地方太平洋沖地震後にテストセンターに投稿されたモデルとなる．テスト結果は，2009年11月1日からの約40ラウンド分である．

CSEPの標準テスト結果は，2017/5/1-8/1のラウンドにおいて，RI10KはS-testをパスしていなかった．また，観測地震数が少ない場合にすべてのモデルでN-Testをパスしていないラウンド等もあった．全ラウンドの各モデル毎の地震1個あたりの情報利得値の平均を計算するとHISTETAS5PA1205, HISTETAS5PA, RI10Kそれぞれ1.419, 1.168, 1.162であった．地震数の予測についてはHISTETA5PA1205は観測地震数をよく予測しているが，他のモデルは学習期間における平均発生数となるためあまりあっていないことがわかる．

複数ラウンドの結果から，地震数の予測についてモデル毎の対応が異なっておりこの精度向上は予測モデルの向上に直結する．また，モデルの評価は、空間予測性能と地震数の予測性能を評価することでよく把握できると思われる．

キーワード：地震予測可能性、CSEP
Keywords: Earthquake Predictability, CSEP

©2019. Japan Geoscience Union. All Right Reserved.



©2019. Japan Geoscience Union. All Right Reserved.

Long-term earthquake risk in North China estimated from a modern catalogue

Long-term earthquake risk in North China estimated from a modern catalogue

熊 子瑶[2]、*庄 建倉[1]、周 仕勇[2]
Ziyao Xiong[2], *Jiancang Zhuang[1], Shiyong Zhou[2]

1. 統計数理研究所、2. 北京大学
1. Institute of Statistical Mathematics, 2. Peking University

In this study, to obtain optimal estimates of the earthquake hazard in North China based on the modern earthquake catalogue, we used two variable kernel function estimation methods and two spatial tessellation methods to calculate the total and background seismic spatial occurrence rates for the study area.

The first problem of this study is to derive the best estimate of the long-term earthquake risk in North China. To address the first problem, we use the kernel function estimation methods of Stock and Smith (2002) and Zhuang et al. (2002), the Bayesian Delaunay-Tessellation Smoothing Method used by Ogata (ODTB) (2003, 2004), and ICVT to estimate the total earthquake hazard for North China. The results were compared and analyzed through the cross-validation method, to ensure accurate reflection of the seismic activity in North China. The sophisticated ODTB method is more stable than the others, but is relatively expensive, in terms of computation demands, while Zhuang et al.’s kernel estimate and the new ICVT method are able to provide reasonable estimates and easier to implement.

For the second problem, of b-value, we use Ogata’s method (2004, 2015) based on free nodes, to calculate the *b*-value spatial distribution. We expect that the obtained results of the spatial distribution of seismic risk and *b*-value provide a reference for the evaluation and prediction of large earthquakes and stress distribution in the study area.

For the third problem, we use two methods to estimate background seismic rates, and compare the results. The first method uses the result of the background seismic event probability, calculated by the epidemic-type aftershock sequence (ETAS) model (Zhuang et al., 2002; Zhuang, 2011), to simulate the background seismic risk distribution. The second method is to calculate the spatial distribution of earthquake hazard by using the HIST-ETAS model (Ogata, 2004).

Using comparative analyses and simulation experiments, we show that all of methods give similar spatial patterns of seismic occurrences.

キーワード：地震リスク、分割、常時地震活動、ETASモデル
Keywords: seismic risk, tessellation, background seismicity, ETAS model

©2019. Japan Geoscience Union. All Right Reserved.

Distributions of focal mechanisms in background seismicity and earthquake clusters in Japan

Distributions of focal mechanisms in background seismicity and earthquake clusters in Japan

*庄 建倉[1,2]、蒔田 恵理[2]
*Jiancang Zhuang[1,2], Eri Maita[2]

1. 統計数理研究所、2. 総合大学院大学
1. Institute of Statistical Mathematics, 2. Graduate University for Advanced Studies

This study tries to find the probability distributions of focal mechanisms in background seismicity and earthquake clusters in Japan by analyzing F-net data. To describe the probability distribution, each focal mechanism is discomposed as the result of a rotation about a particular pole starting from a reference focal mechanism. In this study, DC4 symmetry is considered, i.e., either nodal-plane can be the fault plane and the two sides of the fault plane are distinguishable.

To separate the background and clustering seismicity, we fit the space-time ETAS model (e.g., Zhuang et al, 2011) to the earthquakes with magnitude 4.2+ from 1997 to 2017 in the F-net catalog, and use the stochastic declustering method to estimate the background probabilities that each event is a background event and the triggered probabilities that each event is triggered by other events.

For the background events, the reference focal mechanism is taken as the average focal mechanism in each area, calculated by the method in Kagan (2014). The ration angles between a background event and the mean focal mechanisms at *(x, y)* is reconstructed by

$\zeta(\Delta) \propto \sum_j \phi_j I$(Rotation angle betwen j and the mean focal mechanism is within $(\Delta-\delta, \Delta+\delta)$),

where j runs over all background events near x,y, δ is a small number, and ϕj is the background probability estimated from fitting the space-time ETAS model. For the triggered events, the reference focal mechanism is naturally taken the focal mechanism of the event which triggers it. The rotation angles between the parent event and its direct offspring are reconstructed by

$\xi(\Delta) \propto \sum_{i,j} \rho_{i,j} I$(Rotation angle betwen i and j is within $(\Delta-\delta, \Delta+\delta)$) .

where i and j run over all the event pairs in the catalog, ρij is the probability that event j is triggered by event i estimated based on the ETAS model.

We find that the rotation poles are almost uniformly distributed. The reconstructed results for the rotation angles are shown in Figure 1.

Figure 1 (a) mean focal mechanisms of background seismicity in Japan. (b) Reconstructed distribution of rotation angles for focal mechanisms in the background seismicity and triggered seismicity.

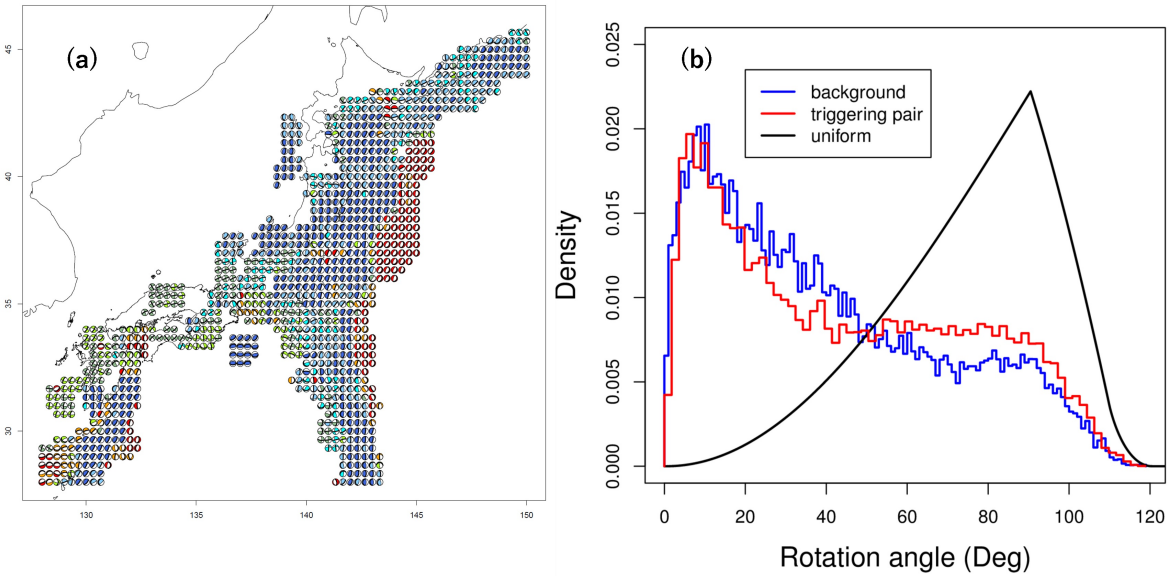
References:

Zhuang J., (2011) , *Next-day earthquake forecasts for the Japan region generated by the ETAS model.*

©2019. Japan Geoscience Union. All Right Reserved.

Earth Planets Space, 63, 207-216. doi:10.5047/eps.2010.12.010.
Kagan Y.Y. and Jackson D. D. (2014) Statistical earthquake focal mechanism forecasts. **Geophys. J. Int.** 197, 620–629. doi: 10.1093/gji/ggu015

キーワード：地震機構、確率分布、地震クラスター、常時地震、ETASモデル
Keywords: earthquake focal mechanism, probability distribution, earthquake cluster, background seismcity, ETAS model



©2019. Japan Geoscience Union. All Right Reserved.

New Ground Motion Prediction Equations for Western Saudi Arabia

*木内 亮太[1,2]、Walter Mooney[1]、Hani Zahran[3]
*Ryota Kiuchi[1,2], Walter Mooney[1], Hani Zahran[3]

1. U.S. Geological Survey、2. 京都大学防災研究所、3. Saudi Geological Survey
1. U.S. Geological Survey, 2. Disaster Prevenetion Research Institute, Kyoto University, 3. Saudi Geological Survey

We developed Ground Motion Prediction Equations (GMPEs) for western Saudi Arabia using 2770 selected records of PGA and PGV from 177 earthquakes of magnitude 3.0 –5.4, recorded at 58 stations in the distance range from 1 km to 400 km. Our GMPEs are developed based on one of the NGA-West2 Project GMPEs (Boore et al., 2014) by employing a mixed effects regression model.

Saudi Arabia is surrounded by several active tectonic regions, including an extension in the Red Sea and left-lateral strike-slip motion in the Gulf of Aqaba and along the Dead Sea Transform Fault (DSTF). In this area, multiple seismic swarms in and around volcanic fields, also known as harrats, have been detected over the past several decades (El-Isa and Shanti, 1989). The most recent large earthquake swarm in the region, which included more than 30,000 earthquakes, occurred from April to June 2009 beneath the volcanic field of Harrat Lunayyir in northwestern Saudi Arabia. The strongest seismic activity occurred May 13-19, 2009 and consisted of events M > 4 (Pallister et al., 2010). The largest earthquake occurred on May 19th, ML 5.4 as estimated by the SGS (Saudi Geological Survey) and Mw 5.7 by the USGS.

The NGA-West2 project used as a reference model mainly consists of shallow crustal earthquakes in active tectonic regions, rather than extensional earthquakes, such as those observed in Saudi Arabia. This deficiency is corrected by calculating a magnitude scaling of the new Saudi Arabia GMPEs compared to those of Boore et al. (2014). Furthermore, there is a clear difference in distance scaling for the Arabian GMPEs in comparison with the NGA-West2 GMPEs. This difference is especially significant at large distances and is mainly due to lower anelastic attenuation in the crystalline crust of western Saudi Arabia. Our empirical data demonstrate that the GMPEs presented here are in good agreement with observed earthquake ground motions in western Saudi Arabia.

キーワード：GMPE、Saudi Arabia、Seismic Hazard
Keywords: GMPE, Saudi Arabia, Seismic Hazard

©2019. Japan Geoscience Union. All Right Reserved.

Study on the spatial and temporal change of velocity structure before and after 2003 Chengkung earthquake, Taiwan

*TING YA LIANG[1], Wen-Yen Chang[1,2,3], Strong Wen[4]

1. National DONG HWA University, 2. Eastern Taiwan Earthquake Research Center, 3. National Center for Research on Earthquake Engineering, 4. National Chung Cheng University

Taiwan is located in the plate converge zone, in which the Longitudinal Valley(LV) is the suture zone between the Eurasian Plate and Philippine Sea Plate. The collision process yields two nearly parallel major fault systems: the Central Range fault (CRF) and the Longitudinal Valley fault(LVF). The Chihshang fault is a creeping thrust fault, which is located in the southern section of the LVF in eastern Taiwan. According to geodetic survey, this fault moves to northwest at a rate approximately 2–3 cm/yr. There were two significant earthquakes occurred nearby the Chihshang fault, the 1951 M7.1 Hualien-Taitung earthquake and the 2003 M6.4 Chengkung earthquake. In this study, the spatial and temporal variations of velocity structure before and after 2003 Chengkung earthquake were obtained through the tomography inversion beneath the southern segment of the Longitudinal Valley. The damping least-square technique and 3D ray tracing scheme were adopted to calculate the most appropriate solution and obtain the velocity structures. The results showed that the Vp values exhibit less significant variations than the parameters Vs and Vp/Vs ratio. But the Vs structures show larger variation after the 2003 mainshock. These results imply that Vp/Vs ratios began to increase before the mainshock, at the hanging wall of the Chihshang fault, which may be related to the increasing density of microcracks and fluid. Previous studies has shown that high Vp/Vs ratio may lead to cracks generating and fluid migration, which can result in changing rock volume and produce partial compensation. Therefore, our results not only give better understanding the seismogenic structures in the ES Taiwan, but also allow us to detect variations of physical parameters caused by crack propagating in stratum during the strong earthquake sequence. Hence, this study shows that the results from temporal and spatial variation of Vp/Vs values in the southern segment of the LVF could allow us to assess the seismic hazard potential in this area, and further explore the relationship between the seismicity and the rheology of fault plane. Finally, long-term monitoring of fault activities will contribute to the research of future earthquake early warning.

Keywords: spatial and temporal variations, Vp/Vs ratio

©2019. Japan Geoscience Union. All Right Reserved.

[E] ポスター発表 | セッション記号 S (固体地球科学)：S-IT 地球内部科学・地球惑星テクトニクス

2019年5月27日(月) 15:30 ~ 17:00 | ポスター会場 幕張メッセ国際展示場 8ホール_12

[S-IT21] 核-マントルの相互作用と共進化

コンビーナ:河合 研志(東京大学大学院理学系研究科地球惑星科学専攻)、飯塚 毅(東京大学)、太田 健二(東京工業大学大学院理工学研究科地球惑星科学専攻)、土屋 卓久(愛媛大学地球深部ダイナミクス研究センター)

近年の高圧実験の進歩で、地球中心部に至る温度圧力条件での鉱物の物性測定が可能となってきた。一方、高精度な古地磁気測定、地球物理学観測、精密地球物理学分析、地球ニュートリノによる地球深部放射性物質の直接観測などの発展と共に、マントル対流や地磁気ダイナモの数値シミュレーション技術も大きく発展して、地球内部の状態の理解が進んできた。本セッションでは、地球及び惑星における核ーマントル相互作用と進化に焦点をあてた、様々な研究分野の成果を一堂に会する機会を提供し、情報交換を進めることを目的とする。異なる分野間の連携を発展させるための日本版地球・惑星深部研究グループ(J-SEDI）の形成に関わる講演も歓迎する。

[SIT21-P01] 茨城県稲田花崗岩における小スケールの岩石組成変化の検討 -日本列島地殻由来の地球ニュートリノフラックスの高精度推定に向けて-

★招待講演

*上木 賢太[1]、南 一輝[2]、飯塚 毅[3]、榎本 三四郎[4]、田中 宏幸[2] (1.海洋研究開発機構、2.東京大学地震研究所、3.東京大学地球惑星科学専攻、4.ワシントン大学)

[SIT21-P02] Towards a better estimation of the temperature distribution beneath the Japanese Islands

*田中 明子[1]、山野 誠[2]、濱元 栄起[3]、後藤 秀作[4]、松本 拓己[5] (1.産業技術総合研究所 活断層・火山研究部門、2.東京大学 地震研究所、3.埼玉県 環境科学国際センター、4.産業技術総合研究所 地圏資源環境研究部門、5.防災科学技術研究所)

[SIT21-P03] 日本列島地殻由来の地殻ニュートリノフラックス推定への地球化学データベース利用

*原口 悟[1]、上木 賢太[1]、岩森 光[1,2,3] (1.海洋研究開発機構、2.東京大学地震研究所、3.東京工業大学)

[SIT21-P04] **Viscosity of potassium titanosilicate melt at high pressure**

*鈴木 昭夫[1] (1.東北大学大学院理学研究科地学専攻)

[SIT21-P05] **Lattice thermal conductivity of wadsleyite and ringwoodite at the mantle transition zone pressures**

*木村 清二[1]、太田 健二[6]、川添 貴章[2]、廣瀬 敬[3]、鍵 裕之[4]、八木 貴志[5] (1.東京工業大学理学院地球惑星科学系、2.広島大学大学院理学研究科地球惑星システム学専攻、3.東京工業大学大学　地球生命研究所、4.東京大学大学院理学系研究科附属地殻化学実験施設 、5.国立研究開発法人産業技術総合研究所、6.東京工業大学大学院理工学研究科地球惑星科学専攻)

[SIT21-P06] In-situ X-ray observations of the olivine-spinel transformation under shear deformation: preliminary results on the reaction-induced weakening

*久保 友明[1]、森山 一哉[1]、森 悠一郎[1]、今村 公裕[1]、小泉 早苗[2]、西原 遊[3]、鈴木 昭夫[4]、肥後 祐司[5] (1.九州大学、2.東大地震研、3.愛媛大学GRC、4.東北大学、5.JASRI)

[SIT21-P07] Internally resistive heated diamond anvil cell experiments with metal encapsulated minerals

*山本 倫也[1]、太田 健二[1]、末広 翔[1]、井上 勇人[1] (1.東京工業大学)

[SIT21-P08] Shear deformation on post-spinel

*山崎 大輔[1]、辻野 典秀[1]、西原 遊[2] (1.岡山大学惑星物質研究所、2.愛媛大学地球深部ダイナミクス研究センター)

[SIT21-P09] **Lattice thermal conductivity of $CaSiO_3$ perovskite at high pressures and high temperatures**

*恩賀 皓太郎[1]、太田 健二[1]、長谷川 暉[1,2]、八木 貴志[2]、廣瀬 敬[3,4]、大石 泰夫[5] (1.東京工業大学理学院地球惑星科学系、2.産業技術総合研究所、3.東京工業大学地球生命研究所、4.東京大学大学院理学系研究科地球惑星科学専攻、5.高輝度光科学研究センター)

[SIT21-P10] **Polycrystalline diamond sintered from ultradispersed nanodiamonds**

*西 真之[1,2]、山本 幸一郎[1]、周 佑黙[1]、入舩 徹男[2,1] (1.愛媛大学地球深部ダイナミクス研究センター、2.東京工業大学地球生命研究所)

[SIT21-P11] Thermal conductivity measurements on iron and MgO periclase at high pressure and high temperature similar to the Earth's mid-lower mantle conditions

*長谷川 暉[1,2]、太田 健二[2]、八木 貴志[1]、廣瀬 敬[3,4] (1.産業技術総合研究所、2.東京工業大学、3.東京工業大学地球生命研究所、4.東京大学)

[SIT21-P12] Azimuthal anisotropy in the lowermost mantle beneath Philippine from ScS-S times

*田中 聡[1] (1.海洋研究開発機構　地球深部ダイナミクス研究分野)

[SIT21-P13] Detailed 3-D S-velocity structure within D" at the western Pacific LLSVP margin: smaller scale plumes and paleoslabs

*鈴木 裕輝[1]、河合 研志[1]、ゲラー ロバート[1]、田中 聡[2]、Weerachai Siripuvaraporn[3]、Songkhun Boonchaisuku[3]、Noisagool Sutthipong[3]、石原 靖[2]、Taweoon Kim、宮川 幸治[4]、竹内 希[4] (1.東京大学、2.海洋研究開発機構、3.Mahidol University、4.東京大学地震研究所)

[SIT21-P14] Possible interaction between the core and mantle inferred from a core surface flow model

*松島 政貴[1] (1.東京工業大学理学院地球惑星科学系)

[SIT21-P15] 高温高圧条件下での金属-ケイ酸塩メルト間の希ガス分配係数の実験的決定

*田中 友崇[1]、桑原 秀治[2]、貴志 智[1]、野村 龍一[3]、三部 賢治[5]、鍵 裕之[4]、舘野 繁彦[6]、角野 浩史[1] (1.東京大学大学院総合文化研究科広域科学専攻相関基礎科学系、2.愛媛大学　地球深部ダイナミクス研究センター、3.京都大学、4.東京大学大学院理学系研究科附属地殻化学実験施設、5.東京大学地震研究所、6.東京工業大学地球生命研究所)

[SIT21-P16] **Measurement of T-dependent electrical resistivity of solid and liquid Fe and Pt at fixed P**

*Innocent Ezenwa[1]、Takashi Yoshino[1] (1.Institute for Planetary Materials, Okayama University)

[SIT21-P17] Ancient, highly depleted mantle constrained by Re-Os isotope and highly-siderophile element compositions of French Polynesian xenoliths

*秋澤 紀克[1]、石川 晃[2]、鈴木 勝彦[3]、小木曽 哲[4] (1.東京大学　大気海洋研究所、2.東京工業大学　理学院地球惑星科学系、3.JAMSTEC　海底資源研究開発センター、4.京都大学　大学院人間・環境学研究科)

[SIT21-P18] First-principles prediction of hydrogen partitioning between the core and mantle

*大場 篤朗[1]、土屋 卓久[1] (1.愛媛大学 地球深部ダイナミクス研究センター)

[SIT21-P19] Microvolume stable isotope measuremetns and its applicaiton for high-pressure high-temperature experimental run products

*Madhusoodhan Satish-Kumar[1]、Shinnosuke Aoyama[1] (1.Department of Geology, Faculty of Science, Niigata University)

[SIT21-P20] Electrical resistivity of hcp Fe-Si alloys at high pressure and temperature

*井上 勇人[1]、末広 翔[1]、太田 健二[1]、廣瀬 敬[2,3]、大石 泰生[4] (1.東京工業大学理学院地球惑星科学系、2.東京工業大学地球生命研究所、3.東京大学大学院理学系研究科地球惑星科学専攻、4.高輝度光科学研究センター)

[SIT21-P21] Electrical resistivity and thermal conductivity of fcc Fe: Implications for the Mercury's core

★Invited Papers

*五味 斎[1]、芳野 極[1] (1.岡山大学)

[SIT21-P22] Lateral heterogeneity in the lowermost outer core (F layer) of the Earth revealed by seismic analyses

*大滝 壽樹[1]、金嶋 聰[2]、土屋 卓久[3] (1.産業技術総合研究所地質情報研究部門、2.九州大学大学院理学研究院地球惑星科学部門、3.愛媛大学地球深部ダイナミクス研究センター)

[SIT21-P23] 内核の不均一成長に伴う地球外核中の流れと軽成分分布

*竹広 真一[1]、佐々木 洋平[2] (1.京都大学数理解析研究所、2.京都大学大学院理学研究科数学教室)

[SIT21-P24] Sharpness of the hemispherical boundary in the inner core beneath the northern Pacific

*入谷 良平[1]、川勝 均[1]、竹内 希[1] (1.東京大学地震研究所)

[SIT21-P25] Stable carbon isotope fractionation in Fe-C system from first principles

*出倉 春彦[1]、土屋 卓久[1] (1.愛媛大学地球深部ダイナミクス研究センター)

茨城県稲田花崗岩における小スケールの岩石組成変化の検討 -日本列島地殻由来の地球ニュートリノフラックスの高精度推定に向けて-
Sample-scale compositional variation of the Inada granite, Ibaraki, Japan -toward the reduction of geoneutrino flux estimation errors from the Japanese crust-

*上木 賢太[1]、南 一輝[2]、飯塚 毅[3]、榎本 三四郎[4]、田中 宏幸[2]
*Kenta Ueki[1], Minami Kazuki[2], Tsuyoshi Iizuka[3], Sanshiro Enomoto[4], Hiroyuki Tanaka[2]

1. 海洋研究開発機構、2. 東京大学地震研究所、3. 東京大学地球惑星科学専攻、4. ワシントン大学
1. Japan Agency for Marine-Earth Science and Technology, 2. Earthquake Research Institute, University of Tokyo, 3. Department of Earth and Planetary Science, University of Tokyo, 4. Center for Experimental Nuclear Physics and Astrophysics, University of Washington

Geoneutrio observed at anti-neutrino observatory "KamLAND" in Kamioka (Hida City, Gifu Prefecture), enables us to directly observe the abundance of radiogenic elements in the deep earth. As crustal rocks exhibit a high concentration of geoneutrino producing radiogenic elements (Uranium and Thorium) than mantle rocks, we have to subtract the contribution of geoneutrino from the Japanese crust from the observation value in Kamioka to estimate geoneutrino flux from core and mantle. For the purpose, we estimated the 3D distribution of uranium and thorium in the Japanese crust by the stochastic modeling using the seismic velocity structure, geological information and geochemical database for the Japanese crustal rock. Geoneutrino flux calculated using the compositional map exhibits a very large error (up to 80%) at present.
We found that information on the compositional heterogeneity (spatial correlation) of various length scale, such as of the single rock suite scale (km to m scale), and sample scale (cm to mm scale) are essential to reduce the estimation error of crustal geoneutrino flux as small as the observation error of the geoneutrino on KamLAND. Therefore, we conducted a grid sampling of the granite of Inada, Ibaraki prefecture, to obtain quantitative knowledge on the small scale compositional heterogeneity. Samples (about 500g) were divided into several centimeter scale split (about 25g). Based on the compositional variations between small splits from one sample, we discuss the small scale sample wise compositional variation. Whole rock chemical composition of each small split was analyzed using XRF. Also, we conducted surface analysis using an ED-XRF to evaluate the spatial distribution of elements in each split. As a result, even within a single sample (about 500g), a compositional variation of about several% at maximum was observed. This result indicates that when conducting the analysis based on the rock chemical composition considering the spatial context, it is necessary to properly evaluate the sample scale heterogeneity, in addition to the tectonic scale, the rock suite scale, and microscopic scale.Also, this result will contribute to the reduction of the estimation error of geoneutrino from the Japanese crust.

キーワード：地球ニュートリノ、花崗岩、岩石化学組成
Keywords: Geoneutrino, Granite, Rock chemical composition

©2019. Japan Geoscience Union. All Right Reserved.

Towards a better estimation of the temperature distribution beneath the Japanese Islands

*田中 明子[1]、山野 誠[2]、濱元 栄起[3]、後藤 秀作[4]、松本 拓己[5]
*Akiko Tanaka[1], Makoto Yamano[2], Hideki Hamamoto[3], Shusaku Goto[4], Takumi Matsumoto[5]

1. 産業技術総合研究所 活断層・火山研究部門、2. 東京大学 地震研究所、3. 埼玉県 環境科学国際センター、4. 産業技術総合研究所 地圏資源環境研究部門、5. 防災科学技術研究所
1. Geological Survey of Japan, National Institute of Advanced Industrial Science and Technology, 2. Earthquake Research Institute, The University of Tokyo, 3. Center for Environmental Science in Saitama, 4. Institute for Geo-Resources and Environment National Institute of Advanced Industrial Science and Technology, 5. National Research Institute for Earth Science and Disaster Resilience

To improve our understanding of the thermal evolution and structure of the deep Earth, it is necessary to know the shallow part of them. Surface heat flow provides important constraint on it. However, the number of heat flow data is limited and spatially very inhomogeneous and even in regions with measurements the data quality varies. For this reason, we have been working on compiling a comprehensive database of heat flow, thermal conductivity, and geothermal gradient. In 2004, Geological Survey of Japan published a digital geoscience map entitled "Geothermal Gradient and Heat Flow Data in and around Japan", which contains heat flow data in the northwestern Pacific area (from 0 to 60°N and from 120 to 160°E) and geothermal gradient data in and around Japan. In 2019, we will be releasing database entitled "Thermal Data Collection in and around Japan", which contains continuously updated of geothermal gradient and heat flow data and adds thermal conductivity data in and around Japan. Thermal conductivity data were compiled from published data and site-specific reports, and measured using the archived cores. This database offers considerable improvements over the previous version released in 2004, and will be published and available at https://www.gsj.jp/en/database/db-portal/index.html. It presents an opportunity to revisit the thermal state of the lithosphere along with other geophysical/geochemical constraints on heat flow extrapolation.

キーワード：地殻熱流量、熱伝導率、地温勾配
Keywords: heat flow, thermal conductivity, geothermal gradient

©2019. Japan Geoscience Union. All Right Reserved.

日本列島地殻由来の地殻ニュートリノフラックス推定への地球化学データベース利用

The estimation of the neutrino flux from the crust of the Japanese islands using the geochemical database

*原口 悟[1]、上木 賢太[1]、岩森 光[1,2,3]
*Satoru Haraguchi[1], Kenta Ueki[1], Hikaru Iwamori[1,2,3]

1. 海洋研究開発機構、2. 東京大学地震研究所、3. 東京工業大学
1. Japan Agency for Marine-Earth Science and Technology, 2. Earthquake Research Institute, the University of Tokyo, 3. Tokyo Institute of Technology

地球深部の構造を直接に示すものとして、「地球深部由来のニュートリノ」が注目されている。地球深部由来のニュートリノを観測する施設として、神岡に設置されている反ニュートリノ検出装置「KamLAND」が稼働しているが、ニュートリノの起源となる放射性物質は、地殻に圧倒的な量が分布しているため、地球深部のU, Th量を推定するためには、ニュートリノフラックスの多くを担う地殻由来フラックスを厳密に区分する必要がある。現時点では、地殻由来ニュートリノは、組成、空間分布ともに単純な地殻化学組成モデルを基に構築されているが、実際の日本列島地殻構成岩石の放射性元素は非常に幅広い組成幅を持ち、複雑に分布している。このため、地球深部由来ニュートリノのより精密な測定には、地殻内の放射性元素分布をより精密に区分する必要があり、地殻内元素分布モデルを構築するための高精度の位置情報を有する岩石地球化学データベースが必要となる。

一方、日本列島の地殻がどのような岩石で構成され、いかなる化学組成をもつかは、地震活動、火山活動や地殻変動を理解する上で基礎的情報であるにも関わらず、地質図にあらわされる以上に系統的な解析（例えば統計解析）はほとんど行われていない。日本列島地殻の化学組成の空間的なバリエーションの解析は、日本列島の進化履歴や、沈み込み帯における化学進化を考える上でも重要である。我々は、日本国内出版文献に掲載されている地球化学データのコンパイルを行うデータベース「DODAI」を地質学雑誌に報告した。本発表では、本データベースを用いた「日本列島の地殻化学構造の解析」の「ニュートリノ地球化学」への貢献について報告したい。日本列島全域をカバーし、高精度の位置情報を有する岩石地球化学データベースである「DODAI」は、データ解析、モデリングに有用である。高精度の位置情報を有する地球化学データベースは地球の化学構造のモデリングに有用であり、本報告では、DODAIデータベースと地球ニュートリノを用いた地球の化学研究のポテンシャルを議論したい。

キーワード：ニュートリノ、地球化学データベース、地殻とマントルの地球化学的構造
Keywords: neutrino, geochemical database, geochemical structure of crust and mantle

©2019. Japan Geoscience Union. All Right Reserved.

Viscosity of potassium titanosilicate melt at high pressure

*鈴木 昭夫[1]
*Akio Suzuki[1]

1. 東北大学大学院理学研究科地学専攻
1. Department of Earth Science, Graduate School of Science, Tohoku University

Viscosity of silicate melt is a fundamental property, which controls volcanic processes, including rates of melt extraction, ascent, and magma mixing. Titanium oxide is contained less than 10 wt% in terrestrial magmatic liquids, however, some lunar magmas contains it over 10 wt%. The addition of titanium to silicate melt affects on the properties such as viscosity, density, and compressibility. Especially the pressure dependence of viscosity is of great interest, because magma is generated in the planetary interiors. The aim of this study is to measure the viscosity of K2TiSi4O11 melt at high pressures to estimate the influence of the pressure-induced structural change of melt.
We performed in situ falling sphere viscometry in the pressure range from 1.3 to 7.4 GPa, by using the MAX-III high pressure apparatus at BL14C2 and NE7A beamlines at Photon Factory in KEK, Tsukuba, Japan. A falling platinum sphere in the melt was monitored by using an X-ray CCD camera with a YAG:Ce fluorescence screen. We observed that the viscosity of KTS4 melt decreased up to 3.3 GPa. In contrast, the pressure dependence in viscosity was not observed above 3.3 GPa. Based on XANES spectra of K2TiSi4O11 glasses quenched under high pressure, Paris et al. (1994) showed that the coordination number of titanium increased with increasing pressure. The present study suggests that the melt becomes depolymerized by the coordination change of titanium under high pressure.

キーワード：マグマ、粘度、高圧力
Keywords: magma, viscosity, high pressure

©2019. Japan Geoscience Union. All Right Reserved.

Lattice thermal conductivity of wadsleyite and ringwoodite at the mantle transition zone pressures

*木村 清二[1]、太田 健二[6]、川添 貴章[2]、廣瀬 敬[3]、鍵 裕之[4]、八木 貴志[5]
*seiji kimura[1], Kenji Ohta[6], Takaaki Kawazoe[2], Kei Hirose[3], Hiroyuki Kagi[4], Takashi Yagi[5]

1. 東京工業大学理学院地球惑星科学系、2. 広島大学大学院理学研究科地球惑星システム学専攻、3. 東京工業大学大学　地球生命研究所、4. 東京大学大学院理学系研究科附属地殻化学実験施設 、5. 国立研究開発法人産業技術総合研究所、6. 東京工業大学大学院理工学研究科地球惑星科学専攻
1. Department of Earth and Planetary Sciences Tokyo Institute of Technology, 2. Department of Earth and Planetary Systems Science, Hiroshima University, 3. Earth-Life Science Institute, Tokyo Institute of Technology, 4. Geochemical Research Center, Graduate School of Science, University of Tokyo, 5. National Institute of Advanced Industrial Science and Technology, 6. Department of Earth and Planetary Sciences, Tokyo Institute of Technology

The lattice thermal conductivities of wadsleyite (Wd) and ringwoodite (Rw), which predominantly occupy the Earth's mantle transition zone, are important transport properties to understand the dynamics and thermal structure of the mantle. In particular, the temperature in the subducting slab is mainly controlled by the thermal conduction of Wd and Rw. Wd and Rw are both thought to preserve a large amount of hydrogen ions, thus should play an important role as the main water reservoir in the Earth. Furthermore, it has been reported that the hydration affects the physical properties of minerals including thermal conductivity, and it is necessary to measure the lattice thermal conductivity of Wd and Rw considering their water content. However, so far, the reported lattice thermal conductivities of Wd and Rw has not been considered their water content (Xu et al., 2004). Here we measured the room temperature lattice thermal conductivity of $(Mg_{0.89}Fe_{0.11})_2SiO_4$ Wd and $(Mg_{0.91}Fe_{0.09})_2SiO_4$ Rw up to 27 GPa, respectively, to clarify their hydration dependence using the pulsed light heating thermoreflectance technique in a diamond anvil cell.The obtained results show similar pressure dependence of the lattice thermal conductivity to the previous study (Xu et al., 2004). However, the absolute values of the thermal conductivity are different; the lattice conductivities of hydrous Wd and Rd are ~52% and ~40% lower than the results of Xu et al. (2004), respectively. Our results suggest strong water content dependence of lattice thermal conductivities of Wd and Rw, implying that the water content in the mantle minerals is key factor for calculating the thermal structure in a subducting slab, mantle dynamics.

キーワード：ウォズレアイト、リングウッダイト、マントル遷移層、含水鉱物、熱伝導率
Keywords: wadsleyite, ringwoodite, mantle transition zone, hydrous minerals, thermal conductivity

©2019. Japan Geoscience Union. All Right Reserved.

In-situ X-ray observations of the olivine-spinel transformation under shear deformation: preliminary results on the reaction-induced weakening

*久保 友明[1]、森山 一哉[1]、森 悠一郎[1]、今村 公裕[1]、小泉 早苗[2]、西原 遊[3]、鈴木 昭夫[4]、肥後 祐司[5]
*Tomoaki Kubo[1], Moriyama Kazuya[1], Yuichiro Mori[1], Masahiro Imamura[1], Sanae Koizumi[2], Yu Nishihara[3], Akio Suzuki[4], Yuji Higo[5]

1. 九州大学、2. 東大地震研、3. 愛媛大学GRC、4. 東北大学、5. JASRI
1. Kyushu Univ., 2. ERI, 3. GRC Ehime Univ., 4. Tohoku Univ., 5. JASRI

It has been suggested that high-pressure transformations cause rheological weakening and large deformation of subducting slabs in mantle transition zone (MTZ) . However, there have been few direct experimental evidences so far largely because of the difficulties in quantitative deformation experiments under such conitions. Here we report preliminary results on the olivine-spinel transformation experiments under shear deformation upto MTZ pressures. D-111 (DT-cup) type high-pressure deformation apparatus was newly used for this purpose combined with high-energy synchrotron mono X-rays (50-60 keV) at Photon Factory (PFAR NE7 beamline), which enables in-situ observations of interactions between transformation and creep behaviors. Sintered Mg_2SiO_4 forsterite was first deformed at 15-25 GPa at 600˚C in shear, and subsequently heated to higher temperatures (~0.2˚C/s) to cause the olivine-spinel transformation under shear deformation. The transformation started at much lower temperatures under shear deformation (~900-1100˚C depending on the overpressure from the phase boundary) compared to that without deformation (~1400˚C), suggesting that the shear deformation enhances the olivine-spinel transition rate. The shear strain rate in the sample monitored by X-ray radiography was ~3-4 x 10^{-6} (s^{-1}) at 600˚C, and increased up to ~2-3 x 10^{-4} (s^{-1}) with ramping temperatures even keeping the anvil displacement rate constant (200 micron/h). We observed that the shear weakening does not occur at the same temperature, but reflects on the initiation of the olivine transition. Also, the weakening effects become significant at larger overpressures (and low T). This implies that the weakening of the shear zone induced by the grain-size reduction due to the olivine-spinel transition, however further evidences from microstructural observations are necessary. We plan to install 8-ch acoustic emission measurement system attached with D-111 apparatus to capture the transformation-induced shear instabitiy. Results of D-DIA shear deformation study on the olivine-spinel transition in Fe_2SiO_4 will also be presented and compared with those of the D-111 study in Mg_2SiO_4 .

©2019. Japan Geoscience Union. All Right Reserved.

Internally resistive heated diamond anvil cell experiments with metal encapsulated minerals

*山本 倫也[1]、太田 健二[1]、末広 翔[1]、井上 勇人[1]
*YAMAMOTO TOMONARI[1], Kenji Ohta[1], Sho Suehiro[1], Hayato Inoue[1]

1. 東京工業大学
1. Tokyo Institute of Technology

Heating technique is crucial for *in-situ* high pressure-temperature (*P-T*) studies into the physical and chemical properties of minerals in the diamond anvil cell (DAC) under deep Earth’s conditions. External resistive heating methods that use resistive heaters such as AlChrom-O wire and graphite surrounding the DAC or just the diamonds (Dubrovinskaia and Dubrovinsky, 2003; Du et al., 2013). This approach creates a homogeneous temperature field in the sample chamber but limits the maximum temperature of about 1200℃ due to graphitization of diamond anvils. Double-sided laser heating with a DAC generates the *P-T* conditions corresponding to the center of the Earth’s (Tateno et al., 2010). However, tightly focused laser beams, instabilities in output laser power and misalignment of the focused beams on the sample surface result in significant temperature variation within the sample in the DAC. Internally resistive heated DAC is an effective heating method to overcome the temperature limitation of external heated DAC and the significant temperature gradients experienced in conventional laser-heated DAC (e.g., Zha and Bassett, 2003). However, the internally resistive heated DAC is mostly applied to metal sample to study the properties of the planetary metallic core despite this technique could be applicable to an insulating mineral.

In this study, we modified the internally resistive heated DAC technique for nonmetallic material. We developed a microfabrication technique for total metal encapsulation of the nonmetallic sample. The sample encapsulated by platinum was loaded in DAC with thermal insulator and connected with two electrical leads to make electrical circuit for resistive heating. We confirmed very stable and homogeneous heating for insulating sample at 30 GPa to 2450 K in the modified internally resistive heated DAC. The highest temperature which this method can generate depends on the metal heater encapsulating the sample. This method offers a larger heating volume with more stable and uniform temperature than laser heating and at temperatures much greater than those that can be generated by external resistive heating methods.

References

Dubrovinskaia, N., & Dubrovinsky, L. (2003). Whole-cell heater for the diamond anvil cell. *Review of Scientific Instruments*, *74*(7), 3433-3437.

Du, Z., Miyagi, L., Amulele, G., & Lee, K. K. (2013). Efficient graphite ring heater suitable for diamond-anvil cells to 1300 K. *Review of Scientific Instruments*, *84*(2), 024502.

Tateno, S., Hirose, K., Ohishi, Y., & Tatsumi, Y. (2010). The structure of iron in Earth’s inner core. *Science*, *330*(6002), 359-361.

Zha, C. S., & Bassett, W. A. (2003). Internal resistive heating in diamond anvil cell for in situ X-ray

©2019. Japan Geoscience Union. All Right Reserved.

diffraction and Raman scattering. *Review of scientific instruments*, *74*(3), 1255-1262.

キーワード：内部抵抗加熱式ダイアモンドアンビルセル、高温高圧実験
Keywords: Internally resistive heated diamond anvil cell, high pressure-temperature experiments

©2019. Japan Geoscience Union. All Right Reserved.

Shear deformation on post-spinel

*山崎 大輔[1]、辻野 典秀[1]、西原 遊[2]
*Daisuke Yamazaki[1], Noriyoshi Tsujino[1], Yu Nishihara[2]

1. 岡山大学惑星物質研究所、2. 愛媛大学地球深部ダイナミクス研究センター
1. Institute for Planetary Materials, Okayama University, 2. GRC, Ehime University

Earth’ s lower mantle is mainly composed of ferro-periclase and bridgmanite. The viscosity of ferro-periclase is considered to be 2-3 orders of magnitude lower than that of bridgmanite. Such large discrepancy in viscosity may cause the significant effect of microstructure of the aggregate of bridgmanite and ferro-periclase on bulk viscosity. For example, bulk viscosity is low when the interconnected weak layer structure is formed, whereas bulk viscosity is as high as the viscosity of bridgmanite when the load bearing framework structure is formed [1].

Microstructural evolution from the load bearing framework structure to the interconnected weak layer structure in post-spinel phase (mixture of bridgmanite and ferro-periclase) during deformation was previously reported based on the rotational Drickamer apparatus [2]. This results suggests the important viscosity reduction during deformation in the lower mantle. We therefore considered that more detailed and precise experiments are necessary to discuss the lower mantle rheology quantitatively.

Deformation experiments under the lower mantle conditions can be conducted by using D111-type deformation Kawai-type high pressure apparatus. This apparatus was previously installed at UCL followed by PF-AR and Misasa. In this study, we use these apparatus for the deformation on post-spinel phase.

Starting material for deformation experiment was well-sintered aggregate of bridgmanite and ferro-periclase synthesized at 24 GPa and 1873 K. For the simple shear deformation, we used 45 degree cut design. In in-situ X-ray experiments at PF-AR, we used tapered and coned anvils for X-ray paths. On the other hand, in “quench” experiments at Misasa, we used a simple cubic anvils (TEL=2.0 mm). All deformation experiments were performed with constant D-rams displacement rate.
We deformed sample up to shear strain of ~0.8 with the 0.4 mm displacements of D-rams. SEM observation on the recovered sample by SEM shows that there is no significant evolution in microstructure, indicating that viscosity reduction is not expected with shear deformation to gamma~1. [1] D. Yamazaki, S. Karato: Am. Mineral., **86**, 385 (2001). [2] J. Girard et al.: Science, **351**, 144 (2016).

©2019. Japan Geoscience Union. All Right Reserved.

Lattice thermal conductivity of $CaSiO_3$ perovskite at high pressures and high temperatures

*恩賀 皓太郎[1]、太田 健二[1]、長谷川 暉[1,2]、八木 貴志[2]、廣瀬 敬[3,4]、大石 泰夫[5]
*Kotaro Onga[1], Kenji Ohta[1], Akira Hasegawa[1,2], Takashi Yagi[2], Kei Hirose[3,4], Yasuo Ohishi[5]

1. 東京工業大学理学院地球惑星科学系、2. 産業技術総合研究所、3. 東京工業大学地球生命研究所、4. 東京大学大学院理学系研究科地球惑星科学専攻、5. 高輝度光科学研究センター
1. Department of Earth and Planetary Sciences, Tokyo Institute of Technology, 2. National Institute of Advanced Industrial Science and Technology, 3. Earth-Life Science Institute, Tokyo Institute of Technology, 4. Department of Earth and Planetary Science, The University of Tokyo, 5. Japan Synchrotron Radiation Research Institute

Laboratory measurements of thermal conductivity of deep Earth materials provide important information on the dynamics and thermal evolution of the mantle and the core. $CaSiO_3$ perovskite (CaPv) is a constituent of pyrolitic lower mantle and of the subducting oceanic crust at depth greater than 560 km. In recent years, there are many reports of the laboratory-based lower mantle thermal conductivity profiles, but the thermal conductivity of CaPv has never been measured and included in the models [1,2,3,4,5] . CaPv is an unquenchable high-pressure phase at ambient conditions, and temperature-induced structure change from tetragonal to cubic occurs at around 500 K [6]. Therefore, *in-situ* high pressure and temperature X-ray diffraction (XRD) and thermal conductivity measurements are required to determine the thermal conductivity of CaPv in the Earth’s deep interior.
In this study, we determined the thermal conductivity of CaPv at about 50 GPa and high temperature to 1950 K by a combination of synchrotron XRD measurements and the pulsed light heating thermoreflectance technique. Based on our experimental results, we consider the effect of the presence of CaPv on the thermal conductivity of the pyrolitic lower mantle and the subducting oceanic crust.

Reference: [1] Manthilake, G. et al., *Proc National Acad Sci.* **108,** 17901–17904 (2011). [2] Ohta, K. et al., *Earth Planet Sc. Lett.* **349,**109–115 (2012). [3] Ohta, K. et al., *Earth Planet Sc. Lett.* **465,** 29–37 (2017). [4] Okuda, Y. et al., *Earth Planet Sc. Lett.* **474,** 25–31 (2017). [5] Hsieh, W.-P. et al., J. Geophys. Res. Solid Earth 122, 4900-4917 (2017). [6] Komabayashi, T. et al., *Earth Planet Sc. Lett.* **260,** 564–569 (2007).

キーワード：カルシウムペロフスカイト、熱伝導率、下部マントル
Keywords: CaPv, thermal conductivity, lower mantle

©2019. Japan Geoscience Union. All Right Reserved.

Polycrystalline diamond sintered from ultradispersed nanodiamonds

*西 真之[1,2]、山本 幸一郎[1]、周 佑黙[1]、入舩 徹男[2,1]
*Masayuki Nishi[1,2], Koichiro Yamamoto[1], Youmo Zhou[1], Tetsuo Irifune[2,1]

1. 愛媛大学地球深部ダイナミクス研究センター、2. 東京工業大学地球生命研究所
1. Geodynamics Research Center, Ehime University, 2. Earth-Life Science Institute, Tokyo Institute of Technology

NPD is a binder-less nanodiamond aggregate (~50 nm) synthesized by direct conversion of graphite under high pressure and temperature [1]. Although NPD has extremely high hardness exceeding that of single-crystalline diamond, it is difficult to obtain the large size of the NPD above 1 cm^3, because extreme high pressure conditions are required. Here we show nanodiamond polyclystalline sintered from ultradispersive nanodiamond under relatively moderate pressure and temperature conditions.

We used a multi-anvil apparatus to sinter the nanodiamonds at 8-15 GPa and 1600-2300˚C, where the diamond is thermodynamically stabilized. The starting materials were enclosed in metal capsules. The microstructures and chemical compositions of the recovered samples were examined using a field-emission scanning electron microscope with energy-dispersive X-ray spectroscopy. Well-sintered polycrystalline were subjected to the Knoop indentation test to evaluate its hardness.

We succeeded in recovering the well-sintered polycrystalline diamonds with grain size of ~10-30 nm in some runs (Figure 1). Full width at half maximum of XRD peaks decreased with increasing temperature due to the grain growth of diamond particles. The color, hardness, and grain size of the sintered polycrystalline changed depending on the capsule materials as well as the pressure and temperature conditions. These features might be affected by the porosity, the grain size, and the impurities. Further studies are required to synthesize the polycrystalline with high hardness comparable to NPD.

References: [1] T. Irifune, A. Kurio, S. Sakamoto, T. Inoue, H. Sumiya., *Nature*, **421**, 599 (2003).

キーワード：multianvil apparatus、nanodiamond、NPD
Keywords: multianvil apparatus, nanodiamond, NPD

©2019. Japan Geoscience Union. All Right Reserved.

Thermal conductivity measurements on iron and MgO periclase at high pressure and high temperature similar to the Earth’s mid-lower mantle conditions

*長谷川 暉[1,2]、太田 健二[2]、八木 貴志[1]、廣瀬 敬[3,4]
*Akira Hasegawa[1,2], Kenji Ohta[2], Takashi Yagi[1], Kei Hirose[3,4]

1. 産業技術総合研究所、2. 東京工業大学、3. 東京工業大学地球生命研究所、4. 東京大学
1. National Institute of Advanced Industrial Science and Technology, 2. Tokyo Institude of Technology, 3. Earth-Life Science Institute, Tokyo Institude of Technology, 4. The University of Tokyo

The thermal transport properties of the Earth’s constituents are important information to constrain the thermal evolution and the heat budget of the Earth. In particular, the thermal conductivity of the core, the largest heat source of the Earth, and the lower mantle, occupying more than half the volume of the whole Earth, are indispensable.

In recent years, thermal conductivity measurement on the sample inside the diamond anvil cell has been carried out utilizing the thermoreflectance phenomenon, the reflectance of metal changes slightly due to the temperature perturbation of several kelvin (e.g. Hsieh et al., 2009 Phys Rev B; Yagi et al., 2011 Meas Sci Technol). However, the reported temperature condition is far from that in Earth’s interior.

In this study, we combined the pulsed light heating thermoreflectance method with high power CW laser heating to obtain the thermal conductivity of material *in-situ* at high pressures and temperatures. As a result of test measurement for Pt, we obtained thermal conductivities of Pt up to 60 GPa and 2000 K, which is in good agreement with the measured values using flash heating method in a laser heated diamond anvil cell (McWilliams et al., 2015 Phys Earth Planet In).

The thermal conductivities of iron and MgO periclase were measured up to 60 GPa and 1700 K with this developed system. We found that the obtained thermal conductivities of iron and MgO have negative temperature dependence, and are consistent with the literatures (Fe: Konôpková et al., 2016 Nature; Ohta et al., 2016 Nature, MgO; Manthilake et al., 2011 Proc National Acad Sci; Dekura and Tsuchiya, 2017 Phys Rev B). The newly developed system here would be a powerful tool to examine the thermal conductivity of Earth’s deep interior.

キーワード：熱伝導率、レーザー加熱式ダイヤモンドアンビルセル、パルス光加熱サーモリフレクタンス法、下部マントル、コア
Keywords: thermal conductivity, laser heated diamond anvil cell, pulsed light heating thermoreflectance method, lower mantle, core

©2019. Japan Geoscience Union. All Right Reserved.

Azimuthal anisotropy in the lowermost mantle beneath Philippine from ScS-S times

*田中 聡[1]
*Satoru Tanaka[1]

1. 海洋研究開発機構　地球深部ダイナミクス研究分野
1. Department of Deep Earth Structure and Dynamics Research Japan Agency for Marine-Earth Science and Technology

Introduction: Seismic anisotropy in the lowermost mantle has been detected by splitting of diffracted S and ScS phases, the discrepancy of shear wave splitting of SKS and SKKS, to date. In many cases, the propagation direction of such seismic waves is restricted due to the combination of sources and receivers. Thus, the azimuthal anisotropy using ray paths passing in multi-directions has been rarely discussed. Now, seismic networks and large-scale seismic arrays have been increasing especially in the eastern Asia where there are also many earthquakes. It is a good opportunity to examine an azimuthal variation of travel times passing through the outside of the Pacific Large Low Shear Velocity Province, where the existence of anisotropy in the lowermost mantle is expected.

Data and Method: I used the seismograms of earthquakes occurred in Mariana, east China, Indonesia, and Vanuatu that are record with the seismic stations belonging to IRIS GSN and PASSCAL, Thai Metrological Department, F-net, JISNET, NECESSArray. This geometry gives a good condition that the mid-points of seismic ray paths are located near Philippine with various azimuths.I measured ScS–S differential travel times using a waveform cross-correlation method, which can effectively cancel the heterogeneity in the crust and upper mantle and the uncertainty of hypocenters. The differential travel times are compared with theoretical travel times by PREM with correction of physical dispersion due to anelasticity for the typical period of 10 s, that for ellipticity of the Earth, finally I obtained about 500 residuals. Even though I used the differential travel times, the ScS–S residuals show the large scattering and the correlation with the residuals of S travel times are much larger than that of ScS phases. This means that the raw ScS–S residuals are affected by heterogeneity in the upper part of the lower mantle where only S waves are propagated. Thus, we applied the further corrections using 3D mantle heterogeneity models.

Results and Discussion: We used S-wave 3D models of S16U6L8, S4BL16, S40RTS, SEMUCB-WM, and a P-wave 3D model of GAP-P4 with conversion rate dlnVs/dlnVp=1.7. I found that the scatter of the ScS–S residuals are much improved and that the correlation coefficient between the residuals of ScS–S and ScS are increased and that between ScS–S and S are much reduced when the GAP-P4 model are used for the correction, probably due to its high spatial resolution in the upper lower mantle. As a result, only the ScS–S residuals corrected with the modified GAP-P4 can be used to infer seismic anisotropy in the lowermost mantle.

Then I fitted cos 2qand cos 4qcurves with least square to obtain the characteristics of the azimuthal variation of the ScS–S residuals, clearly indicating that cos 2qcomponent is significant with the fastest direction (the minimum ScS–S) is along ESE-WNW (N110˚E). This can be explained if [100] axis of post-perovskite is oriented vertically and the direction of [001] axis is ESE-WNW for the incident angle of 45˚. The S-wave fastest direction is nearly parallel to the plate motion directions of the Philippine Sea plate and Sunda block. The amplitude of the azimuthal variation in the ScS–S residual is ±1.1 s, which corresponds to 1.7 % anisotropy if we assume the D” thickness of 300 km based on the previous studies

©2019. Japan Geoscience Union. All Right Reserved.

on the D” discontinuity.

キーワード：マントル最下部、地震波異方性
Keywords: lowermost mantle, seismic anisotropy

©2019. Japan Geoscience Union. All Right Reserved.

Detailed 3-D S-velocity structure within D" at the western Pacific LLSVP margin: smaller scale plumes and paleoslabs

*鈴木 裕輝[1]、河合 研志[1]、ゲラー ロバート[1]、田中 聡[2]、Weerachai Siripuvaraporn[3]、Songkhun Boonchaisuku[3]、Noisagool Sutthipong[3]、石原 靖[2]、Taweoon Kim、宮川 幸治[4]、竹内 希[4]
*Yuki Suzuki[1], Kenji Kawai[1], Robert J. Geller[1], Satoru Tanaka[2], Weerachai Siripuvaraporn[3], Songkhun Boonchaisuku[3], Noisagool Sutthipong[3], Yasushi Ishihara[2], Taweoon Kim, Koji MIYAKAWA[4], Nozomu Takeuchi[4]

1. 東京大学、2. 海洋研究開発機構、3. Mahidol University、4. 東京大学地震研究所
1. The University of Tokyo, 2. Japan Agency for Marine-Earth Science and Technology, 3. Mahidol University, 4. Earthquake Research Institute, The University of Tokyo

Global tomographic models of shear velocity have shown two large-scale low shear velocity provinces (LLSVPs) in D″ beneath the Pacific and Africa. It has been controversial whether these LLSVPs are due to thermal effects, chemical effects, or their combination. The nature and origin of the LLSVPs are of fundamental importance since each of the proposed geodynamical scenarios carries different implications for the thermal, chemical and dynamical evolution of the Earth. Previous seismological studies based on travel-time analysis or forward modeling inferred a sharp-sided velocity contrast of the Pacific LLSVP beneath the western Pacific and suggested that the LLSVP is chemically distinct, although the suggested structures of the western edge of the Pacific LLSVP different from each other. To better understand the origin of LLSVPs, it is essential to infer the detailed three-dimensional (3-D) velocity structure within LLSVP beneath the western Pacific. We recently deployed a seismic array stations in Thailand (Thai Seismic Array—TSAR). We assemble waveforms recorded by TSAR as well as other networks such as TM, AU, MM, and MY, allowing us to sample a wider region than previous studies. We conducted waveform inversion using ~5,300 transverse component records of this dataset for the detailed 3-D shear velocity structure in the lowermost 400 km of the mantle beneath the western Pacific. The inferred model shows a low-velocity anomaly immediately above the core-mantle boundary (CMB) and high-velocity anomalies extending vertically from 400 km to the CMB. Taken into account the previous geodynamical simulation studies, the size of the inferred low velocity anomaly suggests a thermal plume rather than a chemical anomaly. The location of the high velocity anomaly in D″ is consistent with the paleo-Izanagi plate subduction boundary about 200 Ma. This implies that a cold paleo-slab produces the strong lateral velocity contrast at the western edge of the western Pacific LLSVP. Hence, we conclude that the western margin of the Pacific LLSVP and its sharp velocity boundary can be explained mainly by thermal effects, and this implies that the lowermost mantle would be well-mixed and the Pacific LLSVP would not be geochemical reservoir.

キーワード：D" region、Pacific LLSVP、Waveform Inversion、Thai Seismic Array (TSAR)
Keywords: D" region, Pacific LLSVP, Waveform Inversion, Thai Seismic Array (TSAR)

©2019. Japan Geoscience Union. All Right Reserved.

Possible interaction between the core and mantle inferred from a core surface flow model

*松島 政貴[1]
*Masaki Matsushima[1]

1. 東京工業大学理学院地球惑星科学系
1. Department of Earth and Planetary Sciences, School of Science, Tokyo Institute of Technology

Fluid flow in the Earth's liquid outer core is responsible for the dynamo action by which the geomagnetic field is generated and maintained. The fluid flow can be estimated from geomagnetic field data, such as spatial distribution of geomagnetic field and its temporal change referred to as secular variations. This implies that spatial and temporal variations of fluid flow in the core provide information on any interaction between the core and mantle. To investigate possible core-mantle interaction, a core surface flow model is obtained from a geomagnetic field model, COV-OBS.x1 (Gillet et al., 2015) using the method of Matsushima (2015). That is, inside a viscous boundary layer at the core-mantle boundary (CMB), magnetic diffusion is assumed to significantly contribute to temporal change of geomagnetic field, and the radial dependence of core flow is expressed in terms of a spiral similar to the Ekman spiral. Below the boundary layer, magnetic diffusion is neglected as in the frozen-flux approximation, and the tangentially magnetostrophic constraint is imposed on the flow.

Any inhomogeneous structure, such as temperature or heat flux, at the CMB is likely to have a strong effect on the core flow. The inhomogeneity successively influences the flow pattern. Therefore, average of fluid flow is expected to show possible core-mantle interaction. Hence, fluid flows inside and below the boundary layer are averaged over the time from 1840 to 2015 covered by the COV-OBS.x1 model. However, mean amplitudes of upwelling and downwelling flows as well as mean horizontal flows are found to be smaller than those at respective times. This result suggests that possible thermal heterogeneity due to the lowermost mantle structure has little effect on the core surface flow; that is, compositional convection is dominant in the Earth's outer core. It should be noted, however, that there is a noticeable upwelling flow corresponding to a counterclockwise vortex beneath the south of Africa, and that the location is just outside the tangent cylinder, an imaginary cylinder parallel to the rotational axis and attached to the equator of the inner core. This may indicate that the vortex corresponds to an edge of columnar convective motion, although the other edge in the northern hemisphere is unclear.

キーワード：核ーマントル相互作用、コア表面流
Keywords: core-mantle interaction, core surface flow

©2019. Japan Geoscience Union. All Right Reserved.

高温高圧条件下での金属-ケイ酸塩メルト間の希ガス分配係数の実験的決定

Determination of the noble gas partition coefficients between metal-silicate melts under high-pressure and high-temperature conditions

*田中 友崇[1]、桑原 秀治[2]、貴志 智[1]、野村 龍一[3]、三部 賢治[5]、鍵 裕之[4]、舘野 繁彦[6]、角野 浩史[1]
*Tomotaka Tanaka[1], Hideharu Kuwahara[2], Satoshi Kishi[1], Ryuichi Nomura[3], Kenji Mibe[5], Hiroyuki Kagi[4], Shigehiko Tateno[6], Hirochika Sumino[1]

1. 東京大学大学院総合文化研究科広域科学専攻相関基礎科学系、2. 愛媛大学　地球深部ダイナミクス研究センター、3. 京都大学、4. 東京大学大学院理学系研究科附属地殻化学実験施設、5. 東京大学地震研究所、6. 東京工業大学地球生命研究所
1. Department of Basic Science, Graduate School of Arts and Sciences, The University of Tokyo , 2. Geodynamics Research Center, Ehime University, 3. Kyoto University, 4. Geochemical Research Center, Graduate School of Science, University of Tokyo, 5. Earthquake Research Institute, University of Tokyo, 6. Earth-Life Science Institute, Tokyo Institute of Technology

Analyses of ocean island basalts reveal a geochemical reservoir characterized by unradiogenic, “primordial” noble gas signatures (e.g., high $^{3}He/^{4}He$ and low $^{40}Ar/^{36}Ar$ ratios), likely residing in the deep mantle. There has been much debate about the area holding the “primordial” noble gases deep in the Earth (Porcelli & Ballentine, 2002), including that the “primordial” noble gasses have been retained in the deepest region of the mantle since 4.4 Ga (Mukhopadhyay, 2012), or in the core since the core-mantle separation (Trieloff & Kunz, 2005; Bouhifd et al., 2013). However, the validity of latter strongly depends on the quantity of noble gases the core incorporates during accretion and can hold in the present day.
In order to investigate noble gas partitioning behavior between the core and mantle, noble gases were dissolved into metal-silicate melts under high temperature and pressure conditions, and then the samples were quenched, recovered, and analyzed for noble gas concentrations. Sample synthesis was performed at the Geodynamics Research Center, Ehime University. Noble-gas doped silicate glass and iron were melted and equilibrated under high pressure and temperature (3-6 GPa, 1700 and 1800 ˚C) using a multianvil apparatus. The sample capsule was cut and the polished surface of the section was investigated with scanning electron microscope and Raman spectroscopy. The chemical compositions of silicate and metal phases were determined with electron microprobe. And then, the noble gases in the silicate phase were extracted by an ultraviolet laser ablation apparatus and analyzed using a noble gas mass spectrometer at the University of Tokyo.
From the Raman spectra, it was found that crystallization (clinopyroxene) had occurred in samples synthesized at pressures of 6 GPa or higher, indicating that the sample quenching was not enough rapid. There is a possibility that noble gas may not be contained much in the crystallized part because a previous study showed that noble gas content in pyroxene crystal is smaller than those in glass (melt) by about 10^{-4} (Heber *et al.*, 2007). The noble gas concentrations in silicate glass phase are fairly homogeneous, even where a crack is formed during quenching. In future we will measure the noble gases in the iron part and determine the partition coefficient of the noble gases.

References: Bouhifd et al, *Nature Geoscience*. **6**, 982-986, 2013; Mukhopadhyay, *Nature* **486**, 101-104,

©2019. Japan Geoscience Union. All Right Reserved.

2012; Porcelli & Ballentine, *Rev. Mineral. Geochem.* **47**, 411-480, 2002; Trieloff & Kunz, *Phys. Earth Planet. Inter.* **148**, 13-38, 2005; Herber *et al*, *Geochim. Cosmochim. Acta*. **71**, 1041-1061, 2007

©2019. Japan Geoscience Union. All Right Reserved.

Measurement of T-dependent electrical resistivity of solid and liquid Fe and Pt at fixed P

*Innocent Ezenwa[1], Takashi Yoshino[1]

1. Institute for Planetary Materials, Okayama University

Knowledge of the thermal and electrical conductivity of solid and liquid Fe and its relevant alloys at P and T conditions is essential for understanding the cooling history of planetary cores and modelling their dynamo. The general understanding of the electrical transport properties of the transition metals at lower P will perhaps give insight in understanding Fe behavior at the inaccessible planetary core conditions. Theoretical investigation has suggested that the electrical and thermal conductivity of solid and liquid Fe at Earth’ s core conditions are similar in value (Wagle and Steinle-Neumann, (2017). At ambient T, experimental investigation showed that hcp ε -phase of Fe becomes paramagnetic at ~18GPa while Pt is paramagnetic and crystalize fcc at ambient conditions. Since Fe and Pt have an unfilled *d*-band electronic structure and at high P both exhibits closed packed crystal structures, experimental determination of the transport properties of molten Pt at lower P conditions is important for understanding the behavior of molten Fe preceding ε -phase at ~80 GPa. We develop a technique and cell design for the investigation of the electrical resistivity of metals that keeps it free from contamination using multianvil press. And, we report measurements on Fe and Pt. The sample was kept pure by making the electrodes and the sample the same composition while the thermocouple (TC) is placed close to the sample and taking through the gasket. The major challenge of TC breakage during compression and/or heating was overcome by shielding the TC with a cylindrical hollow coiling ring made of the same composition as the TC leads. The use of current polarity reversal to eliminate biased voltage as deployed in previous studies was adopted. On Fe and Pt, resistivity increases and decreases with T and P respectively, was observed. On melting, Fe result at 3 GPa agrees with very recent data by Silber et al. (2018) which showed an increasing difference in the resistivity value of solid and liquid with increasing P. While, Pt resistivity at 3 GPa appears constant comparable to its 1 atm value.

Keywords: Electrical resistivity, Thermal Conductivity, Iron Fe

©2019. Japan Geoscience Union. All Right Reserved.

Ancient, highly depleted mantle constrained by Re-Os isotope and highly-siderophile element compositions of French Polynesian xenoliths

*秋澤 紀克[1]、石川 晃[2]、鈴木 勝彦[3]、小木曽 哲[4]
*Norikatsu Akizawa[1], Akira Ishikawa[2], Katsuhiko Suzuki[3], Tetsu Kogiso[4]

1. 東京大学　大気海洋研究所、2. 東京工業大学　理学院地球惑星科学系、3. JAMSTEC　海底資源研究開発センター、4. 京都大学　大学院人間・環境学研究科
1. Atmosphere and Ocean Research Institute, The University of Tokyo, 2. Department of Earth and Planetary Sciences, Tokyo Institute of Technology, 3. Research and Development Center for Submarine Resources, Japan Agency for Marine-Earth Science and Technology (JAMSTEC), 4. Graduate School of Human and Environmental Studies, Kyoto University

Mantle xenoliths, which are fragmented mantle material trapped by ascending magma, can provide lithological and geochemical information of the inaccessible mantle. In order to better understand the lithological and geochemical characteristics of the mantle, we conducted extensive sampling of mantle xenoliths throughout French Polynesia archipelago: Tahiti, Moorea, and Rurutu islands. We collected a total of 42 mantle xenoliths: 1 lherzolite, 14 harzburgites, 22 dunites, 3 wehrlites, and 2 orthopyroxenites. Here, we present whole-rock rhenium-osmium isotope and highly-siderophile element (Os, Ir, Ru, Pt, Pd, and Re) compositions in addition to whole-rock major-element compositions. Osmium isotope ratio ($^{187}Os/^{188}Os$) of the mantle xenoliths ranges from 0.1172 to 0.1464, where the harzburgites show a statistical bimodal distribution with unradiogenic ($^{187}Os/^{188}Os < 0.125$) and radiogenic ($^{187}Os/^{188}Os > 0.125$) compositions. The harzburgites with unradiogenic $^{187}Os/^{188}Os$ are depleted with regards to whole-rock major-element compositions (< 1.22 wt% Al_2O_3), and chondrite-normalized patterns of highly-siderophile elements. Considering the lithological variation of the mantle xenoliths used herein, the mantle is considerably heterogeneous beneath French Polynesia archipelago. In particular, the contrasting isotopic compositions of the harzburgites suggest different mantle reservoirs with unradiogenic and radiogenic $^{187}Os/^{188}Os$ compositions. We propose a possibility that the harzburgites with unradiogenic $^{187}Os/^{188}Os$ are impinged mantle material beneath normal oceanic lithosphere due probably to ascending plumes.

キーワード：ハルツバーガイト、ダナイト、白金族元素、TIMS、ICP-MS、全岩化学組成
Keywords: Harzburgite, Dunite, PGE, TIMS, ICP-MS, Whole-rock chemical composition

©2019. Japan Geoscience Union. All Right Reserved.

First-principles prediction of hydrogen partitioning between the core and mantle

*大場 篤朗[1]、土屋 卓久[1]
*Atsuroh Ohba[1], Taku Tsuchiya[1]

1. 愛媛大学 地球深部ダイナミクス研究センター
1. Ehime University Geodynamics Research Center

Some recent studies have reported high-P,T hydrous minerals which are stable at the core mantle boundary (CMB) pressure (Sano et al., 2008; Ohhira et al., 2016; Nishi et al., 2017). In order to elucidate the water circulation in the Earth's interior, experiments on the reaction between iron and hydrous minerals or water were also conducted (Iizuka-Oku et al., 2016; Mao et al., 2018; Clesi et al., 2018). However, the partition of hydrogen reported is different in different studies. In this study, we try estimating hydrogen partitioning between molten silicate and liquid iron under the CMB conditions based on the first principles calculation method combined with thermodynamic integration similar to our previous study (Xiong et al., 2018). Here, we assume following the exchange reaction of water between liquid iron and molten silicate is expressed as follows
(16MgSiO3+H2O) + 50Fe ⇔16MgSiO3 + (50Fe+H2O)
as a first example with ensuring the charge neutrality. Here, reaction free energy is calculated by the thermodynamic integration molecular dynamics method (Taniuchi & Tsuchiya, 2018). In the moment, simulations suggest that water prefer liquid iron. Now, additional computations are ongoing for improving numerical accuracy. The mechanism dissolving water into liquid iron is also investigated.

©2019. Japan Geoscience Union. All Right Reserved.

Microvolume stable isotope measuremetns and its applicaiton for high-pressure high-temperature experimental run products

*Madhusoodhan Satish-Kumar[1], Shinnosuke Aoyama[1]

1. Department of Geology, Faculty of Science, Niigata University

Light elements are very important in deep earth processes. Its composition in the lower mantle and core is still not well constrained. Stable isotope composition can be effectively used as an independent proxy. Although isotope fractionation in the deep earth occur in a narrow range, the volume of light element content in the mantle and core are extremely high, which can effectively cause significant natural isotopic compositional variations. It is necessary to accurately measure the isotope composition accurately in micro to nanomole scales, because the high-pressure experimental run products are small in volume. Recent studies have predicted the presence of isotope fractionation even at lower mantle and core *P-T* conditions, especially in magma ocean environment and during the core segregation. Despite the necessity of the micro-volume stable isotope measurement, there is always a tradeoff between the accuracy and the sample size.

At Niigata University, a MAT-253 mass spectrometer (Thermo Fisher Scientific) was installed through the MEXT Grant-in-Aid for Scientific Research on Innovative Areas. Carbon and oxygen isotopic compositions are measured using $CO_2$and multiple sulfur isotopic composition are measured using SF_6gas. A new micro-volume inlet system was installed and fundamental parameters such as pressure effect and capillary flow effect were tested. Using the micro-volume inlet system the minimum volume required for analysis is 1 micro-mole sample gas, and the precession for carbon and oxygen isotopic composition are better than 0.1‰. The precession for sulfur isotopes is ±0.3‰ and ±0.01‰ (1s) for $\delta^{34}S$ and $D^{33}S$, respectively, based on the repeated analyses of standard Ag_2S (IAEA S-1).Multiple sulfur isotope measurement system consists of 1) curie point pyrolyzer for rapid conversion of small volume samples to SF_6gas, 2) vacuum line system for pumping out non-condensable gasses, 3) gas chromatograph for purifying the SF_6gas and 4) micro-volume inlet system for introduction of sample gas to ionization chamber.
Multiple sulfur isotope ratios experimental run products were measured using the new system. Metal phases were separated and sulfur was extracted using Cr(II) reduction method [6]. Preliminary results indicate that S isotope fractionations occur in the pressure range of 3–5 GPa, under high-temperature conditions corresponding to the magma ocean environment. The negative $\delta^{34}S$ of mantle, can hence be explained by sulfur isotope fractionation in a magma ocean environment. Sulfur isotope measurements were also carried out on granitoid samples from the Archean with sulfide sulfur showing positive $\delta^{34}S$ values. Mass independent isotope fractionation, expressed as $\Delta^{33}S$, was also observed, suggesting that sulfur in the mantle alone cannot explain these variations. The incorporation of surface sulfur from sedimentary rocks and seawater is proposed.

Keywords: HPHT experiments, Micro-volume stable isotope measurements, Sulfur isotopes

©2019. Japan Geoscience Union. All Right Reserved.

Electrical resistivity of hcp Fe-Si alloys at high pressure and temperature

*井上 勇人[1]、末広 翔[1]、太田 健二[1]、廣瀬 敬[2,3]、大石 泰生[4]
*Hayato Inoue[1], Sho Suehiro[1], Kenji Ohta[1], Kei Hirose[2,3], Yasuo Ohishi[4]

1. 東京工業大学理学院地球惑星科学系、2. 東京工業大学地球生命研究所、3. 東京大学大学院理学系研究科地球惑星科学専攻、4. 高輝度光科学研究センター
1. Department of Earth and Planetary Sciences, Tokyo Institute of Technology, 2. Earth-Life Science Institute, Tokyo Institute of Technology, 3. Department of Earth and Planetary Science, The University of Tokyo, 4. Japan Synchrotron Radiation Research Institute

Silicon (Si) has been repeatedly suggested to be the major light element in the Earth’s core that mainly consists of iron [1]. Alloying the light element(s) affects a variety of physical properties of iron. Electrical and thermal conductivities strongly constrain the dynamics and thermal evolution of Earth’s core and these parameters are linked by the Wiedemann-Franz law ($\kappa = \sigma LT$; κ: thermal conductivity, σ: electrical conductivity, L: Lorenz number, T: absolute temperature). However, measurements of electrical and thermal conductivities under static condition at extremely high pressures (P) and temperature (T) are limited for pure iron [2], [3]. The estimates of the core conductivity considering the effect of light element(s) have been done based on the resistivity saturation model, but the validity of the model at the core condition is unclear [4], [5].
In this study, we examined electrical resistivity (the reciprocal of electrical conductivity) of Fe-2, 4 and 6.5 wt.%Si at high P-T conditions in an internally-heated diamond anvil cell (IHDAC) up to 99 GPa and 2910 K. Our results of electrical resistivity of hcp Fe-Si alloys showed its nonlinear temperature dependence, indicating the occurrence of the resistivity saturation. The resistivity saturation in Fe-Si alloys observed in this study supports the notion of high core conductivity and resulting molten lowermost mantle and young inner core.

References: [1] Poirier: *Phys. Earth Planet. Inter.* **85**, 319-337 (1994).;[2] Ohta et al.: *Nature* **534**, 95–98 (2016).;[3] Konôpková et al.: *Nature* **534**, 99–101 (2016).;[4] Gomi et al.: *Phys. Earth Planet. Inter.* **224**, 88–103 (2013).;[5] Gomi et al.: *Earth Planet. Sci. Lett.* **451**, 51–61 (2016).

キーワード：電気伝導度、熱伝導率、地球コア
Keywords: Electrical conductivity, Thermal conductivity, Earth's core

©2019. Japan Geoscience Union. All Right Reserved.

Electrical resistivity and thermal conductivity of fcc Fe: Implications for the Mercury’ s core

*五味 斎[1]、芳野 極[1]
*Hitoshi Gomi[1], Takashi Yoshino[1]

1. 岡山大学
1. Okayama University

The Mercury’ s magnetic field may be sustained by the geodynamo motion in the liquid Fe core. However, its strength is about 1% of that of Earth. This weak magnetic field may implies a partly stratified core. Gomi et al. (2013) pointed out that the geometry of the thermal stratification depends critically on the depth dependency of the thermal conductivity. In this study, we conducted first-principles calculations on the face-centered cubic (fcc) Fe to constrain the electrical resistivity and the thermal conductivity of the Mercury’ s core.

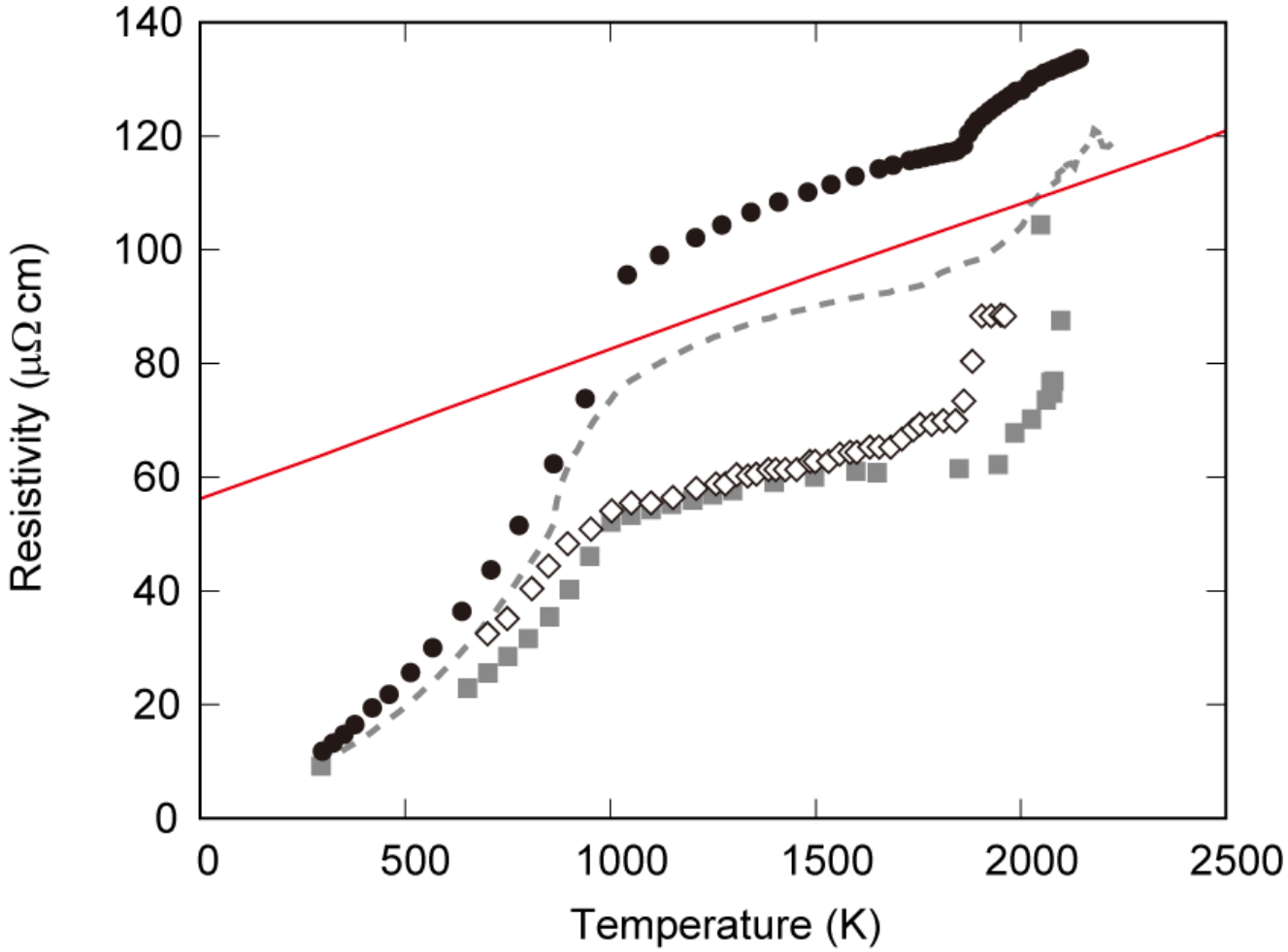
We calculated the electrical resistivity and the thermal conductivity of fcc Fe by means of the Korringa-Kohn-Rostoker method combined with the coherent potential approximation (KKR-CPA) (Akai, 1989). The CPA was adopted to treat the disorder effects due to the atomic vibrations and the magnetic fluctuations on the electronic band structure (Glasbrenner et al., 2014; Ebert et al., 2015; Kou and Akai, 2018). Within the alloy analogy model, the thermal atomic displacements were represented by a discrete set of N_v displacement vectors $\Delta R_v(T)$, where $|\Delta R_v(T)|=\sqrt{<u^2>}$ is the root mean square displacement of atoms, which is based on the Debye model without zero point vibration. The lattice parameter and the Debye temperature are obtained from the equation of state of fcc Fe (Tsujino et al., 2013). In addition to the non-magnetic state, the magnetic disorder was simulated by the local magnetic disorder (LMD) approach. The conductivity was calculated by the Kubo-Greenwood formula with the vertex correction.

The calculated electrical resistivities and thermal conductivities with LMD state are consistent with the literature data at 0 GPa (Ho et al., 1972; 1983), whereas the non-magnetic results show smaller resistivity and larger thermal conductivity. This suggests the importance of the magnetic scattering at low pressures. However, our calculation predicts that the magnetic contribution banishes at higher pressures than 20 GPa. Figure 1 compares the present results and previous experiments (gray broken line; Secco and Scholoessin, 1989, gray square; Deng et al., 2013, open diamond; Pommier, 2018, black circle; Silber et al., 2018) on the electrical resistivity at ~5 GPa. Note that, within the fcc stability field, previous measurements have a large variation. Our calculated resistivity values are between Secco and Scholoessin (1989) and Silber et al. (2018).

We further calculated the electrical resistivity and the thermal conductivity of fcc Fe up to 50 GPa and 3000 K. The thermal conductivity increases with increasing pressure and temperature. This means that, if the inner core is absent, the thermal stratification starts from the bottom, and, after the onset of the inner core, a thick thermal stratified layer may develop at the top of the fluid core (Gomi et al., 2013).

キーワード：電気抵抗率、熱伝導度、水星、核、熱成層
Keywords: electrical resistivity, thermal conductivity, Mercury, core, thermal stratification

©2019. Japan Geoscience Union. All Right Reserved.



©2019. Japan Geoscience Union. All Right Reserved.

Lateral heterogeneity in the lowermost outer core (F layer) of the Earth revealed by seismic analyses

*大滝 壽樹[1]、金嶋 聰[2]、土屋 卓久[3]
*Toshiki Ohtaki[1], Satoshi Kaneshima[2], Taku Tsuchiya[3]

1. 産業技術総合研究所地質情報研究部門、2. 九州大学大学院理学研究院地球惑星科学部門、3. 愛媛大学地球深部ダイナミクス研究センター
1. Geological Survey of Japan, National Institute of Advanced Industrial Science and Technology (AIST), 2. Department of Earth and Planetary Sciences, Kyushu University, 3. Geodynamics Research Center, Ehime University

We have determined seismic velocity structures of the lowermost outer core (F layer) beneath Northeast Pacific and Australia (Ohtaki and Kaneshima, 2015; Ohtaki et al., 2018), and found that the F layer is seismologically heterogeneous. These structures were obtained using a combination of two observations. First one is differential traveltimes between waves that reflect at the inner core boundary (ICB) and that graze the boundary; the second is dispersion (frequency dependence of velocity) of the grazing wave.

Our results show a somewhat strange velocity profile in the F layer beneath Australia, which has a lower-velocity-gradient layer than that of the Preliminary Reference Earth Model (PREM; Dziewonski and Anderson, 1981) on the ICB, and a higher-gradient layer just above the layer. Recent advance in high pressure research enables seismologists to translate lateral seismic velocity variation to relative chemical abundance in the outer core condition. Based on the results of Ichikawa and Tsuchiya (e.g., 2018), we showed light-element enrichment there. This result suggests that lighter fluid exists beneath Australia in the lowermost part of the liquid core, although the outer core is low-viscosity fluid.

The solid inner core of the Earth has quasi-hemispherical structure (e.g., Tanaka and Hamaguchi, 1997). As the origin of this hemispherical structure, uneven growth of the inner core has been proposed (e.g., Aubert et al., 2008; Alboussière et al., 2010; Monnereau et al., 2010). When the liquid in the outer core solidifies at the inner core surface, excess light element is partitioned to residue because the solid inner core is poorer in light elements compared with the liquid outer core. Thus, the uneven growth of the inner core is tied with an uneven release of the light elements to the F layer, which may be related to our results of the heterogeneous F layer. Then, a question arises: this heterogeneity has hemispherical structure like the inner core or local one?

We have not answered it yet because the survey areas of the above studies are restricted. Furthermore, other studies focusing F-layer velocity are not so many. Souriau (2015) determined lateral variations of velocity in the lower outer core using traveltimes of waves that turn there, and suggested that heterogeneity in F has degree-one feature. We also determined the seismic structure of the F layer beneath Antarctica using amplitude ratios between waves that turn just above the inner core and that get into the inner core. Although the resolution and reliability of structure obtained using amplitude ratios is lower than those using the method of our recent papers, the structure beneath Antarctica has a much lower velocity gradient in the F layer compared with PREM. Such a lower gradient is close to the model beneath Australia.

In this paper, we will show the summary of the heterogeneous F-layer structures of velocity and chemical abundance at this stage.

©2019. Japan Geoscience Union. All Right Reserved.

References
Alboussière, T., R. Deguen, and M. Melzani (2010), *Nature*, *466*, 744–747, doi:10.1038/nature09257.
Aubert, J., H. Amit, G. Hulot, and P. Olson (2008), *Nature*, *454*, 758–761, doi:10.1038/nature07109.
Dziewonski, A. M., and D. L. Anderson (1981), *Phys. Earth Planet. Inter.*, 25, 297–356, doi:10.1016/0031-9201(81)90046-7.
Monnereau, M., M. Calvet, L. Margerin, and A. Souriau (2010), *Science*, *328*, 1014–1017, doi:10.1126/science.1186212.
Ichikawa, H., and T. Tsuchiya (2018), J. Geography, 127, 631-646 (in Japanese with English abstract).
Ohtaki, T., S. Kaneshima, and K. Kanjo (2012), *J. Geophys. Res.*, 117, B03312, doi:10.1029/2011JB008717.
Ohtaki, T., and S. Kaneshima (2015), *J. Geophys. Res. Solid Earth*, 120, 7572–7586, doi:10.1002/2015JB012140.
Ohtaki, T., S. Kaneshima, H. Ichikawa, and T. Tsuchiya (2018), *J. Geophys. Res. Solid Earth*, doi:10.1029/2018JB015857.
Tanaka, S., and H. Hamaguchi (1997), *J. Geophys. Res.*, *102*, 2925–2938, doi:10.1029/96JB03187.

キーワード：外核最下部のF層、外核の不均質、オーストラリア下F層での軽元素濃集
Keywords: F layer, lowermost outer core, Heterogeneity of the outer core, Light element concentration in the F layer beneath Australia

©2019. Japan Geoscience Union. All Right Reserved.

内核の不均一成長に伴う地球外核中の流れと軽成分分布
Flows and light element distribution in the outer core associated with heterogeneous growth of the inner core of the Earth

*竹広 真一[1]、佐々木 洋平[2]
*Shin-ichi Takehiro[1], Youhei SASAKI[2]

1. 京都大学数理解析研究所、2. 京都大学大学院理学研究科数学教室
1. Research Institute for Mathematical Sciences, Kyoto University, 2. Department of Mathematics, Kyoto University

近年の地震波解析によると, 内核内の地震波速度の東西不均一な分布が明らかにされ, ICB での相変化が水平一様に生じてはいないという 議論が提唱されるようになった. この観測結果から単純に考えると, 固化半球側の ICB 直上では温度が低く軽成分濃度が高くなり, 溶融半球側で逆に温度が高く軽成分濃度が低くなることが予想される. すなわち, 内核内部の東西不均一分布と ICB 直上の外核内での 熱力学的諸量との相関がみられそうである, しかしながら, 最新の地震波の解析では ICB 直上での地震波速度異常分布は内核内の東西非対称構造とは一致していないことが報告されている.

内核の不均一成長の説明を試みとして外的要因と内的要因の メカニズムがこれまでに提案されてきている. 外的要因説は, 核マントル境界 (CMB) での水平不均一な熱的構造が 外核内に水平熱対流を引き起こし, ICB に水平不均一な温度分布をもたらすと考えるものである. しかしながら, この研究では温度と軽成分をまとめた共密度(co-density)を 用いており, ICB 直上での軽成分分布がどのようになるかが明らかでない. 一方, 内的要因説は, 相変化境界を伴う内核の自発的な不安定性により 横ずれ流れが内核内部に生じるものである. しかしながら, この研究では外核の軽成分がすぐに混合され一様であることを 仮定していおり, ICB 直上での軽成分分布がどのようになるかが明らかでない.

そこで本研究では, 温度と軽成分濃度を独立変数とする回転球殻内の熱組成対流 モデルを用いて, 外的要因および内的要因のそれぞれのストーリーに 沿った熱組成対流の数値実験を行う. 得られる ICB 付近での軽成分濃度分布と 地震波異常分布と比較することにより, もっともらしい外核内の熱組成対流の レジームについて議論する.

キーワード：異方性、内核、核マントル境界
Keywords: Heterogeneity, Inner core, Core-mantle boundary

©2019. Japan Geoscience Union. All Right Reserved.

Sharpness of the hemispherical boundary in the inner core beneath the northern Pacific

*入谷 良平[1]、川勝 均[1]、竹内 希[1]
*Ryohei Iritani[1], Hitoshi Kawakatsu[1], Nozomu Takeuchi[1]

1. 東京大学地震研究所
1. Earthquake Research Institute, Univ. of Tokyo

The hemispherical heterogeneity in the topmost of the Earth’ s inner core, faster velocity and higher attenuation in the eastern hemisphere and slower velocity and weaker attenuation in the western hemisphere, has been revealed by seismological studies. However, how the transition structure between two hemispheres looks like has not been known because of the difficulty to analyze complex core-sensitive data and the limitation of earthquake and seismic array distribution. In this study, we apply the array-based waveform inversion (Iritani et al., 2014) to core phase data that propagate beneath the northern Pacific, and investigate the nature of the transition structure in this region.Dataset used in this study consists of two directional event-station pairs, seismograms observed by the permanent European stations for events at Fiji-Tonga region, and USArray for events near Indonesia. We analyze the broadband vertical component of core phase data containing PKIKP and PKP phases (i.e. the epicentral distance between 145 –155 degree). Resultant analyzed waveforms for EU stations and USArray are 2,108 and 1,172 traces respectively.
In the analysis, waveform inversion approach is employed for each event data to measure traveltime and attenuation in the inner core. As a result, traveltime anomalies observed by EU stations show obvious positive anomaly suggesting mainly propagating the eastern hemisphere, while traveltimes observed by USAray show relatively smaller (or no) anomalies suggesting effects from both of hemispheres. On the other hand, attenuation parameters for both arrays show similar trend that suggests high attenuation corresponding to the eastern hemisphere. To investigate a hemispherical transition boundary in the sampled region, we conduct a ray theory based forward modeling of traveltimes by changing a shape of boundary from meridian boundary to eyeball shaped boundary, and its position. We compute root-mean-square (RMS) of residual between observations and theoretical traveltimes computed with each boundary model. Then, an eyeball shaped boundary, that is located at longitude of 158°W on the equatorial line and latitude of 80°N at the northernmost point, obtained as the preferred boundary model. Finally, we investigate a sharpness of the boundary by varying a width of hemispherical transition. We assume linear variation from the eastern and western hemisphere in a given width and compute RMS. As a result, a width of 600 km at the surface of the inner core shows smaller RMS than sharp boundary. Geophysical significance of this finding will be further discussed.

キーワード：Inner core、Waveform inversion
Keywords: Inner core, Waveform inversion

©2019. Japan Geoscience Union. All Right Reserved.

Stable carbon isotope fractionation in Fe-C system from first principles

*出倉 春彦[1]、土屋 卓久[1]
*Haruhiko Dekura[1], Taku Tsuchiya[1]

1. 愛媛大学地球深部ダイナミクス研究センター
1. Geodynamics Research Center, Ehime University

Carbon is the fourth most abundant element in the solar system and likely one of the constituent light elements in the Earth’s core. Determination of its equilibrium isotope fractionation factor (α) under high pressure (P) and temperature (T) is a key for understanding chemical evolution such as the whole Earth carbon distributions and the amount in the Earth’s core (e.g., Kumar et al., 2011). Because experimental measurement of the isotope fractionation remains technically challenging at the deep mantle condition, attempts to evaluate the α among mantle minerals by first-principles calculations have been made in recent years (e.g., Huang et al., 2014). Recently, our group initiated the theoretical determination of the α in the Fe-C system in the Earth’s deep interior with a full ab initio approach based on the density-functional theory. We performed ab initio lattice dynamics calculations for diamond and iron-carbide (hexagonal Fe7C3) having the two stable carbon isotopes (12C and 13C). The α between the two phases were then determined by using the Gibbs free energies calculated at P ~300 GPa and T ~2000-6000 K. The obtained $10^3 \ln \alpha$ dia-Fe7C3 is found to vary with T from ~+8‰ (2000 K) to ~+5‰ (6000 K). This result indicates that the Fe7C3 is enriched in the heavier isotope (13C) compared with diamond. This trend is qualitatively consistent with low-pressure experimental observations (Kumar et al., 2011).

キーワード：Isotope fractionation、First-principles calculation
Keywords: Isotope fractionation, First-principles calculation

©2019. Japan Geoscience Union. All Right Reserved.

[E] ポスター発表 | セッション記号 S (固体地球科学)：S-IT 地球内部科学・地球惑星テクトニクス

2019年5月27日(月) 17:15 ~ 18:30 | ポスター会場 幕張メッセ国際展示場 8ホール_22

[S-IT21] 核-マントルの相互作用と共進化

コンビーナ:河合 研志(東京大学大学院理学系研究科地球惑星科学専攻)、飯塚 毅(東京大学)、太田 健二(東京工業大学大学院理工学研究科地球惑星科学専攻)、土屋 卓久(愛媛大学地球深部ダイナミクス研究センター)

近年の高圧実験の進歩で、地球中心部に至る温度圧力条件での鉱物の物性測定が可能となってきた。一方、高精度な古地磁気測定、地球物理学観測、精密地球物理学分析、地球ニュートリノによる地球深部放射性物質の直接観測などの発展と共に、マントル対流や地磁気ダイナモの数値シミュレーション技術も大きく発展して、地球内部の状態の理解が進んできた。本セッションでは、地球及び惑星における核ーマントル相互作用と進化に焦点をあてた、様々な研究分野の成果を一堂に会する機会を提供し、情報交換を進めることを目的とする。異なる分野間の連携を発展させるための日本版地球・惑星深部研究グループ(J-SEDI）の形成に関わる講演も歓迎する。

[SIT21-P01] 茨城県稲田花崗岩における小スケールの岩石組成変化の検討 -日本列島地殻由来の地球ニュートリノフラックスの高精度推定に向けて-

★招待講演

*上木 賢太[1]、南 一輝[2]、飯塚 毅[3]、榎本 三四郎[4]、田中 宏幸[2] (1.海洋研究開発機構、2.東京大学地震研究所、3.東京大学地球惑星科学専攻、4.ワシントン大学)

[SIT21-P02] Towards a better estimation of the temperature distribution beneath the Japanese Islands

*田中 明子[1]、山野 誠[2]、濱元 栄起[3]、後藤 秀作[4]、松本 拓己[5] (1.産業技術総合研究所 活断層・火山研究部門、2.東京大学 地震研究所、3.埼玉県 環境科学国際センター、4.産業技術総合研究所 地圏資源環境研究部門、5.防災科学技術研究所)

[SIT21-P03] 日本列島地殻由来の地殻ニュートリノフラックス推定への地球化学データベース利用

*原口 悟[1]、上木 賢太[1]、岩森 光[1,2,3] (1.海洋研究開発機構、2.東京大学地震研究所、3.東京工業大学)

[SIT21-P04] Viscosity of potassium titanosilicate melt at high pressure

*鈴木 昭夫[1] (1.東北大学大学院理学研究科地学専攻)

[SIT21-P05] Lattice thermal conductivity of wadsleyite and ringwoodite at the mantle transition zone pressures

*木村 清二[1]、太田 健二[6]、川添 貴章[2]、廣瀬 敬[3]、鍵 裕之[4]、八木 貴志[5] (1.東京工業大学理学院地球惑星科学系、2.広島大学大学院理学研究科地球惑星システム学専攻、3.東京工業大学大学　地球生命研究所、4.東京大学大学院理学系研究科附属地殻化学実験施設 、5.国立研究開発法人産業技術総合研究所、6.東京工業大学大学院理工学研究科地球惑星科学専攻)

[SIT21-P06] In-situ X-ray observations of the olivine-spinel transformation under shear deformation: preliminary results on the reaction-induced weakening

*久保 友明[1]、森山 一哉[1]、森 悠一郎[1]、今村 公裕[1]、小泉 早苗[2]、西原 遊[3]、鈴木 昭夫[4]、肥後 祐司[5] (1.九州大学、2.東大地震研、3.愛媛大学GRC、4.東北大学、5.JASRI)

[SIT21-P07] Internally resistive heated diamond anvil cell experiments with metal encapsulated minerals

*山本 倫也[1]、太田 健二[1]、末広 翔[1]、井上 勇人[1] (1.東京工業大学)

[SIT21-P08] Shear deformation on post-spinel

*山崎 大輔[1]、辻野 典秀[1]、西原 遊[2] (1.岡山大学惑星物質研究所、2.愛媛大学地球深部ダイナミクス研究センター)

[SIT21-P09] **Lattice thermal conductivity of $CaSiO_3$ perovskite at high pressures and high temperatures**

*恩賀 皓太郎[1]、太田 健二[1]、長谷川 暉[1,2]、八木 貴志[2]、廣瀬 敬[3,4]、大石 泰夫[5] (1.東京工業大学理学院地球惑星科学系、2.産業技術総合研究所、3.東京工業大学地球生命研究所、4.東京大学大学院理学系研究科地球惑星科学専攻、5.高輝度光科学研究センター)

[SIT21-P10] **Polycrystalline diamond sintered from ultradispersed nanodiamonds**

*西 真之[1,2]、山本 幸一郎[1]、周 佑黙[1]、入舩 徹男[2,1] (1.愛媛大学地球深部ダイナミクス研究センター、2.東京工業大学地球生命研究所)

[SIT21-P11] Thermal conductivity measurements on iron and MgO periclase at high pressure and high temperature similar to the Earth's mid-lower mantle conditions

*長谷川 暉[1,2]、太田 健二[2]、八木 貴志[1]、廣瀬 敬[3,4] (1.産業技術総合研究所、2.東京工業大学、3.東京工業大学地球生命研究所、4.東京大学)

[SIT21-P12] Azimuthal anisotropy in the lowermost mantle beneath Philippine from ScS-S times

*田中 聡[1] (1.海洋研究開発機構　地球深部ダイナミクス研究分野)

[SIT21-P13] Detailed 3-D S-velocity structure within D" at the western Pacific LLSVP margin: smaller scale plumes and paleoslabs

*鈴木 裕輝[1]、河合 研志[1]、ゲラー ロバート[1]、田中 聡[2]、Weerachai Siripuvaraporn[3]、Songkhun Boonchaisuku[3]、Noisagool Sutthipong[3]、石原 靖[2]、Taweoon Kim、宮川 幸治[4]、竹内 希[4] (1.東京大学、2.海洋研究開発機構、3.Mahidol University、4.東京大学地震研究所)

[SIT21-P14] Possible interaction between the core and mantle inferred from a core surface flow model

*松島 政貴[1] (1.東京工業大学理学院地球惑星科学系)

[SIT21-P15] 高温高圧条件下での金属-ケイ酸塩メルト間の希ガス分配係数の実験的決定

*田中 友崇[1]、桑原 秀治[2]、貴志 智[1]、野村 龍一[3]、三部 賢治[5]、鍵 裕之[4]、舘野 繁彦[6]、角野 浩史[1] (1.東京大学大学院総合文化研究科広域科学専攻相関基礎科学系、2.愛媛大学　地球深部ダイナミクス研究センター、3.京都大学、4.東京大学大学院理学系研究科附属地殻化学実験施設、5.東京大学地震研究所、6.東京工業大学地球生命研究所)

[SIT21-P16] **Measurement of T-dependent electrical resistivity of solid and liquid Fe and Pt at fixed P**

*Innocent Ezenwa[1]、Takashi Yoshino[1] (1.Institute for Planetary Materials, Okayama University)

[SIT21-P17] Ancient, highly depleted mantle constrained by Re-Os isotope and highly-siderophile element compositions of French Polynesian xenoliths

*秋澤 紀克[1]、石川 晃[2]、鈴木 勝彦[3]、小木曽 哲[4] (1.東京大学　大気海洋研究所、2.東京工業大学　理学院地球惑星科学系、3.JAMSTEC　海底資源研究開発センター、4.京都大学　大学院人間・環境学研究科)

[SIT21-P18] First-principles prediction of hydrogen partitioning between the core and mantle

*大場 篤朗[1]、土屋 卓久[1] (1.愛媛大学 地球深部ダイナミクス研究センター)

[SIT21-P19] Microvolume stable isotope measuremetns and its applicaiton for high-pressure high-temperature experimental run products

*Madhusoodhan Satish-Kumar[1]、Shinnosuke Aoyama[1] (1.Department of Geology, Faculty of Science, Niigata University)

[SIT21-P20] Electrical resistivity of hcp Fe-Si alloys at high pressure and temperature

*井上 勇人[1]、末広 翔[1]、太田 健二[1]、廣瀬 敬[2,3]、大石 泰生[4] (1.東京工業大学理学院地球惑星科学系、2.東京工業大学地球生命研究所、3.東京大学大学院理学系研究科地球惑星科学専攻、4.高輝度光科学研究センター)

[SIT21-P21] Electrical resistivity and thermal conductivity of fcc Fe: Implications for the Mercury's core

★Invited Papers

*五味 斎[1]、芳野 極[1] (1.岡山大学)

[SIT21-P22] Lateral heterogeneity in the lowermost outer core (F layer) of the Earth revealed by seismic analyses

*大滝 壽樹[1]、金嶋 聰[2]、土屋 卓久[3] (1.産業技術総合研究所地質情報研究部門、2.九州大学大学院理学研究院地球惑星科学部門、3.愛媛大学地球深部ダイナミクス研究センター)

[SIT21-P23] 内核の不均一成長に伴う地球外核中の流れと軽成分分布

*竹広 真一[1]、佐々木 洋平[2] (1.京都大学数理解析研究所、2.京都大学大学院理学研究科数学教室)

[SIT21-P24] Sharpness of the hemispherical boundary in the inner core beneath the northern Pacific

*入谷 良平[1]、川勝 均[1]、竹内 希[1] (1.東京大学地震研究所)

[SIT21-P25] Stable carbon isotope fractionation in Fe-C system from first principles

*出倉 春彦[1]、土屋 卓久[1] (1.愛媛大学地球深部ダイナミクス研究センター)

茨城県稲田花崗岩における小スケールの岩石組成変化の検討 -日本列島地殻由来の地球ニュートリノフラックスの高精度推定に向けて-
Sample-scale compositional variation of the Inada granite, Ibaraki, Japan -toward the reduction of geoneutrino flux estimation errors from the Japanese crust-

*上木 賢太[1]、南 一輝[2]、飯塚 毅[3]、榎本 三四郎[4]、田中 宏幸[2]
*Kenta Ueki[1], Minami Kazuki[2], Tsuyoshi Iizuka[3], Sanshiro Enomoto[4], Hiroyuki Tanaka[2]

1. 海洋研究開発機構、2. 東京大学地震研究所、3. 東京大学地球惑星科学専攻、4. ワシントン大学
1. Japan Agency for Marine-Earth Science and Technology, 2. Earthquake Research Institute, University of Tokyo, 3. Department of Earth and Planetary Science, University of Tokyo, 4. Center for Experimental Nuclear Physics and Astrophysics, University of Washington

Geoneutrio observed at anti-neutrino observatory "KamLAND" in Kamioka (Hida City, Gifu Prefecture), enables us to directly observe the abundance of radiogenic elements in the deep earth. As crustal rocks exhibit a high concentration of geoneutrino producing radiogenic elements (Uranium and Thorium) than mantle rocks, we have to subtract the contribution of geoneutrino from the Japanese crust from the observation value in Kamioka to estimate geoneutrino flux from core and mantle. For the purpose, we estimated the 3D distribution of uranium and thorium in the Japanese crust by the stochastic modeling using the seismic velocity structure, geological information and geochemical database for the Japanese crustal rock. Geoneutrino flux calculated using the compositional map exhibits a very large error (up to 80%) at present.
We found that information on the compositional heterogeneity (spatial correlation) of various length scale, such as of the single rock suite scale (km to m scale), and sample scale (cm to mm scale) are essential to reduce the estimation error of crustal geoneutrino flux as small as the observation error of the geoneutrino on KamLAND. Therefore, we conducted a grid sampling of the granite of Inada, Ibaraki prefecture, to obtain quantitative knowledge on the small scale compositional heterogeneity. Samples (about 500g) were divided into several centimeter scale split (about 25g). Based on the compositional variations between small splits from one sample, we discuss the small scale sample wise compositional variation. Whole rock chemical composition of each small split was analyzed using XRF. Also, we conducted surface analysis using an ED-XRF to evaluate the spatial distribution of elements in each split. As a result, even within a single sample (about 500g), a compositional variation of about several% at maximum was observed. This result indicates that when conducting the analysis based on the rock chemical composition considering the spatial context, it is necessary to properly evaluate the sample scale heterogeneity, in addition to the tectonic scale, the rock suite scale, and microscopic scale.Also, this result will contribute to the reduction of the estimation error of geoneutrino from the Japanese crust.

キーワード：地球ニュートリノ、花崗岩、岩石化学組成
Keywords: Geoneutrino, Granite, Rock chemical composition

©2019. Japan Geoscience Union. All Right Reserved.

Towards a better estimation of the temperature distribution beneath the Japanese Islands

*田中 明子[1]、山野 誠[2]、濱元 栄起[3]、後藤 秀作[4]、松本 拓己[5]
*Akiko Tanaka[1], Makoto Yamano[2], Hideki Hamamoto[3], Shusaku Goto[4], Takumi Matsumoto[5]

1. 産業技術総合研究所 活断層・火山研究部門、2. 東京大学 地震研究所、3. 埼玉県 環境科学国際センター、4. 産業技術総合研究所 地圏資源環境研究部門、5. 防災科学技術研究所
1. Geological Survey of Japan, National Institute of Advanced Industrial Science and Technology, 2. Earthquake Research Institute, The University of Tokyo, 3. Center for Environmental Science in Saitama, 4. Institute for Geo-Resources and Environment National Institute of Advanced Industrial Science and Technology, 5. National Research Institute for Earth Science and Disaster Resilience

To improve our understanding of the thermal evolution and structure of the deep Earth, it is necessary to know the shallow part of them. Surface heat flow provides important constraint on it. However, the number of heat flow data is limited and spatially very inhomogeneous and even in regions with measurements the data quality varies. For this reason, we have been working on compiling a comprehensive database of heat flow, thermal conductivity, and geothermal gradient. In 2004, Geological Survey of Japan published a digital geoscience map entitled "Geothermal Gradient and Heat Flow Data in and around Japan", which contains heat flow data in the northwestern Pacific area (from 0 to 60°N and from 120 to 160°E) and geothermal gradient data in and around Japan. In 2019, we will be releasing database entitled "Thermal Data Collection in and around Japan", which contains continuously updated of geothermal gradient and heat flow data and adds thermal conductivity data in and around Japan. Thermal conductivity data were compiled from published data and site-specific reports, and measured using the archived cores. This database offers considerable improvements over the previous version released in 2004, and will be published and available at https://www.gsj.jp/en/database/db-portal/index.html. It presents an opportunity to revisit the thermal state of the lithosphere along with other geophysical/geochemical constraints on heat flow extrapolation.

キーワード：地殻熱流量、熱伝導率、地温勾配
Keywords: heat flow, thermal conductivity, geothermal gradient

©2019. Japan Geoscience Union. All Right Reserved.

日本列島地殻由来の地殻ニュートリノフラックス推定への地球化学データベース利用

The estimation of the neutrino flux from the crust of the Japanese islands using the geochemical database

*原口 悟[1]、上木 賢太[1]、岩森 光[1,2,3]
*Satoru Haraguchi[1], Kenta Ueki[1], Hikaru Iwamori[1,2,3]

1. 海洋研究開発機構、2. 東京大学地震研究所、3. 東京工業大学
1. Japan Agency for Marine-Earth Science and Technology, 2. Earthquake Research Institute, the University of Tokyo, 3. Tokyo Institute of Technology

地球深部の構造を直接に示すものとして、「地球深部由来のニュートリノ」が注目されている。地球深部由来のニュートリノを観測する施設として、神岡に設置されている反ニュートリノ検出装置「KamLAND」が稼働しているが、ニュートリノの起源となる放射性物質は、地殻に圧倒的な量が分布しているため、地球深部のU, Th量を推定するためには、ニュートリノフラックスの多くを担う地殻由来フラックスを厳密に区分する必要がある。現時点では、地殻由来ニュートリノは、組成、空間分布ともに単純な地殻化学組成モデルを基に構築されているが、実際の日本列島地殻構成岩石の放射性元素は非常に幅広い組成幅を持ち、複雑に分布している。このため、地球深部由来ニュートリノのより精密な測定には、地殻内の放射性元素分布をより精密に区分する必要があり、地殻内元素分布モデルを構築するための高精度の位置情報を有する岩石地球化学データベースが必要となる。

一方、日本列島の地殻がどのような岩石で構成され、いかなる化学組成をもつかは、地震活動、火山活動や地殻変動を理解する上で基礎的情報であるにも関わらず、地質図にあらわされる以上に系統的な解析（例えば統計解析）はほとんど行われていない。日本列島地殻の化学組成の空間的なバリエーションの解析は、日本列島の進化履歴や、沈み込み帯における化学進化を考える上でも重要である。我々は、日本国内出版文献に掲載されている地球化学データのコンパイルを行うデータベース「DODAI」を地質学雑誌に報告した。本発表では、本データベースを用いた「日本列島の地殻化学構造の解析」の「ニュートリノ地球化学」への貢献について報告したい。日本列島全域をカバーし、高精度の位置情報を有する岩石地球化学データベースである「DODAI」は、データ解析、モデリングに有用である。高精度の位置情報を有する地球化学データベースは地球の化学構造のモデリングに有用であり、本報告では、DODAIデータベースと地球ニュートリノを用いた地球の化学研究のポテンシャルを議論したい。

キーワード：ニュートリノ、地球化学データベース、地殻とマントルの地球化学的構造
Keywords: neutrino, geochemical database, geochemical structure of crust and mantle

©2019. Japan Geoscience Union. All Right Reserved.

Viscosity of potassium titanosilicate melt at high pressure

*鈴木 昭夫[1]
*Akio Suzuki[1]

1. 東北大学大学院理学研究科地学専攻
1. Department of Earth Science, Graduate School of Science, Tohoku University

Viscosity of silicate melt is a fundamental property, which controls volcanic processes, including rates of melt extraction, ascent, and magma mixing. Titanium oxide is contained less than 10 wt% in terrestrial magmatic liquids, however, some lunar magmas contains it over 10 wt%. The addition of titanium to silicate melt affects on the properties such as viscosity, density, and compressibility. Especially the pressure dependence of viscosity is of great interest, because magma is generated in the planetary interiors. The aim of this study is to measure the viscosity of K2TiSi4O11 melt at high pressures to estimate the influence of the pressure-induced structural change of melt.
We performed in situ falling sphere viscometry in the pressure range from 1.3 to 7.4 GPa, by using the MAX-III high pressure apparatus at BL14C2 and NE7A beamlines at Photon Factory in KEK, Tsukuba, Japan. A falling platinum sphere in the melt was monitored by using an X-ray CCD camera with a YAG:Ce fluorescence screen. We observed that the viscosity of KTS4 melt decreased up to 3.3 GPa. In contrast, the pressure dependence in viscosity was not observed above 3.3 GPa. Based on XANES spectra of K2TiSi4O11 glasses quenched under high pressure, Paris et al. (1994) showed that the coordination number of titanium increased with increasing pressure. The present study suggests that the melt becomes depolymerized by the coordination change of titanium under high pressure.

キーワード：マグマ、粘度、高圧力
Keywords: magma, viscosity, high pressure

©2019. Japan Geoscience Union. All Right Reserved.

Lattice thermal conductivity of wadsleyite and ringwoodite at the mantle transition zone pressures

*木村 清二[1]、太田 健二[6]、川添 貴章[2]、廣瀬 敬[3]、鍵 裕之[4]、八木 貴志[5]
*seiji kimura[1], Kenji Ohta[6], Takaaki Kawazoe[2], Kei Hirose[3], Hiroyuki Kagi[4], Takashi Yagi[5]

1. 東京工業大学理学院地球惑星科学系、2. 広島大学大学院理学研究科地球惑星システム学専攻、3. 東京工業大学大学　地球生命研究所、4. 東京大学大学院理学系研究科附属地殻化学実験施設 、5. 国立研究開発法人産業技術総合研究所、6. 東京工業大学大学院理工学研究科地球惑星科学専攻
1. Department of Earth and Planetary Sciences Tokyo Institute of Technology, 2. Department of Earth and Planetary Systems Science, Hiroshima University, 3. Earth-Life Science Institute, Tokyo Institute of Technology, 4. Geochemical Research Center, Graduate School of Science, University of Tokyo, 5. National Institute of Advanced Industrial Science and Technology, 6. Department of Earth and Planetary Sciences, Tokyo Institute of Technology

The lattice thermal conductivities of wadsleyite (Wd) and ringwoodite (Rw), which predominantly occupy the Earth's mantle transition zone, are important transport properties to understand the dynamics and thermal structure of the mantle. In particular, the temperature in the subducting slab is mainly controlled by the thermal conduction of Wd and Rw. Wd and Rw are both thought to preserve a large amount of hydrogen ions, thus should play an important role as the main water reservoir in the Earth. Furthermore, it has been reported that the hydration affects the physical properties of minerals including thermal conductivity, and it is necessary to measure the lattice thermal conductivity of Wd and Rw considering their water content. However, so far, the reported lattice thermal conductivities of Wd and Rw has not been considered their water content (Xu et al., 2004). Here we measured the room temperature lattice thermal conductivity of $(Mg_{0.89}Fe_{0.11})_2SiO_4$ Wd and $(Mg_{0.91}Fe_{0.09})_2SiO_4$ Rw up to 27 GPa, respectively, to clarify their hydration dependence using the pulsed light heating thermoreflectance technique in a diamond anvil cell.The obtained results show similar pressure dependence of the lattice thermal conductivity to the previous study (Xu et al., 2004). However, the absolute values of the thermal conductivity are different; the lattice conductivities of hydrous Wd and Rd are ~52% and ~40% lower than the results of Xu et al. (2004), respectively. Our results suggest strong water content dependence of lattice thermal conductivities of Wd and Rw, implying that the water content in the mantle minerals is key factor for calculating the thermal structure in a subducting slab, mantle dynamics.

キーワード：ウォズレアイト、リングウッダイト、マントル遷移層、含水鉱物、熱伝導率
Keywords: wadsleyite, ringwoodite, mantle transition zone, hydrous minerals, thermal conductivity

©2019. Japan Geoscience Union. All Right Reserved.

In-situ X-ray observations of the olivine-spinel transformation under shear deformation: preliminary results on the reaction-induced weakening

*久保 友明[1]、森山 一哉[1]、森 悠一郎[1]、今村 公裕[1]、小泉 早苗[2]、西原 遊[3]、鈴木 昭夫[4]、肥後 祐司[5]
*Tomoaki Kubo[1], Moriyama Kazuya[1], Yuichiro Mori[1], Masahiro Imamura[1], Sanae Koizumi[2], Yu Nishihara[3], Akio Suzuki[4], Yuji Higo[5]

1. 九州大学、2. 東大地震研、3. 愛媛大学GRC、4. 東北大学、5. JASRI
1. Kyushu Univ., 2. ERI, 3. GRC Ehime Univ., 4. Tohoku Univ., 5. JASRI

It has been suggested that high-pressure transformations cause rheological weakening and large deformation of subducting slabs in mantle transition zone (MTZ) . However, there have been few direct experimental evidences so far largely because of the difficulties in quantitative deformation experiments under such conitions. Here we report preliminary results on the olivine-spinel transformation experiments under shear deformation upto MTZ pressures. D-111 (DT-cup) type high-pressure deformation apparatus was newly used for this purpose combined with high-energy synchrotron mono X-rays (50-60 keV) at Photon Factory (PFAR NE7 beamline), which enables in-situ observations of interactions between transformation and creep behaviors. Sintered Mg_2SiO_4 forsterite was first deformed at 15-25 GPa at 600˚C in shear, and subsequently heated to higher temperatures (~0.2˚C/s) to cause the olivine-spinel transformation under shear deformation. The transformation started at much lower temperatures under shear deformation (~900-1100˚C depending on the overpressure from the phase boundary) compared to that without deformation (~1400˚C), suggesting that the shear deformation enhances the olivine-spinel transition rate. The shear strain rate in the sample monitored by X-ray radiography was ~3-4 x 10^{-6} (s^{-1}) at 600˚C, and increased up to ~2-3 x 10^{-4} (s^{-1}) with ramping temperatures even keeping the anvil displacement rate constant (200 micron/h). We observed that the shear weakening does not occur at the same temperature, but reflects on the initiation of the olivine transition. Also, the weakening effects become significant at larger overpressures (and low T). This implies that the weakening of the shear zone induced by the grain-size reduction due to the olivine-spinel transition, however further evidences from microstructural observations are necessary. We plan to install 8-ch acoustic emission measurement system attached with D-111 apparatus to capture the transformation-induced shear instabitiy. Results of D-DIA shear deformation study on the olivine-spinel transition in Fe_2SiO_4 will also be presented and compared with those of the D-111 study in Mg_2SiO_4 .

©2019. Japan Geoscience Union. All Right Reserved.

Internally resistive heated diamond anvil cell experiments with metal encapsulated minerals

*山本 倫也[1]、太田 健二[1]、末広 翔[1]、井上 勇人[1]
*YAMAMOTO TOMONARI[1], Kenji Ohta[1], Sho Suehiro[1], Hayato Inoue[1]

1. 東京工業大学
1. Tokyo Institute of Technology

Heating technique is crucial for *in-situ* high pressure-temperature (*P-T*) studies into the physical and chemical properties of minerals in the diamond anvil cell (DAC) under deep Earth’s conditions. External resistive heating methods that use resistive heaters such as AlChrom-O wire and graphite surrounding the DAC or just the diamonds (Dubrovinskaia and Dubrovinsky, 2003; Du et al., 2013). This approach creates a homogeneous temperature field in the sample chamber but limits the maximum temperature of about 1200℃ due to graphitization of diamond anvils. Double-sided laser heating with a DAC generates the *P-T* conditions corresponding to the center of the Earth’s (Tateno et al., 2010). However, tightly focused laser beams, instabilities in output laser power and misalignment of the focused beams on the sample surface result in significant temperature variation within the sample in the DAC. Internally resistive heated DAC is an effective heating method to overcome the temperature limitation of external heated DAC and the significant temperature gradients experienced in conventional laser-heated DAC (e.g., Zha and Bassett, 2003). However, the internally resistive heated DAC is mostly applied to metal sample to study the properties of the planetary metallic core despite this technique could be applicable to an insulating mineral.

In this study, we modified the internally resistive heated DAC technique for nonmetallic material. We developed a microfabrication technique for total metal encapsulation of the nonmetallic sample. The sample encapsulated by platinum was loaded in DAC with thermal insulator and connected with two electrical leads to make electrical circuit for resistive heating. We confirmed very stable and homogeneous heating for insulating sample at 30 GPa to 2450 K in the modified internally resistive heated DAC. The highest temperature which this method can generate depends on the metal heater encapsulating the sample. This method offers a larger heating volume with more stable and uniform temperature than laser heating and at temperatures much greater than those that can be generated by external resistive heating methods.

References

Dubrovinskaia, N., & Dubrovinsky, L. (2003). Whole-cell heater for the diamond anvil cell. *Review of Scientific Instruments*, *74*(7), 3433-3437.

Du, Z., Miyagi, L., Amulele, G., & Lee, K. K. (2013). Efficient graphite ring heater suitable for diamond-anvil cells to 1300 K. *Review of Scientific Instruments*, *84*(2), 024502.

Tateno, S., Hirose, K., Ohishi, Y., & Tatsumi, Y. (2010). The structure of iron in Earth’s inner core. *Science*, *330*(6002), 359-361.

Zha, C. S., & Bassett, W. A. (2003). Internal resistive heating in diamond anvil cell for in situ X-ray

©2019. Japan Geoscience Union. All Right Reserved.

diffraction and Raman scattering. *Review of scientific instruments*, *74*(3), 1255-1262.

キーワード：内部抵抗加熱式ダイアモンドアンビルセル、高温高圧実験
Keywords: Internally resistive heated diamond anvil cell, high pressure-temperature experiments

©2019. Japan Geoscience Union. All Right Reserved.

Shear deformation on post-spinel

*山崎 大輔[1]、辻野 典秀[1]、西原 遊[2]
*Daisuke Yamazaki[1], Noriyoshi Tsujino[1], Yu Nishihara[2]

1. 岡山大学惑星物質研究所、2. 愛媛大学地球深部ダイナミクス研究センター
1. Institute for Planetary Materials, Okayama University, 2. GRC, Ehime University

Earth’ s lower mantle is mainly composed of ferro-periclase and bridgmanite. The viscosity of ferro-periclase is considered to be 2-3 orders of magnitude lower than that of bridgmanite. Such large discrepancy in viscosity may cause the significant effect of microstructure of the aggregate of bridgmanite and ferro-periclase on bulk viscosity. For example, bulk viscosity is low when the interconnected weak layer structure is formed, whereas bulk viscosity is as high as the viscosity of bridgmanite when the load bearing framework structure is formed [1].

Microstructural evolution from the load bearing framework structure to the interconnected weak layer structure in post-spinel phase (mixture of bridgmanite and ferro-periclase) during deformation was previously reported based on the rotational Drickamer apparatus [2]. This results suggests the important viscosity reduction during deformation in the lower mantle. We therefore considered that more detailed and precise experiments are necessary to discuss the lower mantle rheology quantitatively.

Deformation experiments under the lower mantle conditions can be conducted by using D111-type deformation Kawai-type high pressure apparatus. This apparatus was previously installed at UCL followed by PF-AR and Misasa. In this study, we use these apparatus for the deformation on post-spinel phase.

Starting material for deformation experiment was well-sintered aggregate of bridgmanite and ferro-periclase synthesized at 24 GPa and 1873 K. For the simple shear deformation, we used 45 degree cut design. In in-situ X-ray experiments at PF-AR, we used tapered and coned anvils for X-ray paths. On the other hand, in “quench” experiments at Misasa, we used a simple cubic anvils (TEL=2.0 mm). All deformation experiments were performed with constant D-rams displacement rate.
We deformed sample up to shear strain of ~0.8 with the 0.4 mm displacements of D-rams. SEM observation on the recovered sample by SEM shows that there is no significant evolution in microstructure, indicating that viscosity reduction is not expected with shear deformation to gamma~1. [1] D. Yamazaki, S. Karato: Am. Mineral., **86**, 385 (2001). [2] J. Girard et al.: Science, **351**, 144 (2016).

©2019. Japan Geoscience Union. All Right Reserved.

Lattice thermal conductivity of $CaSiO_3$ perovskite at high pressures and high temperatures

*恩賀 皓太郎[1]、太田 健二[1]、長谷川 暉[1,2]、八木 貴志[2]、廣瀬 敬[3,4]、大石 泰夫[5]
*Kotaro Onga[1], Kenji Ohta[1], Akira Hasegawa[1,2], Takashi Yagi[2], Kei Hirose[3,4], Yasuo Ohishi[5]

1. 東京工業大学理学院地球惑星科学系、2. 産業技術総合研究所、3. 東京工業大学地球生命研究所、4. 東京大学大学院理学系研究科地球惑星科学専攻、5. 高輝度光科学研究センター
1. Department of Earth and Planetary Sciences, Tokyo Institute of Technology, 2. National Institute of Advanced Industrial Science and Technology, 3. Earth-Life Science Institute, Tokyo Institute of Technology, 4. Department of Earth and Planetary Science, The University of Tokyo, 5. Japan Synchrotron Radiation Research Institute

Laboratory measurements of thermal conductivity of deep Earth materials provide important information on the dynamics and thermal evolution of the mantle and the core. $CaSiO_3$ perovskite (CaPv) is a constituent of pyrolitic lower mantle and of the subducting oceanic crust at depth greater than 560 km. In recent years, there are many reports of the laboratory-based lower mantle thermal conductivity profiles, but the thermal conductivity of CaPv has never been measured and included in the models [1,2,3,4,5] . CaPv is an unquenchable high-pressure phase at ambient conditions, and temperature-induced structure change from tetragonal to cubic occurs at around 500 K [6]. Therefore, *in-situ* high pressure and temperature X-ray diffraction (XRD) and thermal conductivity measurements are required to determine the thermal conductivity of CaPv in the Earth’s deep interior.
In this study, we determined the thermal conductivity of CaPv at about 50 GPa and high temperature to 1950 K by a combination of synchrotron XRD measurements and the pulsed light heating thermoreflectance technique. Based on our experimental results, we consider the effect of the presence of CaPv on the thermal conductivity of the pyrolitic lower mantle and the subducting oceanic crust.

Reference: [1] Manthilake, G. et al., *Proc National Acad Sci.* **108,** 17901–17904 (2011). [2] Ohta, K. et al., *Earth Planet Sc. Lett.* **349,**109–115 (2012). [3] Ohta, K. et al., *Earth Planet Sc. Lett.* **465,** 29–37 (2017). [4] Okuda, Y. et al., *Earth Planet Sc. Lett.* **474,** 25–31 (2017). [5] Hsieh, W.-P. et al., J. Geophys. Res. Solid Earth 122, 4900-4917 (2017). [6] Komabayashi, T. et al., *Earth Planet Sc. Lett.* **260,** 564–569 (2007).

キーワード：カルシウムペロフスカイト、熱伝導率、下部マントル
Keywords: CaPv, thermal conductivity, lower mantle

©2019. Japan Geoscience Union. All Right Reserved.

Polycrystalline diamond sintered from ultradispersed nanodiamonds

*西 真之[1,2]、山本 幸一郎[1]、周 佑黙[1]、入舩 徹男[2,1]
*Masayuki Nishi[1,2], Koichiro Yamamoto[1], Youmo Zhou[1], Tetsuo Irifune[2,1]

1. 愛媛大学地球深部ダイナミクス研究センター、2. 東京工業大学地球生命研究所
1. Geodynamics Research Center, Ehime University, 2. Earth-Life Science Institute, Tokyo Institute of Technology

NPD is a binder-less nanodiamond aggregate (~50 nm) synthesized by direct conversion of graphite under high pressure and temperature [1]. Although NPD has extremely high hardness exceeding that of single-crystalline diamond, it is difficult to obtain the large size of the NPD above 1 cm^3, because extreme high pressure conditions are required. Here we show nanodiamond polyclystalline sintered from ultradispersive nanodiamond under relatively moderate pressure and temperature conditions.

We used a multi-anvil apparatus to sinter the nanodiamonds at 8-15 GPa and 1600-2300˚C, where the diamond is thermodynamically stabilized. The starting materials were enclosed in metal capsules. The microstructures and chemical compositions of the recovered samples were examined using a field-emission scanning electron microscope with energy-dispersive X-ray spectroscopy. Well-sintered polycrystalline were subjected to the Knoop indentation test to evaluate its hardness.

We succeeded in recovering the well-sintered polycrystalline diamonds with grain size of ~10-30 nm in some runs (Figure 1). Full width at half maximum of XRD peaks decreased with increasing temperature due to the grain growth of diamond particles. The color, hardness, and grain size of the sintered polycrystalline changed depending on the capsule materials as well as the pressure and temperature conditions. These features might be affected by the porosity, the grain size, and the impurities. Further studies are required to synthesize the polycrystalline with high hardness comparable to NPD.

References: [1] T. Irifune, A. Kurio, S. Sakamoto, T. Inoue, H. Sumiya., *Nature*, **421**, 599 (2003).

キーワード：multianvil apparatus、nanodiamond、NPD
Keywords: multianvil apparatus, nanodiamond, NPD

©2019. Japan Geoscience Union. All Right Reserved.

Thermal conductivity measurements on iron and MgO periclase at high pressure and high temperature similar to the Earth’s mid-lower mantle conditions

*長谷川 暉[1,2]、太田 健二[2]、八木 貴志[1]、廣瀬 敬[3,4]
*Akira Hasegawa[1,2], Kenji Ohta[2], Takashi Yagi[1], Kei Hirose[3,4]

1. 産業技術総合研究所、2. 東京工業大学、3. 東京工業大学地球生命研究所、4. 東京大学
1. National Institute of Advanced Industrial Science and Technology, 2. Tokyo Institude of Technology, 3. Earth-Life Science Institute, Tokyo Institude of Technology, 4. The University of Tokyo

The thermal transport properties of the Earth’s constituents are important information to constrain the thermal evolution and the heat budget of the Earth. In particular, the thermal conductivity of the core, the largest heat source of the Earth, and the lower mantle, occupying more than half the volume of the whole Earth, are indispensable.

In recent years, thermal conductivity measurement on the sample inside the diamond anvil cell has been carried out utilizing the thermoreflectance phenomenon, the reflectance of metal changes slightly due to the temperature perturbation of several kelvin (e.g. Hsieh et al., 2009 Phys Rev B; Yagi et al., 2011 Meas Sci Technol). However, the reported temperature condition is far from that in Earth’s interior.

In this study, we combined the pulsed light heating thermoreflectance method with high power CW laser heating to obtain the thermal conductivity of material *in-situ* at high pressures and temperatures. As a result of test measurement for Pt, we obtained thermal conductivities of Pt up to 60 GPa and 2000 K, which is in good agreement with the measured values using flash heating method in a laser heated diamond anvil cell (McWilliams et al., 2015 Phys Earth Planet In).

The thermal conductivities of iron and MgO periclase were measured up to 60 GPa and 1700 K with this developed system. We found that the obtained thermal conductivities of iron and MgO have negative temperature dependence, and are consistent with the literatures (Fe: Konôpková et al., 2016 Nature; Ohta et al., 2016 Nature, MgO; Manthilake et al., 2011 Proc National Acad Sci; Dekura and Tsuchiya, 2017 Phys Rev B). The newly developed system here would be a powerful tool to examine the thermal conductivity of Earth’s deep interior.

キーワード：熱伝導率、レーザー加熱式ダイヤモンドアンビルセル、パルス光加熱サーモリフレクタンス法、下部マントル、コア
Keywords: thermal conductivity, laser heated diamond anvil cell, pulsed light heating thermoreflectance method, lower mantle, core

©2019. Japan Geoscience Union. All Right Reserved.

Azimuthal anisotropy in the lowermost mantle beneath Philippine from ScS-S times

*田中 聡[1]
*Satoru Tanaka[1]

1. 海洋研究開発機構　地球深部ダイナミクス研究分野
1. Department of Deep Earth Structure and Dynamics Research Japan Agency for Marine-Earth Science and Technology

Introduction: Seismic anisotropy in the lowermost mantle has been detected by splitting of diffracted S and ScS phases, the discrepancy of shear wave splitting of SKS and SKKS, to date. In many cases, the propagation direction of such seismic waves is restricted due to the combination of sources and receivers. Thus, the azimuthal anisotropy using ray paths passing in multi-directions has been rarely discussed. Now, seismic networks and large-scale seismic arrays have been increasing especially in the eastern Asia where there are also many earthquakes. It is a good opportunity to examine an azimuthal variation of travel times passing through the outside of the Pacific Large Low Shear Velocity Province, where the existence of anisotropy in the lowermost mantle is expected.

Data and Method: I used the seismograms of earthquakes occurred in Mariana, east China, Indonesia, and Vanuatu that are record with the seismic stations belonging to IRIS GSN and PASSCAL, Thai Metrological Department, F-net, JISNET, NECESSArray. This geometry gives a good condition that the mid-points of seismic ray paths are located near Philippine with various azimuths.I measured ScS–S differential travel times using a waveform cross-correlation method, which can effectively cancel the heterogeneity in the crust and upper mantle and the uncertainty of hypocenters. The differential travel times are compared with theoretical travel times by PREM with correction of physical dispersion due to anelasticity for the typical period of 10 s, that for ellipticity of the Earth, finally I obtained about 500 residuals. Even though I used the differential travel times, the ScS–S residuals show the large scattering and the correlation with the residuals of S travel times are much larger than that of ScS phases. This means that the raw ScS–S residuals are affected by heterogeneity in the upper part of the lower mantle where only S waves are propagated. Thus, we applied the further corrections using 3D mantle heterogeneity models.

Results and Discussion: We used S-wave 3D models of S16U6L8, S4BL16, S40RTS, SEMUCB-WM, and a P-wave 3D model of GAP-P4 with conversion rate dlnVs/dlnVp=1.7. I found that the scatter of the ScS–S residuals are much improved and that the correlation coefficient between the residuals of ScS–S and ScS are increased and that between ScS–S and S are much reduced when the GAP-P4 model are used for the correction, probably due to its high spatial resolution in the upper lower mantle. As a result, only the ScS–S residuals corrected with the modified GAP-P4 can be used to infer seismic anisotropy in the lowermost mantle.

Then I fitted cos 2qand cos 4qcurves with least square to obtain the characteristics of the azimuthal variation of the ScS–S residuals, clearly indicating that cos 2qcomponent is significant with the fastest direction (the minimum ScS–S) is along ESE-WNW (N110˚E). This can be explained if [100] axis of post-perovskite is oriented vertically and the direction of [001] axis is ESE-WNW for the incident angle of 45˚. The S-wave fastest direction is nearly parallel to the plate motion directions of the Philippine Sea plate and Sunda block. The amplitude of the azimuthal variation in the ScS–S residual is ±1.1 s, which corresponds to 1.7 % anisotropy if we assume the D” thickness of 300 km based on the previous studies

©2019. Japan Geoscience Union. All Right Reserved.

on the D” discontinuity.

キーワード：マントル最下部、地震波異方性
Keywords: lowermost mantle, seismic anisotropy

©2019. Japan Geoscience Union. All Right Reserved.

Detailed 3-D S-velocity structure within D" at the western Pacific LLSVP margin: smaller scale plumes and paleoslabs

*鈴木 裕輝[1]、河合 研志[1]、ゲラー ロバート[1]、田中 聡[2]、Weerachai Siripuvaraporn[3]、Songkhun Boonchaisuku[3]、Noisagool Sutthipong[3]、石原 靖[2]、Taweoon Kim、宮川 幸治[4]、竹内 希[4]
*Yuki Suzuki[1], Kenji Kawai[1], Robert J. Geller[1], Satoru Tanaka[2], Weerachai Siripuvaraporn[3], Songkhun Boonchaisuku[3], Noisagool Sutthipong[3], Yasushi Ishihara[2], Taweoon Kim, Koji MIYAKAWA[4], Nozomu Takeuchi[4]

1. 東京大学、2. 海洋研究開発機構、3. Mahidol University、4. 東京大学地震研究所
1. The University of Tokyo, 2. Japan Agency for Marine-Earth Science and Technology, 3. Mahidol University, 4. Earthquake Research Institute, The University of Tokyo

Global tomographic models of shear velocity have shown two large-scale low shear velocity provinces (LLSVPs) in D″ beneath the Pacific and Africa. It has been controversial whether these LLSVPs are due to thermal effects, chemical effects, or their combination. The nature and origin of the LLSVPs are of fundamental importance since each of the proposed geodynamical scenarios carries different implications for the thermal, chemical and dynamical evolution of the Earth. Previous seismological studies based on travel-time analysis or forward modeling inferred a sharp-sided velocity contrast of the Pacific LLSVP beneath the western Pacific and suggested that the LLSVP is chemically distinct, although the suggested structures of the western edge of the Pacific LLSVP different from each other. To better understand the origin of LLSVPs, it is essential to infer the detailed three-dimensional (3-D) velocity structure within LLSVP beneath the western Pacific. We recently deployed a seismic array stations in Thailand (Thai Seismic Array—TSAR). We assemble waveforms recorded by TSAR as well as other networks such as TM, AU, MM, and MY, allowing us to sample a wider region than previous studies. We conducted waveform inversion using ~5,300 transverse component records of this dataset for the detailed 3-D shear velocity structure in the lowermost 400 km of the mantle beneath the western Pacific. The inferred model shows a low-velocity anomaly immediately above the core-mantle boundary (CMB) and high-velocity anomalies extending vertically from 400 km to the CMB. Taken into account the previous geodynamical simulation studies, the size of the inferred low velocity anomaly suggests a thermal plume rather than a chemical anomaly. The location of the high velocity anomaly in D″ is consistent with the paleo-Izanagi plate subduction boundary about 200 Ma. This implies that a cold paleo-slab produces the strong lateral velocity contrast at the western edge of the western Pacific LLSVP. Hence, we conclude that the western margin of the Pacific LLSVP and its sharp velocity boundary can be explained mainly by thermal effects, and this implies that the lowermost mantle would be well-mixed and the Pacific LLSVP would not be geochemical reservoir.

キーワード：D" region、Pacific LLSVP、Waveform Inversion、Thai Seismic Array (TSAR)
Keywords: D" region, Pacific LLSVP, Waveform Inversion, Thai Seismic Array (TSAR)

©2019. Japan Geoscience Union. All Right Reserved.

Possible interaction between the core and mantle inferred from a core surface flow model

*松島 政貴[1]
*Masaki Matsushima[1]

1. 東京工業大学理学院地球惑星科学系
1. Department of Earth and Planetary Sciences, School of Science, Tokyo Institute of Technology

Fluid flow in the Earth's liquid outer core is responsible for the dynamo action by which the geomagnetic field is generated and maintained. The fluid flow can be estimated from geomagnetic field data, such as spatial distribution of geomagnetic field and its temporal change referred to as secular variations. This implies that spatial and temporal variations of fluid flow in the core provide information on any interaction between the core and mantle. To investigate possible core-mantle interaction, a core surface flow model is obtained from a geomagnetic field model, COV-OBS.x1 (Gillet et al., 2015) using the method of Matsushima (2015). That is, inside a viscous boundary layer at the core-mantle boundary (CMB), magnetic diffusion is assumed to significantly contribute to temporal change of geomagnetic field, and the radial dependence of core flow is expressed in terms of a spiral similar to the Ekman spiral. Below the boundary layer, magnetic diffusion is neglected as in the frozen-flux approximation, and the tangentially magnetostrophic constraint is imposed on the flow.

Any inhomogeneous structure, such as temperature or heat flux, at the CMB is likely to have a strong effect on the core flow. The inhomogeneity successively influences the flow pattern. Therefore, average of fluid flow is expected to show possible core-mantle interaction. Hence, fluid flows inside and below the boundary layer are averaged over the time from 1840 to 2015 covered by the COV-OBS.x1 model. However, mean amplitudes of upwelling and downwelling flows as well as mean horizontal flows are found to be smaller than those at respective times. This result suggests that possible thermal heterogeneity due to the lowermost mantle structure has little effect on the core surface flow; that is, compositional convection is dominant in the Earth's outer core. It should be noted, however, that there is a noticeable upwelling flow corresponding to a counterclockwise vortex beneath the south of Africa, and that the location is just outside the tangent cylinder, an imaginary cylinder parallel to the rotational axis and attached to the equator of the inner core. This may indicate that the vortex corresponds to an edge of columnar convective motion, although the other edge in the northern hemisphere is unclear.

キーワード：核ーマントル相互作用、コア表面流
Keywords: core-mantle interaction, core surface flow

©2019. Japan Geoscience Union. All Right Reserved.

高温高圧条件下での金属-ケイ酸塩メルト間の希ガス分配係数の実験的決定

Determination of the noble gas partition coefficients between metal-silicate melts under high-pressure and high-temperature conditions

*田中 友崇[1]、桑原 秀治[2]、貴志 智[1]、野村 龍一[3]、三部 賢治[5]、鍵 裕之[4]、舘野 繁彦[6]、角野 浩史[1]
*Tomotaka Tanaka[1], Hideharu Kuwahara[2], Satoshi Kishi[1], Ryuichi Nomura[3], Kenji Mibe[5], Hiroyuki Kagi[4], Shigehiko Tateno[6], Hirochika Sumino[1]

1. 東京大学大学院総合文化研究科広域科学専攻相関基礎科学系、2. 愛媛大学　地球深部ダイナミクス研究センター、3. 京都大学、4. 東京大学大学院理学系研究科附属地殻化学実験施設、5. 東京大学地震研究所、6. 東京工業大学地球生命研究所
1. Department of Basic Science, Graduate School of Arts and Sciences, The University of Tokyo , 2. Geodynamics Research Center, Ehime University, 3. Kyoto University, 4. Geochemical Research Center, Graduate School of Science, University of Tokyo, 5. Earthquake Research Institute, University of Tokyo, 6. Earth-Life Science Institute, Tokyo Institute of Technology

Analyses of ocean island basalts reveal a geochemical reservoir characterized by unradiogenic, “primordial” noble gas signatures (e.g., high $^{3}He/^{4}He$ and low $^{40}Ar/^{36}Ar$ ratios), likely residing in the deep mantle. There has been much debate about the area holding the “primordial” noble gases deep in the Earth (Porcelli & Ballentine, 2002), including that the “primordial” noble gasses have been retained in the deepest region of the mantle since 4.4 Ga (Mukhopadhyay, 2012), or in the core since the core-mantle separation (Trieloff & Kunz, 2005; Bouhifd et al., 2013). However, the validity of latter strongly depends on the quantity of noble gases the core incorporates during accretion and can hold in the present day.
In order to investigate noble gas partitioning behavior between the core and mantle, noble gases were dissolved into metal-silicate melts under high temperature and pressure conditions, and then the samples were quenched, recovered, and analyzed for noble gas concentrations. Sample synthesis was performed at the Geodynamics Research Center, Ehime University. Noble-gas doped silicate glass and iron were melted and equilibrated under high pressure and temperature (3-6 GPa, 1700 and 1800 ˚C) using a multianvil apparatus. The sample capsule was cut and the polished surface of the section was investigated with scanning electron microscope and Raman spectroscopy. The chemical compositions of silicate and metal phases were determined with electron microprobe. And then, the noble gases in the silicate phase were extracted by an ultraviolet laser ablation apparatus and analyzed using a noble gas mass spectrometer at the University of Tokyo.
From the Raman spectra, it was found that crystallization (clinopyroxene) had occurred in samples synthesized at pressures of 6 GPa or higher, indicating that the sample quenching was not enough rapid. There is a possibility that noble gas may not be contained much in the crystallized part because a previous study showed that noble gas content in pyroxene crystal is smaller than those in glass (melt) by about 10^{-4} (Heber *et al.*, 2007). The noble gas concentrations in silicate glass phase are fairly homogeneous, even where a crack is formed during quenching. In future we will measure the noble gases in the iron part and determine the partition coefficient of the noble gases.

References: Bouhifd et al, *Nature Geoscience*. **6**, 982-986, 2013; Mukhopadhyay, *Nature* **486**, 101-104,

©2019. Japan Geoscience Union. All Right Reserved.

2012; Porcelli & Ballentine, *Rev. Mineral. Geochem.* **47**, 411-480, 2002; Trieloff & Kunz, *Phys. Earth Planet. Inter.* **148**, 13-38, 2005; Herber *et al*, *Geochim. Cosmochim. Acta*. **71**, 1041-1061, 2007

©2019. Japan Geoscience Union. All Right Reserved.

Measurement of T-dependent electrical resistivity of solid and liquid Fe and Pt at fixed P

*Innocent Ezenwa[1], Takashi Yoshino[1]

1. Institute for Planetary Materials, Okayama University

Knowledge of the thermal and electrical conductivity of solid and liquid Fe and its relevant alloys at P and T conditions is essential for understanding the cooling history of planetary cores and modelling their dynamo. The general understanding of the electrical transport properties of the transition metals at lower P will perhaps give insight in understanding Fe behavior at the inaccessible planetary core conditions. Theoretical investigation has suggested that the electrical and thermal conductivity of solid and liquid Fe at Earth’ s core conditions are similar in value (Wagle and Steinle-Neumann, (2017). At ambient T, experimental investigation showed that hcp ε -phase of Fe becomes paramagnetic at ~18GPa while Pt is paramagnetic and crystalize fcc at ambient conditions. Since Fe and Pt have an unfilled *d*-band electronic structure and at high P both exhibits closed packed crystal structures, experimental determination of the transport properties of molten Pt at lower P conditions is important for understanding the behavior of molten Fe preceding ε -phase at ~80 GPa. We develop a technique and cell design for the investigation of the electrical resistivity of metals that keeps it free from contamination using multianvil press. And, we report measurements on Fe and Pt. The sample was kept pure by making the electrodes and the sample the same composition while the thermocouple (TC) is placed close to the sample and taking through the gasket. The major challenge of TC breakage during compression and/or heating was overcome by shielding the TC with a cylindrical hollow coiling ring made of the same composition as the TC leads. The use of current polarity reversal to eliminate biased voltage as deployed in previous studies was adopted. On Fe and Pt, resistivity increases and decreases with T and P respectively, was observed. On melting, Fe result at 3 GPa agrees with very recent data by Silber et al. (2018) which showed an increasing difference in the resistivity value of solid and liquid with increasing P. While, Pt resistivity at 3 GPa appears constant comparable to its 1 atm value.

Keywords: Electrical resistivity, Thermal Conductivity, Iron Fe

©2019. Japan Geoscience Union. All Right Reserved.

Ancient, highly depleted mantle constrained by Re-Os isotope and highly-siderophile element compositions of French Polynesian xenoliths

*秋澤 紀克[1]、石川 晃[2]、鈴木 勝彦[3]、小木曽 哲[4]
*Norikatsu Akizawa[1], Akira Ishikawa[2], Katsuhiko Suzuki[3], Tetsu Kogiso[4]

1. 東京大学　大気海洋研究所、2. 東京工業大学　理学院地球惑星科学系、3. JAMSTEC　海底資源研究開発センター、4. 京都大学　大学院人間・環境学研究科
1. Atmosphere and Ocean Research Institute, The University of Tokyo, 2. Department of Earth and Planetary Sciences, Tokyo Institute of Technology, 3. Research and Development Center for Submarine Resources, Japan Agency for Marine-Earth Science and Technology (JAMSTEC), 4. Graduate School of Human and Environmental Studies, Kyoto University

Mantle xenoliths, which are fragmented mantle material trapped by ascending magma, can provide lithological and geochemical information of the inaccessible mantle. In order to better understand the lithological and geochemical characteristics of the mantle, we conducted extensive sampling of mantle xenoliths throughout French Polynesia archipelago: Tahiti, Moorea, and Rurutu islands. We collected a total of 42 mantle xenoliths: 1 lherzolite, 14 harzburgites, 22 dunites, 3 wehrlites, and 2 orthopyroxenites. Here, we present whole-rock rhenium-osmium isotope and highly-siderophile element (Os, Ir, Ru, Pt, Pd, and Re) compositions in addition to whole-rock major-element compositions. Osmium isotope ratio ($^{187}Os/^{188}Os$) of the mantle xenoliths ranges from 0.1172 to 0.1464, where the harzburgites show a statistical bimodal distribution with unradiogenic ($^{187}Os/^{188}Os < 0.125$) and radiogenic ($^{187}Os/^{188}Os > 0.125$) compositions. The harzburgites with unradiogenic $^{187}Os/^{188}Os$ are depleted with regards to whole-rock major-element compositions (< 1.22 wt% Al_2O_3), and chondrite-normalized patterns of highly-siderophile elements. Considering the lithological variation of the mantle xenoliths used herein, the mantle is considerably heterogeneous beneath French Polynesia archipelago. In particular, the contrasting isotopic compositions of the harzburgites suggest different mantle reservoirs with unradiogenic and radiogenic $^{187}Os/^{188}Os$ compositions. We propose a possibility that the harzburgites with unradiogenic $^{187}Os/^{188}Os$ are impinged mantle material beneath normal oceanic lithosphere due probably to ascending plumes.

キーワード：ハルツバーガイト、ダナイト、白金族元素、TIMS、ICP-MS、全岩化学組成
Keywords: Harzburgite, Dunite, PGE, TIMS, ICP-MS, Whole-rock chemical composition

©2019. Japan Geoscience Union. All Right Reserved.

First-principles prediction of hydrogen partitioning between the core and mantle

*大場 篤朗[1]、土屋 卓久[1]
*Atsuroh Ohba[1], Taku Tsuchiya[1]

1. 愛媛大学 地球深部ダイナミクス研究センター
1. Ehime University Geodynamics Research Center

Some recent studies have reported high-P,T hydrous minerals which are stable at the core mantle boundary (CMB) pressure (Sano et al., 2008; Ohhira et al., 2016; Nishi et al., 2017). In order to elucidate the water circulation in the Earth's interior, experiments on the reaction between iron and hydrous minerals or water were also conducted (Iizuka-Oku et al., 2016; Mao et al., 2018; Clesi et al., 2018). However, the partition of hydrogen reported is different in different studies. In this study, we try estimating hydrogen partitioning between molten silicate and liquid iron under the CMB conditions based on the first principles calculation method combined with thermodynamic integration similar to our previous study (Xiong et al., 2018). Here, we assume following the exchange reaction of water between liquid iron and molten silicate is expressed as follows
(16MgSiO3+H2O) + 50Fe ⇔16MgSiO3 + (50Fe+H2O)
as a first example with ensuring the charge neutrality. Here, reaction free energy is calculated by the thermodynamic integration molecular dynamics method (Taniuchi & Tsuchiya, 2018). In the moment, simulations suggest that water prefer liquid iron. Now, additional computations are ongoing for improving numerical accuracy. The mechanism dissolving water into liquid iron is also investigated.

©2019. Japan Geoscience Union. All Right Reserved.

Microvolume stable isotope measuremetns and its applicaiton for high-pressure high-temperature experimental run products

*Madhusoodhan Satish-Kumar[1], Shinnosuke Aoyama[1]

1. Department of Geology, Faculty of Science, Niigata University

Light elements are very important in deep earth processes. Its composition in the lower mantle and core is still not well constrained. Stable isotope composition can be effectively used as an independent proxy. Although isotope fractionation in the deep earth occur in a narrow range, the volume of light element content in the mantle and core are extremely high, which can effectively cause significant natural isotopic compositional variations. It is necessary to accurately measure the isotope composition accurately in micro to nanomole scales, because the high-pressure experimental run products are small in volume. Recent studies have predicted the presence of isotope fractionation even at lower mantle and core *P-T* conditions, especially in magma ocean environment and during the core segregation. Despite the necessity of the micro-volume stable isotope measurement, there is always a tradeoff between the accuracy and the sample size.

At Niigata University, a MAT-253 mass spectrometer (Thermo Fisher Scientific) was installed through the MEXT Grant-in-Aid for Scientific Research on Innovative Areas. Carbon and oxygen isotopic compositions are measured using $CO_2$and multiple sulfur isotopic composition are measured using SF_6gas. A new micro-volume inlet system was installed and fundamental parameters such as pressure effect and capillary flow effect were tested. Using the micro-volume inlet system the minimum volume required for analysis is 1 micro-mole sample gas, and the precession for carbon and oxygen isotopic composition are better than 0.1‰. The precession for sulfur isotopes is ±0.3‰ and ±0.01‰ (1s) for $\delta^{34}S$ and $D^{33}S$, respectively, based on the repeated analyses of standard Ag_2S (IAEA S-1).Multiple sulfur isotope measurement system consists of 1) curie point pyrolyzer for rapid conversion of small volume samples to SF_6gas, 2) vacuum line system for pumping out non-condensable gasses, 3) gas chromatograph for purifying the SF_6gas and 4) micro-volume inlet system for introduction of sample gas to ionization chamber.
Multiple sulfur isotope ratios experimental run products were measured using the new system. Metal phases were separated and sulfur was extracted using Cr(II) reduction method [6]. Preliminary results indicate that S isotope fractionations occur in the pressure range of 3–5 GPa, under high-temperature conditions corresponding to the magma ocean environment. The negative $\delta^{34}S$ of mantle, can hence be explained by sulfur isotope fractionation in a magma ocean environment. Sulfur isotope measurements were also carried out on granitoid samples from the Archean with sulfide sulfur showing positive $\delta^{34}S$ values. Mass independent isotope fractionation, expressed as $\Delta^{33}S$, was also observed, suggesting that sulfur in the mantle alone cannot explain these variations. The incorporation of surface sulfur from sedimentary rocks and seawater is proposed.

Keywords: HPHT experiments, Micro-volume stable isotope measurements, Sulfur isotopes

©2019. Japan Geoscience Union. All Right Reserved.

Electrical resistivity of hcp Fe-Si alloys at high pressure and temperature

*井上 勇人[1]、末広 翔[1]、太田 健二[1]、廣瀬 敬[2,3]、大石 泰生[4]
*Hayato Inoue[1], Sho Suehiro[1], Kenji Ohta[1], Kei Hirose[2,3], Yasuo Ohishi[4]

1. 東京工業大学理学院地球惑星科学系、2. 東京工業大学地球生命研究所、3. 東京大学大学院理学系研究科地球惑星科学専攻、4. 高輝度光科学研究センター
1. Department of Earth and Planetary Sciences, Tokyo Institute of Technology, 2. Earth-Life Science Institute, Tokyo Institute of Technology, 3. Department of Earth and Planetary Science, The University of Tokyo, 4. Japan Synchrotron Radiation Research Institute

Silicon (Si) has been repeatedly suggested to be the major light element in the Earth’s core that mainly consists of iron [1]. Alloying the light element(s) affects a variety of physical properties of iron. Electrical and thermal conductivities strongly constrain the dynamics and thermal evolution of Earth’s core and these parameters are linked by the Wiedemann-Franz law ($\kappa = \sigma LT$; κ: thermal conductivity, σ: electrical conductivity, L: Lorenz number, T: absolute temperature). However, measurements of electrical and thermal conductivities under static condition at extremely high pressures (P) and temperature (T) are limited for pure iron [2], [3]. The estimates of the core conductivity considering the effect of light element(s) have been done based on the resistivity saturation model, but the validity of the model at the core condition is unclear [4], [5].
In this study, we examined electrical resistivity (the reciprocal of electrical conductivity) of Fe-2, 4 and 6.5 wt.%Si at high P-T conditions in an internally-heated diamond anvil cell (IHDAC) up to 99 GPa and 2910 K. Our results of electrical resistivity of hcp Fe-Si alloys showed its nonlinear temperature dependence, indicating the occurrence of the resistivity saturation. The resistivity saturation in Fe-Si alloys observed in this study supports the notion of high core conductivity and resulting molten lowermost mantle and young inner core.

References: [1] Poirier: *Phys. Earth Planet. Inter.* **85**, 319-337 (1994).;[2] Ohta et al.: *Nature* **534**, 95–98 (2016).;[3] Konôpková et al.: *Nature* **534**, 99–101 (2016).;[4] Gomi et al.: *Phys. Earth Planet. Inter.* **224**, 88–103 (2013).;[5] Gomi et al.: *Earth Planet. Sci. Lett.* **451**, 51–61 (2016).

キーワード：電気伝導度、熱伝導率、地球コア
Keywords: Electrical conductivity, Thermal conductivity, Earth's core

©2019. Japan Geoscience Union. All Right Reserved.

Electrical resistivity and thermal conductivity of fcc Fe: Implications for the Mercury’ s core

*五味 斎[1]、芳野 極[1]
*Hitoshi Gomi[1], Takashi Yoshino[1]

1. 岡山大学
1. Okayama University

The Mercury’ s magnetic field may be sustained by the geodynamo motion in the liquid Fe core. However, its strength is about 1% of that of Earth. This weak magnetic field may implies a partly stratified core. Gomi et al. (2013) pointed out that the geometry of the thermal stratification depends critically on the depth dependency of the thermal conductivity. In this study, we conducted first-principles calculations on the face-centered cubic (fcc) Fe to constrain the electrical resistivity and the thermal conductivity of the Mercury’ s core.

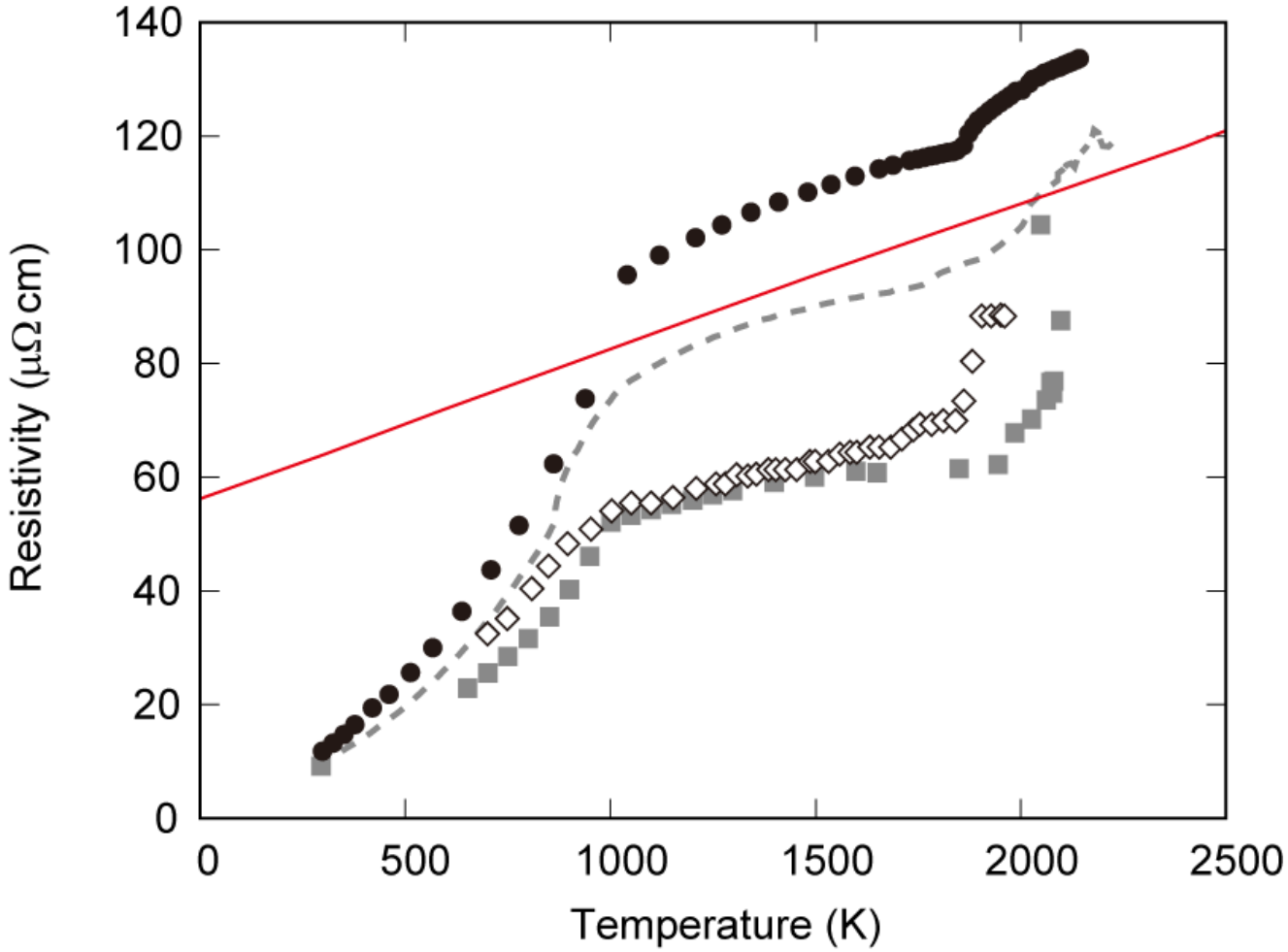
We calculated the electrical resistivity and the thermal conductivity of fcc Fe by means of the Korringa-Kohn-Rostoker method combined with the coherent potential approximation (KKR-CPA) (Akai, 1989). The CPA was adopted to treat the disorder effects due to the atomic vibrations and the magnetic fluctuations on the electronic band structure (Glasbrenner et al., 2014; Ebert et al., 2015; Kou and Akai, 2018). Within the alloy analogy model, the thermal atomic displacements were represented by a discrete set of N_v displacement vectors $\Delta R_v(T)$, where $|\Delta R_v(T)|=\sqrt{<u^2>}$ is the root mean square displacement of atoms, which is based on the Debye model without zero point vibration. The lattice parameter and the Debye temperature are obtained from the equation of state of fcc Fe (Tsujino et al., 2013). In addition to the non-magnetic state, the magnetic disorder was simulated by the local magnetic disorder (LMD) approach. The conductivity was calculated by the Kubo-Greenwood formula with the vertex correction.

The calculated electrical resistivities and thermal conductivities with LMD state are consistent with the literature data at 0 GPa (Ho et al., 1972; 1983), whereas the non-magnetic results show smaller resistivity and larger thermal conductivity. This suggests the importance of the magnetic scattering at low pressures. However, our calculation predicts that the magnetic contribution banishes at higher pressures than 20 GPa. Figure 1 compares the present results and previous experiments (gray broken line; Secco and Scholoessin, 1989, gray square; Deng et al., 2013, open diamond; Pommier, 2018, black circle; Silber et al., 2018) on the electrical resistivity at ~5 GPa. Note that, within the fcc stability field, previous measurements have a large variation. Our calculated resistivity values are between Secco and Scholoessin (1989) and Silber et al. (2018).

We further calculated the electrical resistivity and the thermal conductivity of fcc Fe up to 50 GPa and 3000 K. The thermal conductivity increases with increasing pressure and temperature. This means that, if the inner core is absent, the thermal stratification starts from the bottom, and, after the onset of the inner core, a thick thermal stratified layer may develop at the top of the fluid core (Gomi et al., 2013).

キーワード：電気抵抗率、熱伝導度、水星、核、熱成層
Keywords: electrical resistivity, thermal conductivity, Mercury, core, thermal stratification

©2019. Japan Geoscience Union. All Right Reserved.



©2019. Japan Geoscience Union. All Right Reserved.

Lateral heterogeneity in the lowermost outer core (F layer) of the Earth revealed by seismic analyses

*大滝 壽樹[1]、金嶋 聰[2]、土屋 卓久[3]
*Toshiki Ohtaki[1], Satoshi Kaneshima[2], Taku Tsuchiya[3]

1. 産業技術総合研究所地質情報研究部門、2. 九州大学大学院理学研究院地球惑星科学部門、3. 愛媛大学地球深部ダイナミクス研究センター
1. Geological Survey of Japan, National Institute of Advanced Industrial Science and Technology (AIST), 2. Department of Earth and Planetary Sciences, Kyushu University, 3. Geodynamics Research Center, Ehime University

We have determined seismic velocity structures of the lowermost outer core (F layer) beneath Northeast Pacific and Australia (Ohtaki and Kaneshima, 2015; Ohtaki et al., 2018), and found that the F layer is seismologically heterogeneous. These structures were obtained using a combination of two observations. First one is differential traveltimes between waves that reflect at the inner core boundary (ICB) and that graze the boundary; the second is dispersion (frequency dependence of velocity) of the grazing wave.

Our results show a somewhat strange velocity profile in the F layer beneath Australia, which has a lower-velocity-gradient layer than that of the Preliminary Reference Earth Model (PREM; Dziewonski and Anderson, 1981) on the ICB, and a higher-gradient layer just above the layer. Recent advance in high pressure research enables seismologists to translate lateral seismic velocity variation to relative chemical abundance in the outer core condition. Based on the results of Ichikawa and Tsuchiya (e.g., 2018), we showed light-element enrichment there. This result suggests that lighter fluid exists beneath Australia in the lowermost part of the liquid core, although the outer core is low-viscosity fluid.

The solid inner core of the Earth has quasi-hemispherical structure (e.g., Tanaka and Hamaguchi, 1997). As the origin of this hemispherical structure, uneven growth of the inner core has been proposed (e.g., Aubert et al., 2008; Alboussière et al., 2010; Monnereau et al., 2010). When the liquid in the outer core solidifies at the inner core surface, excess light element is partitioned to residue because the solid inner core is poorer in light elements compared with the liquid outer core. Thus, the uneven growth of the inner core is tied with an uneven release of the light elements to the F layer, which may be related to our results of the heterogeneous F layer. Then, a question arises: this heterogeneity has hemispherical structure like the inner core or local one?

We have not answered it yet because the survey areas of the above studies are restricted. Furthermore, other studies focusing F-layer velocity are not so many. Souriau (2015) determined lateral variations of velocity in the lower outer core using traveltimes of waves that turn there, and suggested that heterogeneity in F has degree-one feature. We also determined the seismic structure of the F layer beneath Antarctica using amplitude ratios between waves that turn just above the inner core and that get into the inner core. Although the resolution and reliability of structure obtained using amplitude ratios is lower than those using the method of our recent papers, the structure beneath Antarctica has a much lower velocity gradient in the F layer compared with PREM. Such a lower gradient is close to the model beneath Australia.

In this paper, we will show the summary of the heterogeneous F-layer structures of velocity and chemical abundance at this stage.

©2019. Japan Geoscience Union. All Right Reserved.

References
Alboussière, T., R. Deguen, and M. Melzani (2010), *Nature*, *466*, 744–747, doi:10.1038/nature09257.
Aubert, J., H. Amit, G. Hulot, and P. Olson (2008), *Nature*, *454*, 758–761, doi:10.1038/nature07109.
Dziewonski, A. M., and D. L. Anderson (1981), *Phys. Earth Planet. Inter.*, 25, 297–356, doi:10.1016/0031-9201(81)90046-7.
Monnereau, M., M. Calvet, L. Margerin, and A. Souriau (2010), *Science*, *328*, 1014–1017, doi:10.1126/science.1186212.
Ichikawa, H., and T. Tsuchiya (2018), J. Geography, 127, 631-646 (in Japanese with English abstract).
Ohtaki, T., S. Kaneshima, and K. Kanjo (2012), *J. Geophys. Res.*, 117, B03312, doi:10.1029/2011JB008717.
Ohtaki, T., and S. Kaneshima (2015), *J. Geophys. Res. Solid Earth*, 120, 7572–7586, doi:10.1002/2015JB012140.
Ohtaki, T., S. Kaneshima, H. Ichikawa, and T. Tsuchiya (2018), *J. Geophys. Res. Solid Earth*, doi:10.1029/2018JB015857.
Tanaka, S., and H. Hamaguchi (1997), *J. Geophys. Res.*, *102*, 2925–2938, doi:10.1029/96JB03187.

キーワード：外核最下部のF層、外核の不均質、オーストラリア下F層での軽元素濃集
Keywords: F layer, lowermost outer core, Heterogeneity of the outer core, Light element concentration in the F layer beneath Australia

©2019. Japan Geoscience Union. All Right Reserved.

内核の不均一成長に伴う地球外核中の流れと軽成分分布
Flows and light element distribution in the outer core associated with heterogeneous growth of the inner core of the Earth

*竹広 真一[1]、佐々木 洋平[2]
*Shin-ichi Takehiro[1], Youhei SASAKI[2]

1. 京都大学数理解析研究所、2. 京都大学大学院理学研究科数学教室
1. Research Institute for Mathematical Sciences, Kyoto University, 2. Department of Mathematics, Kyoto University

近年の地震波解析によると, 内核内の地震波速度の東西不均一な分布が明らかにされ, ICB での相変化が水平一様に生じてはいないという 議論が提唱されるようになった. この観測結果から単純に考えると, 固化半球側の ICB 直上では温度が低く軽成分濃度が高くなり, 溶融半球側で逆に温度が高く軽成分濃度が低くなることが予想される. すなわち, 内核内部の東西不均一分布と ICB 直上の外核内での 熱力学的諸量との相関がみられそうである, しかしながら, 最新の地震波の解析では ICB 直上での地震波速度異常分布は内核内の東西非対称構造とは一致していないことが報告されている.

内核の不均一成長の説明を試みとして外的要因と内的要因の メカニズムがこれまでに提案されてきている. 外的要因説は, 核マントル境界 (CMB) での水平不均一な熱的構造が 外核内に水平熱対流を引き起こし, ICB に水平不均一な温度分布をもたらすと考えるものである. しかしながら, この研究では温度と軽成分をまとめた共密度(co-density)を 用いており, ICB 直上での軽成分分布がどのようになるかが明らかでない. 一方, 内的要因説は, 相変化境界を伴う内核の自発的な不安定性により 横ずれ流れが内核内部に生じるものである. しかしながら, この研究では外核の軽成分がすぐに混合され一様であることを 仮定していおり, ICB 直上での軽成分分布がどのようになるかが明らかでない.

そこで本研究では, 温度と軽成分濃度を独立変数とする回転球殻内の熱組成対流 モデルを用いて, 外的要因および内的要因のそれぞれのストーリーに 沿った熱組成対流の数値実験を行う. 得られる ICB 付近での軽成分濃度分布と 地震波異常分布と比較することにより, もっともらしい外核内の熱組成対流の レジームについて議論する.

キーワード：異方性、内核、核マントル境界
Keywords: Heterogeneity, Inner core, Core-mantle boundary

©2019. Japan Geoscience Union. All Right Reserved.

Sharpness of the hemispherical boundary in the inner core beneath the northern Pacific

*入谷 良平[1]、川勝 均[1]、竹内 希[1]
*Ryohei Iritani[1], Hitoshi Kawakatsu[1], Nozomu Takeuchi[1]

1. 東京大学地震研究所
1. Earthquake Research Institute, Univ. of Tokyo

The hemispherical heterogeneity in the topmost of the Earth’ s inner core, faster velocity and higher attenuation in the eastern hemisphere and slower velocity and weaker attenuation in the western hemisphere, has been revealed by seismological studies. However, how the transition structure between two hemispheres looks like has not been known because of the difficulty to analyze complex core-sensitive data and the limitation of earthquake and seismic array distribution. In this study, we apply the array-based waveform inversion (Iritani et al., 2014) to core phase data that propagate beneath the northern Pacific, and investigate the nature of the transition structure in this region.Dataset used in this study consists of two directional event-station pairs, seismograms observed by the permanent European stations for events at Fiji-Tonga region, and USArray for events near Indonesia. We analyze the broadband vertical component of core phase data containing PKIKP and PKP phases (i.e. the epicentral distance between 145 –155 degree). Resultant analyzed waveforms for EU stations and USArray are 2,108 and 1,172 traces respectively.
In the analysis, waveform inversion approach is employed for each event data to measure traveltime and attenuation in the inner core. As a result, traveltime anomalies observed by EU stations show obvious positive anomaly suggesting mainly propagating the eastern hemisphere, while traveltimes observed by USAray show relatively smaller (or no) anomalies suggesting effects from both of hemispheres. On the other hand, attenuation parameters for both arrays show similar trend that suggests high attenuation corresponding to the eastern hemisphere. To investigate a hemispherical transition boundary in the sampled region, we conduct a ray theory based forward modeling of traveltimes by changing a shape of boundary from meridian boundary to eyeball shaped boundary, and its position. We compute root-mean-square (RMS) of residual between observations and theoretical traveltimes computed with each boundary model. Then, an eyeball shaped boundary, that is located at longitude of 158°W on the equatorial line and latitude of 80°N at the northernmost point, obtained as the preferred boundary model. Finally, we investigate a sharpness of the boundary by varying a width of hemispherical transition. We assume linear variation from the eastern and western hemisphere in a given width and compute RMS. As a result, a width of 600 km at the surface of the inner core shows smaller RMS than sharp boundary. Geophysical significance of this finding will be further discussed.

キーワード：Inner core、Waveform inversion
Keywords: Inner core, Waveform inversion

©2019. Japan Geoscience Union. All Right Reserved.

Stable carbon isotope fractionation in Fe-C system from first principles

*出倉 春彦[1]、土屋 卓久[1]
*Haruhiko Dekura[1], Taku Tsuchiya[1]

1. 愛媛大学地球深部ダイナミクス研究センター
1. Geodynamics Research Center, Ehime University

Carbon is the fourth most abundant element in the solar system and likely one of the constituent light elements in the Earth’s core. Determination of its equilibrium isotope fractionation factor (α) under high pressure (P) and temperature (T) is a key for understanding chemical evolution such as the whole Earth carbon distributions and the amount in the Earth’s core (e.g., Kumar et al., 2011). Because experimental measurement of the isotope fractionation remains technically challenging at the deep mantle condition, attempts to evaluate the α among mantle minerals by first-principles calculations have been made in recent years (e.g., Huang et al., 2014). Recently, our group initiated the theoretical determination of the α in the Fe-C system in the Earth’s deep interior with a full ab initio approach based on the density-functional theory. We performed ab initio lattice dynamics calculations for diamond and iron-carbide (hexagonal Fe7C3) having the two stable carbon isotopes (12C and 13C). The α between the two phases were then determined by using the Gibbs free energies calculated at P ~300 GPa and T ~2000-6000 K. The obtained $10^3 \ln \alpha$ dia-Fe7C3 is found to vary with T from ~+8‰ (2000 K) to ~+5‰ (6000 K). This result indicates that the Fe7C3 is enriched in the heavier isotope (13C) compared with diamond. This trend is qualitatively consistent with low-pressure experimental observations (Kumar et al., 2011).

キーワード：Isotope fractionation、First-principles calculation
Keywords: Isotope fractionation, First-principles calculation

©2019. Japan Geoscience Union. All Right Reserved.

[E] ポスター発表 | セッション記号 B (地球生命科学)：B-BG 地球生命科学・地圏生物圏相互作用

2019年5月27日(月) 13:45 ~ 15:15 | ポスター会場 幕張メッセ国際展示場 8ホール_6

[B-BG01] Elemental cycling in terrestrial and coastal ecosystems- Carbon and Nitrogen perspectives

コンビーナ:Punyasloke Bhadury(Indian Institute of Science Education and Research Kolkata)

Biogeochemical cycling of carbon and nitrogen hold the key to cropping cycle, monsoonal patterns and climate globally. Biological communities that make up the biosphere are essential for cycling of carbon and nitrogen and their functions are regulated by numerous factors including redox conditions, trace metal availability, and energy sources. At the same time temporal and spatial variability of biological communities such as those observed in microbes strongly affect the rate of carbon and nitrogen cycling in various environments including land and marine systems. In this session, submissions are welcomed from scientists including early career scientists working on various aspects of carbon and nitrogen cycling across terrestrial, coastal and oceanic environments. Submissions are also encouraged addressing challenges related to estimation of carbon and nitrogen budgets representing local, regional and global scales.

[BBG01-P01] Forest-CEW: A Forest Ecosystems Model for Carbon-Energy-Water Processes.

*Zhenghong Tan[1] (1.Hainan University China)

[BBG01-P02] **Interdependent Dynamics of LAI-ET across Roofing Landscapes: the Mongolian and Tibetan Plateaus**

*Li Tian[1] (1.Institute of Geographic Sciences and Natural Resources Research, Chinese Academy of Sciences)

[BBG01-P03] **Particle Phase Organic compounds (PAHs and VOCs) at Two Big Cities (Dhaka and Rajshahi) in Bangladesh**

*Islam Nazrul nazrulislam6727@gmail.com[1]、Tanzina Tul Karim[1]、Rasheda Nahida[1]、Nusrat Mousume[1]、Farha Jeba[1]、Abdus Salam[1] (1.Department of Chemistry, University of Dhaka, Dhaka-1000, Bangladesh)

[BBG01-P04] **Diversity and activity of diazotrophs in the coastal waters of Southeastern Arabian Sea (SEAS)**

*JABIR THAJUDEEN[1]、Mohamed Hatha Abdullah (1.Cochin University of Science and Technology India)

[BBG01-P05] **Bloom of *Palmerina hardmaniana*, a marine centric planktonic diatom in a coastal mangrove ecosystem- implication for coastal carbon cycling**

*Punyasloke Bhadury[1] (1.Centre for Climate and Environmental Studies and Department of Biological Sciences, Indian Institute of Science Education and Research Kolkata)

[BBG01-P06] Dynamics of Carbon and Nitrogen influx in large river system: Isotopic study from river Ganga, India

*Anurag Kumar[1]、Prasanta Sanyal[1,2]、Punyasloke Bhadury[3,2] (1.Department of Earth Sciences, Indian Institute of Science Education and Research Kolkata, Mohanpur 741246, India、2.Centre for Climate and Environmental studies, Indian Institute of Science Education and Research Kolkata, Mohanpur 741246, India、3.Department of Biological Sciences, Indian Institute of Science Education and Research Kolkata, Mohanpur 741246, India)

Forest-CEW: A Forest Ecosystems Model for Carbon-Energy-Water Processes.

*Zhenghong Tan[1]

1. Hainan University China

Forest ecosystem models (FEM) are essential tools for studying the forest carbon budget, which is an important subject in the global climate change studies. Although using FEM has a long history and there exist many types of FEM, new models are still being developed for special uses. This presentation introduces Forest-CEW, a forest ecosystems model for carbon-energy-water processes. The model is aimed at having a structure that can be configured flexibly for different forest ecosystems, a graphic interface for inexperienced users, and a command execution mode for experts. The time scale of the model is at the hourly level. Model validation using the data from Tomakomai flux research site (asiaflux.net/index.php?page_id=113) shows that the model can well reconstruct major ecosystem variables including net ecosystem exchange, soil temperature and water content. We also compared Forest-CEW with those include in the TDE ecosystem model intercomparison (cdiac.ess-dive.lbl.gov/epubs/tdemodel/models.html) and the results show that its performance is among the best of the 13 models.

Keywords: Model, Forest Ecosystem, Carbon, Water, Energy

©2019. Japan Geoscience Union. All Right Reserved.

Interdependent Dynamics of LAI-ET across Roofing Landscapes: the Mongolian and Tibetan Plateaus

*Li Tian[1]

1. Institute of Geographic Sciences and Natural Resources Research, Chinese Academy of Sciences

The Mongolian and Tibetan Plateaus have experienced higher-than-global average warming in recent decades, resulting in many significant changes in ecosystem structure and function. Among them are Leaf area index (LAI) and evapotranspiration (ET) that play a fundamental role in shaping many causes and consequences of land surface processes and climate. Here, we focused on the spatiotemporal changes of the LAI, ET and their relationships on these two roofing landscapes. Based on the MODIS products from 2000 through 2014. We found that there existed a general positive relationship between LAI and ET on the Mongolia Plateau (MP), while there was not synergy on the Tibetan Plateau (TP).

Overall, 49.38% (50.62%) of land areas on the TP experienced significant increased (decreased) in LAI, while 94.92% (5.09%) on the MP. For the ET, the increased land area was 21.70% (124.10×10^3 km^2) on the TP and 88.01% (341.60×10^3 km^2) on the MP. More importantly, the relationships varied substantially across the space and over time, with mismatches found in some parts of the landscapes. Substantial additional efforts with observational and/or experimental investigations are need to explore the relationships, including the influences of vegetation characteristics and disturbances.

Keywords: ET, LAI, Eurasian continent, alpine, land surface process

©2019. Japan Geoscience Union. All Right Reserved.

Particle Phase Organic compounds (PAHs and VOCs) at Two Big Cities (Dhaka and Rajshahi) in Bangladesh

*Islam Nazrul nazrulislam6727@gmail.com[1], Tanzina Tul Karim[1], Rasheda Nahida[1], Nusrat Mousume[1], Farha Jeba[1], Abdus Salam[1]

1. Department of Chemistry, University of Dhaka, Dhaka-1000, Bangladesh

Particle Phase Organic compounds (PAHs and VOCs) at Two Big Cities (Dhaka and Rajshahi) in Bangladesh

Md. Nazrul Islam[1*], Tanzina Tul Karim, Rasheda Nahida, Nusrut Mousume, Farha Jeba, and Abdus Salam[2*]

Department of Chemistry, University of Dhaka, Dhaka 1000, Bangladesh

Corresponding Author: [1] nazrulislam6727@gmail.com, Tel: +8801717672748; [2*] asalam@gmail.com, Tel: +880117061160

Atmospheric pollution has a significant impact on human health, climate change, agriculture, and ecosystem. Air quality and the climate change is the top most concern of the World Health Organization (WHO, 2019). Bangladesh is a rapidly developing country with kinds of environmental problems. It became the top most country in the world for the human deaths due to environmental pollution, which was accounted about 27% of the total death (Lancet, 207). Only air pollution caused two thirds of these deaths (Lancet, 2017). Dhaka along with Narayanganj and Gazipur are the top ranking cities in the World for the air pollution (WHO, 2014). Volatile organic compounds (VOCs) and poly aromatic hydrocarbons (PAHs) are the major organic pollutants in the atmosphere. Until now there is no information of VOCs and PAHs regarding their occurrences, sources, seasonal variation and health impact in Bangladesh. In this study we have collected particulate matters samples on quartz filters with a low volume sampler at two big cities in Bangladesh (Capital Dhaka and North West City Rajshahi) from January 2015 to February 2019. Individual organic compounds were extracted with acetone and n-hexane from the particulate matter loaded filters. The chemical analysis was done with Gas Chromatography (GC)-Mass spectrometry (MS). The analyzed organic compounds were naphthalene, anthracene, diazinon, deltramethrin, pyrabenxoime, pyrazosulfuran, prophenophos butachlor, propiconazole, cymoxanil, cypermethrin, lamda cyhalothrin, dimethoate, chloropyriphos, carbofuran, metalaxyl, pentane, hexane, propene, isobutene, 1,3-butadiene, dichloroflouromethane, ethanol, benzene, toluene, ethylbenzene, xylene, styrene, 1,2,3trimethylbenzene, isoprene, cyclopentane, and cyclohexane. Positive matrix factorization (PMF) and air mass trajectory analysis were done for source characterization. Health risk assessment and life time cancer risk (LCR)

©2019. Japan Geoscience Union. All Right Reserved.

were determined with US EPA based model. The elevated concentrations of the determined compounds at both Dhaka and Rajshahi were observed; Dhaka values were slightly higher than Rajshahi. The concentrations of determined compounds were higher during the winter months basically December to February and lower during the monsoon period in the month of July. PMF model revealed that the sources of organic compounds in Bangladesh were diesel exhaust, coal and biomass burning, industry and gasoline exhaust. Ethyl benzene, dichlorouflouromethane, 1,2,3-trimethylbenzene have the potential carcinogenic impact.

Key words: Particle Phase Organics, PAHs, VOCs, PMF, Health Risk Assessment

Keywords: Particle Phase Organics, PAHs and VOCs, PMF and Health Risk Assessment

©2019. Japan Geoscience Union. All Right Reserved.

Diversity and activity of diazotrophs in the coastal waters of Southeastern Arabian Sea (SEAS)

*JABIR THAJUDEEN[1], Mohamed Hatha Abdullah

1. Cochin University of Science and Technology India

In marine environments availability of nitrogen (N2) limits the primary productivity. Nitrogen fixing bacteria (diazotrophs) could convert atmospheric nitrogen to ammonium thereby providing significant input of new nitrogen into the ocean. The knowledge about their diversity, distribution and physiological activity are limited in tropical coastal marine environments. In this study, we determined diversity of nitrogen fixing bacteria and the nitrogen fixation rate through *nifH* based clone library analysis and 15N2 bubble method respectively. We encountered *Trichodesmium*bloom and diatom diazotrophic associations along the coastal environments of SEAS. Nitrogen fixation rate in the coastal waters were varied from 0.15 to 1.02 nmolN/L/h. *Trichodesmium*bloom in the Arabian Sea during pre-monsoon season showed higher nitrogen fixation rate of 3.6 nmolN/L/h. Clone library analysis revealed that 19 Operational Taxonomic Units (OTUs) of nitrogen fixing bacteria were observed from the coastal waters SEAS. The OTUs were related to 7 OTUs of cyanobacteria and 12 OTUs of heterotrophic diazotrophs. Major cyanobacterial OTUs are closely similar to *Trichodesmium*sp., *Richelia*sp., *Synechocystis*sp.. Major heterotrophic diazotrophs belonged to alpha-, beta-, gamma-, epislon-, proteobacteria and firmicutes. Gamma proteobacterial clones were dominating among heterotrophic diazotrophs in the coastal water column of south eastern Arabian Sea. Nitrogen fixation rate in the water column were significantly correlated with dissolved Fe (R^2= 0.66, p= 0.05) and phosphorous (R^2= 0.49, p= 0.05), which revealed these are the major factors controlling nitrogen fixation process in the coastal environments of SEAS.

Keywords: Nitrogen fixation , diazotrophs, Fe, SEAS

©2019. Japan Geoscience Union. All Right Reserved.

Bloom of *Palmerina hardmaniana*, a marine centric planktonic diatom in a coastal mangrove ecosystem- implication for coastal carbon cycling

*Punyasloke Bhadury[1]

1. Centre for Climate and Environmental Studies and Department of Biological Sciences, Indian Institute of Science Education and Research Kolkata

Large celled diatoms play an important role in export of carbon in coastal ecosystems. In the Sundarbans mangrove ecosystem located on the delta of Ganga-Brahmaputra-Meghna riverine systems and facing the coastal Bay of Bengal, a bloom of *Palmerina hardmaniana* (Greville) Hasle was tracked in 2015. The bloom of this centric diatom species was tracked from April- July, 2015 in Sundarbans Biological Observatory Time Series (SBOTS) site of Sundarbans. During pre-bloom (April) dissolved oxygen (DO) concentration was 6.82 mg/L while during bloom (May-June) DO concentration decreased to 3.83 mg/L. This also coincided with Chlorophyll-a concentration which ranged from 0.22-6.28 mg/L during the study period, with highest concentration of 6.28 mg/L in bloom period and overwhelmingly dominated by cells belonging to *Palmerina hardmaniana* (40.8 X 10^4 cells/L). In total 72 phytoplankton species were observed from April-July, 2015 in SBOTS site. The frustules of *Palmerina hardmaniana* ranged from 291-358 μm in length and from 195 to 260 μm in width. Based on *rbc*L phylogeny of RuBISCO, the dominance of *P. hardmaniana* was also confirmed. Increased air and surface water temperatures in SBOTS site showed significant correlation with observed cell abundance of *P. hardmaniana* with the onset of bloom. This is the first report of *P. hardmaniana* bloom in the coastal Sundarbans mangrove ecosystem. Therefore, understanding the physiological success of this centric diatom species in relation to dynamic environmental conditions has consequences for tracking export of carbon by centric diatoms in coastal water and resulting implications for coastal carbon cycling.

Keywords: diatom, phytoplankton bloom, mangrove, carbon cycling

©2019. Japan Geoscience Union. All Right Reserved.

Dynamics of Carbon and Nitrogen influx in large river system: Isotopic study from river Ganga, India

*Anurag Kumar[1], Prasanta Sanyal[1,2], Punyasloke Bhadury[3,2]

1. Department of Earth Sciences, Indian Institute of Science Education and Research Kolkata, Mohanpur 741246, India, 2. Centre for Climate and Environmental studies, Indian Institute of Science Education and Research Kolkata, Mohanpur 741246, India, 3. Department of Biological Sciences, Indian Institute of Science Education and Research Kolkata, Mohanpur 741246, India

Freshwater flux transport large amount of carbon (dissolved and particulate, organic and inorganic) and nitrogen (Dissolved) from continent into the ocean, contributing significantly to the global carbon and nitrogen cycle. The present sources and sinks of naturally as well as anthropogenically produced C and N compounds in the global carbon and nitrogen cycle remains enigmatic. Among the carbon sources in the river ecosystem, the dissolved inorganic carbon (DIC) constitute major component of carbon influx from land to ocean. These fluxes are significantly influenced by the terrestrial and estuary processes. The isotopic composition of DIC can be used to understand the sources and cycling of carbon in rivers and estuaries. In this study, $d^{13}C$ of DIC in river water of Ganga has been used to understand the dissolved inorganic carbon sources into the river. The river Ganga (2500 km) is the largest river of the Indian subcontinent which originates from the Gangotri glacier and drains into Bay of Bengal through its vast delta in the Sunderban. The $d^{13}C_{DIC}$ of river water were measured from source (Gomukh) to sink (Bay of Bengal) of the river Ganga for pre and post-monsoon period. The seasonal variation in the $d^{13}C_{DIC}$ shows enriched isotopic values in pre-monsoon compared to post-monsoon samples, indicating increased biological activities in the riverine system during pre-monsoon. A varied enrichment factor in the $d^{13}C_{DIC}$ values were observed for upper, middle and lower stretch of the river Ganga which might be indicating different sources contributing water in different stretch of the river Ganga. The $d^{18}O$ value of river water, ground water and rain water were used to delineate the different sources of water into the river Ganga. The water budget of the river Ganga shows high glacier melt in the upper stretch, high ground water influx in middle stretch and high rain water input in lower stretch of the river Ganga.

On similar note, the dissolved form of nitrogen in river water (NO_3^-) also significantly impacts the riverine as well as costal ecosystem. The increased influx of nitrate changes the competition between species causing disruption in the biological diversity. The lower stretch of the river Ganga receives maximum rain water input; therefore the region becomes prone to pollutant as result of surface runoff from the catchment areas. The isotopic composition of dissolved nitrate in water can be used to delineate the sources of NO_3^- into the riverine system. The $d^{15}N$ and $d^{18}O$ of the dissolved nitrate in river water from the lower stretch (Kolkata) of the river Ganga indicates the input of anthropogenic activities (pollutant) to river water. The data indicates manure from septic pipe lines as major source of dissolved nitrate present in the river Ganga.

Keywords: DIC, Ganga river, nitrate isotope, India

©2019. Japan Geoscience Union. All Right Reserved.

[E] ポスター発表 | セッション記号 B (地球生命科学)：B-BG 地球生命科学・地圏生物圏相互作用

2019年5月27日(月) 17:15 ~ 18:30 | ポスター会場 幕張メッセ国際展示場 8ホール_31

[B-BG01] Elemental cycling in terrestrial and coastal ecosystems- Carbon and Nitrogen perspectives

コンビーナ:Punyasloke Bhadury(Indian Institute of Science Education and Research Kolkata)

Biogeochemical cycling of carbon and nitrogen hold the key to cropping cycle, monsoonal patterns and climate globally. Biological communities that make up the biosphere are essential for cycling of carbon and nitrogen and their functions are regulated by numerous factors including redox conditions, trace metal availability, and energy sources. At the same time temporal and spatial variability of biological communities such as those observed in microbes strongly affect the rate of carbon and nitrogen cycling in various environments including land and marine systems. In this session, submissions are welcomed from scientists including early career scientists working on various aspects of carbon and nitrogen cycling across terrestrial, coastal and oceanic environments. Submissions are also encouraged addressing challenges related to estimation of carbon and nitrogen budgets representing local, regional and global scales.

[BBG01-P01] Forest-CEW: A Forest Ecosystems Model for Carbon-Energy-Water Processes.

*Zhenghong Tan[1] (1.Hainan University China)

[BBG01-P02] **Interdependent Dynamics of LAI-ET across Roofing Landscapes: the Mongolian and Tibetan Plateaus**

*Li Tian[1] (1.Institute of Geographic Sciences and Natural Resources Research, Chinese Academy of Sciences)

[BBG01-P03] **Particle Phase Organic compounds (PAHs and VOCs) at Two Big Cities (Dhaka and Rajshahi) in Bangladesh**

*Islam Nazrul nazrulislam6727@gmail.com[1]、Tanzina Tul Karim[1]、Rasheda Nahida[1]、Nusrat Mousume[1]、Farha Jeba[1]、Abdus Salam[1] (1.Department of Chemistry, University of Dhaka, Dhaka-1000, Bangladesh)

[BBG01-P04] **Diversity and activity of diazotrophs in the coastal waters of Southeastern Arabian Sea (SEAS)**

*JABIR THAJUDEEN[1]、Mohamed Hatha Abdullah (1.Cochin University of Science and Technology India)

[BBG01-P05] **Bloom of *Palmerina hardmaniana*, a marine centric planktonic diatom in a coastal mangrove ecosystem- implication for coastal carbon cycling**

*Punyasloke Bhadury[1] (1.Centre for Climate and Environmental Studies and Department of Biological Sciences, Indian Institute of Science Education and Research Kolkata)

[BBG01-P06] Dynamics of Carbon and Nitrogen influx in large river system: Isotopic study from river Ganga, India

*Anurag Kumar[1]、Prasanta Sanyal[1,2]、Punyasloke Bhadury[3,2] (1.Department of Earth Sciences, Indian Institute of Science Education and Research Kolkata, Mohanpur 741246, India、2.Centre for Climate and Environmental studies, Indian Institute of Science Education and Research Kolkata, Mohanpur 741246, India、3.Department of Biological Sciences, Indian Institute of Science Education and Research Kolkata, Mohanpur 741246, India)

Forest-CEW: A Forest Ecosystems Model for Carbon-Energy-Water Processes.

*Zhenghong Tan[1]

1. Hainan University China

Forest ecosystem models (FEM) are essential tools for studying the forest carbon budget, which is an important subject in the global climate change studies. Although using FEM has a long history and there exist many types of FEM, new models are still being developed for special uses. This presentation introduces Forest-CEW, a forest ecosystems model for carbon-energy-water processes. The model is aimed at having a structure that can be configured flexibly for different forest ecosystems, a graphic interface for inexperienced users, and a command execution mode for experts. The time scale of the model is at the hourly level. Model validation using the data from Tomakomai flux research site (asiaflux.net/index.php?page_id=113) shows that the model can well reconstruct major ecosystem variables including net ecosystem exchange, soil temperature and water content. We also compared Forest-CEW with those include in the TDE ecosystem model intercomparison (cdiac.ess-dive.lbl.gov/epubs/tdemodel/models.html) and the results show that its performance is among the best of the 13 models.

Keywords: Model, Forest Ecosystem, Carbon, Water, Energy

©2019. Japan Geoscience Union. All Right Reserved.

Interdependent Dynamics of LAI-ET across Roofing Landscapes: the Mongolian and Tibetan Plateaus

*Li Tian[1]

1. Institute of Geographic Sciences and Natural Resources Research, Chinese Academy of Sciences

The Mongolian and Tibetan Plateaus have experienced higher-than-global average warming in recent decades, resulting in many significant changes in ecosystem structure and function. Among them are Leaf area index (LAI) and evapotranspiration (ET) that play a fundamental role in shaping many causes and consequences of land surface processes and climate. Here, we focused on the spatiotemporal changes of the LAI, ET and their relationships on these two roofing landscapes. Based on the MODIS products from 2000 through 2014. We found that there existed a general positive relationship between LAI and ET on the Mongolia Plateau (MP), while there was not synergy on the Tibetan Plateau (TP).

Overall, 49.38% (50.62%) of land areas on the TP experienced significant increased (decreased) in LAI, while 94.92% (5.09%) on the MP. For the ET, the increased land area was 21.70% (124.10×10^3 km^2) on the TP and 88.01% (341.60×10^3 km^2) on the MP. More importantly, the relationships varied substantially across the space and over time, with mismatches found in some parts of the landscapes. Substantial additional efforts with observational and/or experimental investigations are need to explore the relationships, including the influences of vegetation characteristics and disturbances.

Keywords: ET, LAI, Eurasian continent, alpine, land surface process

©2019. Japan Geoscience Union. All Right Reserved.

Particle Phase Organic compounds (PAHs and VOCs) at Two Big Cities (Dhaka and Rajshahi) in Bangladesh

*Islam Nazrul nazrulislam6727@gmail.com[1], Tanzina Tul Karim[1], Rasheda Nahida[1], Nusrat Mousume[1], Farha Jeba[1], Abdus Salam[1]

1. Department of Chemistry, University of Dhaka, Dhaka-1000, Bangladesh

Particle Phase Organic compounds (PAHs and VOCs) at Two Big Cities (Dhaka and Rajshahi) in Bangladesh

Md. Nazrul Islam[1*], Tanzina Tul Karim, Rasheda Nahida, Nusrut Mousume, Farha Jeba, and Abdus Salam[2*]

Department of Chemistry, University of Dhaka, Dhaka 1000, Bangladesh

Corresponding Author: [1] nazrulislam6727@gmail.com, Tel: +8801717672748; [2*] asalam@gmail.com, Tel: +880117061160

Atmospheric pollution has a significant impact on human health, climate change, agriculture, and ecosystem. Air quality and the climate change is the top most concern of the World Health Organization (WHO, 2019). Bangladesh is a rapidly developing country with kinds of environmental problems. It became the top most country in the world for the human deaths due to environmental pollution, which was accounted about 27% of the total death (Lancet, 207). Only air pollution caused two thirds of these deaths (Lancet, 2017). Dhaka along with Narayanganj and Gazipur are the top ranking cities in the World for the air pollution (WHO, 2014). Volatile organic compounds (VOCs) and poly aromatic hydrocarbons (PAHs) are the major organic pollutants in the atmosphere. Until now there is no information of VOCs and PAHs regarding their occurrences, sources, seasonal variation and health impact in Bangladesh. In this study we have collected particulate matters samples on quartz filters with a low volume sampler at two big cities in Bangladesh (Capital Dhaka and North West City Rajshahi) from January 2015 to February 2019. Individual organic compounds were extracted with acetone and n-hexane from the particulate matter loaded filters. The chemical analysis was done with Gas Chromatography (GC)-Mass spectrometry (MS). The analyzed organic compounds were naphthalene, anthracene, diazinon, deltramethrin, pyrabenxoime, pyrazosulfuran, prophenophos butachlor, propiconazole, cymoxanil, cypermethrin, lamda cyhalothrin, dimethoate, chloropyriphos, carbofuran, metalaxyl, pentane, hexane, propene, isobutene, 1,3-butadiene, dichloroflouromethane, ethanol, benzene, toluene, ethylbenzene, xylene, styrene, 1,2,3trimethylbenzene, isoprene, cyclopentane, and cyclohexane. Positive matrix factorization (PMF) and air mass trajectory analysis were done for source characterization. Health risk assessment and life time cancer risk (LCR)

©2019. Japan Geoscience Union. All Right Reserved.

were determined with US EPA based model. The elevated concentrations of the determined compounds at both Dhaka and Rajshahi were observed; Dhaka values were slightly higher than Rajshahi. The concentrations of determined compounds were higher during the winter months basically December to February and lower during the monsoon period in the month of July. PMF model revealed that the sources of organic compounds in Bangladesh were diesel exhaust, coal and biomass burning, industry and gasoline exhaust. Ethyl benzene, dichlorouflouromethane, 1,2,3-trimethylbenzene have the potential carcinogenic impact.

Key words: Particle Phase Organics, PAHs, VOCs, PMF, Health Risk Assessment

Keywords: Particle Phase Organics, PAHs and VOCs, PMF and Health Risk Assessment

©2019. Japan Geoscience Union. All Right Reserved.

Diversity and activity of diazotrophs in the coastal waters of Southeastern Arabian Sea (SEAS)

*JABIR THAJUDEEN[1], Mohamed Hatha Abdullah

1. Cochin University of Science and Technology India

In marine environments availability of nitrogen (N2) limits the primary productivity. Nitrogen fixing bacteria (diazotrophs) could convert atmospheric nitrogen to ammonium thereby providing significant input of new nitrogen into the ocean. The knowledge about their diversity, distribution and physiological activity are limited in tropical coastal marine environments. In this study, we determined diversity of nitrogen fixing bacteria and the nitrogen fixation rate through *nifH* based clone library analysis and 15N2 bubble method respectively. We encountered *Trichodesmium*bloom and diatom diazotrophic associations along the coastal environments of SEAS. Nitrogen fixation rate in the coastal waters were varied from 0.15 to 1.02 nmolN/L/h. *Trichodesmium*bloom in the Arabian Sea during pre-monsoon season showed higher nitrogen fixation rate of 3.6 nmolN/L/h. Clone library analysis revealed that 19 Operational Taxonomic Units (OTUs) of nitrogen fixing bacteria were observed from the coastal waters SEAS. The OTUs were related to 7 OTUs of cyanobacteria and 12 OTUs of heterotrophic diazotrophs. Major cyanobacterial OTUs are closely similar to *Trichodesmium*sp., *Richelia*sp., *Synechocystis*sp.. Major heterotrophic diazotrophs belonged to alpha-, beta-, gamma-, epislon-, proteobacteria and firmicutes. Gamma proteobacterial clones were dominating among heterotrophic diazotrophs in the coastal water column of south eastern Arabian Sea. Nitrogen fixation rate in the water column were significantly correlated with dissolved Fe (R^2= 0.66, p= 0.05) and phosphorous (R^2= 0.49, p= 0.05), which revealed these are the major factors controlling nitrogen fixation process in the coastal environments of SEAS.

Keywords: Nitrogen fixation , diazotrophs, Fe, SEAS

©2019. Japan Geoscience Union. All Right Reserved.

Bloom of *Palmerina hardmaniana*, a marine centric planktonic diatom in a coastal mangrove ecosystem- implication for coastal carbon cycling

*Punyasloke Bhadury[1]

1. Centre for Climate and Environmental Studies and Department of Biological Sciences, Indian Institute of Science Education and Research Kolkata

Large celled diatoms play an important role in export of carbon in coastal ecosystems. In the Sundarbans mangrove ecosystem located on the delta of Ganga-Brahmaputra-Meghna riverine systems and facing the coastal Bay of Bengal, a bloom of *Palmerina hardmaniana* (Greville) Hasle was tracked in 2015. The bloom of this centric diatom species was tracked from April- July, 2015 in Sundarbans Biological Observatory Time Series (SBOTS) site of Sundarbans. During pre-bloom (April) dissolved oxygen (DO) concentration was 6.82 mg/L while during bloom (May-June) DO concentration decreased to 3.83 mg/L. This also coincided with Chlorophyll-a concentration which ranged from 0.22-6.28 mg/L during the study period, with highest concentration of 6.28 mg/L in bloom period and overwhelmingly dominated by cells belonging to *Palmerina hardmaniana* (40.8 X 10^4 cells/L). In total 72 phytoplankton species were observed from April-July, 2015 in SBOTS site. The frustules of *Palmerina hardmaniana* ranged from 291-358 μm in length and from 195 to 260 μm in width. Based on *rbc*L phylogeny of RuBISCO, the dominance of *P. hardmaniana* was also confirmed. Increased air and surface water temperatures in SBOTS site showed significant correlation with observed cell abundance of *P. hardmaniana* with the onset of bloom. This is the first report of *P. hardmaniana* bloom in the coastal Sundarbans mangrove ecosystem. Therefore, understanding the physiological success of this centric diatom species in relation to dynamic environmental conditions has consequences for tracking export of carbon by centric diatoms in coastal water and resulting implications for coastal carbon cycling.

Keywords: diatom, phytoplankton bloom, mangrove, carbon cycling

©2019. Japan Geoscience Union. All Right Reserved.

Dynamics of Carbon and Nitrogen influx in large river system: Isotopic study from river Ganga, India

*Anurag Kumar[1], Prasanta Sanyal[1,2], Punyasloke Bhadury[3,2]

1. Department of Earth Sciences, Indian Institute of Science Education and Research Kolkata, Mohanpur 741246, India, 2. Centre for Climate and Environmental studies, Indian Institute of Science Education and Research Kolkata, Mohanpur 741246, India, 3. Department of Biological Sciences, Indian Institute of Science Education and Research Kolkata, Mohanpur 741246, India

Freshwater flux transport large amount of carbon (dissolved and particulate, organic and inorganic) and nitrogen (Dissolved) from continent into the ocean, contributing significantly to the global carbon and nitrogen cycle. The present sources and sinks of naturally as well as anthropogenically produced C and N compounds in the global carbon and nitrogen cycle remains enigmatic. Among the carbon sources in the river ecosystem, the dissolved inorganic carbon (DIC) constitute major component of carbon influx from land to ocean. These fluxes are significantly influenced by the terrestrial and estuary processes. The isotopic composition of DIC can be used to understand the sources and cycling of carbon in rivers and estuaries. In this study, $d^{13}C$ of DIC in river water of Ganga has been used to understand the dissolved inorganic carbon sources into the river. The river Ganga (2500 km) is the largest river of the Indian subcontinent which originates from the Gangotri glacier and drains into Bay of Bengal through its vast delta in the Sunderban. The $d^{13}C_{DIC}$ of river water were measured from source (Gomukh) to sink (Bay of Bengal) of the river Ganga for pre and post-monsoon period. The seasonal variation in the $d^{13}C_{DIC}$ shows enriched isotopic values in pre-monsoon compared to post-monsoon samples, indicating increased biological activities in the riverine system during pre-monsoon. A varied enrichment factor in the $d^{13}C_{DIC}$ values were observed for upper, middle and lower stretch of the river Ganga which might be indicating different sources contributing water in different stretch of the river Ganga. The $d^{18}O$ value of river water, ground water and rain water were used to delineate the different sources of water into the river Ganga. The water budget of the river Ganga shows high glacier melt in the upper stretch, high ground water influx in middle stretch and high rain water input in lower stretch of the river Ganga.

On similar note, the dissolved form of nitrogen in river water (NO_3^-) also significantly impacts the riverine as well as costal ecosystem. The increased influx of nitrate changes the competition between species causing disruption in the biological diversity. The lower stretch of the river Ganga receives maximum rain water input; therefore the region becomes prone to pollutant as result of surface runoff from the catchment areas. The isotopic composition of dissolved nitrate in water can be used to delineate the sources of NO_3^- into the riverine system. The $d^{15}N$ and $d^{18}O$ of the dissolved nitrate in river water from the lower stretch (Kolkata) of the river Ganga indicates the input of anthropogenic activities (pollutant) to river water. The data indicates manure from septic pipe lines as major source of dissolved nitrate present in the river Ganga.

Keywords: DIC, Ganga river, nitrate isotope, India

©2019. Japan Geoscience Union. All Right Reserved.

[E] ポスター発表 | セッション記号 M (領域外・複数領域)：M-IS ジョイント

2019年5月27日(月) 15:30 ~ 17:00 | ポスター会場 幕張メッセ国際展示場 8ホール_19

[M-IS02] 地球掘削科学

コンビーナ:山田 泰広(海洋研究開発機構　海洋掘削科学研究開発センター)、針金 由美子(産業技術総合研究所)、黒柳 あずみ(東北大学学術資源研究公開センター東北大学総合学術博物館)、山口 耕生(東邦大学, NASA Astrobiology Institute.)

これまでに実施された科学掘削データ・試料の解析・分析結果などの研究成果の報告と、今後の科学掘削計画に関する最新情報の紹介を目的とする。固体地球科学、古環境学、地球生命科学などの様々な分野からの成果を共有し、科学掘削を基軸とした学際的研究を推進する。最近１年間に実施されたICDPプロジェクトとIODP航海の概要報告を中心に、これまでに実施された掘削航海に関連して得られた最新研究成果と、今後数年間に具体化される科学掘削計画、掘削科学に関連する新規手法や技術開発研究等の報告を歓迎する。

[MIS02-P01] 地下生命圏研究における凍結コア試料の活用と名古屋議定書への対応

*肖 楠[1] (1.海洋研究開発機構)

[MIS02-P02] In-situ rock strength calculated from drilling parameters. Comparison of results from various sites.

*Adam Wspanialy[1]、Yasuhiro Yamada[1]、Saneatsu Saito[1]、KYAW MOE[1] (1.Japan Agency for Marine-Earth Science and Technology)

[MIS02-P03] Interaction between submarine landslides and subseafloor sedimentary microbiome: Chikyu SCORE Expedition 910 off Cape Erimo

*星野 辰彦[1]、浦本 豪一郎[2]、藤内 智士[2]、諸野 祐樹[1]、井尻 暁[1]、鈴木 志野[1]、久保 雄介[1]、稲垣 史生[1]、Chikyu SCORE Exp. 910 研究者一同 (1.独立行政法人海洋研究開発機構、2.高知大学)

[MIS02-P04] 襟裳岬沖SCORE掘削コアのXRFコアスキャナー連続化学分析

*村山 雅史[1]、矢生 晋介[3]、藤内 智士[2]、浦本 豪一郎[3]、山田 泰広[4]、稲垣 史生[4]、久保 雄介[5] (1.高知大学　農林海洋科学部海洋資源科学科、2.高知大学　理工学部、3.高知大学　海洋コア総合研究センター、4.海洋研究開発機構　海洋掘削科学研究開発センター, 、5.海洋研究開発機構　地球深部探査センター)

[MIS02-P05] 熊本地震震源断層掘削コアを用いた熱物性測定

*佐野 暉[1]、林 為人[1]、渋谷 奨[1,2]、神谷 奈々[1]、杉本 達洋[1]、石塚 師也[1]、林 愛明[3] (1.京都大学大学院工学研究科、2.地圏総合コンサルタント、3.京都大学大学院理学研究科)

[MIS02-P06] 東オーストラリア沖ロードハウライズ地域で採取された浅部コアの物性・強度試験結果：将来のロードハウライズライザー掘削に向けて

*杉原 孝充[1]、青池 寛[1]、斎藤 実篤[2]、村山 達也[1]、武田 研太郎[1]、小野寺 拓也[3]、澄川 あゆみ[3]、木戸 ゆかり[1]、真田 佳典[1] (1.海洋研究開発機構　地球深部探査センター、2.海洋研究開発機構　海洋掘削科学研究開発センター、3.日本海洋事業)

[MIS02-P07] ICDP DSeis 4: Drilling, core logging, and in-hole geophysical logging of ICDP DSeis drilling into the M5.5 aftershock zones in a South African gold mines.

*吉田 峻輔[1]、田所 遼悟[1]、杉村 幸祐[1]、兼松 慎[1]、東 充也[1]、Liebenberg Benni[2]、 van Heerden Esterhuizen[2]、Stephen Tau[3]、Siyanda Mngadi[3]、Ray Durrheim[3]、Martin Ziegler[4]、椋平 祐輔[5]、Ronald Conze[6]、矢部 康男[7]、金木 俊也[8]、Yokoyama Yuki[9]、Nomqhele Nkosi[10]、Dave Roberts[10]、Sifiso Buccio[11]、小笠原 宏[1] (1.Graduate school of science and engineering, Ritsumeikan、2.Moab Khotsong mine, Vijoenskroon、3.Univ. Witwatersrand, School of Geoscience、4.ETH, Zurich Dep. Earth Sciences、5.Inst. Fluid Science, Tohoku Univ.、6.GFZ, Potzdam、7.Graduate School of Science, Tohoku Univ.、8.Disaster Prevention Research Inst., Kyoto Univ.、9.Graduate School of Science,Osaka Univ.、10.Mandela Mining Precinct, CSIR、11.Council for Geoscience)

[MIS02-P08] ICDP DSeis 5: Diametrical Core Deformation Analysis of the M5.5 aftershock zone core - stress concentration at reflective intrusives and transition in stress regimes.

*杉村 幸祐[1]、吉田 峻輔[1]、田所 遼悟[1]、小笠原 宏[2]、石田 亮壮、矢部 康男[3]、伊藤 高敏[4]、明雄 船戸[5]、Siyanda Mngadi[6]、Ray Durrheim[6] (1.立命館大学大学院　理工学研究科、2.立命館大学　理工学部、3.東北大学　理学部、4.東北大学　流体科学研究所、5.深田地質研究所、6.Univ. Witwatersrand, School of Geoscience)

[MIS02-P09] ICDP DSeis 6: Deformation Rate Analysis of the M5.5 aftershock zone core - stress concentration at reflective intrusives

*兼松 慎[1]、東 充也[1]、矢部 康男[2]、阿部 周平[2]、Watson Bryan[3]、Durrheim Ray[3]、小笠原 宏[1] (1.立命館大学 理工学部　物理科学科、2.東北大学理学研究科、3.Witwatersrand大)

[MIS02-P10] ICDP DSeis 7: compilation of stress information and comparison with calculated stresses in the M5.5 aftershock zones

*東 充也[1]、矢部 康男[2]、杉村 幸佑[1]、石田 亮壮、兼松 慎[1]、吉田 峻輔[1]、田所 遼悟[1]、伊藤 高敏[4]、船戸 明雄[5]、小笠原 宏[3] (1.立命館大学大学院理工学研究科、2.東北大学大学院理学研究科・理学部 附属地震・噴火予知研究観測センター、3.立命館大学理工学部、4.東北大学流体科学研究所、5.深田地質研究所)

[MIS02-P11] ICDP DSeis 8: the M5.5 fault structure and reflective intrusives in legacy 3D seismic reflection data

*野田 拓[1]、Manzi Musa[2]、Ogasawara Hiroyuki[1]、Linzer Lindsay[2]、Enslin Stephanie[2]、Durrheim Ray[2]、小笠原 宏[1] (1.立命館大学、2.Witwatersrand大)

[MIS02-P12] ICDP DSeis 9: are streaks in the M5.5 aftershocks potentially located on highly stressed intrusive?

*Ryogo Tadokoro[1]、Katsuya Ishibashi[2]、Horiuchi Shigeki[3]、Hiroshi Ogasawara[4] (1.Graduate School of Science and Engineering, Ritsumeikan Univ.、2.School of Science and Engineering, Ritsumeikan Univ.、3.Homeseismo ltd.、4.College of Science and Engineering, Ritsumeikan Univ.)

地下生命圏研究における凍結コア試料の活用と名古屋議定書への対応
Utilization and curation of frozen core samples in IODP and implementation of the Nagoya Protocol in ocean drilling science

*肖 楠[1]
*Nan XIAO[1]

1. 海洋研究開発機構
1. Japan Agency for Marine Earthe Science and Technology

Deep biosphere research has become one of the major scientific focuses in ocean drilling science. How to access to core samples with sufficient quality has been a changes for scientists. Currently there are two methods of accessing to deep biosphere samples which are participating in drilling expeditions and requesting samples from core repositories. The Kochi Core Center has curated deep biosphere samples that were processed aseptically and stored at deep frozen (-80 degree C) condition from more than 10 drilling expeditions. Increased scientific attention to microbiological research of the subseafloor envrionment raises the complications and concerns related to adherence to the Nagoya Protocol of the Convention on Biological Diversity (CBD). The Nagoya Protocol is an international agreement that aims to guide countries in developing standart protocols and protections for accessing biological materials, and sharing benefits derived from their utilization. Since its commencement, the Nagoya Protocol has placed international biological research, especially fieldwork, under greater political scrutiny and increased its complexity due to the variation in implementation between nations. We present the central points of the Nagoya Protocol on access and benefit-sharing (ABS) and discuss their relationship to ocean drilling research. In addition, we address the challenges faced by ocean drilling in complying with this internation convention.

キーワード：海洋掘削、凍結コア試料、名古屋議定書、生物多様性
Keywords: ocean drilling program, frozen core sample, Nagoya Protocol, convention on biological diversity

©2019. Japan Geoscience Union. All Right Reserved.

In-situ rock strength calculated from drilling parameters. Comparison of results from various sites.

*Adam Wspanialy[1], Yasuhiro Yamada[1], Saneatsu Saito[1], KYAW MOE[1]

1. Japan Agency for Marine-Earth Science and Technology

Drilling parameters are excellent datasets to understand in-situ physical properties of the rock. Continuous core samples along with parameters such as Torque, RPM, WOB and ROP have been collected during drilling operations. The borehole data acquisition was complemented with full LWD/MWD and wireline logging. After core delivery to surface core scratch tests have been carried out to measure Unconfined Compressive Strength (UCS). Our comprehensive approach enabled us to integrate all data and conduct detailed analysis of the in-situ subsurface physical and mechanical properties of a rock cut by a drill bit.

Here we present some results from offshore and onshore drilling experiments carried out in Japan, Oman and Australia. Methods such as Specific Energy (SE) and Equivalent Strength (EST) have been used to estimate in-situ rock properties, namely UCS and analyse drilling process.

Our results demonstrate that the calculated in-situ rock strength based on SE/EST methods correlates well with sonic derived UCS and core scratch derived UCS. Utilised methods also successfully detect fractures in the formation, show developing drilling dysfunctions such as vibration, and bit balling.

Keywords: rock strength, drilling parameters, Specific Energy

©2019. Japan Geoscience Union. All Right Reserved.

Interaction between submarine landslides and subseafloor sedimentary microbiome: Chikyu SCORE Expedition 910 off Cape Erimo

*星野 辰彦[1]、浦本 豪一郎[2]、藤内 智士[2]、諸野 祐樹[1]、井尻 暁[1]、鈴木 志野[1]、久保 雄介[1]、稲垣 史生[1]、Chikyu SCORE Exp. 910 研究者一同
*Tatsuhiko Hoshino[1], Go-Ichiro Uramoto[2], Satoshi Tonai[2], Yuki Morono[1], Akira Ijiri[1], Shino Suzuki[1], Yusuke Kubo[1], Fumio Inagaki[1], Chikyu SCORE Exp. 910 Scientists .

1. 独立行政法人海洋研究開発機構、2. 高知大学
1. Japan Agency for Marine-Earth Science and Technology, 2. Kochi University

During the past decades, scientific ocean drilling has explored the subseafloor sedimentary biosphere down to over 2 kilometers below seafloor (Inagaki et al., 2015). The total biomass and diversity of microbial community in the subseafloor biosphere are comparable to those in the hydrosphere (Kallmeyer et al., 2012). Taxonomic composition of subseafloor microbial communities are distinct from those of other habitats on Earth’ s surface, such as ocean and soil, inferring that adaptive evolution of microbial community to the energy-limited deep sedimentary habitats have occurred. In a previous study of bioturbated layers in surface marine sediments, it has been reported that seawater-migration by macrofauna activity during the initial depositional stage notably affected microbial community structures (Chen et al. 2017). Similarly, it can be hypothesized that submarine landslides have introduced easily degradable fresh organic matter and dissolved electron acceptors (e.g., oxygen, sulfate) to the sedimentary habitats, and consequently caused a shift of microbial communities and its function.

In 2017, we conducted the Chikyu’ s first SCORE Expedition 910 at the Hidaka Trough off Cap Erimo and obtained sediment cores down to 100 meters below the seafloor. In the core column, four intervals of deformed sediments were identified, indicating the occurrences of multiple submarine landslides in this area. In those deformed sediment intervals, we observed no clear anomaly in the profile of cell abundance, which decrease with sediment depth as generally seen in the other subserfloor sediments. In addition, pore water chemistry data do not show clear anomaly either, indicating recovery of sediment geochemistry from the turbation caused by landslides. While both profiles of microbial cell abundance and pore water geochemistry did not show anomaly in the deformed sediment intervals, the DNA-based analyses, showed some unusual appearances of microbial taxa relative to the depth, suggesting the potential migration of microbes from the upper horizons by submarine landslides.

Reference

Inagaki F, et al (2015). Science 349: 420-424; Kallmeyer J, et al (2012). Proc Natl Acad Sci U S A 109: 16213-16216; Chen X, et al (2017). Sci Rep 7: 2400.

キーワード：Chikyu SCORE、Deep biosphere、Mass transport deposit
Keywords: Chikyu SCORE, Deep biosphere, Mass transport deposit

©2019. Japan Geoscience Union. All Right Reserved.

襟裳岬沖SCORE掘削コアのXRFコアスキャナー連続化学分析
High-resolution continuous records of the chemical composition of the marine sediment off Cape Erimo, Hokkaido, Japan

*村山 雅史[1]、矢生 晋介[3]、藤内 智士[2]、浦本 豪一郎[3]、山田 泰広[4]、稲垣 史生[4]、久保 雄介[5]
*Masafumi MURAYAMA[1], Shinsuke Yagyu[3], Satoshi Tonai[2], Go-Ichiro Uramoto[3], Yasuhiro Yamada[4], Fumio Inagaki[4], Yusuke Kubo[5]

1. 高知大学　農林海洋科学部海洋資源科学科、2. 高知大学　理工学部、3. 高知大学　海洋コア総合研究センター、4. 海洋研究開発機構　海洋掘削科学研究開発センター, 、5. 海洋研究開発機構　地球深部探査センター
1. Faculty of Agriculture and Marine Science, Kochi University, 2. Faculty of Science and Technology, Kochi University, 3. Center for Advanced Marine Core Research, Kochi University, 4. Research and Development Center for Ocean Drilling Science, JAMSTEC, 5. Center for Deep Earth Exploration, JAMSTEC

About 100 m sediment cores were taken from off Cape Erimo, Hokkaido, Japan on the Shallow Core Program (SCORE) by D/V Chikyu in 2017. The sedimentary sequence is intercalated with mass transport deposits caused by earthquake-triggered submarine landslides and/or climate changes. Here we report a result of high-resolution continuous geochemical composition of these cores using XRF core scanning technique.

キーワード：襟裳岬沖掘削コア、XRFコアスキャナー、SCOREプログラム、地球深部探査船「ちきゅう」
Keywords: sediment core off Cape Erimo, XRF core scanner (ITARX), Shallow Core Program (SCORE), D/V Chikyu

©2019. Japan Geoscience Union. All Right Reserved.

熊本地震震源断層掘削コアを用いた熱物性測定
Thermal property measurements of core samples retrieved from Futagawa fault drilling

*佐野 暉[1]、林 為人[1]、渋谷 奨[1,2]、神谷 奈々[1]、杉本 達洋[1]、石塚 師也[1]、林 愛明[3]
*Terasu Sano[1], Weiren Lin[1], Susumu Shibutani[1,2], Nana Kamiya[1], Tatsuhiro Sugimoto[1], Kazuya Ishitsuka[1], Aiming Lin[3]

1. 京都大学大学院工学研究科、2. 地圏総合コンサルタント、3. 京都大学大学院理学研究科
1. Graduate School of Engineering, Kyoto University, 2. Chi-ken Sogo Consultants Co., Ltd.,, 3. Graduate School of Science, Kyoto University

地球科学の分野では、地下の温度構造を理解することは重要である。地下の温度構造を決定するのは地殻熱流量と地層の熱伝導率であるため、地下深部から採取される岩石試料を用いて、熱伝導率ならびに熱拡散率、比熱を測定する必要がある。2017年から2018年にかけて熊本地震本震の震源断層である布田川断層を貫くように掘削された最大深度約700 mの掘削孔内の温度を測定したところ、明らかな温度異常が見られた（林ほか, 2019 JpGU）。この温度異常の原因を解明することは、阿蘇火山帯に位置する当該地域の地下温度構造を理解するだけでなく、地震メカニズムの更なる解明にもつながると期待される。そこで、当該掘削孔の岩石コア試料を用いて、深度約300～700 mに分布する地層を構成する主要な岩種の熱物性を測定し、この温度構造の異常を熱物性の観点から考察した。

熱物性測定用の試料として、熊本県益城町にある布田川断層掘削孔の前述深度区間において、主要な岩種から計20個のコア試料を採取した。このコアのサンプリングは、掘削された岩種のうちなるべく多くの種類を選びつつ、サンプリングした深度が大きく開きすぎないように留意して行った。なお、サンプリングした深度区間の主な岩種は、300 m～353 mが基底堆積物、353 m～514 mが安山岩、514 m～562 mが砂・礫岩、562 m～700 mが凝灰岩である。熱物性測定に用いた全岩石試料の基本物性として、密度と有効空隙率を測定した。その結果、含水飽和状態の湿潤密度は、基底堆積物層が1.57 g/㎤～2.02 g/㎤、安山岩層が2.31 g/㎤～2.95 g/cm^3、砂・礫岩層が2.29 g/㎤～2.41 g/cm^3、、凝灰岩層が1.99 g/㎤～2.29 g/cm^3となった。また、有効空隙率を測定したところ、基底堆積物層が40.0 %～47.8 %、安山岩層が3.1　%～25.5 %、砂・礫岩層が21.6%～29.4 %、凝灰岩層が19.4 %～35.8 %となり、非常に大きく変動することが判明した。

熱物性の測定には、非定常面熱源法（ホットディスク法）を用いた。ホットディスク法において、２つの試料でセンサーを挟んで測定する手法は、１つの試料を用いる手法より精度がよいと考えられるため、コア試料を3 cmの厚さに切り分け、1つのコアから４つのサブサンプルを取得、隣り合う２つのサブサンプルで１回の測定を行った。１つのコアにつき３回の測定を行い、平均値をそのコアの熱物性値とした。また、熱物性の測定は含水飽和と完全乾燥状態でそれぞれ行った。熱伝導率の測定結果は、基底堆積物層が0.88 W/(mK)～1.10 W/(mK)、安山岩層が1.00 W/(mK)～1.81 W/(mK)、砂・礫岩層が1.26 W/(mK)～1.31 W/(mK)、凝灰岩層が0.96 W/(mK)～1.27 W/(mK)となった。この値を用いて、温度構造に関する考察を行った。また、熱拡散率、比熱の測定結果は、基底堆積物層が0.26 ㎟/s～1.28 ㎟/s, 0.85 J/(g・K)～3.46 J/(g・K)、安山岩層が0.48 ㎟/s～0.91 ㎟/s, 1.36 J/(g・K)～2.60 J/(g・K)、砂・礫岩層が0.49 ㎟/s～0.66 ㎟/s, 1.95 J/(g・K)～2.70 J/(g・K)、凝灰岩層が0.40 ㎟/s～0.99 ㎟/s, 1.40 J/(g・K)～2.93 J/(g・K)となった。

林ほか（2019 JpGU）が行った掘削孔内の温度測定結果によれば、深部の約430～650 mの区間では、深くなるにつれ地層の温度がほぼ直線的に高くなる温度構造が認められ、その地温勾配は55 ℃/km程度であった。採取したコアの熱伝導率を、そのコアと同じ地質の層厚によって重みづけして平均熱伝導率を計算し

©2019. Japan Geoscience Union. All Right Reserved.

たうえ、フーリエの法則（j=λgradT、jは熱流量、λは熱伝導率、gradTは地温勾配）を用いて、当該深度範囲における地殻熱流量を求めた。さらに、当該掘削孔の深度範囲では、この熱流量以外の熱源がないと仮定し、かつ、熱伝導の定常状態として、同じフーリエの法則を用いて、実測した最深の温度からスタートし、各地層の熱伝導率を用いて、温度の深度プロファイルを試算した。

実測の温度プロファイルは深度約310～430 mの区間においては、ほぼ一定であり、その地温勾配が約1 ℃/kmという異常な温度分布の結果が得られた（林ほか, 2019 JpGU）。450 m以深では、試算の温度構造は実測の温度構造とよく一致しており、その深度区間では用いた仮定が正しいことが示唆された。一方、深度430 mと310 m付近では、熱物性値からの試算では、実測値の急激な温度勾配の変化を再現できなかった。すなわち、この温度異常は熱物性値の変化によるものではないと確認された。現段階では、この温度異常の原因として、地下水流動に伴う熱の移動の可能性があると推測される。今後は、さらに多くのコアの熱物性の測定を進め、より正確な熱物性の深度プロファイルを構築するとともに、この温度異常の原因究明に貢献したい。

キーワード：掘削孔、熱物性、温度
Keywords: Drilling, thermal properties, Temperature

©2019. Japan Geoscience Union. All Right Reserved.

東オーストラリア沖ロードハウライズ地域で採取された浅部コアの物性・強度試験結果：将来のロードハウライズライザー掘削に向けて
Results of geotechnical tests on shallow sediment cores recovered from Lord Howe Rise, off eastern Australia: Implications for future Lord Howe Rise riser drilling

*杉原 孝充[1]、青池 寛[1]、斎藤 実篤[2]、村山 達也[1]、武田 研太郎[1]、小野寺 拓也[3]、澄川 あゆみ[3]、木戸 ゆかり[1]、真田 佳典[1]
*Takamitsu Sugihara[1], Kan Aoike[1], Saneatsu Saito[2], Tatsuya Murayama[1], Kentaro Takeda[1], Takuya Onodera[3], Ayumi Sumikawa[3], Yukari Kido[1], Yoshinori Sanada[1]

1. 海洋研究開発機構　地球深部探査センター、2. 海洋研究開発機構　海洋掘削科学研究開発センター、3. 日本海洋事業
1. Center for deep earth exploration, Japan Agency for Marine-Science and Technology, 2. Research and development center for ocean drilling science, Japan Agency for Marine-Science and Technology, 3. Nippon Marine Enterprises, Ltd.

Lord Howe Rise (LHR) Drilling Project (871-CPP2) is an accepted IODP drilling proposal to reconstruct Cretaceous tectonic history of northern Zealandia, designated as a Chikyu riser drilling project. In order to plan a riser drilling operation, it is important to evaluate mechanical strength and physical properties of shallow sediment (0 to 100 or 200 meters below sea floor, mbsf) for setting Blow-out Prevention (BOP) system and riser with heavy weight on the seafloor. Geotechnical core test (e.g., triaxial compressive test and consolidation test) is an essential work to directly measure rock strength and physical properties of geological materials. Therefore, the geotechnical core tests are usually conducted for the surface sediment to evaluate their mechanical and physical properties. In the LHR region, calcareous sediment is broadly and predominantly distributed, and clayey sediment is not observed in shallow sediments. In general, deep seafloor is composed of clayey sediment, and their mechanical and physical properties are well understood. However, mechanical and physical properties of calcareous sediment in both ambient and confined pressure conditions are not well known.

In this study, results of geotechnical test for shallow cores taken in the LHR region are presented, and characteristics of mechanical and physical properties (especially shear strength and permeability) are discussed.

Shallow cores for geotechnical test were taken by R/V Kairei with a gravity piston corer in KR17-15C and by D/V JOIDES Resolution with a rotary core barrel (RCB) in Expedition 371. The gravity piston coring by R/V Kairei was conducted at the proposed riser drilling sites DLHR-5A and -3A, and two cores with approximately 7 m length were taken at each site. The RCB coring by D/V JOIDES Resolution was conducted at Site U1506 in Expedition 371. A whole-round sample with 40 cm length was taken from U1506A-13R for our investigation, and depth of the whole-round sample is 116.5 mbsf. In order to measure physical and mechanical properties for the core samples, geotechnical tests of Penetrometer test, Bulk density, Grain density, Liquid limit, Plastic limit, Grain size distribution, Constant rate of strain consolidation test (CRSC test), and Triaxial compressive strength test with pore pressure measurement (Consolidated-Undrained conditions) were carried out.

Most of the tests except penetrometer test were carried out by OYO Co. Procedures of those

©2019. Japan Geoscience Union. All Right Reserved.

measurements and tests were based on the regulations established by Japanese Geotechnical Society (JGS) and Japanese Industrial Standards (JIS). Those are almost the same as their regulations in the ASTM.

All of core samples are composed of calcareous ooze, and grain size distribution of the core samples shows clay size fraction (less than 5 micro meters) is dominant (more than 80 %).

Based on the bulk density data, overburden stresses were calculated and consolidation pressures corresponding to depth of 10 to 240 mbsf for the triaxial test were estimated assuming k0 compaction (k0 factor = 0.5). The result of the triaxial test show shear strength profile gradually increases with depth and is almost identical to those of clayey sediment from Kumano Basin and Nankai Trough. However, the result of the penetrometer test indicates that shear strength of calcareous ooze under ambient condition is quite lower than those of clayey sediment. This observation suggests mechanical strength of calcareous ooze is easily released with depressurizing of sediment.

Based on the result of the CRSC test, it is indicated that calcareous ooze shows no obvious preconsolidation stress, and this result is in good agreement with the result of the triaxial test mentioned above. Permeability of calcareous ooze calculated from the CRSC test results is similar to sandy sediment and the results indicate calcareous ooze is more permeable as compared with clayey sediment.

Those results will be dedicated to analysis for the riser operation in the LHR area.

キーワード：ロードハウライズ、ライザー掘削、岩石強度試験、剪断強度、透水率
Keywords: Lord Howe Rise, Riser drilling, Rock strength test, Shear strength, Permeability

©2019. Japan Geoscience Union. All Right Reserved.

ICDP DSeis 4: Drilling, core logging, and in-hole geophysical logging of ICDP DSeis drilling into the M5.5 aftershock zones in a South African gold mines.

*吉田 峻輔[1]、田所 遼悟[1]、杉村 幸祐[1]、兼松 慎[1]、東 充也[1]、Liebenberg Benni[2]、 van Heerden Esterhuizen[2]、Stephen Tau[3]、Siyanda Mngadi[3]、Ray Durrheim[3]、Martin Ziegler[4]、椋平 祐輔[5]、Ronald Conze[6]、矢部 康男[7]、金木 俊也[8]、Yokoyama Yuki[9]、Nomqhele Nkosi[10]、Dave Roberts[10]、Sifiso Buccio[11]、小笠原 宏[1]
*Shunsuke YOSHIDA[1], Tadokoro Ryogo[1], Kosuke Sugimura[1], Kanematsu Makoto[1], Mitsuya Higashi[1], Benni Liebenberg[2], Esterhuizen van Heerden[2], Stephen Tau[3], Siyanda Mngadi[3], Ray Durrheim[3], Martin Ziegler[4], Yusuke Mukuhira[5], Ronald Conze[6], Yasuo Yabe[7], Shunya Kaneki[8], Yuki Yokoyama[9], Nomqhele Nkosi[10], Dave Roberts[10], Sifiso Buccio[11], Hiroshi Ogasawara[1]

1. Graduate school of science and engineering, Ritsumeikan、2. Moab Khotsong mine, Vijoenskroon、3. Univ. Witwatersrand, School of Geoscience、4. ETH, Zurich Dep. Earth Sciences、5. Inst. Fluid Science, Tohoku Univ.、6. GFZ, Potzdam、7. Graduate School of Science, Tohoku Univ.、8. Disaster Prevention Research Inst., Kyoto Univ.、9. Graduate School of Science,Osaka Univ.、10. Mandela Mining Precinct, CSIR、11. Council for Geoscience
1. Graduate school of science and engineering, Ritsumeikan , 2. Moab Khotsong mine, Vijoenskroon, 3. Univ. Witwatersrand, School of Geoscience, 4. ETH, Zurich Dep. Earth Sciences, 5. Inst. Fluid Science, Tohoku Univ., 6. GFZ, Potzdam, 7. Graduate School of Science, Tohoku Univ., 8. Disaster Prevention Research Inst., Kyoto Univ., 9. Graduate School of Science,Osaka Univ., 10. Mandela Mining Precinct, CSIR, 11. Council for Geoscience

ICDP drilling into the aftershock zone of the 2014 M5.5 earthquake near Orkney, South Africa commenced on 2017 and was completed in 2018. This M5.5 earthquake started from a depth about 5 km and ruptured West Rand Group below mining horizon on unknown geological structure in a deep gold mine. The mechanism of left-lateral slip of this M5.5 earthquake contradicted normal-faulting mechanisms of typical mining-induced earthquakes on mining horizons. The upper fringe of the aftershock zone was several hundreds of meters from the deepest level of the mine. Two NQ holes were collared at a depth of 2.9 km (95 level) below surface at a deep gold mine. Hole A (817m) deviated too much to intersect the M5.5 fault but Hole B (700m) intersected the M5.5 fault. A 3-m double-tube couldn't recover the fault material much, while a 1.5m triple-tube could recover the fault material more in Hole C branched from 544 m in Hole B. Geophysical logging, core logging, and water/gas monitoring followed drilling. All the core was transported to Mandela Mining Precinct, CSIR, Johannesburg and systematically described and scanned by the ICDP DMT scanner. Some of the core were selected for core stress measurements.

In JpGU 2019 meeting, nine papers (ICDP DSeis 1-9) report on the outcomes. This poster (ICDP DSeis 4) compiles drilling, core logging, and in-hole geophysical logging of ICDP DSeis drilling into the M5.5 aftershock zones in a South African gold mines. A core orientation tool was used during drilling but not 100% reliable because there was a case that a bottom line in a core run was different by more than 90 degrees from the bottom line in the next core run. We elaborated to compare OTV image with core to carefully check the core orientation. The modified core orientation allowed us to modify the maximum stress direction that Ishida et al. (2018) measured. We could confirm good consistency with borehole breakout analysis (Richenbacher 2018; ETH master thesis). We will report on other associated outcomes. Refer other papers (ICDP DSeis 1-3, 5-9) for other related outcomes.

©2019. Japan Geoscience Union. All Right Reserved.

Acknowledgement: The DSeis team includes co-authors of the papers ICDP DSeis 2-9 and members shown at https://www.icdp-online.org/projects/world/africa/orkney-s-africa/details/. We thank Harmony Gold, Anglogold Ashanthi, Lesedi, Digital Surveying, OHMS, Seismogen, 3D Geoscience. ICDP, JSPS, SA NRF, MEXT Japan, US NSF, German DRF, and Ritsumeikan Univ. financially support the project.

©2019. Japan Geoscience Union. All Right Reserved.

ICDP DSeis 5: Diametrical Core Deformation Analysis of the M5.5 aftershock zone core - stress concentration at reflective intrusives and transition in stress regimes.

*杉村 幸祐[1]、吉田 峻輔[1]、田所 遼悟[1]、小笠原 宏[2]、石田 亮壮、矢部 康男[3]、伊藤 高敏[4]、明雄 船戸[5]、Siyanda Mngadi[6]、Ray Durrheim[6]
*Kosuke Sugimura[1], Shunsuke YOSHIDA[1], Ryogo Tadokoro[1], Hiroshi Ogasawara[2], Akimasa Ishida, Yasuo Yabe[3], Takatoshi Ito[4], Akio Funato[5], Siyanda Mngadi[6], Ray Durrheim[6]

1. 立命館大学大学院　理工学研究科、2. 立命館大学　理工学部、3. 東北大学　理学部、4. 東北大学　流体科学研究所、5. 深田地質研究所、6. Univ. Witwatersrand, School of Geoscience
1. Graduate school of science and engineering, Ritsumeikan, 2. College of Science and Engineering, Ritsumeikan Univ., 3. Graduate School of Science, Tohoku Univ., 4. Inst. Fluid Science, Tohoku Univ., 5. Fukada Geological Institute, 6. Univ. Witwatersrand, School of Geoscience

ICDP drilling into the aftershock zone of the 2014 M5.5 earthquake near Orkney, South Africa commenced on 2017 and was completed in 2018. Drilling was designed to minimize damage on core and borehole, being able to maximize core recovery. Hole A (817m) was drilled in 2017. It unfortunately didn't intersect the M5.5 fault, running eventually sub-parallel and roughly 100m from the aftershock zone. As the hole was stable we could recover almost 100% of core from the area traversing the periphery of the M5.5 aftershock zone for a distance of several hundreds of meters. Ishida et al. (2018) carried out Diametrical Core Diameter Analysis (Ito and Funato, 2017). This analysis measures the change in core diameter with roll angle around the core axis, which was caused by a relief of anisotropic stress during drilling. We used this analysis because (1) the expected stress was too high for hydrofracturing method, (2) uncertainty in stress magnitude is unavoidable in damage interpretations, (3) DSeis hole were too long for overcoring technique, and (4) DCDA is non-destructive and very easy to make if core is recovered. Ishida et al. (2018) measured 186 pieces of core from Hole A (817m collared at 2.9km depth) that were recovered near the M5.5 aftershock zone. They successfully illustrated spatial variation in differential stress in a plane perpendicular to Hole A axis. They found stress concentration at intrusives with one located at the depth of the upper fringe of the M5.5 aftershock zone. We carried out additional measurement for the remaining part of Hole A and Hole B. With additional data measured at adjacent locations, we could confirm that the stress concentration Ishida et al (2018) found at intrusives was not an outlier. We will report how Hole B that intersected the M5.5 fault differ from Hole A stress.

This is one of nine ICDP DSeis papers (ICDP DSeis 1-9) presented in JpGU 2019. Refer other papers for other topic on drilling, logging, other stress measurement, fault materials, comparison with calculated stress, legacy 3D seismic reflection data, and relocated aftershocks.

©2019. Japan Geoscience Union. All Right Reserved.

ICDP DSeis 6: Deformation Rate Analysis of the M5.5 aftershock zone core - stress concentration at reflective intrusives

*兼松 慎[1]、東 充也[1]、矢部 康男[2]、阿部 周平[2]、Watson Bryan[3]、Durrheim Ray[3]、小笠原 宏[1]
*Kanematsu Makoto[1], Mitsuya Higashi[1], Yasuo Yabe[2], Shuhei Abe[2], Bryan Watson[3], Ray Durrheim[3], Hiroshi Ogasawara[1]

1. 立命館大学 理工学部　物理科学科、2. 東北大学理学研究科、3. Witwatersrand大
1. Ritsumeikan Univ., 2. Tohoku Univ., 3. Univ. Witwatersrand

ICDP drilling into the aftershock zone of the 2014 M5.5 earthquake near Orkney, South Africa commenced on 2017 and was completed in 2018. Ishida et al. (2018) and Sugimura et al. (2019; ICDP DSeis 5) report on spatial variation of differential stress in a plane perpendicular to the borehole axis. It is ideal to have different stress component especially at critical location where significant characteristics were found. Deformation Rate Analysis (Yamamoto, 2009) can measure stress in any direction although the method takes time and the specimen are not reusable for other test. So, we planned to selected samples where characteristic spatial variation was found by DCDA method (Ishida et al. 2018 and Sugimura et al. 2019). It was confirmed also in normal stress component along the borehole axis that stress was concentrated at the intrusive at about 400m.

This is one of nine ICDP DSeis papers (ICDP DSeis 1-9) presented in JpGU 2019. Refer other papers for other topics on drilling, logging, other stress measurement, fault materials, comparison with calculated stress, legacy 3D seismic reflection data, and relocated aftershocks.

Acknowledgement: The DSeis team includes co-authors of the papers ICDP DSeis 2-9 and members shown at https://www.icdp-online.org/projects/world/africa/orkney-s-africa/details/. We thank Harmony Gold, Anglogold Ashanthi, Lesedi, Digital Surveying, OHMS, Seismogen, 3D Geoscience. ICDP, JSPS, SA NRF, MEXT Japan, US NSF, German DRF, and Ritsumeikan Univ. financially support the project.

キーワード：地震発生場、応力測定、DRA
Keywords: Seismogenic zone, Stress Measurement, DRA

©2019. Japan Geoscience Union. All Right Reserved.

ICDP DSeis 7: compilation of stress information and comparison with calculated stresses in the M5.5 aftershock zones

*東 充也[1]、矢部 康男[2]、杉村 幸佑[1]、石田 亮壮、兼松 慎[1]、吉田 峻輔[1]、田所 遼悟[1]、伊藤 高敏[4]、船戸 明雄[5]、小笠原 宏[3]
*Mitsuya Higashi[1], Yasuo Yabe[2], Kosuke Sugimura[1], Akimasa Ishida, Makoto Kanematsu[1], Shunsuke YOSHIDA[1], Ryogo Tadokoro[1], Takatoshi Ito[4], Akio Funato[5], Hiroshi Ogasawara[3]

1. 立命館大学大学院理工学研究科、2. 東北大学大学院理学研究科・理学部 附属地震・噴火予知研究観測センター、3. 立命館大学理工学部、4. 東北大学流体科学研究所、5. 深田地質研究所
1. Graduate School of Science and Engineering, Ritsumeikan Univ., 2. Research Center for Prediction of Earthquakes and Volcanic Eruptions, Graduate School of Science, Tohoku University, 3. College of Science and Engineering, Ritsumeikan Univ., 4. Inst. Fluid Science, Tohoku Univ., 5. Fukada Geological Institute

ICDP drilling into the aftershock zone of the 2014 M5.5 earthquake near Orkney, South Africa commenced on 2017 and was completed in 2018. Spatial variation in stress was measured by Ishida et al. (2018) and Sugimura et al. (2019; ICDP DSeis 5) by DCDA method (Funato and Ito, 2017) and Kanematsu et al. (2019; ICDP DSeis 6). This poster reports on compilation of stress information including the other information sources and compares with calculated stress.

We first compared with a 3D stress state that Ogasawara et al. (2012) measured in 2011 at 98L (3.0 km depth from surface). We assume zero stress on surface, the measured 3D stress (normal faulting stress regime) at 3.0 km, and stress linearly increasing with depth. The calculated stress was consistent with DCDA results measured in the initial 100m section in Hole A, while inconsistent in deeper section. The calculated direction of maximum stress in a plane perpendicular to the borehole axis was also inconsistent with the measured stress information (Yoshida et al. 2019 JpGU; ICDP DSeis 5). Except for the stress concentration measured at intrusives, the measured DCDA results were systematically lower than the calculated stress. In a stress regime that caused the left-lateral horizontal slip on the M5.5 fault, horizontal stress should be larger, which will increase horizontal stress component in a plane perpendicular to the Hole A axis. This increase should decrease difference in stress in the plane perpendicular to the Hole A axis. By JpGU 2019, we will make additional effort to interpret more from the comparison between the measured and calculated stress.

This is one of nine papers (ICDP DSeis 1-9). Refer other papers for other topic on drilling, logging, other stress measurement, fault materials, legacy 3D seismic reflection data, and relocated aftershocks.

Acknowledgement: The DSeis team includes co-authors of the papers ICDP DSeis 2-9 and members shown at https://www.icdp-online.org/projects/world/africa/orkney-s-africa/details/. We thank Harmony Gold, Anglogold Ashanthi, Lesedi, Digital Surveying, OHMS, Seismogen, 3D Geoscience. ICDP, JSPS, SA NRF, MEXT Japan, US NSF, German DRF, and Ritsumeikan Univ. financially support the project.

©2019. Japan Geoscience Union. All Right Reserved.

©2019. Japan Geoscience Union. All Right Reserved.

ICDP DSeis 8: the M5.5 fault structure and reflective intrusives in legacy 3D seismic reflection data

*野田 拓[1]、Manzi Musa[2]、Ogasawara Hiroyuki[1]、Linzer Lindsay[2]、Enslin Stephanie[2]、Durrheim Ray[2]、小笠原 宏[1]
*Noda Taku[1], Musa Manzi[2], Hiroyuki Ogasawara[1], Lindsay Linzer[2], Stephanie Enslin[2], Ray Durrheim[2], Hiroshi Ogasawara[1]

1. 立命館大学、2. Witwatersrand大
1. Ritsumeikan Univ., 2. Univ. Witwatersrand

ICDP drilling into the aftershock zone of the 2014 M5.5 earthquake near Orkney, South Africa commenced on 2017 and was completed in 2018. Hiroyuki et al. (2017 AGU) reported on legacy seismic reflection to analyze geological structures in the southern most area of the M5.5 aftershock zones. They found vertical structures in four 2-D lines that were potentially responsible for the M5.5 earthquake and illustrated cross-cutting relations of the M5.5 structure and other known faults that dislocated gold reefs more than several hundreds of meters both horizontally and vertically. Another legacy seismic reflection data which was recorded in 1996 and covered much wider area of the M5.5 aftershock zone was found. We calibrated velocity structure by tying with borehole data including DSeis Holes A and B, we found some of intrusives (sills) that Hole A and B were strong reflectors in the legacy 3D seismic reflection data.

Aftershocks located by in-mine 46 geophones are dense at the southern upper fringe, with a sharp cut-off dipping about 20 degrees to the south; some clear stripes of aftershocks are also seen, in parallel to the upper fringe (Tadokoro et al., JpGU2019, ICDP DSeis 9). It is interesting to note that the reflector (sills) are also in parallel to the upper fringe of the aftershock zone and the aftershock stripes. It is also notable that stress concentration is reported at the intrusives by Sugimura et al. (JpGU2019; ICDP DSeis 5) and Kanematsu et al. (JpGU2019; ICDP DSeis 6). Some mechanism that controls the extent of the aftershocks should exist.

This paper is one of nine papers (ICDP DSeis 1-9). Refer other papers for other topics, e.g. on drilling, logging, stress measurements and evaluation, fault materials, and relocated aftershocks.

Acknowledgement: The DSeis team includes co-authors of the papers ICDP DSeis 2-9 and members shown at https://www.icdp-online.org/projects/world/africa/orkney-s-africa/details/. We thank Harmony Gold, Anglogold Ashanthi, Lesedi, Digital Surveying, OHMS, Seismogen, 3D Geoscience. ICDP, JSPS, SA NRF, MEXT Japan, US NSF, German DRF, and Ritsumeikan Univ. financially support the project.

キーワード：ICDP DSeis、M5.5地震発生場、地震反射法探査
Keywords: ICDP DSeis, The M5.5 seismogenic zone, Seismic reflection

©2019. Japan Geoscience Union. All Right Reserved.

ICDP DSeis 9: are streaks in the M5.5 aftershocks potentially located on highly stressed intrusive?

*Ryogo Tadokoro[1], Katsuya Ishibashi[2], Horiuchi Shigeki[3], Hiroshi Ogasawara[4]

1. Graduate School of Science and Engineering, Ritsumeikan Univ., 2. School of Science and Engineering, Ritsumeikan Univ., 3. Homeseismo ltd., 4. College of Science and Engineering, Ritsumeikan Univ.

ICDP drilling into the aftershock zone of the 2014 M5.5 earthquake near Orkney, South Africa commenced on 2017 and was completed in 2018. Aftershocks located by in-mine 46 geophones are dense at the southern upper fringe, with a sharp cut-off dipping about 20 degrees to the south. Some clear stripes of aftershocks are also seen, in parallel to the upper fringe. It is interesting to note that the reflector (sills) are also in parallel to the upper fringe of the aftershock zone and the aftershock stripes. It is also notable that stress concentration is reported at the intrusives by Sugimura et al. (JpGU2019; ICDP DSeis 5) and Kanematsu et al. (JpGU2019; ICDP DSeis 6). Some mechanism that controls the extent of the aftershocks should exist.

In order to discuss further, we relocated aftershocks with the Double-Difference method (Waldhouser and Ellsworth, 2004). At the moment, we could relocate only 60 events at the upper fringe of the aftershocks. We used in-mine seismic network data of Anglogold Ashanti. P- and S- arrival times that the algorithm of Horiuchi et al. (2011) was used. A sharper alignment of aftershocks is successfully illustrated. By JpGU 2019, we will make additional efforts to extend the area of relocation to discuss more.

Acknowledgement: The DSeis team includes co-authors of the papers ICDP DSeis 2-9 and members shown at https://www.icdp-online.org/projects/world/africa/orkney-s-africa/details/. We thank Harmony Gold, Anglogold Ashanthi, Lesedi, Digital Surveying, OHMS, Seismogen, 3D Geoscience. ICDP, JSPS, SA NRF, MEXT Japan, US NSF, German DRF, and Ritsumeikan Univ. financially support the project.

©2019. Japan Geoscience Union. All Right Reserved.

[E] ポスター発表 | セッション記号 M (領域外・複数領域)：M-IS ジョイント

2019年5月27日(月) 17:15 ~ 18:30 | ポスター会場 幕張メッセ国際展示場 8ホール_32

[M-IS02] 地球掘削科学

コンビーナ:山田 泰広(海洋研究開発機構　海洋掘削科学研究開発センター)、針金 由美子(産業技術総合研究所)、黒柳 あずみ(東北大学学術資源研究公開センター東北大学総合学術博物館)、山口 耕生(東邦大学, NASA Astrobiology Institute.)

これまでに実施された科学掘削データ・試料の解析・分析結果などの研究成果の報告と、今後の科学掘削計画に関する最新情報の紹介を目的とする。固体地球科学、古環境学、地球生命科学などの様々な分野からの成果を共有し、科学掘削を基軸とした学際的研究を推進する。最近１年間に実施されたICDPプロジェクトとIODP航海の概要報告を中心に、これまでに実施された掘削航海に関連して得られた最新研究成果と、今後数年間に具体化される科学掘削計画、掘削科学に関連する新規手法や技術開発研究等の報告を歓迎する。

[MIS02-P01] 地下生命圏研究における凍結コア試料の活用と名古屋議定書への対応

*肖 楠[1] (1.海洋研究開発機構)

[MIS02-P02] In-situ rock strength calculated from drilling parameters. Comparison of results from various sites.

*Adam Wspanialy[1]、Yasuhiro Yamada[1]、Saneatsu Saito[1]、KYAW MOE[1] (1.Japan Agency for Marine-Earth Science and Technology)

[MIS02-P03] Interaction between submarine landslides and subseafloor sedimentary microbiome: Chikyu SCORE Expedition 910 off Cape Erimo

*星野 辰彦[1]、浦本 豪一郎[2]、藤内 智士[2]、諸野 祐樹[1]、井尻 暁[1]、鈴木 志野[1]、久保 雄介[1]、稲垣 史生[1]、Chikyu SCORE Exp. 910 研究者一同 (1.独立行政法人海洋研究開発機構、2.高知大学)

[MIS02-P04] 襟裳岬沖SCORE掘削コアのXRFコアスキャナー連続化学分析

*村山 雅史[1]、矢生 晋介[3]、藤内 智士[2]、浦本 豪一郎[3]、山田 泰広[4]、稲垣 史生[4]、久保 雄介[5] (1.高知大学　農林海洋科学部海洋資源科学科、2.高知大学　理工学部、3.高知大学　海洋コア総合研究センター、4.海洋研究開発機構　海洋掘削科学研究開発センター, 、5.海洋研究開発機構　地球深部探査センター)

[MIS02-P05] 熊本地震震源断層掘削コアを用いた熱物性測定

*佐野 暉[1]、林 為人[1]、渋谷 奨[1,2]、神谷 奈々[1]、杉本 達洋[1]、石塚 師也[1]、林 愛明[3] (1.京都大学大学院工学研究科、2.地圏総合コンサルタント、3.京都大学大学院理学研究科)

[MIS02-P06] 東オーストラリア沖ロードハウライズ地域で採取された浅部コアの物性・強度試験結果：将来のロードハウライズライザー掘削に向けて

*杉原 孝充[1]、青池 寛[1]、斎藤 実篤[2]、村山 達也[1]、武田 研太郎[1]、小野寺 拓也[3]、澄川 あゆみ[3]、木戸 ゆかり[1]、真田 佳典[1] (1.海洋研究開発機構　地球深部探査センター、2.海洋研究開発機構　海洋掘削科学研究開発センター、3.日本海洋事業)

[MIS02-P07] ICDP DSeis 4: Drilling, core logging, and in-hole geophysical logging of ICDP DSeis drilling into the M5.5 aftershock zones in a South African gold mines.

*吉田 峻輔[1]、田所 遼悟[1]、杉村 幸祐[1]、兼松 慎[1]、東 充也[1]、Liebenberg Benni[2]、 van Heerden Esterhuizen[2]、Stephen Tau[3]、Siyanda Mngadi[3]、Ray Durrheim[3]、Martin Ziegler[4]、椋平 祐輔[5]、Ronald Conze[6]、矢部 康男[7]、金木 俊也[8]、Yokoyama Yuki[9]、Nomqhele Nkosi[10]、Dave Roberts[10]、Sifiso Buccio[11]、小笠原 宏[1] (1.Graduate school of science and engineering, Ritsumeikan、2.Moab Khotsong mine, Vijoenskroon、3.Univ. Witwatersrand, School of Geoscience、4.ETH, Zurich Dep. Earth Sciences、5.Inst. Fluid Science, Tohoku Univ.、6.GFZ, Potzdam、7.Graduate School of Science, Tohoku Univ.、8.Disaster Prevention Research Inst., Kyoto Univ.、9.Graduate School of Science,Osaka Univ.、10.Mandela Mining Precinct, CSIR、11.Council for Geoscience)

[MIS02-P08] ICDP DSeis 5: Diametrical Core Deformation Analysis of the M5.5 aftershock zone core - stress concentration at reflective intrusives and transition in stress regimes.

*杉村 幸祐[1]、吉田 峻輔[1]、田所 遼悟[1]、小笠原 宏[2]、石田 亮壮、矢部 康男[3]、伊藤 高敏[4]、明雄 船戸[5]、Siyanda Mngadi[6]、Ray Durrheim[6] (1.立命館大学大学院　理工学研究科、2.立命館大学　理工学部、3.東北大学　理学部、4.東北大学　流体科学研究所、5.深田地質研究所、6.Univ. Witwatersrand, School of Geoscience)

[MIS02-P09] ICDP DSeis 6: Deformation Rate Analysis of the M5.5 aftershock zone core - stress concentration at reflective intrusives

*兼松 慎[1]、東 充也[1]、矢部 康男[2]、阿部 周平[2]、Watson Bryan[3]、Durrheim Ray[3]、小笠原 宏[1] (1.立命館大学 理工学部　物理科学科、2.東北大学理学研究科、3.Witwatersrand大)

[MIS02-P10] ICDP DSeis 7: compilation of stress information and comparison with calculated stresses in the M5.5 aftershock zones

*東 充也[1]、矢部 康男[2]、杉村 幸佑[1]、石田 亮壮、兼松 慎[1]、吉田 峻輔[1]、田所 遼悟[1]、伊藤 高敏[4]、船戸 明雄[5]、小笠原 宏[3] (1.立命館大学大学院理工学研究科、2.東北大学大学院理学研究科・理学部 附属地震・噴火予知研究観測センター、3.立命館大学理工学部、4.東北大学流体科学研究所、5.深田地質研究所)

[MIS02-P11] ICDP DSeis 8: the M5.5 fault structure and reflective intrusives in legacy 3D seismic reflection data

*野田 拓[1]、Manzi Musa[2]、Ogasawara Hiroyuki[1]、Linzer Lindsay[2]、Enslin Stephanie[2]、Durrheim Ray[2]、小笠原 宏[1] (1.立命館大学、2.Witwatersrand大)

[MIS02-P12] ICDP DSeis 9: are streaks in the M5.5 aftershocks potentially located on highly stressed intrusive?

*Ryogo Tadokoro[1]、Katsuya Ishibashi[2]、Horiuchi Shigeki[3]、Hiroshi Ogasawara[4] (1.Graduate School of Science and Engineering, Ritsumeikan Univ.、2.School of Science and Engineering, Ritsumeikan Univ.、3.Homeseismo ltd.、4.College of Science and Engineering, Ritsumeikan Univ.)

地下生命圏研究における凍結コア試料の活用と名古屋議定書への対応
Utilization and curation of frozen core samples in IODP and implementation of the Nagoya Protocol in ocean drilling science

*肖 楠[1]
*Nan XIAO[1]

1. 海洋研究開発機構
1. Japan Agency for Marine Earthe Science and Technology

Deep biosphere research has become one of the major scientific focuses in ocean drilling science. How to access to core samples with sufficient quality has been a changes for scientists. Currently there are two methods of accessing to deep biosphere samples which are participating in drilling expeditions and requesting samples from core repositories. The Kochi Core Center has curated deep biosphere samples that were processed aseptically and stored at deep frozen (-80 degree C) condition from more than 10 drilling expeditions. Increased scientific attention to microbiological research of the subseafloor envrionment raises the complications and concerns related to adherence to the Nagoya Protocol of the Convention on Biological Diversity (CBD). The Nagoya Protocol is an international agreement that aims to guide countries in developing standart protocols and protections for accessing biological materials, and sharing benefits derived from their utilization. Since its commencement, the Nagoya Protocol has placed international biological research, especially fieldwork, under greater political scrutiny and increased its complexity due to the variation in implementation between nations. We present the central points of the Nagoya Protocol on access and benefit-sharing (ABS) and discuss their relationship to ocean drilling research. In addition, we address the challenges faced by ocean drilling in complying with this internation convention.

キーワード：海洋掘削、凍結コア試料、名古屋議定書、生物多様性
Keywords: ocean drilling program, frozen core sample, Nagoya Protocol, convention on biological diversity

©2019. Japan Geoscience Union. All Right Reserved.

In-situ rock strength calculated from drilling parameters. Comparison of results from various sites.

*Adam Wspanialy[1], Yasuhiro Yamada[1], Saneatsu Saito[1], KYAW MOE[1]

1. Japan Agency for Marine-Earth Science and Technology

Drilling parameters are excellent datasets to understand in-situ physical properties of the rock. Continuous core samples along with parameters such as Torque, RPM, WOB and ROP have been collected during drilling operations. The borehole data acquisition was complemented with full LWD/MWD and wireline logging. After core delivery to surface core scratch tests have been carried out to measure Unconfined Compressive Strength (UCS). Our comprehensive approach enabled us to integrate all data and conduct detailed analysis of the in-situ subsurface physical and mechanical properties of a rock cut by a drill bit.

Here we present some results from offshore and onshore drilling experiments carried out in Japan, Oman and Australia. Methods such as Specific Energy (SE) and Equivalent Strength (EST) have been used to estimate in-situ rock properties, namely UCS and analyse drilling process.

Our results demonstrate that the calculated in-situ rock strength based on SE/EST methods correlates well with sonic derived UCS and core scratch derived UCS. Utilised methods also successfully detect fractures in the formation, show developing drilling dysfunctions such as vibration, and bit balling.

Keywords: rock strength, drilling parameters, Specific Energy

©2019. Japan Geoscience Union. All Right Reserved.

Interaction between submarine landslides and subseafloor sedimentary microbiome: Chikyu SCORE Expedition 910 off Cape Erimo

*星野 辰彦[1]、浦本 豪一郎[2]、藤内 智士[2]、諸野 祐樹[1]、井尻 暁[1]、鈴木 志野[1]、久保 雄介[1]、稲垣 史生[1]、Chikyu SCORE Exp. 910 研究者一同
*Tatsuhiko Hoshino[1], Go-Ichiro Uramoto[2], Satoshi Tonai[2], Yuki Morono[1], Akira Ijiri[1], Shino Suzuki[1], Yusuke Kubo[1], Fumio Inagaki[1], Chikyu SCORE Exp. 910 Scientists .

1. 独立行政法人海洋研究開発機構、2. 高知大学
1. Japan Agency for Marine-Earth Science and Technology, 2. Kochi University

During the past decades, scientific ocean drilling has explored the subseafloor sedimentary biosphere down to over 2 kilometers below seafloor (Inagaki et al., 2015). The total biomass and diversity of microbial community in the subseafloor biosphere are comparable to those in the hydrosphere (Kallmeyer et al., 2012). Taxonomic composition of subseafloor microbial communities are distinct from those of other habitats on Earth’ s surface, such as ocean and soil, inferring that adaptive evolution of microbial community to the energy-limited deep sedimentary habitats have occurred. In a previous study of bioturbated layers in surface marine sediments, it has been reported that seawater-migration by macrofauna activity during the initial depositional stage notably affected microbial community structures (Chen et al. 2017). Similarly, it can be hypothesized that submarine landslides have introduced easily degradable fresh organic matter and dissolved electron acceptors (e.g., oxygen, sulfate) to the sedimentary habitats, and consequently caused a shift of microbial communities and its function.

In 2017, we conducted the Chikyu’ s first SCORE Expedition 910 at the Hidaka Trough off Cap Erimo and obtained sediment cores down to 100 meters below the seafloor. In the core column, four intervals of deformed sediments were identified, indicating the occurrences of multiple submarine landslides in this area. In those deformed sediment intervals, we observed no clear anomaly in the profile of cell abundance, which decrease with sediment depth as generally seen in the other subserfloor sediments. In addition, pore water chemistry data do not show clear anomaly either, indicating recovery of sediment geochemistry from the turbation caused by landslides. While both profiles of microbial cell abundance and pore water geochemistry did not show anomaly in the deformed sediment intervals, the DNA-based analyses, showed some unusual appearances of microbial taxa relative to the depth, suggesting the potential migration of microbes from the upper horizons by submarine landslides.

Reference

Inagaki F, et al (2015). Science 349: 420-424; Kallmeyer J, et al (2012). Proc Natl Acad Sci U S A 109: 16213-16216; Chen X, et al (2017). Sci Rep 7: 2400.

キーワード：Chikyu SCORE、Deep biosphere、Mass transport deposit
Keywords: Chikyu SCORE, Deep biosphere, Mass transport deposit

©2019. Japan Geoscience Union. All Right Reserved.

襟裳岬沖SCORE掘削コアのXRFコアスキャナー連続化学分析
High-resolution continuous records of the chemical composition of the marine sediment off Cape Erimo, Hokkaido, Japan

*村山 雅史[1]、矢生 晋介[3]、藤内 智士[2]、浦本 豪一郎[3]、山田 泰広[4]、稲垣 史生[4]、久保 雄介[5]
*Masafumi MURAYAMA[1], Shinsuke Yagyu[3], Satoshi Tonai[2], Go-Ichiro Uramoto[3], Yasuhiro Yamada[4], Fumio Inagaki[4], Yusuke Kubo[5]

1. 高知大学　農林海洋科学部海洋資源科学科、2. 高知大学　理工学部、3. 高知大学　海洋コア総合研究センター、4. 海洋研究開発機構　海洋掘削科学研究開発センター, 、5. 海洋研究開発機構　地球深部探査センター
1. Faculty of Agriculture and Marine Science, Kochi University, 2. Faculty of Science and Technology, Kochi University, 3. Center for Advanced Marine Core Research, Kochi University, 4. Research and Development Center for Ocean Drilling Science, JAMSTEC, 5. Center for Deep Earth Exploration, JAMSTEC

About 100 m sediment cores were taken from off Cape Erimo, Hokkaido, Japan on the Shallow Core Program (SCORE) by D/V Chikyu in 2017. The sedimentary sequence is intercalated with mass transport deposits caused by earthquake-triggered submarine landslides and/or climate changes. Here we report a result of high-resolution continuous geochemical composition of these cores using XRF core scanning technique.

キーワード：襟裳岬沖掘削コア、XRFコアスキャナー、SCOREプログラム、地球深部探査船「ちきゅう」
Keywords: sediment core off Cape Erimo, XRF core scanner (ITARX), Shallow Core Program (SCORE), D/V Chikyu

©2019. Japan Geoscience Union. All Right Reserved.

熊本地震震源断層掘削コアを用いた熱物性測定
Thermal property measurements of core samples retrieved from Futagawa fault drilling

*佐野 暉[1]、林 為人[1]、渋谷 奨[1,2]、神谷 奈々[1]、杉本 達洋[1]、石塚 師也[1]、林 愛明[3]
*Terasu Sano[1], Weiren Lin[1], Susumu Shibutani[1,2], Nana Kamiya[1], Tatsuhiro Sugimoto[1], Kazuya Ishitsuka[1], Aiming Lin[3]

1. 京都大学大学院工学研究科、2. 地圏総合コンサルタント、3. 京都大学大学院理学研究科
1. Graduate School of Engineering, Kyoto University, 2. Chi-ken Sogo Consultants Co., Ltd.,, 3. Graduate School of Science, Kyoto University

地球科学の分野では、地下の温度構造を理解することは重要である。地下の温度構造を決定するのは地殻熱流量と地層の熱伝導率であるため、地下深部から採取される岩石試料を用いて、熱伝導率ならびに熱拡散率、比熱を測定する必要がある。2017年から2018年にかけて熊本地震本震の震源断層である布田川断層を貫くように掘削された最大深度約700 mの掘削孔内の温度を測定したところ、明らかな温度異常が見られた（林ほか, 2019 JpGU）。この温度異常の原因を解明することは、阿蘇火山帯に位置する当該地域の地下温度構造を理解するだけでなく、地震メカニズムの更なる解明にもつながると期待される。そこで、当該掘削孔の岩石コア試料を用いて、深度約300～700 mに分布する地層を構成する主要な岩種の熱物性を測定し、この温度構造の異常を熱物性の観点から考察した。

熱物性測定用の試料として、熊本県益城町にある布田川断層掘削孔の前述深度区間において、主要な岩種から計20個のコア試料を採取した。このコアのサンプリングは、掘削された岩種のうちなるべく多くの種類を選びつつ、サンプリングした深度が大きく開きすぎないように留意して行った。なお、サンプリングした深度区間の主な岩種は、300 m～353 mが基底堆積物、353 m～514 mが安山岩、514 m～562 mが砂・礫岩、562 m～700 mが凝灰岩である。熱物性測定に用いた全岩石試料の基本物性として、密度と有効空隙率を測定した。その結果、含水飽和状態の湿潤密度は、基底堆積物層が1.57 g/㎤～2.02 g/㎤、安山岩層が2.31 g/㎤～2.95 g/cm^3、砂・礫岩層が2.29 g/㎤～2.41 g/cm^3、、凝灰岩層が1.99 g/㎤～2.29 g/cm^3となった。また、有効空隙率を測定したところ、基底堆積物層が40.0 %～47.8 %、安山岩層が3.1　%～25.5 %、砂・礫岩層が21.6%～29.4 %、凝灰岩層が19.4 %～35.8 %となり、非常に大きく変動することが判明した。

熱物性の測定には、非定常面熱源法（ホットディスク法）を用いた。ホットディスク法において、２つの試料でセンサーを挟んで測定する手法は、１つの試料を用いる手法より精度がよいと考えられるため、コア試料を3 cmの厚さに切り分け、1つのコアから４つのサブサンプルを取得、隣り合う２つのサブサンプルで１回の測定を行った。１つのコアにつき３回の測定を行い、平均値をそのコアの熱物性値とした。また、熱物性の測定は含水飽和と完全乾燥状態でそれぞれ行った。熱伝導率の測定結果は、基底堆積物層が0.88 W/(mK)～1.10 W/(mK)、安山岩層が1.00 W/(mK)～1.81 W/(mK)、砂・礫岩層が1.26 W/(mK)～1.31 W/(mK)、凝灰岩層が0.96 W/(mK)～1.27 W/(mK)となった。この値を用いて、温度構造に関する考察を行った。また、熱拡散率、比熱の測定結果は、基底堆積物層が0.26 ㎟/s～1.28 ㎟/s, 0.85 J/(g・K)～3.46 J/(g・K)、安山岩層が0.48 ㎟/s～0.91 ㎟/s, 1.36 J/(g・K)～2.60 J/(g・K)、砂・礫岩層が0.49 ㎟/s～0.66 ㎟/s, 1.95 J/(g・K)～2.70 J/(g・K)、凝灰岩層が0.40 ㎟/s～0.99 ㎟/s, 1.40 J/(g・K)～2.93 J/(g・K)となった。

林ほか（2019 JpGU）が行った掘削孔内の温度測定結果によれば、深部の約430～650 mの区間では、深くなるにつれ地層の温度がほぼ直線的に高くなる温度構造が認められ、その地温勾配は55 ℃/km程度であった。採取したコアの熱伝導率を、そのコアと同じ地質の層厚によって重みづけして平均熱伝導率を計算し

©2019. Japan Geoscience Union. All Right Reserved.

たうえ、フーリエの法則（j=λgradT、jは熱流量、λは熱伝導率、gradTは地温勾配）を用いて、当該深度範囲における地殻熱流量を求めた。さらに、当該掘削孔の深度範囲では、この熱流量以外の熱源がないと仮定し、かつ、熱伝導の定常状態として、同じフーリエの法則を用いて、実測した最深の温度からスタートし、各地層の熱伝導率を用いて、温度の深度プロファイルを試算した。

実測の温度プロファイルは深度約310～430 mの区間においては、ほぼ一定であり、その地温勾配が約1 ℃/kmという異常な温度分布の結果が得られた（林ほか, 2019 JpGU）。450 m以深では、試算の温度構造は実測の温度構造とよく一致しており、その深度区間では用いた仮定が正しいことが示唆された。一方、深度430 mと310 m付近では、熱物性値からの試算では、実測値の急激な温度勾配の変化を再現できなかった。すなわち、この温度異常は熱物性値の変化によるものではないと確認された。現段階では、この温度異常の原因として、地下水流動に伴う熱の移動の可能性があると推測される。今後は、さらに多くのコアの熱物性の測定を進め、より正確な熱物性の深度プロファイルを構築するとともに、この温度異常の原因究明に貢献したい。

キーワード：掘削孔、熱物性、温度
Keywords: Drilling, thermal properties, Temperature

©2019. Japan Geoscience Union. All Right Reserved.

東オーストラリア沖ロードハウライズ地域で採取された浅部コアの物性・強度試験結果：将来のロードハウライズライザー掘削に向けて
Results of geotechnical tests on shallow sediment cores recovered from Lord Howe Rise, off eastern Australia: Implications for future Lord Howe Rise riser drilling

*杉原 孝充[1]、青池 寛[1]、斎藤 実篤[2]、村山 達也[1]、武田 研太郎[1]、小野寺 拓也[3]、澄川 あゆみ[3]、木戸 ゆかり[1]、真田 佳典[1]
*Takamitsu Sugihara[1], Kan Aoike[1], Saneatsu Saito[2], Tatsuya Murayama[1], Kentaro Takeda[1], Takuya Onodera[3], Ayumi Sumikawa[3], Yukari Kido[1], Yoshinori Sanada[1]

1. 海洋研究開発機構　地球深部探査センター、2. 海洋研究開発機構　海洋掘削科学研究開発センター、3. 日本海洋事業
1. Center for deep earth exploration, Japan Agency for Marine-Science and Technology, 2. Research and development center for ocean drilling science, Japan Agency for Marine-Science and Technology, 3. Nippon Marine Enterprises, Ltd.

Lord Howe Rise (LHR) Drilling Project (871-CPP2) is an accepted IODP drilling proposal to reconstruct Cretaceous tectonic history of northern Zealandia, designated as a Chikyu riser drilling project. In order to plan a riser drilling operation, it is important to evaluate mechanical strength and physical properties of shallow sediment (0 to 100 or 200 meters below sea floor, mbsf) for setting Blow-out Prevention (BOP) system and riser with heavy weight on the seafloor. Geotechnical core test (e.g., triaxial compressive test and consolidation test) is an essential work to directly measure rock strength and physical properties of geological materials. Therefore, the geotechnical core tests are usually conducted for the surface sediment to evaluate their mechanical and physical properties. In the LHR region, calcareous sediment is broadly and predominantly distributed, and clayey sediment is not observed in shallow sediments. In general, deep seafloor is composed of clayey sediment, and their mechanical and physical properties are well understood. However, mechanical and physical properties of calcareous sediment in both ambient and confined pressure conditions are not well known.

In this study, results of geotechnical test for shallow cores taken in the LHR region are presented, and characteristics of mechanical and physical properties (especially shear strength and permeability) are discussed.

Shallow cores for geotechnical test were taken by R/V Kairei with a gravity piston corer in KR17-15C and by D/V JOIDES Resolution with a rotary core barrel (RCB) in Expedition 371. The gravity piston coring by R/V Kairei was conducted at the proposed riser drilling sites DLHR-5A and -3A, and two cores with approximately 7 m length were taken at each site. The RCB coring by D/V JOIDES Resolution was conducted at Site U1506 in Expedition 371. A whole-round sample with 40 cm length was taken from U1506A-13R for our investigation, and depth of the whole-round sample is 116.5 mbsf. In order to measure physical and mechanical properties for the core samples, geotechnical tests of Penetrometer test, Bulk density, Grain density, Liquid limit, Plastic limit, Grain size distribution, Constant rate of strain consolidation test (CRSC test), and Triaxial compressive strength test with pore pressure measurement (Consolidated-Undrained conditions) were carried out.

Most of the tests except penetrometer test were carried out by OYO Co. Procedures of those

©2019. Japan Geoscience Union. All Right Reserved.

measurements and tests were based on the regulations established by Japanese Geotechnical Society (JGS) and Japanese Industrial Standards (JIS). Those are almost the same as their regulations in the ASTM.

All of core samples are composed of calcareous ooze, and grain size distribution of the core samples shows clay size fraction (less than 5 micro meters) is dominant (more than 80 %).

Based on the bulk density data, overburden stresses were calculated and consolidation pressures corresponding to depth of 10 to 240 mbsf for the triaxial test were estimated assuming k0 compaction (k0 factor = 0.5). The result of the triaxial test show shear strength profile gradually increases with depth and is almost identical to those of clayey sediment from Kumano Basin and Nankai Trough. However, the result of the penetrometer test indicates that shear strength of calcareous ooze under ambient condition is quite lower than those of clayey sediment. This observation suggests mechanical strength of calcareous ooze is easily released with depressurizing of sediment.

Based on the result of the CRSC test, it is indicated that calcareous ooze shows no obvious preconsolidation stress, and this result is in good agreement with the result of the triaxial test mentioned above. Permeability of calcareous ooze calculated from the CRSC test results is similar to sandy sediment and the results indicate calcareous ooze is more permeable as compared with clayey sediment.

Those results will be dedicated to analysis for the riser operation in the LHR area.

キーワード：ロードハウライズ、ライザー掘削、岩石強度試験、剪断強度、透水率
Keywords: Lord Howe Rise, Riser drilling, Rock strength test, Shear strength, Permeability

©2019. Japan Geoscience Union. All Right Reserved.

ICDP DSeis 4: Drilling, core logging, and in-hole geophysical logging of ICDP DSeis drilling into the M5.5 aftershock zones in a South African gold mines.

*吉田 峻輔[1]、田所 遼悟[1]、杉村 幸祐[1]、兼松 慎[1]、東 充也[1]、Liebenberg Benni[2]、 van Heerden Esterhuizen[2]、Stephen Tau[3]、Siyanda Mngadi[3]、Ray Durrheim[3]、Martin Ziegler[4]、椋平 祐輔[5]、Ronald Conze[6]、矢部 康男[7]、金木 俊也[8]、Yokoyama Yuki[9]、Nomqhele Nkosi[10]、Dave Roberts[10]、Sifiso Buccio[11]、小笠原 宏[1]
*Shunsuke YOSHIDA[1], Tadokoro Ryogo[1], Kosuke Sugimura[1], Kanematsu Makoto[1], Mitsuya Higashi[1], Benni Liebenberg[2], Esterhuizen van Heerden[2], Stephen Tau[3], Siyanda Mngadi[3], Ray Durrheim[3], Martin Ziegler[4], Yusuke Mukuhira[5], Ronald Conze[6], Yasuo Yabe[7], Shunya Kaneki[8], Yuki Yokoyama[9], Nomqhele Nkosi[10], Dave Roberts[10], Sifiso Buccio[11], Hiroshi Ogasawara[1]

1. Graduate school of science and engineering, Ritsumeikan、2. Moab Khotsong mine, Vijoenskroon、3. Univ. Witwatersrand, School of Geoscience、4. ETH, Zurich Dep. Earth Sciences、5. Inst. Fluid Science, Tohoku Univ.、6. GFZ, Potzdam、7. Graduate School of Science, Tohoku Univ.、8. Disaster Prevention Research Inst., Kyoto Univ.、9. Graduate School of Science,Osaka Univ.、10. Mandela Mining Precinct, CSIR、11. Council for Geoscience
1. Graduate school of science and engineering, Ritsumeikan , 2. Moab Khotsong mine, Vijoenskroon, 3. Univ. Witwatersrand, School of Geoscience, 4. ETH, Zurich Dep. Earth Sciences, 5. Inst. Fluid Science, Tohoku Univ., 6. GFZ, Potzdam, 7. Graduate School of Science, Tohoku Univ., 8. Disaster Prevention Research Inst., Kyoto Univ., 9. Graduate School of Science,Osaka Univ., 10. Mandela Mining Precinct, CSIR, 11. Council for Geoscience

ICDP drilling into the aftershock zone of the 2014 M5.5 earthquake near Orkney, South Africa commenced on 2017 and was completed in 2018. This M5.5 earthquake started from a depth about 5 km and ruptured West Rand Group below mining horizon on unknown geological structure in a deep gold mine. The mechanism of left-lateral slip of this M5.5 earthquake contradicted normal-faulting mechanisms of typical mining-induced earthquakes on mining horizons. The upper fringe of the aftershock zone was several hundreds of meters from the deepest level of the mine. Two NQ holes were collared at a depth of 2.9 km (95 level) below surface at a deep gold mine. Hole A (817m) deviated too much to intersect the M5.5 fault but Hole B (700m) intersected the M5.5 fault. A 3-m double-tube couldn't recover the fault material much, while a 1.5m triple-tube could recover the fault material more in Hole C branched from 544 m in Hole B. Geophysical logging, core logging, and water/gas monitoring followed drilling. All the core was transported to Mandela Mining Precinct, CSIR, Johannesburg and systematically described and scanned by the ICDP DMT scanner. Some of the core were selected for core stress measurements.

In JpGU 2019 meeting, nine papers (ICDP DSeis 1-9) report on the outcomes. This poster (ICDP DSeis 4) compiles drilling, core logging, and in-hole geophysical logging of ICDP DSeis drilling into the M5.5 aftershock zones in a South African gold mines. A core orientation tool was used during drilling but not 100% reliable because there was a case that a bottom line in a core run was different by more than 90 degrees from the bottom line in the next core run. We elaborated to compare OTV image with core to carefully check the core orientation. The modified core orientation allowed us to modify the maximum stress direction that Ishida et al. (2018) measured. We could confirm good consistency with borehole breakout analysis (Richenbacher 2018; ETH master thesis). We will report on other associated outcomes. Refer other papers (ICDP DSeis 1-3, 5-9) for other related outcomes.

©2019. Japan Geoscience Union. All Right Reserved.

Acknowledgement: The DSeis team includes co-authors of the papers ICDP DSeis 2-9 and members shown at https://www.icdp-online.org/projects/world/africa/orkney-s-africa/details/. We thank Harmony Gold, Anglogold Ashanthi, Lesedi, Digital Surveying, OHMS, Seismogen, 3D Geoscience. ICDP, JSPS, SA NRF, MEXT Japan, US NSF, German DRF, and Ritsumeikan Univ. financially support the project.

©2019. Japan Geoscience Union. All Right Reserved.

ICDP DSeis 5: Diametrical Core Deformation Analysis of the M5.5 aftershock zone core - stress concentration at reflective intrusives and transition in stress regimes.

*杉村 幸祐[1]、吉田 峻輔[1]、田所 遼悟[1]、小笠原 宏[2]、石田 亮壮、矢部 康男[3]、伊藤 高敏[4]、明雄 船戸[5]、Siyanda Mngadi[6]、Ray Durrheim[6]
*Kosuke Sugimura[1], Shunsuke YOSHIDA[1], Ryogo Tadokoro[1], Hiroshi Ogasawara[2], Akimasa Ishida, Yasuo Yabe[3], Takatoshi Ito[4], Akio Funato[5], Siyanda Mngadi[6], Ray Durrheim[6]

1. 立命館大学大学院　理工学研究科、2. 立命館大学　理工学部、3. 東北大学　理学部、4. 東北大学　流体科学研究所、5. 深田地質研究所、6. Univ. Witwatersrand, School of Geoscience
1. Graduate school of science and engineering, Ritsumeikan, 2. College of Science and Engineering, Ritsumeikan Univ., 3. Graduate School of Science, Tohoku Univ., 4. Inst. Fluid Science, Tohoku Univ., 5. Fukada Geological Institute, 6. Univ. Witwatersrand, School of Geoscience

ICDP drilling into the aftershock zone of the 2014 M5.5 earthquake near Orkney, South Africa commenced on 2017 and was completed in 2018. Drilling was designed to minimize damage on core and borehole, being able to maximize core recovery. Hole A (817m) was drilled in 2017. It unfortunately didn't intersect the M5.5 fault, running eventually sub-parallel and roughly 100m from the aftershock zone. As the hole was stable we could recover almost 100% of core from the area traversing the periphery of the M5.5 aftershock zone for a distance of several hundreds of meters. Ishida et al. (2018) carried out Diametrical Core Diameter Analysis (Ito and Funato, 2017). This analysis measures the change in core diameter with roll angle around the core axis, which was caused by a relief of anisotropic stress during drilling. We used this analysis because (1) the expected stress was too high for hydrofracturing method, (2) uncertainty in stress magnitude is unavoidable in damage interpretations, (3) DSeis hole were too long for overcoring technique, and (4) DCDA is non-destructive and very easy to make if core is recovered. Ishida et al. (2018) measured 186 pieces of core from Hole A (817m collared at 2.9km depth) that were recovered near the M5.5 aftershock zone. They successfully illustrated spatial variation in differential stress in a plane perpendicular to Hole A axis. They found stress concentration at intrusives with one located at the depth of the upper fringe of the M5.5 aftershock zone. We carried out additional measurement for the remaining part of Hole A and Hole B. With additional data measured at adjacent locations, we could confirm that the stress concentration Ishida et al (2018) found at intrusives was not an outlier. We will report how Hole B that intersected the M5.5 fault differ from Hole A stress.

This is one of nine ICDP DSeis papers (ICDP DSeis 1-9) presented in JpGU 2019. Refer other papers for other topic on drilling, logging, other stress measurement, fault materials, comparison with calculated stress, legacy 3D seismic reflection data, and relocated aftershocks.

©2019. Japan Geoscience Union. All Right Reserved.

ICDP DSeis 6: Deformation Rate Analysis of the M5.5 aftershock zone core - stress concentration at reflective intrusives

*兼松 慎[1]、東 充也[1]、矢部 康男[2]、阿部 周平[2]、Watson Bryan[3]、Durrheim Ray[3]、小笠原 宏[1]
*Kanematsu Makoto[1], Mitsuya Higashi[1], Yasuo Yabe[2], Shuhei Abe[2], Bryan Watson[3], Ray Durrheim[3], Hiroshi Ogasawara[1]

1. 立命館大学 理工学部　物理科学科、2. 東北大学理学研究科、3. Witwatersrand大
1. Ritsumeikan Univ., 2. Tohoku Univ., 3. Univ. Witwatersrand

ICDP drilling into the aftershock zone of the 2014 M5.5 earthquake near Orkney, South Africa commenced on 2017 and was completed in 2018. Ishida et al. (2018) and Sugimura et al. (2019; ICDP DSeis 5) report on spatial variation of differential stress in a plane perpendicular to the borehole axis. It is ideal to have different stress component especially at critical location where significant characteristics were found. Deformation Rate Analysis (Yamamoto, 2009) can measure stress in any direction although the method takes time and the specimen are not reusable for other test. So, we planned to selected samples where characteristic spatial variation was found by DCDA method (Ishida et al. 2018 and Sugimura et al. 2019). It was confirmed also in normal stress component along the borehole axis that stress was concentrated at the intrusive at about 400m.

This is one of nine ICDP DSeis papers (ICDP DSeis 1-9) presented in JpGU 2019. Refer other papers for other topics on drilling, logging, other stress measurement, fault materials, comparison with calculated stress, legacy 3D seismic reflection data, and relocated aftershocks.

Acknowledgement: The DSeis team includes co-authors of the papers ICDP DSeis 2-9 and members shown at https://www.icdp-online.org/projects/world/africa/orkney-s-africa/details/. We thank Harmony Gold, Anglogold Ashanthi, Lesedi, Digital Surveying, OHMS, Seismogen, 3D Geoscience. ICDP, JSPS, SA NRF, MEXT Japan, US NSF, German DRF, and Ritsumeikan Univ. financially support the project.

キーワード：地震発生場、応力測定、DRA
Keywords: Seismogenic zone, Stress Measurement, DRA

©2019. Japan Geoscience Union. All Right Reserved.

ICDP DSeis 7: compilation of stress information and comparison with calculated stresses in the M5.5 aftershock zones

*東 充也[1]、矢部 康男[2]、杉村 幸佑[1]、石田 亮壮、兼松 慎[1]、吉田 峻輔[1]、田所 遼悟[1]、伊藤 高敏[4]、船戸 明雄[5]、小笠原 宏[3]
*Mitsuya Higashi[1], Yasuo Yabe[2], Kosuke Sugimura[1], Akimasa Ishida, Makoto Kanematsu[1], Shunsuke YOSHIDA[1], Ryogo Tadokoro[1], Takatoshi Ito[4], Akio Funato[5], Hiroshi Ogasawara[3]

1. 立命館大学大学院理工学研究科、2. 東北大学大学院理学研究科・理学部 附属地震・噴火予知研究観測センター、3. 立命館大学理工学部、4. 東北大学流体科学研究所、5. 深田地質研究所
1. Graduate School of Science and Engineering, Ritsumeikan Univ., 2. Research Center for Prediction of Earthquakes and Volcanic Eruptions, Graduate School of Science, Tohoku University, 3. College of Science and Engineering, Ritsumeikan Univ., 4. Inst. Fluid Science, Tohoku Univ., 5. Fukada Geological Institute

ICDP drilling into the aftershock zone of the 2014 M5.5 earthquake near Orkney, South Africa commenced on 2017 and was completed in 2018. Spatial variation in stress was measured by Ishida et al. (2018) and Sugimura et al. (2019; ICDP DSeis 5) by DCDA method (Funato and Ito, 2017) and Kanematsu et al. (2019; ICDP DSeis 6). This poster reports on compilation of stress information including the other information sources and compares with calculated stress.

We first compared with a 3D stress state that Ogasawara et al. (2012) measured in 2011 at 98L (3.0 km depth from surface). We assume zero stress on surface, the measured 3D stress (normal faulting stress regime) at 3.0 km, and stress linearly increasing with depth. The calculated stress was consistent with DCDA results measured in the initial 100m section in Hole A, while inconsistent in deeper section. The calculated direction of maximum stress in a plane perpendicular to the borehole axis was also inconsistent with the measured stress information (Yoshida et al. 2019 JpGU; ICDP DSeis 5). Except for the stress concentration measured at intrusives, the measured DCDA results were systematically lower than the calculated stress. In a stress regime that caused the left-lateral horizontal slip on the M5.5 fault, horizontal stress should be larger, which will increase horizontal stress component in a plane perpendicular to the Hole A axis. This increase should decrease difference in stress in the plane perpendicular to the Hole A axis. By JpGU 2019, we will make additional effort to interpret more from the comparison between the measured and calculated stress.

This is one of nine papers (ICDP DSeis 1-9). Refer other papers for other topic on drilling, logging, other stress measurement, fault materials, legacy 3D seismic reflection data, and relocated aftershocks.

Acknowledgement: The DSeis team includes co-authors of the papers ICDP DSeis 2-9 and members shown at https://www.icdp-online.org/projects/world/africa/orkney-s-africa/details/. We thank Harmony Gold, Anglogold Ashanthi, Lesedi, Digital Surveying, OHMS, Seismogen, 3D Geoscience. ICDP, JSPS, SA NRF, MEXT Japan, US NSF, German DRF, and Ritsumeikan Univ. financially support the project.

©2019. Japan Geoscience Union. All Right Reserved.

©2019. Japan Geoscience Union. All Right Reserved.

ICDP DSeis 8: the M5.5 fault structure and reflective intrusives in legacy 3D seismic reflection data

*野田 拓[1]、Manzi Musa[2]、Ogasawara Hiroyuki[1]、Linzer Lindsay[2]、Enslin Stephanie[2]、Durrheim Ray[2]、小笠原 宏[1]
*Noda Taku[1], Musa Manzi[2], Hiroyuki Ogasawara[1], Lindsay Linzer[2], Stephanie Enslin[2], Ray Durrheim[2], Hiroshi Ogasawara[1]

1. 立命館大学、2. Witwatersrand大
1. Ritsumeikan Univ., 2. Univ. Witwatersrand

ICDP drilling into the aftershock zone of the 2014 M5.5 earthquake near Orkney, South Africa commenced on 2017 and was completed in 2018. Hiroyuki et al. (2017 AGU) reported on legacy seismic reflection to analyze geological structures in the southern most area of the M5.5 aftershock zones. They found vertical structures in four 2-D lines that were potentially responsible for the M5.5 earthquake and illustrated cross-cutting relations of the M5.5 structure and other known faults that dislocated gold reefs more than several hundreds of meters both horizontally and vertically. Another legacy seismic reflection data which was recorded in 1996 and covered much wider area of the M5.5 aftershock zone was found. We calibrated velocity structure by tying with borehole data including DSeis Holes A and B, we found some of intrusives (sills) that Hole A and B were strong reflectors in the legacy 3D seismic reflection data.

Aftershocks located by in-mine 46 geophones are dense at the southern upper fringe, with a sharp cut-off dipping about 20 degrees to the south; some clear stripes of aftershocks are also seen, in parallel to the upper fringe (Tadokoro et al., JpGU2019, ICDP DSeis 9). It is interesting to note that the reflector (sills) are also in parallel to the upper fringe of the aftershock zone and the aftershock stripes. It is also notable that stress concentration is reported at the intrusives by Sugimura et al. (JpGU2019; ICDP DSeis 5) and Kanematsu et al. (JpGU2019; ICDP DSeis 6). Some mechanism that controls the extent of the aftershocks should exist.

This paper is one of nine papers (ICDP DSeis 1-9). Refer other papers for other topics, e.g. on drilling, logging, stress measurements and evaluation, fault materials, and relocated aftershocks.

Acknowledgement: The DSeis team includes co-authors of the papers ICDP DSeis 2-9 and members shown at https://www.icdp-online.org/projects/world/africa/orkney-s-africa/details/. We thank Harmony Gold, Anglogold Ashanthi, Lesedi, Digital Surveying, OHMS, Seismogen, 3D Geoscience. ICDP, JSPS, SA NRF, MEXT Japan, US NSF, German DRF, and Ritsumeikan Univ. financially support the project.

キーワード：ICDP DSeis、M5.5地震発生場、地震反射法探査
Keywords: ICDP DSeis, The M5.5 seismogenic zone, Seismic reflection

©2019. Japan Geoscience Union. All Right Reserved.

ICDP DSeis 9: are streaks in the M5.5 aftershocks potentially located on highly stressed intrusive?

*Ryogo Tadokoro[1], Katsuya Ishibashi[2], Horiuchi Shigeki[3], Hiroshi Ogasawara[4]

1. Graduate School of Science and Engineering, Ritsumeikan Univ., 2. School of Science and Engineering, Ritsumeikan Univ., 3. Homeseismo ltd., 4. College of Science and Engineering, Ritsumeikan Univ.

ICDP drilling into the aftershock zone of the 2014 M5.5 earthquake near Orkney, South Africa commenced on 2017 and was completed in 2018. Aftershocks located by in-mine 46 geophones are dense at the southern upper fringe, with a sharp cut-off dipping about 20 degrees to the south. Some clear stripes of aftershocks are also seen, in parallel to the upper fringe. It is interesting to note that the reflector (sills) are also in parallel to the upper fringe of the aftershock zone and the aftershock stripes. It is also notable that stress concentration is reported at the intrusives by Sugimura et al. (JpGU2019; ICDP DSeis 5) and Kanematsu et al. (JpGU2019; ICDP DSeis 6). Some mechanism that controls the extent of the aftershocks should exist.

In order to discuss further, we relocated aftershocks with the Double-Difference method (Waldhouser and Ellsworth, 2004). At the moment, we could relocate only 60 events at the upper fringe of the aftershocks. We used in-mine seismic network data of Anglogold Ashanti. P- and S- arrival times that the algorithm of Horiuchi et al. (2011) was used. A sharper alignment of aftershocks is successfully illustrated. By JpGU 2019, we will make additional efforts to extend the area of relocation to discuss more.

Acknowledgement: The DSeis team includes co-authors of the papers ICDP DSeis 2-9 and members shown at https://www.icdp-online.org/projects/world/africa/orkney-s-africa/details/. We thank Harmony Gold, Anglogold Ashanthi, Lesedi, Digital Surveying, OHMS, Seismogen, 3D Geoscience. ICDP, JSPS, SA NRF, MEXT Japan, US NSF, German DRF, and Ritsumeikan Univ. financially support the project.

©2019. Japan Geoscience Union. All Right Reserved.

[E] ポスター発表 | セッション記号 M (領域外・複数領域)：M-TT 計測技術・研究手法

2019年5月27日(月) 13:45 ~ 15:15 | ポスター会場 幕張メッセ国際展示場 8ホール_10

[M-TT46] 統合地球観測システムとしてのGPS/GNSSの新展開

コンビーナ:小司 禎教(気象研究所気象衛星・観測システム研究部第２研究室)、市川 香(九州大学応用力学研究所)、太田 雄策(東北大学大学院理学研究科附属地震・噴火予知研究観測センター)、津川 卓也(情報通信研究機構)

GNSSは、大気圏、電離圏、固体地球の基盤となる統合観測システムとなっている。地上及び宇宙基地型GNSS観測は、2006年より数値気象予報の改善に貢献している。近年では反射波を用いて高度、地面粗度、土壌水分、積雪深、湿度や植生インデックスを導出する研究が発展している。船舶やブイなど海洋上のGNSS観測は、海面高度に加えて海洋上の水蒸気観測の能力を持つ。Multi-GNSSがもたらす観測データの増加は、統合地球観測システムとしてのGNSSの能力を拡大させる。
本セッションの目的は、GNSS研究の最新成果を共有し、あらたな学際研究を促進することにある。GNSSを用いた大気（対流圏、電離圏）、GNSS-R、またGNSS-音響観測による海底測位のようなの異なる観測の統合に関する投稿を歓迎する。

[MTT46-P01] 新たな海底地殻変動観測手法のためのGNSSブイからの連続音響測距

*田所 敬一[1]、衣笠 菜月[1]、加藤 照之[2]、寺田 幸博[3]、二村 彰[4]、松廣 健二郎[1] (1.名古屋大学地震火山研究センター、2.神奈川県温泉地学研究所、3.高知工業高等専門学校、4.弓削商船高等専門学校)

[MTT46-P02] Accuracy and precision assessment of the real-time kinematic GNSS time series for moored buoy using three-axis programable moving table

*太田 雄策[1]、今野 美冴[1]、木戸 元之[2] (1.東北大学大学院理学研究科附属地震・噴火予知研究観測センター、2.東北大学災害科学国際研究所)

[MTT46-P03] 静止衛星によるGNSS-R海面高度計測

*市川 香[1]、奥村 立樹[2]、根田 昌典[3]、馬場 康之[4] (1.九州大学応用力学研究所、2.九州大学総合理工学府大気海洋環境システム学専攻、3.京都大学大学院理学研究科、4.京都大学防災研究所)

[MTT46-P04] **Estimation of typhoon wind speed using CYGNSS observations: A case study of Typhoon Lan in 2017**

*加古 真一郎[1]、富田 裕之[2]、市川 香[3] (1.鹿児島大学大学院理工学研究科、2.名古屋大学 宇宙地球環境研究所、3.九州大学応用力学研究所)

[MTT46-P05] Ionospheric and seismic effects caused by the North Korea nuclear tests realized on 2006-2017

Nataliia Perevalova[2]、*Nikolai Shestakov[1]、Anna Dobrynina[3,4]、Dmitry Kostylev[7]、Meng Guojie[5]、Wei-Wei Wu[5,6] (1.Institute for Applied Mathematics FEB RAS, Vladivostok, Russia; Far Eastern Federal University, Vladivostok, Russia、2.Institute of Solar-Terrestrial Physics SB RAS, Irkutsk, Russia、3.Institute of the Earth's Crust SB RAS, Irkutsk, Russia 、4.Geological institute SB RAS, Ulan-Ude, Russia 、5.Institute of Earthquake Forecasting, China Earthquake Administration, Beijing, China、6.College of Surveying and Geo-informatics, Tongji University, Shanghai, China、7.Sakhalin Branch of Federal Research Center Geophysical Survey RAS, Yuzhno_Sakhalinsk, Russia)

[MTT46-P06] Relationships between Water Vapor Concentration Index derived from GNSS and Surface Wind Convergence during Localized Heavy Rainfall in Tokyo in Summer

*瀬戸 芳一[1]、小司 禎教[2]、常松 展充[3]、高橋 日出男[1] (1.首都大学東京大学院都市環境科学研究科地理環境学域、2.気象庁気象研究所、3.東京都環境科学研究所)

[MTT46-P07] 次世代高感度マイクロ波放射計の開発-序報-

*市川 隆一[1]、氏原 秀樹[1]、佐藤 晋介[1]、雨谷 純[1]、太田 雄策[2]、宮原 伐折羅[3]、宗包 浩志[3]、長崎 岳人[4]、田島 治[5]、荒木 健太郎[6]、田尻 拓也[6]、瀧口 博士[7]、松島 健[8]、松島 喜雄[9]、桃谷 辰也[10]、宇都宮 健志[10] (1.情報通信研

究機構、2.東北大学、3.国土地理院、4.高エネルギー加速器研究機構、5.京都大学、6.気象研究所、7.宇宙航空研究開発機構、8.九州大学、9.産業技術総合研究所、10.日本気象協会)

[MTT46-P08] Refractivity Distributions over the Kanto Plain Obtained by Dual-polarization Radar

*瀬古 弘[1]、佐藤 英一[1]、山内 洋[2] (1.気象研究所、2.気象庁)

[MTT46-P09] Spatial and temporal distribution of tropospheric water vapor observed by a Raman lidar and a GNSS receiver network over Shigaraki, Japan

*矢吹 正教[1]、津田 敏隆[1]、河野 邑弥[2]、鳥取 裕作[2]、塚本 誠[2]、竹内 栄治[2] (1.京都大学生存圏研究所、2.英弘精機株式会社)

[MTT46-P10] **Study of the Mechanisms of Severe Thunderstorm in Tokyo Metropolitan Area using High Frequent Assimilation of GNSS and Other Ground-based Observations**

*小司 禎教[1]、酒井 哲[2]、足立 アホロ[1]、吉田 智[2]、永井 智広[2] (1.気象研究所気象衛星・観測システム研究部第２研究室、2.気象研究所気象衛星・観測システム研究部第３研究室)

新たな海底地殻変動観測手法のためのGNSSブイからの連続音響測距
Continuous acoustic ranging from a GNSS buoy for the new method of seafloor crustal deformation measurements

*田所 敬一[1]、衣笠 菜月[1]、加藤 照之[2]、寺田 幸博[3]、二村 彰[4]、松廣 健二郎[1]
*Keiichi Tadokoro[1], Natsuki Kinugasa[1], Teruyuki Kato[2], Yukihiro Terada[3], Akira Futamura[4], Kenjiro Matsuhiro[1]

1. 名古屋大学地震火山研究センター、2. 神奈川県温泉地学研究所、3. 高知工業高等専門学校、4. 弓削商船高等専門学校
1. Research Center for Seismology, Volcanology and Earthquake and Volcano Research Center, Nagoya University, 2. Hot Springs Research Institute of Kanagawa Prefecture, 3. Kochi National College of Technology, 4. National Institute of Technology, Yuge College

Our research group has been testing a measurement system for the continuous seafloor crustal deformation at a moored buoysite operated by Kochi prefecture, located 32 km off Cape Ashizuri, Japan.An acoustic transducer was fixed at about 1.7 m beneath the sea surface with a pole mounted on the buoy body.Three ocean bottom acoustic transponders had been installed around the moored point of the buoy. The acoustic signals are sequentially transmitted to these three transponders every three minutes. The recorded data on the buoy are planned to transmitted to a ground base station through a commercial communication satellite operated by Thuraya Telecommunications Company.
We performed a test for the continuous acoustic ranging between the buoy and the ocean bottom transponders from March 28 to 31 and from June 2 to July 12 (1st period), and from November 16to December 17 (2nd period) in 2018. The acoustic ranging was continuously possible throughout the above periods when power was supplied whereas it was unexpectedly terminated because of power failure during the winter season. The acoustic signals were transmitted 27,856 times in total, and the buoy-mounted acoustic ranging unit received 23,342 signals from the ocean bottom transponders. However, the acoustic data sent to the ground base station was only 12 % because of some trouble of the satellite communication modem.
The reflected signals from the buoy body and/or the seafloor sometimes contaminated the received acoustic signals; also multiple reflections inside of an anti-reflection cover attached to the buoy-mounted transducer, whose purpose is to cut off the reflection from the sea surface, were remarkable during the 1st period. The multiple reflections caused the misidentification of the direct wave from the sea-bottom units. We, therefore, removed the anti-reflection cover during the 2nd period, which remarkably reduced the confused reflections.
We coded a program for detecting the arrival time of direct acoustic wave automatically on the basis of thresholds of cross-correlation coefficient and energy ratio (the ratio of the squared amplitudes preceding and following a test point) to reduce the capacity of data transferred via satellite communication using the acoustic waveform recorded during the 1st period. The program successfully picked the correct direct wave onset for more than 99 % of the waveforms recorded during the 2nd period.

©2019. Japan Geoscience Union. All Right Reserved.

Accuracy and precision assessment of the real-time kinematic GNSS time series for moored buoy using three-axis programable moving table

*太田 雄策[1]、今野 美冴[1]、木戸 元之[2]
*Yusaku Ohta[1], Misae Imano[1], Motoyuki Kido[2]

1. 東北大学大学院理学研究科附属地震・噴火予知研究観測センター、2. 東北大学災害科学国際研究所
1. Research Center for Prediction of Earthquakes and Volcanic Eruptions, Graduate School of Science, Tohoku University, 2. IRIDeS, Tohoku University

Rapid understanding of the magnitude of large earthquakes and their associated fault dimensions are extremely important. Especially, capture of the coseismic deformation in the offshore region will be key information to understand the fault dimensions for the large interplate earthquake. Based on this background, Tohoku University and JAMSTEC are jointly developing the on-demand crustal deformation monitoring system using moored buoy system. The buoy can measure the sea-floor horizontal crustal deformation by GNSS/Acoustic technique and vertical deformation using ocean bottom pressure sensor. One of the key technology in our developed system is the real-time kinematic GNSS which can measure three-dimensional position of the buoy in real-time. In contrast, it is difficult to understand quantitatively the precision and accuracy of estimated buoy position because no reference for the position. Thus, we assess the precision and accuracy of real-time kinematic GNSS time series using programable three-axis movable table.

We have developed the single-axis precise programable movable table (Ohta et al., 2016). We expanded this developed system to three-axis. For the real-time kinematic analysis, we adopted Trimble CenterPoint RTX (hereafter, RTX) with 10Hz sampling interval. The correction message for the analysis was received via a stationary satellite. We also estimated the GNSS antenna position using very short-baseline kinematic analysis as reference solution. The developed movable table can operate single axis horizontal displacement, rotational movement, and tilt deformation. To simulate the actual buoy movement, we gave the motion to the movable table based on the actual buoy movement. We conducted the experiment in 24 hours duration.

We calculated the residual time series between obtain time series by RTX and short-baseline kinematic solution. The difference between averaged absolute position was quite good in the horizontal components which was less than 10mm. In contrast, the vertical component shows the clear discrepancy between them. RTX time series shows systemically higher than the baseline analysis which reached approximately 230mm. In contrast, the precision of the calculated residual time series was good in both of the components. Calculated standard deviations were 10-11mm and 28mm in horizontal components and vertical component, respectively. We will show the more detailed results from our experiment and discuss the ability of the real-time kinematic analysis in our developed buoy.

©2019. Japan Geoscience Union. All Right Reserved.

静止衛星によるGNSS-R海面高度計測
GNSS-R altimetry using a Geostationary Satellite

*市川 香[1]、奥村 立樹[2]、根田 昌典[3]、馬場 康之[4]
*Kaoru Ichikawa[1], Tatsuki Okumura[2], Masanori Konda[3], Yasuyuki Baba[4]

1. 九州大学応用力学研究所、2. 九州大学総合理工学府大気海洋環境システム学専攻、3. 京都大学大学院理学研究科、4. 京都大学防災研究所
1. Res. Inst. Appl. Mech., Kyushu Univ., 2. Dept. ESST, Interdicipl. Grad. School Eng. Sc., Kyushu Univ., 3. Graduate School of Science, Kyoto Univ., 4. Disaster Prevention Res. Inst., Kyoto Univ.

The GNSS reflectometry (GNSS-R) uses GNSS signals reflected at the sea surface, which are usually eliminated as the multipath error. The reflected GNSS path received at an antenna is always longer than the direct path, so that the height of the antenna from the sea surface is geometrically determined from the excess path length. The excess path length can be either directly determined by measuring the temporal delay of the reflected signals, or indirectly estimated from interferometric cyclic modulations of the received power (often referred as signal-to-noise ratio; SNR) induced by phase differences between the direct and reflected GNSS signals. In the latter method, as the elevation angle of an earth orbiting GNSS satellite changes in time, the geometric reflection point on the sea surface temporally displaces, which results in interferometric changes of the path length during a period while the satellite is in sight. Meanwhile, for a geostationary satellite in BeiDou constellations that are always in sight, the path length changes not by the movement of the satellite but the elevation of the reflection surface, *i.e.* the sea level rise. In this study, we used the three-month time series (2016/09-11) of the 1Hz SNR of the geostationary BeiDou #02 satellite observed by a GNSS-R system deployed to the Shirahama Oceanographic Observatory Tower owned by Kyoto University (33deg, 42’ 32’’ N, 135deg, 19’ 58’’ E) at the height of ~20m. The geostationary GNSS-R altimetry observed significant flood tides when the wind speed is stably low; the 0.6m sea level rise was successfully determined by the SNR interferometry with 0.05m rms difference. However, significant interferometric SNR changes by tides were not recorded at high or low tides since at least 0.25m sea level change is required for the interferometry cycle. Consequently, the cyclic periods of the geostationary GNSS-R altimetry for tides become long (1-4 hours for 0.25m change in Shirahama), the interferometric variations were usually contaminated by SNR changes induced by the other factors such as winds. On the contrary, faster sea level changes by wave motions could be recognized by the geostationary GNSS-R altimetry, although the temporal sampling intervals of the present data were not adequate.

キーワード：GNSS-R、海面高度計、BeiDou静止GNSS衛星
Keywords: GNSS-R , altimetry, BeiDou geostationary GNSS satellite

©2019. Japan Geoscience Union. All Right Reserved.

Estimation of typhoon wind speed using CYGNSS observations: A case study of Typhoon Lan in 2017

*加古 真一郎[1]、富田 裕之[2]、市川 香[3]
*Kako Shinichiro[1], Hiroyuki Tomita[2], Kaoru Ichikawa[3]

1. 鹿児島大学大学院理工学研究科、2. 名古屋大学 宇宙地球環境研究所、3. 九州大学応用力学研究所
1. Graduate School of Science and Engineering, Kagoshima University, 2. Institute for Space-Earth Environment, Nagoya University, 3. Research institute for Applied Mechanics, Kyushu University

We conducted a case study of Typhoon Lan, which occurred in 2017, to investigate the impact of the Cyclone Global Navigation Satellite System (CYGNSS) on the estimation of extremely high wind speeds, such as those occurring during typhoons. We studied CYGNSS because it is expected to be capable of observing wind speeds in regions with extremely high wind speeds and heavy rains (i.e., typhoons) where it is difficult to perform measurements using the current microwave instrument. Firstly, we compared CYGNSS-derived wind speeds produced by NASA with those derived from AMSR2 produced by the Japan Aerospace Exploration Agency. CYGNSS was found to underestimate the wind speeds around Typhoon Lan compared with AMSR2. We then attempted to estimate the wind speeds using the leading edge slope (LES) and mean square slope (MSS) derived from the CYGNSS observations. Although the relationship between the MSS and wind speed differs depending on the wave age (Zhao and Tobe, 2003), it is difficult to estimate the wave age because this estimation is required the wind and wave speeds. We used the wave period as a substitute for the wave age since the wave period is expected to be similar to the wave age. We therefore first computed the fourth power of the wave period (T4) in line with Wang and Ichikawa (2016). Next, we classified the ocean into three regions based on T4 to investigate the relationship between the MSS and the wind speed observed by AMSR2 in each region. Finally, we approximated the curves relating the MSS to the wind speed using exponential functions in the three regions and estimated the wind speed using these curves. The comparison between the wind speeds produced by NASA and those estimated in this study demonstrated that our method can estimate high wind speeds more accurate than the CYGNSS wind speeds produced by NASA.

キーワード：CYGNSS、AMSR2、台風
Keywords: CYGNSS, AMSR2, tyhoon

©2019. Japan Geoscience Union. All Right Reserved.

Ionospheric and seismic effects caused by the North Korea nuclear tests realized on 2006-2017

Nataliia Perevalova[2], *Nikolai Shestakov[1], Anna Dobrynina[3,4], Dmitry Kostylev[7], Meng Guojie[5], Wei-Wei Wu[5,6]

1. Institute for Applied Mathematics FEB RAS, Vladivostok, Russia; Far Eastern Federal University, Vladivostok, Russia, 2. Institute of Solar-Terrestrial Physics SB RAS, Irkutsk, Russia, 3. Institute of the Earth's Crust SB RAS, Irkutsk, Russia , 4. Geological institute SB RAS, Ulan-Ude, Russia , 5. Institute of Earthquake Forecasting, China Earthquake Administration, Beijing, China, 6. College of Surveying and Geo-informatics, Tongji University, Shanghai, China, 7. Sakhalin Branch of Federal Research Center Geophysical Survey RAS, Yuzhno_Sakhalinsk, Russia

Using data from GPS/GLONASS receivers and seismic networks, we studied the ionospheric and lithospheric effects caused by six underground nuclear tests realized in North Korea on 2006-2017.
To investigate the ionospheric disturbances, we analyzed data from several continuous GNSS-networks (GPS and GLONASS) operating in Asia - Western Pacific region: IGS, GEONET, FEB RAS and FEFU complex geodynamic network, a set of stations belonging to China and South Korea GNSS-networks. Sites close to the Korean Peninsula were selected for the analysis. Series of total electron content (TEC) in the ionosphere were calculated on the base of dual-frequency phase measurements of GNSS receivers. To detect disturbances caused by the nuclear tests, TEC series were filtered in the range of periods from 1 to 10 minutes. Despite the small magnitudes of seismic events associated with the nuclear tests, we were able to identify ionospheric disturbances which were most likely generated by these explosions. Such disturbances were detected for 4 out of 6 nuclear tests. The main parameters of the disturbances were determined. From our analysis we concluded that characteristics of ionospheric disturbances caused by the underground nuclear tests differed significantly from the parameters of disturbances that are usually observed after earthquakes.
For seismic analysis, we used data from the broadband seismic station networks located at distances up to 23 degrees from the Korean Peninsula: II, IC, IU, TW, JP, G, KS, and KG given by IRIS, and regional seismic network BY. The frequency content of P and surface Rayleigh waves registered by 46 broadband stations was analyzed. For some events, the P-wave frequency content showed the prevalence of low frequencies in spectra (~0.45 Hz). The peak frequencies of the surface Rayleigh waves was in the 0.05-0.45 Hz range. Preliminary analysis of the peak frequencies spatial distribution showed that the continental massive area is characterized by the relatively high frequencies (0.14-0.50 Hz) while for the areas adjacent to marginal seas the low values of peak frequencies are observed (from 0.13 Hz and less).
Acknowledgments. We are deeply indebted to Scripps Orbit and Permanent Array Center (SOPAC) for the IGS-network data, to Geospatial Information Authority of Japan for GEONET network data, to Korea Astronomy & Space Science Institute for access to GNSS data on the Korean Peninsula, CCU CC FEB RAS for access to data from the FEB RAS and FEFU complex geodynamic network; Institute of Earthquake Forecasting, China Earthquake Administration for access to GNSS data in China. The facilities of the IRIS Data Management System, and specifically the IRIS Data Management Center, and Baikal Regional Seismological Center and Sakhalin Branch of Federal Research Center Geophysical Survey RAS were used to get waveform and metadata required in this study. This work was performed with budgetary funding of Basic Research program II.16 and was also partially supported by RFBR grants 17-45-388072_p_a, 17-45-388049_ p_a, 17-55-53110_GFEN_a, 19-05-00889_a.

Keywords: North Korea nuclear tests, ionospheric and lithospheric effects, GPS/GLONASS-observations

©2019. Japan Geoscience Union. All Right Reserved.

©2019. Japan Geoscience Union. All Right Reserved.

Relationships between Water Vapor Concentration Index derived from GNSS and Surface Wind Convergence during Localized Heavy Rainfall in Tokyo in Summer

*瀬戸 芳一[1]、小司 禎教[2]、常松 展充[3]、高橋 日出男[1]
*Yoshihito Seto[1], Yoshinori Shoji[2], Nobumitsu Tsunematsu[3], Hideo Takahashi[1]

1. 首都大学東京大学院都市環境科学研究科地理環境学域、2. 気象庁気象研究所、3. 東京都環境科学研究所
1. Department of Geography, Graduate School of Urban Environmental Sciences, Tokyo Metropolitan University, 2. Meteorological Research Institute, 3. Tokyo Metropolitan Research Institute for Environmental Protection

In recent years, short-term heavy-rainfall events that have caused severe damages such as flooding have frequently occurred in the Tokyo Metropolitan area in summer. In view of the development process of cumulonimbus clouds, the convergence of surface winds and the spatial concentration of water vapor are supposed to have taken place prior to the occurrence of heavy rainfall. This study aims to clarify the evolutionary process of short-term heavy rainfall as a contribution to short-range forecasting of heavy rainfall that occurs locally.

The relationships between the occurrence of heavy rainfall and the convergence of surface winds and water vapor concentration for heavy-rainfall cases were examined using data from July to September obtained from high-density meteorological observations in Tokyo, Japan. We used the water vapor concentration (WVC) index derived from the global navigation satellite system (GNSS) analysis as indices for the degree of divergence and convergence of water vapor in the lower troposphere (Shoji 2013).

Corresponding to heavy-rainfall areas, the convergence of surface winds tended to increase for several tens of minutes prior to the heavy rainfall. The peak time of wind convergence was observed 10–30 min before the heavy-rainfall occurrence, and the convergence continued to increase for approximately 30 min until the convergence peak time (Seto et al. 2018). Around the heavy-rainfall area, the increase in the WVC index coincided with the increase in convergence. On the other hand, it was considered that the temporal and spatial scales of the WVC index are larger than those of wind convergence. From these results, by monitoring the temporal variations and distributions of these parameters using a high-density observation network, it should be possible to predict the occurrence of heavy rainfall rapidly and accurately.

References

Seto, Y., Yokoyama, H., Nakatani, T., Ando, H., Tsunematsu, N., Shoji, Y., Kusunoki, K., Nakayama, M., Saitoh, Y. and Takahashi, H. 2018. Relationships among rainfall distribution, surface wind, and precipitable water vapor during heavy rainfall in central Tokyo in summer. J. Meteor. Soc. Japan, 96A, 35–49.
Shoji, Y. 2013. Retrieval of water vapor inhomogeneity using the Japanese nationwide GPS array and its potential for prediction of convective precipitation. J. Meteor. Soc. Japan, 91, 43–62.

キーワード：短時間強雨、地上風収束、水蒸気、高密度観測
Keywords: localized heavy rainfall, wind convergence, water vapor, high-density observation

©2019. Japan Geoscience Union. All Right Reserved.

次世代高感度マイクロ波放射計の開発-序報-
Development of novel ground-based microwave radiometer for earth science -preliminary report-

*市川 隆一[1]、氏原 秀樹[1]、佐藤 晋介[1]、雨谷 純[1]、太田 雄策[2]、宮原 伐折羅[3]、宗包 浩志[3]、長崎 岳人[4]、田島 治[5]、荒木 健太郎[6]、田尻 拓也[6]、瀧口 博士[7]、松島 健[8]、松島 喜雄[9]、桃谷 辰也[10]、宇都宮 健志[10]
*Ryuichi Ichikawa[1], Hideki Ujihara[1], Shinsuke Satoh[1], Jun Amagai[1], Yusaku Ohta[2], Basara Miyahara[3], Hiroshi Munekane[3], Taketo Nagasaki[4], Osamu Tajima[5], Kentaro Araki[6], Takuya Tajiri[6], Hiroshi Takiguchi[7], Takeshi Matsushima[8], Nobuo Matsushima[9], Tatsuya Momotani[10], Kenji Utsunomiya[10]

1. 情報通信研究機構、2. 東北大学、3. 国土地理院、4. 高エネルギー加速器研究機構、5. 京都大学、6. 気象研究所、7. 宇宙航空研究開発機構、8. 九州大学、9. 産業技術総合研究所、10. 日本気象協会
1. National Institute of Information and Communications Technology, 2. Tohoku University, 3. Geospatial Information Authority of Japan, 4. High Energy Accelerator Research Organization, 5. Kyoto University, 6. Meteorological Research Institute, JMA, 7. Japan Aerospace eXploration Agency, 8. Kyushu University, 9. National Institute of Advanced Industrial Science and Technology, 10. Japan Weather Association

中性大気中の水蒸気変動を高時空分解能で把握するために、次世代高感度マイクロ波放射計の開発に着手した。このマイクロ波放射計は、マイクロ波を用いたGNSSやVLBIといった宇宙測地技術の高精度化に加え、火山活動監視や積乱雲の発達過程観測への寄与を念頭に置いている。同放射計の基本的な設計概念は、高エネルギー加速器研究機構(KEK)が開発したKUMODeSのそれを踏襲する。KUMODeSは、20-30 GHz帯と50-60 GHz帯の2つの帯域を受信する広帯域受信機を搭載し、前者の低雑音アンプを10Kまで冷却することで、水蒸気及び液水の吸収帯での高感度化を実現している。一方、後者の受信系は、酸素の吸収帯を同時観測することで大気放射を把握し、双方の放射温度を解析することで水蒸気に寄与する放射スペクトルを正確に推定出来る。我々は、KUMODeS観測で得られた可降水量をGNSS、ラジオゾンデ、あるいは数値予報データから得られた可降水量と比較し、KUMODeSが水蒸気時空変動を高精度に把握できる可能性を示した。これを踏まえ、新たに開発する放射計では、20-60 GHzを一気に受信可能な広帯域フィードを搭載し、得られた信号を導波管型偏波分離器(OMT)を用いて分離した水平・直交のそれぞれの偏波成分を20-30 GHz及び50-60 GHzの各々の低雑音増幅器(LNA)で受ける受信系を考えている。さらに、受信系全体をスターリング冷凍機を用いた冷凍容器に格納し、これにより信号対雑音比の向上を図ることで感度向上を目指す。この受信系の開発完了は今年の年末を目標としており、既存のパラボラアンテナ受信部に搭載して評価観測を行う予定である。

キーワード：GNSS、マイクロ波放射計、水蒸気
Keywords: GNSS, microwave radiometer, water vapor

©2019. Japan Geoscience Union. All Right Reserved.

Refractivity Distributions over the Kanto Plain Obtained by Dual-polarization Radar

*瀬古 弘[1]、佐藤 英一[1]、山内 洋[2]
*Hiromu Seko[1], Eiichi Sato[1], Hiroshi Yamauchi[2]

1. 気象研究所、2. 気象庁
1. Meteorological Research Institute, 2. Japan Meteorological Agency

Temperature and water vapor near the surface play crucial roles for the generation of convection cells. However, their variations just before the generations of convection cells still are not understood completely. In this study the temporal variations of refractivity index were obtained by MRI dual-polarization Doppler radar. The features of temperature and water vapor including generation period of convection cells will be shown in this presentation. On 19th August 2017, the sea breeze invaded from Kashima-Nada and the refractivity increased along the front of the sea breeze. The scattered weak echoes that appeared around the front seem to be related with the increase of refractivity. These are the features near the surface. The comparison with other data such as GNSS PWV will be also presented.

キーワード：観測手法、ドップラーレーダ、屈折率
Keywords: Observation method, Doppler radar, Refractivity index

©2019. Japan Geoscience Union. All Right Reserved.

Spatial and temporal distribution of tropospheric water vapor observed by a Raman lidar and a GNSS receiver network over Shigaraki, Japan

*矢吹 正教[1]、津田 敏隆[1]、河野 邑弥[2]、鳥取 裕作[2]、塚本 誠[2]、竹内 栄治[2]
*Masanori Yabuki[1], Toshitaka Tsuda[1], Yuya Kawano[2], Yusaku Tottori[2], Makoto Tsukamoto[2], Eiji Takeuchi[2]

1. 京都大学生存圏研究所、2. 英弘精機株式会社
1. Research Institute for Sustainable Humanosphere, Kyoto University, 2. EKO Instruments Co., Ltd.

Understanding the spatial and temporal distributions of water vapor in the atmosphere is critical for unveiling the fundamental mechanisms of localized extreme weather events. Besides, it is highly beneficial for improving the accuracy of weather forecasts by mesoscale numerical weather prediction models. To achieve the continuous monitoring of water vapor distributions, we performed simultaneous measurements by Raman lidar in the UV-C region and a dense Global Navigation Satellite System (GNSS) network. The former is a novel technology that can be utilized for profiling the vertical distribution of the water vapor mixing ratio for twenty-four hours, while the latter can be used for detecting the horizontal distribution of precipitable water vapor. The Raman lidar employs a laser at a wavelength of 266 nm and detects the light separated into an elastic backscatter signal and vibrational Raman signals of oxygen, nitrogen, and water vapor at wavelengths of 266, 277, 284, and 295 nm, respectively. The use of these wavelengths is convenient because of the low background noise during daytime, since most of the solar radiation in the ultraviolet range below 300 nm is absorbed by the ozone layer in the stratosphere. The lidar was encased in a temperature-controlled compact container, resistant to a variety of environmental conditions. Continuous observation of water vapor profiles by lidar has been conducted at the Shigaraki MU radar observatory (34˚51’ N, 136˚06’ E, 385 m a.s.l.) since November 2017. The dense GNSS receiver network consisted of 10 dual-frequency GNSS stations which were installed with a horizontal spacing of 3-4 km near the observatory on July 2017. In this study, we present our water vapor monitoring system as well as the preliminary results on the spatio-temporal water vapor distributions in 2018.

Acknowledgements
A part of this study is supported by JSPS KAKENHI Grant Number 15H03724.

キーワード：水蒸気、ラマンライダー、稠密GNSSネットワーク
Keywords: water vapor, Raman lidar, dense GNSS network

©2019. Japan Geoscience Union. All Right Reserved.

Study of the Mechanisms of Severe Thunderstorm in Tokyo Metropolitan Area using High Frequent Assimilation of GNSS and Other Ground-based Observations

Study of the Mechanisms of Severe Thunderstorm in Tokyo Metropolitan Area using High Frequent Assimilation of GNSS and Other Ground-based Observations

*小司 禎教[1]、酒井 哲[2]、足立 アホロ[1]、吉田 智[2]、永井 智広[2]
*Yoshinori Shoji[1], Tetsu Sakai[2], Ahoro Adachi[1], Satoru Yoshida[2], Tomohiro Nagai[2]

1. 気象研究所気象衛星・観測システム研究部第２研究室、2. 気象研究所気象衛星・観測システム研究部第３研究室
1. The Second Laboratory of Meteorological Satellite and Observation System Research Department, Meteorological Research Institute, 2. The Third Laboratory of Meteorological Satellite and Observation System Research Department, Meteorological Research Institute

Highly urbanized Tokyo metropolitan area is vulnerable to severe storms such as local torrential rainfall, thunder lightning and tornado. Recently, the number of days with thunderstorms has been increasing in Tokyo. Elucidation of the mechanism of extreme weather in Tokyo is urgent matter (Nakatani et al. 2013). To study the rolls of water vapor and wind for the rapid life-cycle (initiation, development and dissipation) of hazardous cumulus convection, we installed a mobile Raman-lidar (Sakai et al. 2018), a wind profiler, and five GNSS stations in and around Tokyo.

Using 3DVAR capability of WRF data assimilation system (WRFDA)(Barker et al. 2012) , three-dimensional atmospheric fields with 1 km horizontal resolution were produced at every 10min throughout the August 2017 and 2018. Background fields were produced by JMA nonhydrostatic model (NHM)(Saito et al. 2007). In addition to the observed data at these campaign observation instruments, Japan Meteorological Agency’ s operational surface meteorological stations, wind-profiler stations and GNSS PWV derived at dense GNSS network of Geospatial Information Authority of Japan are assimilated. We confirmed that the reproduced atmospheric fields (Temperature, humidity, and wind) showed better agreement with observations of radiosonde, lidar derived water vapor mixing ratio, and wind-profiler than background fields at altitudes lower than 2 km. Assimilation of surface meteorological observations (atmospheric pressure, temperature, humidity and wind) introduced better agreement mainly at altitude lower than 0.5 km. Inclusion of GNSS derived PWV resulted better agreement of humidity at altitude higher than 0.5 km and inclusion of wind field from wind-profiler led better agreement of wind field.

We have investigated roles of water vapor for several local heavy rainfall events occurred in Tokyo in August 2017 and 2018 and found that convergence of water vapor flux at 0.5 km altitude had intensified prior to the occurrence of torrential precipitation. Statistical and quantitative results will be discussed at the symposium.

This study is supported by JSPS KAKENHI Grants 17H00852.

©2019. Japan Geoscience Union. All Right Reserved.

キーワード：水蒸気、データ同化、局地豪雨
Keywords: Water vapor, Data assimilation, Localized heavy rainfall

©2019. Japan Geoscience Union. All Right Reserved.

[E] ポスター発表 | セッション記号 M (領域外・複数領域)：M-TT 計測技術・研究手法

2019年5月27日(月) 17:15 ~ 18:30 | ポスター会場 幕張メッセ国際展示場 8ホール_43

[M-TT46] 統合地球観測システムとしてのGPS/GNSSの新展開

コンビーナ:小司 禎教(気象研究所気象衛星・観測システム研究部第２研究室)、市川 香(九州大学応用力学研究所)、太田 雄策(東北大学大学院理学研究科附属地震・噴火予知研究観測センター)、津川 卓也(情報通信研究機構)

GNSSは、大気圏、電離圏、固体地球の基盤となる統合観測システムとなっている。地上及び宇宙基地型GNSS観測は、2006年より数値気象予報の改善に貢献している。近年では反射波を用いて高度、地面粗度、土壌水分、積雪深、湿度や植生インデックスを導出する研究が発展している。船舶やブイなど海洋上のGNSS観測は、海面高度に加えて海洋上の水蒸気観測の能力を持つ。Multi-GNSSがもたらす観測データの増加は、統合地球観測システムとしてのGNSSの能力を拡大させる。
本セッションの目的は、GNSS研究の最新成果を共有し、あらたな学際研究を促進することにある。GNSSを用いた大気（対流圏、電離圏）、GNSS-R、またGNSS-音響観測による海底測位のようなの異なる観測の統合に関する投稿を歓迎する。

[MTT46-P01] 新たな海底地殻変動観測手法のためのGNSSブイからの連続音響測距

*田所 敬一[1]、衣笠 菜月[1]、加藤 照之[2]、寺田 幸博[3]、二村 彰[4]、松廣 健二郎[1] (1.名古屋大学地震火山研究センター、2.神奈川県温泉地学研究所、3.高知工業高等専門学校、4.弓削商船高等専門学校)

[MTT46-P02] Accuracy and precision assessment of the real-time kinematic GNSS time series for moored buoy using three-axis programable moving table

*太田 雄策[1]、今野 美冴[1]、木戸 元之[2] (1.東北大学大学院理学研究科附属地震・噴火予知研究観測センター、2.東北大学災害科学国際研究所)

[MTT46-P03] 静止衛星によるGNSS-R海面高度計測

*市川 香[1]、奥村 立樹[2]、根田 昌典[3]、馬場 康之[4] (1.九州大学応用力学研究所、2.九州大学総合理工学府大気海洋環境システム学専攻、3.京都大学大学院理学研究科、4.京都大学防災研究所)

[MTT46-P04] **Estimation of typhoon wind speed using CYGNSS observations: A case study of Typhoon Lan in 2017**

*加古 真一郎[1]、富田 裕之[2]、市川 香[3] (1.鹿児島大学大学院理工学研究科、2.名古屋大学 宇宙地球環境研究所、3.九州大学応用力学研究所)

[MTT46-P05] Ionospheric and seismic effects caused by the North Korea nuclear tests realized on 2006-2017

Nataliia Perevalova[2]、*Nikolai Shestakov[1]、Anna Dobrynina[3,4]、Dmitry Kostylev[7]、Meng Guojie[5]、Wei-Wei Wu[5,6] (1.Institute for Applied Mathematics FEB RAS, Vladivostok, Russia; Far Eastern Federal University, Vladivostok, Russia、2.Institute of Solar-Terrestrial Physics SB RAS, Irkutsk, Russia、3.Institute of the Earth's Crust SB RAS, Irkutsk, Russia 、4.Geological institute SB RAS, Ulan-Ude, Russia 、5.Institute of Earthquake Forecasting, China Earthquake Administration, Beijing, China、6.College of Surveying and Geo-informatics, Tongji University, Shanghai, China、7.Sakhalin Branch of Federal Research Center Geophysical Survey RAS, Yuzhno_Sakhalinsk, Russia)

[MTT46-P06] Relationships between Water Vapor Concentration Index derived from GNSS and Surface Wind Convergence during Localized Heavy Rainfall in Tokyo in Summer

*瀬戸 芳一[1]、小司 禎教[2]、常松 展充[3]、高橋 日出男[1] (1.首都大学東京大学院都市環境科学研究科地理環境学域、2.気象庁気象研究所、3.東京都環境科学研究所)

[MTT46-P07] 次世代高感度マイクロ波放射計の開発-序報-

*市川 隆一[1]、氏原 秀樹[1]、佐藤 晋介[1]、雨谷 純[1]、太田 雄策[2]、宮原 伐折羅[3]、宗包 浩志[3]、長崎 岳人[4]、田島 治[5]、荒木 健太郎[6]、田尻 拓也[6]、瀧口 博士[7]、松島 健[8]、松島 喜雄[9]、桃谷 辰也[10]、宇都宮 健志[10] (1.情報通信研

究機構、2.東北大学、3.国土地理院、4.高エネルギー加速器研究機構、5.京都大学、6.気象研究所、7.宇宙航空研究開発機構、8.九州大学、9.産業技術総合研究所、10.日本気象協会)

[MTT46-P08] Refractivity Distributions over the Kanto Plain Obtained by Dual-polarization Radar

*瀬古 弘[1]、佐藤 英一[1]、山内 洋[2] (1.気象研究所、2.気象庁)

[MTT46-P09] Spatial and temporal distribution of tropospheric water vapor observed by a Raman lidar and a GNSS receiver network over Shigaraki, Japan

*矢吹 正教[1]、津田 敏隆[1]、河野 邑弥[2]、鳥取 裕作[2]、塚本 誠[2]、竹内 栄治[2] (1.京都大学生存圏研究所、2.英弘精機株式会社)

[MTT46-P10] **Study of the Mechanisms of Severe Thunderstorm in Tokyo Metropolitan Area using High Frequent Assimilation of GNSS and Other Ground-based Observations**

*小司 禎教[1]、酒井 哲[2]、足立 アホロ[1]、吉田 智[2]、永井 智広[2] (1.気象研究所気象衛星・観測システム研究部第２研究室、2.気象研究所気象衛星・観測システム研究部第３研究室)

新たな海底地殻変動観測手法のためのGNSSブイからの連続音響測距
Continuous acoustic ranging from a GNSS buoy for the new method of seafloor crustal deformation measurements

*田所 敬一[1]、衣笠 菜月[1]、加藤 照之[2]、寺田 幸博[3]、二村 彰[4]、松廣 健二郎[1]
*Keiichi Tadokoro[1], Natsuki Kinugasa[1], Teruyuki Kato[2], Yukihiro Terada[3], Akira Futamura[4], Kenjiro Matsuhiro[1]

1. 名古屋大学地震火山研究センター、2. 神奈川県温泉地学研究所、3. 高知工業高等専門学校、4. 弓削商船高等専門学校
1. Research Center for Seismology, Volcanology and Earthquake and Volcano Research Center, Nagoya University, 2. Hot Springs Research Institute of Kanagawa Prefecture, 3. Kochi National College of Technology, 4. National Institute of Technology, Yuge College

Our research group has been testing a measurement system for the continuous seafloor crustal deformation at a moored buoysite operated by Kochi prefecture, located 32 km off Cape Ashizuri, Japan.An acoustic transducer was fixed at about 1.7 m beneath the sea surface with a pole mounted on the buoy body.Three ocean bottom acoustic transponders had been installed around the moored point of the buoy. The acoustic signals are sequentially transmitted to these three transponders every three minutes. The recorded data on the buoy are planned to transmitted to a ground base station through a commercial communication satellite operated by Thuraya Telecommunications Company.
We performed a test for the continuous acoustic ranging between the buoy and the ocean bottom transponders from March 28 to 31 and from June 2 to July 12 (1st period), and from November 16to December 17 (2nd period) in 2018. The acoustic ranging was continuously possible throughout the above periods when power was supplied whereas it was unexpectedly terminated because of power failure during the winter season. The acoustic signals were transmitted 27,856 times in total, and the buoy-mounted acoustic ranging unit received 23,342 signals from the ocean bottom transponders. However, the acoustic data sent to the ground base station was only 12 % because of some trouble of the satellite communication modem.
The reflected signals from the buoy body and/or the seafloor sometimes contaminated the received acoustic signals; also multiple reflections inside of an anti-reflection cover attached to the buoy-mounted transducer, whose purpose is to cut off the reflection from the sea surface, were remarkable during the 1st period. The multiple reflections caused the misidentification of the direct wave from the sea-bottom units. We, therefore, removed the anti-reflection cover during the 2nd period, which remarkably reduced the confused reflections.
We coded a program for detecting the arrival time of direct acoustic wave automatically on the basis of thresholds of cross-correlation coefficient and energy ratio (the ratio of the squared amplitudes preceding and following a test point) to reduce the capacity of data transferred via satellite communication using the acoustic waveform recorded during the 1st period. The program successfully picked the correct direct wave onset for more than 99 % of the waveforms recorded during the 2nd period.

©2019. Japan Geoscience Union. All Right Reserved.

Accuracy and precision assessment of the real-time kinematic GNSS time series for moored buoy using three-axis programable moving table

*太田 雄策[1]、今野 美冴[1]、木戸 元之[2]
*Yusaku Ohta[1], Misae Imano[1], Motoyuki Kido[2]

1. 東北大学大学院理学研究科附属地震・噴火予知研究観測センター、2. 東北大学災害科学国際研究所
1. Research Center for Prediction of Earthquakes and Volcanic Eruptions, Graduate School of Science, Tohoku University, 2. IRIDeS, Tohoku University

Rapid understanding of the magnitude of large earthquakes and their associated fault dimensions are extremely important. Especially, capture of the coseismic deformation in the offshore region will be key information to understand the fault dimensions for the large interplate earthquake. Based on this background, Tohoku University and JAMSTEC are jointly developing the on-demand crustal deformation monitoring system using moored buoy system. The buoy can measure the sea-floor horizontal crustal deformation by GNSS/Acoustic technique and vertical deformation using ocean bottom pressure sensor. One of the key technology in our developed system is the real-time kinematic GNSS which can measure three-dimensional position of the buoy in real-time. In contrast, it is difficult to understand quantitatively the precision and accuracy of estimated buoy position because no reference for the position. Thus, we assess the precision and accuracy of real-time kinematic GNSS time series using programable three-axis movable table.

We have developed the single-axis precise programable movable table (Ohta et al., 2016). We expanded this developed system to three-axis. For the real-time kinematic analysis, we adopted Trimble CenterPoint RTX (hereafter, RTX) with 10Hz sampling interval. The correction message for the analysis was received via a stationary satellite. We also estimated the GNSS antenna position using very short-baseline kinematic analysis as reference solution. The developed movable table can operate single axis horizontal displacement, rotational movement, and tilt deformation. To simulate the actual buoy movement, we gave the motion to the movable table based on the actual buoy movement. We conducted the experiment in 24 hours duration.

We calculated the residual time series between obtain time series by RTX and short-baseline kinematic solution. The difference between averaged absolute position was quite good in the horizontal components which was less than 10mm. In contrast, the vertical component shows the clear discrepancy between them. RTX time series shows systemically higher than the baseline analysis which reached approximately 230mm. In contrast, the precision of the calculated residual time series was good in both of the components. Calculated standard deviations were 10-11mm and 28mm in horizontal components and vertical component, respectively. We will show the more detailed results from our experiment and discuss the ability of the real-time kinematic analysis in our developed buoy.

©2019. Japan Geoscience Union. All Right Reserved.

静止衛星によるGNSS-R海面高度計測
GNSS-R altimetry using a Geostationary Satellite

*市川 香[1]、奥村 立樹[2]、根田 昌典[3]、馬場 康之[4]
*Kaoru Ichikawa[1], Tatsuki Okumura[2], Masanori Konda[3], Yasuyuki Baba[4]

1. 九州大学応用力学研究所、2. 九州大学総合理工学府大気海洋環境システム学専攻、3. 京都大学大学院理学研究科、4. 京都大学防災研究所
1. Res. Inst. Appl. Mech., Kyushu Univ., 2. Dept. ESST, Interdicipl. Grad. School Eng. Sc., Kyushu Univ., 3. Graduate School of Science, Kyoto Univ., 4. Disaster Prevention Res. Inst., Kyoto Univ.

The GNSS reflectometry (GNSS-R) uses GNSS signals reflected at the sea surface, which are usually eliminated as the multipath error. The reflected GNSS path received at an antenna is always longer than the direct path, so that the height of the antenna from the sea surface is geometrically determined from the excess path length. The excess path length can be either directly determined by measuring the temporal delay of the reflected signals, or indirectly estimated from interferometric cyclic modulations of the received power (often referred as signal-to-noise ratio; SNR) induced by phase differences between the direct and reflected GNSS signals. In the latter method, as the elevation angle of an earth orbiting GNSS satellite changes in time, the geometric reflection point on the sea surface temporally displaces, which results in interferometric changes of the path length during a period while the satellite is in sight. Meanwhile, for a geostationary satellite in BeiDou constellations that are always in sight, the path length changes not by the movement of the satellite but the elevation of the reflection surface, *i.e.* the sea level rise. In this study, we used the three-month time series (2016/09-11) of the 1Hz SNR of the geostationary BeiDou #02 satellite observed by a GNSS-R system deployed to the Shirahama Oceanographic Observatory Tower owned by Kyoto University (33deg, 42’ 32’’ N, 135deg, 19’ 58’’ E) at the height of ~20m. The geostationary GNSS-R altimetry observed significant flood tides when the wind speed is stably low; the 0.6m sea level rise was successfully determined by the SNR interferometry with 0.05m rms difference. However, significant interferometric SNR changes by tides were not recorded at high or low tides since at least 0.25m sea level change is required for the interferometry cycle. Consequently, the cyclic periods of the geostationary GNSS-R altimetry for tides become long (1-4 hours for 0.25m change in Shirahama), the interferometric variations were usually contaminated by SNR changes induced by the other factors such as winds. On the contrary, faster sea level changes by wave motions could be recognized by the geostationary GNSS-R altimetry, although the temporal sampling intervals of the present data were not adequate.

キーワード：GNSS-R、海面高度計、BeiDou静止GNSS衛星
Keywords: GNSS-R , altimetry, BeiDou geostationary GNSS satellite

©2019. Japan Geoscience Union. All Right Reserved.

Estimation of typhoon wind speed using CYGNSS observations: A case study of Typhoon Lan in 2017

*加古 真一郎[1]、富田 裕之[2]、市川 香[3]
*Kako Shinichiro[1], Hiroyuki Tomita[2], Kaoru Ichikawa[3]

1. 鹿児島大学大学院理工学研究科、2. 名古屋大学 宇宙地球環境研究所、3. 九州大学応用力学研究所
1. Graduate School of Science and Engineering, Kagoshima University, 2. Institute for Space-Earth Environment, Nagoya University, 3. Research institute for Applied Mechanics, Kyushu University

We conducted a case study of Typhoon Lan, which occurred in 2017, to investigate the impact of the Cyclone Global Navigation Satellite System (CYGNSS) on the estimation of extremely high wind speeds, such as those occurring during typhoons. We studied CYGNSS because it is expected to be capable of observing wind speeds in regions with extremely high wind speeds and heavy rains (i.e., typhoons) where it is difficult to perform measurements using the current microwave instrument. Firstly, we compared CYGNSS-derived wind speeds produced by NASA with those derived from AMSR2 produced by the Japan Aerospace Exploration Agency. CYGNSS was found to underestimate the wind speeds around Typhoon Lan compared with AMSR2. We then attempted to estimate the wind speeds using the leading edge slope (LES) and mean square slope (MSS) derived from the CYGNSS observations. Although the relationship between the MSS and wind speed differs depending on the wave age (Zhao and Tobe, 2003), it is difficult to estimate the wave age because this estimation is required the wind and wave speeds. We used the wave period as a substitute for the wave age since the wave period is expected to be similar to the wave age. We therefore first computed the fourth power of the wave period (T4) in line with Wang and Ichikawa (2016). Next, we classified the ocean into three regions based on T4 to investigate the relationship between the MSS and the wind speed observed by AMSR2 in each region. Finally, we approximated the curves relating the MSS to the wind speed using exponential functions in the three regions and estimated the wind speed using these curves. The comparison between the wind speeds produced by NASA and those estimated in this study demonstrated that our method can estimate high wind speeds more accurate than the CYGNSS wind speeds produced by NASA.

キーワード：CYGNSS、AMSR2、台風
Keywords: CYGNSS, AMSR2, tyhoon

©2019. Japan Geoscience Union. All Right Reserved.

Ionospheric and seismic effects caused by the North Korea nuclear tests realized on 2006-2017

Nataliia Perevalova[2], *Nikolai Shestakov[1], Anna Dobrynina[3,4], Dmitry Kostylev[7], Meng Guojie[5], Wei-Wei Wu[5,6]

1. Institute for Applied Mathematics FEB RAS, Vladivostok, Russia; Far Eastern Federal University, Vladivostok, Russia, 2. Institute of Solar-Terrestrial Physics SB RAS, Irkutsk, Russia, 3. Institute of the Earth's Crust SB RAS, Irkutsk, Russia , 4. Geological institute SB RAS, Ulan-Ude, Russia , 5. Institute of Earthquake Forecasting, China Earthquake Administration, Beijing, China, 6. College of Surveying and Geo-informatics, Tongji University, Shanghai, China, 7. Sakhalin Branch of Federal Research Center Geophysical Survey RAS, Yuzhno_Sakhalinsk, Russia

Using data from GPS/GLONASS receivers and seismic networks, we studied the ionospheric and lithospheric effects caused by six underground nuclear tests realized in North Korea on 2006-2017.
To investigate the ionospheric disturbances, we analyzed data from several continuous GNSS-networks (GPS and GLONASS) operating in Asia - Western Pacific region: IGS, GEONET, FEB RAS and FEFU complex geodynamic network, a set of stations belonging to China and South Korea GNSS-networks. Sites close to the Korean Peninsula were selected for the analysis. Series of total electron content (TEC) in the ionosphere were calculated on the base of dual-frequency phase measurements of GNSS receivers. To detect disturbances caused by the nuclear tests, TEC series were filtered in the range of periods from 1 to 10 minutes. Despite the small magnitudes of seismic events associated with the nuclear tests, we were able to identify ionospheric disturbances which were most likely generated by these explosions. Such disturbances were detected for 4 out of 6 nuclear tests. The main parameters of the disturbances were determined. From our analysis we concluded that characteristics of ionospheric disturbances caused by the underground nuclear tests differed significantly from the parameters of disturbances that are usually observed after earthquakes.
For seismic analysis, we used data from the broadband seismic station networks located at distances up to 23 degrees from the Korean Peninsula: II, IC, IU, TW, JP, G, KS, and KG given by IRIS, and regional seismic network BY. The frequency content of P and surface Rayleigh waves registered by 46 broadband stations was analyzed. For some events, the P-wave frequency content showed the prevalence of low frequencies in spectra (~0.45 Hz). The peak frequencies of the surface Rayleigh waves was in the 0.05-0.45 Hz range. Preliminary analysis of the peak frequencies spatial distribution showed that the continental massive area is characterized by the relatively high frequencies (0.14-0.50 Hz) while for the areas adjacent to marginal seas the low values of peak frequencies are observed (from 0.13 Hz and less).
Acknowledgments. We are deeply indebted to Scripps Orbit and Permanent Array Center (SOPAC) for the IGS-network data, to Geospatial Information Authority of Japan for GEONET network data, to Korea Astronomy & Space Science Institute for access to GNSS data on the Korean Peninsula, CCU CC FEB RAS for access to data from the FEB RAS and FEFU complex geodynamic network; Institute of Earthquake Forecasting, China Earthquake Administration for access to GNSS data in China. The facilities of the IRIS Data Management System, and specifically the IRIS Data Management Center, and Baikal Regional Seismological Center and Sakhalin Branch of Federal Research Center Geophysical Survey RAS were used to get waveform and metadata required in this study. This work was performed with budgetary funding of Basic Research program II.16 and was also partially supported by RFBR grants 17-45-388072_p_a, 17-45-388049_ p_a, 17-55-53110_GFEN_a, 19-05-00889_a.

Keywords: North Korea nuclear tests, ionospheric and lithospheric effects, GPS/GLONASS-observations

©2019. Japan Geoscience Union. All Right Reserved.

©2019. Japan Geoscience Union. All Right Reserved.

Relationships between Water Vapor Concentration Index derived from GNSS and Surface Wind Convergence during Localized Heavy Rainfall in Tokyo in Summer

*瀬戸 芳一[1]、小司 禎教[2]、常松 展充[3]、高橋 日出男[1]
*Yoshihito Seto[1], Yoshinori Shoji[2], Nobumitsu Tsunematsu[3], Hideo Takahashi[1]

1. 首都大学東京大学院都市環境科学研究科地理環境学域、2. 気象庁気象研究所、3. 東京都環境科学研究所
1. Department of Geography, Graduate School of Urban Environmental Sciences, Tokyo Metropolitan University, 2. Meteorological Research Institute, 3. Tokyo Metropolitan Research Institute for Environmental Protection

In recent years, short-term heavy-rainfall events that have caused severe damages such as flooding have frequently occurred in the Tokyo Metropolitan area in summer. In view of the development process of cumulonimbus clouds, the convergence of surface winds and the spatial concentration of water vapor are supposed to have taken place prior to the occurrence of heavy rainfall. This study aims to clarify the evolutionary process of short-term heavy rainfall as a contribution to short-range forecasting of heavy rainfall that occurs locally.

The relationships between the occurrence of heavy rainfall and the convergence of surface winds and water vapor concentration for heavy-rainfall cases were examined using data from July to September obtained from high-density meteorological observations in Tokyo, Japan. We used the water vapor concentration (WVC) index derived from the global navigation satellite system (GNSS) analysis as indices for the degree of divergence and convergence of water vapor in the lower troposphere (Shoji 2013).

Corresponding to heavy-rainfall areas, the convergence of surface winds tended to increase for several tens of minutes prior to the heavy rainfall. The peak time of wind convergence was observed 10–30 min before the heavy-rainfall occurrence, and the convergence continued to increase for approximately 30 min until the convergence peak time (Seto et al. 2018). Around the heavy-rainfall area, the increase in the WVC index coincided with the increase in convergence. On the other hand, it was considered that the temporal and spatial scales of the WVC index are larger than those of wind convergence. From these results, by monitoring the temporal variations and distributions of these parameters using a high-density observation network, it should be possible to predict the occurrence of heavy rainfall rapidly and accurately.

References

Seto, Y., Yokoyama, H., Nakatani, T., Ando, H., Tsunematsu, N., Shoji, Y., Kusunoki, K., Nakayama, M., Saitoh, Y. and Takahashi, H. 2018. Relationships among rainfall distribution, surface wind, and precipitable water vapor during heavy rainfall in central Tokyo in summer. J. Meteor. Soc. Japan, 96A, 35–49.
Shoji, Y. 2013. Retrieval of water vapor inhomogeneity using the Japanese nationwide GPS array and its potential for prediction of convective precipitation. J. Meteor. Soc. Japan, 91, 43–62.

キーワード：短時間強雨、地上風収束、水蒸気、高密度観測
Keywords: localized heavy rainfall, wind convergence, water vapor, high-density observation

©2019. Japan Geoscience Union. All Right Reserved.

次世代高感度マイクロ波放射計の開発-序報-
Development of novel ground-based microwave radiometer for earth science -preliminary report-

*市川 隆一[1]、氏原 秀樹[1]、佐藤 晋介[1]、雨谷 純[1]、太田 雄策[2]、宮原 伐折羅[3]、宗包 浩志[3]、長崎 岳人[4]、田島 治[5]、荒木 健太郎[6]、田尻 拓也[6]、瀧口 博士[7]、松島 健[8]、松島 喜雄[9]、桃谷 辰也[10]、宇都宮 健志[10]
*Ryuichi Ichikawa[1], Hideki Ujihara[1], Shinsuke Satoh[1], Jun Amagai[1], Yusaku Ohta[2], Basara Miyahara[3], Hiroshi Munekane[3], Taketo Nagasaki[4], Osamu Tajima[5], Kentaro Araki[6], Takuya Tajiri[6], Hiroshi Takiguchi[7], Takeshi Matsushima[8], Nobuo Matsushima[9], Tatsuya Momotani[10], Kenji Utsunomiya[10]

1. 情報通信研究機構、2. 東北大学、3. 国土地理院、4. 高エネルギー加速器研究機構、5. 京都大学、6. 気象研究所、7. 宇宙航空研究開発機構、8. 九州大学、9. 産業技術総合研究所、10. 日本気象協会
1. National Institute of Information and Communications Technology, 2. Tohoku University, 3. Geospatial Information Authority of Japan, 4. High Energy Accelerator Research Organization, 5. Kyoto University, 6. Meteorological Research Institute, JMA, 7. Japan Aerospace eXploration Agency, 8. Kyushu University, 9. National Institute of Advanced Industrial Science and Technology, 10. Japan Weather Association

中性大気中の水蒸気変動を高時空分解能で把握するために、次世代高感度マイクロ波放射計の開発に着手した。このマイクロ波放射計は、マイクロ波を用いたGNSSやVLBIといった宇宙測地技術の高精度化に加え、火山活動監視や積乱雲の発達過程観測への寄与を念頭に置いている。同放射計の基本的な設計概念は、高エネルギー加速器研究機構(KEK)が開発したKUMODeSのそれを踏襲する。KUMODeSは、20-30 GHz帯と50-60 GHz帯の2つの帯域を受信する広帯域受信機を搭載し、前者の低雑音アンプを10Kまで冷却することで、水蒸気及び液水の吸収帯での高感度化を実現している。一方、後者の受信系は、酸素の吸収帯を同時観測することで大気放射を把握し、双方の放射温度を解析することで水蒸気に寄与する放射スペクトルを正確に推定出来る。我々は、KUMODeS観測で得られた可降水量をGNSS、ラジオゾンデ、あるいは数値予報データから得られた可降水量と比較し、KUMODeSが水蒸気時空変動を高精度に把握できる可能性を示した。これを踏まえ、新たに開発する放射計では、20-60 GHzを一気に受信可能な広帯域フィードを搭載し、得られた信号を導波管型偏波分離器(OMT)を用いて分離した水平・直交のそれぞれの偏波成分を20-30 GHz及び50-60 GHzの各々の低雑音増幅器(LNA)で受ける受信系を考えている。さらに、受信系全体をスターリング冷凍機を用いた冷凍容器に格納し、これにより信号対雑音比の向上を図ることで感度向上を目指す。この受信系の開発完了は今年の年末を目標としており、既存のパラボラアンテナ受信部に搭載して評価観測を行う予定である。

キーワード：GNSS、マイクロ波放射計、水蒸気
Keywords: GNSS, microwave radiometer, water vapor

©2019. Japan Geoscience Union. All Right Reserved.

Refractivity Distributions over the Kanto Plain Obtained by Dual-polarization Radar

*瀬古 弘[1]、佐藤 英一[1]、山内 洋[2]
*Hiromu Seko[1], Eiichi Sato[1], Hiroshi Yamauchi[2]

1. 気象研究所、2. 気象庁
1. Meteorological Research Institute, 2. Japan Meteorological Agency

Temperature and water vapor near the surface play crucial roles for the generation of convection cells. However, their variations just before the generations of convection cells still are not understood completely. In this study the temporal variations of refractivity index were obtained by MRI dual-polarization Doppler radar. The features of temperature and water vapor including generation period of convection cells will be shown in this presentation. On 19th August 2017, the sea breeze invaded from Kashima-Nada and the refractivity increased along the front of the sea breeze. The scattered weak echoes that appeared around the front seem to be related with the increase of refractivity. These are the features near the surface. The comparison with other data such as GNSS PWV will be also presented.

キーワード：観測手法、ドップラーレーダ、屈折率
Keywords: Observation method, Doppler radar, Refractivity index

©2019. Japan Geoscience Union. All Right Reserved.

Spatial and temporal distribution of tropospheric water vapor observed by a Raman lidar and a GNSS receiver network over Shigaraki, Japan

*矢吹 正教[1]、津田 敏隆[1]、河野 邑弥[2]、鳥取 裕作[2]、塚本 誠[2]、竹内 栄治[2]
*Masanori Yabuki[1], Toshitaka Tsuda[1], Yuya Kawano[2], Yusaku Tottori[2], Makoto Tsukamoto[2], Eiji Takeuchi[2]

1. 京都大学生存圏研究所、2. 英弘精機株式会社
1. Research Institute for Sustainable Humanosphere, Kyoto University, 2. EKO Instruments Co., Ltd.

Understanding the spatial and temporal distributions of water vapor in the atmosphere is critical for unveiling the fundamental mechanisms of localized extreme weather events. Besides, it is highly beneficial for improving the accuracy of weather forecasts by mesoscale numerical weather prediction models. To achieve the continuous monitoring of water vapor distributions, we performed simultaneous measurements by Raman lidar in the UV-C region and a dense Global Navigation Satellite System (GNSS) network. The former is a novel technology that can be utilized for profiling the vertical distribution of the water vapor mixing ratio for twenty-four hours, while the latter can be used for detecting the horizontal distribution of precipitable water vapor. The Raman lidar employs a laser at a wavelength of 266 nm and detects the light separated into an elastic backscatter signal and vibrational Raman signals of oxygen, nitrogen, and water vapor at wavelengths of 266, 277, 284, and 295 nm, respectively. The use of these wavelengths is convenient because of the low background noise during daytime, since most of the solar radiation in the ultraviolet range below 300 nm is absorbed by the ozone layer in the stratosphere. The lidar was encased in a temperature-controlled compact container, resistant to a variety of environmental conditions. Continuous observation of water vapor profiles by lidar has been conducted at the Shigaraki MU radar observatory (34˚51’ N, 136˚06’ E, 385 m a.s.l.) since November 2017. The dense GNSS receiver network consisted of 10 dual-frequency GNSS stations which were installed with a horizontal spacing of 3-4 km near the observatory on July 2017. In this study, we present our water vapor monitoring system as well as the preliminary results on the spatio-temporal water vapor distributions in 2018.

Acknowledgements
A part of this study is supported by JSPS KAKENHI Grant Number 15H03724.

キーワード：水蒸気、ラマンライダー、稠密GNSSネットワーク
Keywords: water vapor, Raman lidar, dense GNSS network

©2019. Japan Geoscience Union. All Right Reserved.

Study of the Mechanisms of Severe Thunderstorm in Tokyo Metropolitan Area using High Frequent Assimilation of GNSS and Other Ground-based Observations

Study of the Mechanisms of Severe Thunderstorm in Tokyo Metropolitan Area using High Frequent Assimilation of GNSS and Other Ground-based Observations

*小司 禎教[1]、酒井 哲[2]、足立 アホロ[1]、吉田 智[2]、永井 智広[2]
*Yoshinori Shoji[1], Tetsu Sakai[2], Ahoro Adachi[1], Satoru Yoshida[2], Tomohiro Nagai[2]

1. 気象研究所気象衛星・観測システム研究部第２研究室、2. 気象研究所気象衛星・観測システム研究部第３研究室
1. The Second Laboratory of Meteorological Satellite and Observation System Research Department, Meteorological Research Institute, 2. The Third Laboratory of Meteorological Satellite and Observation System Research Department, Meteorological Research Institute

Highly urbanized Tokyo metropolitan area is vulnerable to severe storms such as local torrential rainfall, thunder lightning and tornado. Recently, the number of days with thunderstorms has been increasing in Tokyo. Elucidation of the mechanism of extreme weather in Tokyo is urgent matter (Nakatani et al. 2013). To study the rolls of water vapor and wind for the rapid life-cycle (initiation, development and dissipation) of hazardous cumulus convection, we installed a mobile Raman-lidar (Sakai et al. 2018), a wind profiler, and five GNSS stations in and around Tokyo.

Using 3DVAR capability of WRF data assimilation system (WRFDA)(Barker et al. 2012) , three-dimensional atmospheric fields with 1 km horizontal resolution were produced at every 10min throughout the August 2017 and 2018. Background fields were produced by JMA nonhydrostatic model (NHM)(Saito et al. 2007). In addition to the observed data at these campaign observation instruments, Japan Meteorological Agency’ s operational surface meteorological stations, wind-profiler stations and GNSS PWV derived at dense GNSS network of Geospatial Information Authority of Japan are assimilated. We confirmed that the reproduced atmospheric fields (Temperature, humidity, and wind) showed better agreement with observations of radiosonde, lidar derived water vapor mixing ratio, and wind-profiler than background fields at altitudes lower than 2 km. Assimilation of surface meteorological observations (atmospheric pressure, temperature, humidity and wind) introduced better agreement mainly at altitude lower than 0.5 km. Inclusion of GNSS derived PWV resulted better agreement of humidity at altitude higher than 0.5 km and inclusion of wind field from wind-profiler led better agreement of wind field.

We have investigated roles of water vapor for several local heavy rainfall events occurred in Tokyo in August 2017 and 2018 and found that convergence of water vapor flux at 0.5 km altitude had intensified prior to the occurrence of torrential precipitation. Statistical and quantitative results will be discussed at the symposium.

This study is supported by JSPS KAKENHI Grants 17H00852.

©2019. Japan Geoscience Union. All Right Reserved.

キーワード：水蒸気、データ同化、局地豪雨
Keywords: Water vapor, Data assimilation, Localized heavy rainfall

©2019. Japan Geoscience Union. All Right Reserved.

[E] ポスター発表 | セッション記号 M (領域外・複数領域)：M-TT 計測技術・研究手法

2019年5月27日(月) 13:45 ~ 15:15 | ポスター会場 幕張メッセ国際展示場 8ホール_11

[M-TT47] 人新世における高精細地形・地球物理データの活用

コンビーナ:早川 裕弋(北海道大学地球環境科学研究院)、楠本 成寿(富山大学大学院理工学研究部(都市デザイン学))、Gomez Christopher(神戸大学 海事科学部 海域火山リスク科学研究室)

Recent technical developments of high-definition topographic and geophysical data acquisition have enabled us to further investigate geoscientific issues including land surface processes, subsurface structures, submarine and aerial environments, geo-ecological interactions, and disaster mitigation. Such high-definition or high-resolution data are particularly useful for studies in short-term temporal scales, and future predictions such as numerical modelings. In this session, we expect submissions on topics challenging such issues in the Anthropocene, the most recent geological era of the Earth. A range of topics would fit the session framework, including theoretical work, improvements in data acquisition, extensive data preservation and archiving, pre- and post-processing, statistical analysis, modeling, and simulation for geoscientific research and geohazard assessments in the Anthropocene. The methodological approaches may include, but not limited to, laser scanning, SfM-MVS photogrammetry, GNSS precise positioning, SAR interferometry, multi-beam sonar, and electromagnetic sensors, based on terrestrial (fixed or mobile) and aerial (UAV or manned airborne) platforms.

[MTT47-P01] High-definition topography monitoring after riverbed cultivation in the Echi River, central Japan

*小倉 拓郎[1,2]、淺野 悟史[3]、水野 敏明[3]、東 善広[3]、北井 剛[4]、早川 裕弋[5,6]、飯塚 浩太郎[6] (1.東京大学大学院新領域創成科学研究科、2.北海道大学大学院環境科学院、3.滋賀県琵琶湖環境科学研究センター、4.滋賀県立琵琶湖博物館、5.北海道大学地球環境研究院、6.東京大学空間情報科学研究センター)

[MTT47-P02] **Spatial distribution of land surface displacements in the crater of Tateyama Midagahara Volcano using high-definition topographic data**

*早川 裕弋[1]、楠本 成寿[2]、小倉 拓郎[3,4] (1.北海道大学地球環境科学研究院、2.富山大学大学院理工学研究部、3.東京大学新領域創成科学研究科、4.北海道大学大学院環境科学院)

[MTT47-P03] SfM/MVSを用いた簡易的な河床形状復元および水深評価に関する検討

*大澤 幸太[1]、新里 忠史[2]、三田地 勝昭[3]、川村 淳[1]、大川 真弘[1] (1.三菱マテリアルテクノ株式会社、2.日本原子力研究開発機構、3.エイ・ティ・エス株式会社)

[MTT47-P04] Ground Penetrating Radar Imaging of Moisture and Water movement in volcanic soil

*Christopher A Gomez[1] (1.Kobe University Faculty of Maritime Sciences Volcanic Risk at Sea Research Group)

[MTT47-P05] **Estimating Eruptive Volumes of Mud Volcano Southwestern Taiwan by Using UAV and SfM-MVS Photogrammetry**

*CHIA-YING LIU[1]、Ray Y Chuang[1]、Horng-Yue Chen[2] (1.Department of Geography, National Taiwan University、2.Academia Sinica, Institute of Earth Sciences)

[MTT47-P06] Increasing temporal depth of urban Land-Use Regression Models by wind-data driven dynamic buffer generation

*Tilman Leo Hohenberger[1]、King Wai Leung[1] (1.Division of Environment and Sustainability, Hong Kong University of Science and Technology)

High-definition topography monitoring after riverbed cultivation in the Echi River, central Japan

*小倉 拓郎[1,2]、淺野 悟史[3]、水野 敏明[3]、東 善広[3]、北井 剛[4]、早川 裕弋[5,6]、飯塚 浩太郎[6]
*Takuro Ogura[1,2], Satoshi Asano[3], Toshiaki Mizuno[3], Yoshihiro Azuma[3], Takeshi Kitai[4], Yuichi S Hayakawa[5,6], Kotaro Iizuka[6]

1. 東京大学大学院新領域創成科学研究科、2. 北海道大学大学院環境科学院、3. 滋賀県琵琶湖環境科学研究センター、4. 滋賀県立琵琶湖博物館、5. 北海道大学地球環境研究院、6. 東京大学空間情報科学研究センター
1. Graduate School of Frontier Sciences, The University of Tokyo, 2. Graduate School of Environmental Science, Hokkaido University, 3. Lake Biwa Environmental Research Institute , 4. Lake Biwa Museum, 5. Faculty of Environmental Earth Science, Hokkaido University, 6. Center for Spatial information Science, The University of Tokyo

Natural processes of erosion and deposition on riverbeds are generally limited in Japan due to large-scale public constructions including dams and banks. As a result of the construction of dams, sediment transport may dramatically decrease in the downstream area are, and the river ecosystem can also be affected. To make sediment move more vigorously, we cultivated the armored gravel riverbed with heavy machinery. We then explore the effects of riverbed cultivating by monitoring the topographic changes with high-frequency and high-definition measurements (HF-HD measurements), whereas conventional measurement technologies do not compensate spatial resolution and temporal resolution to capture the topographic change. Using UAS (Unmanned Aerial Vehicle) and SfM-MVS (Structure-from-Motion –Multi-view Stereo) photogrammetry, we found the transportation of the fixed gravels were occurring after cultivating the riverbed in 2017. The temporal and spatial resolutions of the HF-HD topographic data was approximately 2 months and 10 cm, respectively. In July 2018, water flow at 130 m^3/s was discharged from the upstream dam, and we confirmed that a part of the gravels in the cultivated area was eroded and replaced with new sediments (Fig. 1). These observations indicate that riverbed monitoring using UAV and SfM - MVS can be a practical tool for proper management of riverbeds. Applying this result, we will further clarify the relationships between the water quantity discharged from the dam and the riverbed topographic changes.

キーワード：高精細地形情報、河床耕耘、UAV、SfM多視点ステレオ写真測量、愛知川
Keywords: High-definition topographic data, riverbed cultivation, UAV, SfM-MVS photogrammetry, Echi river

©2019. Japan Geoscience Union. All Right Reserved.

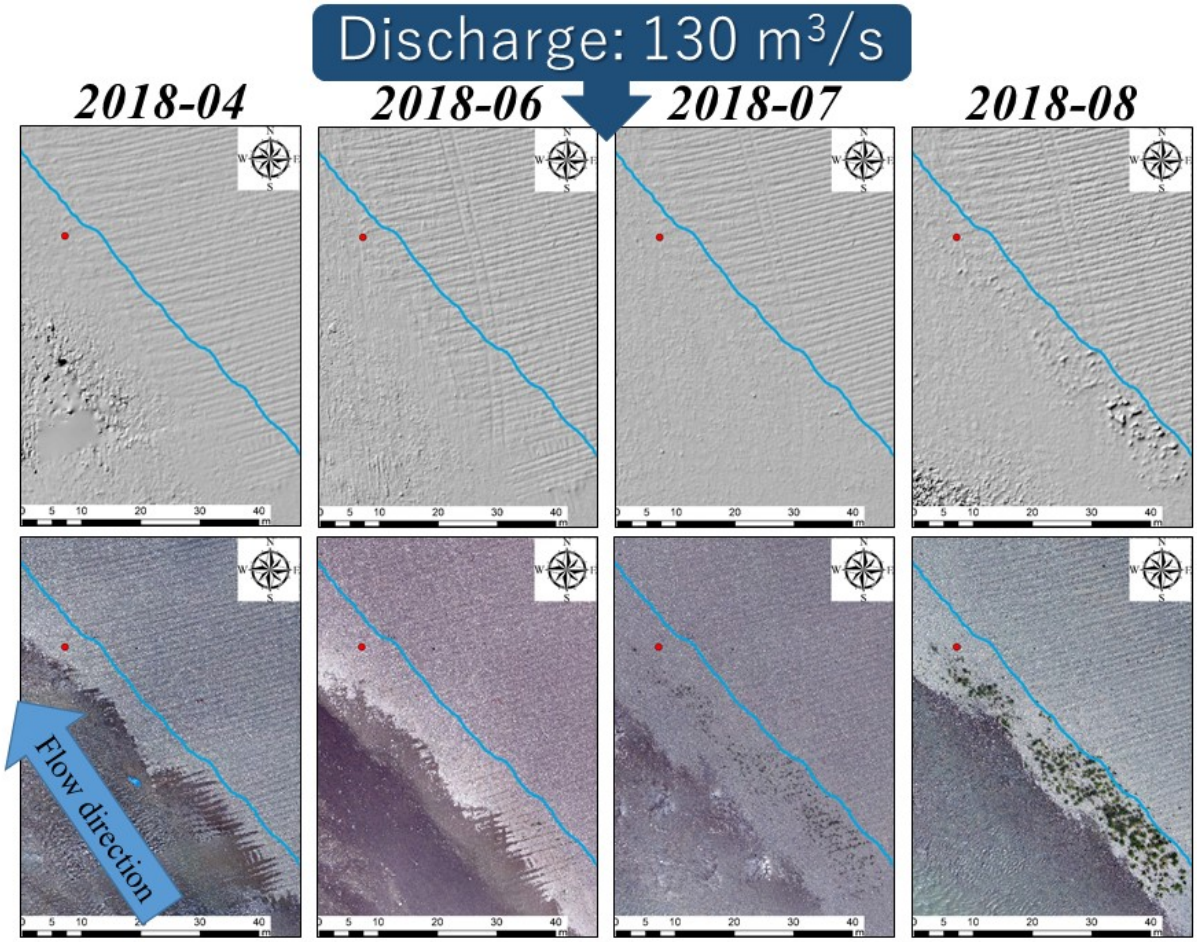


Fig.1. Hillshade images and ortho images of cultivated area.

©2019. Japan Geoscience Union. All Right Reserved.

Spatial distribution of land surface displacements in the crater of Tateyama Midagahara Volcano using high-definition topographic data

*早川 裕弌[1]、楠本 成寿[2]、小倉 拓郎[3,4]
*Yuichi S. Hayakawa[1], Shigekazu Kusumoto[2], Takuro Ogura[3,4]

1. 北海道大学地球環境科学研究院、2. 富山大学大学院理工学研究部、3. 東京大学新領域創成科学研究科、4. 北海道大学大学院環境科学院
1. Faculty of Environmental Earth Science, Hokkaido University, 2. Graduate School of Science and Engineering for Research, University of Toyama, 3. Graduate School of Frontier Science, The University of Tokyo, 4. Graduate School of Environmental Science, Hokkaido University

Detailed monitoring of land surface displacements is crucial for the assessment of activities of a volcano, especially in its crater area. Close-range remote sensing of high-definition topographic data is advantageous in the detection of centimeter-scale ground-surface displacements in a wide spacial extent, whereas the conventional leveling method is capable of detecting millimeter-scale displacements along a measurement line. We investigated the spatial distribution of land surface displacements in the Jigoku-Dani crater area of Mt. Tateyama Midagahara Volcano in Toyama Prefecture, central Japan by high-definition topographic measurements including terrestrial laser scanning and unmanned aerial vehicle-based structure-from-motion photogrammetry. The annual measurements were performed for three years (2015 to 2017). The range of uplift detected by terrestrial laser scanning corresponds with that by leveling. Together with the analytical results of the leveling data, the spatial pattern of the uplift suggests the extent of an underground pressured zone to cause the exhumation. For the prediction of the volcanic activities, further monitoring is required to reveal the spatiotemporal patterns of the displacements.

キーワード：地上レーザ測量、UAS-SfM、点群
Keywords: terrestrial laser scanning, unmanned aerial system structure-from-motion, point cloud

©2019. Japan Geoscience Union. All Right Reserved.

SfM/MVSを用いた簡易的な河床形状復元および水深評価に関する検討
Study on a simplified measurement of water depth and reconstruction of the riverbed form by using SfM and MVS.

*大澤 幸太[1]、新里 忠史[2]、三田地 勝昭[3]、川村 淳[1]、大川 真弘[1]
*OSAWA KOTA[1], Tadafumi Niizato [2], Katsuaki Mitachi[3], Makoto Kawamura[1], Masahiro Ohkawa[1]

1. 三菱マテリアルテクノ株式会社、2. 日本原子力研究開発機構、3. エイ・ティ・エス株式会社
1. Mitsubishi Materials Techno corporation , 2. Japan Atomic Energy Agency, 3. ATOM TRANSPORT SERVICE CO., LTD

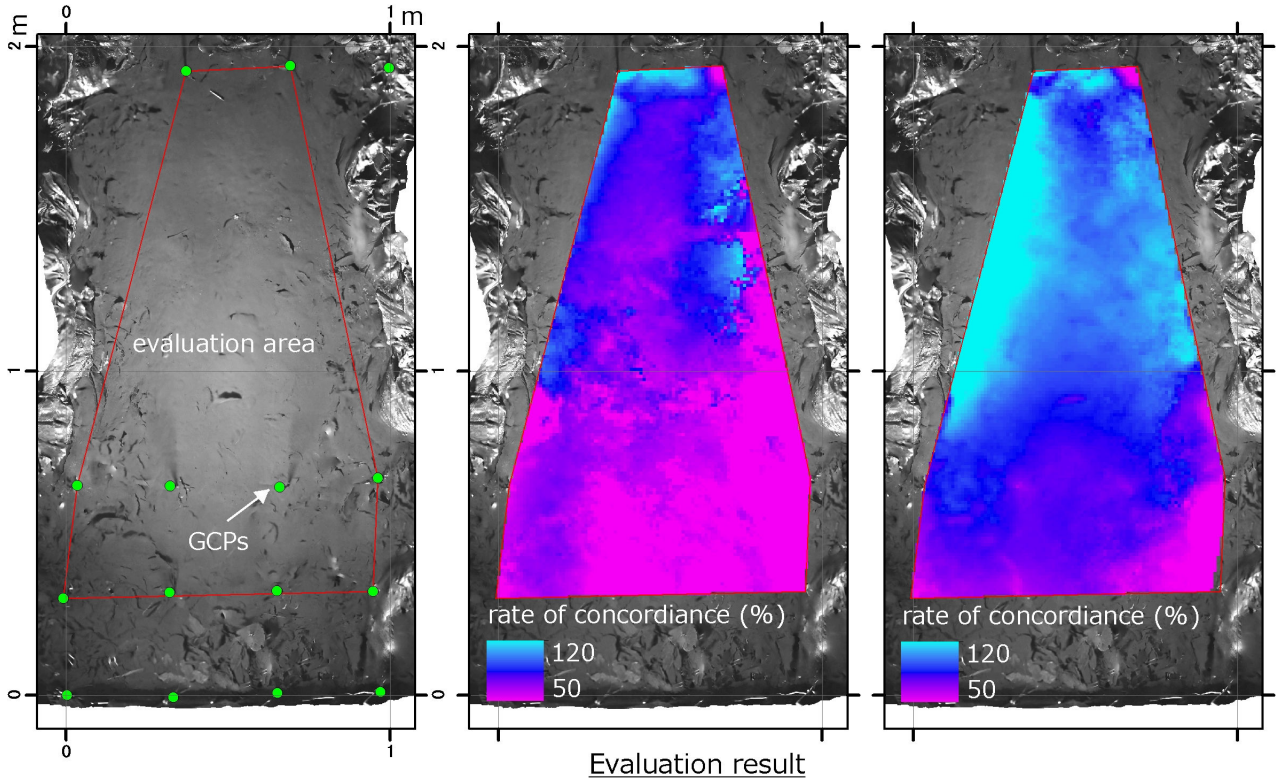
【はじめに】
東京電力ホールディングス福島第一原子力発電所の事故により山地森林内に沈着した放射性セシウムの林外への移動は、森林斜面から渓流などの小河川に流入した懸濁物による運搬過程が主要であると考えられている。そのため、自然環境中の放射性セシウムの移動や分布の変化を評価するうえで、山地森林内における小河川の河床形状や土砂の堆積量の変化を詳細に把握することは重要である。
小河川の河床における堆積量の変化は、観測開始時に基準水面を設定の上、計測時における基準水面に対する水面の距離と水深から求められる。小流域河川における水深計測方法としてはスタッフやメジャーを用いた直接計測手法が一般的であるが、詳細な河床形状を把握する場合、調査に多くの時間と労力を必要とする。また、近年ではレーザーを用いた高密度で水深を計測する手法もあるが、機器が高価であり、高度な計測技術を要する。そこで、本研究では画像を用いて立体構造を復元することが可能なSfM(Structure from Motion)およびMVS(Multi View Stereo)技術（以降SfM/MVS）を用いて、簡易的、効率的かつ詳細に水深および河床形状を復元することとした。水中で取得した画像や空中から河床を撮影した画像を用いた構造復元の例は少なく、また、本研究同等の小流域河川を対象とした実地検証事例はこれまで報告されていない。本研究では通常の画像撮影方法とあわせて、水面や水中における光の特性を考慮した独自の撮影方法を実験的に採用し、両手法で撮影された画像からSfM/MVSを用いて復元した河床形状と水深について評価した。
【調査対象及び手法】
調査対象は福島県阿武隈山地南部のスギ林内を流下する河道幅1 m程度の小河川である。河道に対し直交方向に三角堰を設置し、土砂を堆積させた。
陸上から水面下を撮影する場合、水面や水中での光の特性が水面下の構造復元に悪影響を与える。特に水深は実際の値より浅くなる傾向がある。そこで本研究では、1)水面反射を考慮し、薄暮において投光機およびサーキュラーPLフィルタ使用した撮影、2)水中での光の減衰を考慮し、光源に市販されている青色フィルムを被せるとともに、RバンドとGバンドを除外する手法を試みた（以下、TM）。一方で、日中に通常の手法により撮影した画像を用いてモデルを復元し（以下、DM）、比較した。なお、調査時には従来手法である1 mm目盛メジャーを用いた水深の計測も実施し、復元精度の評価に使用した。
薄暮時における撮影では265枚、日中は297枚の画像を取得した。それぞれの撮影時間は30分程度である。本研究におけるSfM/MVS処理にはAgisoft社のPhotoScan Professionalを用いた。取得した画像の内部評定の要素補正は同ソフト付随するセルフキャリブレーション機能を用いて行い、復元したモデルの外部評定要素の補正には、対象範囲を内包する形で配置した測量用紅白ポールと水面の交点を補正点として用いた。復元されたモデルよりDSM(Digital Surface Model)を作成した。なお、三角堰近傍は落ち葉などが多く堆積しており、周囲で実測した水深よりかなり浅く、SfM/MVSより復元したDSMには落ち葉の高さや形状が含まれることから、復元精度の評価からは除外した。
【結果及び考察】
薄暮時に撮影した画像は、水面反射が大きく低減し河床の状況を詳細に表現できた。モデルの再現性に関して面的な評価を実施するために、実測値を内挿した値を基準とする一致率[（各モデル水深÷内挿値）×100]を算出した（図）。すなわち、100%で内挿値と一致、それ以上で深く復元、それ以下で浅く復元されているこ

©2019. Japan Geoscience Union. All Right Reserved.

とを示す。水深20~25cmでDMは46%、TMは73%、水深10~15cmではDMは62%、TMは93%の一致率を示した。

TMはDMに対し高い一致率を示し、簡易的な手法ではあるものの、投光器等を用いた撮影手法は、画像の質を向上させ水深の復元性能を高めることが示唆された。またTMは堆積した落ち葉や枝などが復元されており、細かな河床形状や変化を把握することが可能であった。一方で、両モデルとも水深が増加するに伴い水深の復元性は一様に悪くなった。これは水面における光の屈折などの影響によるものと考えられる。更なる補正、撮影方法については今後の検討課題である。

キーワード：SfM/MVS、水深計測、河床形状
Keywords: SfM/MVS, measurement of water depth, riverbed form



Left: Orthographic Image, Evaluation area (red polygon) and location of GCPs (green dot),
Center: Discrepancy between measured and analysis (DM),
Right: Discrepancy between measured and analysis (TM)

©2019. Japan Geoscience Union. All Right Reserved.

Ground Penetrating Radar Imaging of Moisture and Water movement in volcanic soil

*Christopher A Gomez[1]

1. Kobe University Faculty of Maritime Sciences Volcanic Risk at Sea Research Group

Ground Penetrating Radar is a non-invasive subsurface method that provides results on the dielectric properties of the ground between 0 and 30 m on average in sediments. Working from sediments from Mt Unzen in Japan, tests over the moisture content and the air content change were conducted on the material in order to infer further data during field measurement. The GPR used in the survey is a Ramac Mala mounted with an antenna of 800 Mhz and a stack signal over time. The data were processed using Matlab using data filtering and time-depth conversion, and calculation of the dielectric properties variations. The signal analysis shows that the velocity does change over time depending on the moisture content and the change in air/void ratio. For a given homogeneous material, like at volcanoes, multiplying such analysis is a step forward the development of relatable tables for various environments.

Keywords: Ground Penetrating Radar, Soil moisture content, Volcanic material

©2019. Japan Geoscience Union. All Right Reserved.

Estimating Eruptive Volumes of Mud Volcano Southwestern Taiwan by Using UAV and SfM-MVS Photogrammetry

*CHIA-YING LIU[1], Ray Y Chuang[1], Horng-Yue Chen[2]

1. Department of Geography, National Taiwan University, 2. Academia Sinica, Institute of Earth Sciences

Mud volcanoes are special geologic features occurred in tectonic areas with horizontal compression. Complete research for mud volcanos can help us to understand the interaction of the crust and surface. In Taiwan, mud volcanoes are present on-land and off-shore southwestern Taiwan around the transitional area from subduction to orogeny. Among all mud volcanoes in Taiwan, the Wandan mud volcano erupts sporadically with significantly large amount of effluent mud. However, the mechanism of the eruption remains unclear because we lack fundamental information such as eruptive volumes, duration of mud eruption, impact factors and recurrence intervals. Therefore, it is important to estimate the eruptive volumes and further to examine the spatiotemporal pattern of the Wandan mud volcano eruption. We first compile literature and newspapers for historic eruption events to estimate two groups of recurrence interval: 150-180 days for highly active period and 300-600 days for less active period.

Since the sporadic eruption make different for rapid survey by using traditional methods, we take advantage of unmanned aerial vehicles (UAV) to design a survey network specifically. Therefore, we estimate the eruptive volumes of recent eruptions for the Wandan mud volcano by using aerial images taken from UAV, and 3D models derived from the structure-from-motion (SfM) photogrammetry technique. We use RTK-GPS and leveling for horizontal and vertical measurements of ground control point, respectively. We use the SfM software to generate DSMs, point clouds, and orthophotos with cm-level accuracy. We estimate the eruptive volume by subtracting the pre-eruption DSM from the post-eruption DSM. Our results show that for the event on 15 May, 2018, the eruptive area is 12,761 m^2 and the volume is 13,106.3625 ±13.0105m^3.

Keywords: UAS, GNSS, digital surface modeling, control survey

©2019. Japan Geoscience Union. All Right Reserved.

Increasing temporal depth of urban Land-Use Regression Models by wind-data driven dynamic buffer generation

*Tilman Leo Hohenberger[1], King Wai Leung[1]

1. Division of Environment and Sustainability, Hong Kong University of Science and Technology

Land-use regression (LUR) models are commonly used as an inexpensive and easy to set-up way to predict spatial variability in air-pollution. They are successfully applied to regional and, more and more, urban settings, making use of spatial predictors such as land-use, vegetation, morphology and geography. New approaches include an improved use of wind-data for buffer-creation and predictor calculation.

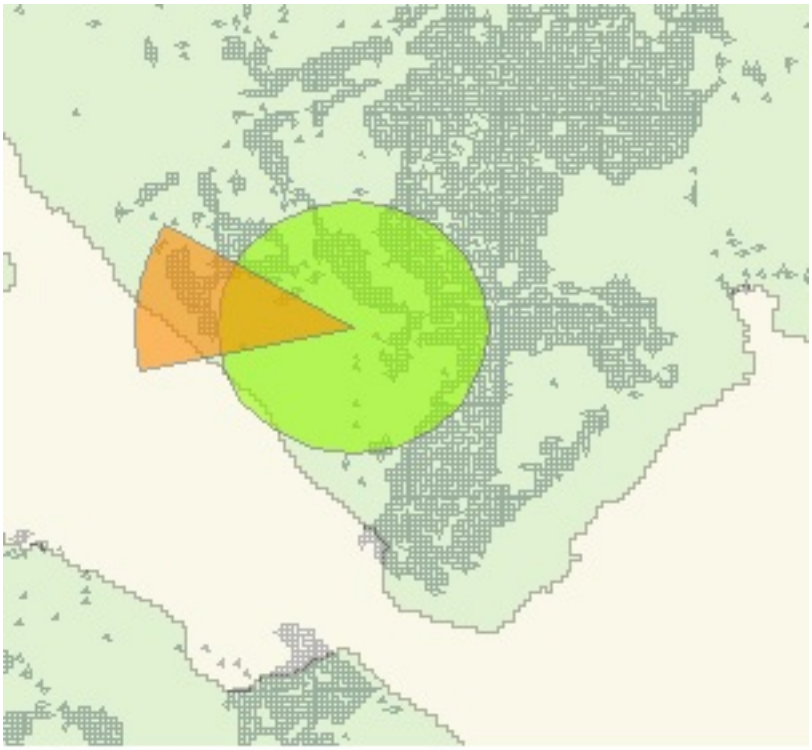
Traditionally, LUR models are used to generate annual or seasonal concentration averages and are not able cover deeper temporal variability. We aim at increasing temporal depth by using a novel approach in generating dynamic buffers for predictor calculation using both monthly wind-speed and wind-direction averages. The traditional circular buffers are replaced by wedges, whose orientation and radius are bound to these meteorological variables.

Here, Hong Kong’ s diverse territory is taken as a study site, and our model is trained with 5 years data from 16 government air quality monitoring stations and deployed portable sensors network. We compare our novel approach to both traditional LUR models and a sophisticated urban chemical transport model (ADMS-Urban).

Results will highlight the opportunities in using LUR models for monthly air-quality pollution concentration as an alternative to chemical transport modelling.

Keywords: Wind, Land Use Regression, Spatial Data, Meteorology

©2019. Japan Geoscience Union. All Right Reserved.



Dynamic and circular LUR buffer in Hong Kong's urban environment

©2019. Japan Geoscience Union. All Right Reserved.

[E] ポスター発表 | セッション記号 M (領域外・複数領域)：M-TT 計測技術・研究手法

2019年5月27日(月) 17:15 ~ 18:30 | ポスター会場 幕張メッセ国際展示場 8ホール_44

[M-TT47] 人新世における高精細地形・地球物理データの活用

コンビーナ:早川 裕弋(北海道大学地球環境科学研究院)、楠本 成寿(富山大学大学院理工学研究部(都市デザイン学))、Gomez Christopher(神戸大学 海事科学部 海域火山リスク科学研究室)

Recent technical developments of high-definition topographic and geophysical data acquisition have enabled us to further investigate geoscientific issues including land surface processes, subsurface structures, submarine and aerial environments, geo-ecological interactions, and disaster mitigation. Such high-definition or high-resolution data are particularly useful for studies in short-term temporal scales, and future predictions such as numerical modelings. In this session, we expect submissions on topics challenging such issues in the Anthropocene, the most recent geological era of the Earth. A range of topics would fit the session framework, including theoretical work, improvements in data acquisition, extensive data preservation and archiving, pre- and post-processing, statistical analysis, modeling, and simulation for geoscientific research and geohazard assessments in the Anthropocene. The methodological approaches may include, but not limited to, laser scanning, SfM-MVS photogrammetry, GNSS precise positioning, SAR interferometry, multi-beam sonar, and electromagnetic sensors, based on terrestrial (fixed or mobile) and aerial (UAV or manned airborne) platforms.

[MTT47-P01] High-definition topography monitoring after riverbed cultivation in the Echi River, central Japan

*小倉 拓郎[1,2]、淺野 悟史[3]、水野 敏明[3]、東 善広[3]、北井 剛[4]、早川 裕弋[5,6]、飯塚 浩太郎[6] (1.東京大学大学院新領域創成科学研究科、2.北海道大学大学院環境科学院、3.滋賀県琵琶湖環境科学研究センター、4.滋賀県立琵琶湖博物館、5.北海道大学地球環境研究院、6.東京大学空間情報科学研究センター)

[MTT47-P02] **Spatial distribution of land surface displacements in the crater of Tateyama Midagahara Volcano using high-definition topographic data**

*早川 裕弋[1]、楠本 成寿[2]、小倉 拓郎[3,4] (1.北海道大学地球環境科学研究院、2.富山大学大学院理工学研究部、3.東京大学新領域創成科学研究科、4.北海道大学大学院環境科学院)

[MTT47-P03] SfM/MVSを用いた簡易的な河床形状復元および水深評価に関する検討

*大澤 幸太[1]、新里 忠史[2]、三田地 勝昭[3]、川村 淳[1]、大川 真弘[1] (1.三菱マテリアルテクノ株式会社、2.日本原子力研究開発機構、3.エイ・ティ・エス株式会社)

[MTT47-P04] Ground Penetrating Radar Imaging of Moisture and Water movement in volcanic soil

*Christopher A Gomez[1] (1.Kobe University Faculty of Maritime Sciences Volcanic Risk at Sea Research Group)

[MTT47-P05] **Estimating Eruptive Volumes of Mud Volcano Southwestern Taiwan by Using UAV and SfM-MVS Photogrammetry**

*CHIA-YING LIU[1]、Ray Y Chuang[1]、Horng-Yue Chen[2] (1.Department of Geography, National Taiwan University、2.Academia Sinica, Institute of Earth Sciences)

[MTT47-P06] Increasing temporal depth of urban Land-Use Regression Models by wind-data driven dynamic buffer generation

*Tilman Leo Hohenberger[1]、King Wai Leung[1] (1.Division of Environment and Sustainability, Hong Kong University of Science and Technology)

High-definition topography monitoring after riverbed cultivation in the Echi River, central Japan

*小倉 拓郎[1,2]、淺野 悟史[3]、水野 敏明[3]、東 善広[3]、北井 剛[4]、早川 裕弋[5,6]、飯塚 浩太郎[6]
*Takuro Ogura[1,2], Satoshi Asano[3], Toshiaki Mizuno[3], Yoshihiro Azuma[3], Takeshi Kitai[4], Yuichi S Hayakawa[5,6], Kotaro Iizuka[6]

1. 東京大学大学院新領域創成科学研究科、2. 北海道大学大学院環境科学院、3. 滋賀県琵琶湖環境科学研究センター、4. 滋賀県立琵琶湖博物館、5. 北海道大学地球環境研究院、6. 東京大学空間情報科学研究センター
1. Graduate School of Frontier Sciences, The University of Tokyo, 2. Graduate School of Environmental Science, Hokkaido University, 3. Lake Biwa Environmental Research Institute , 4. Lake Biwa Museum, 5. Faculty of Environmental Earth Science, Hokkaido University, 6. Center for Spatial information Science, The University of Tokyo

Natural processes of erosion and deposition on riverbeds are generally limited in Japan due to large-scale public constructions including dams and banks. As a result of the construction of dams, sediment transport may dramatically decrease in the downstream area are, and the river ecosystem can also be affected. To make sediment move more vigorously, we cultivated the armored gravel riverbed with heavy machinery. We then explore the effects of riverbed cultivating by monitoring the topographic changes with high-frequency and high-definition measurements (HF-HD measurements), whereas conventional measurement technologies do not compensate spatial resolution and temporal resolution to capture the topographic change. Using UAS (Unmanned Aerial Vehicle) and SfM-MVS (Structure-from-Motion –Multi-view Stereo) photogrammetry, we found the transportation of the fixed gravels were occurring after cultivating the riverbed in 2017. The temporal and spatial resolutions of the HF-HD topographic data was approximately 2 months and 10 cm, respectively. In July 2018, water flow at 130 m^3/s was discharged from the upstream dam, and we confirmed that a part of the gravels in the cultivated area was eroded and replaced with new sediments (Fig. 1). These observations indicate that riverbed monitoring using UAV and SfM - MVS can be a practical tool for proper management of riverbeds. Applying this result, we will further clarify the relationships between the water quantity discharged from the dam and the riverbed topographic changes.

キーワード：高精細地形情報、河床耕耘、UAV、SfM多視点ステレオ写真測量、愛知川
Keywords: High-definition topographic data, riverbed cultivation, UAV, SfM-MVS photogrammetry, Echi river

©2019. Japan Geoscience Union. All Right Reserved.

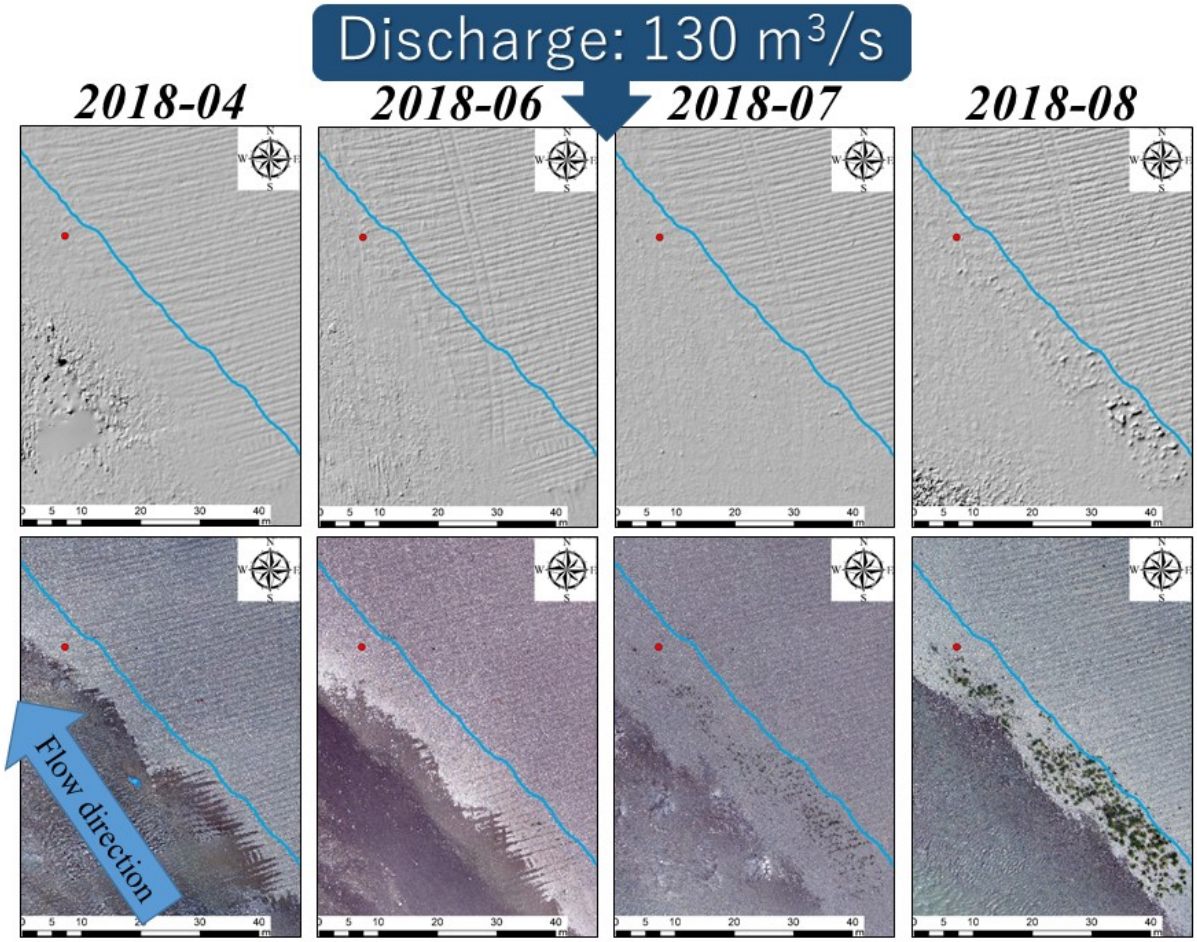


Fig.1. Hillshade images and ortho images of cultivated area.

©2019. Japan Geoscience Union. All Right Reserved.

Spatial distribution of land surface displacements in the crater of Tateyama Midagahara Volcano using high-definition topographic data

*早川 裕弌[1]、楠本 成寿[2]、小倉 拓郎[3,4]
*Yuichi S. Hayakawa[1], Shigekazu Kusumoto[2], Takuro Ogura[3,4]

1. 北海道大学地球環境科学研究院、2. 富山大学大学院理工学研究部、3. 東京大学新領域創成科学研究科、4. 北海道大学大学院環境科学院
1. Faculty of Environmental Earth Science, Hokkaido University, 2. Graduate School of Science and Engineering for Research, University of Toyama, 3. Graduate School of Frontier Science, The University of Tokyo, 4. Graduate School of Environmental Science, Hokkaido University

Detailed monitoring of land surface displacements is crucial for the assessment of activities of a volcano, especially in its crater area. Close-range remote sensing of high-definition topographic data is advantageous in the detection of centimeter-scale ground-surface displacements in a wide spacial extent, whereas the conventional leveling method is capable of detecting millimeter-scale displacements along a measurement line. We investigated the spatial distribution of land surface displacements in the Jigoku-Dani crater area of Mt. Tateyama Midagahara Volcano in Toyama Prefecture, central Japan by high-definition topographic measurements including terrestrial laser scanning and unmanned aerial vehicle-based structure-from-motion photogrammetry. The annual measurements were performed for three years (2015 to 2017). The range of uplift detected by terrestrial laser scanning corresponds with that by leveling. Together with the analytical results of the leveling data, the spatial pattern of the uplift suggests the extent of an underground pressured zone to cause the exhumation. For the prediction of the volcanic activities, further monitoring is required to reveal the spatiotemporal patterns of the displacements.

キーワード：地上レーザ測量、UAS-SfM、点群
Keywords: terrestrial laser scanning, unmanned aerial system structure-from-motion, point cloud

©2019. Japan Geoscience Union. All Right Reserved.

SfM/MVSを用いた簡易的な河床形状復元および水深評価に関する検討
Study on a simplified measurement of water depth and reconstruction of the riverbed form by using SfM and MVS.

*大澤 幸太[1]、新里 忠史[2]、三田地 勝昭[3]、川村 淳[1]、大川 真弘[1]
*OSAWA KOTA[1], Tadafumi Niizato [2], Katsuaki Mitachi[3], Makoto Kawamura[1], Masahiro Ohkawa[1]

1. 三菱マテリアルテクノ株式会社、2. 日本原子力研究開発機構、3. エイ・ティ・エス株式会社
1. Mitsubishi Materials Techno corporation , 2. Japan Atomic Energy Agency, 3. ATOM TRANSPORT SERVICE CO., LTD

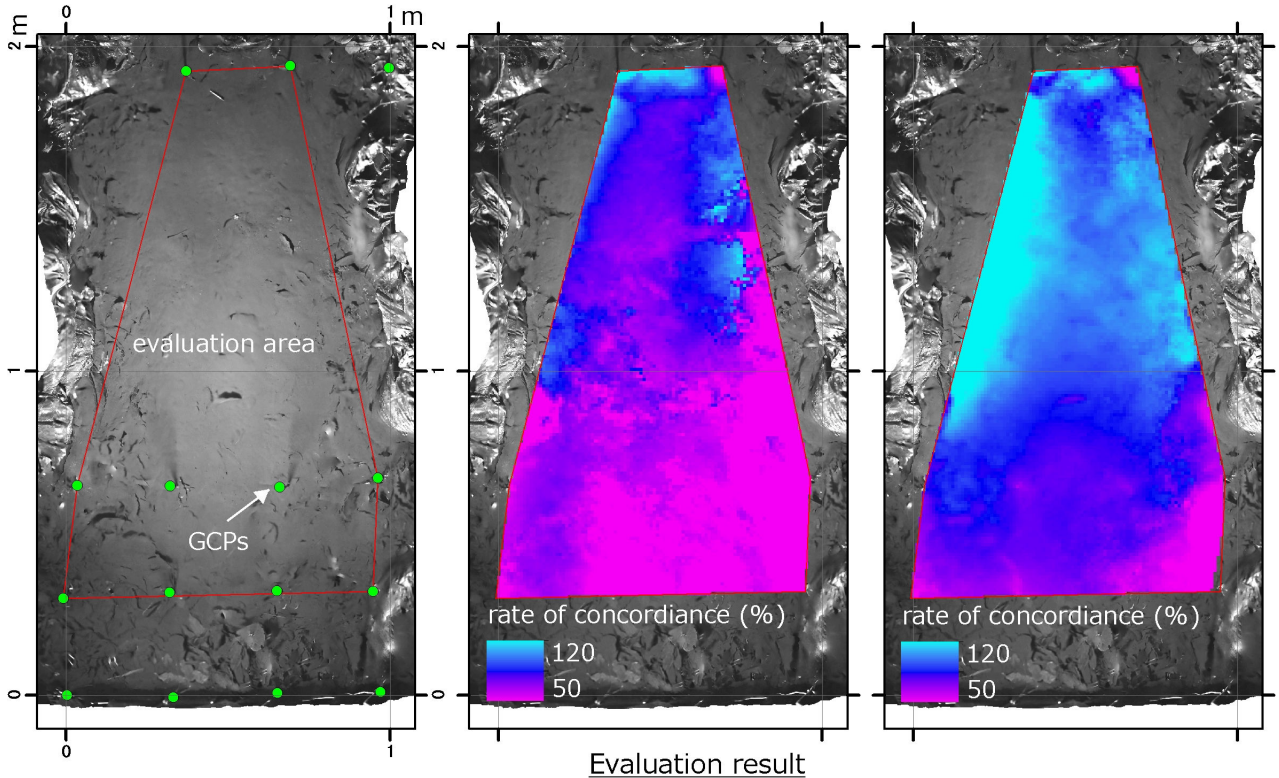
【はじめに】
東京電力ホールディングス福島第一原子力発電所の事故により山地森林内に沈着した放射性セシウムの林外への移動は、森林斜面から渓流などの小河川に流入した懸濁物による運搬過程が主要であると考えられている。そのため、自然環境中の放射性セシウムの移動や分布の変化を評価するうえで、山地森林内における小河川の河床形状や土砂の堆積量の変化を詳細に把握することは重要である。
小河川の河床における堆積量の変化は、観測開始時に基準水面を設定の上、計測時における基準水面に対する水面の距離と水深から求められる。小流域河川における水深計測方法としてはスタッフやメジャーを用いた直接計測手法が一般的であるが、詳細な河床形状を把握する場合、調査に多くの時間と労力を必要とする。また、近年ではレーザーを用いた高密度で水深を計測する手法もあるが、機器が高価であり、高度な計測技術を要する。そこで、本研究では画像を用いて立体構造を復元することが可能なSfM(Structure from Motion)およびMVS(Multi View Stereo)技術（以降SfM/MVS）を用いて、簡易的、効率的かつ詳細に水深および河床形状を復元することとした。水中で取得した画像や空中から河床を撮影した画像を用いた構造復元の例は少なく、また、本研究同等の小流域河川を対象とした実地検証事例はこれまで報告されていない。本研究では通常の画像撮影方法とあわせて、水面や水中における光の特性を考慮した独自の撮影方法を実験的に採用し、両手法で撮影された画像からSfM/MVSを用いて復元した河床形状と水深について評価した。
【調査対象及び手法】
調査対象は福島県阿武隈山地南部のスギ林内を流下する河道幅1 m程度の小河川である。河道に対し直交方向に三角堰を設置し、土砂を堆積させた。
陸上から水面下を撮影する場合、水面や水中での光の特性が水面下の構造復元に悪影響を与える。特に水深は実際の値より浅くなる傾向がある。そこで本研究では、1)水面反射を考慮し、薄暮において投光機およびサーキュラーPLフィルタ使用した撮影、2)水中での光の減衰を考慮し、光源に市販されている青色フィルムを被せるとともに、RバンドとGバンドを除外する手法を試みた（以下、TM）。一方で、日中に通常の手法により撮影した画像を用いてモデルを復元し（以下、DM）、比較した。なお、調査時には従来手法である1 mm目盛メジャーを用いた水深の計測も実施し、復元精度の評価に使用した。
薄暮時における撮影では265枚、日中は297枚の画像を取得した。それぞれの撮影時間は30分程度である。本研究におけるSfM/MVS処理にはAgisoft社のPhotoScan Professionalを用いた。取得した画像の内部評定の要素補正は同ソフト付随するセルフキャリブレーション機能を用いて行い、復元したモデルの外部評定要素の補正には、対象範囲を内包する形で配置した測量用紅白ポールと水面の交点を補正点として用いた。復元されたモデルよりDSM(Digital Surface Model)を作成した。なお、三角堰近傍は落ち葉などが多く堆積しており、周囲で実測した水深よりかなり浅く、SfM/MVSより復元したDSMには落ち葉の高さや形状が含まれることから、復元精度の評価からは除外した。
【結果及び考察】
薄暮時に撮影した画像は、水面反射が大きく低減し河床の状況を詳細に表現できた。モデルの再現性に関して面的な評価を実施するために、実測値を内挿した値を基準とする一致率[（各モデル水深÷内挿値）×100]を算出した（図）。すなわち、100%で内挿値と一致、それ以上で深く復元、それ以下で浅く復元されているこ

©2019. Japan Geoscience Union. All Right Reserved.

とを示す。水深20~25cmでDMは46%、TMは73%、水深10~15cmではDMは62%、TMは93%の一致率を示した。

TMはDMに対し高い一致率を示し、簡易的な手法ではあるものの、投光器等を用いた撮影手法は、画像の質を向上させ水深の復元性能を高めることが示唆された。またTMは堆積した落ち葉や枝などが復元されており、細かな河床形状や変化を把握することが可能であった。一方で、両モデルとも水深が増加するに伴い水深の復元性は一様に悪くなった。これは水面における光の屈折などの影響によるものと考えられる。更なる補正、撮影方法については今後の検討課題である。

キーワード：SfM/MVS、水深計測、河床形状
Keywords: SfM/MVS, measurement of water depth, riverbed form



Left: Orthographic Image, Evaluation area (red polygon) and location of GCPs (green dot),
Center: Discrepancy between measured and analysis (DM),
Right: Discrepancy between measured and analysis (TM)

©2019. Japan Geoscience Union. All Right Reserved.

Ground Penetrating Radar Imaging of Moisture and Water movement in volcanic soil

*Christopher A Gomez[1]

1. Kobe University Faculty of Maritime Sciences Volcanic Risk at Sea Research Group

Ground Penetrating Radar is a non-invasive subsurface method that provides results on the dielectric properties of the ground between 0 and 30 m on average in sediments. Working from sediments from Mt Unzen in Japan, tests over the moisture content and the air content change were conducted on the material in order to infer further data during field measurement. The GPR used in the survey is a Ramac Mala mounted with an antenna of 800 Mhz and a stack signal over time. The data were processed using Matlab using data filtering and time-depth conversion, and calculation of the dielectric properties variations. The signal analysis shows that the velocity does change over time depending on the moisture content and the change in air/void ratio. For a given homogeneous material, like at volcanoes, multiplying such analysis is a step forward the development of relatable tables for various environments.

Keywords: Ground Penetrating Radar, Soil moisture content, Volcanic material

©2019. Japan Geoscience Union. All Right Reserved.

Estimating Eruptive Volumes of Mud Volcano Southwestern Taiwan by Using UAV and SfM-MVS Photogrammetry

*CHIA-YING LIU[1], Ray Y Chuang[1], Horng-Yue Chen[2]

1. Department of Geography, National Taiwan University, 2. Academia Sinica, Institute of Earth Sciences

Mud volcanoes are special geologic features occurred in tectonic areas with horizontal compression. Complete research for mud volcanos can help us to understand the interaction of the crust and surface. In Taiwan, mud volcanoes are present on-land and off-shore southwestern Taiwan around the transitional area from subduction to orogeny. Among all mud volcanoes in Taiwan, the Wandan mud volcano erupts sporadically with significantly large amount of effluent mud. However, the mechanism of the eruption remains unclear because we lack fundamental information such as eruptive volumes, duration of mud eruption, impact factors and recurrence intervals. Therefore, it is important to estimate the eruptive volumes and further to examine the spatiotemporal pattern of the Wandan mud volcano eruption. We first compile literature and newspapers for historic eruption events to estimate two groups of recurrence interval: 150-180 days for highly active period and 300-600 days for less active period.

Since the sporadic eruption make different for rapid survey by using traditional methods, we take advantage of unmanned aerial vehicles (UAV) to design a survey network specifically. Therefore, we estimate the eruptive volumes of recent eruptions for the Wandan mud volcano by using aerial images taken from UAV, and 3D models derived from the structure-from-motion (SfM) photogrammetry technique. We use RTK-GPS and leveling for horizontal and vertical measurements of ground control point, respectively. We use the SfM software to generate DSMs, point clouds, and orthophotos with cm-level accuracy. We estimate the eruptive volume by subtracting the pre-eruption DSM from the post-eruption DSM. Our results show that for the event on 15 May, 2018, the eruptive area is 12,761 m^2 and the volume is 13,106.3625 ±13.0105m^3.

Keywords: UAS, GNSS, digital surface modeling, control survey

©2019. Japan Geoscience Union. All Right Reserved.

Increasing temporal depth of urban Land-Use Regression Models by wind-data driven dynamic buffer generation

*Tilman Leo Hohenberger[1], King Wai Leung[1]

1. Division of Environment and Sustainability, Hong Kong University of Science and Technology

Land-use regression (LUR) models are commonly used as an inexpensive and easy to set-up way to predict spatial variability in air-pollution. They are successfully applied to regional and, more and more, urban settings, making use of spatial predictors such as land-use, vegetation, morphology and geography. New approaches include an improved use of wind-data for buffer-creation and predictor calculation.

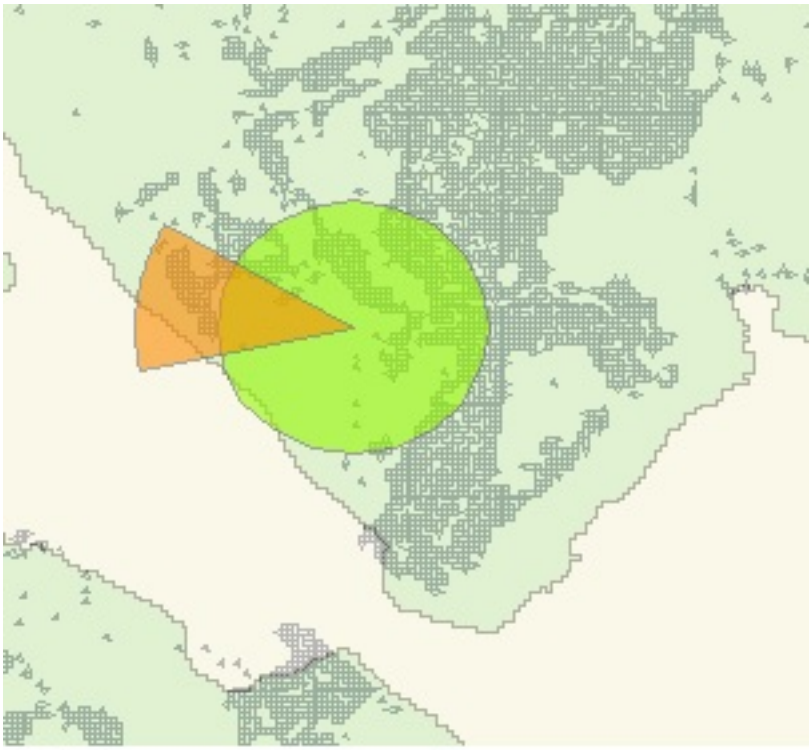
Traditionally, LUR models are used to generate annual or seasonal concentration averages and are not able cover deeper temporal variability. We aim at increasing temporal depth by using a novel approach in generating dynamic buffers for predictor calculation using both monthly wind-speed and wind-direction averages. The traditional circular buffers are replaced by wedges, whose orientation and radius are bound to these meteorological variables.

Here, Hong Kong’ s diverse territory is taken as a study site, and our model is trained with 5 years data from 16 government air quality monitoring stations and deployed portable sensors network. We compare our novel approach to both traditional LUR models and a sophisticated urban chemical transport model (ADMS-Urban).

Results will highlight the opportunities in using LUR models for monthly air-quality pollution concentration as an alternative to chemical transport modelling.

Keywords: Wind, Land Use Regression, Spatial Data, Meteorology

©2019. Japan Geoscience Union. All Right Reserved.



Dynamic and circular LUR buffer in Hong Kong's urban environment

©2019. Japan Geoscience Union. All Right Reserved.